Formation waters in petroleum reservoirs; their controls and applications

Stephanie Jane Houston

Submitted in accordance with the requirements for the degree of

Doctor of Philosophy (PhD)

The University of Leeds

School of Earth and Environment

March 2007

THESIS CONTAINS CD/DVD

ACKNOWLEGDMENTS

I would like to thank my supervisors, Bruce Yardley, Quentin Fisher, Craig Smalley and Ian Collins for all their help and support. I would like to thank BP for providing me with a substantial proportion of the data necessary for my studies; as well as granting me permission to study core samples from Miller and San Juan. I am also indebted to academic and technical staff at the University of Leeds for their assistance and advice: Lesley Neve, Neil Cundall, Robert Marshall, Linda Forbes and Eric Condliffe. Non-supervisor staff at BP have also been invaluable in providing me with the advice, information and support I needed, especially Rob Bruant, Dave Mercer and Kevin Webb. Thanks also to Sasha Haddad and Richard Worden at the University of Liverpool.

I would not have completed this work were it not for the mutual support from the occupiers of the railway carriage, Sally, Rosie, Claire, Luciana and Caco, as well as other Leeds geochemists Lois and Murray. My family have been unbelievably strong and understanding over the past years, through some difficult times. The various occupants of Manor Drive, Village Place and Burley Hill Drive have all helped me maintain my good humour, and special thanks go to Sarah. Finally, the most heartfelt thanks to Mark who has not only been with me every step of the way, but also deigned to read sections of the thesis and even voiced some brave opinions.

ABSTRACT

Abundant water chemistry analyses from nine different locations (predominantly petroleum reservoirs) on five continents were evaluated. This information, together with local mineralogy, depth and temperature relations provided a sound basis from which to investigate the most important controls on formation water composition. In particular, the detailed study of two very different hydrocarbon reservoir case studies (the Central US coalbed methane reservoir, the San Juan Basin and the North Sea oilfield Miller) provided an insight not only into the fundamental controls on formation water composition, but also into the effects of active oilfield development on systems that are very sensitive to change on rapid timescales.

The geochemistry of San Juan waters is controlled by the introduction of bicarbonate through carbonate dissolution and methane/coal oxidation leading to leaching of Na-bearing clay minerals, and by ion exchange on clay minerals and dilution by meteoric waters in certain locations. The time series of produced waters from Miller enabled detailed study of fluid mixing in the field and the physical, chemical and thermodynamic response of the system to the injection of seawater. Changes occur in the concentrations of many water components through time that cannot be explained by linear mixing between formation water and injected water and require dissolution or precipitation reactions to have occurred between injection and production sites. For example Ba, and SO_4 concentrations are affected by equilibrium with barite and what is likely to be sulphate reduction. Also, excess Si present in the fluid is due to dissolution of the silicate phases in the reservoir, and demonstrates reactions between silicate minerals occur on a fast enough timescale to buffer the pH of the water.

Integration of all available data shows consistent patterns of behaviour, which implicate mineral-fluid interactions in the subsurface as a major control on formation water chemistry. For example, globally, Ca concentrations are shown to behave in one of three ways, all of which depend on water interaction with the host rock, be it silicate or carbonate, clastic or evaporite. Distinct trends arise for bicarbonate waters, brines derived by halite dissolution and formation brines that have evolved extensively with silicates. In addition, K concentrations are closely related to feldspar-clay equilibria and Mg concentrations are influenced predominantly by carbonate minerals with significant contribution from clays. It is likely that initial Ba concentration is related to interaction with K-feldspars and SO_4 is controlled by equilibrium with sulphate mineral phases as well as by redox.

A greater understanding of formation water chemistry leads to an improved perception of the importance of these systems in terms of both furthering scientific progress and the technological development of the oil and gas industry. In particular, produced water chemistry analyses from Miller were used to appraise and improve the most important aspects of both generic and specific reservoir models. A set of simple models emphasised the point that small variations in reservoir property parameters can have significant effects on model outputs, and thus the highlighted the importance of thorough reservoir characterisation, particularly permeability heterogeneity, capillary pressure and relative fluid permeabilities.

Geochemical models of three different systems from the integrated database (the Alberta Basin, a Colombian onshore oilfield and an oilfield from offshore Gulf of Mexico) illustrate that reservoir rocks containing a wide variety of minerals are the most effective at limiting pH decrease following the injection of CO_2 into the system. The geochemistry, in particular the salinity, of the formation water present also has a significant bearing on the processes that are likely to occur during CO_2 sequestration.

CONTENTS

Contents

FIGURES

TABLES

A. OVERVIEW

1.0 INTRODUCTION

"Formation water" is a term for water, saline or otherwise, present within the pore spaces of a sedimentary rock, and can include locally recharged waters of meteoric origin as well as that originally present when the sediment was deposited. Pore waters are ubiquitous in sediments and sedimentary rocks and exhibit significant variation in composition. They can vary in terms of salinity as well as in the relative concentrations of the dissolved species, but the reasons for this extreme variability are not fully understood. Many authors have speculated on what might control formation water composition, and certain theories have now become generally accepted. These theories include: the increase in cation concentration with chloride constrained by charge balance, the conservative nature of halides and their use in determining fluid origins and the effect of some diagenetic processes and water-rock interactions on formation water chemistry. However, some noteworthy questions regarding the nature of formation waters still remain unanswered.

A great deal of emphasis is now being placed on improving the understanding of the controls on waters in systems such as groundwater aquifers and oil and gas reservoirs. In the petroleum industry in particular, formation water composition can affect the likelihood of mineral scale precipitating, give an indication as to the extent of fluid mixing in producing reservoirs and provide information about the homogeneity of the reservoir and the nature of any mineralogically controlled reactions. In addition, the co-existence of water with hydrocarbons results in both chemical and physical interactions during production (e.g. wettability, dissolution of organic acids, gas souring through H_2S production etc) the understanding of which are critical to the industry.

The objectives of this thesis are to identify the main variations in formation water chemistry on global, regional and local scales, to identify the controls on particular fluid characteristics and to apply knowledge of formation water chemistry to practical, industrial problems. This thesis will: summarise the current understanding of the nature of, and controls on, formation waters, highlighting those aspects of the subject that remain uncertain; use detailed data from specific locations (case studies) to understand better the subsurface processes that may be extrapolated to similar locations worldwide; use a portion of the global formation water data available to evaluate further the degree to which formation water compositions reflect water-rock interaction processes; and apply new understanding to practical problems experienced by petroleum companies present day. Furthermore, the extent to which formation waters are predictable and affected by changing mineralogy and temperature will be evaluated, together with the extent to which they remain unpredictable due to the importance of basin history and kinetic factors.

In this study I have attempted to bring together information from a number of different sources from the last ~50 years. Detailed knowledge of the processes occurring in one specific location can provide information about the likelihood of such processes taking place elsewhere. The core of the thesis is comprised of two case studies of hydrocarbon reservoirs in two very different geological settings, with different exploitative potential and which are at different stages in their production life cycle. The case studies are: the oil-producing Miller field in the North Sea and the coal-bed methane-bearing northern San Juan Basin in Colorado/New Mexico. In both cases the data used is primarily the analyses of the inorganic elemental composition of the formation waters, but additional information on geology and mineralogy has been utilised extensively, as well as isotopic data where available. Similar methods of data analysis used on different datasets highlight differences and similarities in the systems and provide a detailed understanding of specific, important processes occurring in each.

The next stage is to draw on the detailed local information and apply it to a larger global scale. In doing so, it is possible to make use of the abundant formation water chemistry data available in the literature, together with that provided by BP for this project. From this analysis, a series of predictive guildines can be identified and applied successfully to regions on a basin scale. The "rules" are constructed through explaining ion concentrations in terms of their relation to water-rock interactions. It will be argued that the overall formation water composition of a particular location acts as a "fingerprint" and reflects the mineralogy of the relevant lithologies, the burial conditions and the chlorinity of the formation waters.

Once a reasonable level of understanding has been reached, this knowledge benefits possible applications that are of direct use in the petroleum industry and contributes to the current push towards producing abundant, sustainable and renewable energy sources. CO_2 sequestration has been mooted as a possible short term solution to emissions-induced climate change. The safe introduction of any gas to a system containing rocks, hydrocarbons and chemically complex formation waters requires detailed understanding of the likely chemical consequences of such a process.

Similarly, water (saline or fresh) is often introduced into reservoirs as part of the production process. Water present in the reservoir is produced along with hydrocarbons from oil and gas reservoirs. Monitoring the change (or lack thereof) in the chemical composition of the produced water will be shown to provide information as to the chemical and physical processes occurring within the formation.

2. CONTROLS ON FORMATION WATER COMPOSITIONS

2.1 Introduction

A great deal of literature has been published on the subject of formation waters, dating back over 50 years. This chapter summarises the main findings of past studies, highlights remaining controversies and uncertainties and sets the scene for the new work that forms the bulk of the thesis. The chapter begins by outlining the basic characteristics of formation waters and how they vary. It then discusses what are accepted to be the dominant controls on formation water composition, detailing the most important of these controls.

2.2 Formation water basics

2.2.1 Definitions

Formation water is water that occurs naturally within the pores of sedimentary rock and is free to move under appropriate hydrodynamic conditions (Worden *et al.*, 1990). If a formation water is the same water that was included in the pore spaces at the time of deposition, it is known as *connate water* (Hanor, 1994). All formation waters contain soluble salts to some degree, but the variation in the concentration and nature of these dissolved salts is considerable: waters range in salinity from almost fresh to dense, saline brines. In order to distinguish easily the different types of formation waters and consistently describe them, it is necessary to define the relevant terms commonly used in the literature. The word "*brine*" is commonly used to describe any water containing dissolved salts, however Carpenter (1978) set out a classification scheme which maybe easily applied to formation waters. It requires that a brine must contain over 100,000 mg/L total dissolved salts, water containing between 10,000 and 100,000 mg/L dissolved salts is termed *saline*, and any water containing less than 10,000 mg/L is either *fresh* or *brackish*. By these definitions seawater (at ~35,000 mg/L dissolved salts) is saline, but not a brine. *Salinity* is a measure of the total dissolved salts (usually of Na, K, Ca and Mg) in solution, but is often used interchangeably with *total dissolved solids* (TDS), which is the sum of all inorganic and organic non-particulate material. In addition to these terms, *chlorinity* is the concentration of all dissolved chloride in solution, but because chloride is the dominant anion in most saline waters, chlorinity is often used as a proxy for salinity.

2.2.2 The dynamic subsurface

The water included in sediment pore spaces is only very rarely true connate water, because of both chemical alteration and physical migration (Hanor, 1994). Formation water may have originated very close to where it currently resides and have evolved chemically in situ, or may have been introduced to the rock through large scale physical migration linked to compaction, tectonic deformation, meteoric recharge or magmatic activity. There are various processes by

which aqueous components are concentrated to produce fluids with high ionic strength, including, at the surface: evaporation of H_2O from saline water (e.g. seawater), and at depth: dissolution of evaporite minerals; incongruent alteration of hydrous evaporite minerals; and incorporation of water into hydrous minerals (Carpenter, 1978). Sources of dissolved salts in formation fluids of sedimentary basins are central to interpreting fluid origin, evolution and migration in the crust (Walter *et al.*, 1990).

Formation waters are further subject to a number of different physical, chemical and thermodynamic processes in the subsurface that permanently alter their character, and often cause them to change so much that the original nature of the fluid can no longer be recognised. Physical transport of the fluids can cause changes in composition through dispersion and diffusion, as well as through inducing thermodynamic disequilibrium.

In addition to the natural process of fluid evolution, sampling or hydrocarbon production practices can cause significant inaccuracies in estimating and measuring the ion concentration of formation waters and some uncertainty about whether a fluid analysed at surface is representative of fluid at depth. Boiling and degassing caused by pressure reduction seriously affects bicarbonate and carbon dioxide content, which in turn affects pH (Carpenter and Miller, 1969). Mixing of incompatible waters can result in the precipitation of mineral scales and the consequent reduction in concentration of species such as sulphate and carbonate.

2.2.3 Typical formation water compositions

Although there is significant variation in the nature of formation waters globally, there are a number of features common to all such fluids, for example, formation waters are commonly enriched in Ca and Cl and depleted in Na, SO_4 and K relative to seawater ratios (Davisson and Criss, 1996). The overall concentration of the major ions, Na, Ca, Cl etc in a basinal brine tends to increase with depth (Pearson, 1994). Hanor (1994) states that there is a "*profound and progressive change in the cationic makeup of sedimentary formation waters with increasing salinity*". The following sections describe the features typical of all formation waters.

2.2.3.1 *Anionic composition*

Chloride is the predominant anion in oilfield brines (Collins, 1969), making up 95% by mass of the anions in most sedimentary formation waters that have salinities greater than 10,000mg/L (Hanor, 1994). The concentration of Cl affects the concentrations of all the cations, but not their relative abundance (Stefánsson and Anórsson, 2000).

Waters with salinities of less than 10,000 mg/L may have bicarbonate, sulphate or acetate as the dominant anion (Hanor, 1994). Carbonate waters are generally associated with the dissolution

of limestones, silicate hydrolysis, or volcanic gases (Jones and Bodine, 1987; Land, 1987). Alkalinity tends to decrease with increasing salinity but sulphate in formation waters generally shows little or no systematic variation with TDS (Hanor, 1994). Although in most brines sulphate is rarely dominant, it is often the most abundant anion in solution after chloride and can contribute significantly to the overall charge balance of the system.

Table 2.1. Representative water analyses from sedimentary basins around the world, together with the composition of seawater for comparison. (na designates not analysed, GOM is Gulf of Mexico). Data from: Warren and Smalley, 1994; Bazin et al., 1997; Carpenter et al. 1974 and Land et al. 1988

Fluid component mg/L (except pH)	Seawater	Miller, North Sea	Statfjord, North Sea	Thames, North Sea	Mahakam Basin, Indonesia	Central Mississippi	Offshore Louisiana, GOM
Li	0.170	na	na	na	na	63	2.3
Na	10760	28800	8165	70360	2328.9	66700	29600
K	399	1820	121	9020	43.1	7860	144
Mg	1290	115	68	3560	86	2840	620
Ca	411	1060	1050	10860	131.5	47200	2080
Sr	8.1	110	na	390	na	2190	49
Ba	0.021	1030	41	na	na	80	33
Fe	0.034	10	na	160	na	414	8.6
Zn	0.005	na	na	na	na	19	0.06
SiO_2	3	32	na	na	0.058	45	51
Cl	19350	47680	14286	145630	2816.8	207400	48250
SO_4	2700	7	29	1500	190.3	36	21
HCO_3	142	2070	360	70	2934.7	na	226
pH	7.5	6.7	6.18	5.73	6.44	na	na

2.2.3.2 *Cations - Alkali metals*

Most oilfield waters contain more sodium by weight than any other cation (Collins, 1969). During evaporation, the overall Na content of brines increases with salinity until halite starts to precipitate at approximately 300,000mg/L. Lower salinity waters tend to be Na-dominated because the silicate minerals that buffer its concentration are relatively soluble (Hanor, 1994). Potassium forms another major component of many reservoir fluids and though present only in very small quantities, lithium is also a common constituent of formation water. Figure 2.1 illustrates the variation in cation concentration with changing TDS.

2.2.3.3 *Cations - Alkali earth metals*

In waters whose salinities exceed 300,000 mg/L, following removal of Na through halite precipitation and through mineralogical buffering of the Ca/Na^2 ratio, calcium can become the dominant cation by mass (for example in the saline brines of the Gulf of Mexico). In particular, Ca concentrations are often enhanced through albitisation of Ca-rich plagioclase or dolomitisation of calcite, which will be discussed further below. However, waters in which chloride is the predominant anion and Ca is the most abundant cation are relatively uncommon. Modern seawater itself does not have a significant $CaCl_2$ component.

The highest relative concentrations of magnesium are in seawater but, in unusually oxidising conditions, Mg can be important in waters interacting with mafic rocks containing ferromagnesian minerals as well as marine muds (Jones and Bodine, 1987). Strontium and barium are also commonly found in formation waters, though generally subordinate to Ca and Mg. There are however, some examples of reservoir fluids being extremely rich in Sr and Ba (e.g. Miller Field, North Sea), and this has significant implications for predicting the likelihood of the formation of mineral scales through mixing of incompatible waters.

2.2.3.4 *Silica*

Although only a trace component in seawater (Table 2.1), silica can reach levels of 10s to 100s ppm in oil field reservoir waters. Although quartz is ubiquitous in sedimentary basins, Hanor (1994) asserts that most basinal waters are not in thermodynamic equilibrium with quartz However, levels of silica in some fluids are remarkably constant, varying only with pressure, temperature and dissolved gas concentration (Jamtveit and Yardley, 1997).

2.2.3.5 *Transition metals*

Formation waters typically also contain detectable amounts of transition metals, in particular lead, zinc iron and copper. The behaviour of these ions in formation waters is complex, however there is a clear trend of preferential association with highly saline brines and higher temperatures (Hanor, 1994; Yardley *et al.*, 2003; Yardley, 2005).

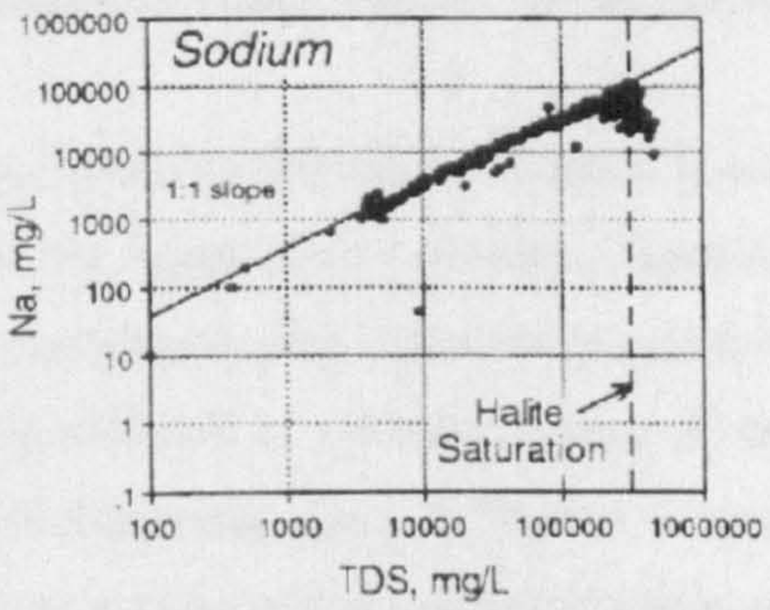

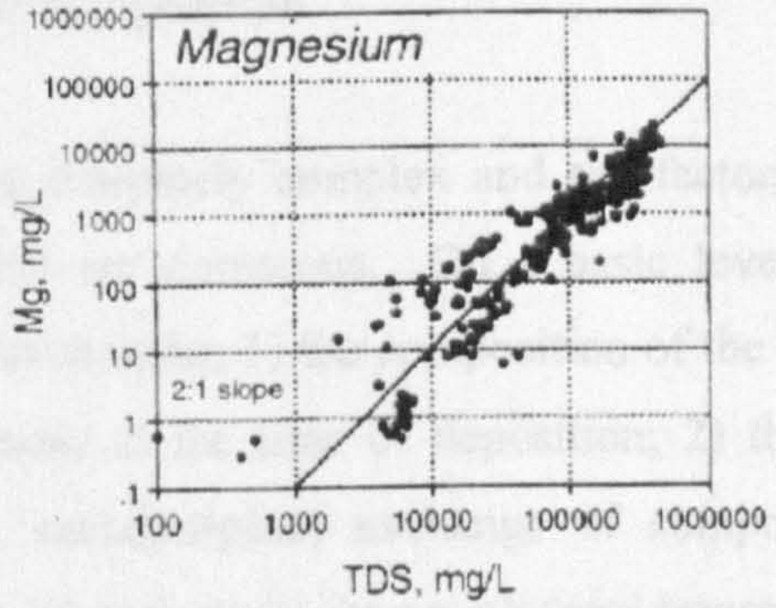

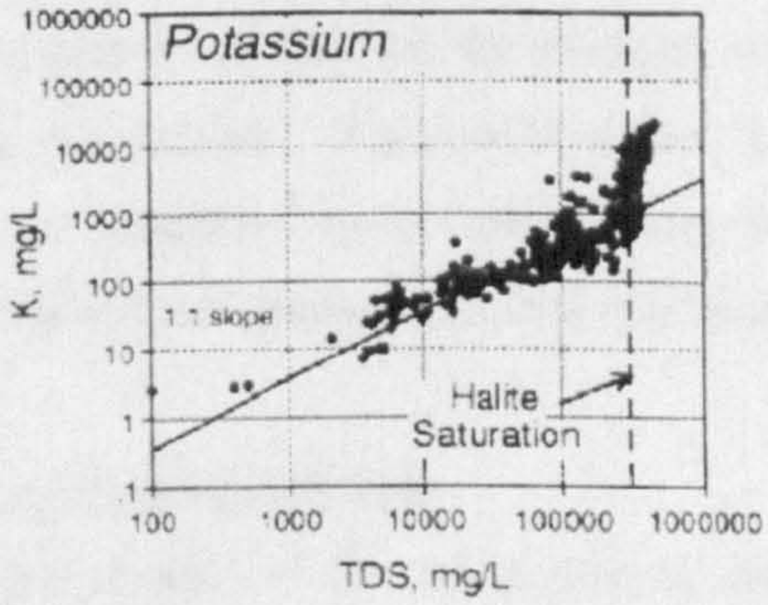

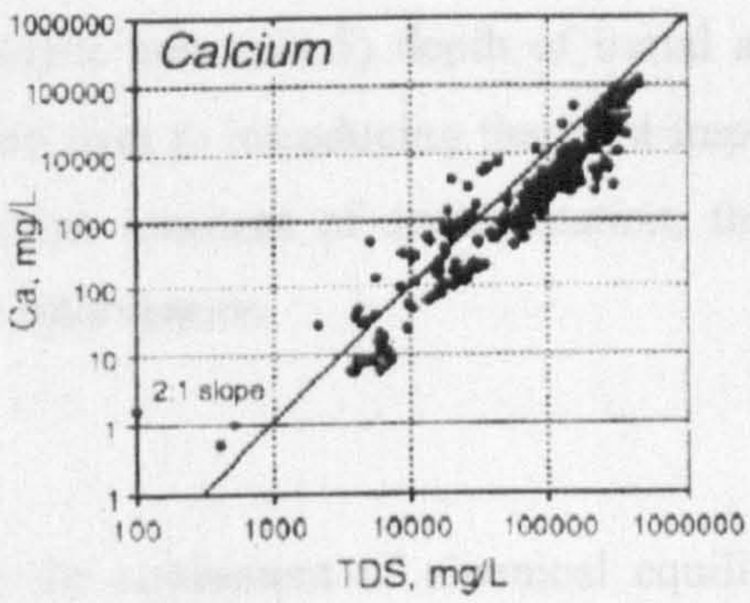

Figure 2.1 Scatter plots showing the covariance of log Na, K, Mg and Ca with log TDS for typical saline fluids. Note the 1:1 slopes for Na and K and the 2:1 slopes for the divalent cations. From Hanor, 1994, using data from Connolly *et al*., (1990); Kharaka *et al*., (1987); Stueber and Walter (1991); Wilson and Long (1991); Case (1945); Moldovanyi and Walter (1992); Land *et al.,* (1988); Land and Macpherson (1989); Michard and Bastide (1988); Lundegard and Trevena (1990); Fisher and Boles (1990); White (1965), Egeberg and Aagaard (1989) and Hanor, (1994).

2.2.3.6 *Organic components of brine*

Although they are the most abundant species, inorganic ions are not always the only components of pore waters; formation waters are often in prolonged contact with hydrocarbons and contain dissolved organic species. The concentration of organic acids in oilfield waters is often very low, but concentrations of up to ~10,000 ppm acetate have been reported with up to ~4400 ppm of other organic acids (Helgeson *et al*, 1993). The most significant organic components of formation waters include minor amounts of neutral organic molecules of hydrocarbons and charged anionic species (Hanor, 1994) in addition to dissolved gases such as methane.

2.3 Introduction to the controls on formation water composition

Subsurface systems containing formation waters are extremely complex and the factors that influence the composition of those formation waters are numerous. On a basic level, the ultimate controls on pore water composition are believed to be: 1) the composition of the water physically included in the pore spaces of the sediment at the time of deposition; 2) the net effects of diagenetic (and at higher temperatures, metamorphic) exchange of components between the water and a) the ambient solids or b) any other fluid; 3) the net physical transport of material into and out of the sediment by bulk flow and the mixing of waters (Hanor, 1993); and 4) the proportion of fluid to the reactive mineral surface area and 5) depth of burial and in particular, temperature. The rest of section 2.3 is given over to introducing the most important controls on formation water composition from the first moment of sedimentation, through complex subsurface processes, to the effects of human intervention.

2.3.1 Initial fluid composition

The dissolved load of formation waters, and hence the attainment of chemical equilibrium between such fluids and their host rocks is affected by the concentration of ligands (predominantly chloride) in the fluid initially (Jamtveit and Yardley, 1997). This is inherited and is a function of the origin of the sedimentary pore fluid. Changing chloride concentration can have a significant effect on driving diagenetic exchange of major solutes. Any change in the total anionic charge of formation water will cause it to attempt to re-equilibrate with its surroundings and as a result various solids may be dissolved or precipitated (Hanor, 1994).

2.3.1.1 *Evaporation and dissolution of evaporites*

Hanor, (1993) states that salinity is primarily the result of physical processes of mixing of meteoric, marine and subaerially evaporated fluids with those derived by subsurface dehydration reactions and the dissolution of evaporites. Evaporation and dissolution are the most widely invoked mechanisms to explain the source of saline waters. However, it has also been suggested in the past that increase in the ion content of brines is due to the process of membrane filtration (or reverse chemical osmosis) as fluids migrate through clay-rich sediments (e.g. Graf, 1982; Hanor, 1994).

2.3.1.2 *Depositional environment*

Climate, sedimentation rate, location of sedimentation and sediment source are among factors relating to depositional environment that have an effect on the nature of the initial pore fluid and sediment, and the subsequent reactions that alter their nature (Burley, 1984). Early shallow diagenetic processes generally occur in the presence of a great deal of water, but the nature of the fluid present varies considerably. In humid areas with a higher degree of rainfall unstable

minerals dissolve easily because water flushing prevents solutes building up in solution and the system coming to equilibrium (Bjørlykke, 1998). On the continents, a great deal of evaporation occurs which promotes the formation of calcretes and dolocretes, however in marine environments, minerals are able to react with seawater to varying degrees. For example, fluvial and shallow marine sediments may be flushed by meteoric water after deposition while more distal shelf facies and turbidites normally will be subjected to much less meteoric flushing. In the North Sea Basin it has been shown that the distribution of kaolinite in sandstones can be related to facies and climate; the Permian and Triassic sandstones in the North Sea region which were deposited in a dry climate generally contain little kaolinite compared to the Jurassic fluvial and shallow marine sandstones deposited in a more humid environment (Bjørlykke, 1998). Eogenetic (early diagenetic) cement growth can be a function of climate, vegetation cover, rainfall and fluvial activity, evaporation rate and degree, regional gradient and river-, and groundwater flow rate as well as of mineralogy in the active weathering zone in the upland portions of valleys and in the aquifer (Figure 2.2, Schmid *et al.*, 2006). Silcretes are silica-cemented duricrusts formed by geochemical sedimentation processes operating at or near the Earth's surface and are an example of the direct effect of climate on sedimentation. Pedogenic silcretes may be laterally extensive and typically indicate episodes of landscape stability. They appear to be restricted to tropical or sub-tropical environments with alternating dry and wet seasons or periods. Groundwater silcretes form in a range of environments and their formation is less climate-specific; they have been reported from temperate, monsoonal and arid palaeoenvironments (Ullyott and Nash, 2006).

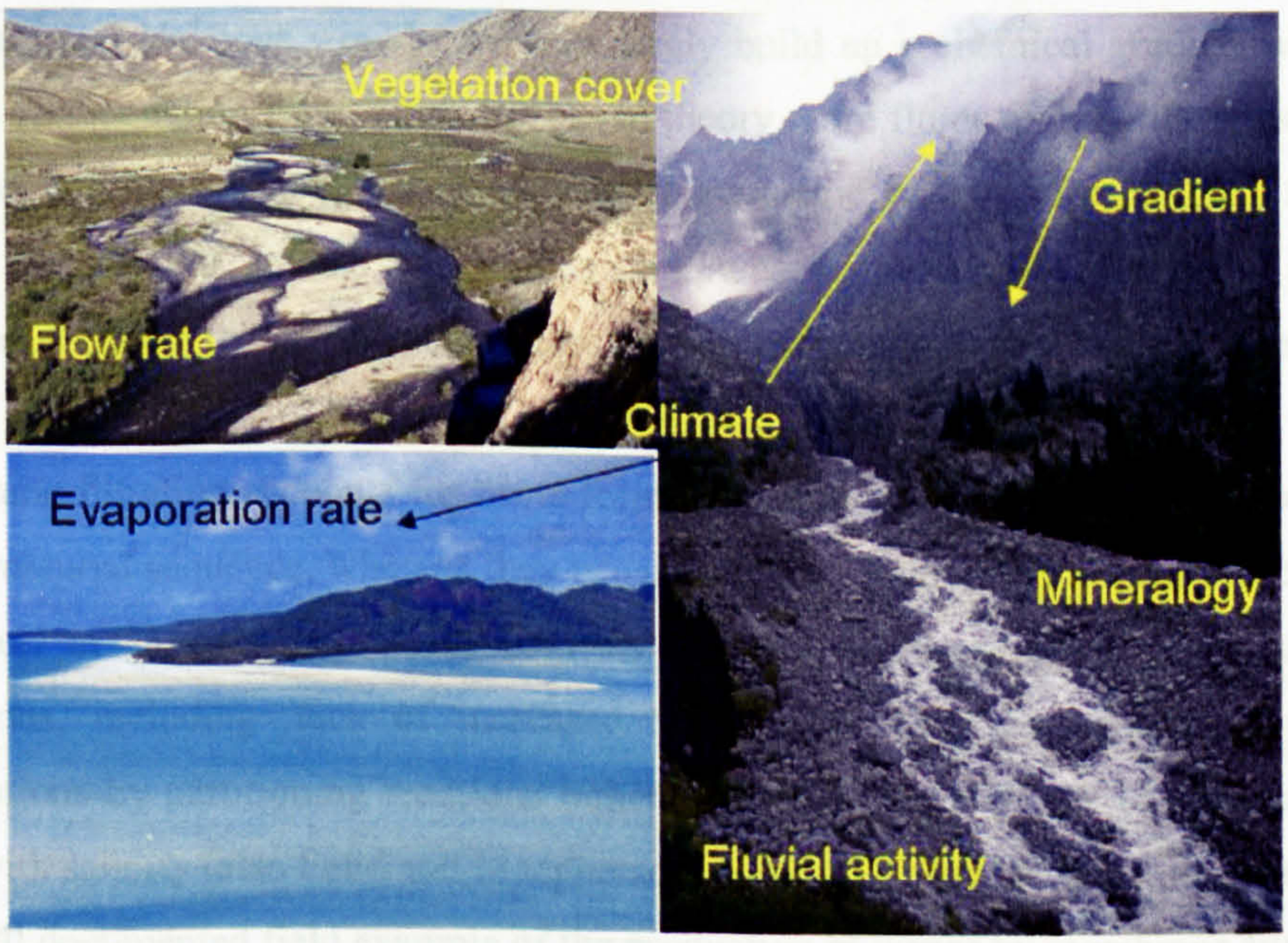

Figure 2.2. Illustrating different potential depositional environments (braided rivers, Kyrgystan [http://www.uoregon.edu/~millerm/braided.html]; shallow marine/beach, Queensland) and the various processes that might affect the composition of formation waters. For example, these fluvial sediments may be flushed by meteoric water after deposition and are likely to be of lower salinity.

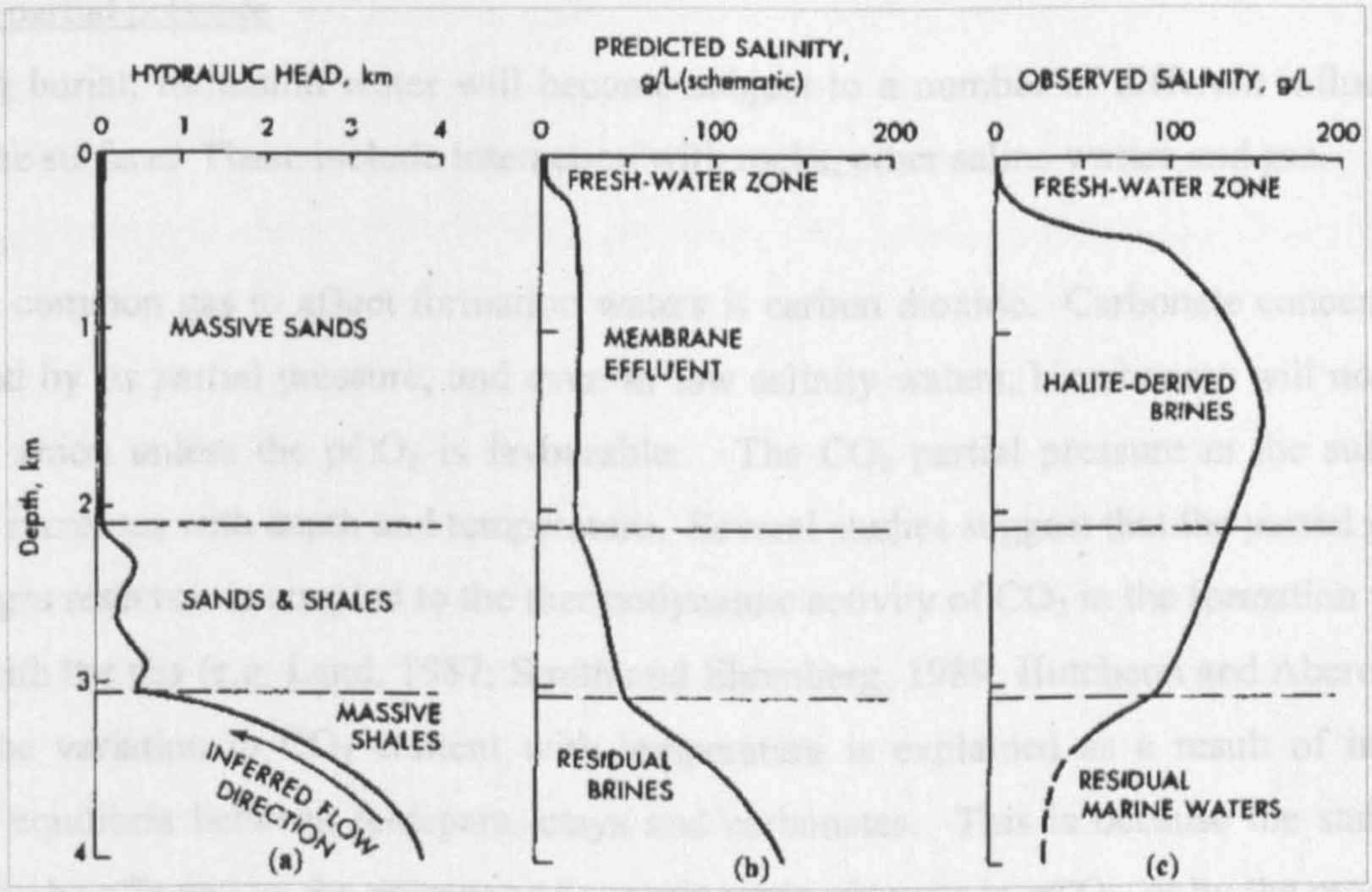

Figure 2.3 Diagram showing vertical variation in isodensity hydraulic head in a typical section of the South Louisiana Gulf Coast. a) Hydraulic head is used as a proxy for hydraulic force, if membrane filtration were an important brine-forming process here, residual brines should be accumulating within the massive shales of the overpressured zone at the base of the section shown (b). Instead, observed salinities decrease downward (c). Hanor, (1994).

2.3.1.3 *Membrane filtration*

The membrane filtration hypothesis proposes the formation of brines by hydraulically driven flow of fluid across semi-permeable shale or clay beds. Since shale has pore walls with a net negative charge, Cl^- ions would suffer electrical repulsion and be unable to pass through narrow pore throats and Na^+ ions would correspondingly build up a chemical gradient along the pore that stops further cation flow (Graf, 1982). In theory, pore fluids on the influent side of a shale membrane will thus become progressively more saline as cross-formational flow and the selective filtration of cations and anions continues (Figure 2.3). However, although this mechanism works in the lab, in recent years its viability in nature has been called into question.

If membrane filtration accounts for brine formation, salinities should decrease upward through an overpressured sequence, whereas they usually decrease with depth. Land (1995) reports that in the Gulf of Mexico the reverse osmosis model fails to explain a great many chemical observations, including: lack of increased Sr and Ba ions; the control of univalent ion concentrations by partitioning reactions rather than filtration, and lack of correlation of boron species with salinity (also Land and Macpherson, 1992). Hanor (1994) argues that there is not a single well documented field example of the production of brines by membrane filtration.

2.3.2 Gas partial pressure

Following burial, formation water will become subject to a number of different influences to those at the surface. These include interaction with rocks, other saline waters and gas.

The most common gas to affect formation waters is carbon dioxide. Carbonate concentrations are limited by its partial pressure, and even in low salinity waters, bicarbonate will not be the dominant anion unless the pCO_2 is favourable. The CO_2 partial pressure in the subsurface generally increases with depth and temperature. Several studies suggest that the partial pressure CO_2 in a gas reservoir is coupled to the thermodynamic activity of CO_2 in the formation water in contact with the gas (e.g. Land, 1987; Smith and Ehrenberg, 1989; Hutcheon and Abercrombie, 1990). The variation in CO_2 content with temperature is explained as a result of inorganic chemical equilibria between feldspars, clays and carbonates. This is because the stability of calcite may be affected by the presence of organic acids, changes in pCO_2, or by the progression of silicate reactions (Hutcheon *et al.*, 1993). Silicate (feldspar and clay) reactions cause major increases in acidity with increasing temperature during diagenesis in clastic reservoir systems and the H^+ generated should be continuously consumed by carbonate (which has more rapid reaction rates) to produce CO_2 (Hutcheon and Abercrombie, 1990), explaining why CO_2 partial pressure will generally increase as the temperature increases. However, it has been noted by Baines and Worden (2004) that although the CO_2 partial pressure increases with depth and temperature, it is not so much the quantity of CO_2 but the fluid pressure that increases. Thus, the studies that concluded CO_2 has been produced, resulting in increasing CO_2 partial pressure (e.g. Smith and Ehrenberg, 1989; Hutcheon and Abercrombie, 1990, etc) may be wrong.

The influence of gas presence on formation water composition is strongly dependent on the pressure of the system. For example, as gas-bearing water travels to the surface, the carbon dioxide begins to outgas a result of the drop in pressure and the accompanying increase in pH can cause supersaturation with respect to calcium carbonate, resulting in its precipitation (Carpenter and Miller, 1969; Hutcheon *et al.*, 1993).

2.3.3 Pressure and Temperature effects

Most reactions are dependent on pressure and temperature which vary with depth, e.g. the present-day geothermal gradients in the North Sea are between 30-40°C/km (Bjørlykke, 1998). The direct effect of these variations is on mineral solubility (Von Damm *et al.*, 1991) or equilibrium element ratios. Indeed, the concentration of dissolved silica in solution has been used in a number of different systems as a geothermometer (Fournier, 1983; 1985), as have the K/Na and Li/Na ratios (Fournier, 1979; Fouillac and Michard, 1981 and Verma and Santoyo, 1997).

Temperature has a significant effect on thermodynamic mineral stability. For example, feldspar composition is extremely sensitive to temperature effects. Some waters can be in equilibrium with both K-feldspar and albite, however, at higher temperatures any removal of K can cause fluid compositions to move into the albite stability field, causing albitisation (Aagaard *et al.*, 1990; Bjørlykke *et al.*, 1995).

Milliken *et al.,* (1989) noted that temperature is a major control on the degree of grain alteration. Sandstones buried to less than 2.7 km typically have negligible quartz cement (Fisher *et al.*, 2000), but the extent of silica cementation increases with depth and temperature (Oelkers *et al.*, 1996). The rate of these reactions also increases with temperature.

Temperature also affects organic processes that often occur in the subsurface. These processes may include bacterially mediated reduction reactions.

2.3.4 redox and pH

Most solid phases and waters deposited in continental and open marine sedimentary environments contain elemental components in relatively high oxidation states because they have been transported in water (Coleman, 1985; Hanor, 1994). Authigenic minerals and the activities of dissolved species in redox equilibrium can provide information as to the oxidation state of a sediment and its formation water (Hanor, 1994). For example: detrital sedimentary organic matter is oxidised initially by aerobic bacteria and subsequently by successive microbial reactions involving the oxidising agents: manganese, nitrate, ferric iron and sulphate, each being used to exhaustion before the next one is used (Coleman, 1985). The eventual product of oxidation of carbon may be authigenic carbonate minerals that vary in zones according to depth and the mechanism of oxidation. Diagenetic products with increasing depth include calcite (non-ferroan), rhodochrosite, siderite, calcite (non-ferroan + pyrite) and ferroan dolomite (Coleman, 1985).

In most formation waters, sulphate is the species that is most likely to be directly affected by the redox state of the system. Although it is rarely the dominant anion in reservoir formation waters, sulphate levels between 5 and >3000 mg/L commonly occur. Sulphate is an important component of seawater but sulphate dominated formation waters may have formed due to the oxidation of reduced sulphur; conversely, sulphate may be lost from a brine by the process of reduction to form dissolved sulphide as well as by sulphate precipitation. However, the concentration of dissolved sulpide in brines is generally very low, and the loss of H_2S from the brine may be attributed to precipitation as iron sulphide (Carpenter, 1978). Sulphate reduction could be bacterially mediated (BSR) in the upper parts of a reservoir, where lower temperatures would be more conducive to bacterial activity, or be thermochemical (TSR) in the hotter parts of

the reservoir (McCartney *et al.*, 2005). Estimates of the initiation temperature for TSR range widely between 80 and >160°C (Cross *et al.*, 2004) however, Worden *et al.* (2003) argue that thermodynamic and kinetic factors are favourable for TSR in petroleum systems with sulphate-rich waters at temperature >120°C. Experiments indicate that the rate of TSR is rapid on a geological timescale and imply that many more sulphate-bearing gas reservoirs should be soured by high concentrations of H_2S than actually are. Extrapolated sulphate half lives for gas and oil reservoirs are 23-1650 and 1650-372,000 years respectively (Cross *et al.*, 2004). Mineral-fluid equilibria may also play an important role in buffering f_{O2}, if stable or metastable equilibria exist between reduced and oxidised forms of C, Fe or S (Hanor, 1994).

pH and redox conditions can be used to characterise the predominant aqueous speciation, mineral reactions and stabilities in a wide range of natural environments (Glynn and Plummer, 2005). The pH of formation waters decreases with increasing salinity from typical values of 7-9 in moderately saline waters to 3-4 in saline brines (Hanor, 1994). In sedimentary basins it is likely that chloride acts as a master variable, its changing concentration driving water-rock reactions to preserve charge balance, and pH is fixed by a combination of mineralogy and charge balance with Cl (Helgeson, 1970; Hanor, 1994). Common pH controlling equilibria include the relations between K-feldspar, kaolinite and illite (see sections 2.4.3 and 4.5). The ability of mineral-fluid equilibria to control pH depends on the rate of reaction of the buffer system which must be fast enough to respond to internally or externally imposed changes in H^+ concentration (Hutcheon *et al.*, 1993).

2.3.5 Equilibrium with hydrocarbons

Formation waters in oilfield reservoirs co-exist with a great variety of hydrocarbons and organic species may form a significant proportion of the dissolved components of a water. Organic acids have been proposed as pH buffers that control the dissolution of carbonate and contribute CO_2 during diagenesis (Hutcheon and Abercrombie, 1990) although silicate equilibria generally have higher pH buffering capacities than carbonates or organic acids.

Within the temperature range 80 – 100°C, aliphatic acids may contribute close to 100% of the alkalinity of the water. Helgeson *et al.* (1993) suggest that there is metastable equilibrium between dissolved carboxylate and carbonate species in oilfield formation waters. There is a marked decrease in aqueous solubility with increasing carbon number for each class of hydrocarbons present in petroleum and the solubility of dissolved hydrocarbons mostly increases with increasing temperature but decreases with increasing salinity (Hanor, 1994). Organic acid anions, of which acetate (CH_3COO^-) is the most abundant, have an apparent preferential association with low salinity waters (Collins, 1975; Hanor, 1994; Lundegard and Land, 1989).

Hydrocarbon species in formation waters can be generated at the oil-water interface in deeper reservoirs by the hydrolytic disproportionation of hydrocarbons in petroleum to produce oxidised carbon-bearing aqueous species and hydrocarbons in crude oil with lower molecular weights, which generally favours dissolution of carbonates and detrital silicates by lowering the pH of the aqueous phase (Helgeson *et al.*, 1993).

2.3.6 Fluid-rock interactions

There is a large body of evidence which indicates that the concentration of many aqueous components in shallow crustal waters is controlled at least in part by mineral-buffering, even at relatively low temperatures (Hanor, 2002). Changes in chlorinity and salinity, that is, in the total concentration of anionic charge in aqueous solution, cause the broad systematic increase in dissolved Na, K, Mg and Ca and decrease in pH and carbonate alkalinity, suggesting that thermodynamic buffering by silicate-carbonate (± halide) mineral assemblages is a first order control on subsurface fluid compositions. The case has been made above that in sedimentary basins chloride is the dominant master variable and pH is more likely to be buffered or limited by mineral assemblages (Helgeson, 1969; 1970; Hanor, 1993; 1994).

After deposition, sediment is buried, and undergoes various textural and compositional changes in the process of diagenesis and lithification. The net effects of diagenesis are the result of eogenetic processes, defining the initial textural, mineralogical and geochemical composition; temperature and pressure changes with mechanical and chemical compaction; "import" or "export" of components through fluid flow or diffusion (sometimes due to the re-introduction of surface waters – telogenetic processes) and precipitation of cements (Burley, 1984; Bjørlykke *et al*, 1995; Bjørkum *et al.*, 1998). Local factors influencing diagenesis are important, particularly the composition, temperature and flux of the formation water (Milliken *et al.*, 1989). Consequently, the diagenetic processes also exert a profound control over the nature of the fluid present in the rock.

Though diagenetic processes vary according to different geological situations, they include reactions and interactions that are almost ubiquitous and are well constrained. Some reactions and processes include: 1) formation of secondary porosity from feldspar dissolution and precipitation of diagenetic kaolinite; 2) quartz cementation; 3) precipitation of illite and its dependence on precursor minerals (as mentioned above) and 4) effects of hydrocarbon saturation on diagenesis (Bjørlykke *et al*, 1995). Specific examples of diagenetic processes are discussed further below.

Diagenetic reactions in lower temperature environments are driven towards greater thermodynamic stability at a rate which is controlled by the kinetics of the mineral reactions (Bjørlykke, 1989; Dove and Rimstidt, 1994). It is principally the solution and precipitation rates that are important in diagenesis, rather then solid diffusion which is too slow.

2.3.7 Physical transport and mixing: diffusion and dispersion

Pore water compositions are dictated by both chemical and physical factors, including: the net physical transport of material into and out of the sediments by bulk flow and the mixing of waters (Hanor, 1994). Geochemical reactions along ground-water flow paths can lead to regional variations in water composition that evolve in the direction of flow (Glynn and Plummer, 2005) and pore fluid flow rates can affect fluid equilibrium with minerals (Bjørlykke, 1997).

Bjørlykke and Grant (1994), suggest that one of the most critical factors controlling diagenetic processes may be the amount of mass transfer by pore water flow over long distances (>100 m) in sedimentary basins. Large fluxes of pore water would be required to move significant volumes of solids, given the low solubilities of quartz and calcite. At low temperatures and high flow rates the pore water may be undersaturated or supersaturated with respect to the mineral phases, in particular the silicate minerals which have slow reaction rates (Bjørlykke and Grant, 1994). However, significant quantities of silicate and carbonate mineral phases can be redistributed under isothermal and isobaric conditions, without large volumes of fluids being involved, as the relative proportions of minerals in various metastable phase assemblages adjust to changes in fluid composition required by changes in chloride or total anionic charge (Hanor, 2002). Egeberg and Aagaard (1989) observe that waters from clastic and chalk reservoirs define the same trends, indicating that they may have evolved through parallel paths and serve to constrain the number of possible alteration mechanisms.

Mass transport in porous rocks is controlled by 4 processes: advection, dispersion and diffusion, sorption onto mineral surfaces and reactions (Jamtveit and Yardley, 1997, Chapter 1). Each transport mechanism involves different volumes of water (Aplin and Warren, 1994) and has different transport efficiencies coupled to the water volume. For example, 10^4-10^6 pore volumes of water are required to precipitate 5 vol% quartz cement by updip migration and associated cooling of a quartz-saturated fluid, depending on precipitation temperature. In contrast, only one pore volume of fluid is required if transport is effected by convection or diffusion (Aplin and Warren, 1994). The δO^{18} values of formation waters reflects the relative importance of these processes. Enrichment of formation waters in ^{18}O is generally ascribed to seawater evaporation and/or diagenetic reaction with clay minerals and carbonates. In both cases, the absolute volume of water is limited. Because evaporites compose <10% of basin fill and

because they are normally found in the basal sections of basins, the total volume of evaporated seawater is less then one pore volume of the sands in the basin. Hence, any enrichment in $\delta^{18}O$ over the initial value normally implies low water-rock ratios (Aplin and Warren, 1994).

Although Cl can be said to be a master variable in most formation waters, and though it drives fluid-rock exchange and controls bulk fluid compositions, chloride itself is controlled by the physical processes of fluid advection and dispersion (Hanor, 1994). Fluid compositional differences that are purely chemical in nature will mix through diffusion (Smalley *et al.*, 2004). Pore water flow will also normally cause the water to be heated or cooled and this will itself cause the dissolution or precipitation of minerals.

2.3.8 Fluid mixing

Sedimentary systems are dynamic. Fluid can move through basins in response to thermal variation, sediment compaction, displacement of less dense pore waters and tectonic deformation (Carpenter, 1978). Formation waters can potentially move great distances over time in permeable sedimentary units (Worden *et al.*, 1999). Mixing occurs where a permeable pathway (permanent or transient) can draw down fluids from more than one reservoir. In produced systems, it is common practice in industry to inject fluids into producing hydrocarbon reservoirs as a form of pressure support or secondary oil recovery technique, inducing mixing between the formation water and the injected fluid. In addition, mixing can arise in a porous medium through density differences generated by temperature or composition. Thus, the potential for two or more fluids to interact and mix in the subsurface is very high.

If there were no mixing of formation waters in sedimentary basins, then most subsurface waters today would either be fresh, have normal marine salinities, or be saturated with respect to halite. In fact, most waters in most sedimentary basins have salinities or Br-Cl systematics which can only be accounted for by mixing of these end-member water types (Hanor, 1994). Although waters can mix by both advective and diffusive processes, mixing due to compositionally-driven diffusion is very inefficient and will rarely produce a homogeneous mass of fluid (Smalley *et al.*, 2004; Hanor, 1994).

There are many effects of fluid mixing on formation water composition (e.g. Fontes and Matray, 1993; McCartney *et al.*, 2005) and the simplest of these is dilution. Dilution reduces the concentration of dissolved species and may cause the water become undersaturated with respect to the minerals with which it is in contact, thus causing dissolution and associated reactions.

The dilution of fluids may also cause formation waters to become undersaturated in certain species, forcing the fluid-rock system out of thermodynamic equilibrium and causing the

dissolution of reservoir silicates and carbonates. Some natural waters that appear to be at or near equilibrium with a given mineral phase may in fact be undergoing significant dissolution/precipitation of the mineral as a result of other irreversible reactions (Glynn and Plummer, 2005). In addition, mixing thermodynamically incompatible fluids may cause certain minerals to precipitate, thus reducing the concentration of the relevant species in solution, e.g. barium-rich formation water and sulphate-rich seawater combining to form barite scale in oil reservoirs (Todd *et al.*, 1994).

2.3.9 Density stratification

It is generally accepted that fluids in sedimentary basins may either be dominated by continuous or episodic throughput flow, or may be a sandstone-pore water system near the closed-system end of the diagenetic spectrum and experience little throughflow (Macaulay *et al*, 1992). Fluid flow in sedimentary basins may be caused by meteoric influx driven by hydrostatic head, episodic dewatering, upward compactional fluid drive, sediment subsidence etc in an open sediment-pore water system. It is also possible that meteoric water can recharge a sedimentary basin at depth, if there is a continuous permeable horizon that outcrops at the surface (Snyder *et al.*, 2003).

Fluid salinity in many sedimentary basins increases with depth (Egeberg and Aagaard, 1989; Hanor, 1993; 1994), and this could be because fluid flow is sufficiently uninhibited over geological time that sedimentary basins simply become density stratified (Land, 1987). Many old, quiescent sedimentary basins are filled with dense, ponded brines and formation waters in those basins now co-exist with relatively stable assemblages of minerals (Land, 1995).

2.3.10 Influence of production operations

The composition of produced water is affected by many factors, including: a) the different types of water present in the reservoir (e.g. formation water from the oil leg or aquifer, injection water, residual drilling mud filtrate fluid etc), the composition of these waters, and their proportions in the produced flow, b) reactions occurring between injection water and formation water or reservoir minerals, c) fluid flow conditions in the reservoir (McCartney *et al.*, 2005).

Engineering-induced temperature and pressure drops and fluid injection are chiefly responsible for carbonate scale precipitation and chemical incompatibility – the most common cause of sulphate scaling – and cause significant concentrations of dissolved species to be removed from solution (Todd *et al.*, 1994).

The principal scaling risks have often been identified as being caused by mixing of aquifer-type water with injected seawater in the production wells. An alternative concept needs to be

considered whereby any future scaling risk is associated with mixing between oil leg formation waters of variable compositions, aquifer waters and injected water. An understanding of any variations in oil leg formation water salinity is important for the reliable estimation of initial hydrocarbon volumes (McCartney *et al*., 2005).

Most of the information available in the literature and from primary sources referring to formation waters from oilfield reservoirs actually refers to produced waters sampled at the well-head before the onset of production. There is a distinction between formation water compositions based on samples taken prior to the onset of production and produced water composition. It is important to note that although processes 2.3.1 – 2.3.9 ultimately control the composition of formation water, produced waters will necessarily be affected by the process of removal of oil from the reservoir.

2.4 Current understanding: implications for novel formation water studies

2.4.1 Variation in palaeoseawater versus chemical reaction

The majority of the discussion on controls on formation water composition hinges on the premise that fluid-rock interactions are the key process. However, Lowenstein *et al.* (2003) argue that some typical formation water characteristics are the result not of alteration of water post-burial, but of variations in composition of surface waters through time. They suggest that the high Ca/Na ratio in most oilfield brines arises because past seawater had a very different composition to that found today. These authors propose that many Ca-rich fluids are evaporated palaeoseawater from when the oceans were Ca rich and SO_4^{2-} poor (Figure 2.4) and reject the argument that $CaCl_2$ brines are highly altered fluids (e.g. Carpenter, 1978; Hanor, 1994 etc). Their basis for secular variation in the major ion chemistry of Phanerozoic seawater comes from fluid inclusions in marine halites (Lowenstein *et al.*, 2001), fossil echinoderms (Dickson, 2002) and strontium in biological calcites (Steuber and Vezier, 2002). During times when seafloor spreading rates were high (Cambrian to Devonian and Jurassic to Cretaceous), Lowenstein *et al.* (2003) claim that a combination of circumstances favoured the accumulation of $CaCl_2$ in marine evaporites and brines in marginal and interior basins of continents. Evaporative concentration in a marine basin with restricted circulation and an arid climate would have produced $CaCl_2$ brines with elevated concentrations of Na, Ca, Mg, K and Cl (Lowenstein *et al.*, 2003).

If this hypothesis were proved to be correct, it would call in to question a great deal of the understanding on which most formation water studies are based. The model however, is restricted geographically to some very specific conditions and despite its simplicity, nevertheless relies on a certain degree of water-rock interaction. The example provided is the Illinois Basin, where the rocks have been dolomitized, which Lowenstein *et al.* (2003) use to explain the depletion in Mg relative to the predicted concentration for evaporated $CaCl_2$ seawater.

The general premise behind this theory is an attractive one that it would be interesting to consider in more situations. However, it is unlikely that dolomitization is the only water-rock interaction occurring in these places. In addition, Lowenstein *et al.* (2003) only consider water samples from less than 2000m depth and temperatures less than 100°C; at greater depths and higher temperatures more diagenetic reactions are likely to be taking place.

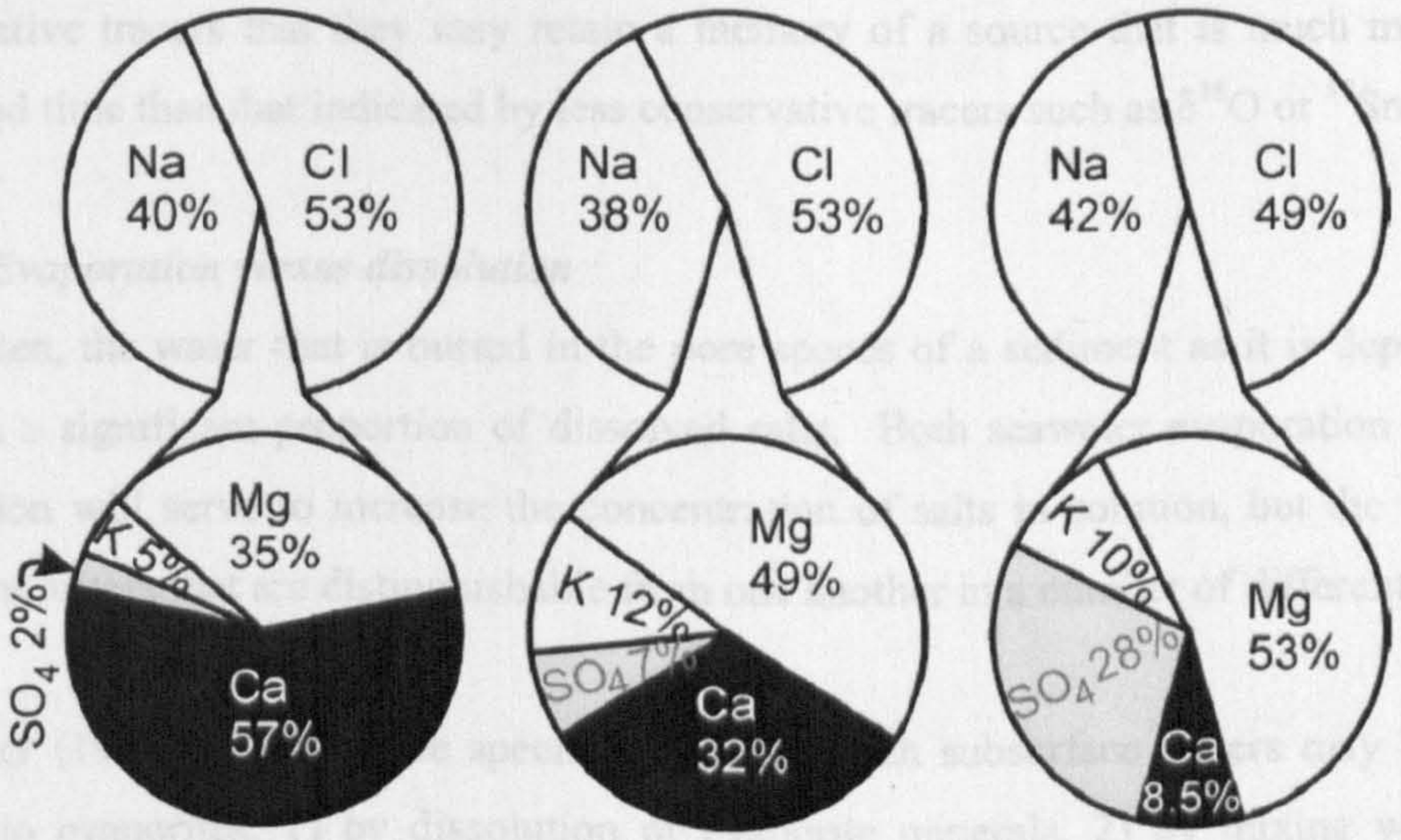

Figure 2.4 Chemical compositions of typical Illinois basin brine (sample 257 in Stueber and Walter, 1991), Silurian seawater (Brennan and Lowenstein, 2002), and modern seawater (in molal percent). Silurian and modern seawater are shown evaporated 3.6 and 3.9 times, respectively, to same Cl molality (2183 mmol) as Illinois basin brine 257.

2.4.2 Origin and variation in formation water salinity

The salinity of pore waters in sedimentary basins worldwide varies by over four orders of magnitude from <10 mg/L to >300,000 mg/L. The evolution of fresh surface waters to saline brines is a critical stage in the creation of subsurface formation waters. It has already been highlighted that Cl is a master variable that may influence the chemical reactions that occur between water and rock. The origin of salinity is thus the starting point in the discussion on the controls on formation water composition.

This discussion of the origin of formation brines hinges on conservative solutes, i.e. those components whose initial concentrations in groundwater may normally only be modified by fluid mixing (Fontes and Matray, 1993), including addition or removal of water by hydration or dehydration reactions, because they are not normally present in solids. Dissolved chloride is an extremely valuable conservative solute because its concentration is controlled by the physical processes of advection, dispersion and molecular diffusion, rather than by chemical reaction (Hanor, 2002) since it does not normally enter solid phases apart from halite. It is thus an excellent indicator of mixing and dilution (Böhlke and Irwin, 1992), but cannot alone identify the source of salinity in brines (Frape and Fritz, 1987). Generally, halogen ratios and halogen:cation ratios (e.g. Cl/Br, Na/Br) are used to distinguish how a brine may have originated (Carpenter, 1978; Walter *et al.*, 1990). In recent years, Cl stable isotopes ($\delta^{37}Cl$) have provided a valuable additional tracer of chloride source and evolution (Kaufmann *et al.*, 1984; Eggenkamp *et al.*, 1995; Eastoe *et al.*, 1999). It follows from the character of

conservative tracers that they may retain a memory of a source that is much more remote in space and time than that indicated by less conservative tracers such as $\delta^{18}O$ or $^{87}Sr/^{86}Sr$.

2.4.2.1 *Evaporation versus dissolution*

Very often, the water that is buried in the pore spaces of a sediment as it is deposited already contains a significant proportion of dissolved salts. Both seawater evaporation and evaporite dissolution will serve to increase the concentration of salts in solution, but the two processes will form waters that are distinguishable from one another in a number of different ways.

Carpenter (1978) defined three specific ways in which subsurface waters may be genetically related to evaporites: 1) by dissolution of evaporite minerals, 2) by mixing with interstitial waters expelled from evaporites during compaction and 3) by incongruent alteration of hydrous evaporite minerals. Subsurface dissolution of mixed evaporite assemblages may produce brines which have compositions reflecting preferential or incongruent dissolution of the bulk evaporite sediment (Hanor, 1994). Subaerial evaporation of seawater produces two basic types of waters in terms of dominant components: from a salinity of 35 – 333g/L, the waters are dominated by Na-Cl and at higher salinities (see Table 1) the waters become progressively dominated by Mg-Cl-SO_4 (Hanor, 1994).

Studying bromine (usually as Br^-) is a common method of distinguishing evaporite-related fluids of different origin as it generally increases with total dissolved solids (TDS). Cl is preferentially partitioned over Br into Na, K and Mg halogen salts during their precipitation and Br preferentially remains behind in solution until the final stages of evaporation (Rittenhouse, 1967; Hanor, 1994). During seawater evaporation, Br, Cl and TDS increase in the residual brines and the Cl/Br ratio does not vary from the original seawater ratio of ~ 650 until halite begins to precipitate (Rittenhouse, 1967; Böhlke and Irwin, 1992; Banks *et al.*, 2000). Brines formed by subaerial evaporation of seawater should thus have Cl/Br ratios lower than ~650, whereas brines formed by the dissolution of halite should have low Br/TDS (Rittenhouse, 1967) and a Cl/Br ratio of more than ~650 (Hanor, 1994; Böhlke and Irwin, 1992; Cann and Banks, 2001). The Br content of halite is approximately 70 ppm, thus congruent dissolution of halite can produce fluids with Cl/Br ratios up to thirty times those of seawater (Walter *et al.*, 1990).

Some authors have suggested however, that there are some alternative influences on Br/Cl ratios. In particular, Wilson and Long (1984) showed experimentally that fluids with Cl/Br ratios close to those of seawater can in principle be produced by incongruent halite dissolution (halite recrystallization) (Walter *et al.*, 1990; Stueber and Walter, 1991; Land, 1995).

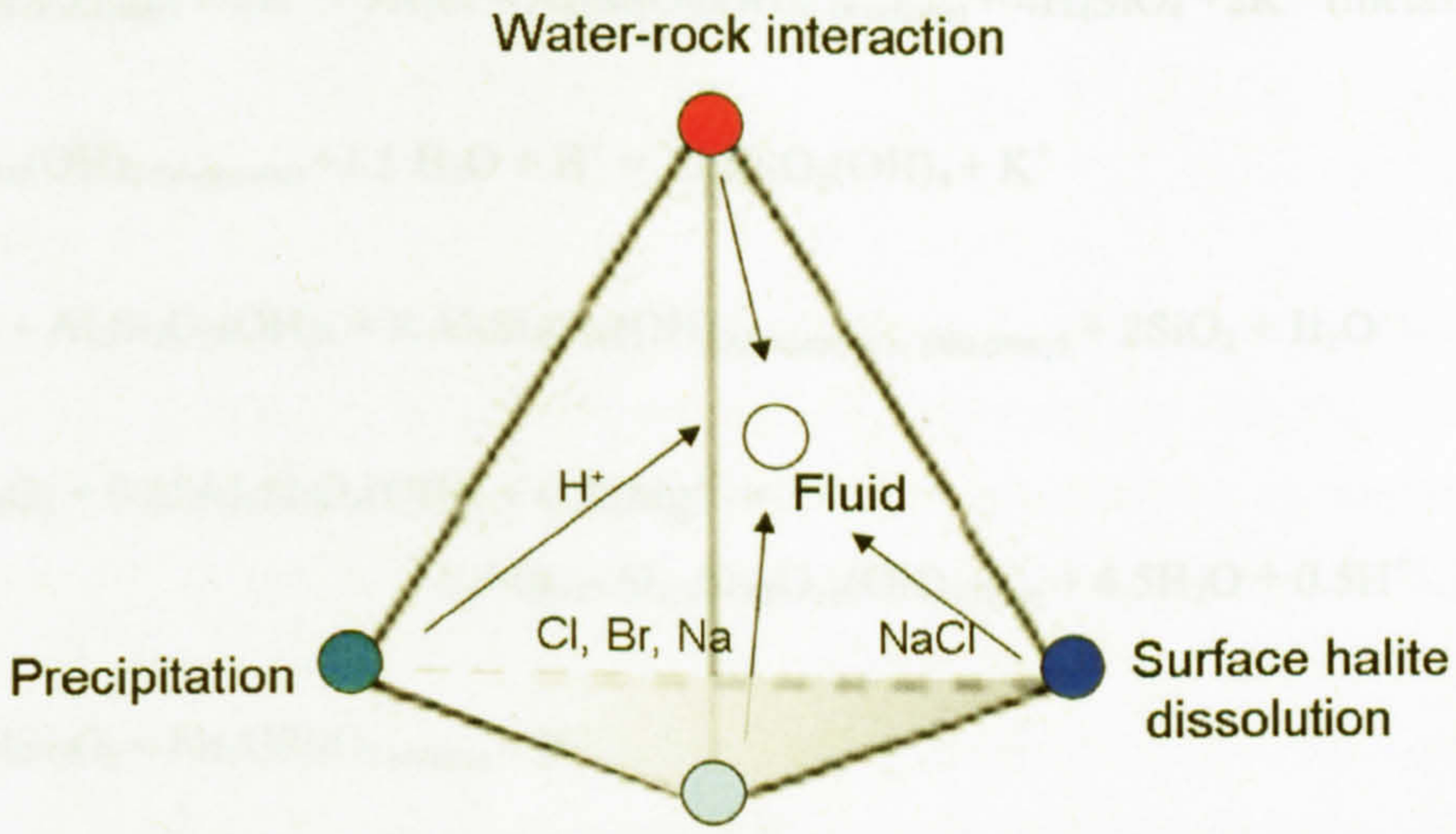

Figure 2.5. Schematic diagram illustrating potential controls on surface waters. Fluid compositions are affected by precipitation, evaporation and halite dissolution at the surface, but are altered by water-rock interaction following burial.

2.4.3 Fluid-rock interactions and diagenesis

As discussed in Section 2.3, there are a number of factors/processes controlling the composition of fluids in the subsurface, often after an initial increase in salinity due to subaerial evaporation or halite dissolution, and the most complex of these processes are fluid-rock interactions. Pore waters are often a more sensitive indicator of mineral reactions than the mineral assemblage itself, although there will often be evidence of reactions preserved in the rock. Each particular fluid component or ion pair is influenced by a number of specific, and often mutually dependent water-rock interaction processes. The following discussion outlines what are thought to be the main controls on the concentration of the most important species in formation waters.

2.4.3.1 *Potassium, feldspar equilibrium and associated reactions*

Potassium is a major component of many feldspars, micas and clays. It participates in solid solutions and is easily removed from both rocks and solution (Collins, 1975). Any depletion in K in subsurface brines relative to other fluid components may be due to its uptake by clays in processes such as thermal diagenesis. Diagenetic reactions that may affect the concentration of K include: 1) kaolinization of K-feldspar and mica (reactions 2 and 3), 2) illitization of kaolinite (reaction 5), and 3) albitisation of detrital K-feldspar (Egeberg and Aagaard, 1989) as is shown below (reaction 6). A major limitation on K variability is buffering of K^+/H^+ and Na^+/H^+ ratios by mineral equilibria. Na/K ratios often approach feldspar equilibrium and these ratios are used as a geothermometer (Fournier, 1979).

$$2KAlSi_3O_{8\ (K\text{-feldspar})} + 2H^+ + 9H_2O = Al_2Si_2O_5(OH)_{4\ (Kaolinite)} + 4H_4SiO_4 + 2K^+ \quad \text{(metastable)} \quad (2)$$

$$KAl_3Si_3O_{10}(OH)_{2\ (Muscovite)} + 1.5\ H_2O + H^+ = Al_2Si_2O_5(OH)_4 + K^+ \quad (3)$$

$$KAlSi_3O_8 + Al_2Si_2O_5(OH)_4 = KAl_3Si_3O_{10}(OH)_{2(\text{Muscovite as Illite proxy})} + 2SiO_2 + H_2O \quad (4)$$

$$0.6KAlSi_3O_8 + 0.85Al_2Si_2O_5(OH)_4 + 0.25Mg^{2+} =$$
$$_{0.6}Mg_{0.25}Al_{2.3}Si_{3.5}O_{10}(OH)_{2(Illite)} + 4.5H_2O + 0.5H^+ \quad (5)$$

$$Na^+ + KAlSi_3O_8 = NaAlSi_3O_{8\ (Albite)} + K^+ \quad (6)$$

Reactions involving detrital feldspars often have a significant effect on K concentrations and these minerals are normally unstable in diagenetic temperature, pressure and pore fluid chemistry conditions (Worden and Morad, 2003). The rate of feldspar dissolution in aqueous solutions is a function of effective surface area and pH at constant pressure and temperature. The rate is limited by reactions at the solution/mineral interface (Helgeson *et al.*, 1984) and by the presence of dissolved species such as the alkali cations (Na^+, K^+, Li^+) and Al, which may adsorb onto mineral surfaces, compete with H^+ for reactive sites, or affect the formation and stability of rate-controlling activated surface complexes (Blake and Walter, 1999). The presence of organic acids increases rates of feldspar dissolution (Oelkers and Schott, 1998). K-feldspar is particularly susceptible to dissolution (Milliken *et al.*, 1989) or albitisation and loss of K-feldspars creates porosity and liberates K as well as Ba ions.

In sufficiently alkaline conditions, K-feldspar can be stable under diagenetic conditions at temperatures ranging from 50-80°C (Aagaard *et al.*, 1990). However, it can also be transformed to illite or kaolinite which releases silica to the pore fluid (Ehrenberg and Nadeau, 1989; Worden and Morad, 2000; Chuhan *et al.*, 2000). Dissolution of feldspar and precipitation of kaolinite require large fluxes of water so that K^+ and silica are removed and the pore-water can remain sufficiently acid (Bjørlykke, 1998). This is a metastable transformation and so the two can subsequently react together, forming the clay mineral illite (reactions 3 and 5, Chuhan *et al.*, 2000; 2001). In addition, the disappearance of smectite and formation of illite with depth in sedimentary basins is a common and important diagenetic reaction (Abercrombie *et al.*, 1994).

As the rate of illite precipitation increases, dissolution of kaolinite and smectite and precipitation of illite will remove K from solution and the K concentration may fall below that which represents equilibrium with K-feldspar. Aagard *et al.* (1990) and Bjørlykke *et al.* (1995) suggest that this may serve as a driving force for albitisation, and albitisation can occur at temperatures from ~65°C, close to the estimated onset temperatures for illitization (70-80°C).

Sometimes the formation of quartz and kaolinite/illite is accompanied by the co-precipitation of carbonate cements (Worden and Morad, 2000).

2.4.3.2 *Lithium*

Micas and pyroxenes are a major reservoir for crustal lithium, which tends to be associated with the silicate phase in rocks. An enrichment of Li in pore water can indicate some interaction with the basement (Banks *et al.*, 2002), and because Li concentration in magmatic waters is related to volcanic emanations, the increase in the Li content of deeper waters might be related to the same cause (Collins, 1975). Li has been used with Na in an empirical geothermometer (Fouillac and Michard, 1981), where temperature is given using the Na/Li ratio, but this geothermometer lacks the rigorous foundation of the Na/K geothermometer and is often clearly inapplicable (as in the study of Banks *et al.*, 2002).

2.4.3.3 *Sodium and relations with calcium*

There are many potential controls on the concentration of such a reactive element as sodium in pore waters, however these controls are limited in that as the dominant cation, charge balance considerations are paramount. High values of Na/Cl are extremely rare and significant absolute Na contributions can only be gained from halite dissolution (Fontes and Matray, 1993). An external/extra source of Na, such as albite dissolution, cannot be invoked to account for high values of Na/Cl (relative to seawater) without an equal removal of K and/or Mg to maintain charge balance (for example, in diagenesis).

In addition to K-feldspar dissolution, plagioclase is altered during diagenesis to albite, consuming Na and releasing Ca ions, because albite is stable at diagenetic temperatures and pressures while Ca bearing feldspars are not. Davisson and Criss (1996) found that many basinal fluids exhibited simple seawater dilution or concentration behaviour accompanied by Ca enrichment and a Na deficit, which they believed to be caused by Ca and Na abundances being modified by these authigenic albite-forming reactions with detrital plagioclase or clay minerals (reaction 7):

$$CaAl_2Si_2O_{8\,(anorthite)} + 4SiO_{2\,(Quartz)} + 2Na^+ = 2NaAlSi_3O_{8\,(albite)} + Ca^{2+} \qquad (7)$$

It should be noted however, that this is a trend common to most sedimentary formation waters and not all sedimentary basins contain abundant Ca-plagioclase. A very similar trend can also arise from exchange of Ca for Mg, as would occur in dolomitisation (see reaction 8, Figures 2.6 and 2.7.)

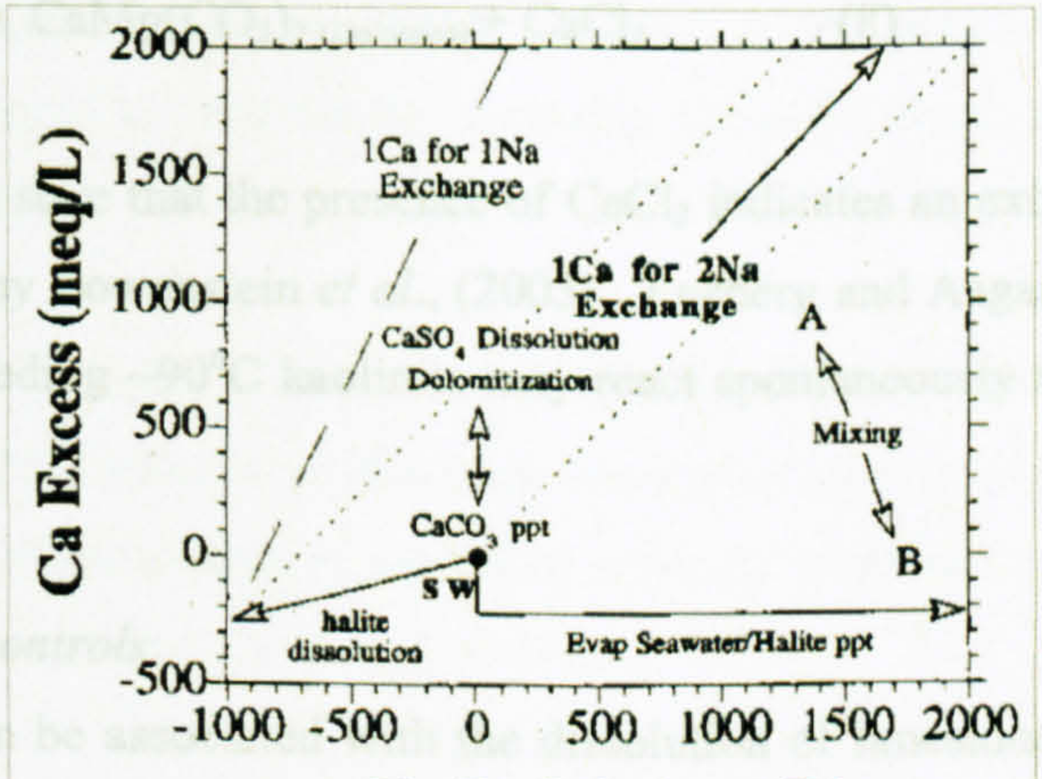

Figure 2.6 Excess-deficit plot showing model predictions for different processes. Halite dissolution into seawater or freshwater produces negative values along a slope of 1:4. Reactions involving 2 Na for 1 Ca exchange produce slope of 2:1. Mixing on the excess-deficit plot forms a straight line between any two endmembers A and B. From Davisson and Criss, 1996.

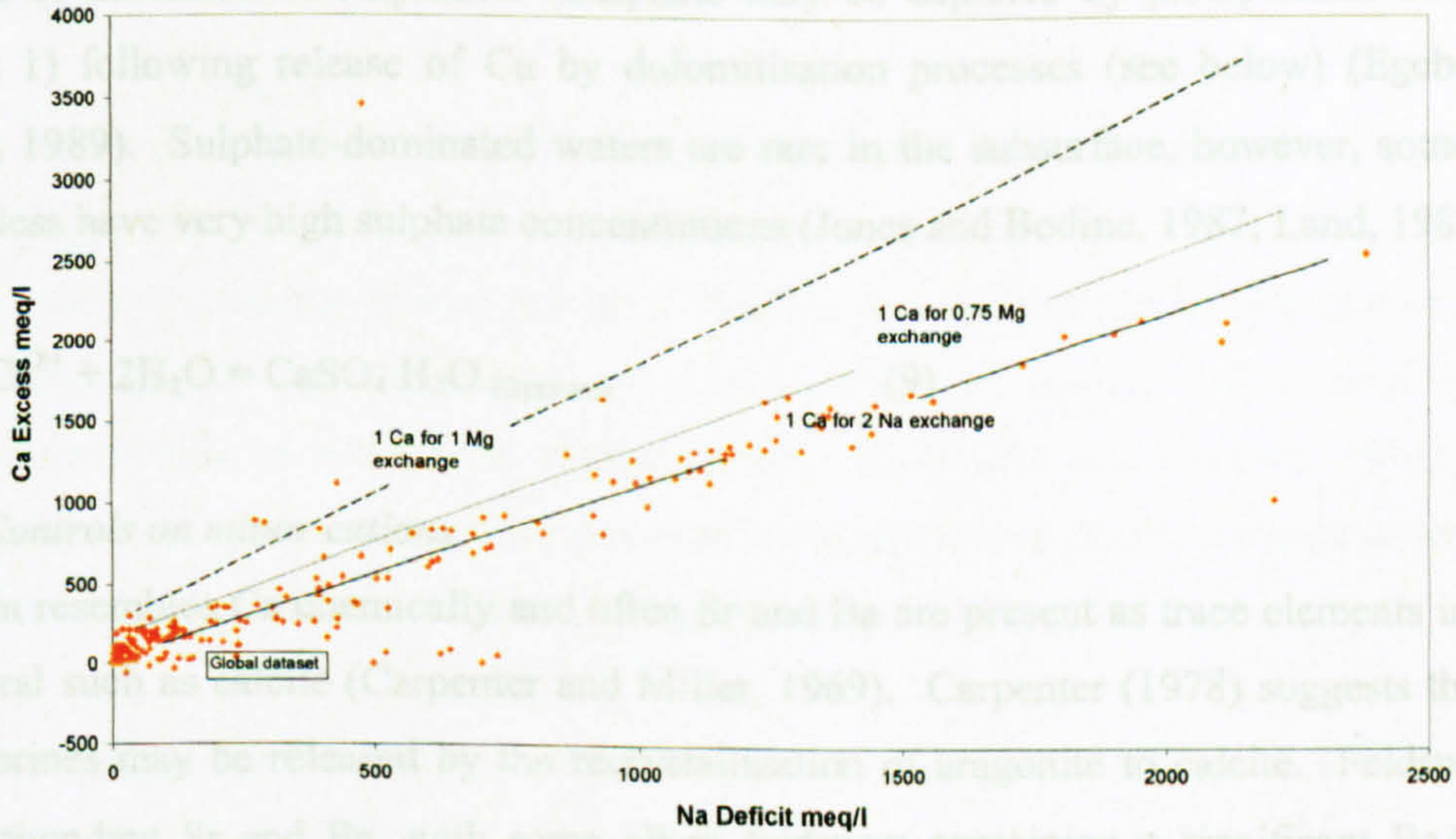

Figure 2.7 An alternative plot showing the Davisson and Criss 1 Ca for 2 Na trend together with a similar trend arising from the 1:1 exchange of Ca for Mg as would occur during dolomitisation.

2.4.3.4 *Calcium and relations with magnesium*

It is the relatively high concentration of calcium in many brines that is a good indication that they are not derived simply by halite dissolution (Land, 1995). Ca tends to be dominant in waters from carbonate and plagioclase-rich rocks (Jones and Bodine, 1987) but Ca-rich waters are also present where no plagioclase or carbonate remains. High Ca/Mg and Ca/Na ratios in some oilfield brines are often attributed to the conversion of calcite to dolomite by Mg-rich water (Collins, 1975; Carpenter, 1978; Lowenstein *et al.*, 2003) although if molar Ca/Na in formation water exceeds molar Mg/Na in seawater, an additional source of Ca is required. The highest relative concentrations of magnesium are in seawater. Relative depletion of Mg is believed to be a result of the replacement reaction to form dolomite e.g. (Collins, 1975):

$$2CaCO_{3\ (Calcite)} + MgCl_2 = CaMg(CO_3)_{2\ (Dolomite)} + CaCl_2 \qquad (8)$$

Jones and Bodine, (1987) state that the presence of $CaCl_2$ indicates an extremely highly altered fluid, a view challenged by Lowenstein *et al.*, (2003). Egeberg and Aagaard (1989) noted also that at temperatures exceeding ~90°C kaolinite may react spontaneously with dissolved Mg to form high-Mg chlorites.

2.4.3.5 *Anions and their controls*

Carbonate-rich waters can be associated with the dissolution of limestones, silicate hydrolysis (through pH buffering – see section 2.3.2), or volcanic gases. Bicarbonate concentrations in solution may be limited by externally imposed CO_2 partial pressures (above) or by the availability of alkali earth cations through the solubility of carbonates (Jones and Bodine, 1987; Land, 1987). Sulphate-dominated waters generally reflect the dissolution of gypsum or anhydrite or oxidation of sulphides. Sulphate may be depleted by precipitation of gypsum (reaction 1) following release of Ca by dolomitisation processes (see below) (Egeberg and Aagaard, 1989). Sulphate-dominated waters are rare in the subsurface, however, some brines nevertheless have very high sulphate concentrations (Jones and Bodine, 1987; Land, 1987).

$$SO_4^{2-} + Ca^{2+} + 2H_2O = CaSO_4.H_2O_{\ (Gypsum)} \qquad (9)$$

2.4.3.6 *Controls on minor cations*

Strontium resembles Ca chemically and often Sr and Ba are present as trace elements in a high Ca mineral such as calcite (Carpenter and Miller, 1969). Carpenter (1978) suggests that Sr in oilfield brines may be released by the recrystallization of aragonite to calcite. Feldspars also contain abundant Sr and Ba, with some alkali feldspars containing a significant $BaAl_2Si_2O_8$ (celsian) component. Plagioclase is one important reservoir for Sr in Gulf Coast sandstones, which typically contain approximately 1000ppm Sr (Land and Macpherson, 1992). The origin of Sr and Ba in saline brines is almost certainly related in part to extensive clay-feldspar-water reaction (Land, 1987; Worden *et al.*, 1999). Egeberg and Aagaard (1989) suggest that high levels of Sr are a secondary result of the process of dolomitisation, caused by celestite dissolution in response to lowering of the SO_4 concentration by precipitation of gypsum as Ca is released. However, celestite is a rare component of reservoir rocks. The $^{87}Sr/^{86}Sr$ ratio is an important natural tracer of water-rock interaction processes (Smalley *et al*, 1995; Worden *et al.*, 1999). The $^{87}Sr/^{86}Sr$ ratio of fluids reflects the integration of the different sources of Sr that have contributed to the fluids e.g. seawater is non-radiogenic, but radiogenic values are derived from older basement rocks or detritus (Hanor, 1994; Cann and Banks, 2001). It had long been thought that the only significant trend between barium and salinity was a decrease in Ba due to fluid mixing causing barite saturation and that Ba was not typically buffered by silicate-

carbonate equilibrium reactions (Hanor, 1994); however, it has been shown that in modern oceanic basins seawater is at or near barite saturation (Monnin *et al.*, 1999, 2001; Monnin, 1999).

As well as the significant variation of transition metal concentration with temperature (Yardley *et al.*, 2003), there is a clear trend of preferential association of transition metals with highly saline brines; due to the solubilization of metals by chloride complexing and the lower pH of more saline fluids arising from equilibria such as 3-6.

2.4.3.7 *Quartz and formation waters*

Quartz cement is responsible for much of the porosity and permeability reduction in well-sorted, quartz-rich sandstones that have been buried deeper than around 3km. Fluid inclusion data from North Sea reservoirs indicate that most of the quartz cement forms at temperatures exceeding 90-100°C (Bjørlykke and Egeberg, 1993; Oelkers *et al.*, 1996).

There are many possible local sources of quartz cements in sandstones including: clay mineral transformations e.g. the illitization and chloritization of smectite; biogenic sources such as siliceous bioclasts; feldspar-related reactions (Barclay and Worden, 2000); dissolution of more soluble silica phases e.g. amorphous silica; dissolution of quartz, and mineral reactions involving the release of silica from silicate minerals (Bjørlykke and Egeberg, 1993). All of these processes are likely to affect the composition of associated pore water and some may be considered as external sources if linked with large advective fluxes.

In most sandstones, the observed abundance of secondary quartz exceeds the amount that can be drawn from illitization of silicates. Thus, grain contact quartz dissolution "pressure solution" has long been invoked by some as the major source of silica (e.g. Bjørlykke and Egeberg, 1993; Brosse *et al.*, 2000), who note that under certain conditions substantial quartz dissolution can occur at quartz-clay interfaces.

Quartz cementation in sandstones has long been the subject of much controversy. The main controversy surrounding pressure dissolution is whether it is initiated by increasing lithostatic pressure, increasing temperature, or the presence of clay minerals along grain interfaces (Worden and Morad, 2000). Oelkers *et al.* (1996) suggest that temperature controlled quartz dissolution/precipitation rates and aqueous diffusion coefficients are of far more importance than the negligible role of pressure in this process (despite the term pressure solution). That is, quartz cement is most likely derived from quartz dissolution at clay or mica surfaces of stylolites by a process also known as illite-mica induced dissolution (I-MID, Figure 2.8) (Oelkers *et al.*, 1996; Bjørkum *et al.*, 1998; Oelkers *et al.*, 2000).

In the past, some authors have suggested that some quartz is derived from sources external to the sandstone; the diagenesis of shales and sandstones may be closely related and, during diagenesis, the shales would act as the sources of SiO_2 for diagenetic quartz in the sandstones (Lynch *et al*., 1997). Land and Milliken (2000) have also presented data showing that silica released from clay reactions appears to have, in some places, been lost from the mudrocks, which supports the contention that this commonly occurs as burial progresses (Land and Milliken, 2000). However, silica is only sparingly soluble in water (Worden and Morad, 2000). Thus, it is believed that insufficient volumes of water would be available to transport the quantity of quartz found in sedimentary basins advectively, even with the help of extensive fracture networks (Bjørkum *et al*, 1998; Fisher *et al*., 2000).

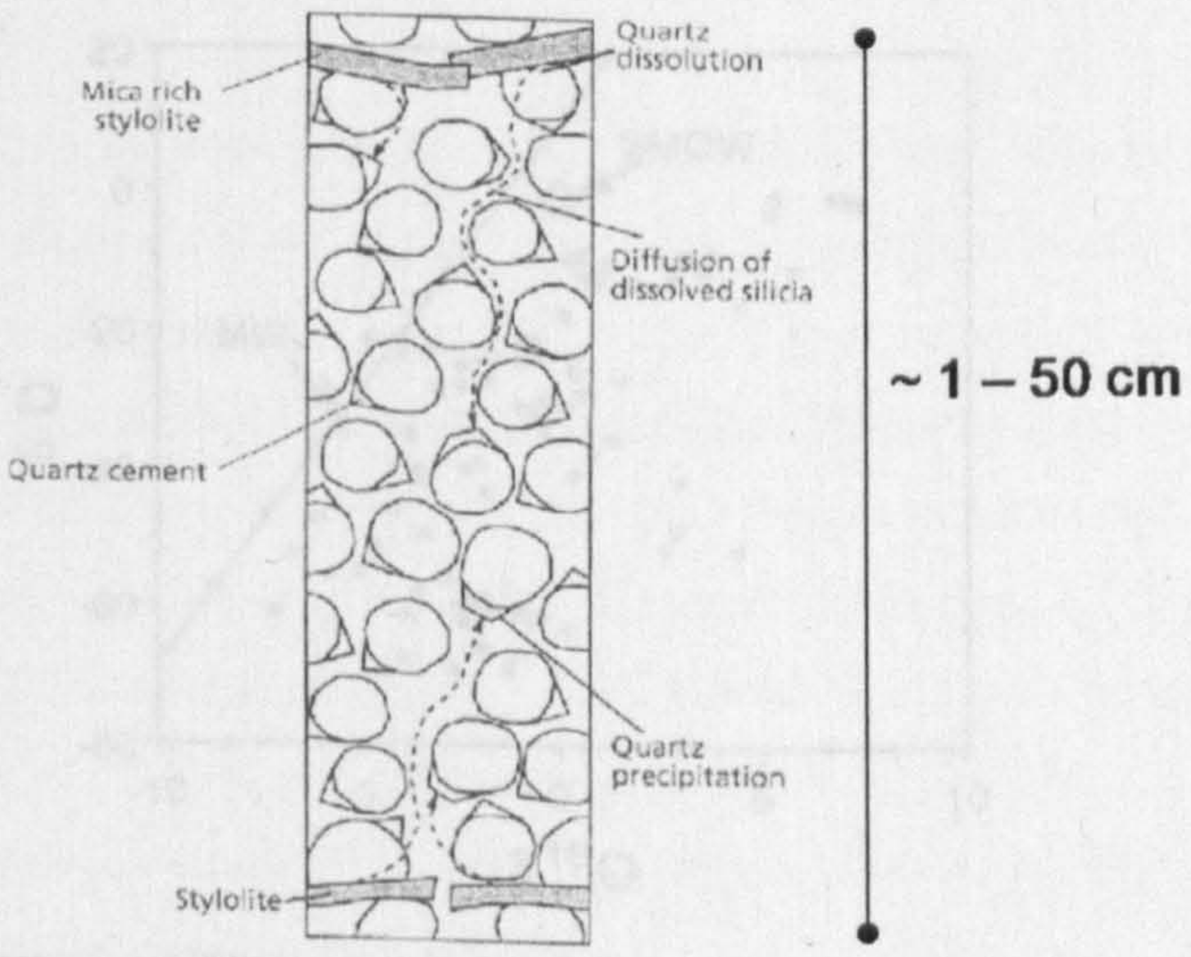

Figure 2.8. Schematic illustration of the theoretical mechanism of silica dissolution/transport and precipitation in quartz-rich sandstones, involving quartz dissolution occurs at stylolite interfaces catalyzed by the interaction of quartz grains and mica/illitic clay surfaces. After Oelkers *et al*., 1996.

2.4.4 Stable Isotopes

A plot of global water $\delta^{18}O$ and δD values and standard mean ocean water defines the Global Meteoric Water Line (Craig, 1961; Figure 2.9). Formation waters commonly plot to the right of the meteoric water line due to exchange of $\delta^{18}O$ with minerals (Lawrence and Taylor, 1971; Drever, 1997; Worden *et al*., 1999). The reason that $\delta^{18}O$ is affected but not δD is that overall rocks contains large amounts of oxygen but very little hydrogen (Taylor, 1997; Drever, 1997). In a water-saturated sediment, most oxygen is in the rock and in isotopic exchange the total mass of each isotope remains constant. In some basins there is a covariance in δD and $\delta^{18}O$ which may reflect mixing of light waters having a meteoric component with heavier ones (Hanor, 1994). In coal-bed methane reservoirs, well waters that fall below the global meteoric

water line for δD and $\delta^{18}O$ line may contain hydrogen expelled from the peats during coal formation, resulting in net deuterium depletion (Riese *et al.*, 2005).

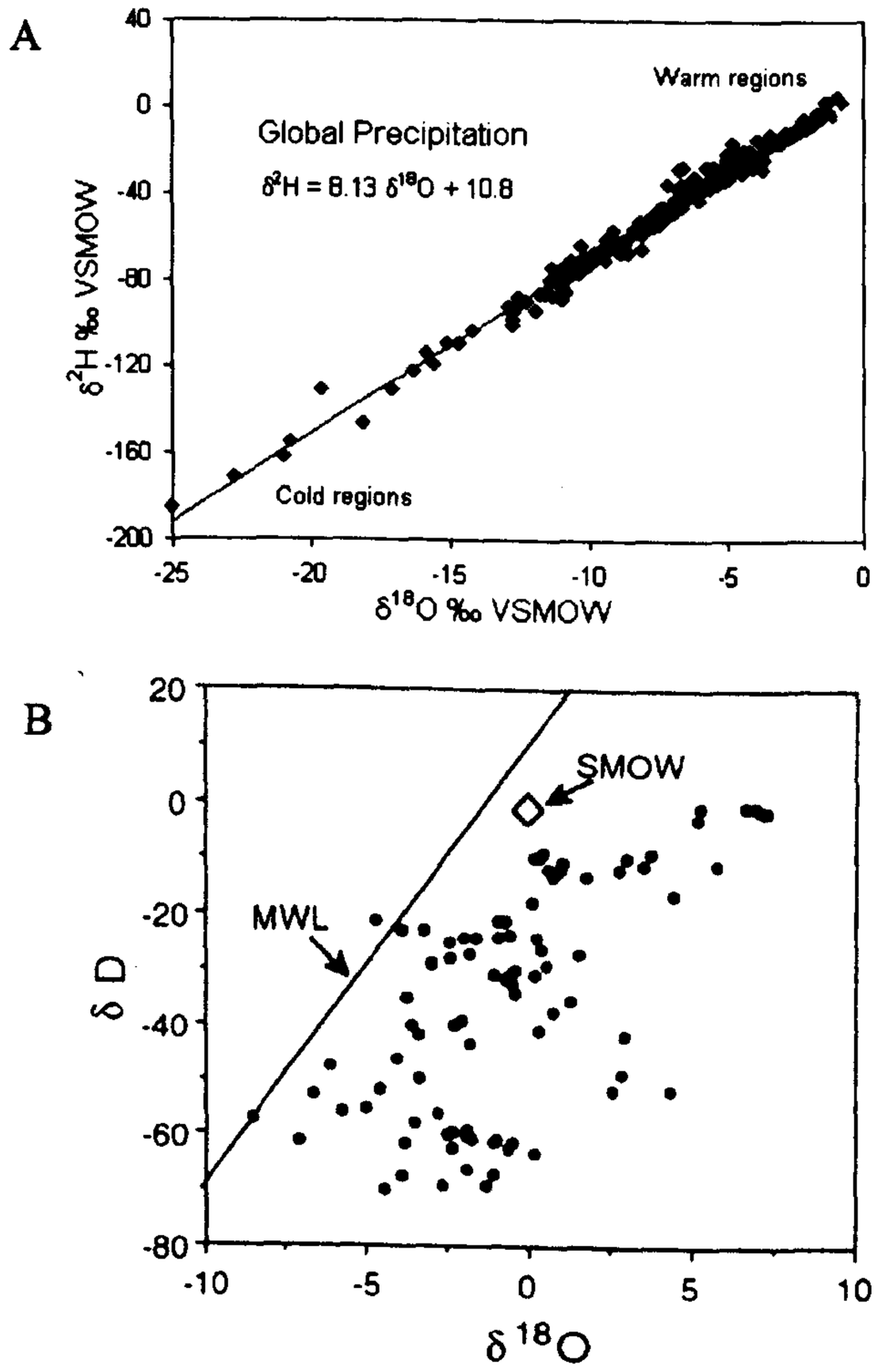

Figure 2.9. A) δD and $\delta^{18}O$ variation in global meteoric waters lying along a global trend and B) the same isotopic variation in formation waters, relatively enriched in ^{18}O (from Hanor, 1994, using data as in Figure 2.1.

Stable H and O isotope data document increasing water-rock interaction with depth (Eastoe *et al.*, 2001), and are often used to distinguish a fluid in equilibrium in a closed system from one that has been involved in large-scale infiltration. For example, high $\delta^{18}O$ and δD values are consistent with isotopic exchange with minerals and would indicate a more closed system.

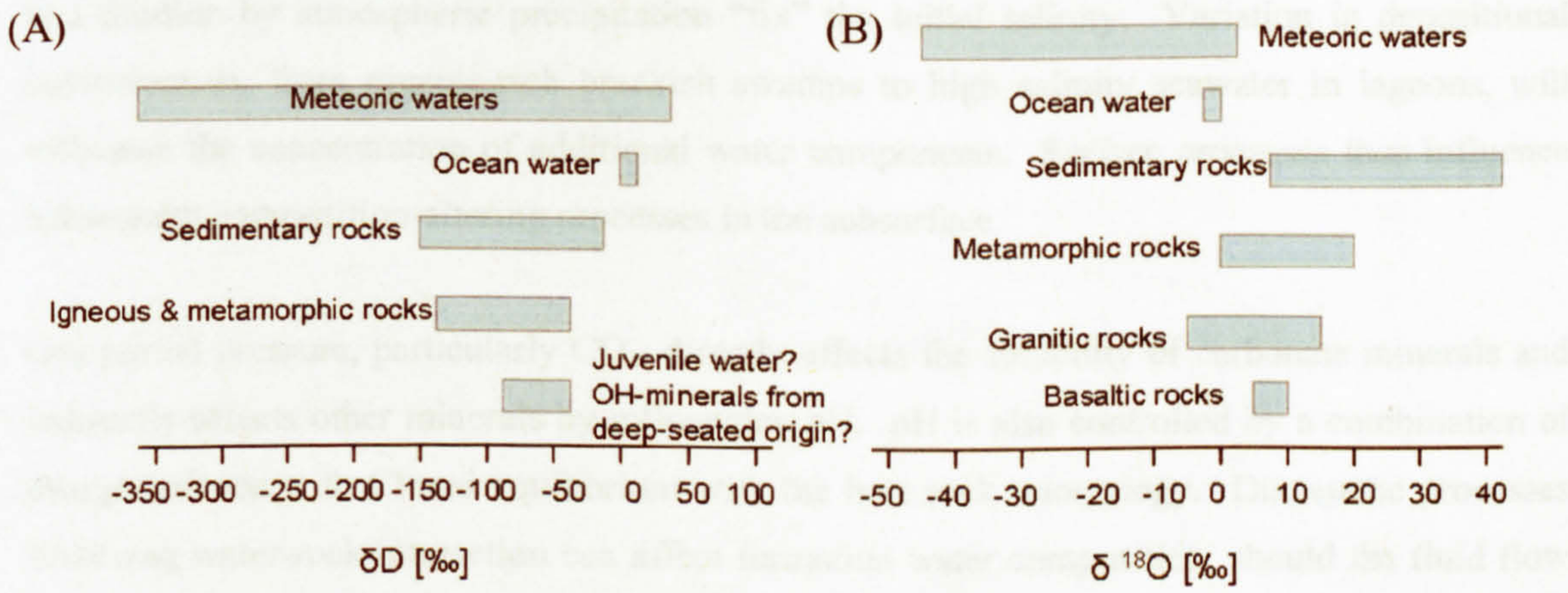

Figure 2.10 (A) D/H ratios of some geologically important reservoirs (δD) relative to SMOW), (B) $\delta^{18}O$ values of important geological reservoirs. After Hoefs, 2004.

The oxygen isotope composition of a rock depends on the ^{18}O contents of the constituent minerals and the mineral proportions. Minerals can be arranged according to their tendency to concentrate ^{18}O, with quartz having a high tendency and hematite a low tendency. This order has been explained in terms of the bond type and strength in the crystal structure (Hoefs, 2004). The average $\delta^{18}O$ of quartz in igneous rocks is ~ +9‰, in metamorphic rocks ~ +13 to +14‰, and in sandstones, ~ +11‰ (Figure 2.10). Meteoric fluids have $\delta^{18}O \approx -7‰$, becoming more ^{18}O enriched with increasing temperature, and basinal type fluids typically have $\delta^{18}O \approx +2$ to +5‰ (Marchand *et al.*, 2002). Sediment pore waters depend on the reactivity of different minerals and will be in equilibrium with diagenetic minerals, not detrital ones. Hence quartz cements are much heavier than sand grains.

2.5 Summary

Global variation in formation water composition reflects variation in depositional setting, burial history, fluid-rock interaction, fluid flow regime, and after production has begun, engineering practice. The processes following the onset of burial enhance formation water variability through reactions specific to each system. The systems in question are easily differentiated through variations in mineralogy. Thus, depending on the degree of mineralogical influence, the formation waters from different systems should also be easily distinguished.

Producing an accurate picture of the most important controls on one particular formation water is challenging, but it should be possible. There are a number of rules, trends and reactions that are common to most sedimentary basins.

These processes are controlled by several factors which can generally not be considered independently. Prior to burial, surface processes of evaporation of marine and lacustrine water

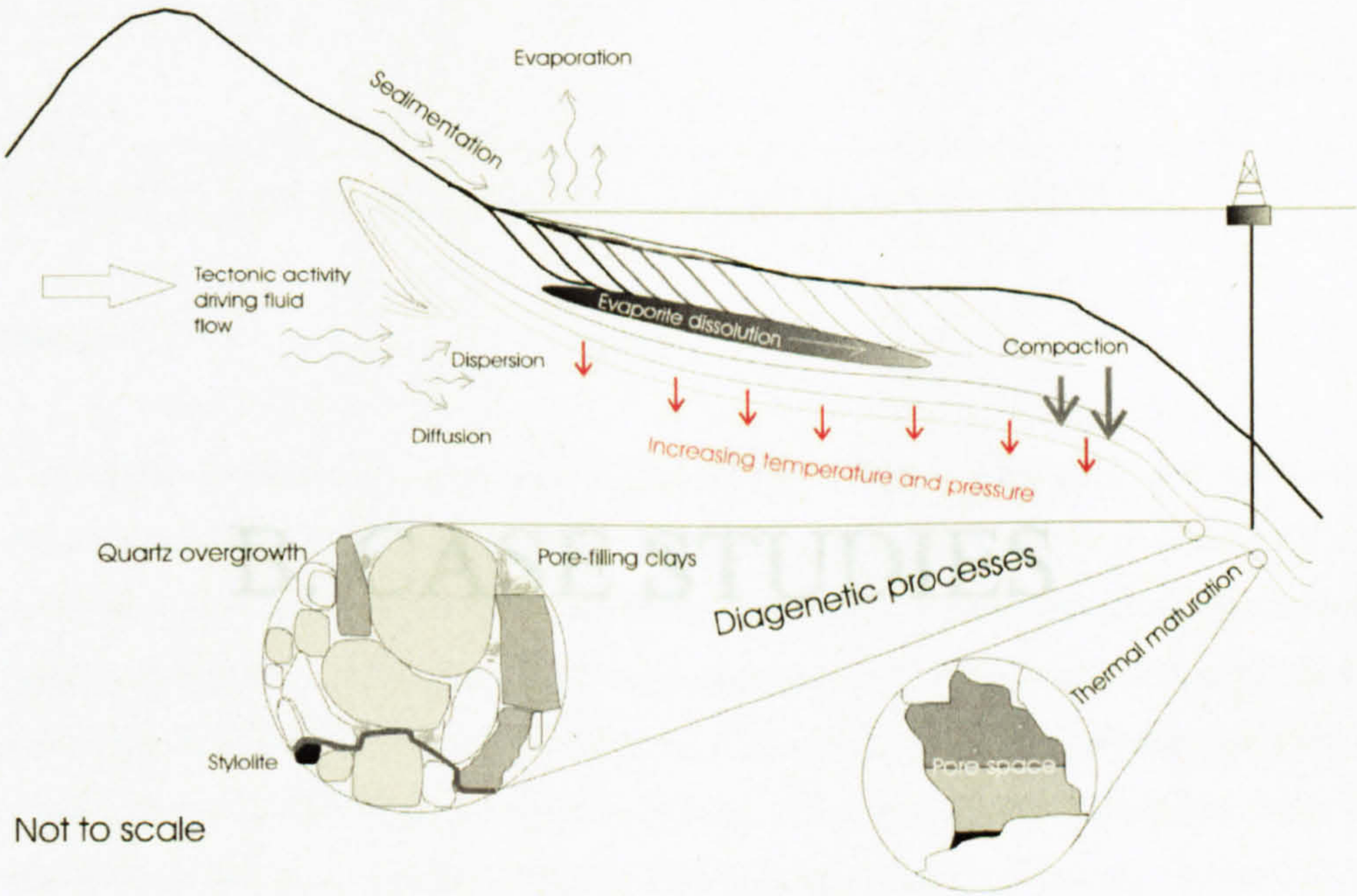

Figure 2.11. A schematic diagram illustrating the main processes that can affect the composition of formation water.

2.6 Note on data quality

The data used in this study of formation water geochemistry is from a number of different sources. In particular, reports in the literature and produced water analyses from working oil fields. Data obtained from literature is likely to be of high quality and reliable, while more recent oil field data will not be as good. In addition, samples from working oil fields may be obtained through a number of different processes. These include: drill-stem tests (pressurised and uncontaminated); other down-hole tools (pressurised but likely to be contaminated) and well-head and separator samples (depressurised). Depressurisation of samples will cause CO_2 to degas and thus pH and bicarbonate concentrations will be affected. Another potential source of uncertainty associated with oil field water samples is the timing of sampling. Analyses made of samples from exploration or appraisal wells, very early in the production cycle are likely to be better representations of formation waters than those made later which may have been subject to some contamination through production processes. Thus there is significant uncertainty related to the use of this data.

However, every effort has been made to reduce uncertainty and to use only the most reliable analyses. Each analysis was charge balanced and those that showed more than 1% discrepancy were rejected. The exception to this being very low salinity waters from San Juan and Colombia which failed to charge balance because in these cases only a very small inaccuracy in analysis can lead to a big charge balance discrepancy. It is important to note that this study focuses on very broad trends which are unaffected by minor inaccuracies and scatter. The scatter will not have a significant effect when water variability is so great and the salinity range is so large.

B. CASE STUDIES

3. CASE STUDY 1: SAN JUAN BASIN, COLORADO AND NEW MEXICO

3.1 Introduction

The San Juan Basin occupies the east-central part of the Colorado Plateau in northwestern New Mexico and southwestern Colorado (Figure 3.1; Laubach and Tremain, 1994). It is roughly circular and covers an area of about 17,353 km^2. Rocks in the basin range in age from Precambrian to Cenozoic and coal is present throughout the Cretaceous system (Laubach and Tremain, 1994). The Upper Cretaceous Fruitland Formation is the largest coal and coal-bed methane resource in the Basin and methane production began in the area in 1951 at the Ignacio Blanco-Fruitland gas field at Ignacio, Colorado (Marroquìn and Hart, 2004). The San Juan Basin is presently the second largest gas-producing basin in the United States with approximately 0.28 x 10^{12} m^3 derived annually from the coalbed methane reservoirs of the Fruitland Formation (Snyder *et al.*, 2003).

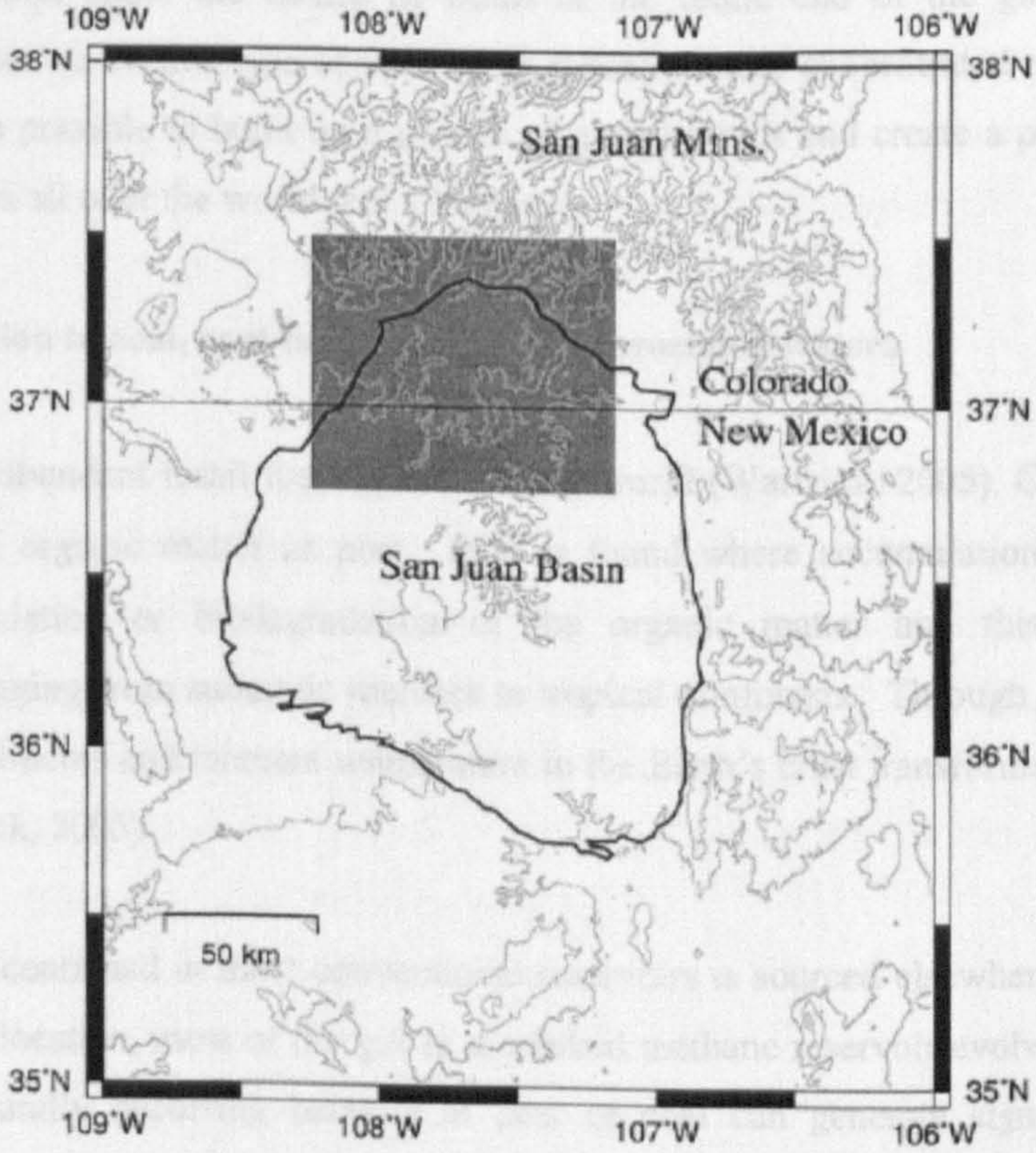

Figure 3.1. Location of the San Juan Basin in west-central US, and the area from which the samples were collected. From Snyder *et al.*, 2003.

3.2 Aims

Although a great deal of work has been undertaken concerning the isotope geochemistry of the San Juan Basin formation waters, understanding of other aspects of the fluid chemistry remains limited. Isotopes have provided a great deal of information regarding the "plumbing" of the reservoir and the extent of heterogeneities affecting fluid flow, and this study aims to continue this work making use of the anionic and cationic components of the formation waters. Because groundwater evolves chemically along its flow path, hydrochemistry can be used to help define recharge and discharge areas. Detailed study of the composition of formation waters of San Juan will also provide a better understanding of the water-rock reactions occurring. The chapter will initially summarise the nature of this coalbed system, outline the results of previous studies into the area and then go on to investigate additional insights into the formation water chemistry and host rock mineralogy.

Of wider significance, the San Juan formation waters are extremely low salinity and provide valuable information about the nature of fluids at the dilute end of the global spectrum. In comparing the controls on this type of water with those on more concentrated brines in other parts of the world, it is possible to build up a picture of global trends and create a predictive model for fluids in reservoirs all over the world (see Chapter 5).

3.3 An introduction to coal, coal-bed methane and associated waters

Coal is the most abundant fossil fuel resource in the world (Warwick, 2005). Coal is formed from accumulations of organic matter as peat. Peat is found where accumulation of organic matter exceeds the oxidation or biodegradation of the organic matter and this occurs in many environments, ranging from subarctic marshes to tropical rainforests. Through time, the weight of the overlying sediments and inherent temperature in the Earth's crust transforms the organic matter into coal (Warwick, 2005).

Whereas the gas contained in most conventional reservoirs is sourced elsewhere and has migrated from its original location, most of the gas in a coalbed methane reservoir evolved in situ (Riese *et al.*, 2005). Naturally occurring bacteria in peat or coal can generate significant amounts of methane. The methane produced from organic matter associated with coal beds is a mixture of biogenic and thermogenic gas. The formation of this methane involves a combination of acetate fermentation and CO_2 reduction as well as thermocatalytic degradation of organic matter (Scott *et*

al., 1994; Riese *et al.*, 2005). Methanogenesis occurs throughout all the coal rank stages, and if significant amounts of the gas are trapped in the coal or an adjacent reservoir, such as porous sandstone beds, it may eventually become an economic gas resource i.e. coalbed methane (CBM) (Warwick, 2005).

Methane and other gases such as CO_2 and ethane in CBM reservoirs are largely adsorbed within the coal matrix and are prevented from desorbing by high formation pressures. The micropores that form during coal diagenesis are generally an order of magnitude smaller than conventional pores (95% of micropores are less than 0.5 nm in diameter), severely limiting permeability (Snyder *et al.*, 2003) however, permeable pathways are provided by diagenetic fracture networks known as cleats (Riese *et al.*, 2005).

The migration of gas from coalbed systems, through desorbtion or diffusion, requires either an increase in temperature or a decrease in pressure to transfer free gas to the cleats within the coals. The production of coalbed methane therefore requires the release of confining pressure on the adsorbed gases (Snyder *et al.*, 2003). Each gas component in a coalbed reservoir has unique sorption characteristics and some gases, such as CO_2 and ethane are more strongly sorbed to coal surfaces, than others (nitrogen and methane). Therefore, the percentage of CO_2 in the produced gas will increase as reservoir pressures decrease during production (Scott *et al.*, 1994). Coalbeds below the regional water table are usually water saturated.

The produced water from coal beds with associated methane tends to have a very characteristic chemical composition. In his 2003 study, Van Voast identified six different coal- and methane-bearing basins (including San Juan), all with very similar water compositions. The waters are typically very low in Ca and Mg with SO_4 almost totally absent, and Na, HCO_3 and Cl are predominant. Concentrations nearer the recharge areas are generally lower for Na and Cl and somewhat higher for Ca and Mg. These water compositions are attributed to microbial SO_4 reduction and accompanying reactions of this process.

3.4 Tectonics and evolution of the San Juan Basin

The San Juan Basin is a Laramide tectonic feature whose predominant structures formed beginning ca. 73-30 Ma (Riese *et al.*, 2005). Basin subsidence began during the Late Cretaceous and continued into the early Eocene. Significant accommodation space allowed accumulation of beach sands and back-barrier, marginal marine lagoonal sediments during the Cretaceous (Riese *et al.*, 2005).

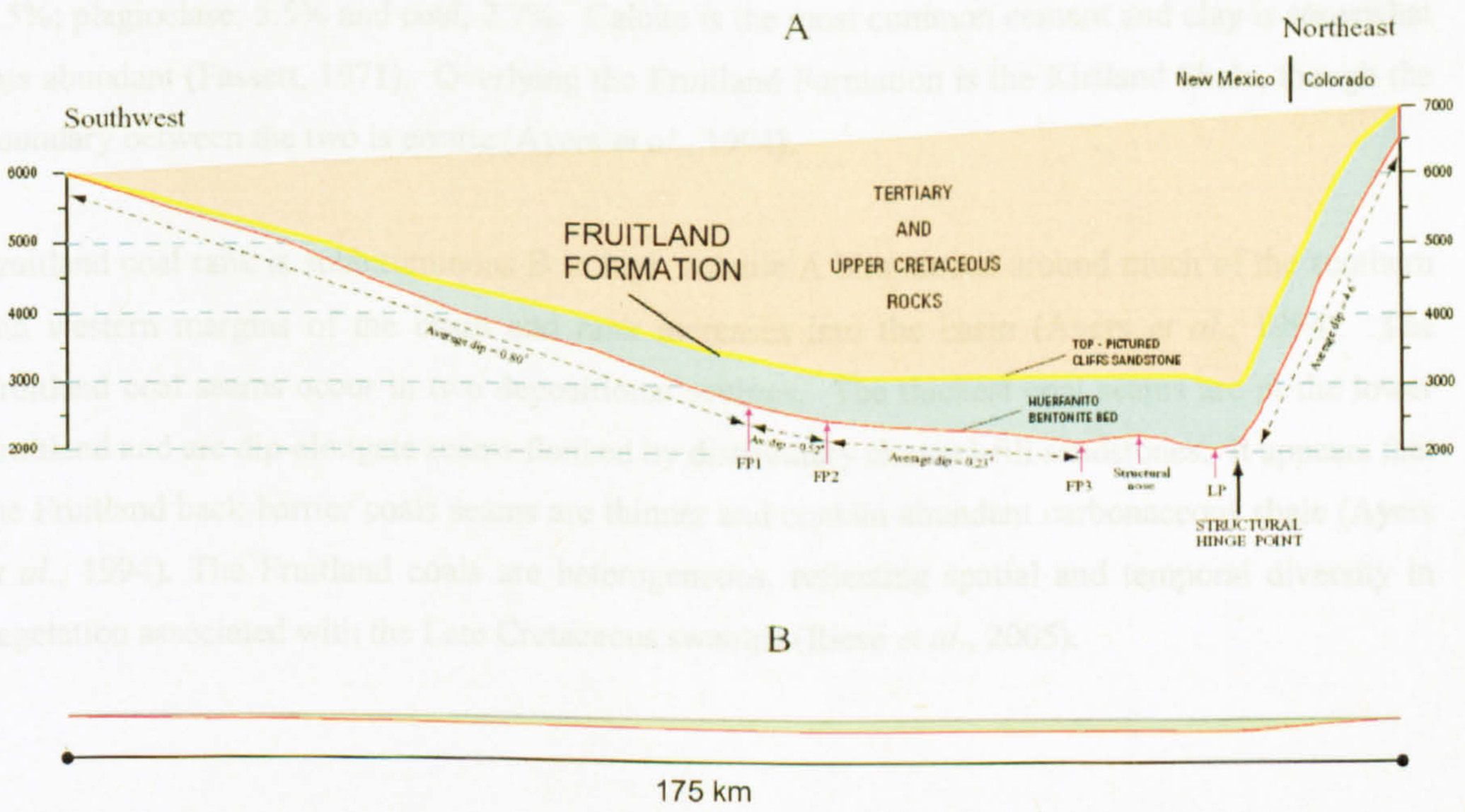

Figure 3.2. A: Cross section through the major stratigraphic features of the San Juan Basin, with exaggerated vertical scale in feet, B: schematic representation of the basin at scale. From Fassett, 1971

The Fruitland coals were deposited in a coastal swamp environment (Fassett, 1975) during regressive cycles of sedimentation. The underlying Pictured Cliffs Sandstone is a coastal facies that was formed as the Late Cretaceous coastline prograded northeastward into the Western Interior seaway (Scott *et al.*, 1994; Ayers *et al.*, 1994) and a vertical succession of shelf through to coal-bearing sediments was deposited. The more massive sandstone units of the upper part of the Pictured Cliffs Formation are medium- to fine-grained and are composed of quartz, K-feldspar, plagioclase feldspar and coal (~ 4% average). In places, the Pictured Cliffs Sandstone is capped by a red-brown iron-cemented sandstone layer (Fassett, 1971).

Intermittent transgressive-regressive shifts of the shoreline resulted in the deposition of the Fruitland Formation coals. The formation is composed of interbedded sandstone, siltstone, shale, carbonaceous shale, carbonaceous sandstone and siltstone, coal, and some limestone but the coal beds are the most continuous rock units in the Fruitland (Fassett, 1971). These reach individual bed thickness of >18m and interfinger and interbed freely with the upper tongues of the Pictured Cliffs Sandstone back-barrier, marginal marine facies, and the continental facies of the Fruitland Formation (Marroquìn and Hart, 2004; Riese *et al.*, 2005; Ayers *et al.*, 1994). The average composition of the Fruitland sandstone beds in the north of the basin is: quartz, 85%; K-feldspar, 6.5%; plagioclase, 5.5% and coal, 2.7%. Calcite is the most common cement and clay is somewhat less abundant (Fassett, 1971). Overlying the Fruitland Formation is the Kirtland Shale, though the boundary between the two is erratic (Ayers *et al.*, 1994).

Fruitland coal rank is subbituminous B to high volatile A bituminous around much of the southern and western margins of the basin and rank increases into the basin (Ayers *et al.*, 1994). The Fruitland coal seams occur in two depositional settings. The thickest coal seams are in the lower Fruitland and are dip-elongate seams flanked by distributary channel-fill sandstones. It appears that the Fruitland back-barrier coals seams are thinner and contain abundant carbonaceous shale (Ayers *et al.*, 1994). The Fruitland coals are heterogeneous, reflecting spatial and temporal diversity in vegetation associated with the Late Cretaceous swamps (Riese *et al.*, 2005).

3.5 Hydrogeology

The Fruitland coals are generally layered and discontinuous, punctuated by clastic interbeds of fluvial and marine origin and by bentonites. This heterogeneity is reflected in the cases of adjacent wells showing significant variations in production history of both natural gas and the co-produced waters (Riese *et al.*, 2005).

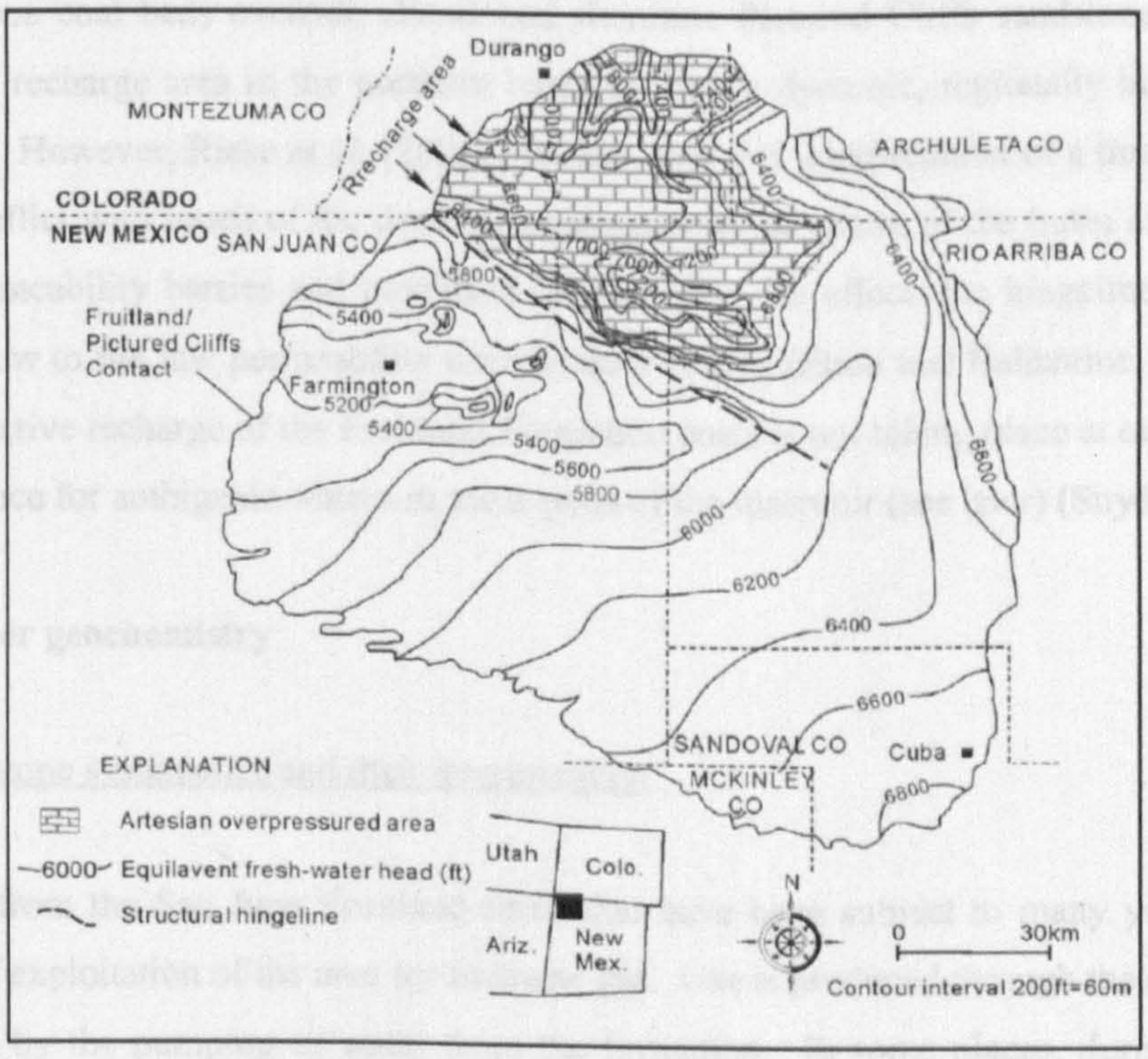

Figure 3.3. The main hydrogeological features of the San Juan Basin, including the northern area of artesian overpressure and the northwest-southeast trending structural hingeline. After Zhou and Ballantine, 2006.

The nature of the hydrogeology of the basin remains contentious, but is important because groundwater interaction with hydrocarbons may play an important role in their migration and quality. It is generally agreed that recharge does occur at the elevated northern margin of the basin where numerous thick coal seams outcrop in the wettest part of the basin outcrop (Figure 3.3), but not anywhere else (Kaiser *et al.*, 1994; Snyder *et al.*, 2003; Riese *et al.*, 2005). The Fruitland Formation is abnormally pressured relative to the freshwater hydrostatic gradient and the San Juan Basin can be divided into north-central overpressured and west-central underpressured areas (Scott *et al.*, 1994; (Kaiser *et al.*, 1994). Overpressuring is thought to be artesian in origin, the result of

recharge at an elevated outcrop and aquifer confinement (Scott *et al.*, 1994). The transition between the pressure regimes is marked by a pronounced steeping of the potentiometric surface and coincides with pinch-out of thick coal seams and possible faulting along the basin's structural hingeline (Figure 3.3).

The Fruitland Formation coals have historically been considered to constitute a regionally interconnected hydrologic unit. Scott *et al.* (1994) suggested that highly permeable, laterally continuous coal beds override abandoned shoreline Pictured Cliffs sandstones and extend to the elevated recharge area in the northern basin to form a dynamic, regionally interconnected aquifer system. However, Riese *et al.* (2005) maintain that this interpretation of a through-flowing system is in conflict with much of the data. Overpressure in the centre of the basin indicates the presence of a permeability barrier and precludes throughflow. In effect, the hingeline forms a barrier for water flow to the low permeability underpressured area (Zhou and Ballantine, 2006). It is thought that effective recharge of the Fruitland Formation coals is not taking place at outcrop although there is evidence for authigenic waters in some parts of the reservoir (see later) (Snyder *et al.*, 2003).

3.6 Water geochemistry

3.6.1 Isotope systematics and their interpretation

Waters from the San Juan Fruitland formation have been subject to many years of scrutiny as a result of exploitation of the area for methane gas. Gas is produced through the reduction of pressure initiated by the pumping of water from the formation. In some places, during the production of coalbed gas, a large amount of water is produced in order to recover the gas (Warwick, 2005). The water must then be safely disposed of, hence the concern about the impact of removing the produced water.

Isotope studies of the waters have been carried out in an effort to define better the origin, history and nature of the formation water as well as the hydrogeology of the reservoir. In a study by Snyder *et al.* (2003) long-lived cosmogenic and stable isotopes, including $^{129}I/I$ (^{129}I/total iodide), $^{36}Cl/Cl$ (^{36}Cl/total Cl), δD, $\delta^{18}O$ and $^{87}Sr/^{86}Sr$, were used to establish the age of the formation waters over a large geographical area and trace the evolution of the chemistry of the waters.

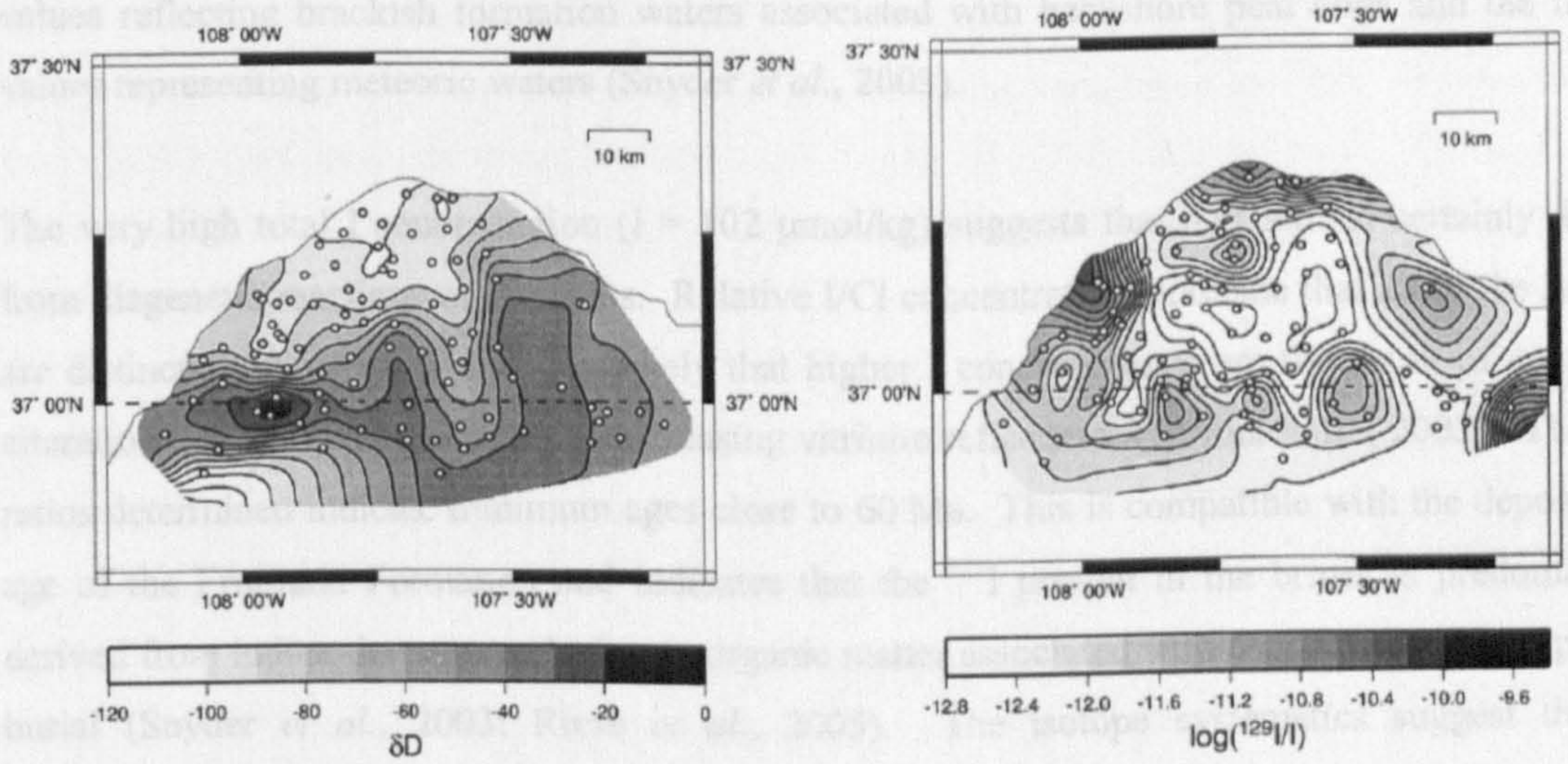

Figure 3.4. From Snyder *et al.* (2003), the distribution of δD and $^{129}I/I$ ratios in the northern part of the basin. Dots represent where δD and ^{129}I were analysed.

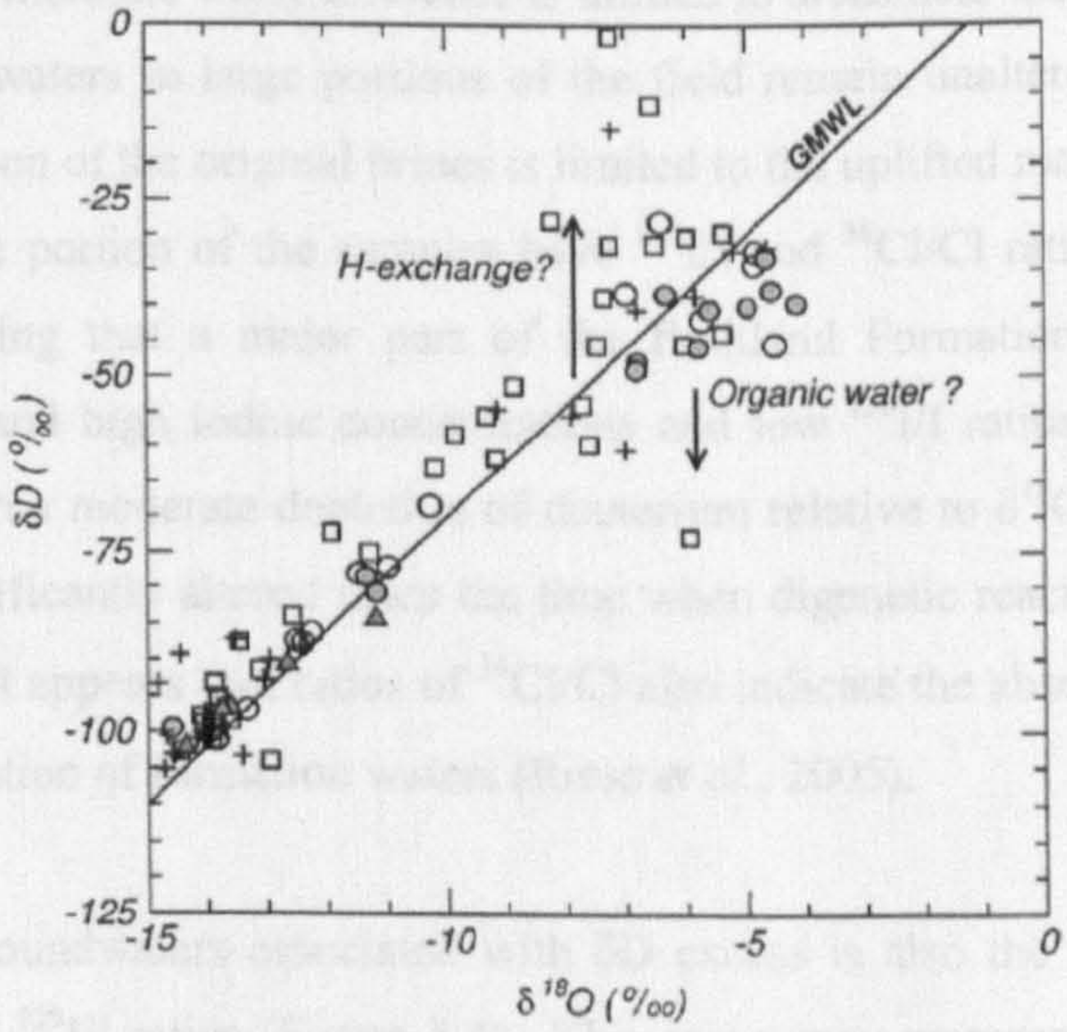

Figure 3.5. From Snyder *et al*, 2003, values of δD and $\delta^{18}O$ for the Fruitland waters. Filled triangles = local surface waters, plus = waters with total iodine <1 μM, squares = 1–10 μM total iodine, open circles = 10–30 μM total iodine, filled circles >30 μM total iodine.

The isotopic studies of Snyder *et al.* (2003) suggest that there are a number of different sets of waters present in the reservoir; however, values of δD and $\delta^{18}O$ generally plot along the GMWL (global meteoric water line), indicating a predominantly meteoric source for the waters (Figure 3.5). The variation along the line is believed to be due to different sources for the water with the heaviest

values reflecting brackish formation waters associated with backshore peat bogs and the lightest values representing meteoric waters (Snyder *et al.*, 2003).

The very high total I concentration (I = 102 μmol/kg) suggests that it is almost certainly derived from diagenetic reactions of the peats. Relative I/Cl concentrations indicate that all of the samples are distinct from seawater and it is likely that higher I concentrations are the result of diagenetic alteration that also had the effect of increasing vitrinite reflectance (Snyder *et al.*, 2003). The $^{129}I/I$ ratios determined indicate minimum ages close to 60 Ma. This is compatible with the depositional age of the Fruitland Formation and indicates that the ^{129}I present in the brines is predominantly derived from iodine that was sorbed onto organic matter associated with coal-forming peats prior to burial (Snyder *et al.*, 2003; Riese *et al.*, 2005). The isotope systematics suggest that the composition of Fruitland brines was modified both during ongoing coal diagenesis, and through the subsequent involvement of water of a meteoric origin. Some ^{129}I results indicate the presence of anthropogenic waters in some of the samples; however, Snyder *et al.* (2003) maintain that the evidence for recent meteoric water influence is limited to areas near the western outcrop of the field and the formation waters in large portions of the field remain unaltered. Thus, they suggest that meteoric modification of the original brines is limited to the uplifted margins of the basin (Snyder *et al.*, 2003). A large portion of the samples have $^{129}I/I$ and $^{36}Cl/Cl$ ratios below pre-anthropogenic values, demonstrating that a major part of the Fruitland Formation has preserved its original isotopic signature and high iodine concentrations and low $^{129}I/I$ ratios of waters elsewhere in the basin, together with a moderate depletion of deuterium relative to $\delta^{18}O$, suggests that these waters have not been significantly altered since the time when digenetic reactions occurred in the deepest part of the basin. It appears that ratios of $^{36}Cl/Cl$ also indicate the absence of recent surface waters involved in the dilution of formation waters (Riese *et al.*, 2005).

A group of old groundwaters associated with δD excess is also the group of groundwaters with somewhat elevated $^{129}I/I$ ratios (Figure 3.4). This group may represent upward migration of fluids into the Fruitland Formation along basement fractures, perhaps from deeper formation waters (Snyder *et al.*, 2003). In addition, it is suggested that a group of deuterium enriched, low chloride formation waters are likely to be the product of near-outcrop methanogenesis through CO_2 reduction during a period of groundwater incursion (Riese *et al.*, 2005). Finally, a group of waters with a moderate enrichment of I may contain waters which infiltrated the coals at the time of the Laramide uplift, between 25 and 30 Ma (Snyder *et al.*, 2003). With regard to strontium isotopic composition, production wells show mixing between a seawater-carbonate end-member with an

additional strontium-rich end-member with $^{87}Sr/^{86}Sr = 0.713$ (Riese *et al.*, 2005). The observation that deuterium excesses in portions of the basins are also accompanied by $^{87}Sr/^{86}Sr$ ratios that are much higher than seawater values has been used to suggest that the original connate waters have at some point received an influx of waters from another source that was in contact with basement rocks (Riese *et al.*, 2005).

A recent study by Zhou and Ballantine (2006) using ^{4}He dating of waters from the same area, has provided formation water ages of between 2.33×10^4 and 1.06×10^5 years in the underpressured area of the basin and between 1.65×10^4 and 4.48×10^5 years in the overpressured area. These ages are 2-3 orders of magnitude smaller than those obtained using $^{129}I/I$ and $^{36}Cl/Cl$ ratios and are consistent with ages of major recharge events previously reported (Phillips *et al.*, 1986), ^{14}C dates and hydrological modelling dates (Mavor *et al.*, 1991). However, these events were established for different stratigraphic horizons (in particular the Cretaceous-Tertiary Ojo Alamo Sandstone) and while the discrepancies may have implications for the interpretation of the hydrogeology of the area, the transient nature of helium gas in the reservoir would probably be expected to produced younger ages than the more static halides.

3.6.2 Water geochemistry

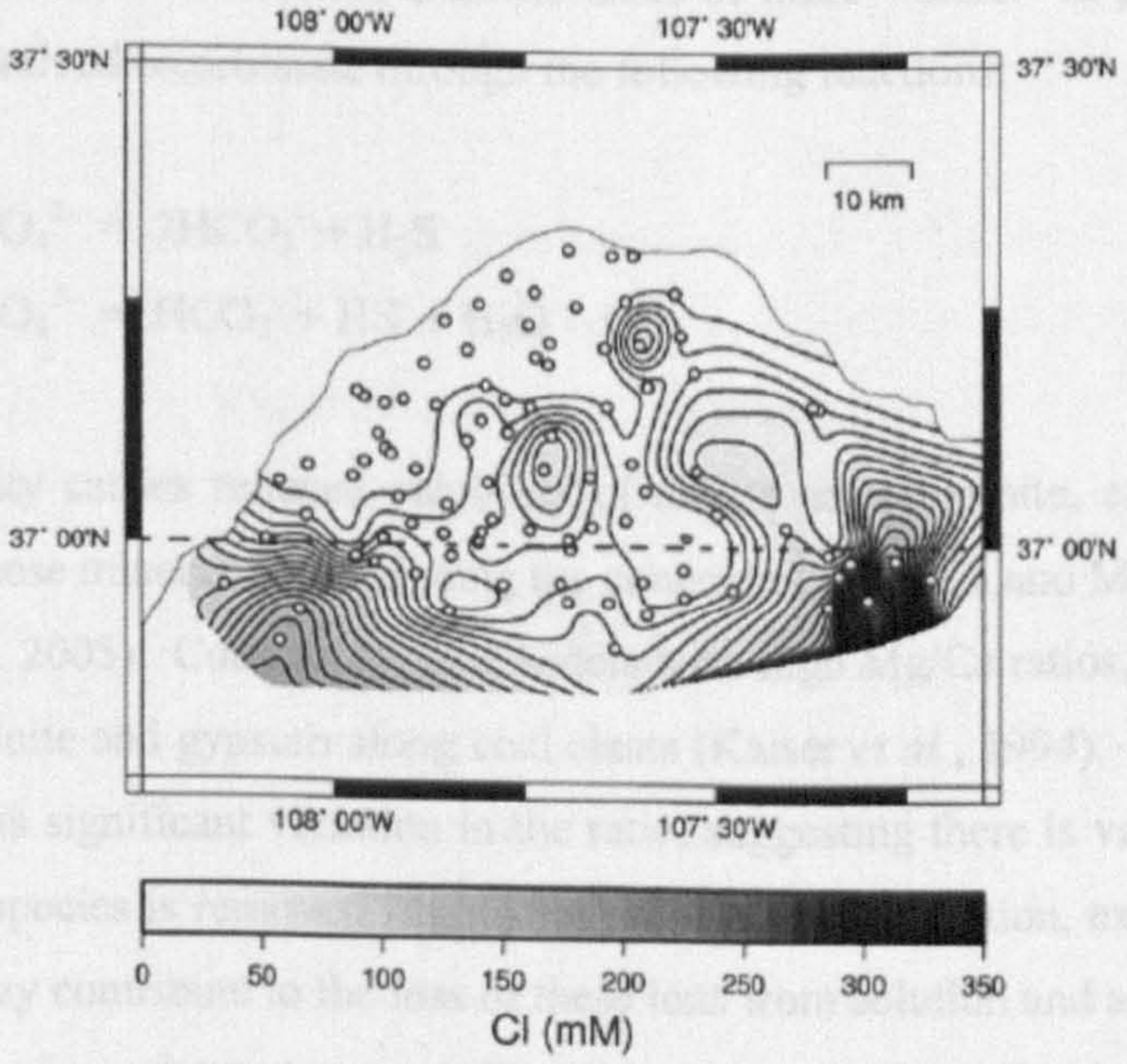

Figure 3.6. The distribution of Cl within the Fruitland coals, dots represent where Cl was analysed. Note the northwest-southeast trending area of low Cl. From Snyder *et al.*, 2003.

The chemical and isotopic makeup of the waters associated with coalbed methane is influenced by a variety of factors including contributions from connate waters that were originally deposited with the peats, the expulsion of certain elements during the formation of the coal, water-rock interactions both locally and along the path of flowing groundwater, and microbially mediated reactions involving both methanogenesis and anaerobic oxidation of methane (Riese *et al.*, 2005).

Formation waters associated with coalbed methane are generally sodium chloride-bicarbonate dominated and depleted in calcium, magnesium and sulphate (Van Voast, 2003; Riese *et al.*, 2005). Kaiser *et al.* (1994) report that in the north-central part of the San Juan basin waters are fresh to brackish Ca-Mg-HCO_3 and Na-HCO_3 types and rarely exceed TDS contents of 30,000 mg/L. In the south, waters are more saline Na-HCO_3, $NaSO_4$ and NaCl types exceeding 35,000 mg/L in some cases. Waters in the north-central part of the basin are unique in their very high HCO_3 contents, high Na, low Ca, Mg and Cl contents, negligible SO_4 and Ba enrichment (Appendix I). Kaiser *et al,* (1994) suggest that very high HCO_3 contents, neutral to slightly alkaline pHs and lack of SO_4 indicate an open chemical system and addition of organically sourced CO_2. Van Voast (2003) maintains that relatively high SO_4 levels can be obtained through dissolution of sulphide minerals along the paths of flow. The subsequent reduction of this sulphate is said to be a prerequisite reaction for the biogenesis of methane, is an attendant condition in its thermogenesis and is responsible for the distinct chemical characteristics of these waters. In particular it enhances the enrichment of dissolved bicarbonate through the following reactions:

$$2CH_4 + SO_4^{2-} = 2HCO_3^- + H_2S \quad (1)$$

$$2CH_4 + SO_4^{2-} = HCO_3^- + HS^- + H_2O + CO_2 \quad (2)$$

Increased alkalinity causes reduced solubility of calcite and dolomite, encouraging the inorganic precipitation of these minerals and reducing the concentration of Ca and Mg in solution (Van Voast, 2003; Riese *et al.*, 2005). Commonly, coal waters have high Mg/Ca ratios, likely due to preferential Ca removal in calcite and gypsum along coal cleats (Kaiser *et al.*, 1994). San Juan is no exception to this, but there is significant variation in the ratio, suggesting there is variability in how much of which dissolved species is removed from solution, where. In addition, exchange of Na from clays for Ca and Mg may contribute to the loss of these ions from solution and account for the high levels of Na observed. In recharge areas, infiltrating waters readily dissolve soluble salts, building commonly high concentrations of Ca, Mg and Na. Progressively along the flow paths and the water's contact with reactive clay minerals, the Ca and Mg ions adsorb to the clay and are replaced

in the water solution by equivalent molar concentrations of Na previously adsorbed onto the clay (Van Voast, 2003).

A set of waters with unusually low chloride concentrations have caused Synder *et al.* (2003) to suggest that post-Eocene basin uplift increased the hydraulic gradient within the reservoir and initially gave rise to incursion of meteoric water. Chlorinity data show a fresh-water plume of possibly meteoric origin extending basinward from the northern and northwestern margins (Kaiser *et al.*, 1994). Because high HCO_3 waters coincide with overpressure and high Cl waters coincide with underpressure, Kaiser *et al.* (1994) suggest that formation water chemistry cannot be used to infer completion lithology.

3.7 Investigating the San Juan Basin

3.7.1 Aims

The following sections of this chapter are dedicated to evaluating the conclusions drawn in previous studies; in particular, that the majority of the waters are brackish in origin, that there is very little meteoric input to the basin and subsequent through-flow, that major cation concentrations (Ca, Mg, Na) are controlled by cation exchange processes and the high bicarbonate concentration of the waters is due to sulphate reduction. The study also aims to illustrate that, on a basin scale, formation waters will reflect the nature of the host lithology, contrary to previous assertions.

3.7.2 San Juan Mineralogy

In order to establish the possible main mineralogical controls on the formation water composition in the San Juan Basin, it was essential to have a good understanding of mineralogical make-up of the reservoir rocks. Core samples taken from the Fruitland and Pictured Cliffs Formations in the Northern part of the basin were generously provided by BP.

Five samples of the sandstones between coal layers were studied using scanning electron microscopy (SEM) and analysed using X-ray diffraction (XRD). The samples were taken from 3 different drill cores, at varying depths and in variable lithologies and provide a useful overall picture of the most important aspects of the mineralogy. The rocks reflect their original shoreline depositional setting. Samples are predominantly sandstones with some shales and coal material. The sandstones are all quartz rich (up to ~80%) and also contain substantial amounts of detrital albite, K-feldspar, mica and lithic fragments as well as authigenic siderite, dolomite, detrital and

authigenic clays and quartz overgrowths. Where the samples also contain coal, this occurs in layers between highly compacted sands and shales.

Significant compaction and chemical diagenesis has substantially reduced porosity, although there are a number of large secondary pores formed from the dissolution of an unknown phase (Figures 3.7A and B). Most pore spaces are filled with kaolin or illite (Figure 3.7B). Proximity to coal layers appears to have an effect on the nature of authigenic clay present. In areas with a high organic content, the dominant clay type appears to be kaolin with illite more important elsewhere. Calcite is rare in these rocks though there are substantial amounts of dolomite present. Much of the dolomite is altered to siderite (Figures 3.7B, C and D). There is evidence of the earlier presence of significant amounts of smectite (Figures 3.7B and 3.8F), now largely transformed to illite, possibly derived from bentonites thought to be present which are the devitrification products of ash falls.

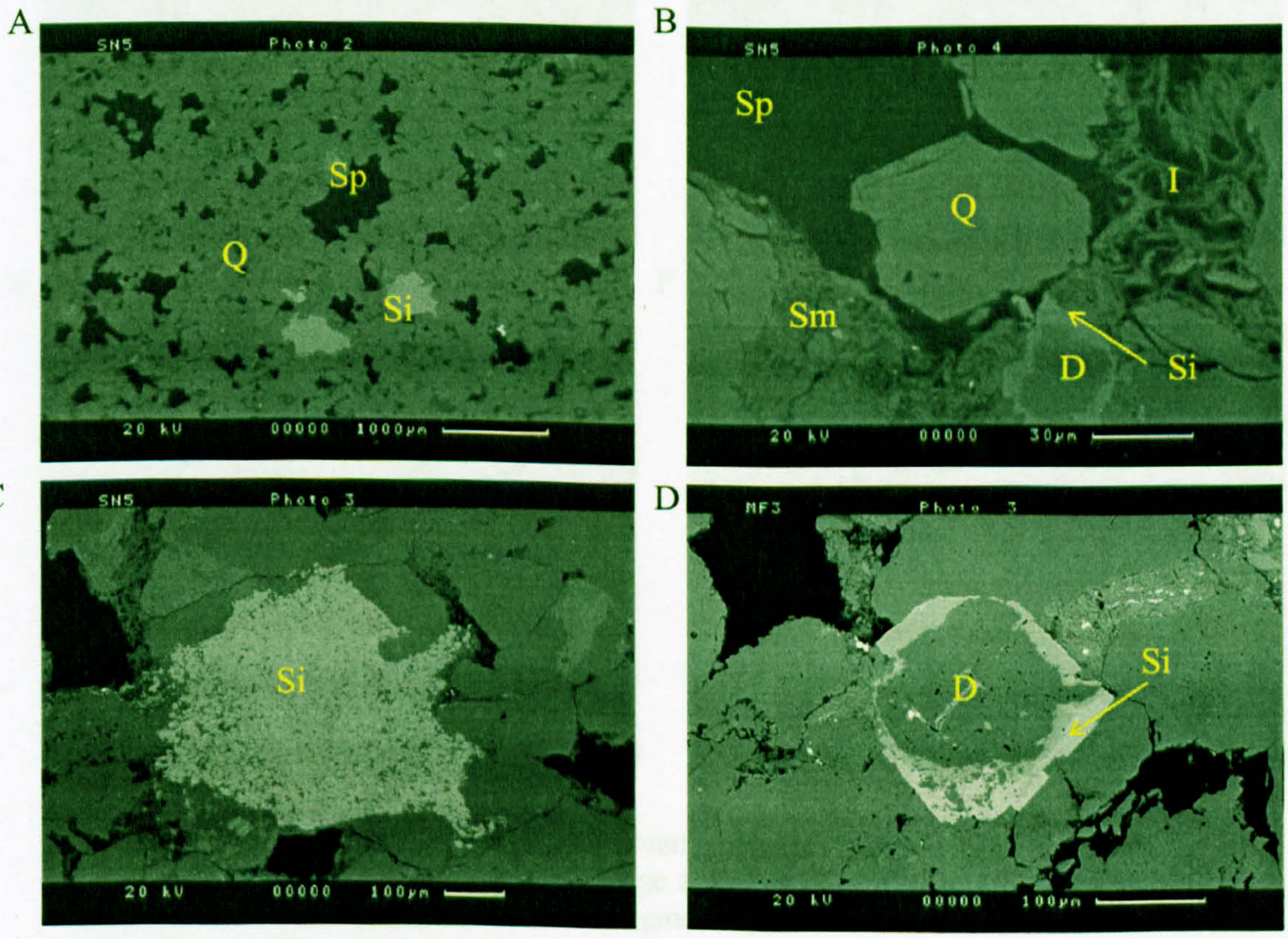

Figure 3.7.
A. SN (707.2m) Quartz (Q) rich sand containing large secondary pores (Sp) and abundant siderite (Si)
B. SN (707.2m) Angular quartz clasts with pore-filling illite (I) and smectite (Sm). In places dolomite is altered to siderite (Si)
C. SN (707.2m) Late stage siderite (Si) surrounded by quartz
D. MF (816.3m) Early authigenic dolomite altered to later siderite

A

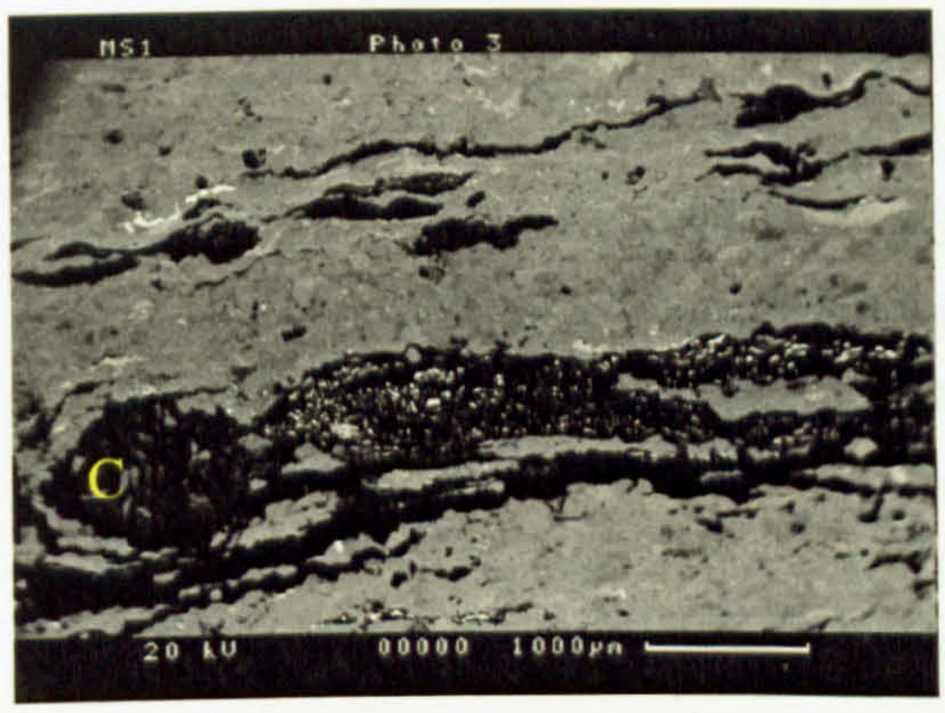

B

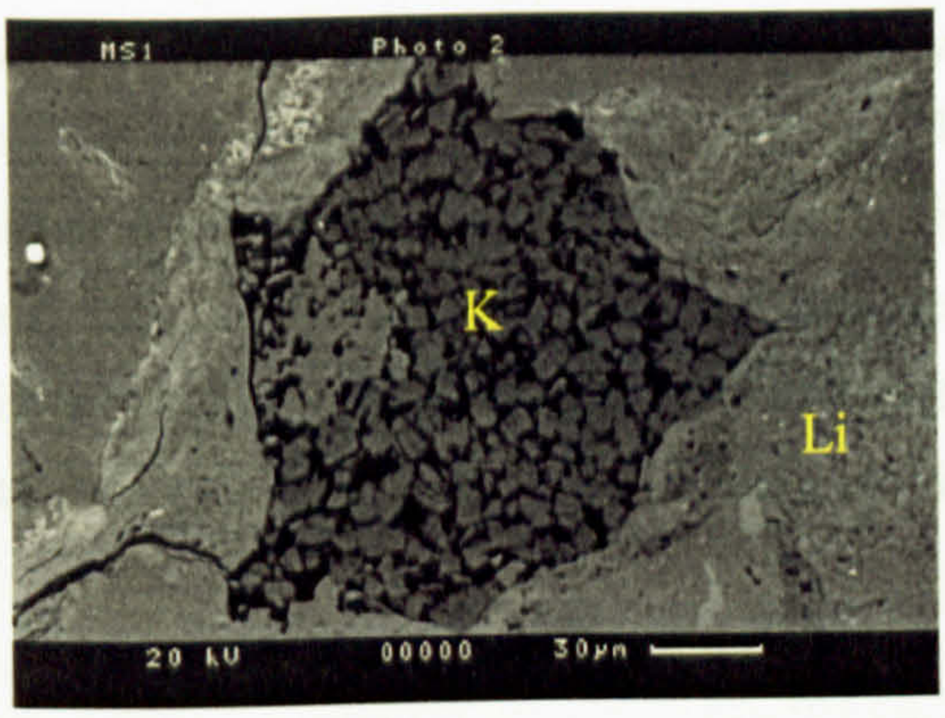

C

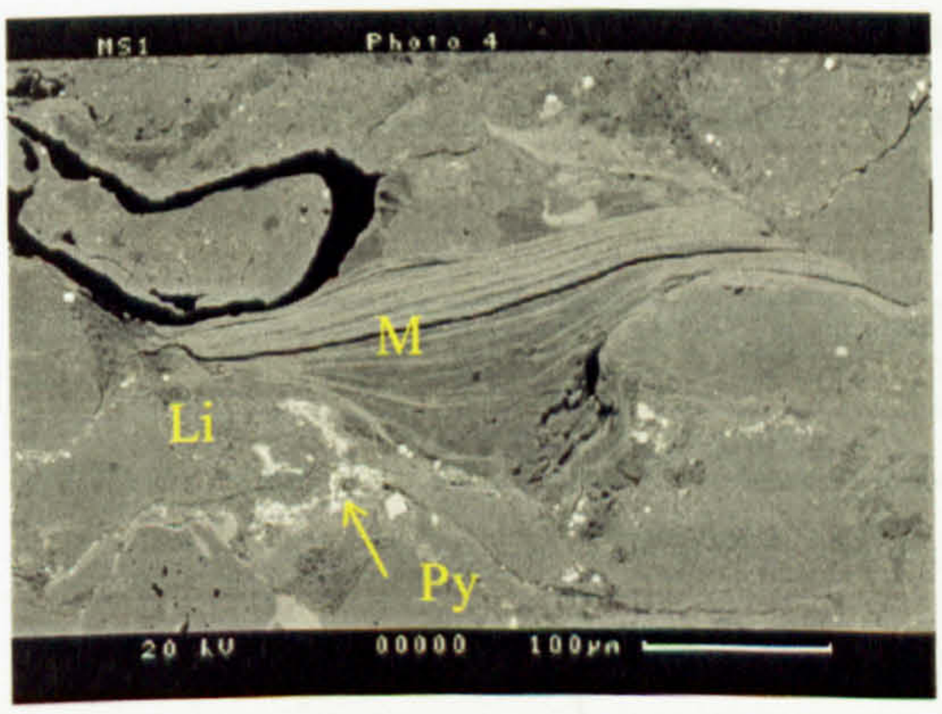

D

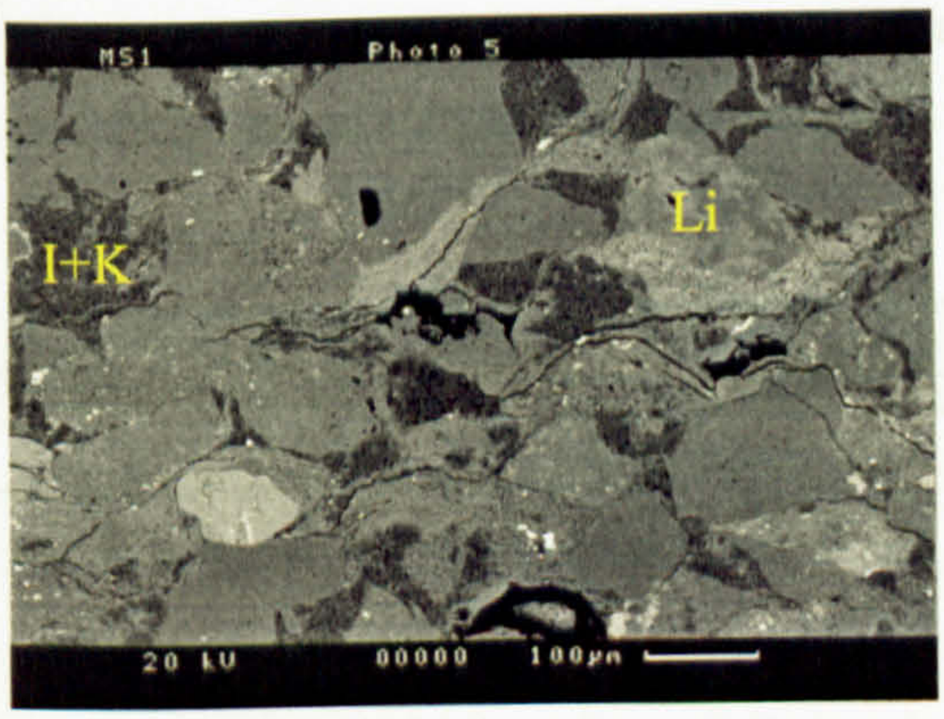

E

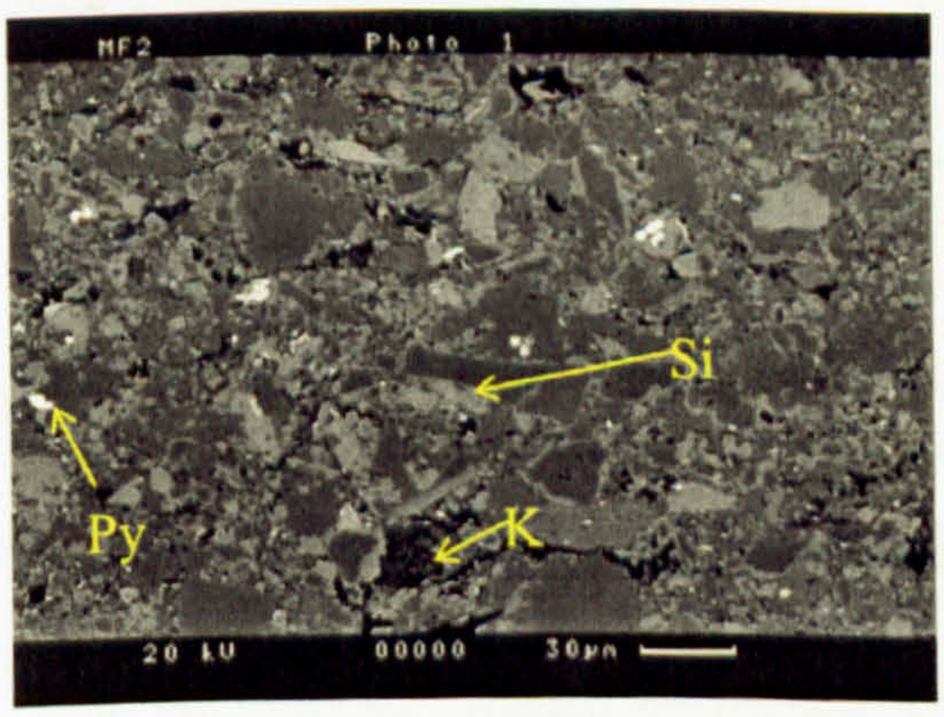

F

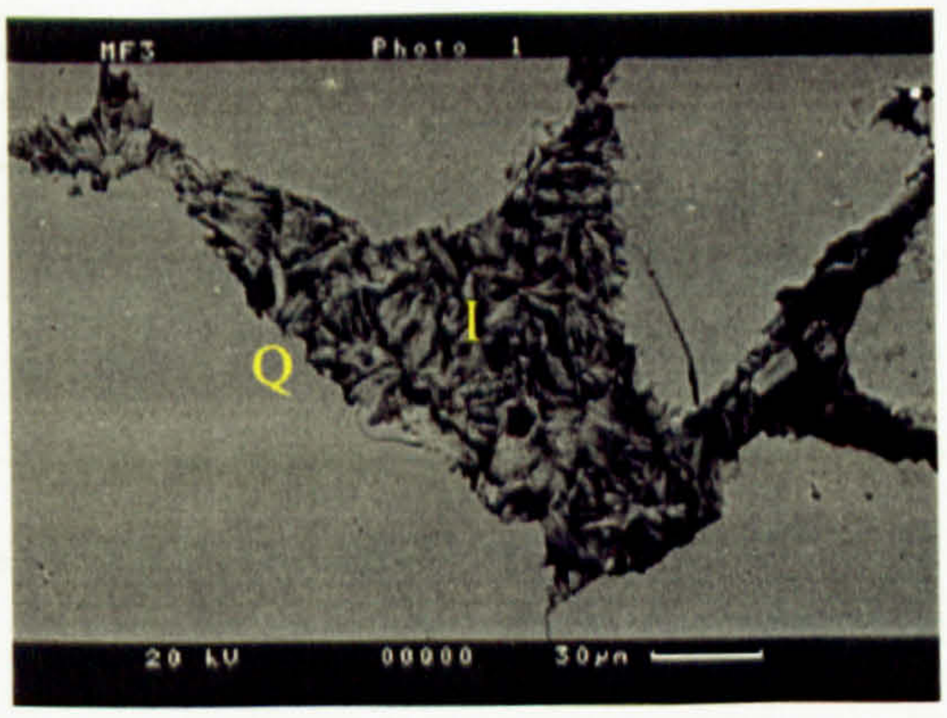

Figure 3.8.
A. MS (891.2m) Coal (C) occurs in the San Juan reservoir rocks as elongate bands
B. MS (891.2m) Some locations contain large amounts of pore-filling illitised kaolin (K) together with metamorphic and igneous lithic rock fragments (Li)
C. MS (891.2m) Fibrous mica (M) with associated lithic fragments and early pyrite (Py)
D. MS (891.2m) San Juan reservoir rocks can be very mineralogically complex. Here the pore spaces between quartz, siderite and lithic fragments (Li) are filled by illitised kaolin (I+K)
E. MF (773.5m) Finer siltstone consisting of angular clasts, containing abundant siderite cement (Si) and small amounts of pyrite (Py) authigenic kaolin (K).
F. MF (816.3m) Some locations contain more abundant quartz overgrowths than others (Q) and many of the pore spaces contain authigenic illite.

In some places lithic fragments comprise up to 40% of the rock, though more commonly they amount to around 15%. These consist of igneous and metamorphic clasts, mostly heavily illitised (Figures 3.8B, D and E). The presence of significant quartz overgrowths (5-10% in places) (Figure 3.8F) and illitised kaolin (Figure 3.8B) suggests that the rocks have undergone diagenesis at temperatures exceeding ~90°C. The facts that the rocks have clearly reached thermal maturity and methane generation has occurred also indicate that the rocks must have experienced higher temperatures and been subsequently uplifted.

XRD analysis of the samples studied in the SEM indicates that the dominant mineralogy of the reservoir rocks includes quartz, albite, dolomite, muscovite, chlorite, pyrite, siderite, kaolinite and mixed layer illite-smectite (Appendix II contains the XRD traces for all the samples analysed).

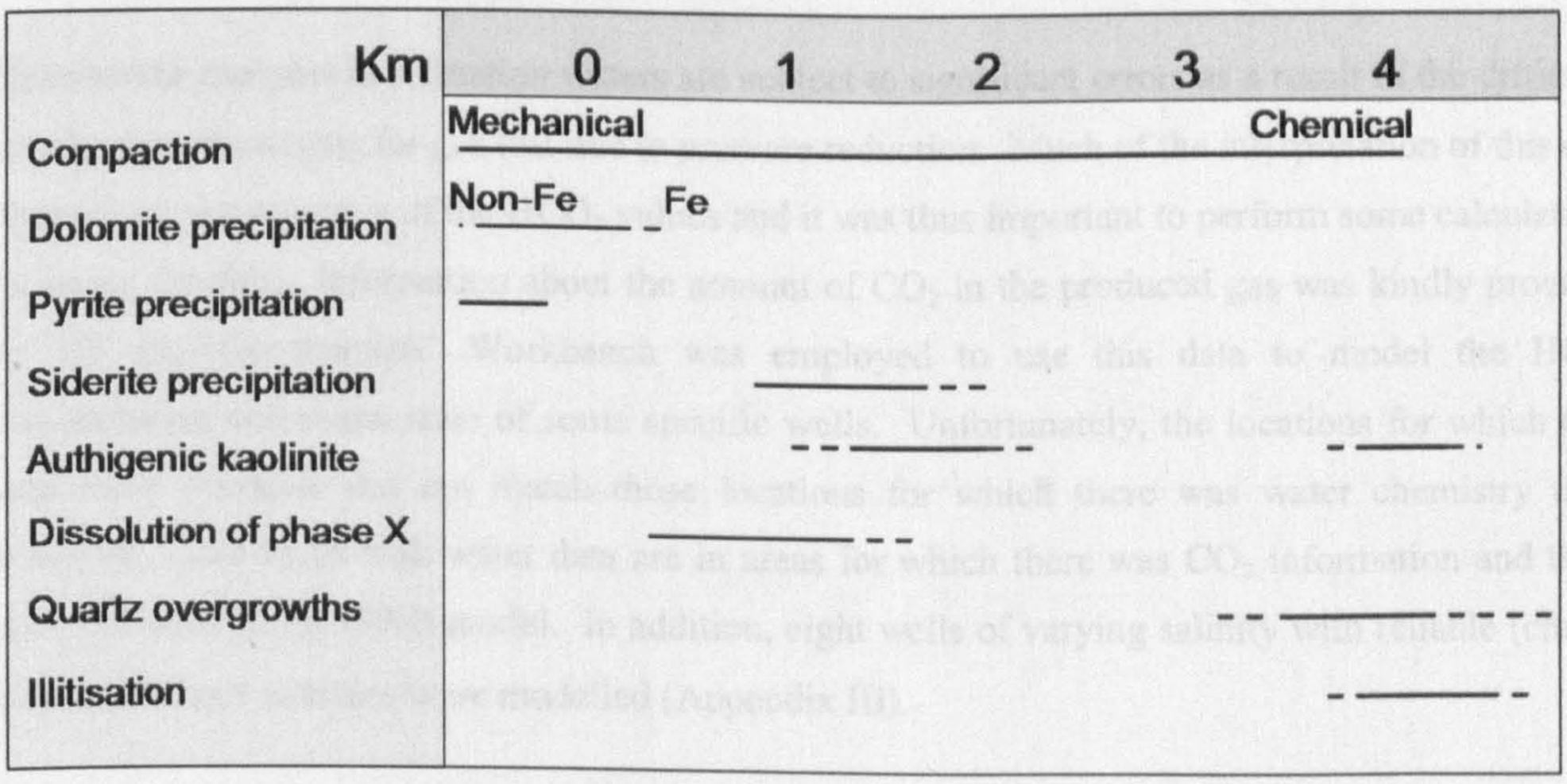

Figure 3.9. Paragenetic sequence for minerals in the San Juan reservoir rocks

3.7.3 The water analysis dataset

A dataset consisting of samples from 129 wells and surface waters in the northern part of the San Juan Basin has been generously provided by BP. All the samples were collected during one summer season and each was analysed for major cations, anions and radiogenic and stable isotopes. The results of the detailed isotope study of the waters are outlined above, but little work has been carried out in the past to analyse the nature of the other dissolved inorganic species. The following section outlines the basic character of the San Juan formation waters, and provides a basis for further, more detailed study into fully understanding water chemistry in this kind of system.

3.7.3.1 *Data quality analysis*

All the data were subject to charge balance testing, however, due to the very low salinities involved, the analyses often did not balance at all well. In addition, the waters were not analysed for pH.

Bicarbonate analyses in formation waters are subject to significant errors as a result of the difficulty involved in accounting for gas lost due to pressure reduction. Much of the interpretation of this data depends on the accuracy of the HCO_3 values and it was thus important to perform some calculations to assess the data. Information about the amount of CO_2 in the produced gas was kindly provided by BP and Geochemists' Workbench was employed to use this data to model the HCO_3 concentration and redox state of some specific wells. Unfortunately, the locations for which CO_2 data were available did not match those locations for which there was water chemistry data. However, three wells with water data are in areas for which there was CO_2 information and these were included in the GWB model. In addition, eight wells of varying salinity with reliable (charge balanced) water analyses were modelled (Appendix III).

For each well, the precise water chemistry was specified, CO_2 was swapped into the basis replacing HCO_3, CH_4 was swapped into the basis replacing $O_{2(aq)}$ (thus controlling redox state) and pH was set to be controlled by equilibrium with dolomite. Charge balance was controlled by Cl in the most saline waters, or by Ca or Mg in the more dilute waters. The fluid for each well was then allowed to come to equilibrium and the results noted.

Table 1 presents some of the model basis inputs and results. Calculated HCO_3 values do not match the input values but are always of the same order of magnitude and differ only by up to 7000 mg/kg (average = 300 mg/kg). This confirms that, while the measured HCO_3 values may not be completely accurate, they can be relied on to help identify general trends. Oxygen fugacity is very

low, and where sulphur species are present, they tend to exist as H_2S, indicating a reducing environment.

Table 1. Showing the major basis input species and results from the GWB model identifying HCO_3 concentrations and redox state, highlighted analyses exhibited some charge balance discrepancy

Well name	Charge balanced on	Partial Pressure CO2 (bar)	Partial Pressure CH4 (bar)	HCO3 measured (mg/kg)	HCO3 calculated (mg/kg)		pH	log fO2	H2S (mg/kg)	H2S (Mol)
24-5;32-9	Cl	2.2	97.0	9020.0	1969.0		6.0	-66.462	0.272	8.1E-06
32-4;33-8	Cl	2.2	84.4	5120.0	2408.0		6.1	-66.425	0.209	6.2E-06
Allison 102	*Cl*	*4.2*	*95.5*	*2644.0*	*2810.0*		*5.9*	*-65.870*		
Allison 127	*Cl (Ca)*	*4.2*	*95.5*	*2929.0*	*1685.0*	*6274*	*5.5*	*-72.335*		
Dusenberry Com	Cl (Ca)	2.2	84.4	1226.0	2804.0	2139	6.2	-66.426		
Animas 35-2	*Ca*			*1122.0*	*2126.0*		*5.8*	*-66.282*		
Arado 1-13	Ca	2.2	84.4	441.0	902.3		5.7	-66.424		
Federal 4-1	Ca	2.2	84.4	1369.0	2587.0		6.2	-66.424		
Royce State 36-2	Ca	2.2	84.4	1389.0	2386.0		6.1	-66.424		
Huber 2-34	Mg	2.2	84.4	877.0	1761.0		6.0	-66.424	0.339	1.0E-05

3.7.3.2 *Basic data features*

The data were plotted on a series of simple diagrams to illustrate their most obvious chemical characteristics. In most cases, though not all, these diagrams support the observations noted in the literature. The waters are extremely low salinity, with variable chloride compositions, high levels of bicarbonate and sodium and low concentrations of calcium and magnesium (Figure 3.10) as would be expected from coal-bed waters. Cation concentrations increase with increasing salinity, but correlation is poor, suggesting an alternative control on the cation composition of the waters.

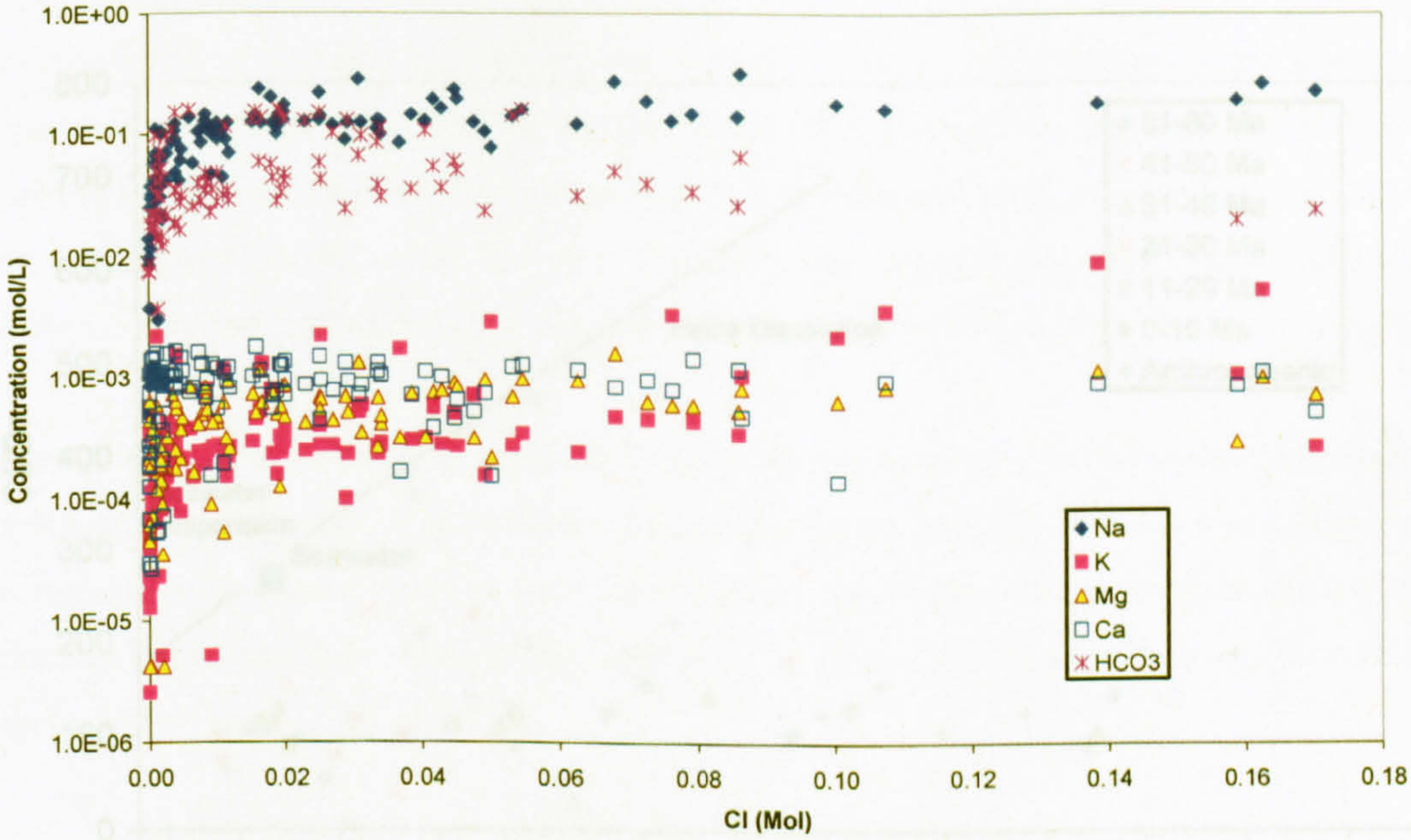

Figure 3.10. Varying concentrations of cations and anions with Cl in Fruitland formation water, including Na, K, Ca, Mg and HCO_3. Note the log scale.

Fluid origins

The traditional method of tracking the evolution of water of marine origin, Cl/Br and Na/Br ratios (see Chapter 2), shows that the San Juan formation waters are severely enriched in Br relative to Ca and Na (Figure 3.11). A plot of Br systematics will not establish the original nature of the water, but assuming a marine-brackish origin, simple dilution and thus the preservation of the ratios, it is clear that water-rock interaction has had a great influence on the composition of the waters. The very high Br/Cl implies a distinct supply of Br and the organic matter in the coal would have been the most likely source (Spears, 2005; Biester *et al.*, 2006). This is in accordance with the assertion of Snyder *et al.* (2003) that high I concentrations are derived from diagenetic reactions with the peats.

Dominant anions

Significant deviation from charge balance (charge imbalance reaches an average of 86% when Cl is considered alone, compared with 34% when all anions are considered) indicates an additional anion is needed to maintain charge balance (Appendix I). A plot of Cl and HCO_3 concentration vs. TDS tells much about the major controls on the formation water composition (Figure 3.12). Both species show a positive correlation, however, the rapid initial increase in bicarbonate with TDS suggests that this is the dominant anion at lower salinities.

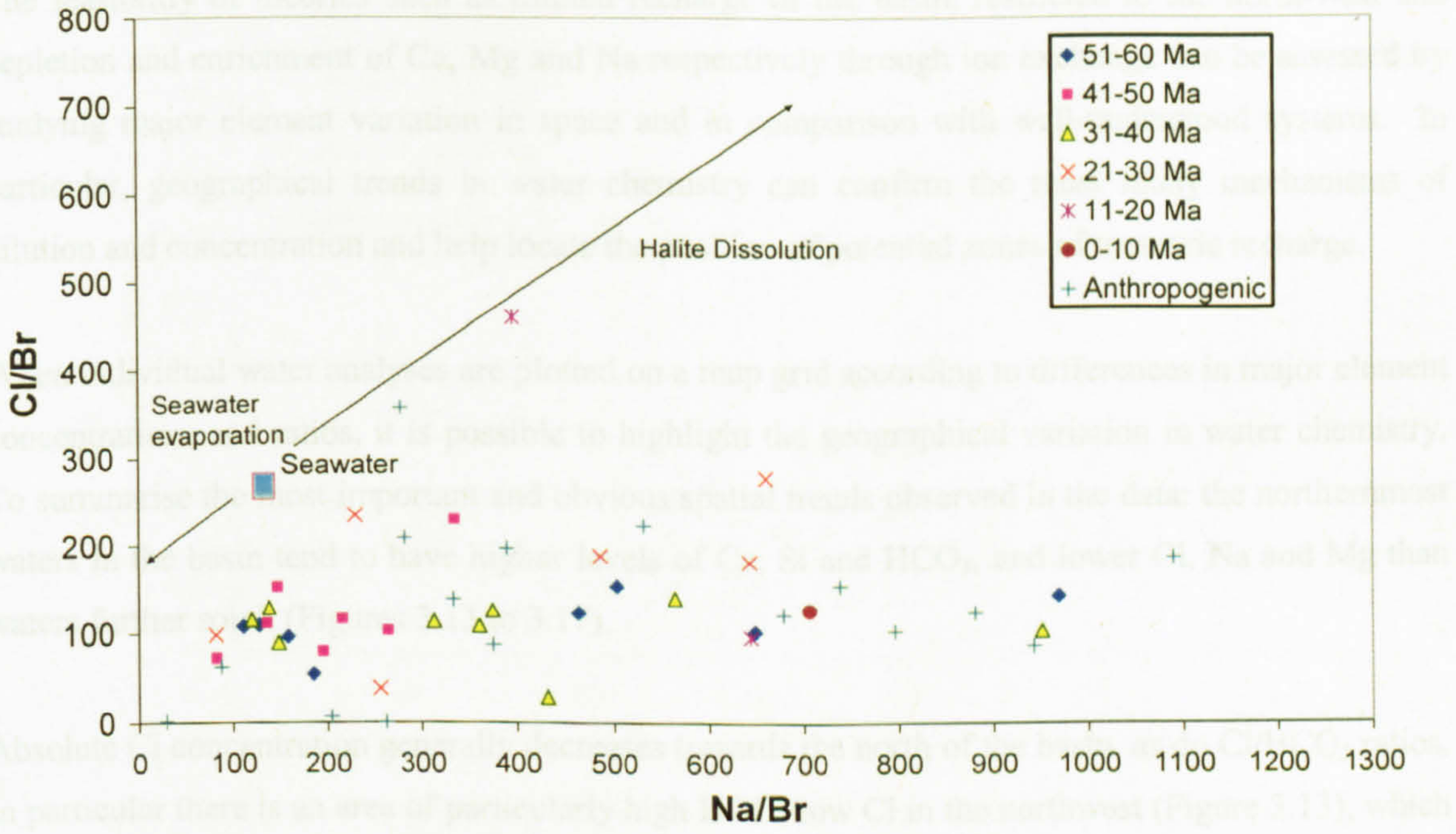

Figure 3.11. San Juan data do not lie on the trend predicted either by seawater evaporation or halite dissolution, due to high levels of Br derived from organic matter. There is very little correlation based on ages of samples analysed

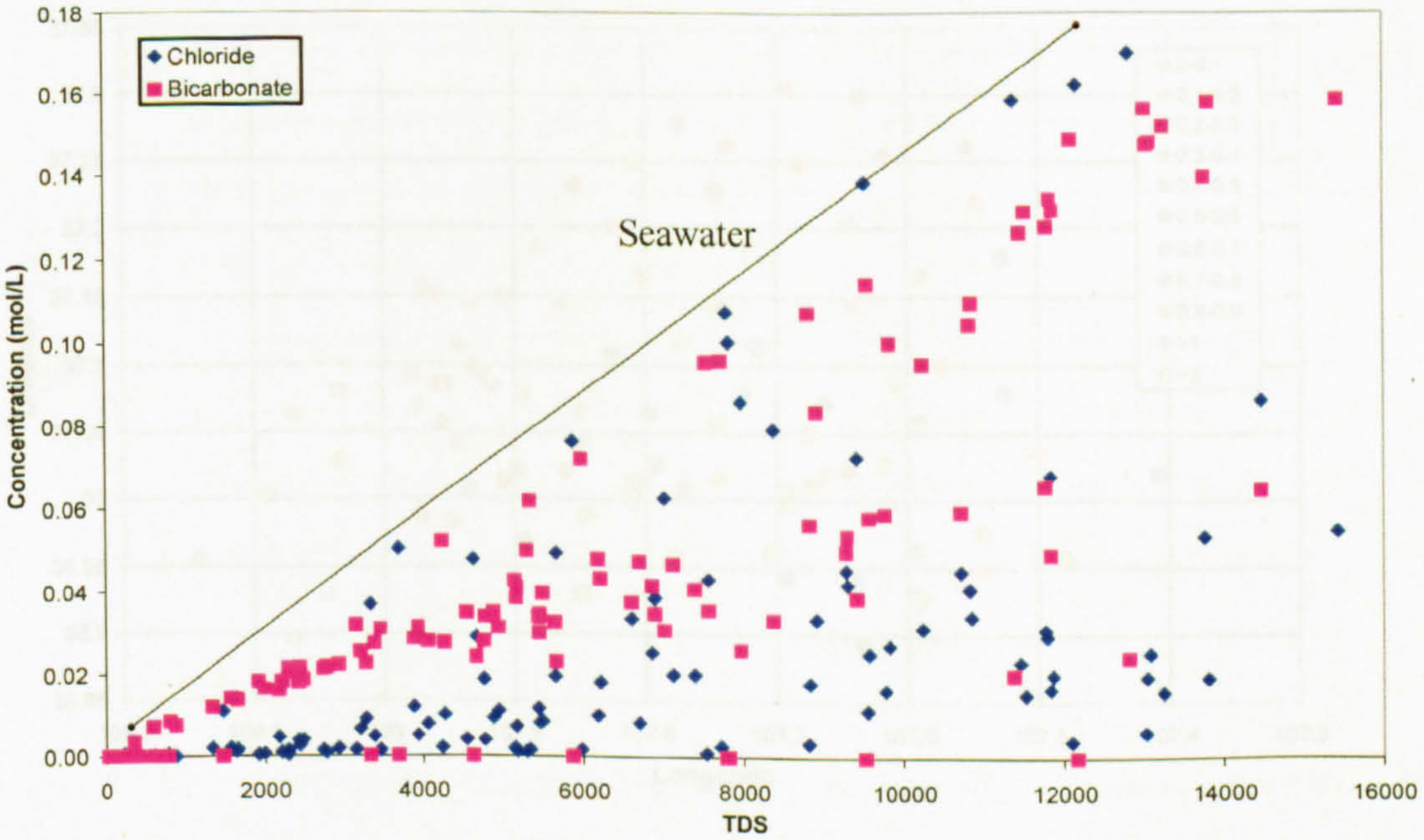

Figure 3.12. Relative Cl and HCO_3 concentrations with changing TDS. Note the importance of HCO_3 at low TDS values and the fence formed at seawater concentrations

3.7.4 Spatial variations

The feasibility of theories such as limited recharge of the basin, restricted to the north-west and depletion and enrichment of Ca, Mg and Na respectively through ion exchange can be assessed by studying major element variation in space and in comparison with well-understood systems. In particular, geographical trends in water chemistry can confirm the most likely mechanisms of dilution and concentration and help locate the position of potential zones of meteoric recharge.

When individual water analyses are plotted on a map grid according to differences in major element concentrations and ratios, it is possible to highlight the geographical variation in water chemistry. To summarise the most important and obvious spatial trends observed in the data: the northernmost waters in the basin tend to have higher levels of Ca, Si and HCO_3, and lower Cl, Na and Mg than waters further south (Figures 3.13 to 3.17).

Absolute Cl concentration generally decreases towards the north of the basin, as do Cl/HCO_3 ratios. In particular there is an area of particularly high HCO_3/low Cl in the northwest (Figure 3.13), which was also highlighted in the study by Snyder *et al.* (2003) who also used Cl concentrations as well as δD and ^{129}I (Figures 3.4 and 3.6). This area is interpreted as the main site of meteoric recharge into the basin.

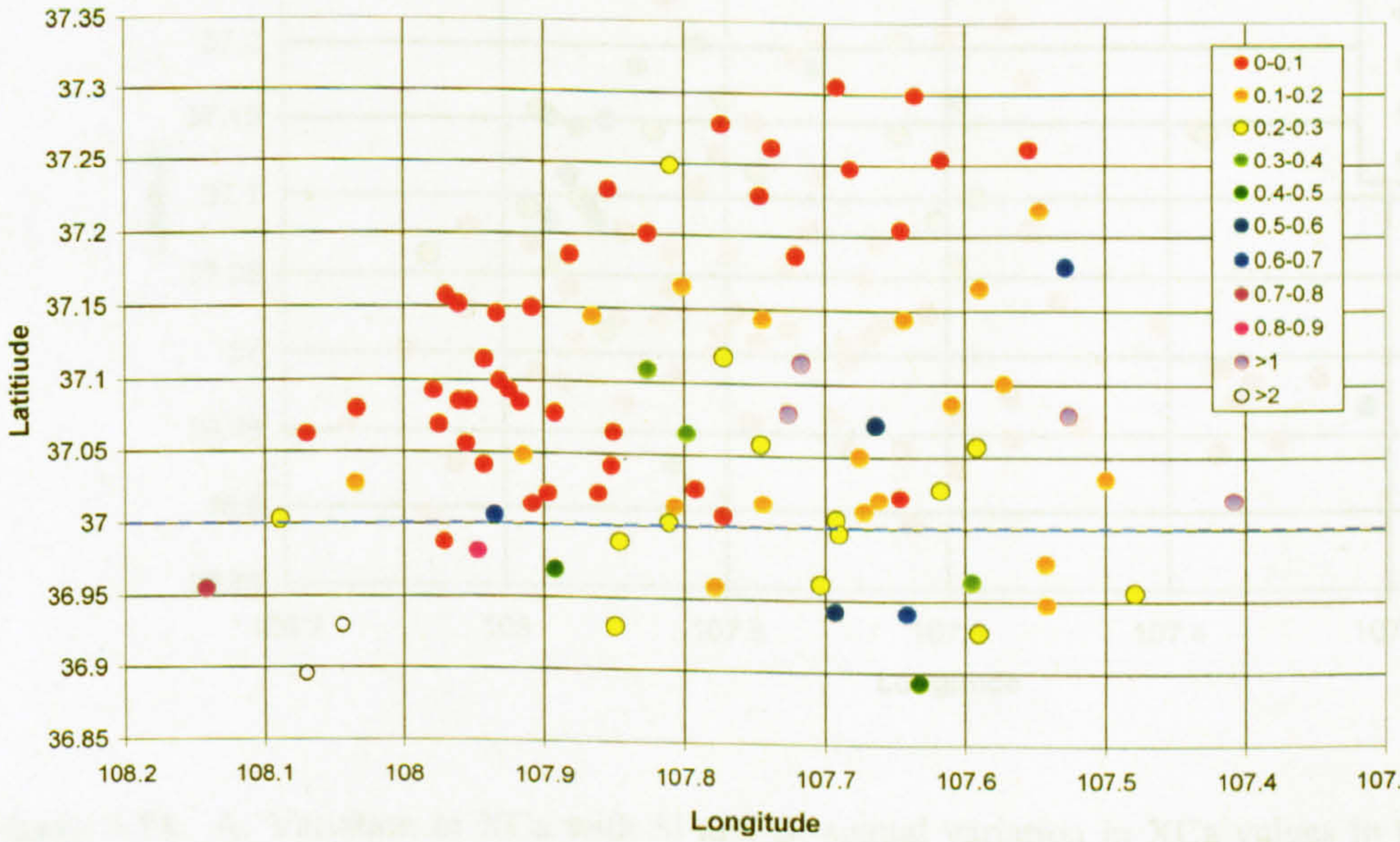

Figure 3.13. The variation in Cl/HCO_3 ratio in the San Juan Basin, areas of relatively lower Cl/higher HCO_3 correspond with the assumed locations of meteroric influx into the basin (c.f. Figure 3.6)

A

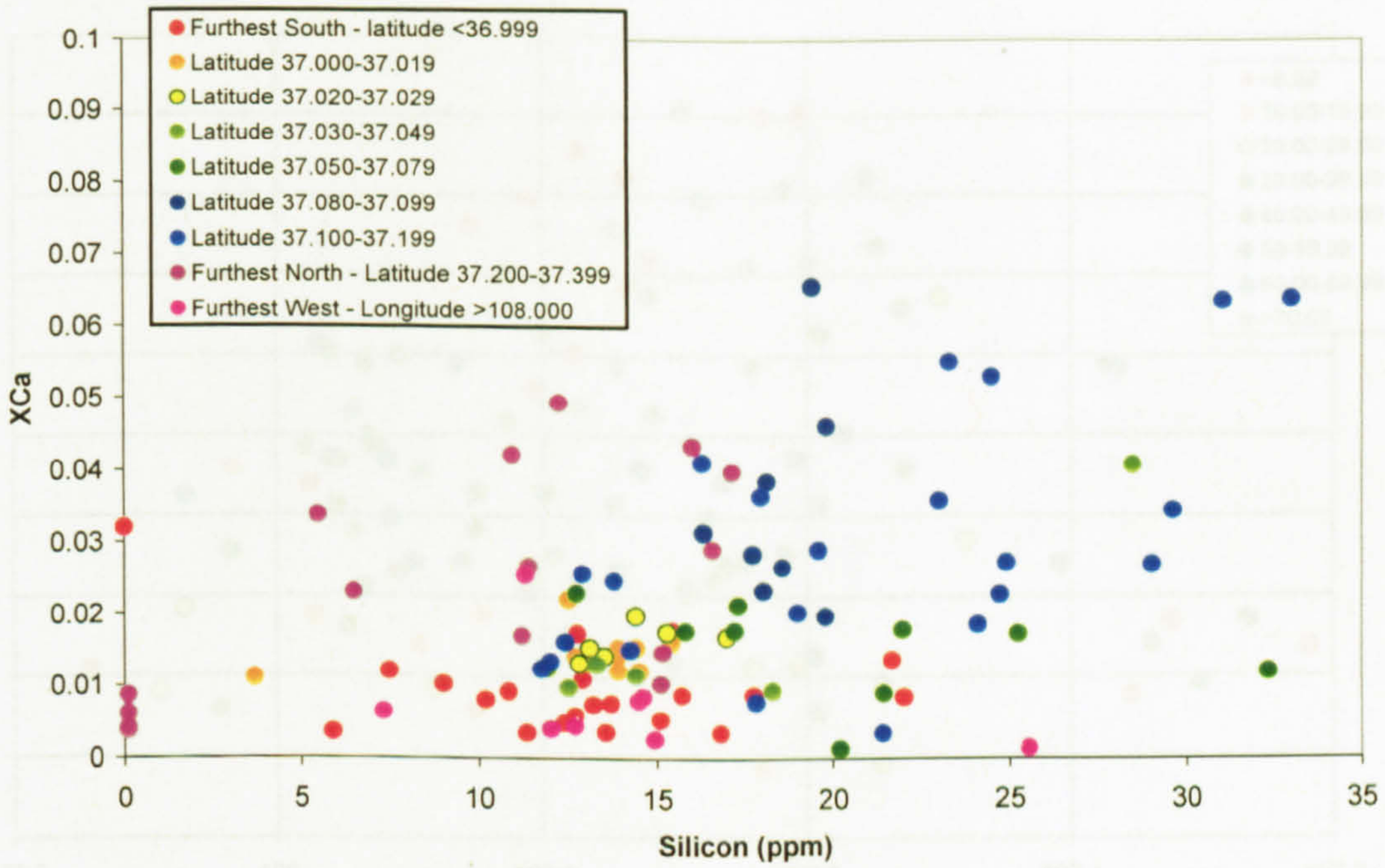

B

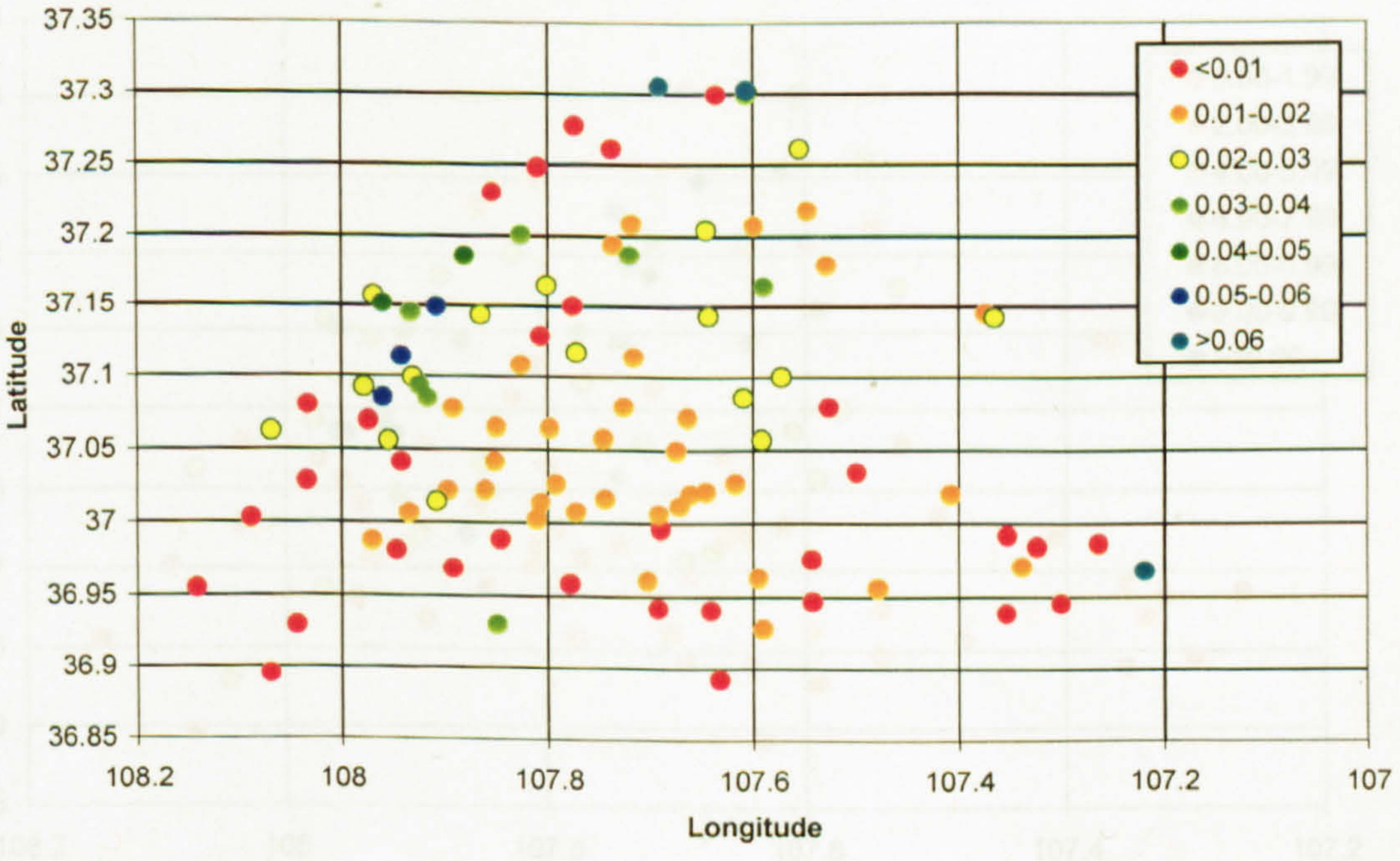

Figure 3.14. A: Variation in XCa with Si and B: spatial variation in XCa values in the northern part of the San Juan.

A

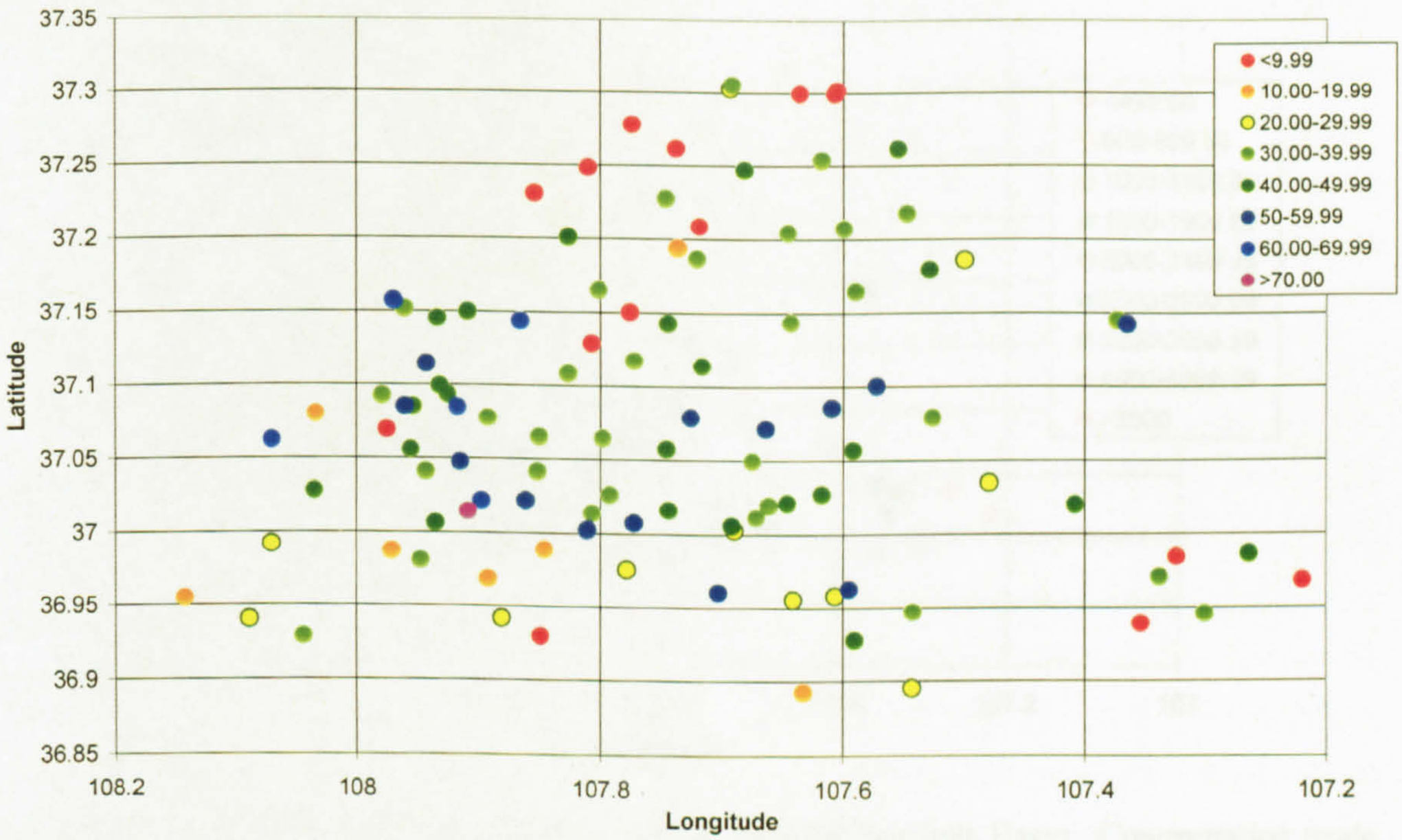

B

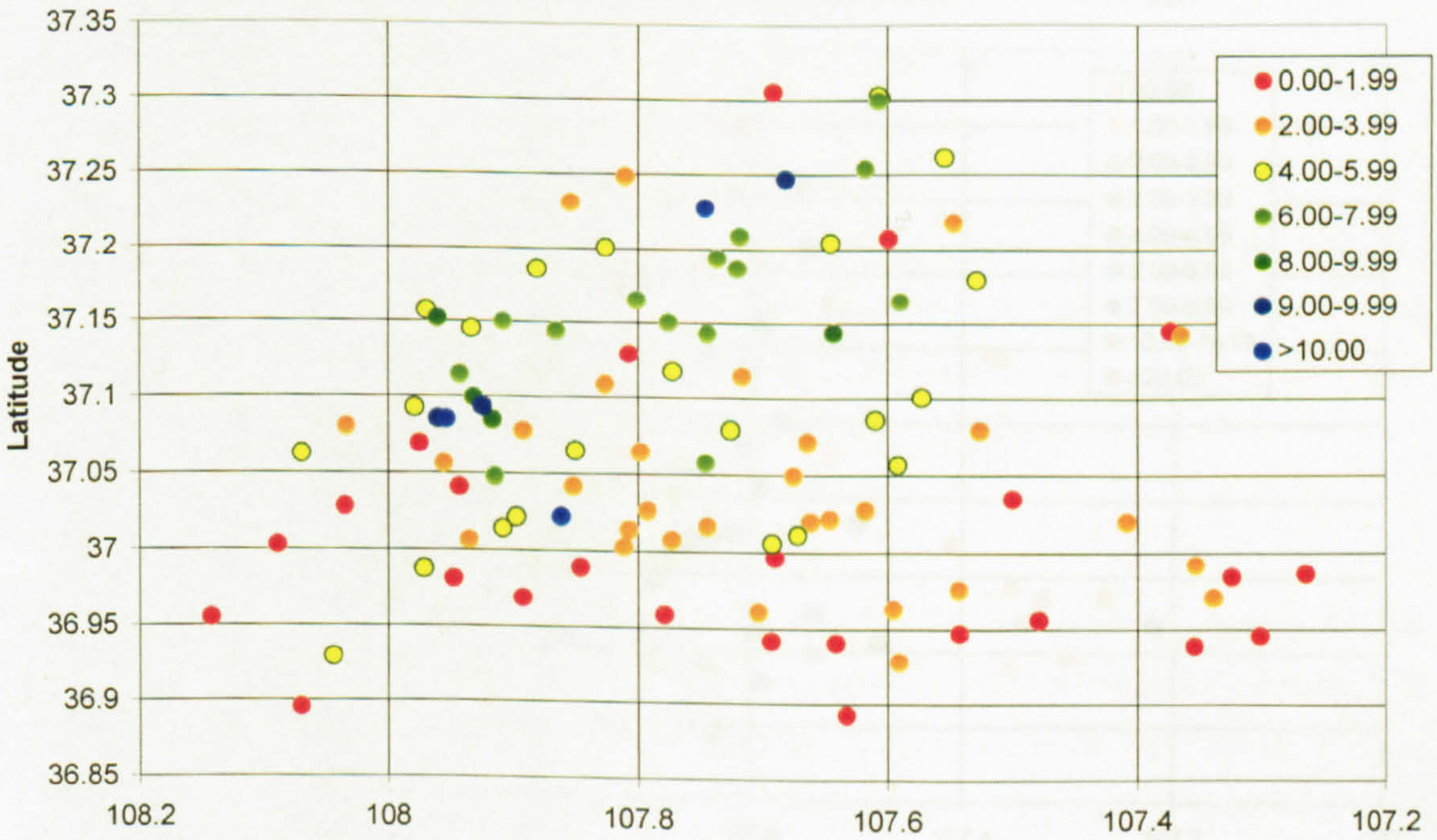

Figure 3.15. A: Variation in Ca concentration (in ppm) over the northern part of the San Juan Basin, note higher values in the west-central area, B: variation in the Ca/Mg ratio in the same area, high values correspond to areas with high Ca concentration, suggesting Mg concentrations are relatively constant over the northern part of the basin.

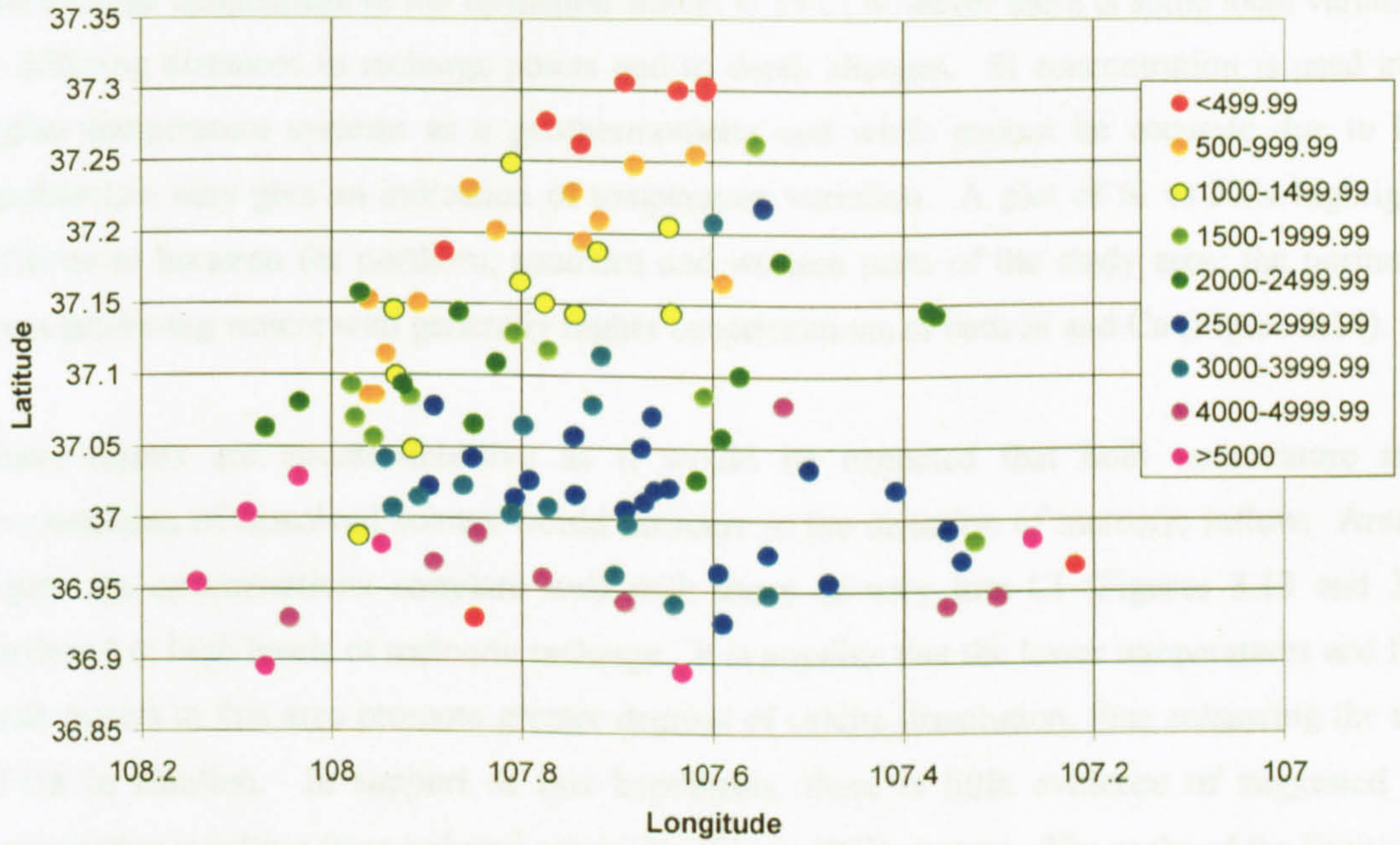

Figure 3.16. Variation in Na concentration (in ppm) over the San Juan Basin. Concentration tends to increase steadily southwards without being affected by areas of meteoric recharge.

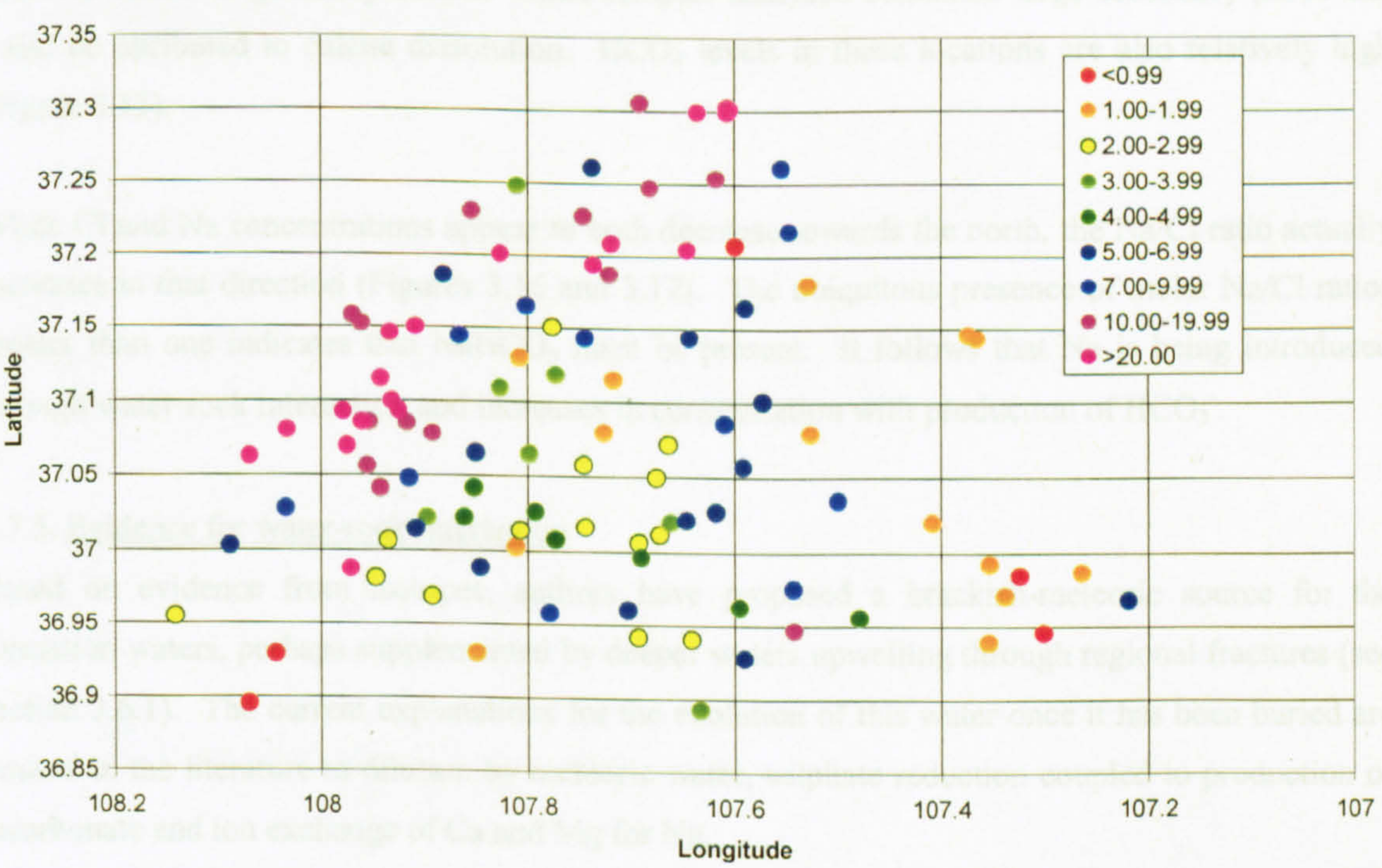

Figure 3.17. Variation in the Na/Cl ratio by weight. The ratio increases dramatically to the North west indicating that Na (as NaHCO3) is being introduced to the system in these locations through diagenetic processes

The average temperature of the formation waters is 55°C, however there is some local variation due to differing distances to recharge points and to depth changes. Si concentration is used in many higher temperature systems as a geothermometer and while cannot be accurate due to lack of equilibrium, may give an indication of temperature variation. A plot of Si vs XCa highlights the differences between the northern, southern and western parts of the study area; the northernmost areas producing waters with generally higher concentrations of both Si and Ca (Figure 3.14).

These results are counter-intuitive as it would be expected that both temperature and the concentration of dissolved solutes would decrease in the direction of meteoric inflow. Areas with higher Ca concentrations correlate well with those of very low Cl (Figures 3.13 and 3.15) – attributed to high levels of meteoric recharge. It is possible that the lower temperatures and flowing fresh waters in this area promote greater degrees of calcite dissolution, thus enhancing the amount of Ca in solution. In support of this hypothesis, there is little evidence of suggested calcite precipitation resulting from reduced solubility of high-HCO_3 waters. The rocks of the Fruitland and Pictured Cliffs Formations contain abundant carbonate minerals including dolomite and siderite, however calcite is generally absent. Most samples analysed contained large secondary pores that could be attributed to calcite dissolution. HCO_3 levels in these locations are also relatively high (Figure 3.13).

While Cl and Na concentrations appear to both decrease towards the north, the Na/Cl ratio actually increases in that direction (Figures 3.16 and 3.17). The ubiquitous presence of molar Na/Cl ratios greater than one indicates that $NaHCO_3$ must be present. It follows that Na is being introduced through water-rock interaction and increases in concentration with production of HCO_3^-.

3.7.5. Evidence for water-rock interaction

Based on evidence from isotopes, authors have proposed a brackish-meteoric source for the formation waters, perhaps supplemented by deeper waters upwelling through regional fractures (see section 3.6.1). The current explanations for the evolution of this water once it has been buried are limited in the literature to dilution by meteoric water, sulphate reduction coupled to production of bicarbonate and ion exchange of Ca and Mg for Na.

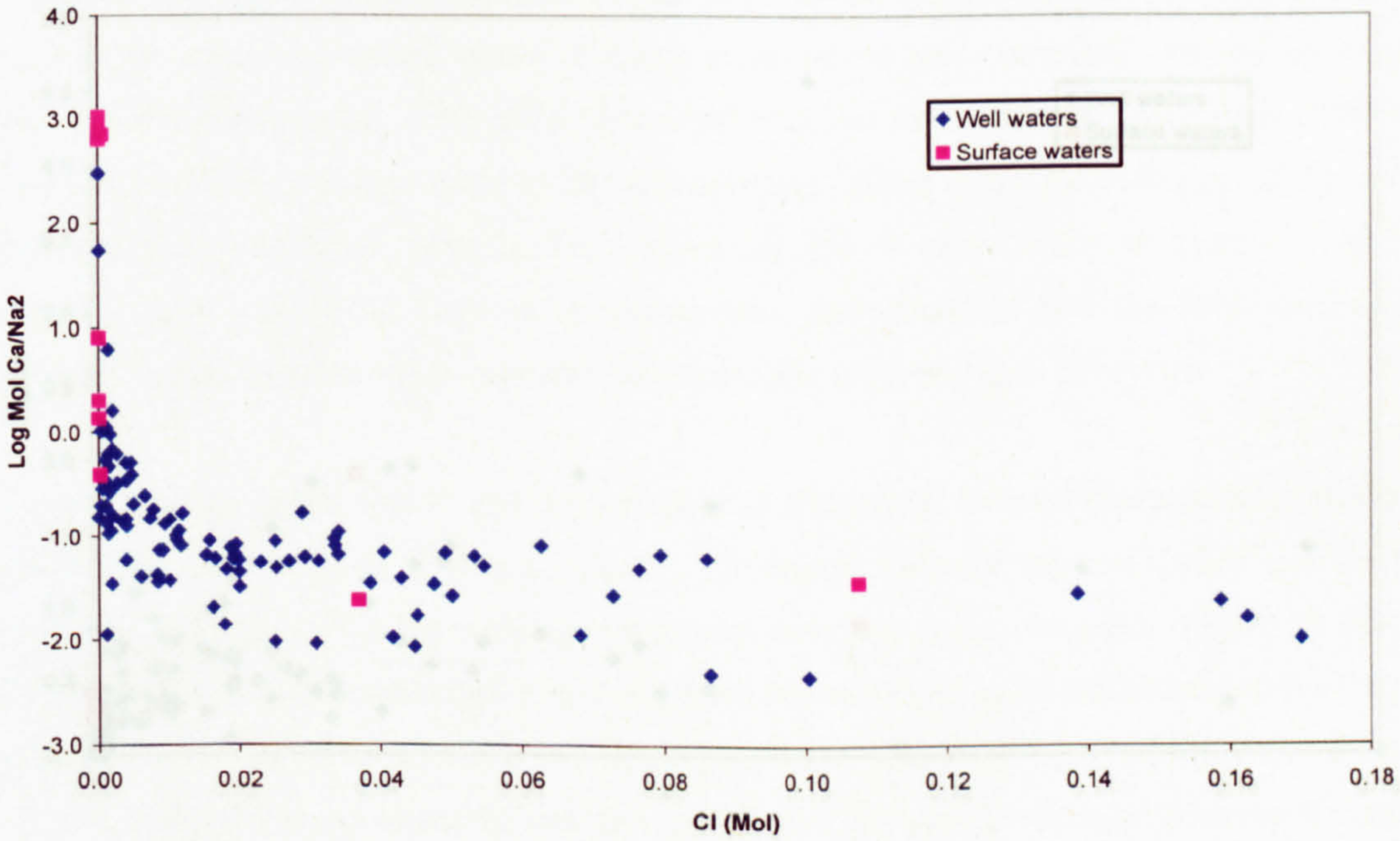

Figure 3.18. Variation in the parameter log mol Ca/Na^2 with Cl. Note the inverse correlation and lack of consistency in the lower salinity region of data indicating that buffering by Ca-silicates is not an important feature of this system.

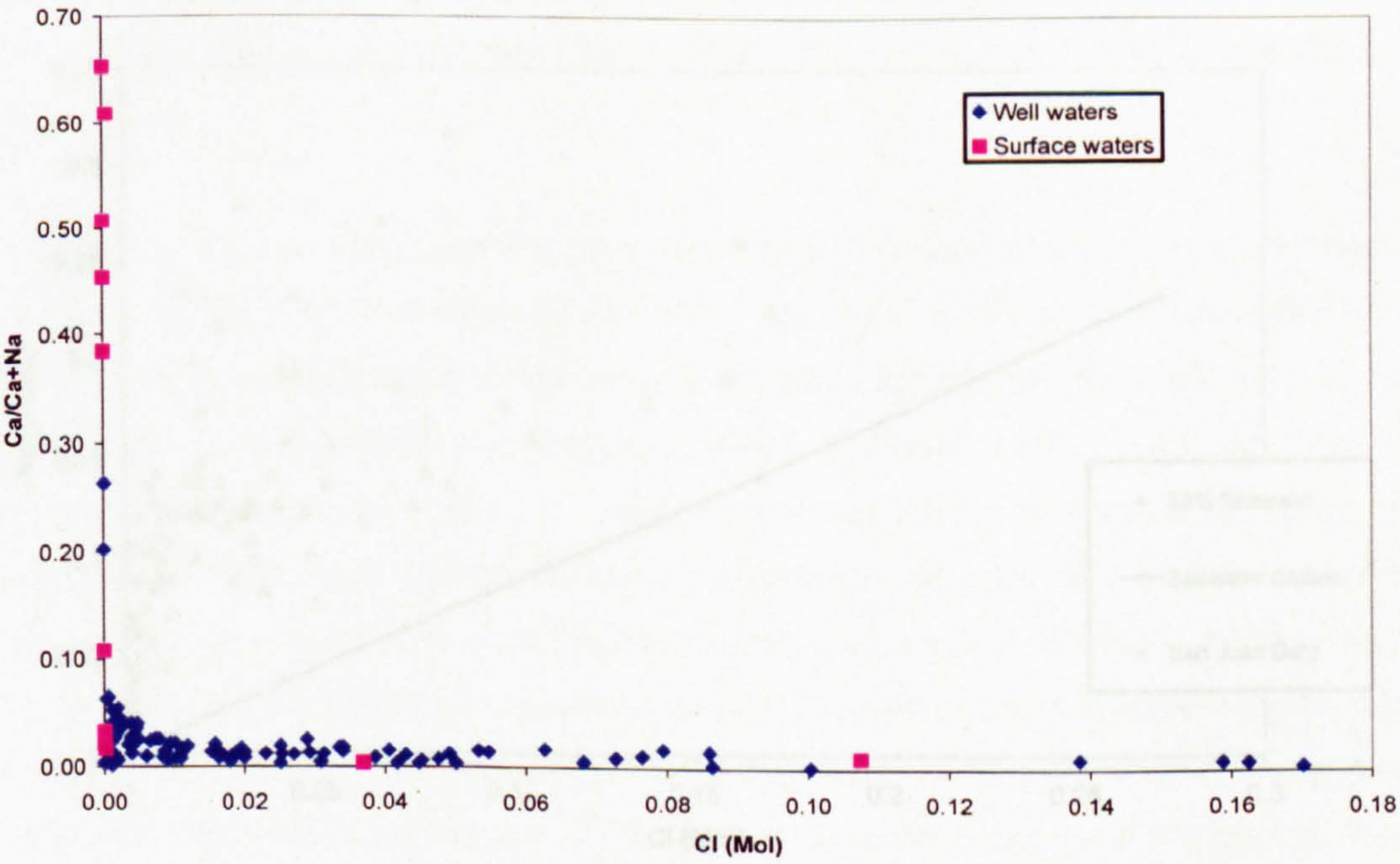

Figure 3.19. The importance of Ca as a cation appears to decrease with increasing Cl, in contrast with what is observed in chloride dominated waters.

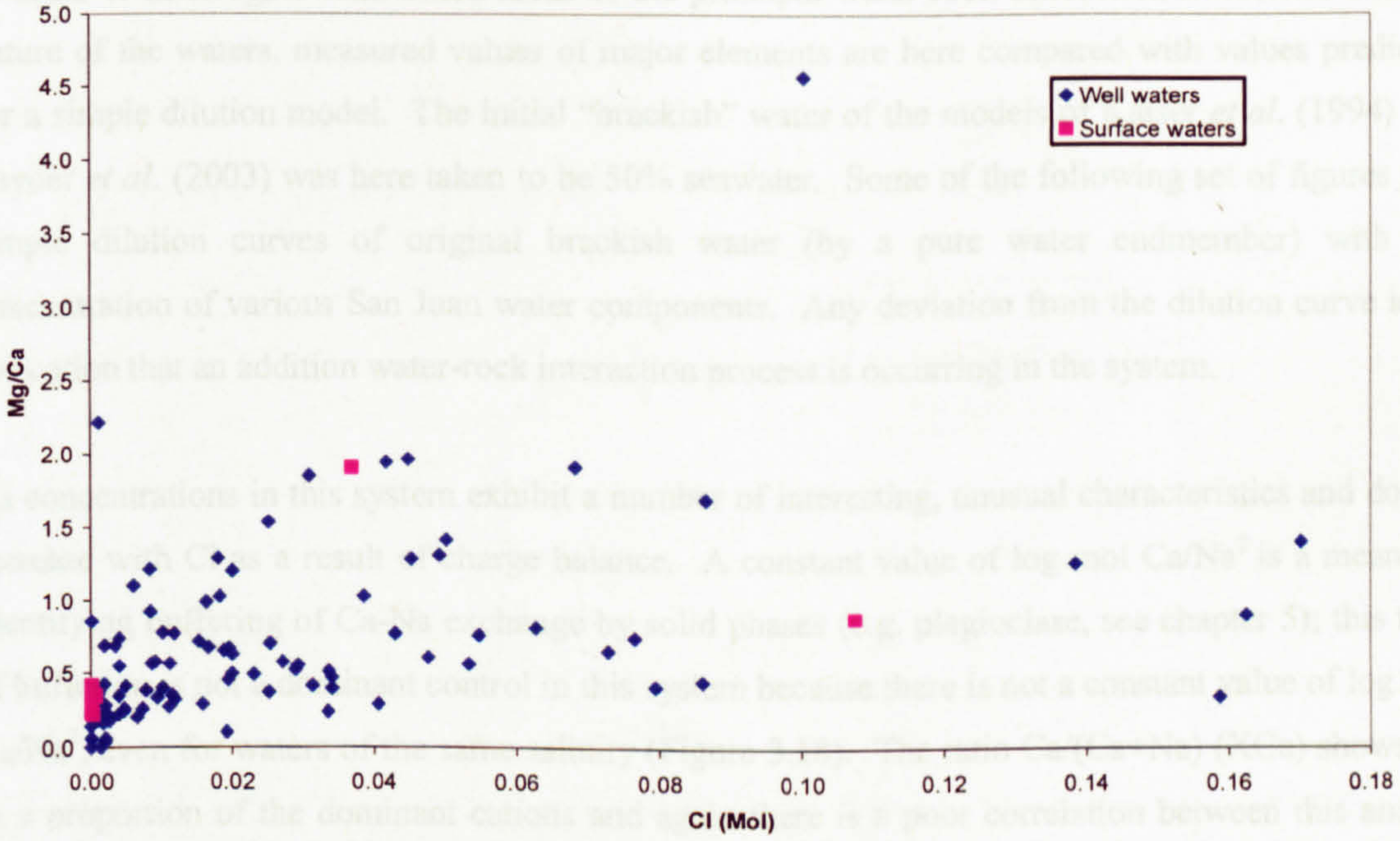

Figure 3.20. There is significant variation in the Mg/Ca ratio with changing Cl concentration, though there is a generally positive correlation suggesting a source of Mg or sink for Ca impacted by increasing Cl concentration

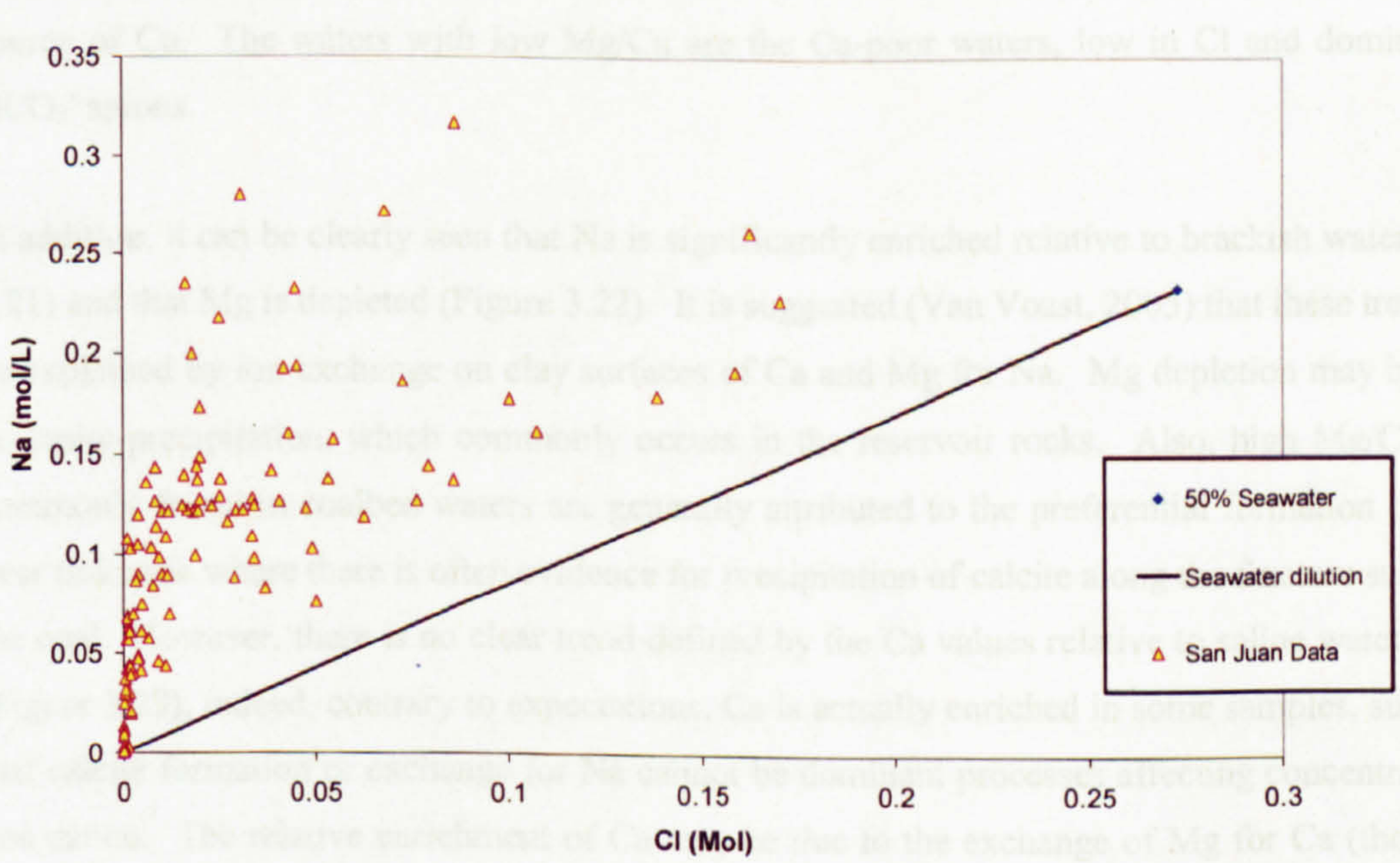

Figure 3.21. Variation in Cl and Na assuming simple dilution of modern seawater with no water-rock interaction, and data from San Juan formation waters. Note higher than predicted levels of Na in the formation waters.

In order to interrogate established ideas of the principal water-rock interaction influences and the nature of the waters, measured values of major elements are here compared with values predicted for a simple dilution model. The initial "brackish" water of the models of Kaiser *et al.* (1994) and Snyder *et al.* (2003) was here taken to be 50% seawater. Some of the following set of figures plot simple dilution curves of original brackish water (by a pure water endmember) with the concentration of various San Juan water components. Any deviation from the dilution curve is an indication that an addition water-rock interaction process is occurring in the system.

Ca concentrations in this system exhibit a number of interesting, unusual characteristics and do not increase with Cl as a result of charge balance. A constant value of log mol Ca/Na^2 is a means of identifying buffering of Ca-Na exchange by solid phases (e.g. plagioclase, see chapter 5); this type of buffering is not a dominant control in this system because there is not a constant value of log mol Ca/Na^2, even for waters of the same salinity (Figure 3.18). The ratio Ca/(Ca+Na) (XCa) shows Ca as a proportion of the dominant cations and again there is a poor correlation between this and Cl concentration, with the highest values in very low salinity surface waters (Figure 3.19). Furthermore, there is significant variation in the Mg/Ca ratio (Figure 3.20), and lower values suggest either that more Mg than Ca has been lost from solution, or that there is an additional source of Ca. The waters with low Mg/Ca are the Ca-poor waters, low in Cl and dominated by HCO_3^- anions.

In addition, it can be clearly seen that Na is significantly enriched relative to brackish water (Figure 3.21) and that Mg is depleted (Figure 3.22). It is suggested (Van Voast, 2005) that these trends may be explained by ion exchange on clay surfaces of Ca and Mg for Na. Mg depletion may be due to dolomite precipitation, which commonly occurs in the reservoir rocks. Also, high Mg/Ca values commonly found in coalbed waters are generally attributed to the preferential formation of calcite over dolomite where there is often evidence for precipitation of calcite along the fracture surfaces of the coal. However, there is no clear trend defined by the Ca values relative to saline water dilution (Figure 3.23), indeed, contrary to expectations, Ca is actually enriched in some samples, suggesting that calcite formation or exchange for Na cannot be dominant processes affecting concentrations of this cation. The relative enrichment of Ca may be due to the exchange of Mg for Ca (though this would result in low Mg/Ca ratios), or as mentioned above, localised calcite dissolution at sites of meteoric water recharge.

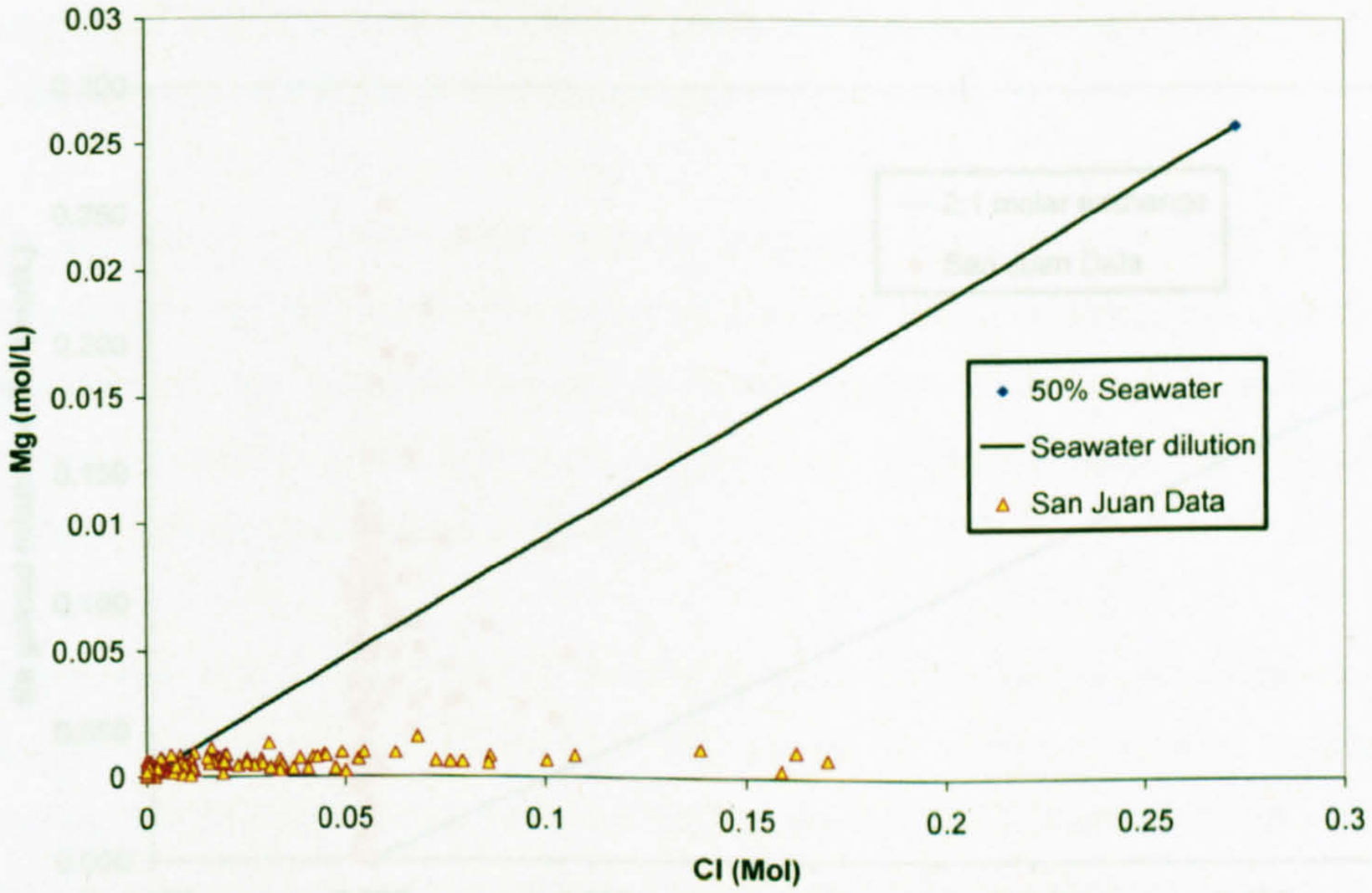

Figure 3.22. Mg data from the San Juan formation waters. Mg is strongly depleted in the formation waters relative to predicted values from a brackish water dilution model

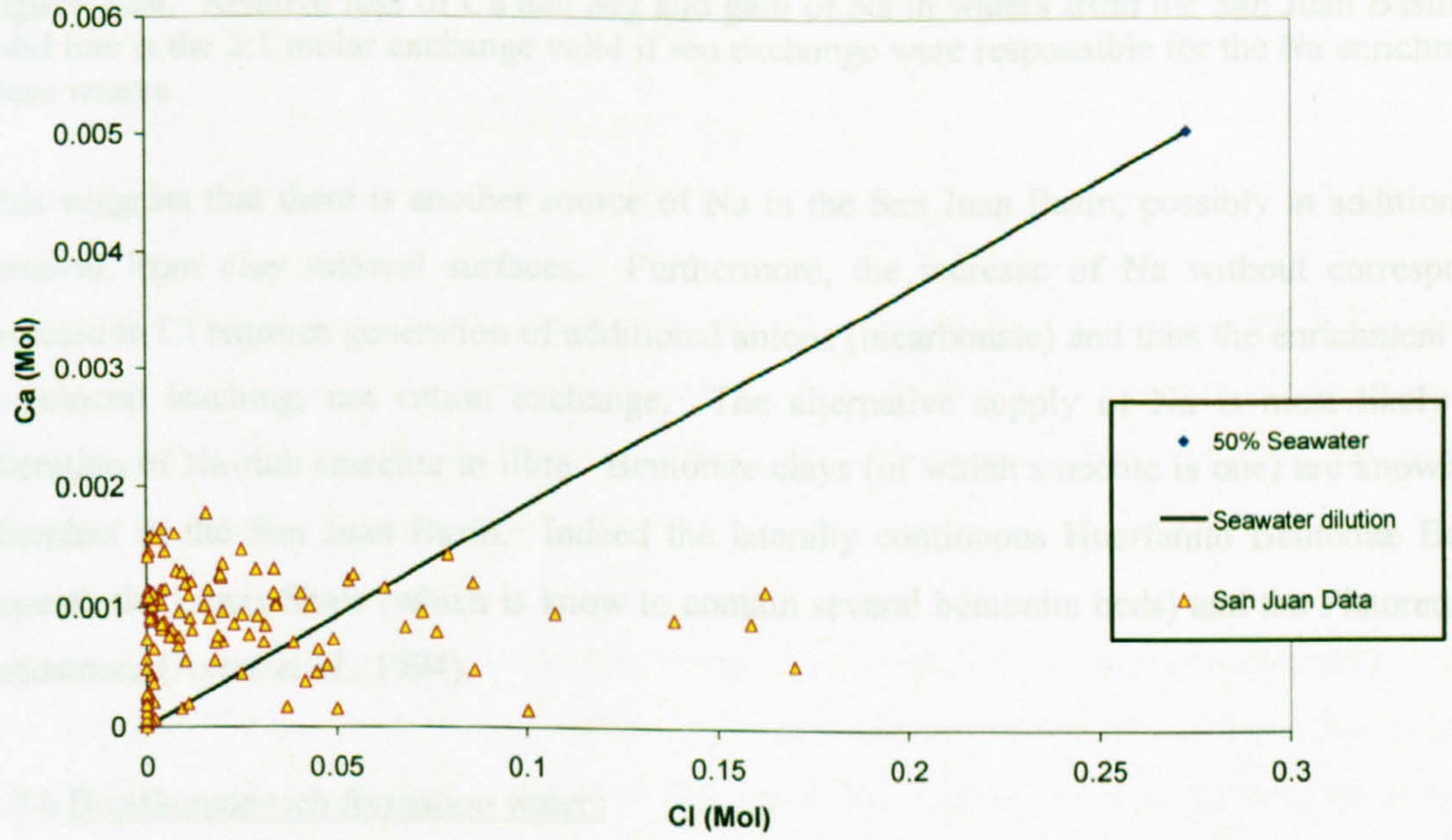

Figure 3.23. Ca data from the San Juan formation waters. Ca varies independently of Cl and hence sometimes appears depleted and sometimes enriched in the formation waters relative, to predicted values from brackish water dilution.

Figure 3.24 shows the predicted trend line for diluted brackish water if equal molar amounts of Ca and Mg were removed from solution and Na added through cation exchange. The data from San Juan all show that far more Na has been gained than Ca and Mg lost, despite the fact that the figure does not account for Ca and Mg lost through precipitation of carbonates.

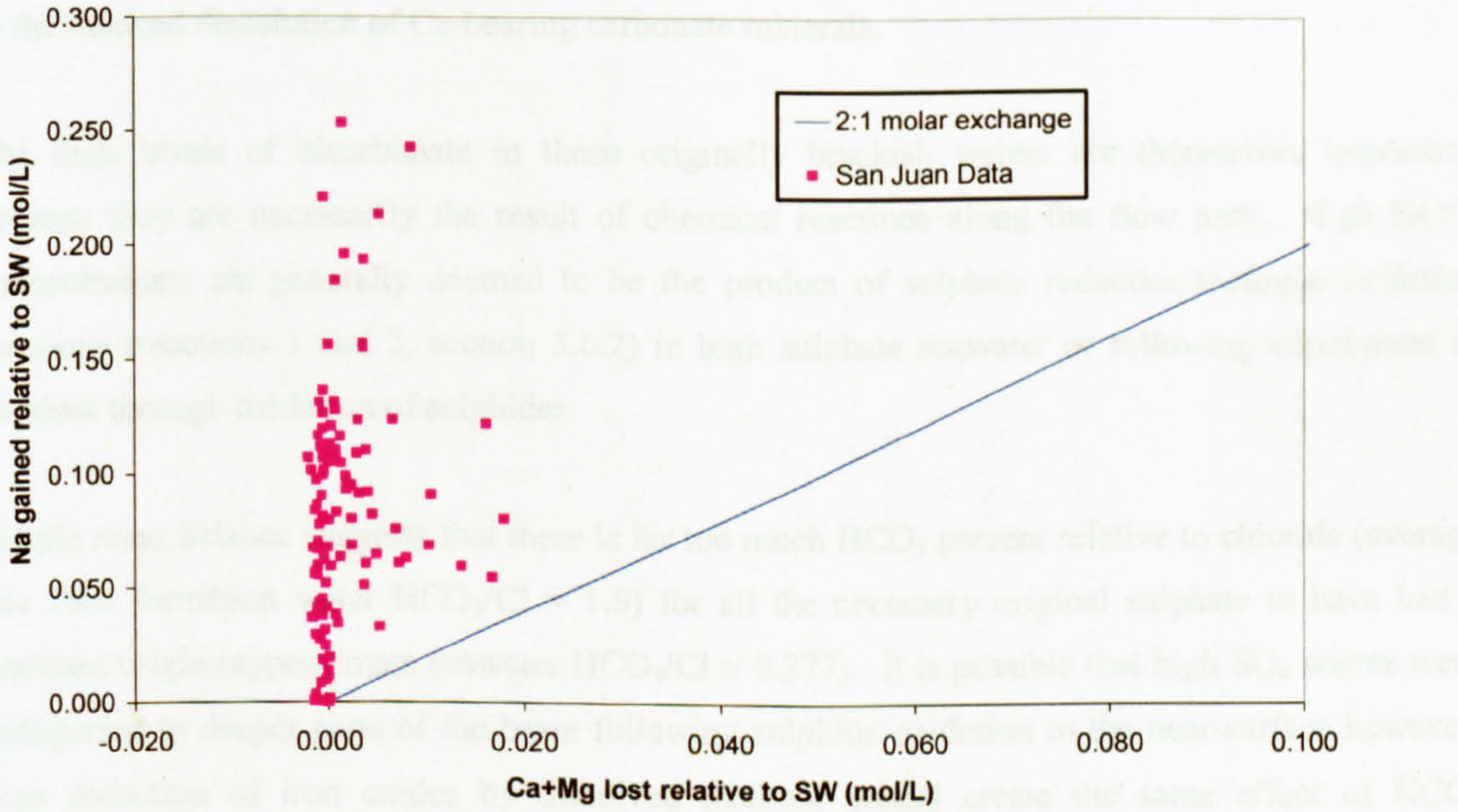

Figure 3.24. Relative loss of Ca and Mg and gain of Na in waters from the San Juan Basin. The solid line is the 2:1 molar exchange valid if ion exchange were responsible for the Na enrichment in these waters

This suggests that there is another source of Na in the San Juan Basin, possibly in addition to its removal from clay mineral surfaces. Furthermore, the increase of Na without corresponding increase in Cl requires generation of additional anions (bicarbonate) and thus the enrichment is due to mineral leaching, not cation exchange. The alternative supply of Na is most likely to be alteration of Na-rich smectite to illite. Bentonite clays (of which smectite is one) are known to be abundant in the San Juan Basin. Indeed the laterally continuous Huerfanito Bentonite Bed lies beneath the Lewis Shale (which is know to contain several bentonite beds) and the Pictured Cliffs sandstones (Ayers *et al.,* 1994).

3.7.6 Bicarbonate-rich formation waters

The low Cl waters are also extremely high in HCO_3. Figure 3.12 showed that at the very lowest salinities bicarbonate is more abundant in solution than chloride. Figures 3.25 and 3.26 show the results of calculating the speciation of 19 representative San Juan water samples at calcite saturation using the geochemical modelling programme, the Geochemists' Workbench. Figure 3.25 indicates that sodium concentration is exclusively related to the amount of bicarbonate present. However, calcium is more associated with bicarbonate at the lowest salinities and with chloride at higher salinities (Figure 3.26). This may be a result of geographical influence, because the lower salinity

waters exist in places where bicarbonate levels are high and Ca concentration is being enriched due to the inferred dissolution of Ca-bearing carbonate minerals.

The high levels of bicarbonate in these originally brackish waters are themselves interesting because they are necessarily the result of chemical reactions along the flow path. High HCO_3 concentrations are generally deemed to be the product of sulphate reduction/methane oxidation reactions (reactions 1 and 2, section 3.6.2) in high sulphate seawater or following enrichment of sulphate through oxidation of sulphides.

Simple mass balance suggests that there is far too much HCO_3 present relative to chloride (average San Juan formation water $HCO_3/Cl = 1.9$) for all the necessary original sulphate to have had a seawater origin (approximate seawater $HCO_3/Cl = 0.277$). It is possible that high SO_4 waters were transported to deeper parts of the basin following sulphide oxidation in the near-surface however, deep reduction of iron oxides by dissolved methane would create the same effect of HCO_3 enrichment:

$$4Fe_2O_3 + CH_4 = 8FeO + HCO_3^- + H^+ + H_2O \qquad (3)$$

$$4Fe_2O_3 + CH_4 = 8FeO + CO_2 + 2H_2O \qquad (4)$$

When sulphate reduction occurs, significant amounts of pyrite might be expected in the reservoir sandstones as a result of the sulphate reduction. In fact, there are only very limited amounts of pyrite present. Oxidation of methane by iron oxide does not produce sulphide so this process is consistent with the lack of pyrite present.

Alternatively, there may be an additional source for the HCO_3. Furthermore, sulphate reduction producing bicarbonate ions does not affect the charge balance of the water. Thus, the increase in Na should be accompanied by a decrease in Ca and Mg, because there is no increase in negative charge. However, this behaviour is not seen. The dissolution of calcite at meteoric recharge points is a potential source of bicarbonate, evidenced by the increase in Ca concentration towards the north-west of the Basin.

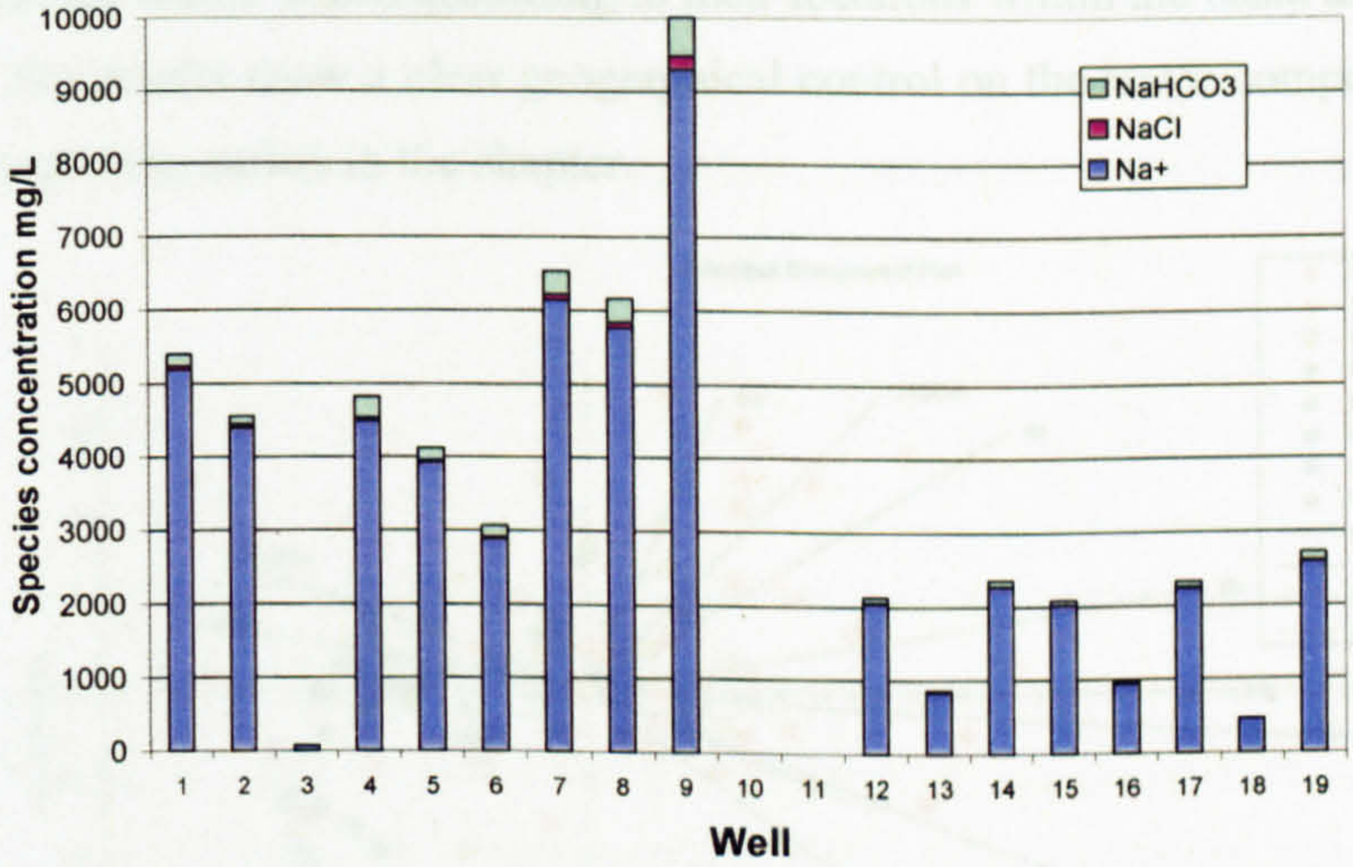

Figure 3.25. Sodium speciation in waters from 19 representative wells in the San Juan Basin, selected for variation in location and Cl content. Excluding Na^+ note the consistent dominance of $NaHCO_3$ rather than NaCl.

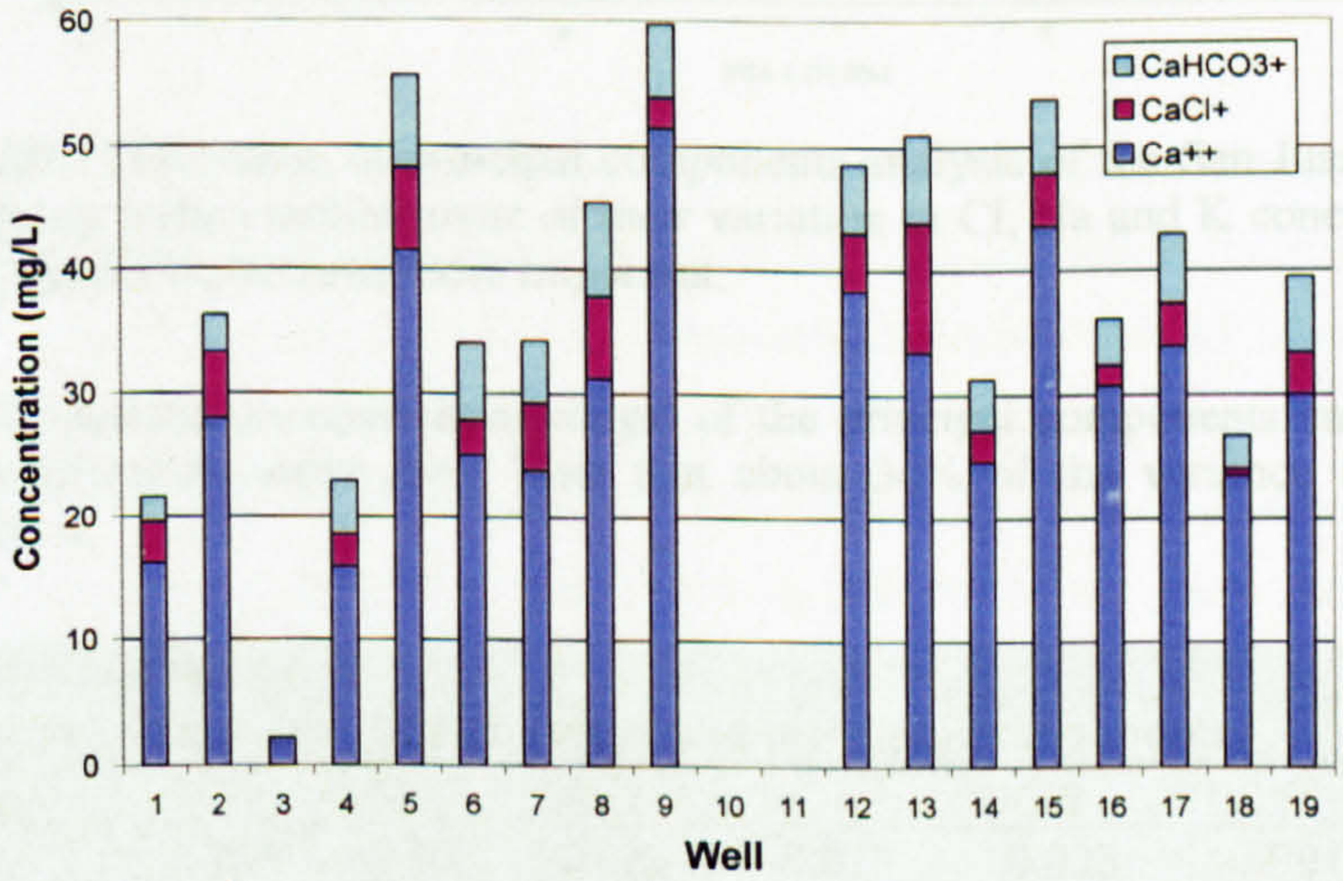

Figure 3.26. Calcium speciation in waters from the same 19 representative wells in the San Juan Basin. Excluding Ca^{2+} note the bimodal importance of $CaHCO_3^+$ and $CaCl^+$

3.7.7 Principal components analysis

In order to further assess the controls on the San Juan formation water compositions, principal components analysis – PCA – (see chapter 5 for a full discussion of the technique) was carried out on the water data. The cause for the majority of variance in the dataset is likely to be the most important aspect of the water chemistry and can be determined by PCA. In this case the data were analysed based on the concentrations of K, Na, Mg, Ca, Sr, Ba, Fe, Mn, Cl, HCO_3 and ratios of XCa, Ca/Mg and Na/K.

The waters are colour coded according to their locations within the basin and Figure 3.27 shows the results. The results show a clear geographical control on the water compositions that supplements the evidence from earlier in the chapter.

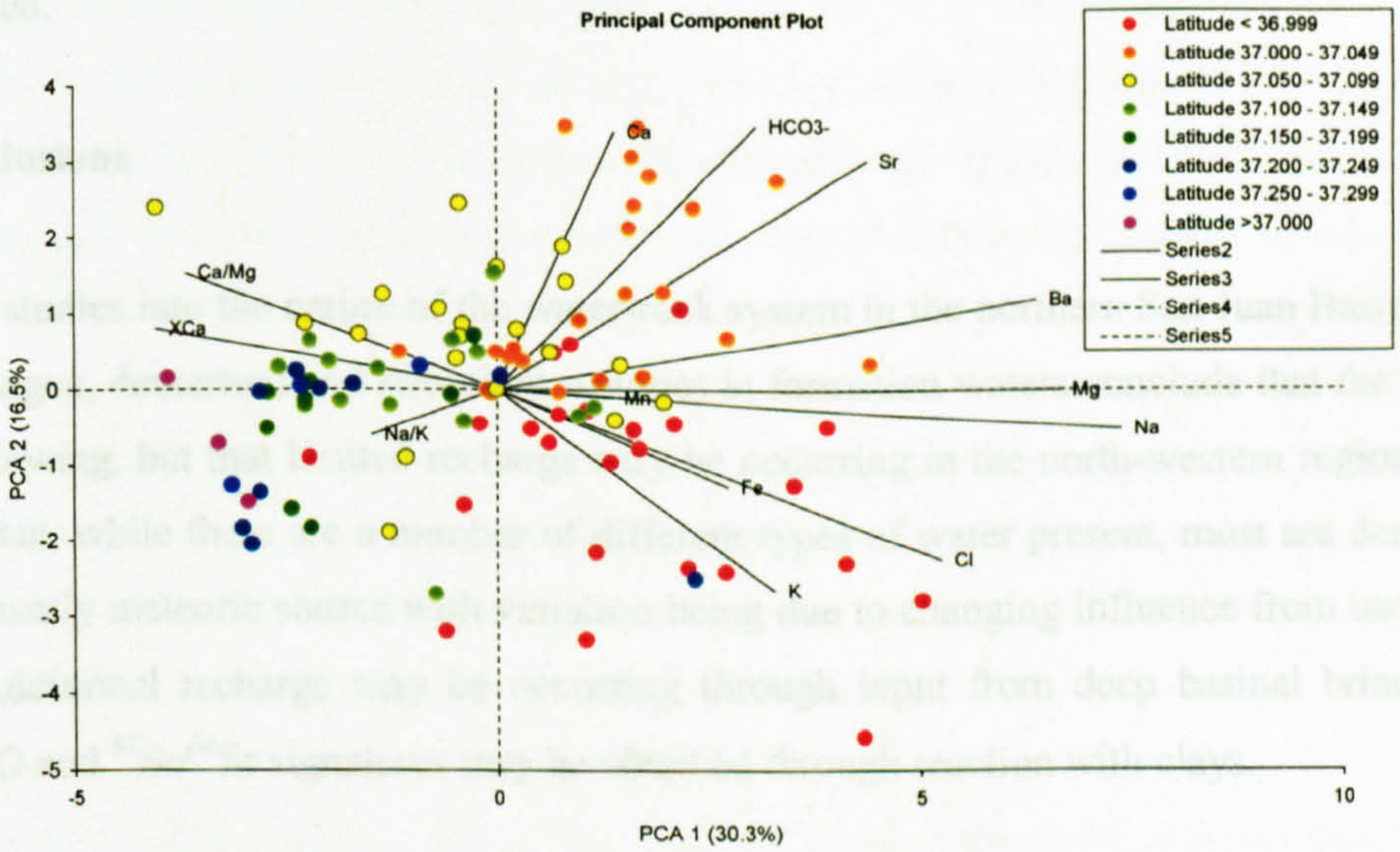

Figure 3.27. The results of principal components analysis of the San Juan formation waters. The most northerly waters exhibit most of their variation in Cl, Na and K concentrations, while further south, HCO_3 and Ca become more important.

Table 3.2. Results (component loadings) of the principal components analysis performed on the San Juan formation water data. Note that about 30% of the variance is explained by the Na concentration.

Component Loadings
(correlations between initial variables and principal components)

Variable	PC 1	PC 2	PC 3	PC 4	PC 5	PC 6
Na	0.928	-0.107	-0.039	-0.078	0.023	-0.091
K	0.410	-0.543	0.085	0.396	0.231	0.037
Mg	0.837	-0.003	-0.356	0.063	-0.108	0.137
Ca	0.174	0.692	-0.132	0.411	0.189	0.061
Sr	0.549	0.617	0.171	-0.033	0.070	0.136
Ba	0.801	0.241	-0.283	-0.061	-0.018	-0.136
Fe	0.341	-0.262	0.413	0.060	-0.677	-0.111
Mn	0.168	-0.022	0.857	0.060	0.071	0.240
Cl	0.660	-0.460	0.199	0.235	0.355	0.125
HCO3-	0.384	0.708	0.336	-0.246	-0.093	0.057
XCa	-0.506	0.161	-0.147	0.479	-0.211	0.549
Ca/Mg	-0.462	0.313	0.337	0.284	0.255	-0.446
Na/K	-0.186	-0.124	0.051	-0.727	0.276	0.301

In addition, the component loadings (Table 3.2) suggest that most of the variance is related to Na and then the alkali earth metals (Ca+Mg) and bicarbonate. Thus, the importance of the excess Na in solution and the dissolution/precipitation/ion exchange reactions controlling Ca and Mg is emphasised.

3.8 Conclusions

Previous studies into the nature of the water-rock system in the northern San Juan Basin, conducted using halogen, deuterium and strontium isotopes in formation waters conclude that the Basin is not throughflowing, but that limited recharge may be occurring in the north-western regions. Isotopes suggest that, while there are a number of different types of water present, most are derived from a predominantly meteoric source with variation being due to changing influence from backshore peat bogs. Additional recharge may be occurring through input from deep basinal brines, although similar δD and $^{87}Sr/^{86}Sr$ signatures may be obtained through reaction with clays.

Isotopes have only limited use when considered independently from other aspects of water chemistry. Typically, formation waters associated with coalbed methane are always thought to be similar, being sodium chloride-bicarbonate dominated and depleted in calcium, magnesium and sulphate. However, there is some chemical variation within the formation waters of the San Juan Basin itself and they have been shown to behave differently from what was expected.
The conservative components of the water, including Cl, can track the dilution of waters and influence of fluid mixing. Study of the dissolved halides alone cannot support or contradict the theory that the waters are of brackish origin, altered by waters flowing in at the northern basin margin and through deep fractures. However, the geographical pattern of lower Cl concentrations towards the north-west of the basin corresponds well with previous hypotheses that this area is experiencing significant meteoric recharge.

The origin of the formation waters in the San Juan Basin is difficult to determine by studying the behaviour of the water components. This is because even at the low temperatures in this system, the chemistry of the waters is dominated by the results of ongoing water-rock reactions which mask any older chemical signature. In particular, the coal present in the reservoir contributes significantly to halogen concentrations, particularly bromide. This means they are not conservative enough to have remained constant through time and therefore cannot be used to identify fluid origins. However, variation in the concentrations of the cations Na, Ca and Mg can provide a useful

picture of the processes occurring. Low values of Ca and Mg and high values of Na have previously been attributed to cation exchange, however a simple mass balance calculation suggests that there is far more Na in the system than can be accounted for by this process. Instead, while ion exchange is probably occurring, the most likely source for the elevated Na concentrations in the San Juan Basin is leaching of the abundant bentonite clay, present in the area as the devitrification product of ash falls. The high Na/Cl ratio is also evidence that Na is being introduced into the system through diagenetic leaching processes, possibly driven by the generation of carbonic acid from coal.

The Ca concentration is not as consistently low as has been previously suggested, in fact it is highly variable. The variability is due to a combination of cation exchange processes and the dissolution of Ca-bearing minerals. The latter process is especially prevalent in the colder meteoric waters in the north-west, as indicated by higher Ca values in this area.

Geochemical modelling and the presence of coal and pyrite in the rocks indicates that the system is reducing. Extremely high bicarbonate concentrations are therefore likely the result of iron oxide and sulphate reduction, however, the lack of pyrite present suggests that the former process is more important. In addition, it is possible that carbonate dissolution at the basin margins contributes to the bicarbonate content of the waters. The introduction of large amounts of bicarbonate to the system affects the behaviour of the cations present and the fluids contain a significant proportion of $NaHCO_3$ and $CaHCO_3^+$.

The importance of low salinity-high bicarbonate waters as part of a continuous global trend in water compositions cannot be overestimated and will be examined in more detail in Chapter 5.

4. CASE STUDY 2: THE MILLER OIL FIELD, NORTH SEA

4.1 Introduction

Formation waters in petroleum reservoirs could potentially have residence times that are significant on geological timescales of tens to hundreds of millions of years, or are relatively brief at tens of thousands of years. Although fluid migration in the subsurface can and does occur, flow is believed to happen slowly enough to allow for the equilibration of waters with their host rocks (Hanor, 1994). When hydrocarbon resources are exploited, changes are induced in the system on a timescale that can be as short as a few days. The impact of human activity on such systems has huge implications for the efficiency of the industrial processes, for the environment and for our understanding of the nature of fluid-rock interaction on geological and human timescales.

The following chapter is a case study of a particular oil field in the North Sea, Miller, which can provide an insight into processes occurring on a human timescale. Using an extensive dataset of produced water chemical analyses, integrated with a detailed mineralogical study of the reservoir sandstones, I illustrate the types of fluid-rock and fluid-fluid interaction that occur in a typical North Sea oil field in response to the production and injection over a period of 14 years.

4.2 Background to the Miller field

The Miller Oil Field covers an area of 45km^2 in the South Viking Graben in the North Sea, and is situated in blocks 16/7b and 16/8b (Figure 4.1). First oil was produced in 1992, with estimated recoverable reserves at the time of 240MMbbl (Warren and Smalley, 1994; Marchand, 2001). The temperature is relatively high (120°C) and a wide range of elements occur in the formation water at significant concentrations (Warren and Smalley, 1994). Hydrocarbon production is supported by water/gas injection wells. Waterflooding was initiated shortly after first oil and has continued to date. This production strategy has created some problems in relation to the formation of barite scale. The oilfield is one of several whose main producing reservoir is contained within the Upper Jurassic Brae Formation sandstones at the margin of the Viking Graben; the others include South Brae, Central Brae, North Brae, East Brae and Kingfisher.

In the past, several different aspects of the diagenesis of the Miller field have been studied (e.g. Gluyas *et* al., 2000; Marchand, 2001). The origin of quartz cements has been of particular scientific interest (e.g. Gluyas *et al.*, 2000). The problem of barite scaling has also been subject

to a great deal of scrutiny. In this study a number of different data analysis and mineralogical investigation methods are brought together in order to understand fully the Miller field in its complexity.

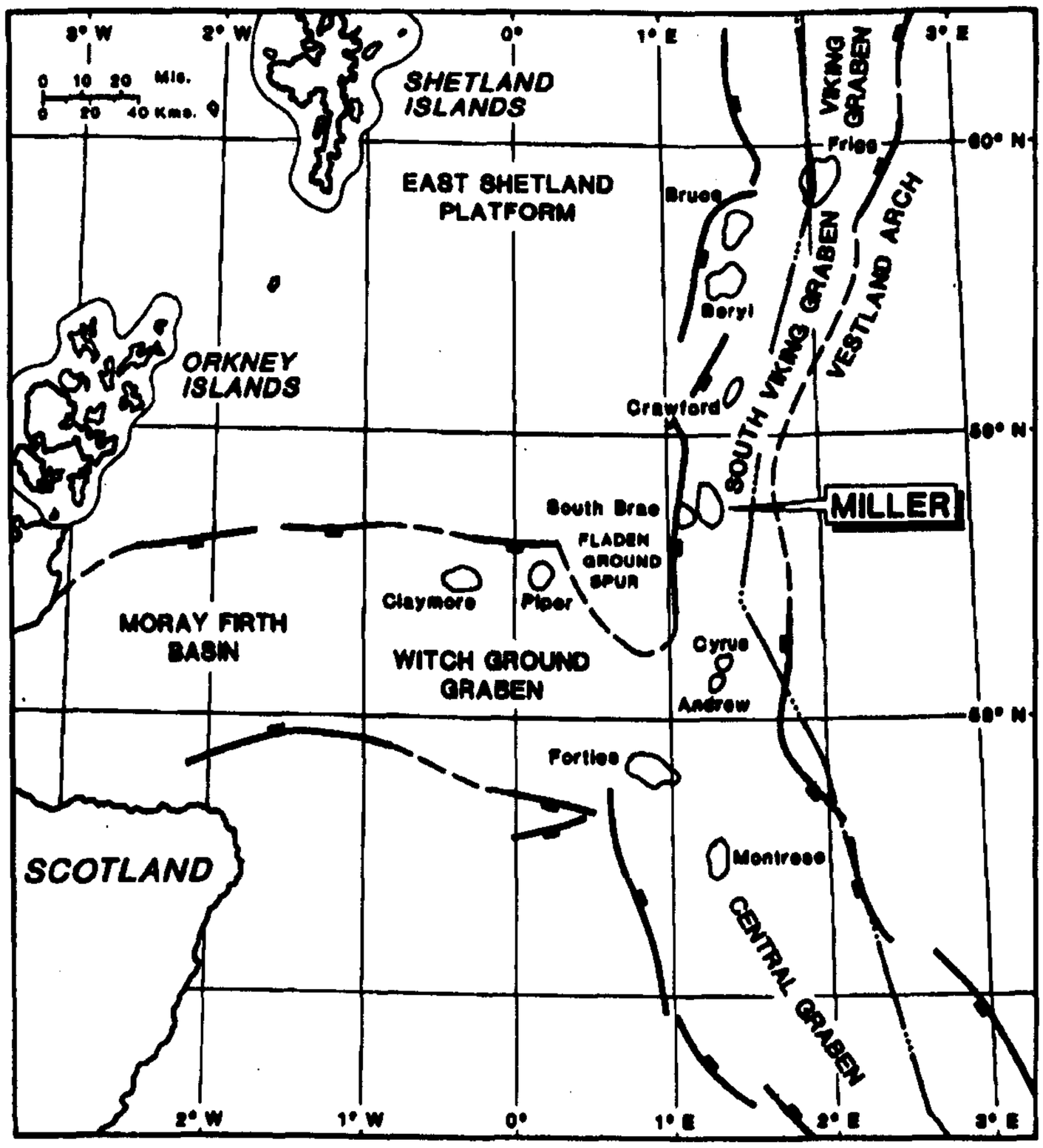

Figure 4.1. Location of the Miller field in the North Sea

4.2.1 Stratigraphy

The Miller reservoir rocks are part of the Upper Jurassic Brae Formation at the western margin of the South Viking Graben at a depth of c. 4km (Prosser, *et al.*, 1995; Marchand, 2001). The Viking Graben is a North-South trending half-graben that is fault bounded to the west against the Devonian Fladen Ground Spur basement. Of the more than 3km of Late Jurassic and Cretaceous sediments that are estimated to be at the graben margin, approximately half form the Brae Formation.

There are three chronostratigraphic members of the Brae Formation, that also broadly relate to three lithostratigraphic reservoir units. The three units range in age from Oxfordian to Volgian (157-143Ma), with Unit 3 comprising the lowermost unit of the Formation. On a regional scale the Formation is both overlain and underlain by and interdigitates with the Kimmeridge Clay Formation which is both source and seal for the oil accumulation (Garland, 1993; Prosser *et al.*,

1995; Gluyas *et al.*, 2000). In the south, north and northwest, stratigraphic pinchout of the submarine fan sequence into the Kimmeridge Clay provides the trapping mechanism (Prosser *et al.*, 1995).

In Miller the Brae Formation Unit 2 sandstones form the reservoir rocks (Garland, 1993). The sands in this area are medium grained, finer than in the Brae Fields to the west. There are five major lithological facies in the Brae area, three of which are represented in the Miller Field. In general the reservoir is dominated by clean, fine- to medium-grained, well sorted quartzose sandstones (Garland, 1993). The first of the three facies is a medium-thick bedded sandstone, with beds 10 to>30cm thick of clean, fine- to very coarse-grained sandstone, in places containing granules and small pebbles. The second lithofacies consists of thin alternating beds of sandstone and mudstone which are up to 20cm and 0.1-5cm thick respectively. Sands are fine- to medium-grained and are tabular or lenticular and bed boundaries are generally sharp. The final facies comprises isolated dark grey-black, micaceous, carbonaceous mudstone layers of between 20 and 50cm in thickness. The three lithofacies described correspond to Facies 3 to 5 of the five major facies in the Brae area (Lithofacies A-C as described by Prosser *et al.*, 1995). The best quality reservoir sandstones in the Miller Field are the massive sandstones, which have a paucity of clearly defined sedimentary structures. Poorer quality interbedded sands and muds typically separate out the more massive units and are potential barriers to vertical fluid flow (Prosser *et al.*, 1995).

4.2.2 Depositional Setting

Miller represents the distal part of an extensive system of tectonically controlled sub-marine fans. The Fladen Ground Spur in the west was the source of the sediment and at the time was a shallow marine to sub-aerial shelf area (Garland, 1993). The main reservoir interval in Miller, situated further away from the foot of the fault scarp, accumulated as a lobe-shaped fan and received finer grained sediments than the proximal areas of the fan (e.g. East, North, South and Central Brae Fields). The thickly bedded sands of the facies described above correspond to high density turbidite currents; the interbedded sands and muds represent hemipelagic settling between turbidity flows in relatively quiescent areas of the mid- to outer-fan or inter-channel areas (Prosser *et al.*, 1995; Gluyas *et al.*, 2000); and the laminated muds also correspond to hemipelagic settling with rare sand laminae and graded silts deposited from very dilute turbidity flows.

4.2.3 Porosity and permeability

In the North Sea hydrocarbon provinces, porosity in most sandstone reservoirs appears to follow a linear porosity versus depth trend. Overall, a regional North Sea porosity loss gradient of

about 8% provides a good estimate. Miller exhibits exceptionally high porosities of up to 22% which deviate significantly from the expected values of between 12 and 13% porosity. The oil leg in the Miller Field has a higher average porosity value (19±1.4%) than the water leg (14±0.5%) which some authors suggest is indicative of the oil filling inhibiting quartz cementation (Emery *et al.*, 1993; Marchand *et al.*, 2000).

Pressure surveys have identified permeability baffles, expressed as "steps" in the pressure gradient (Garland, 1993). The highest permeabilities occur within clean, medium grained massive sandstones and the lowest within the shaly, heterolithic lithofacies (A or 2). It is important to note that most of the Miller lithofacies contain spatial variability at the cm-scale (i.e. caused by laminations) that will cause permeability variation that cannot be accounted for in a reservoir simulation model: even the massive sandstones are not homogeneous with respect to permeability. It may also be that lateral correlation of permeability may be poor and hence high permeability conduits are unlikely to be laterally continuous over large distances (Prosser *et al.*, 1995).

4.2.4 Mineralogy and Reservoir Sandstone Composition

The Brae reservoir within Miller is classified in the literature as a quartz arenite to subarkose and sublith-arenite (Marchand, 2001; Garland, 1993). Quartz and polycrystalline quartz (including chert) typically form about 90% of the detrital framework in the Unit 2 reservoir. Detrital clay is present in the rock, though its abundance varies significantly according to the lithofacies. Where it is present, detrital clay forms around 3% of the rock volume, however, it can be completely absent in some of the thickly bedded sands. Rock fragments are also present in significant quantities, (up to 6%) and are most commonly comprised of siltstone, and mudstone clasts. Potassium feldspar forms 1-2 % of the rock (Gluyas *et al.*, 2000; Marchand, 2001).

Analysis of several samples from varying depths demonstrate that the Brae Formation is composed predominantly of quartz, both detrital and authigenic. Figure 4.2 presents two views of samples from different depths in the same well and it is immediately evident that the deeper sample (B, P sand) has less porosity than the shallower sample (A, Unit 1).

In accordance with the literature, an SEM study of the rocks revealed that the mineralogy of the Brae Formation in Miller is very simple and the main other mineral phases present are K-feldspar, calcite, kaolinite, illite and pyrite. There was no evidence of any plagioclase feldspar at all. Porosity varies between ~ 11 % in areas with a high proportion of overgrowths to > 17 % in areas with very few quartz overgrowths. In a number of samples large secondary pore spaces

are present, formed from the dissolution of individual mineral grains (Figure 4.3.A). Pyrite occurs as authigenic framboids (Figure 4.3.A) as well as in relatively large masses in pore spaces and replacing other minerals (Figure 4.3.G).

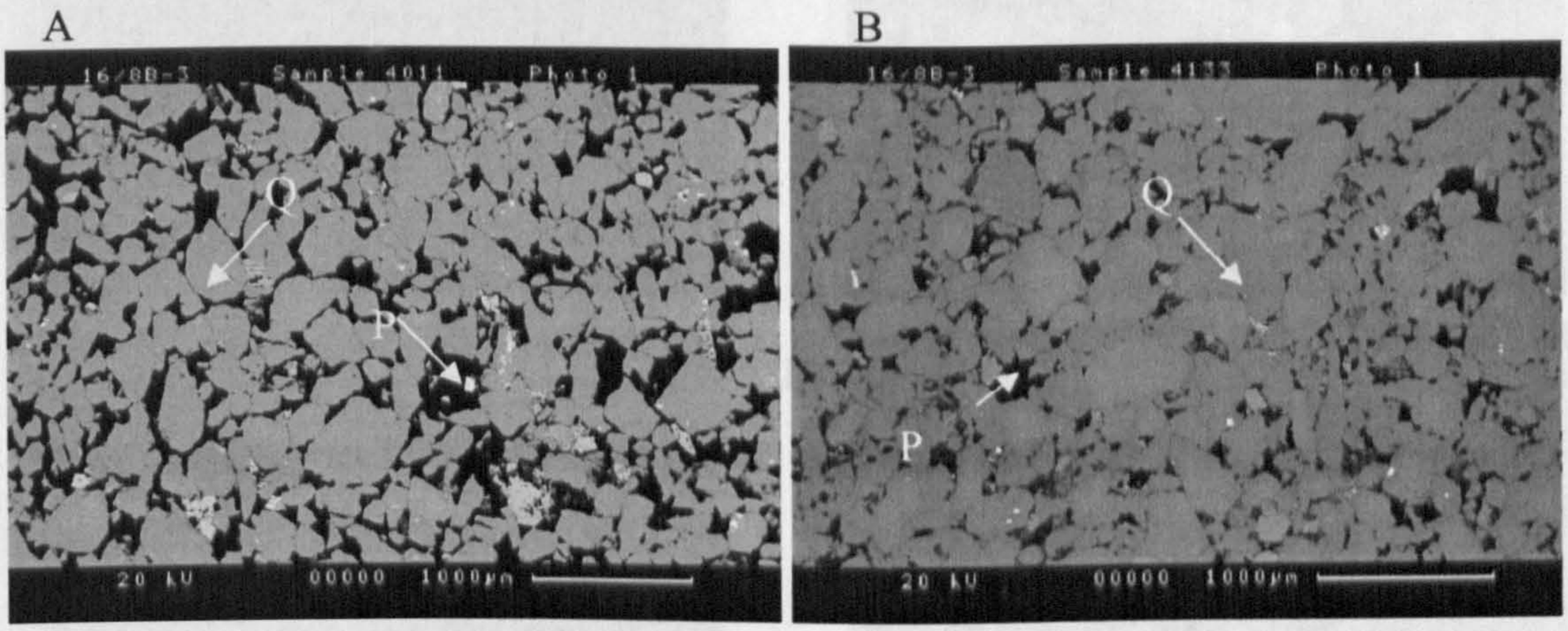

Figure 4.2. SEM image of general mineralogy in well 16/8B-3 at: (A) 4011 m and (B) 4133 m. Note smaller pore spaces in deeper sample. P = pore space, Q = quartz

K-feldspar makes up between 1 and 5 % of the rock and is formed from both detrital and authigenic grains (Figure 4.3.A and B). Early circulation of meteoric water in sandstones will often result in feldspar dissolution during shallow burial (20-55°C), though complete dissolution is not thought to occur below 130°C (Glassman, 1992). Hence, much of the K-feldspar is partially (or fully) dissolved but some grains remain completely intact (Figures 4.3.B and 4.5.D). A portion of the large secondary pore spaces may have been formed through dissolution of K-feldspar or calcite. Kaolinite occurs as detrital grains and authigenic pore-filling material, and in both cases has a fibrous morphology and is consistently partially illitised (Figures 4.3.C, D and 4.5.E and F). Kaolinite is often, but not always, associated with K-feldspar, because at moderate temperatures (<90-100°C) K-feldspar is frequently transformed to kaolinite thereby producing silica (Worden and Morad, 2000). Authigenic kaolinite is also occasionally found overgrown by authigenic quartz on the surface of detrital grains (Figure 4.3.E), indicating the two phases were precipitating at the same time.

Illite is either precipitated in an open system through leaching of K-feldspar, or within a closed system through reaction between K-feldspar and kaolinite as shown in chapter 2 (Chuhan *et al.*, 2001) and the rate of precipitation increases with depth on approaching temperatures of 120-140°C (Bjørlykke, 1996). As the rate of illite precipitation increases, dissolution of kaolinite and smectite and precipitation of illite will remove K from solution and the K concentration may fall below that which represents equilibrium with K-feldspar. Sometimes the formation of quartz and kaolinite/illite is accompanied by the co-precipitation of carbonate cements (Worden and Morad, 2000).

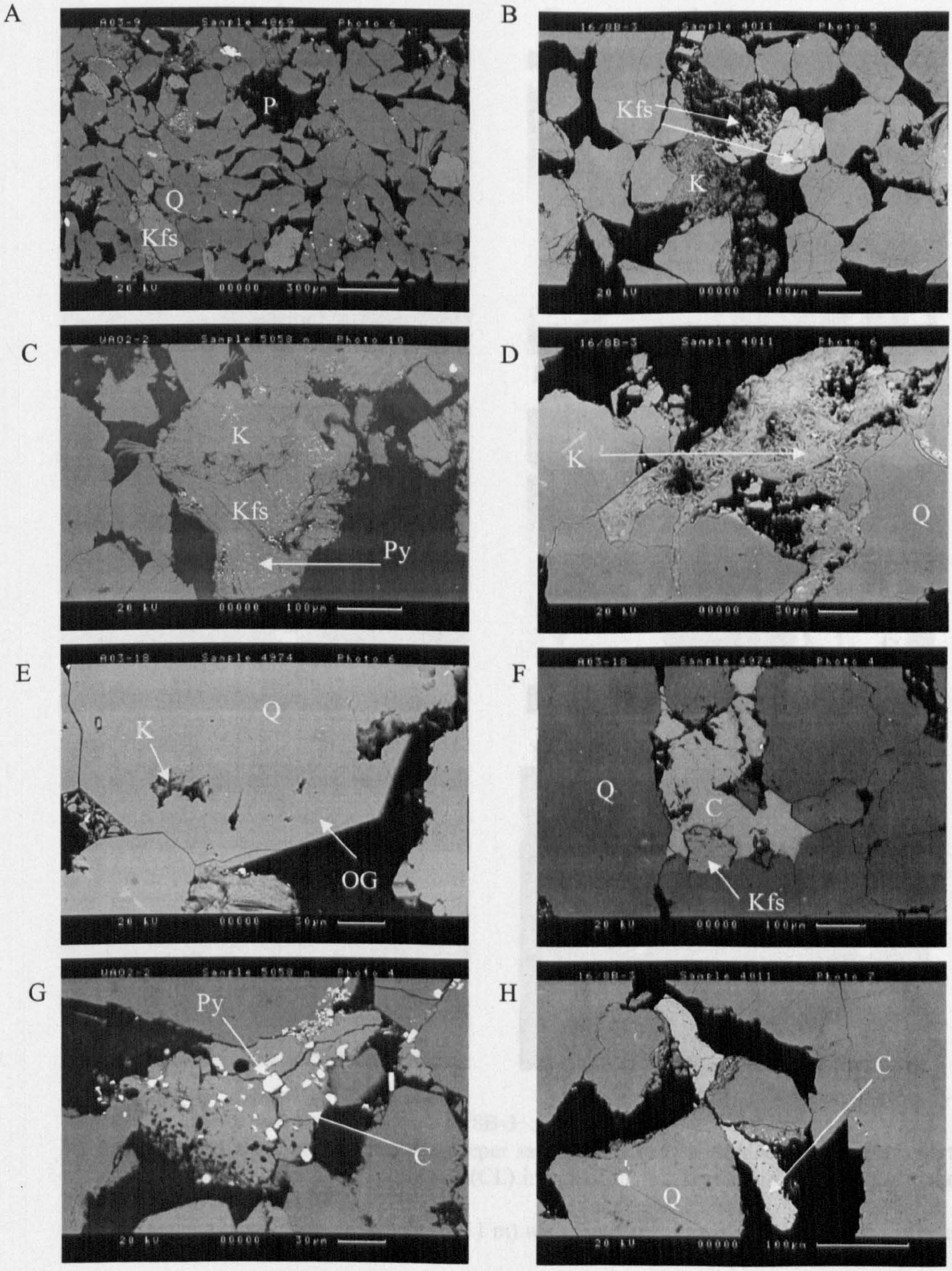

Figure 4.3. Backscatter electron SEM (BSE) images of thin sections from Miller. A) (A03) Quartz (Q) dominates the mineralogy, note large pore spaces (P) resulting from dissolution of K-feldspar (Kfs) or calcite, B) (16/8B-3) preferential dissolution of some K-feldspar grains (Kfs) over others, note association of dissolving K-feldspar and kaolinite (K), C) (A02) and D) (16/8B-3) (detrital and authigenic illitised kaolinite (K), E) (A03) kaolinite trapped by quartz overgrowth (OG) indicating coincidental precipitation, F) (A03), G) (A02) and H) (16/8B-3) varying growth morphologies of calcite (C) with pyrite (Py) in places and sometimes partially dissolved.

A

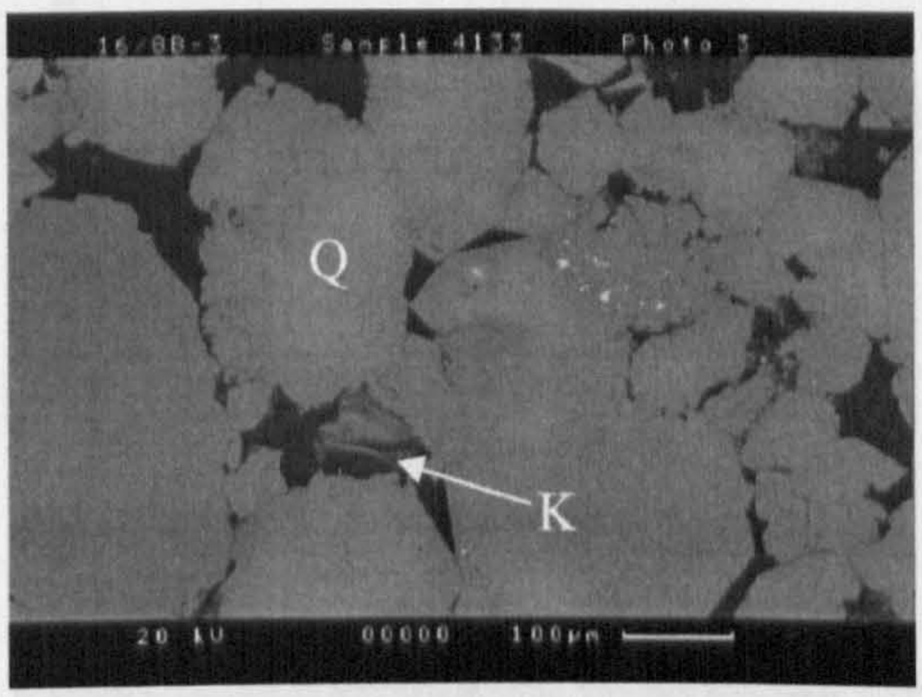

B

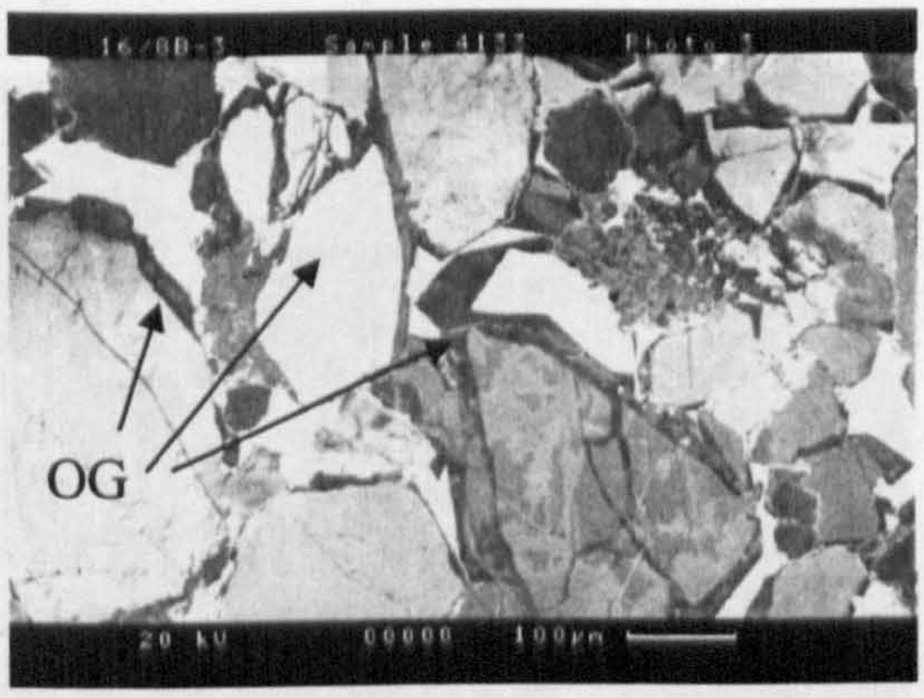

C

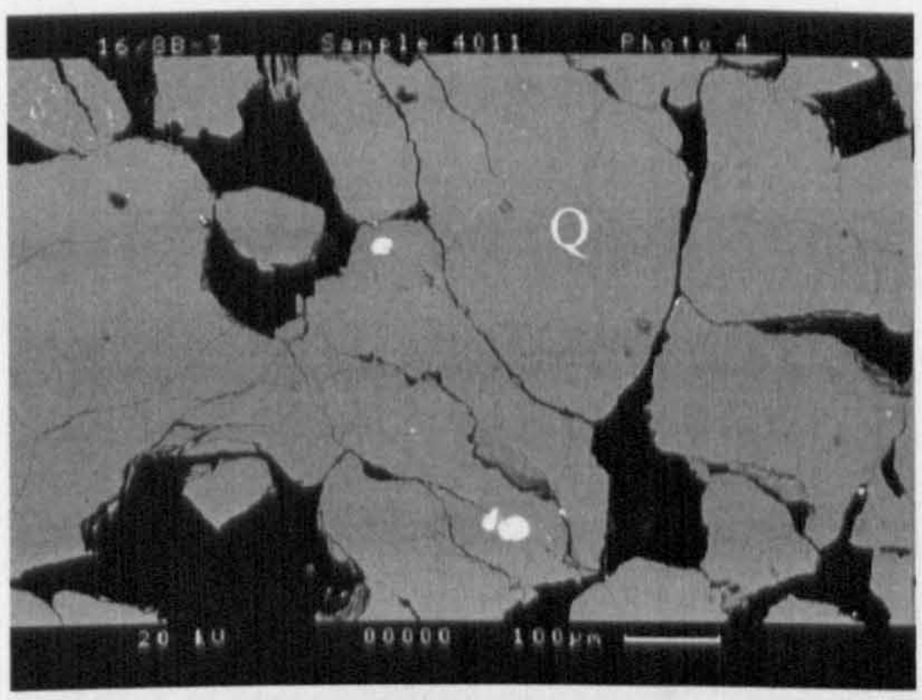

D

E

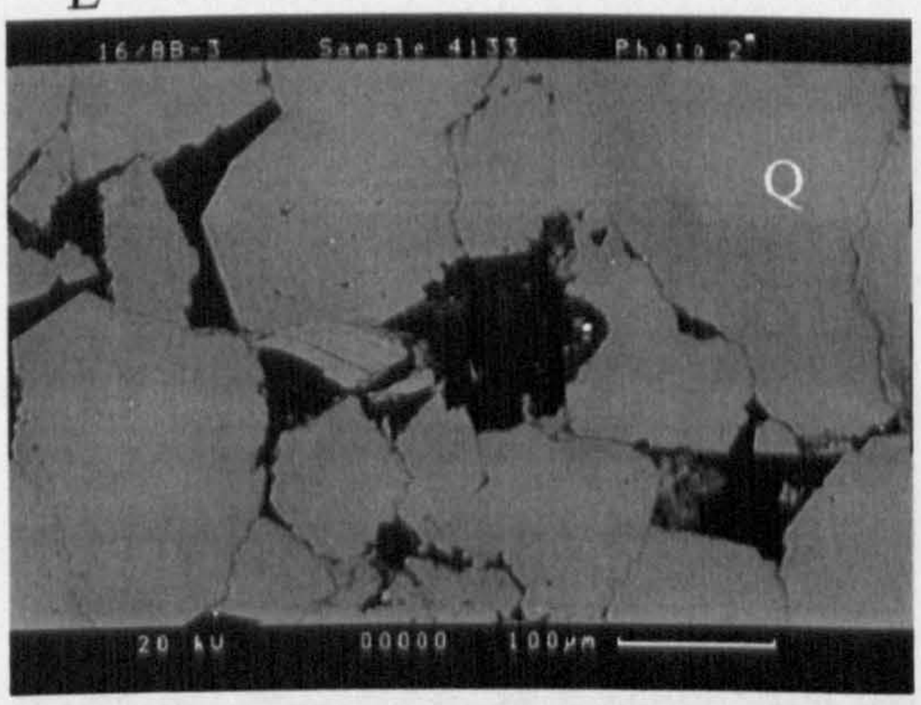

F

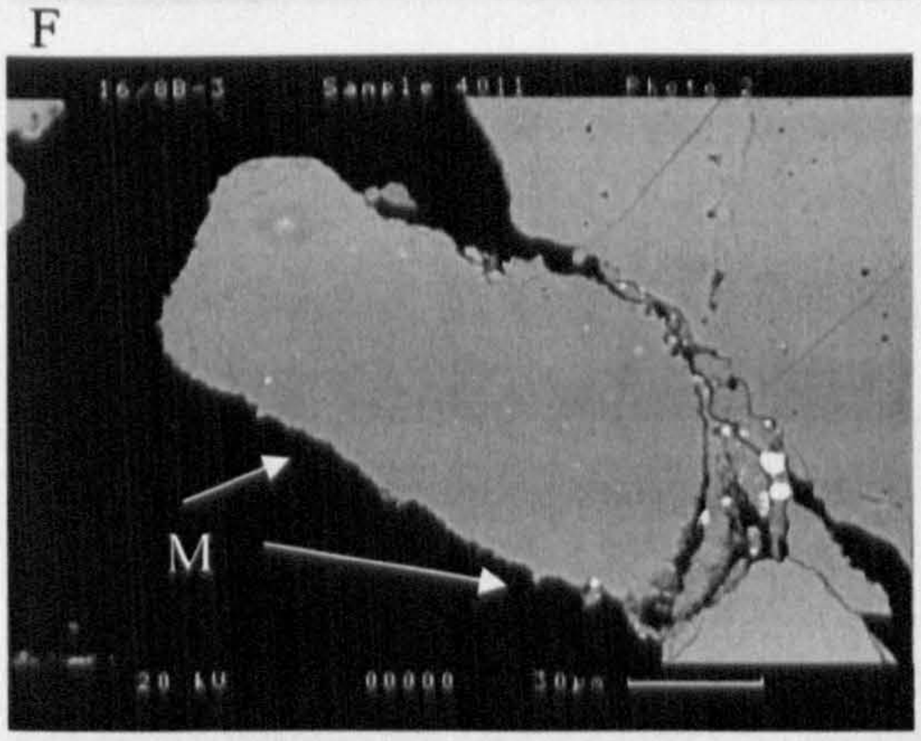

Figure 4.4. Quartz overgrowths in well 16/8B-3
A) Backscattered electron image of the deeper sample (4133 m) with large amounts of quartz overgrowths and, B) cathodoluminescence (CL) image of the same area highlighting the darker quartz of the overgrowths (OG)
C) BSE image of the shallower sample (4011 m) with fewer overgrowths and, B) a CL image of the same area
E) Deeper sample with significant overgrowths and little evidence of microcrystalline quartz
F) Shallower sample exhibiting the characteristic "furry" texture of microcrystalline quartz coated quartz grains (M).

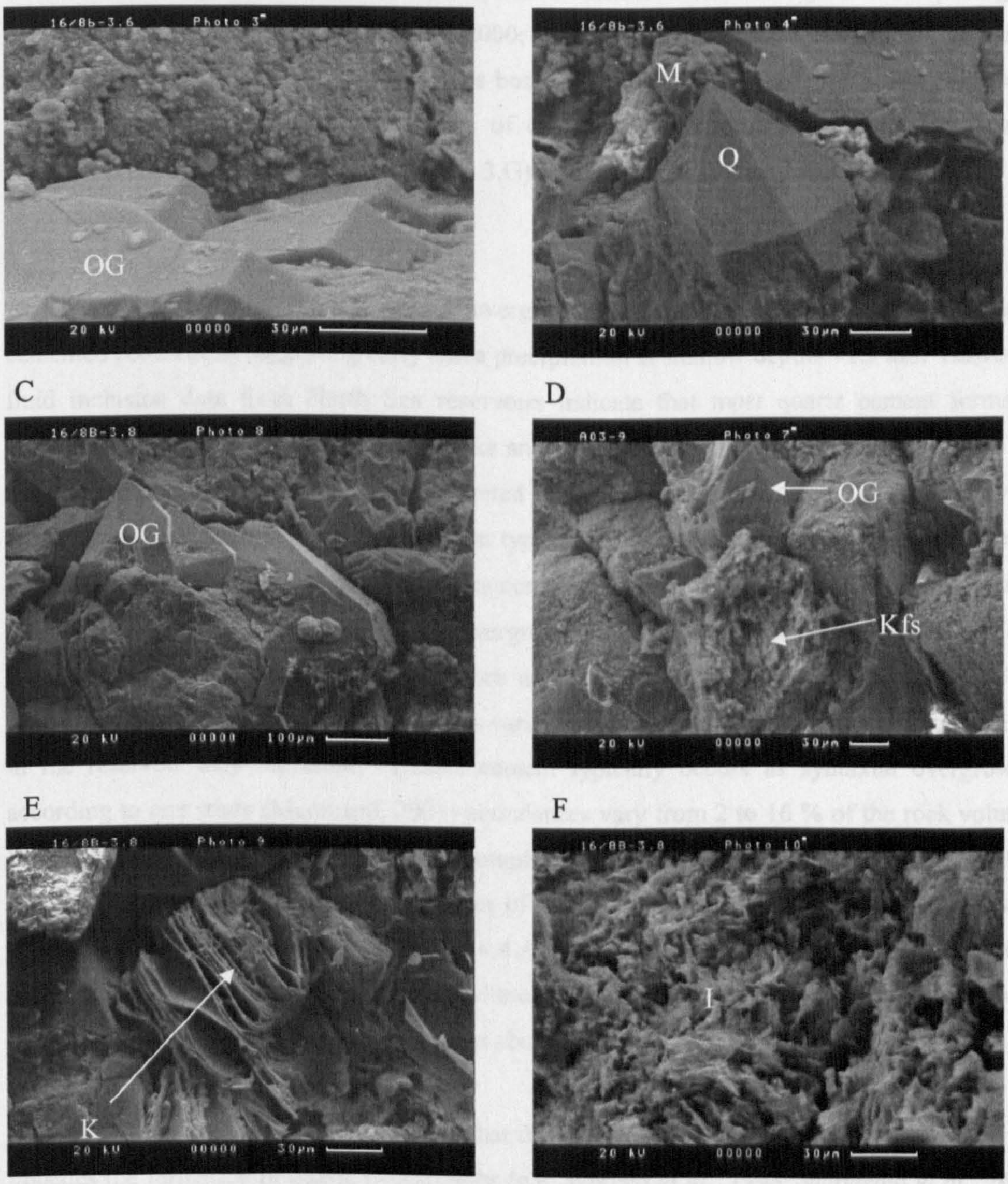

Figure 4.5. Secondary electron images of broken surfaces of the Miller samples, highlighting features illustrated in Figures 4.3 and 4.4.

A) (16/8B-3) Isolated euhedral quartz overgrowth (OG) surrounded by microcrystalline quartz (M)

B) (16/8B-3) Initially well formed quartz crystal whose continued growth is inhibited by the presence of microcrystalline quartz.

C) (16/8B-3) More abundant quartz overgrowth in the deeper sample

D) (A03) Partially dissolved K-feldspar grain (Kfs), note microcrystalline quartz on mineral surfaces

E) (16/8B-3) Platey kaolinite (K) in a pore space

F) (16/8B-3) Fibrous illite (I), altered from kaolinite

Authigenic calcite forms about 0.5 – 2 % of the rock and was the first to form at relatively shallow burial depths. Calcite cement exhibits a number of different growth morphologies, including concretionary masses (Gluyas, 2000; Marchand, 2001) (4.3.F and H) and generally acts as a pore filling cement. It overgrows both original detrital quartz grains and those with quartz overgrowths indicating two stages of calcite precipitation. Calcite in many places exhibits evidence of dissolution (Figure 4.3.G) and its removal may have contributed to the large secondary pore spaces.

According to Marchand (2001) quartz overgrowths have been observed in early calcite cemented concretions suggesting early silica precipitation at shallow depths <1.5 km. However, fluid inclusion data from North Sea reservoirs indicate that most quartz cement forms at temperatures exceeding 90-100°C (Bjørlykke and Egeberg, 1993; Oelkers *et al.*, 1996), and the main phase of quartz cementation is interpreted to have occurred at relatively deep burial (>2.5 km). Sandstones buried to less than 2.7 km typically have negligible quartz cement (Fisher *et al.*, 2000), indicating that the extent of silica cementation increases with depth and temperature (Oelkers *et al.*, 1996). Angular quartz overgrowths are present in all samples studied (e.g. Figures 4.5.A - C), however they are more abundant in some places than in others. The proportion of authigenic quartz overgrowths varies between samples according to which horizon in the reservoir they represent. Quartz cement typically occurs as syntaxial overgrowths according to one study (Marchand, 2001) abundances vary from 2 to 16 % of the rock volume. Figure 4.4 shows BSE and CL images of samples from different depths in well 16/8b-3, while Figure 4.5 shows secondary electron images of the broken sample surfaces. The sample with abundant quartz overgrowths (Figures 4.4.A, B and 4.5.C) contains only very little microcrystalline quartz (Figure 4.4.E), whereas the sample with few quartz overgrowths (Figures 4.4. C, D and 4.5.A and B) contains abundant microcrystalline quartz (Figure 4.4.F).

Several authors in the past have suggested that the migration of hydrocarbons into a porous rock impedes the formation of quartz overgrowths (e.g. Worden *et al.*, 1998; Marchand *et al.*, 2000, 2001, 2002). Marchand (2000) suggested that areas with high porosity preservation in Miller are due to impedance of quartz cementation by early emplacement of hydrocarbons. This theory has been questioned by several Norwegian authors, including Aase and Walderhaug (2005). They suggest instead that variable quartz cementation and porosity distribution in the reservoir is mainly controlled by the amount of coatings, including microcrystalline quartz, on the quartz grains. Evidence from this brief study presented here could support this hypothesis, although the evidence is not conclusive and the microcrystalline quartz may be a result of the presence of oil i.e. an effect rather than a cause. Microcrystalline quartz is thought to be derived

from sponge spicules. The random orientations of the small crystallites interfere with the formation of normal quartz overgrowths (Bloch *et al.*, 2002).

Table 4.1. Suggested paragenetic sequence of diagenetic events in the Brae Formation sandstones using data obtained from direct observation of rock samples and from the literature.

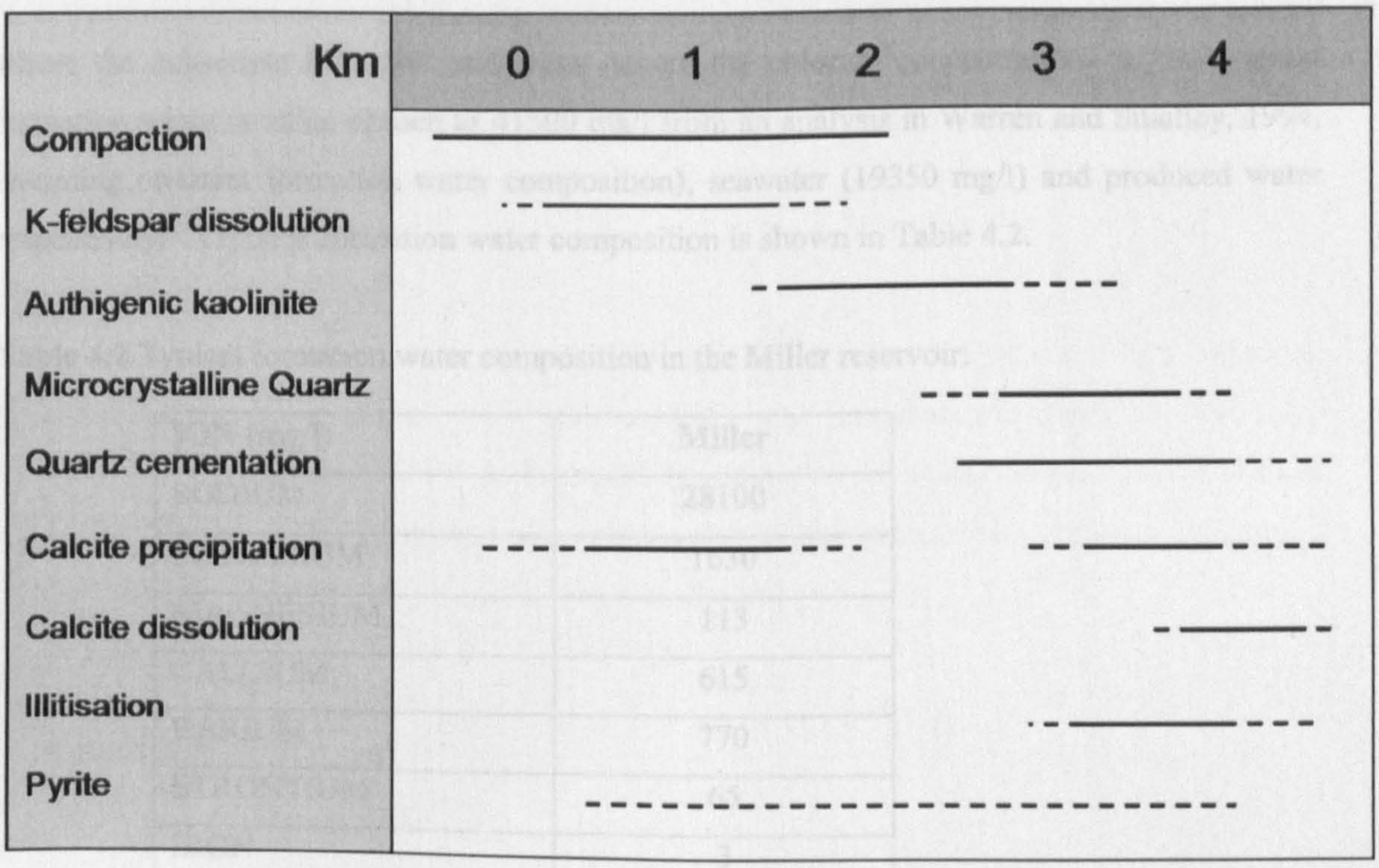

4.3 Introduction to dataset and methods

The produced water from each well in Miller was sampled and analysed on an almost daily basis for approximately 10 years, for major cations, anions and transition metals, and this data was made available for this project by BP. The main aim of this intensive sampling strategy was to track the progress of injected seawater through the reservoir and mitigate the effects of barite scaling due to water mixing. The results of a separate study into the physical nature of water mixing in the Miller reservoir are included in Chapter 7; however the method used for identifying seawater in the produced water is also applicable to identifying water-rock and water mixing reactions.

The reservoir is at a relatively high temperature (~120°C) with formation water of high salinity (an NaCl-$CaCl_2$ brine), with low sulphate and high barium. In contrast, injected seawater is initially at surface temperatures with lower salinity, high sulphate and low barium. Because Cl is a conservative ion, unlikely to be involved in any water-rock interactions in this reservoir, changes in the concentration of the Cl ion in the produced water can be used to estimate the

proportion of injected seawater to original formation water in any produced water mixture. Lower chloride in the produced water is assumed to indicate a higher seawater component, i.e. the percentage seawater in each produced water sample is:

$$\%Seawater = ([Cl_{FW} - Cl_{meas}]/[Cl_{FW} - Cl_{SW}]) \times 100 \qquad (1)$$

where the subscripts FW, SW and meas denote the chloride concentrations in the original formation water (a value chosen as 41500 mg/l from an analysis in Warren and Smalley, 1994, assuming constant formation water composition), seawater (19350 mg/l) and produced water respectively. A typical formation water composition is shown in Table 4.2.

Table 4.2 Typical formation water composition in the Miller reservoir.

ION (mg/l)	Miller
SODIUM	28100
POTASSIUM	1630
MAGNESIUM	113
CALCIUM	615
BARIUM	770
STRONTIUM	65
IRON	3
CHLORIDE	46050
SULPHATE	4
BICARBONATE	1655
CARBON DIOXIDE	20 (mol%)
pH	7.5

If produced waters were simply binary mixtures of formation water and injected water, all ions, when plotted against Cl, should show linear mixing relations. To monitor any potential reactions, the deviation between the analysed concentration of each component in the produced water and the value predicted from linear mixing of seawater and formation water to produce the observed chloride was calculated (equation 2) and graphs were plotted to illustrate the results of these calculations.

$$N_{(P)}\ (mg/l) = N_{(FW)}(mg/l) - ((N_{(FW)}\ (mg/l) - N_{(SW)}(mg/l))/100 * \%\ Seawater)$$

Where $N_{(P)}$ is the predicted concentration of species N, and $N_{(FW)}$ and $N_{(SW)}$ are the concentrations of species N in pure formation water and pure seawater respectively.

4.4 Results

Figures 4.6-4.12 show field-representative results from well A14 (see Appendix IV for well locations). Many ions do not show linear mixing relations with varying Cl; this indicates that dissolution or precipitation, occurred in the reservoir (water-rock interaction) and/or in the well bore (e.g. precipitation of barite scale through water-water interaction). Figures 4.6-4.12 plot measured and predicted values for each of the major water components and what follows is a description of their behaviour, particularly those that show some evidence for reaction in the reservoir.

Potassium

The water mixing trend for Potassium (K) is complicated (Figure 4.6); some data follows a linear mixing trend, but the plots also exhibit large amounts of scatter in the data. Concentrations of K recorded are so high and the scatter is so random in time that it is most likely that many of the K-analyses are spurious due to the presence of additives containing potassium in the injected water (Collins, pers.comm. 2005).

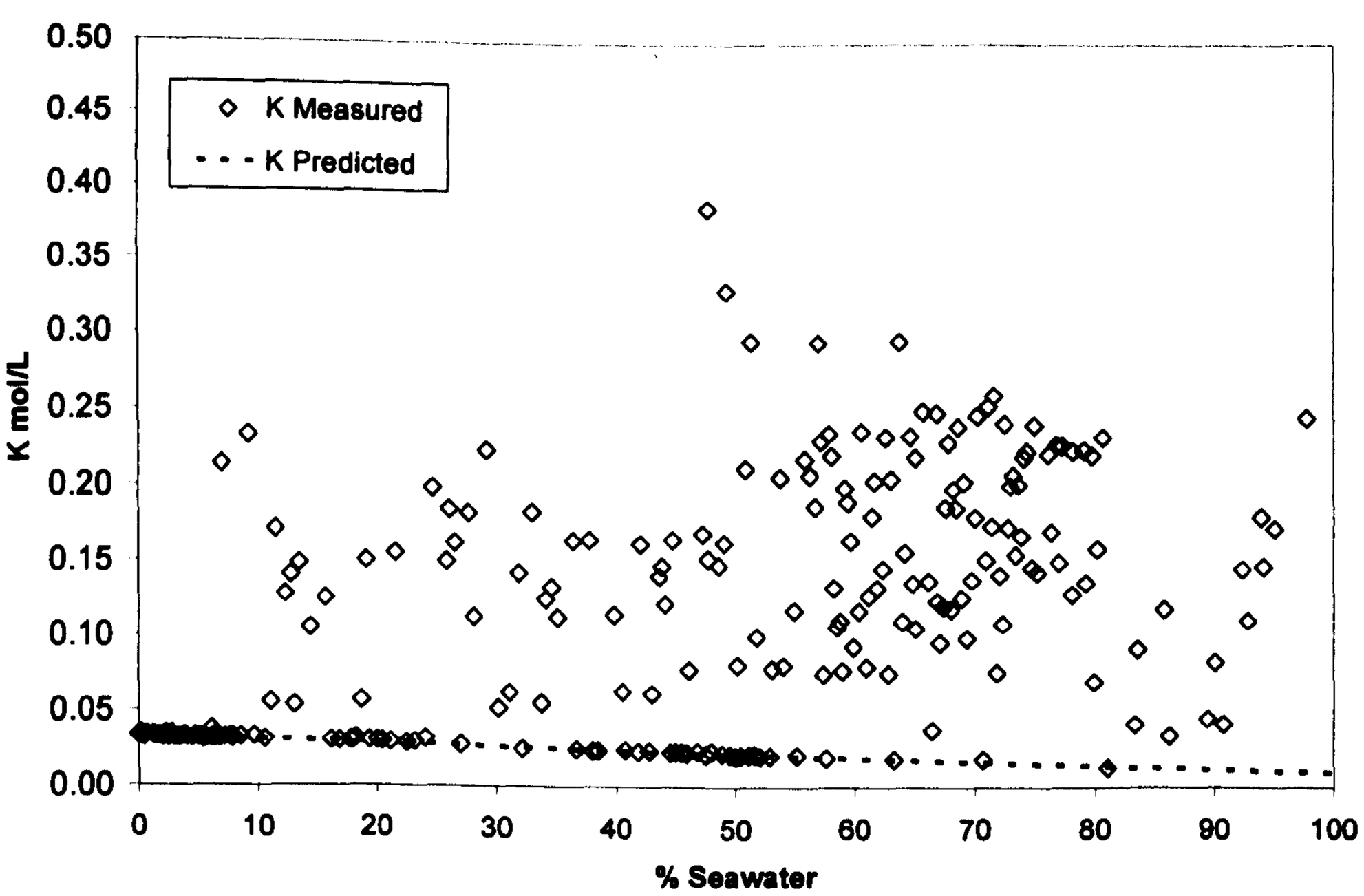

Figure 4.6 Variation in K concentration with proportion of seawater in the produced water, relative to a linear mixing line between seawater and formation water, from representative well A14. Note, despite elevated levels and scatter in the data, some data points follow the linear mixing line

Sodium

Sodium (Na) appears to follow a simple mixing trend, increasing in concentration only as chloride does (Figure 4.7). However, sodium is not known as a conservative ion, and the simple mixing trend exhibited by Na ions may merely be a reflection of the fact that its concentration is particularly high in these fluids. That is, the higher the concentration of ions present, the more extensive any reaction will need to be in order for its effects to become detectable above the effects of fluid mixing.

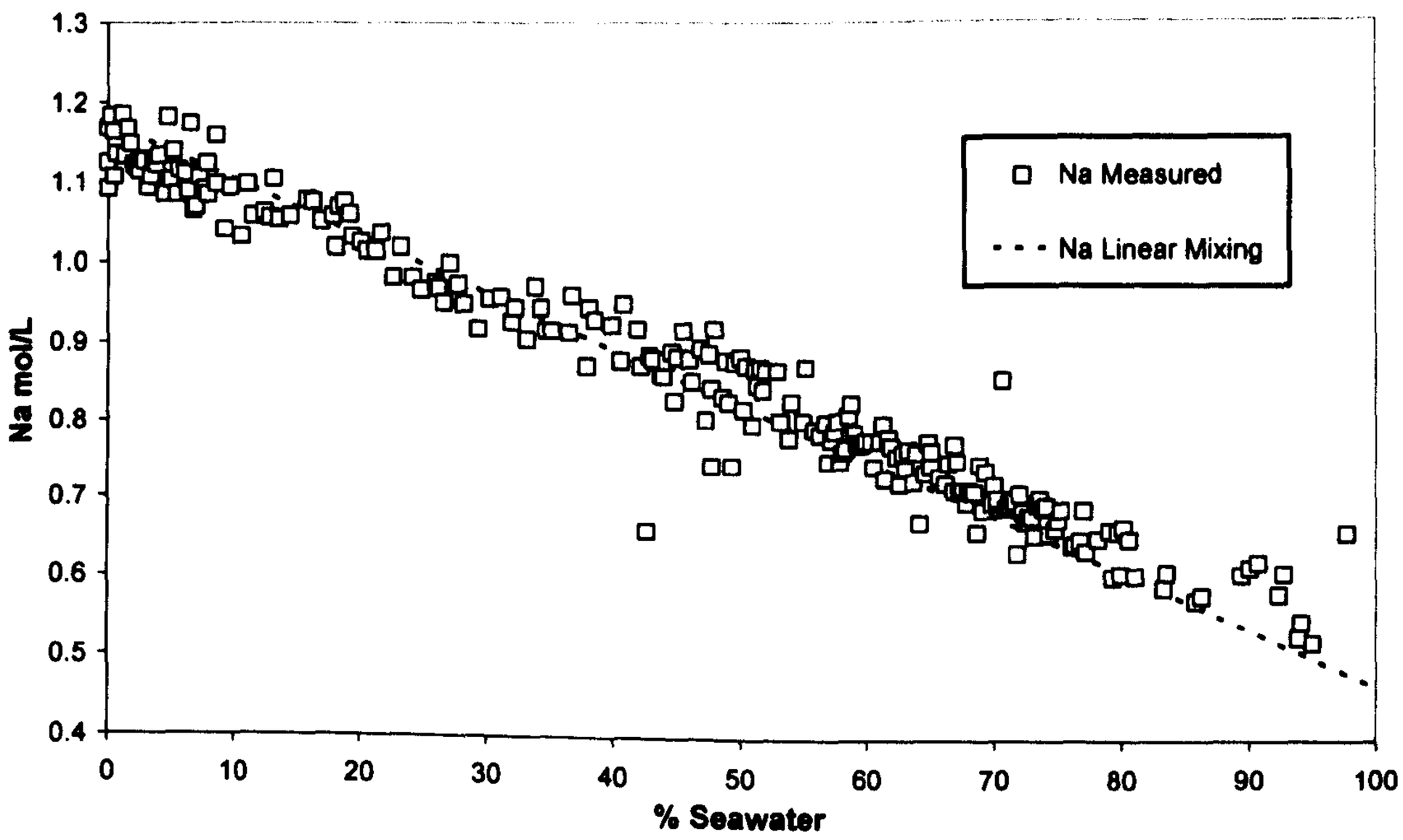

Figure 4.7 Variation in Na concentration with proportion of seawater in the produced water, relative to a linear mixing line between seawater and formation water, from representative well A14. Note the appearance of conservative behaviour despite slight elevation in Na levels

Calcium and Magnesium

Calcium (Ca) tends to show a general increase with increasing seawater, though the increase is greater than would be expected for simple mixing and appears often to be split into two components (Figure 4.8). This suggests that while there is an element of fluid mixing occurring, there is also a source of calcium in the system. The increase in Ca above the mixing line is particularly apparent when % seawater is >20%, suggesting it may arise through seawater-rock interactions.

Magnesium (Mg), in contrast, shows at a trend (possibly two) defining arcs which correspond to the mixing line close to the 2 end members, but show strong depletion for intermediate compositions (Figure 4.9).

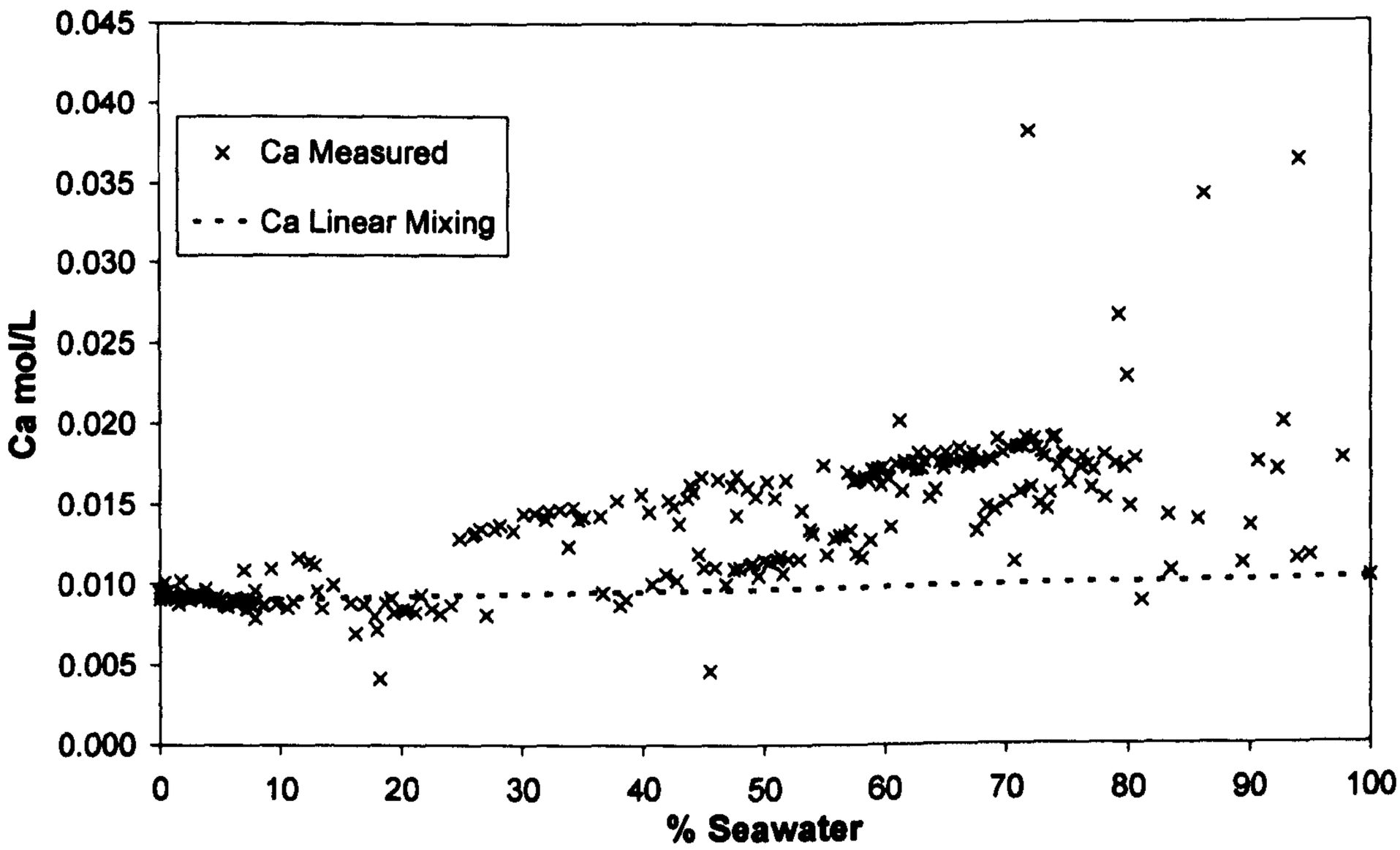

Figure 4.8 Variation in Ca concentration with proportion of seawater in the produced water, relative to a linear mixing line between seawater and formation water, from representative well A14. Note the two separate trends and the relatively high levels of Ca present

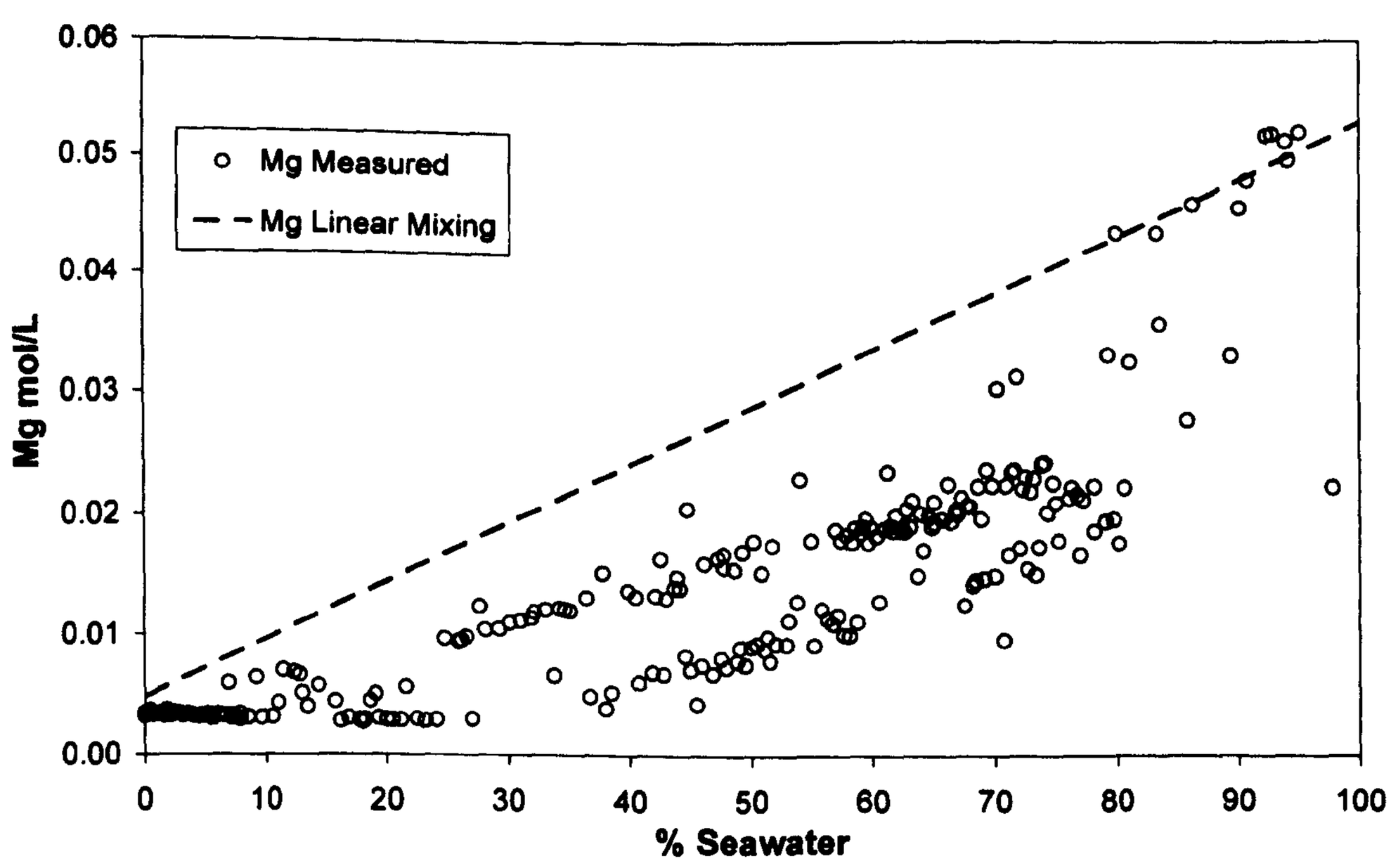

Figure 4.9 Variation in Mg concentration with proportion of seawater in the produced water, relative to a linear mixing line between seawater and formation water, from representative well A14. Note the two separate trends and the significant depletion in Mg relative to the linear mixing line

Barium

There is a large overall decrease in the amount of barium (Ba) in produced water with increasing seawater, but the position of the measured data below the mixing line (Figure 4.10) indicates that there has been significant removal of Ba from the mixed fluid (up to about 450mg/l from predicted levels).

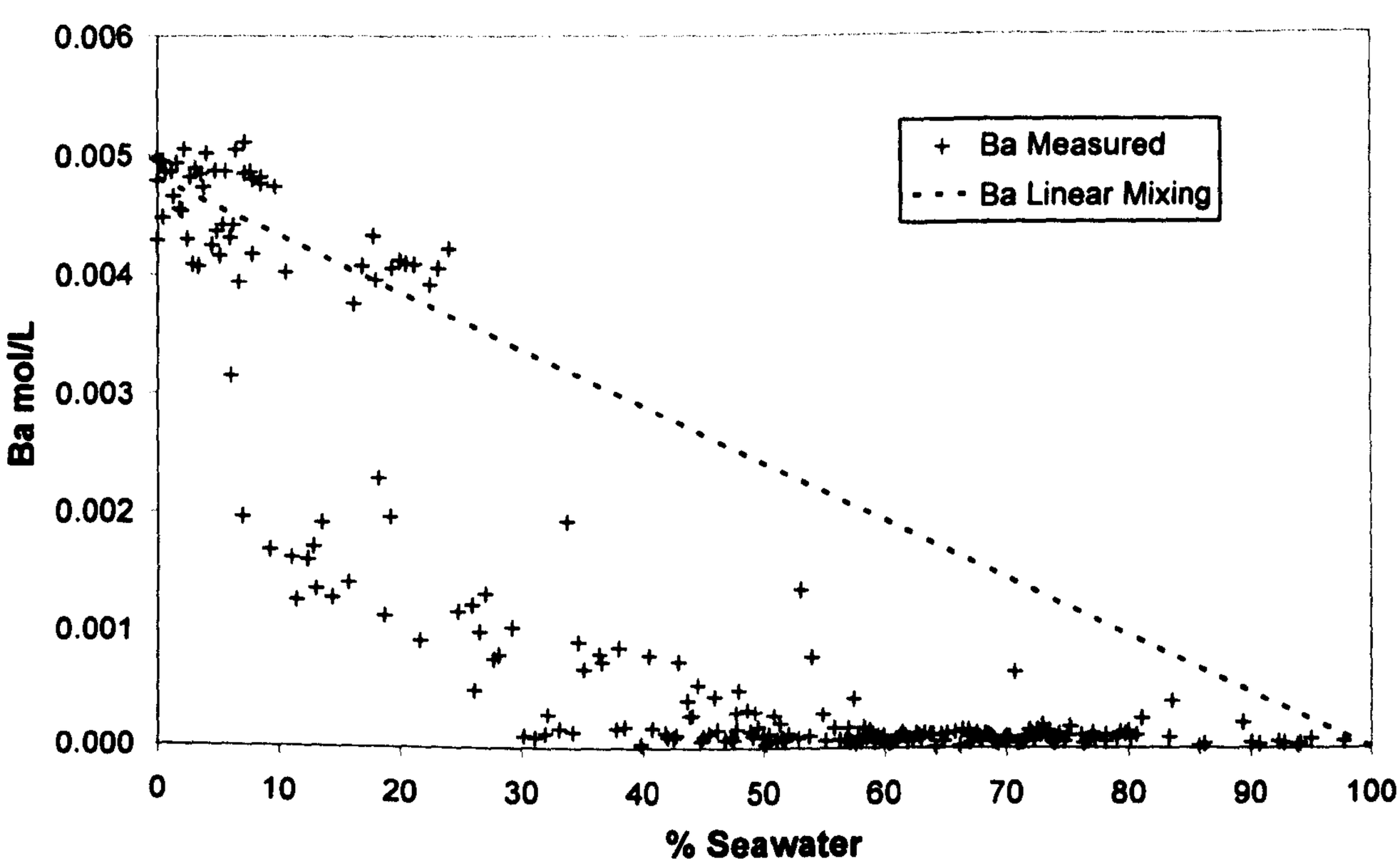

Figure 4.10 Variation in Ba concentration with proportion of seawater in the produced water, relative to a linear mixing line between seawater and formation water, from representative well A14. Note the significant depletion in Ba relative to the linear mixing line

4.5 Interpretation of fluid processes between the injection and production well heads

Where measured ion concentrations deviate significantly from the calculated linear mixing lines, the discrepancies are most likely due to the precipitation or dissolution of minerals.

Potassium and sodium

Potassium is a major component of the drilling mud used in the completion of oil field wells. The scatter in the data may therefore be ascribed to contamination. However, a substantial proportion of the measured values lie on the linear mixing line, indicating either that K does not participate in water-rock reactions, or that, as with Na, it is too concentrated. Although reactions involving Na may be difficult to observe, it may also be that the conservative trend suggests there is neither a source nor a sink for Na in this system. This is supported by the fact that there is very little plagioclase in the system so processes such as the albitisation of plagioclase cannot be important here.

Calcium and magnesium

Calcite is present in the reservoir rocks as authigenic cement and concretions and hence elevated Ca levels in the formation water may be derived from the dissolution of calcite. Seawater is slightly undersaturated with respect to calcite and, although formation water will be in equilibrium with calcite (and potentially other Ca-bearing minerals) present, a mixture of injected seawater and formation water would dissolve calcite, increasing the concentration of Ca in solution. Dissolving calcite would also increase the pH of the fluid mixture. As the pH increases, the solubility of calcite decreases so the reaction should be self-limiting. Temperature is also a factor that can be taken into account. Calcite shows retrograde solubility, suggesting that most dissolution is likely to occur in shallower parts of the reservoir, where temperatures are lower. Ultimately though, the system is dynamic and dissolution of calcite is limited by the degree to which it comes into contact with undersaturated fluid for the requisite period of time.

Conversely, Mg is depleted relative to the linear mixing curve (Figure 4.9), a feature common to the North Sea (Bazin *et al.*, 1997). It is probable that the observed increase in Ca and decrease in Mg concentrations are at least partially the result of a coupled reaction. Rapid dolomitisation of the authigenic calcite would account for the pattern observed, however, when relative molar losses and gains in Mg and Ca respectively are compared (Figure 4.11) it becomes evident that removal of Mg is far greater that the gain of Ca. This implies that though dolomitisation is likely to be occurring, there is an additional sink for Mg in the system.

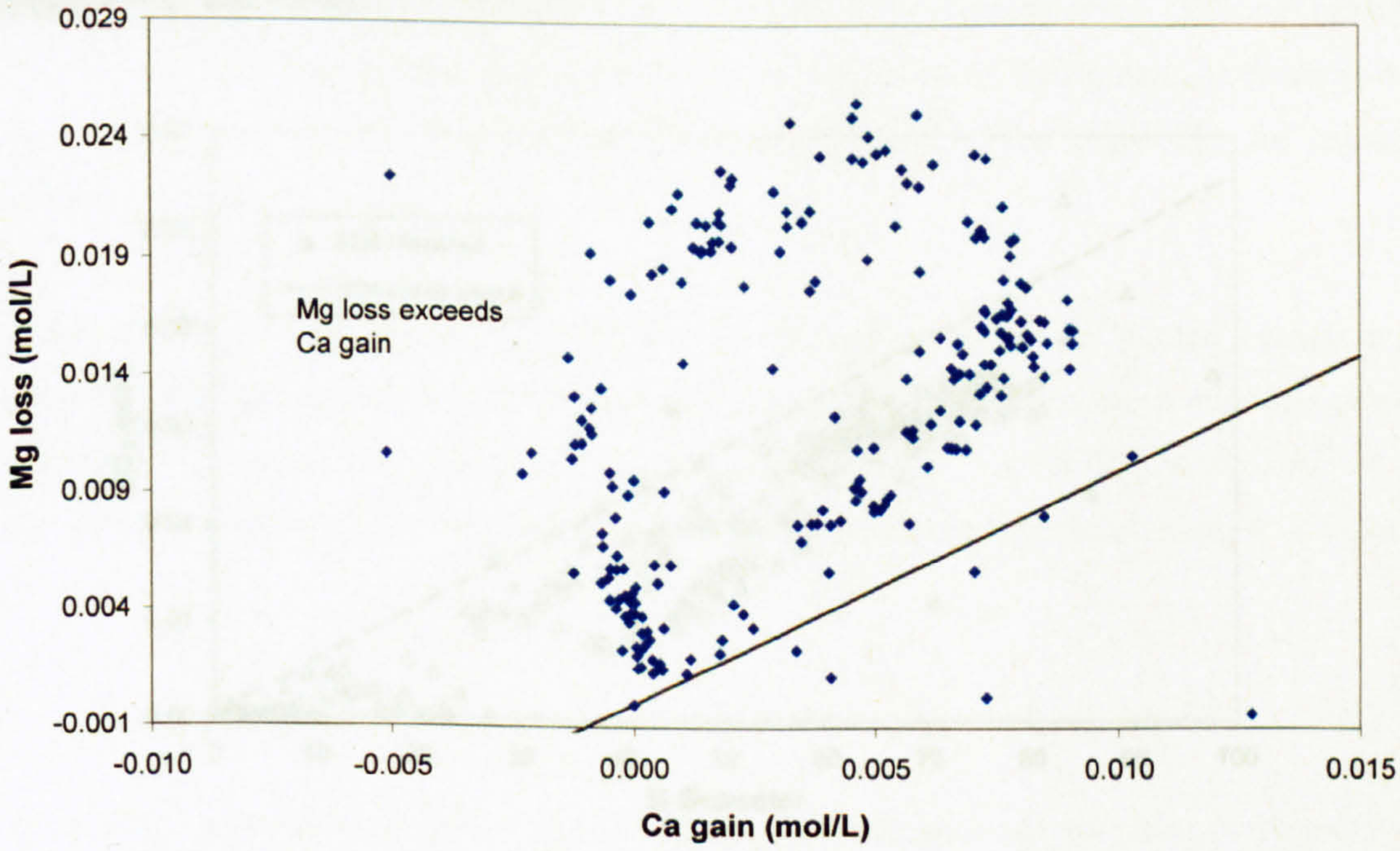

Figure 4.11. Ca and Mg concentrations relative to a 1:1 stoichiometric exchange (straight line) representative of simple dolomitisation

Mg is known to be removed from solution in smectites or chlorite or may also be removed through ion exchange reactions. However, the presence of chlorite in these rocks has not been recognised and the only corresponding increase in ion concentration necessary to account for ion exchange processes (Ca) is more likely due to mineral dissolution or alteration reactions.

It is not possible to unequivocally identify which process is most important in controlling Mg concentrations and Ca/Mg ratios. However, mass balance and kinetics suggest that dolomitisation cannot be a dominant process and a combination of clay formation and calcite dissolution is likely.

Barium

The loss of Ba is most likely accounted for by its reaction with sulphate to form barite, known to be an important scaling process in this field because sulphate and barium decrease together relative to the linear mixing line.

$$N_{(l)}\ (mg/l) = N_{(P)}\ (mg/l) - N_{(meas)}\ (mg/l) \qquad (3)$$

Where $N_{(l)}$ is the amount of species N (in this case, Ba) lost from the system, $N_{(P)}$ is the predicted concentration of N (see equation 2) and $N_{(meas)}$ is the measured concentration of N. The calculation can be performed for any dissolved species and if molar concentrations are used as an alternative to mg/l then the results can be used to establish the stoichiometric relations as in Figures 4.11 and 4.14B.

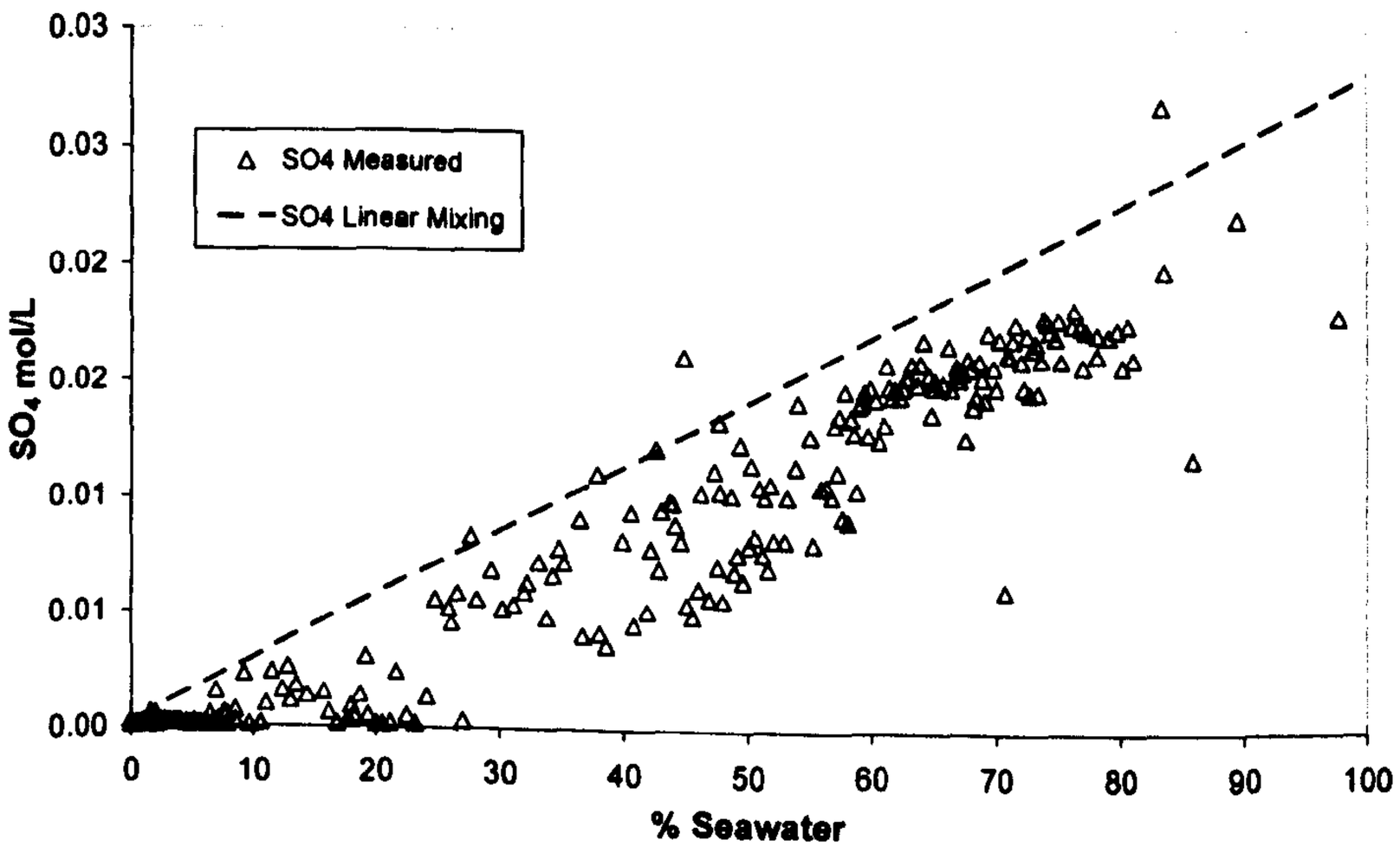

Figure 4.12 Variation in sulphate concentration with proportion of seawater in the produced water, relative to a linear mixing line between seawater and formation water, from representative well A14. Note the depletion in sulphate relative to the linear mixing line

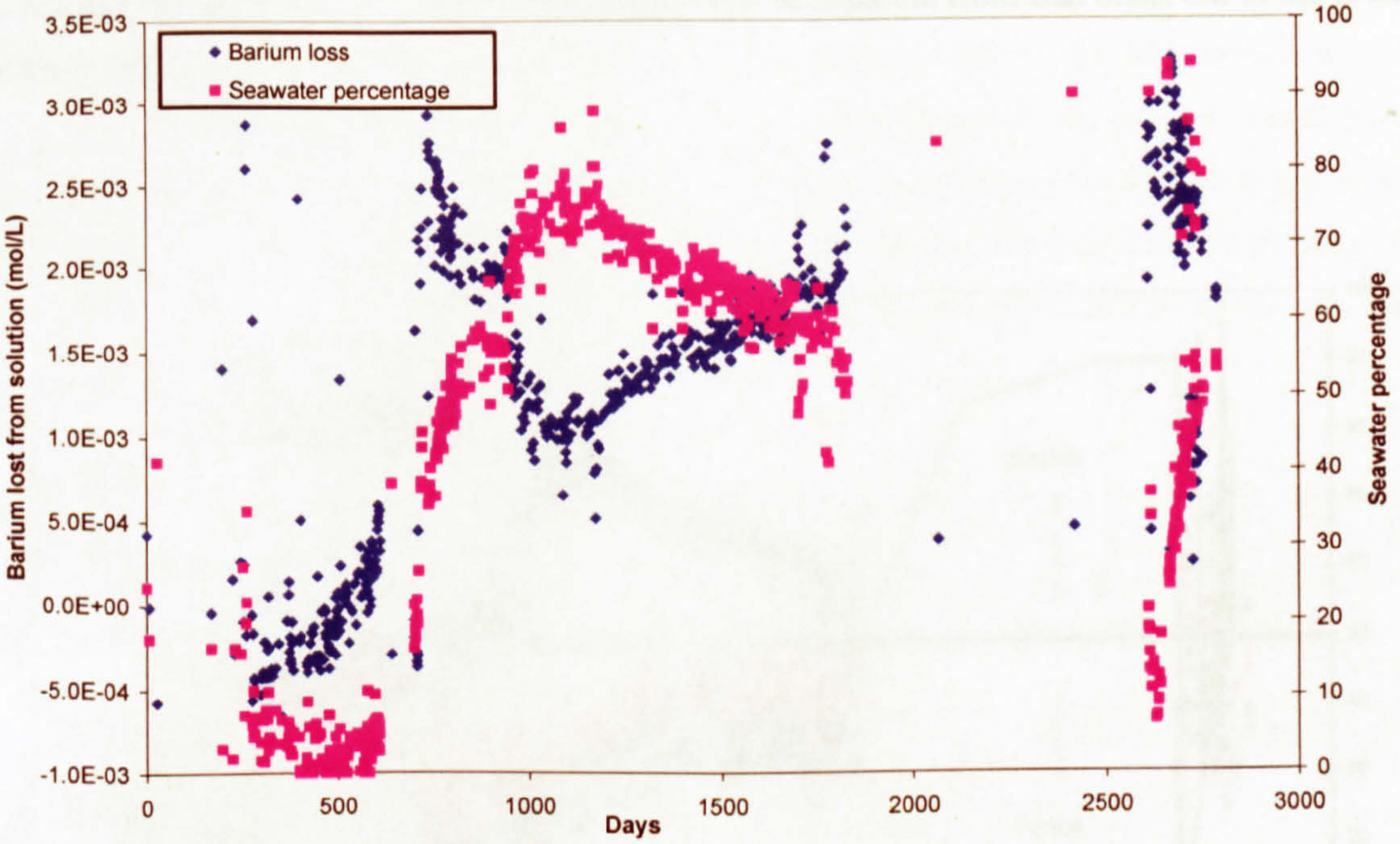

Figure 4.13. Time series plot showing both the seawater percentage and the amount of barium that has been lost from solution relative to linear mixing between seawater and formation water. Well A14.

Sulphate

Due to the large difference in sulphate concentration between seawater and formation water, this ion has potential to be another useful indicator of seawater incursion. However, sulphate is not a conservative component and the predicted sulphate is consistently very different (usually much higher) from the amount of sulphate actually measured in the system, indicating that sulphate has been removed from the mixed fluid (Figure 4.12). One possibility for sulphate removal is barite precipitation.

When the difference between the predicted and measured sulphate is plotted against time (Figure 4.14B), the biggest differences correspond to changes either in the production rate of water, or the proportion of seawater in the produced water. The deficit in the amount of sulphate in the system relative to what would be expected after barite precipitation, is calculated by:

$$SO_{4(D)}\ (mg/l) = 0 - ((SO_{4(P)}\ (mg/l) - (0.70073Ba_{(l)}(mg/l)) - SO_{4(meas)}(mg/l)) \qquad (4)$$

Where $SO_{4(D)}$ is the sulphate deficit in mg/l, $SO_{4(P)}$ is the sulphate concentration predicted from seawater percentage, $Ba_{(l)}$ is the amount of Ba lost from the system as barite and $SO_{4(meas)}$ is the measured sulphate concentration. Most commonly, there is an increase in the sulphate deficit (i.e. more sulphate is removed from the system) when the amount of seawater in the system

increases. This pattern of sulphate deficit appears to be separate from that observed in the lower salinity waters.

A

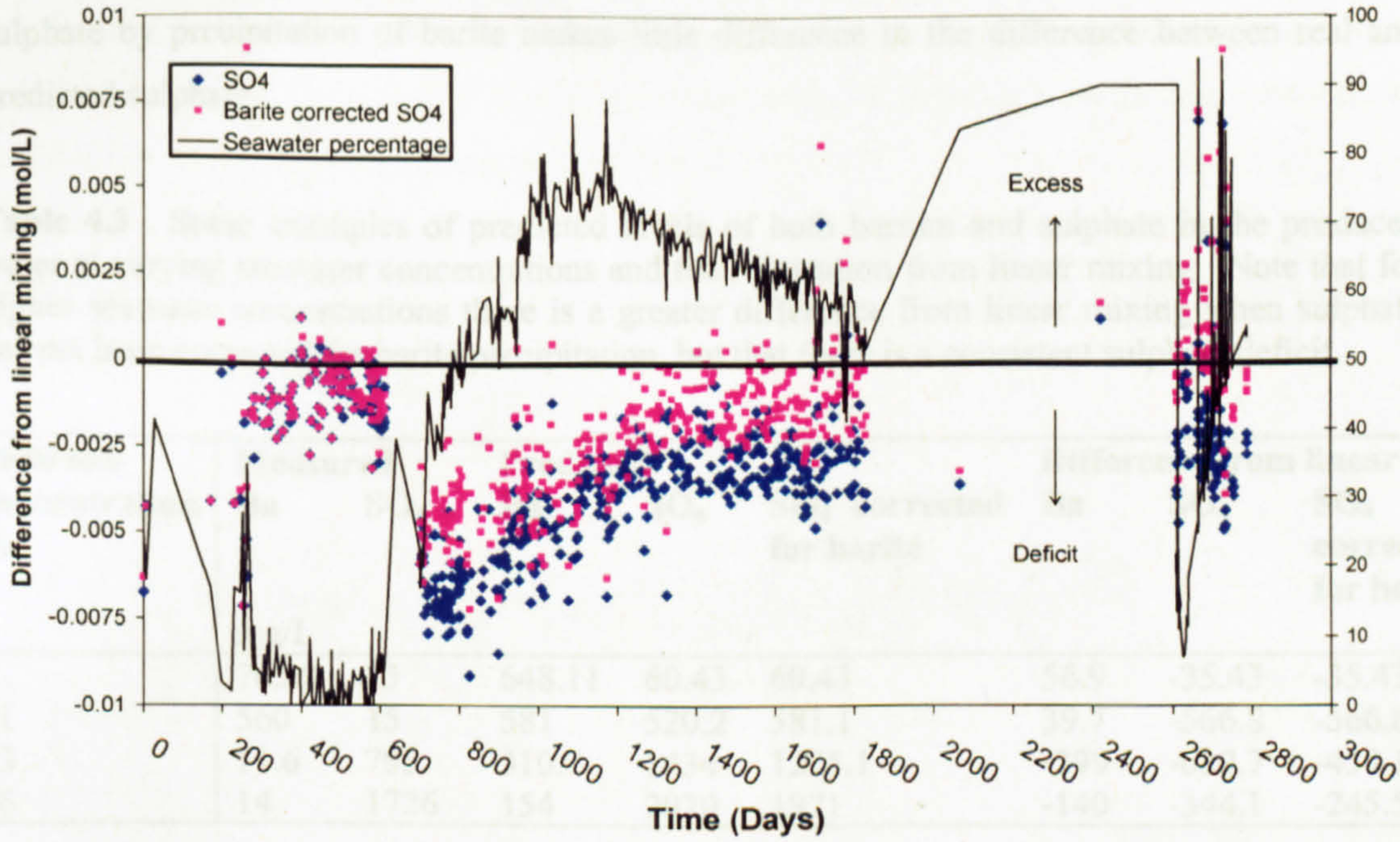

B

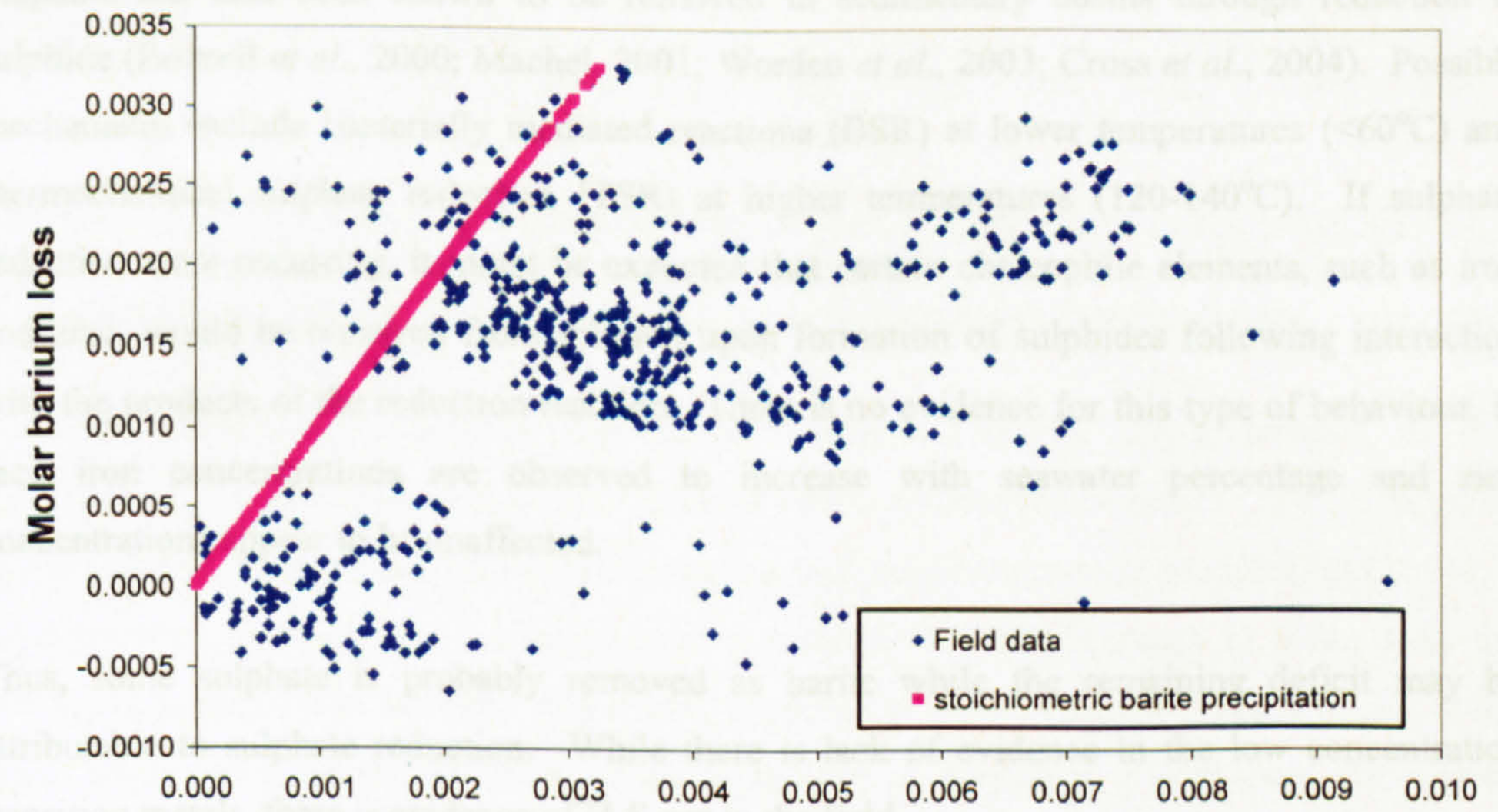

Figure 4.14. A: Variation in sulphate deficit (in mg/l) with seawater, taking into account sulphate removed by precipitation as barite, B: excess sulphate loss from solution relative to the trend for stoichiometric barite precipitation if all the Ba removed from solution is precipitated as barite

Although the main sink for sulphate is its reaction with Ba to form barite, the SO_4 deficit is not always matched by a corresponding Ba deficit, and thus not all of the SO_4 deficit can be explained by barite precipitation. Table 4.3 provides selected results of calculations determining the size of the remaining sulphate deficit once barite precipitation has been accounted for. These data, along with Figures 4.16A and B and illustrate that the removal of sulphate by precipitation of barite makes little difference to the difference between real and predicted sulphate.

Table 4.3 . Some examples of predicted levels of both barium and sulphate in the produced water at varying seawater concentrations and their deviation from linear mixing. Note that for higher seawater concentrations there is a greater difference from linear mixing when sulphate has not been corrected for barite precipitation, but that there is a consistent sulphate deficit.

Seawater concentration %	Measured		Predicted			Difference from linear mixing		
	Ba	SO_4	Ba	SO_4	SO_4 corrected for barite	Ba	SO_4	SO_4 corrected for barite
	mg/L							
2	705.0	25	648.11	60.43	60.43	56.9	-35.43	-35.43
21	560	15	581	520.2	581.1	39.7	-566.8	-566.8
53	11.6	795	310.7	1434	1225.1	-299	-639.7	-430.1
76	14	1726	154	2070	1971	-140	-344.1	-245.5

Sulphate has also been shown to be removed in sedimentary basins through reduction to sulphide (Bottrell *et al.*, 2000; Machel, 2001; Worden *et al.*, 2003; Cross *et al.*, 2004). Possible mechanisms include bacterially mediated reactions (BSR) at lower temperatures (<60°C) and thermochemical sulphate reduction (TSR) at higher temperatures (120-140°C). If sulphate reduction were occurring, it might be expected that certain chalcophile elements, such as iron and zinc, would be removed from solution upon formation of sulphides following interaction with the products of the reduction reaction. There is no evidence for this type of behaviour, in fact, iron concentrations are observed to increase with seawater percentage and zinc concentrations appear to be unaffected.

Thus, some sulphate is probably removed as barite while the remaining deficit may be attributable to sulphate reduction. While there is lack of evidence in the low concentration transition metals, there is evidence of H_2S gas in the field.

Silicon

Figure 4.15 shows that the silicon concentration remains almost constant in the produced water irrespective of the proportion of seawater present, and is always close to quartz saturation at 120°C (~60 mg/l $SiO_{2(aq)}$). Based on the produced water from one well (proportionally <1% of

the field), this requires dissolution of ~80 tonnes of silica from the formation over the production cycle, equivalent to removal of ~30 m^3 of quartz.

Silica solubility is extremely temperature dependent: the hotter the temperature, the more silica is expected in solution. So, increasing depth tends to cause an increase in silica solubility and this facilitates quartz cementation. The addition of low-silicon seawater to such a system would therefore be expected to dilute the silicon concentration, whereas in fact the concentration of this species varies very little throughout the life of a well.

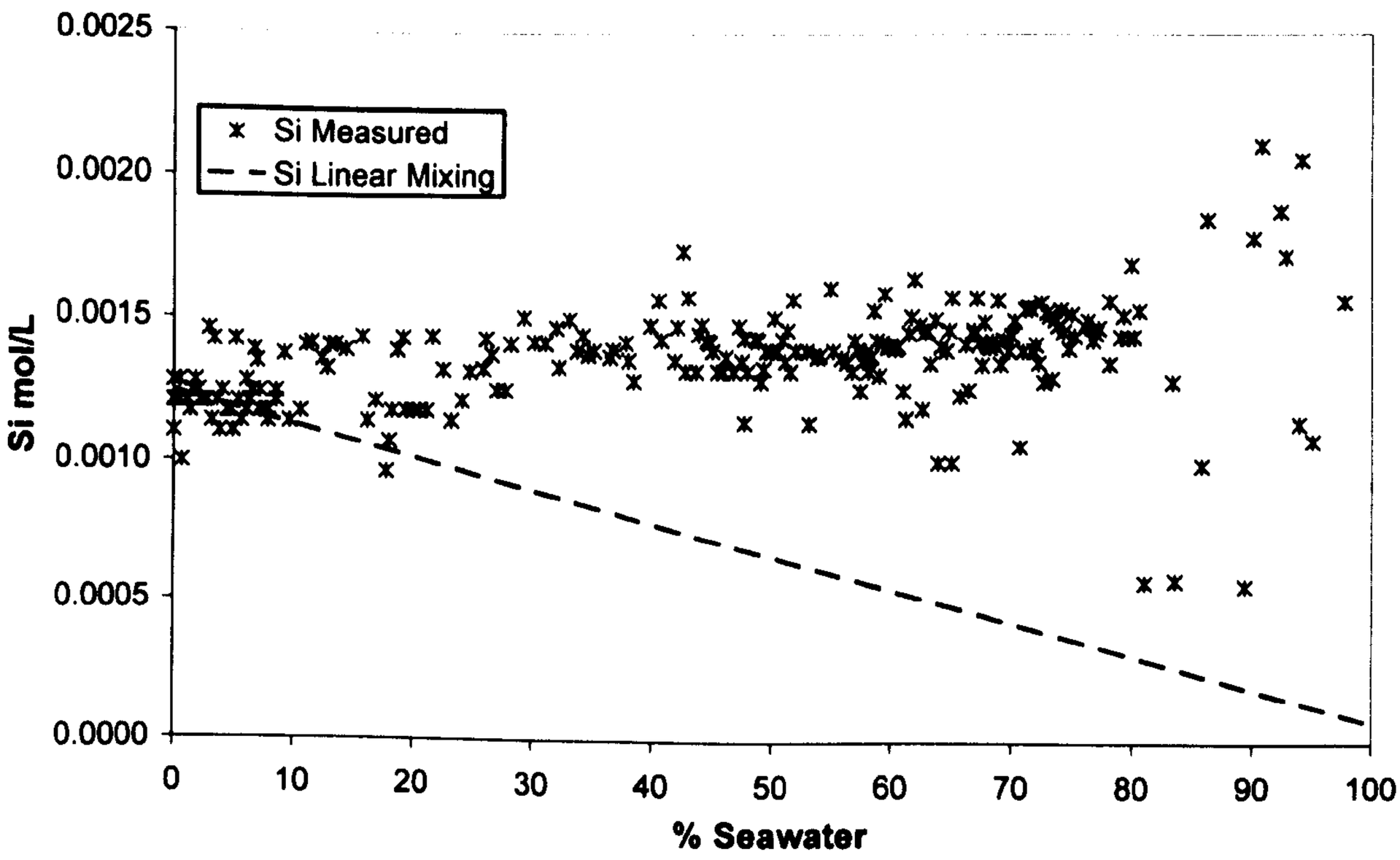

Figure 4.15 Variation in Si concentration with proportion of seawater in the produced water, relative to a linear mixing line between seawater and formation water, from representative well A14. Note the consistently high Si levels and the slight increase in Si with seawater percentage

The mechanisms controlling silica saturation in the reservoir are not fully understood, but it is clear that silica dissolution must occur rapidly at relatively low temperatures (120°C), possibly on the order of days to weeks in order to maintain high concentrations in produced fluids with a high seawater percentage. In detail, there is actually a slight increase in silica with the increasing proportion of seawater in the later produced waters. A possible cause of this is the lower salinity of these waters, because silica solubility is subject to a salting-out effect (Von Damm *et al,*. 1991; Schmulovich *et* al, 2006), that is silica is more soluble in less saline waters with a lower water activity. This can be tested as follows: if quartz dissolution can be written as:

$$SiO_2 + 4H_2O = SiO_2.4H_2O \qquad (5)$$

Hence calculations based on a solvation number of 4 (reaction 5, Schmulovich *et* al, 2006) indicate that the lowered water activity (0. 966 in formation water as opposed to 0.982 in seawater) can account for only 4-5 mg/l of the increase in silicon observed in the more dilute waters. Alternatively, metastable enhancement of the degree of silica saturation may provide alternative explanation of elevated silicon concentrations. There is evidence for the presence of reactive metastable sponge spicules in trace amounts in Miller (Bjørlykke and Egeberg, 1993) and cases of rapid silica dissolution have elsewhere been ascribed to their presence in the rocks (Ichenhower and Dove, 2000; Aase and Walderhaug, 2005; Bjørlykke and Egeberg, 1993). However, their dissolution cannot account for the fact that Si concentrations in the produced water actually *exceed* that in the original formation water which was itself buffered by coexistence with the same spicules.

An alternative and preferred mechanism for enhanced silica in solution is the breakdown of silicates in response to the ingress of cold seawater which is heated as it passes through the formation. For example, K-feldspar dissolution and illitization are known to have occurred in Miller as a diagenetic process (Marchand, 2001; Gluyas, 2000). K-feldspar dissolution occurs more rapidly than quartz dissolution at temperatures as low as 65°C, partly as a result of the high surface area caused by abundant microtextures on feldspar overgrowths (Aagaard *et al,*. 1989; Worden and Rushton, 1992) and porous alteration of detrital grains. Feldspar alteration to illite can be written to a first approximation as:

$$3KAlSi_3O_8 + 2H^+ = KAl_3Si_3O_{10}(OH)_2 + SiO_{2(aq)} + 2K^+ \qquad (6)$$

Provided this reaction is overstepped by the infiltration of low pH fluid, it can drive the concentration of silica in solution above the equilibrium level for quartz saturation and account for the increase in silica level during production.

4.5.1 Variations in formation water

All previous calculations have been based on the assumption that the composition of the formation water is constant throughout the field. There is evidence however, that this is not always strictly the case.

When the concentrations of species in solution are plotted against percentage seawater (Figure 4.16) some trends are evident that appear not to be related to fluid mixing. At low seawater percentages, magnesium and sulphate in particular show characteristic downward trends that appear to behave independently of the influence of mixing. When low seawater % points with anomalously low Mg concentrations are picked out, they correspond to those points also

exhibiting particularly low sulphate. This suggests that there is a separate, high chloride (therefore suggesting low % seawater), low Mg and low SO_4 water that is being produced in places as well as the analysed high chloride formation water.

It may also be that produced water with a lower Cl concentration doesn't represent invariably mixed water, but may be a different formation water with a lower salinity. Though most ions do show behaviour that is most easily interpreted as mixing between seawater and formation water with some fluid-rock interaction, some show a slightly different pattern that could represent mixing between two different formation waters. It is likely that the apparent increase in chloride through time in well A16 (Figure 6.21, Chapter 6) may be due to formation water being produced from different parts of the reservoir unit through time.

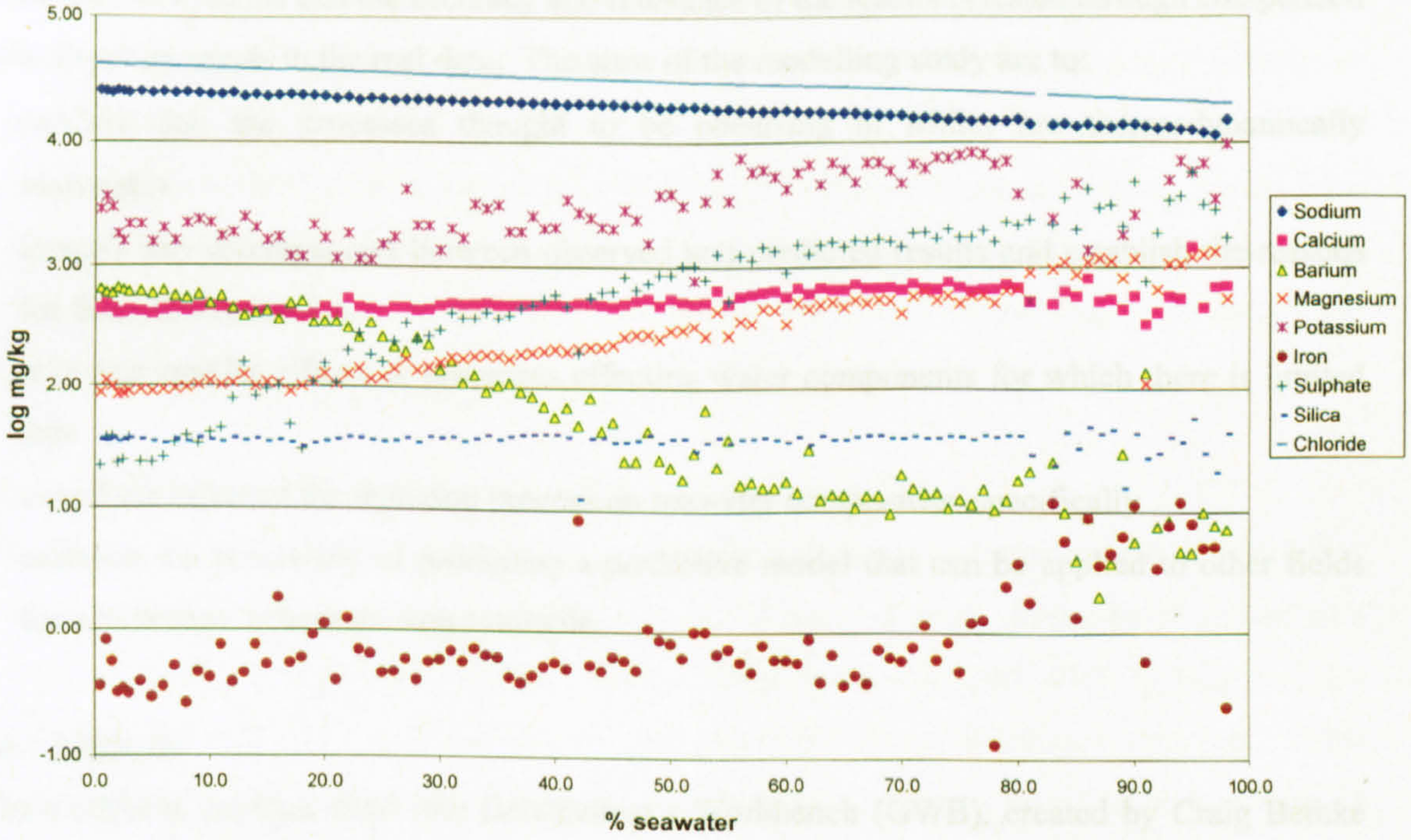

Figure 4.16. A, the simplified variation in fluid components with increasing seawater for three wells in Miller.

Strontium isotope data indicates that there is vertical variation in the nature of the formation water in particular places in the field (Smalley, 2005; personal communication). The waters have $^{87}Sr/^{86}Sr$ values ranging from 0.710074 to 0.723693, increasing with depth. Unfortunately the strontium data does not correspond directly with the water composition data for the ten producing wells. It is therefore not possible to conclude that slight variation in aqueous species concentration in the produced water is due to separate formation waters, but it is likely that the

different layers in the reservoir rocks that have distinctive $^{87}Sr/^{86}Sr$ values also have distinctive formation water compositions.

4.6 Geochemical modelling of water mixing in Miller

Section 4.5 outlined in detail evidence provided by real data for the most likely reactions occurring in the Brae Formation reservoir rocks of the Miller Field, North Sea. These reactions: barite precipitation, sulphate reduction, dolomitisation, clay dissolution, clay formation and silicate dissolution, are all processes that could potentially occur in any similar system with a typical sandstone reservoir, saline formation water and injection of seawater for pressure support and EOR. Geochemical modelling is an additional tool to improve understanding of processes affecting water compositions in such a system. Real data is used to produce models of theoretical systems and the accuracy and relevance of the results is tested through comparison with observed trends in the real data. The aims of the modelling study are to:

- confirm that the processes thought to be occurring in Miller are thermodynamically reasonable
- identify any discrepancies between observed and predicted results and establish the reasons for these discrepancies
- note any smaller effects or processes affecting water components for which there is limited data
- model the effect of the injection process on seawater composition specifically
- establish the possibility of producing a predictive model that can be applied to other fields for which there is enough data available.

4.6.1 Methods

The modelling package used was Geochemist's Workbench (GWB), created by Craig Bethke (1994), which can be used to show how a system should evolve geochemically in terms of mineral, water and gas chemistry (Bethke, 1994; Barclay and Worden, 2000). An initial basis must be specified, including fluid components, the amounts of any minerals in the equilibrium system, the activity of a species such as H^+ (pH), etc. Other parameters may also be set, or may be allowed to vary to a specified degree, for example temperature or the fugacity of any gases present. The system is then allowed to proceed to equilibrium and/or along a precise reaction path. Although differential reaction rates can be input, the modelling was done assuming that the system came to equilibrium at each step in the model.

All plots in the following sections were created using Gtplot as part of the Geochemist's Workbench.

4.6.1.1. *Water-mixing: no water-rock interaction*

In any situation, mixing two waters of differing composition will cause a number of precipitation and/or dissolution reactions to occur in order to restore equilibrium in the system. The simplest type of model that can be applied to the Miller reservoir system is to assume simple mixing of two different waters with no influence exerted by the minerals present in the system. An analogy for this type of model would be to mix the two waters in a beaker in a lab.

In order to create this model, the composition of typical seawater (Table 4.4) was specified in the basis at 25°C and was added gradually to water with a composition typical of the Miller field (Table 4.5). The model was set to continue until the formation water was completely replaced by seawater using the "flash option"; that is the original fluid (formation water) was removed from the equilibrium system and the reactant fluid (seawater) was added, assuming 100% mixing. The initial formation water analysis lacked measurements for silica and aluminium therefore values of $SiO_{2\,(aq)} = 27$ and $Al^{3+} = 1$ mg/kg were taken from subsequent water analyses taken prior to seawater incursion (data provided by BP). From this model, mixing curves were produced that demonstrate how each fluid component is expected to behave throughout the process of seawater addition in this case (assuming no water-rock interaction). The results can be seen in Figure 4.17.

4.6.1.2. *Water-mixing including water-rock interaction*

The next stage in the modelling process is to assume that any mixture of waters in a reservoir will come into contact, and react, with the surfaces of host minerals. In the basis, as part of a typical seawater composition, $quartz_{(S)}$ and $calcite_{(S)}$ were swapped with $SiO_{2(aq)}$ and Ca respectively, to simulate equilibration of seawater with these ubiquitous minerals. This seawater composition, with redox fixed by equilibrium with hematite, was then heated from 25 to 120°C. That is, from ambient temperature to the temperature reported for the pore water at depth in the Miller field in the North Sea Formation Waters Atlas (Warren and Smalley, 1994). The second column in Table 4.4 shows the concentration of the principal components after equilibration and Figure 4.18 shows the minerals that precipitated as seawater was heated.

Following equilibration, the resulting fluid was then taken (using the "pickup" option) and added to a fluid of a composition presumed to be similar to that of the formation water at 120°C. The waters were mixed in varying proportions using the "flash" option, introduced above.

Assumptions. The purpose of a model is not to be an exact replica of a natural system, but rather a reflection and interpretation of how that system might behave under specific defined

conditions. This means that when a model is constructed certain assumptions must be made and compromises accepted. This study was no exception and a number of unknown parameters have been defined with reference to known facts about the system. The mineralogy of the Miller field includes detrital quartz and minor k-feldspar with major authigenic quartz and calcite and some authigenic illite, ferroan dolomite, kaolinite and pyrite. Thus, the formation water was set to be saturated with quartz, calcite, k-feldspar and illite. It was also assumed that the seawater had time to equilibrate as it was gradually heated with depth and that the temperature and composition of the formation water were measured accurately.

Table 4.4. The composition of seawater used in the geochemical modelling compared with the endmember seawater calculated from real data.

Parameter	**Seawater**	**Model heated seawater (Section 4.6.2.2)**	**Miller seawater end-member (section 4.6.2.3)**
	(mg/kg)		
Na^+	10760	10410	13530
K^+	399	385.8	524
Mg^{2+}	1290	658.7	900
Ca^+	411	827.2 (after swapping with 50 free gram Calcite)	620
Fe^{2+}	0.0034	0.003308	9
$SiO_{2\,(aq)}$	1	62.07 (after swapping with 100 free gram Quartz)	37.5
Cl^-	19350	18770	21740
Br^-	30	29.01	--
SO_4^{2-}	2700	1161	2443
HCO_3^-	142	1141	--
pH	7.5	5.67	
Temperature	25°C	120°C	120°C

Suppression of precipitating phases. Although small amounts of ferroan dolomite were reported to be present in the rocks of Miller and there is evidence that dolomitisation of calcite is occurring in the reservoir, the precipitation of any kind of dolomite was suppressed to prevent it forming in unrealistic amounts. The precipitation of talc ($Mg_3Si_4O_{10}(OH)_2$), witherite ($BaCO_3$), magnesite ($Mg(CO_3)$) and strontianite ($SrCO_3$) were also suppressed.

Problems and Limitations. Though both the formation water and the seawater were set to be saturated with various minerals, the two mineral assemblages were not precisely the same because it was assumed that it was seawater was more likely to have been in contact only with quartz and calcite for longer than with the other minerals. The consequence of this is that the model would behave as though the fluid was moving from one rock type into another of slightly differing mineralogy. In order to assess the problems this might cause, another model was run with both fluids in contact with the same amount of the same minerals. The results of this model showed negligible differences to the original.

Another problem with using a model in this way is that the quality of the data input cannot be guaranteed. In particular, the amount of bicarbonate a fluid contains at the well head will not be the same as at depth due to pressure affecting solubility. This may mean that predicted levels of bicarbonate in the fluid or of carbonate bearing minerals may be slightly skewed.

4.6.1.3. *Changes in injected seawater composition*

In order to assess the effect of injection on seawater composition specifically, a number of analyses interpreted as >80% seawater incursion from the time-series data for various wells were studied. From this data, a typical, representative "reacted seawater" composition was constructed, which is compared with typical injected seawater data in Table 4.4 (third column).

4.6.2 Results

4.6.2.1 *Water-mixing no water-rock interaction*

Figure 4.17 shows the varying concentrations of the major fluid components as formation water is replaced by, and mixes with seawater. When these curves are compared to the real data (Figure 4.14), a number of interesting features can be noted. Measured Cl, Na, K, Mg, Ba and SO_4 ions all show the same general trends predicted by the mixing curves, although the absolute values differ somewhat. As would be expected, conservative Cl decreases with increasing seawater, as does the concentration of Na. Mg shows a significant increase, and Ba and SO_4 show a decrease and an increase respectively, though the values are relatively level until about 25% seawater.

Though there are some important similarities between the model and the data from the real field, it is the differences that provide the most interesting information about processes occurring in the system.

4.6.2.2 *Water-mixing including water-rock interaction*

Figure 4.18 and Table 4.4 show that, while most of the seawater components remain at constant concentration during heating from 25-120°C, the overall composition undergoes some significant changes. Large stage precipitation of Mg-rich antigorite and huntite with sulphate-rich anhydrite correlates with changes in Mg^{2+}, SO_4^{2-} and HCO_3^- and the dissolution of calcite.

GWB produces results in two formats, a text (numerical) output and a graphical output using the Gtplot programme. Figures 4.19, 4.20 and 4.21 show changes in the fluid components and minerals precipitated with increasing seawater and decreasing formation water proportion. It is useful to study the three graphs (and the text output) together.

Table 4.5 Original basis of the model fluids for the Miller, Central Brae and Ekofisk Fields, North Sea

Parameter	**Value (Miller)**	**Value (Central Brae)**	**Value (Ekofisk)**
Na^+	23950 mg/kg	36700 mg/kg	23989 mg/kg
K^+	Swap for 100 free gram k-feldspar	Swap for 50 free gram K-feldspar	Swap for 50 free gram K-feldspar
Mg^{2+}	100 mg/kg	48 mg/kg	469 mg/kg
Ca^{2+}	Swap for 50 free gram Calcite	Swap for 25 free gram Calcite	Swap for 25 free gram Calcite
Ba^{2+}	700 mg/kg	1030 mg/kg	14 mg/kg
Sr^{2+}	55mg/kg	50 mg/kg	762 mg/kg
Fe^{2+}	2 mg/kg	39 mg/kg	1×10^{-6} mg/kg
Al^{3+}	Swap for 50 free gram Illite	20 mg/kg	10 mg/kg
$SiO_2(aq)$	Swap for 2 free gram Quartz	Swap for 12 free gram Quartz	Swap for 15 free gram Quartz
Cl^-	40100 mg/kg	57660 mg/kg	47751 mg/kg
SO_4^{2-}	30 mg/kg	6 mg/kg	38 mg/kg
HCO_3^-	2200mg/kg	3310 mg/kg	525 mg/kg
pH	7.5	6.39	6.46
Temperature	120°C	123°C	162°C

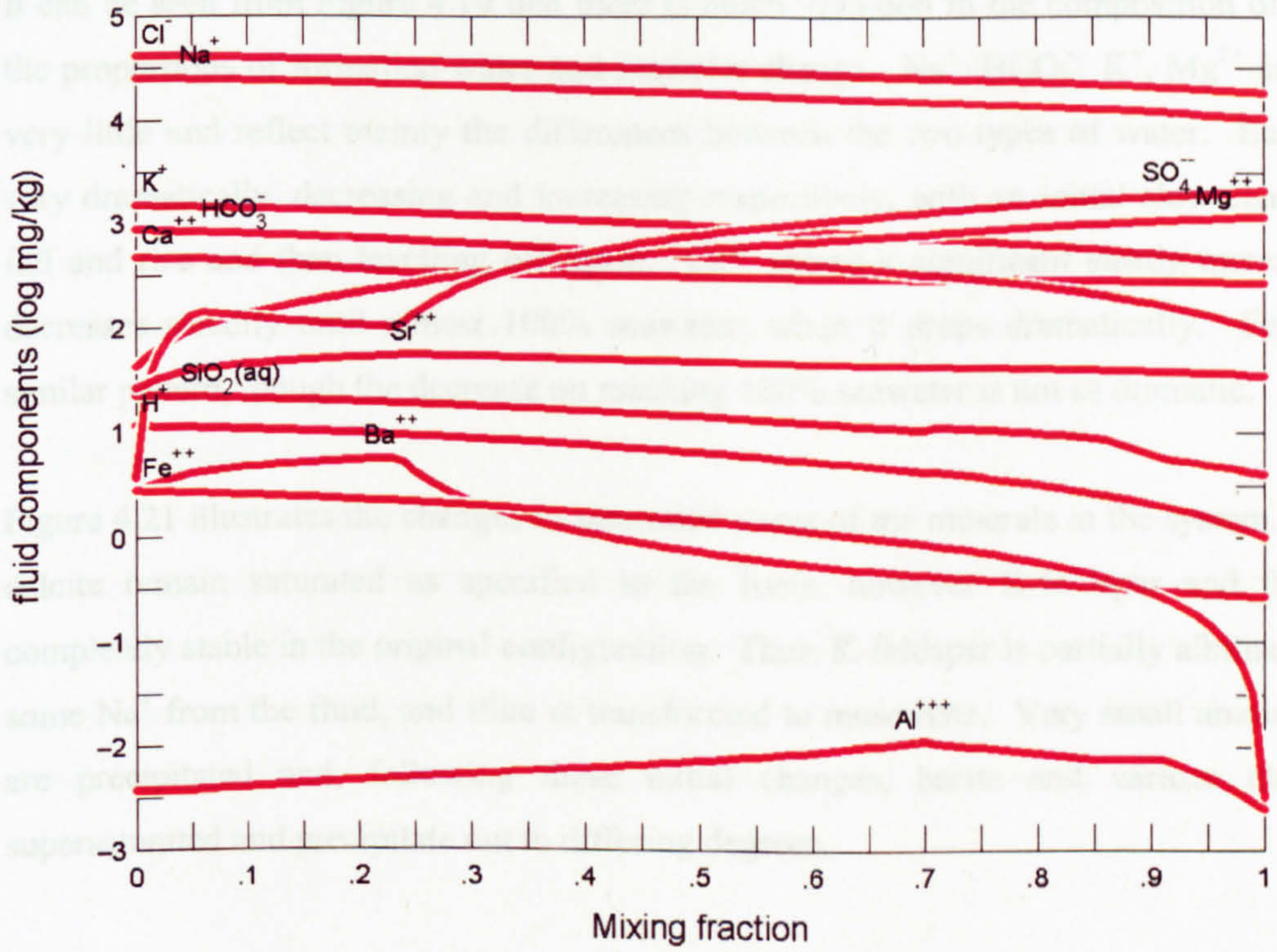

Figure 4.17 Curves to show the compositions of model fluids produced by mixing of pure formation (left) water and pure seawater (right)

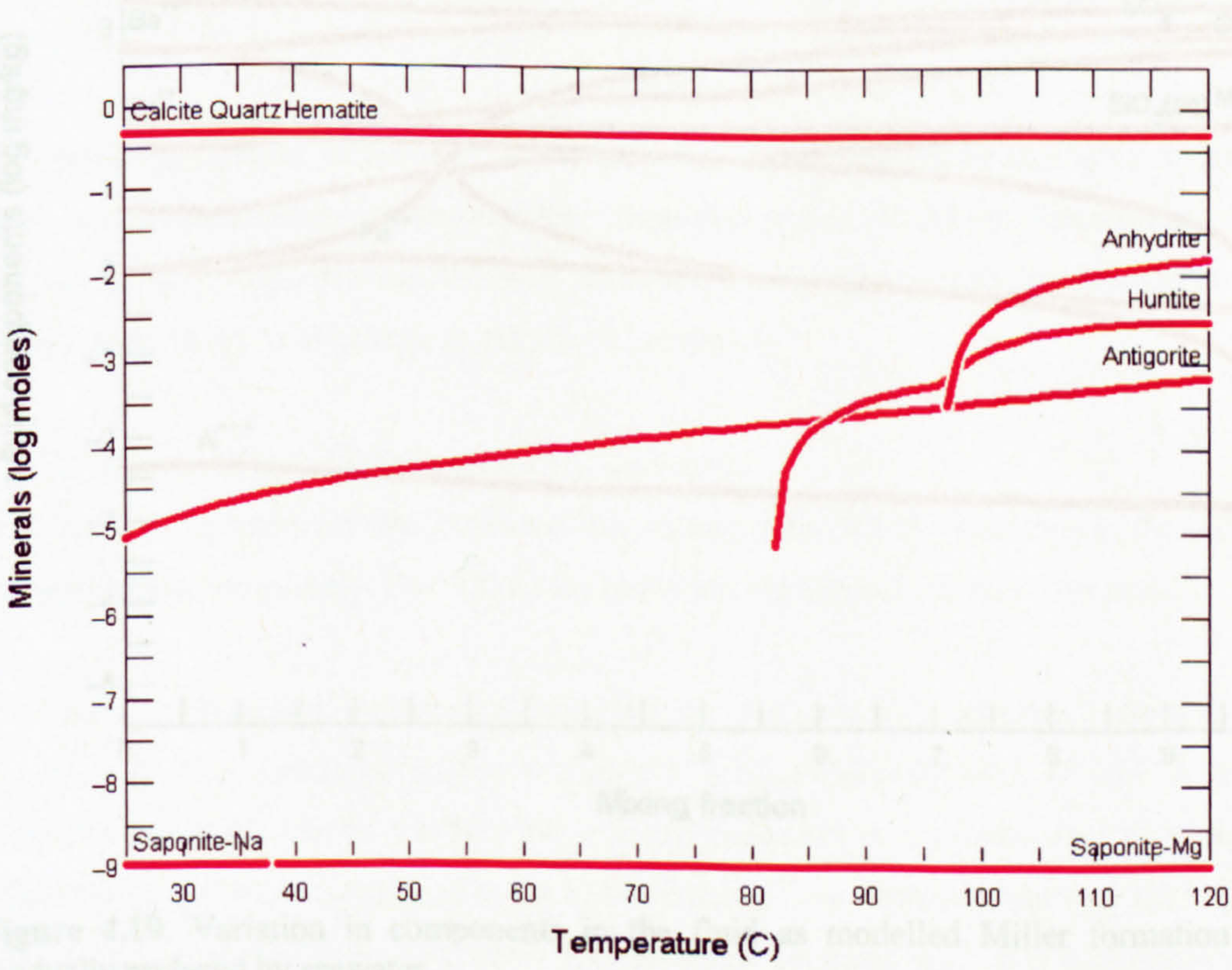

Figure 4.18 Minerals that precipitate on heating typical seawater in equilibrium with quartz, calcite and hematite.

It can be seen from Figure 4.19 that there is much variation in the composition of the fluid as the proportions of formation water and seawater change. Na^+, HCO_3^-, K^+, Mg^{2+} and Al^{3+} vary very little and reflect mainly the differences between the two types of water. Ba^{2+} and SO_4^{2-} vary dramatically, decreasing and increasing respectively, with an initial slow change, a sharp fall and rise and then levelling off again. Ca^{2+} shows a significant steady increase and Sr^{2+} decreases steadily until almost 100% seawater, when it drops dramatically. Fe^{2+} follows a similar pattern, though the decrease on reaching 100% seawater is not as dramatic.

Figure 4.21 illustrates the changes in saturation states of the minerals in the system. Quartz and calcite remain saturated as specified in the basis, however K-feldspar and illite are not completely stable in the original configuration. Thus, K-feldspar is partially albitised, removing some Na^+ from the fluid, and illite is transformed to muscovite. Very small amounts of pyrite are precipitated and, following these initial changes, barite and various clays become supersaturated and precipitate out to differing degrees.

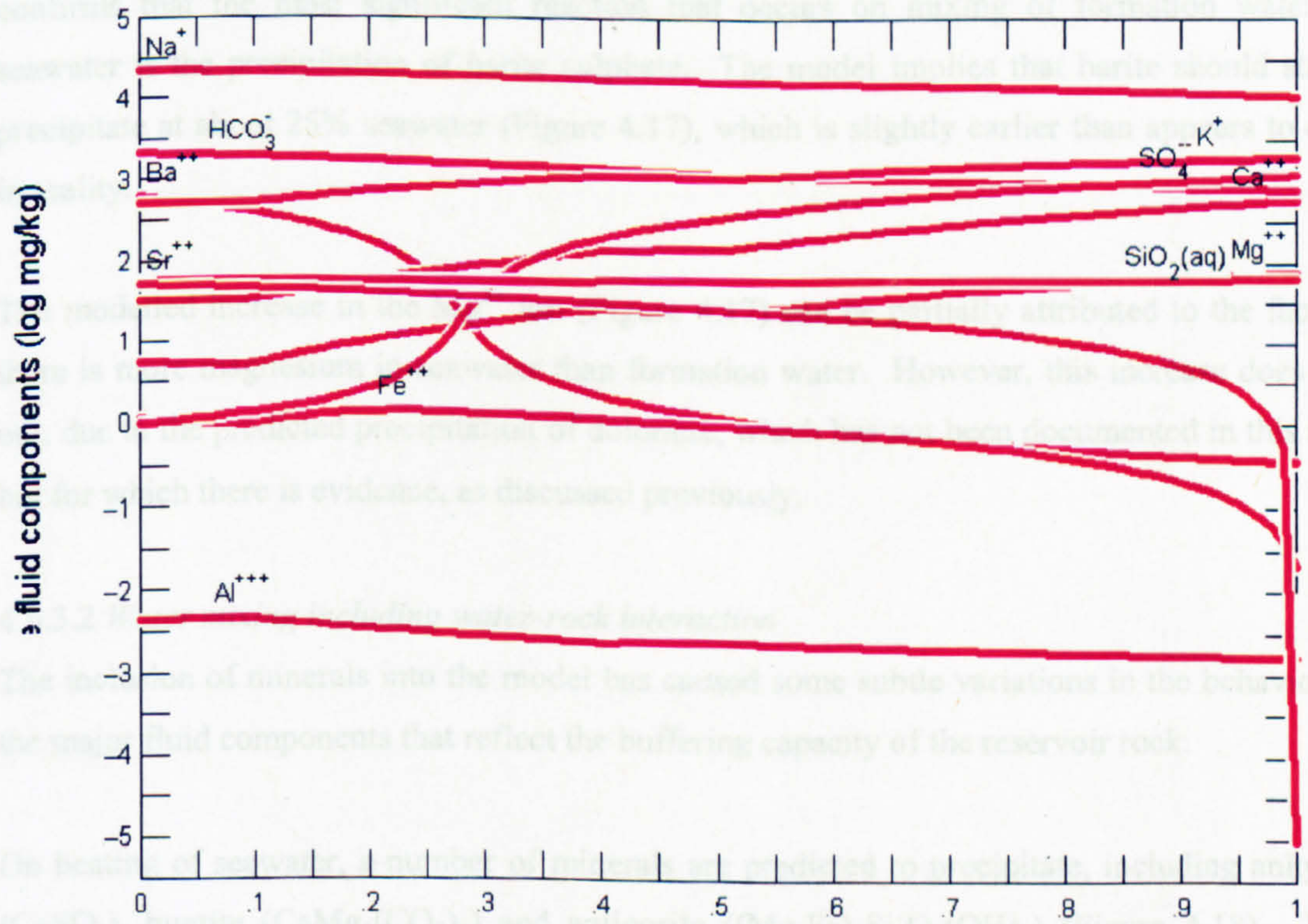

Figure 4.19. Variation in components in the fluid as modelled Miller formation water is gradually replaced by seawater.

4.6.2.3 *Changes in injected seawater composition*

The reacted seawater composition in the third column of Table 4.4 shows some significant variation from both real seawater, and the modelled seawater. There is far more Fe^{2+} in the reacted seawater than either the typical- or the equilibrated-seawater. In addition, the amount of sulphate present is similar to a typical seawater composition, but far more than predicted by the heating model. The reacted water also contains more $SiO_{2(aq)}$ than the typical seawater.

4.6.3 Discussion

4.6.3.1 *Water-mixing no water-rock interaction*

The modelled change in concentration of each component in the fluid can be explained by the precipitation and dissolution of minerals and the interaction of the two different types of water. For example, seawater contains less Na^+, K and HCO_3^-, and more Mg^{2+} than formation water, as is reflected in the changes in these components of the fluid as the relative proportion of seawater increases (Figure 4.17).

It is well established that Miller is subject to a serious barite scale problem and the model confirms that the most significant reaction that occurs on mixing of formation water and seawater is the precipitation of barite sulphate. The model implies that barite should start to precipitate at about 25% seawater (Figure 4.17), which is slightly earlier than appears to occur in reality.

The modelled increase in the Mg^{2+} ion (Figure 4.17) can be partially attributed to the fact that there is more magnesium in seawater than formation water. However, this increase does level out, due to the predicted precipitation of dolomite, which has not been documented in this study but for which there is evidence, as discussed previously.

4.6.3.2 *Water mixing including water-rock interaction*

The inclusion of minerals into the model has caused some subtle variations in the behaviour of the major fluid components that reflect the buffering capacity of the reservoir rock.

On heating of seawater, a number of minerals are predicted to precipitate, including anhydrite ($CaSO_4$), huntite ($CaMg_3(CO_3)_4$) and antigorite ($(Mg,Fe)_3Si_2O_5(OH)_4$) (Figure 4.18). These minerals precipitate due to the fact that although seawater is supersaturated with dolomite its precipitation has been suppressed in the basis. The Mg^{2+} ion deviates only very slightly from the mixing line between formation water and seawater (Figures 4.17 and 4.19) because of the suppression of dolomite and magnesite, which would have caused a significant loss in that ion,

had they been allowed to precipitate. Anhydrite precipitates because seawater is relatively rich in Ca and SO_4 and the solubility of the mineral decreases as the temperature increases.

As in the "no-mineral" model, barite precipitates due to the interaction of Ba^{2+} ions from the formation water and SO_4^{2-} ions in from the seawater as the two mix. The amount of barite that precipitates reaches a maximum at around 40% seawater and then decreases again as the supply of Ba^{2+} ions from the formation water is reduced. Ba^{2+} decreases slowly with the deceasing amount of Ba^{2+}-rich formation water present until about 35% seawater when the decrease becomes more rapid as barite precipitation reaches a maximum. The decrease then levels off again as the supply of Ba^{2+} ions becomes further reduced. SO_4^{2-} follows an opposite pattern (Figure 4.19). The general increase is due to the greater amount of sulphate in seawater than formation water and the sudden release of SO_4^{2-} ions into solution at ~40% seawater is probably due to the dissolution of a sulphate bearing mineral.

Though the modelled amount of Ca^{2+} in the water mixture increases with increasing seawater (Figure 4.19), this cannot be attributed to differing levels in the two types of fluid as both seawater and formation water have been set to be saturated with calcite. However, calcite is the only possible source of Ca^{2+} ions so this increase must be due to the progressive dissolution of calcite.

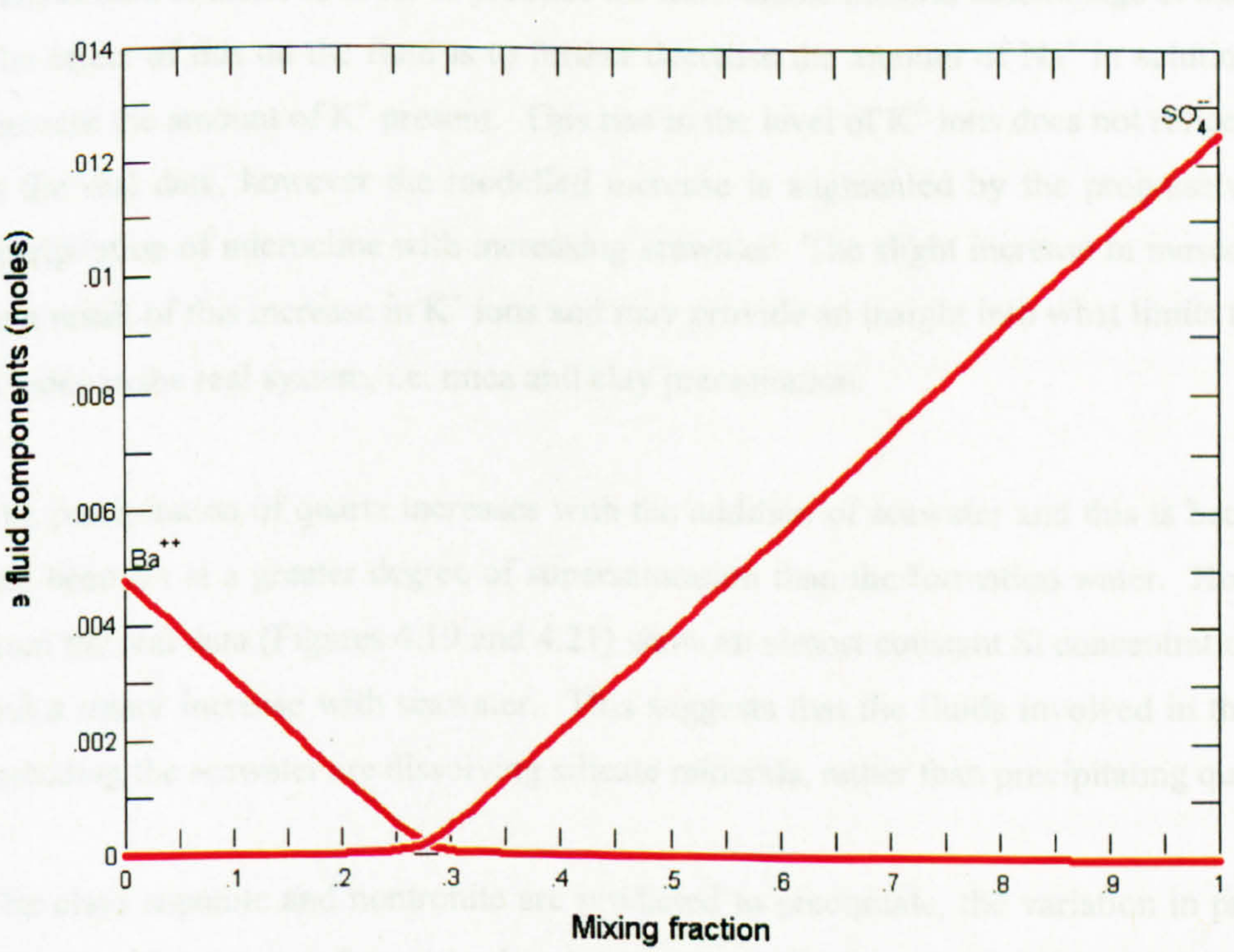

Figure 4.20 The general trend of the Ba^{2+} and SO_4^{2-} ions in solution with increasing seawater.

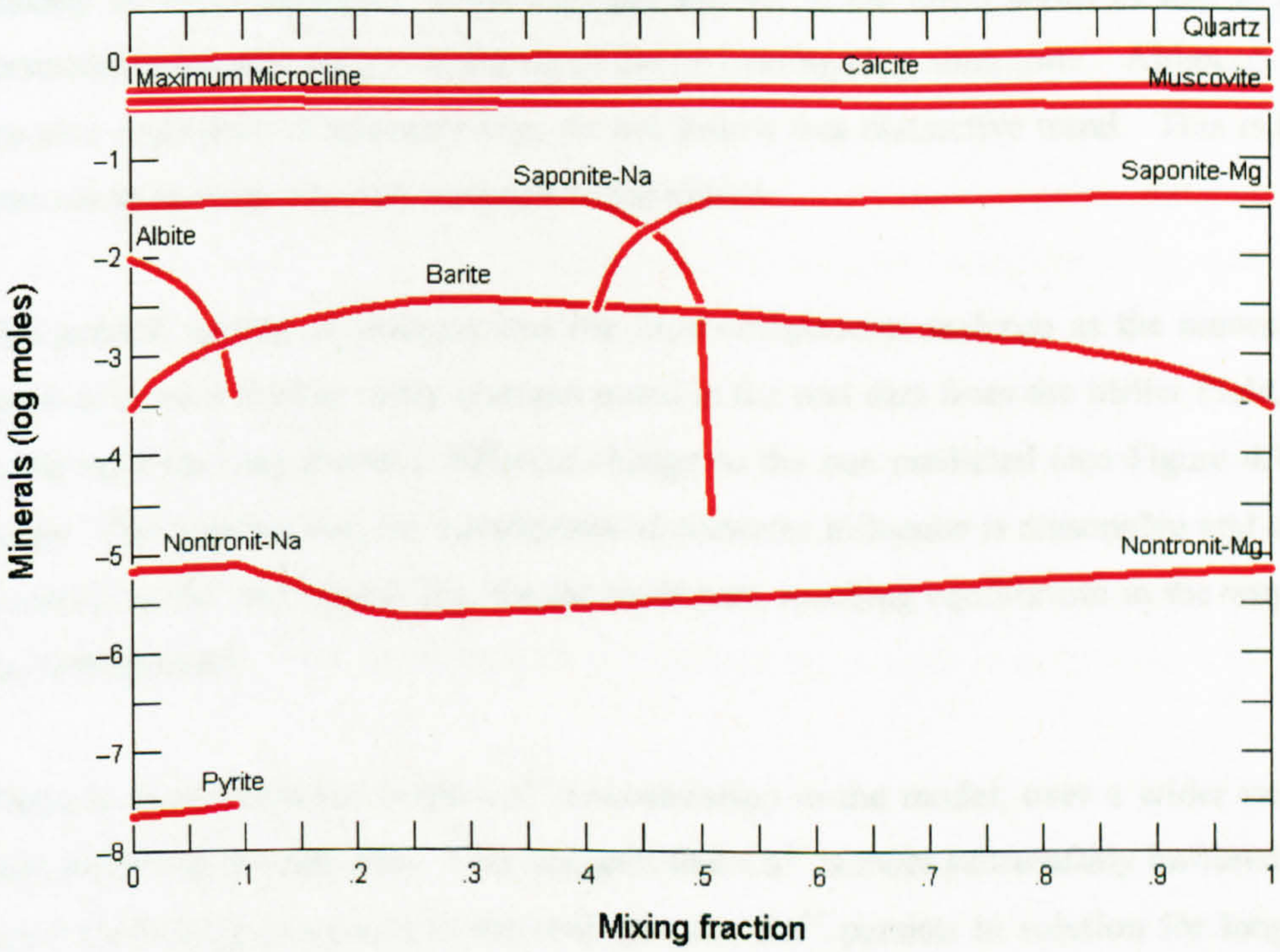

Figure 4.21. Minerals that precipitate as Miller formation water is gradually replaced by seawater

Figure 4.21 shows that at the onset of water mixing, part of the alkali feldspar (microcline) is transformed to albite in order to produce the most stable mineral assemblage at this temperature. The effect of this on the fluid is to further decrease the amount of Na^+ in solution and slightly increase the amount of K^+ present. This rise in the level of K^+ ions does not reflect observations in the real data, however the modelled increase is augmented by the progressive decrease in precipitation of microcline with increasing seawater. The slight increase in muscovite may also be a result of this increase in K^+ ions and may provide an insight into what limits the increase of K^+ ions in the real system, i.e. mica and clay precipitation.

The precipitation of quartz increases with the addition of seawater and this is because seawater had been set at a greater degree of supersaturation than the formation water. However, results from the real data (Figures 4.19 and 4.21) show an almost constant Si concentration in the water and a minor increase with seawater. This suggests that the fluids involved in the real system, including the seawater are dissolving silicate minerals, rather than precipitating quartz.

The clays saponite and nontronite are predicted to precipitate, the variation in principal cation (Na, Ca, Mg) being reflected in the changing composition of the fluid with which they are in equilibrium (Figures 4.19 and 4.21). Sr^{2+} decreases gradually until about 90% seawater when its levels drop dramatically. This distinct pattern is due to the extremely low levels of strontium in seawater. Fe^{2+} exhibits a very similar, pattern whereby it decreases slowly and then more

quickly at ~90% seawater. These changes are due to the lower levels of iron in seawater than formation water and the precipitation of the Fe bearing clay nontronite. Although Ba^{2+} and Al^{3+} are also negligible in seawater they do not follow this distinctive trend. This is because these ions are in equilibrium with minerals in the system.

The general pattern of changes that the fluid components undergo as the amount of seawater increase is very similar to the changes noted in the real data from the Miller Field. In fact, Fe^{2+} is the only ion that shows a different change to the one predicted (see Figure 4.19 and Figure 4.14). This implies that the assumption of seawater influence is reasonable and that fluids and minerals in the real system are, for the most part, reaching equilibrium in the way predicted by the GWB model.

There is more variation in the Ca^{2+} concentration in the model, over a wider range of values, than shown by the real data. This suggests that Ca^{2+} is more successfully buffered by calcite (or other Ca-bearing minerals) in the real system. Ba^{2+} persists in solution for longer in the real data, indicating that the precipitation of barite is delayed or slower than that predicted. K^{+} does not show a smooth variation in the real data, but rather fluctuates, but this is most likely due to contamination by K-rich drilling mud.

4.6.3.3 *Changes in injected seawater composition*

The dramatically elevated Fe and Si concentrations in seawater in the real data (Figure 4.16) are indications of rapid water-rock reactions that affect these fluid components but not others. The fact that sulphate is so high suggests that anhydrite has not precipitated as seawater heated in the reservoir, even though it should be supersaturated (e.g. Figure 4.18.). The increased levels of Fe^{2+} and SiO_2 indicate that the water has come to equilibrium with Fe-bearing (silicate) phases or Fe-sulphide phases; this is also not predicted by the model. It is likely that these changes are affected by kinetic limitations. Thus, the GWB model is not sufficient to describe in detail all the reactions occurring in the real system.

4.6.4 Modelling other fields

The GWB model of water mixing in the Miller Field has been shown to adequately describe the most important processes occurring in the reservoir as a result of seawater injection. Miller is in close geological association with the Central and South Brae oil fields and consists of the Brae Formation sandstone. It is therefore reasonable to assume that these fields will have undergone a similar set of diagenetic processes to Miller and that the same model applied to their respective formation water compositions would yield similar results. Conversely, the Ekofisk Field (also in the North Sea) has a reservoir consisting of Cretaceous and Danian age chalks of

the Ekofisk and Tor Formations (Warren and Smalley, 1994), and would therefore be expected to yield substantially different results.

The same "water-mixing including water-rock interaction" model was applied to each alternative reservoir, with only very few alterations made to accommodate the differences in reservoir mineralogy.

1) Central Brae. Figures 4.22 and 4.23 show the results of such a model applied to the Central Brae Field. Alterations made to the basis of this version of the model include: illite remaining undersaturated (Table 4.4) to prevent the water becoming too supersaturated. The figures show some striking similarities to the Miller model, with some notable exceptions.

The constant level of Fe^{2+} ions is partly a reflection of the fact that seawater contains a similar amount of these ions to the formation water. The more significant presence of iron in this case however, has caused siderite to precipitate on the reaction of Fe^{2+} ions with HCO_3^-. It is also reflected in the precipitation of the clays annite and nontronite, which both contain iron, and pyrite. Mg^{2+} ions can be seen to increase. This is because seawater contains significantly more magnesium than the formation water, although the precipitation of Mg-bearing nontronite is probably causing the increase of Mg^{2+} ions to be slowed.

As in the Miller example, the precipitation of alkali feldspar appears to be intimately linked with the precipitation of muscovite, and both of these are linked with the amount of K^+ in solution. The K^+ component of the fluid remains almost steady as the reaction progresses and seems to be buffered by the changing amounts of potassium-bearing minerals present. The variation in the proportions of K-feldspar and muscovite are probably due to the availability of Al^{3+} ions in solution.

Despite any differences, the fundamental reactions appear to have remained the same and most of the other ions in the fluid, particularly Ba^{2+} and SO_4^{2+}, follow precisely the same patterns as in the Miller example.

The implication of these observations is that, if the original model was realistic, the reactions occurring in Miller and Central Brae must be very similar, with only a few exceptions. This would be a reasonable conclusion to draw, as the two fields are contained within the one Upper Jurassic Brae Formation.

2) Ekofisk. Figures 4.24 and 4.25 show the results of applying the mixing model to the Ekofisk Field. As for Central Brae, very little was changed from the original model, but again illite was not set to be saturated and the temperature was significantly higher at 162°C (Table 4.4).

The results are clearly different to those from the previous examples, though some similarities persist. The Na^+, K^+, Sr^{2+}, Mg^{2+} and Ca^{2+} components of the fluid all behave in a similar way to the Miller model, however, the trend for the Fe^{2+} ions is the reverse of that exhibited by the Miller and Central Brae examples, reflecting the very low levels in formation water relative to seawater. Other big differences are in the HCO_3^-, Ba^{2+} and SO_4^{2-} concentrations.

Though the overall trend of an increase in SO_4^- and a decrease in Ba^{2+} can still be observed, these two fluid components show none of the distinctive variation pattern of the Miller and Central Brae experiments. Instead, Ba^{2+} ions behave in the same way as Sr^{2+}, reflecting the low levels of barium in seawater, and SO_4^{2-} ions increase at a steady rate. In addition, very little barite forms, and only at the beginning of the mixing process, while sufficient Ba^{2+} ions are still available. For the first time, celestite ($SrSO_4$) is observed, and its mode of precipitation mirrors that of barite. This is because at Ekofisk there is much more Sr^{2+} than Ba^{2+}, whereas at Miller and Central Brae there is only slightly more Ba^{2+} than Sr^{2+}. The excess Sr at Ekofisk is probably due to the substitution of Sr into the abundant calcite of the chalk.

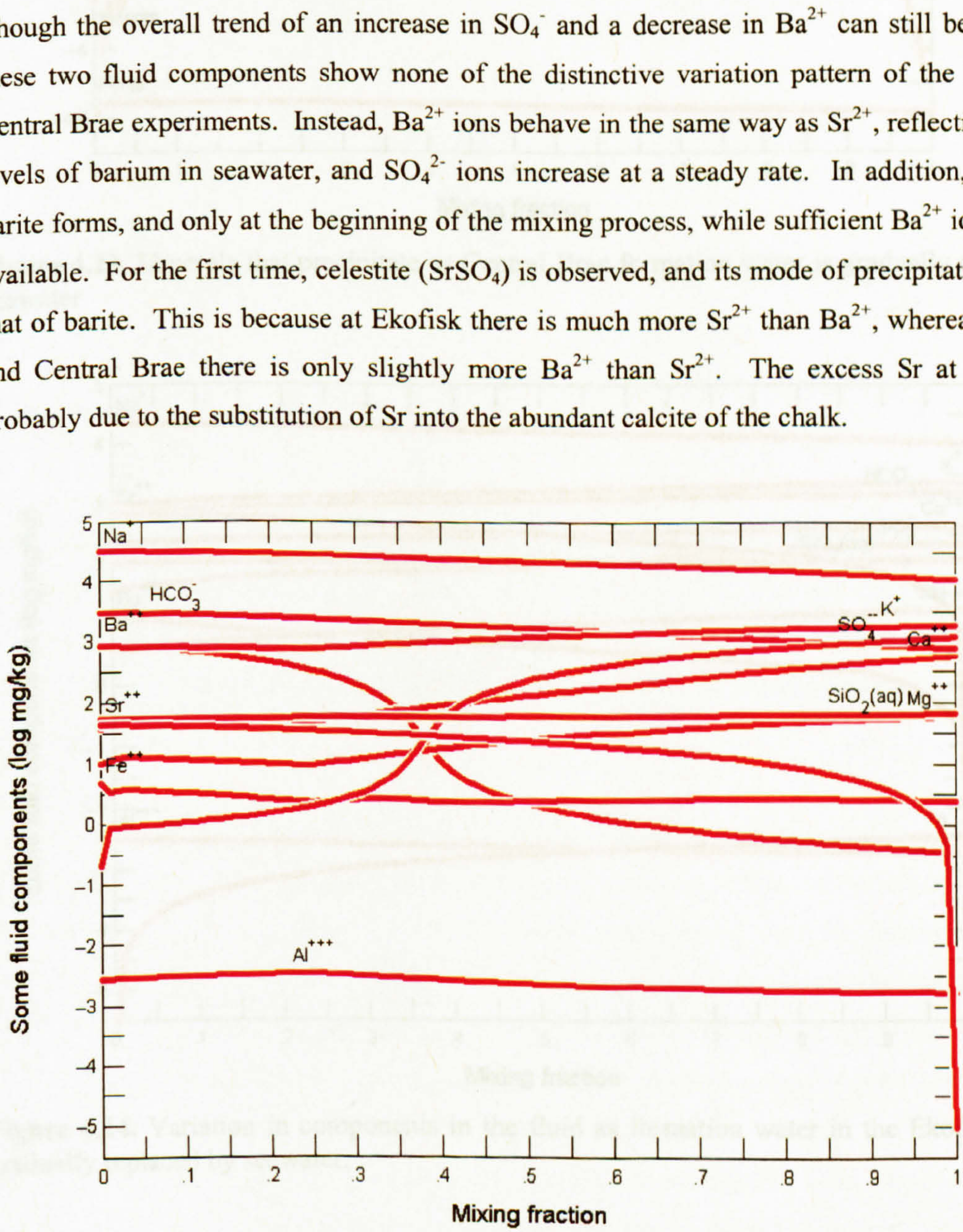

Figure 4.22. Variation in components in the fluid as formation water in the Central Brae Field is gradually replaced by seawater.

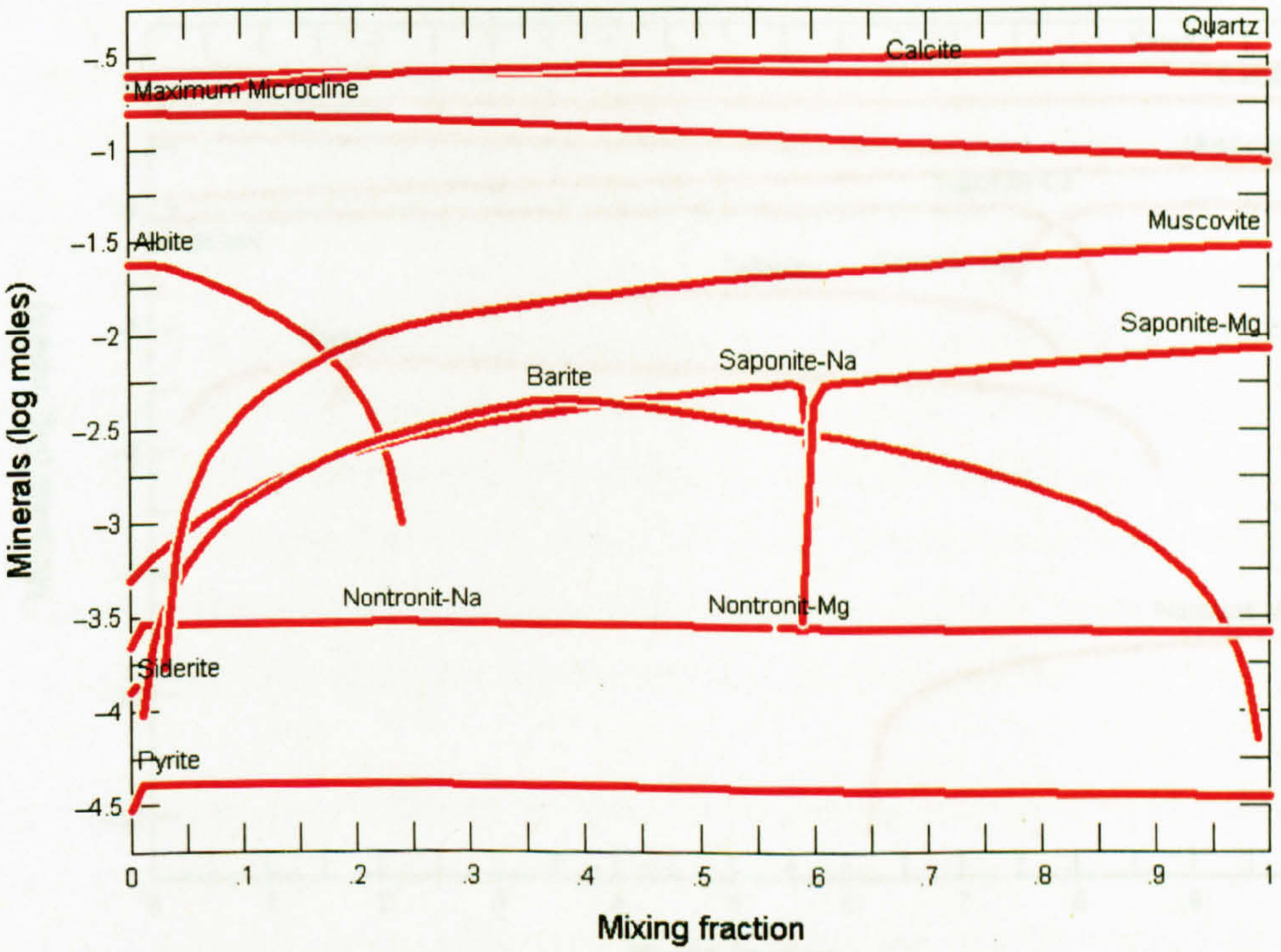

Figure 4.23. Minerals that precipitate as Central Brae formation water is gradually replaced by seawater

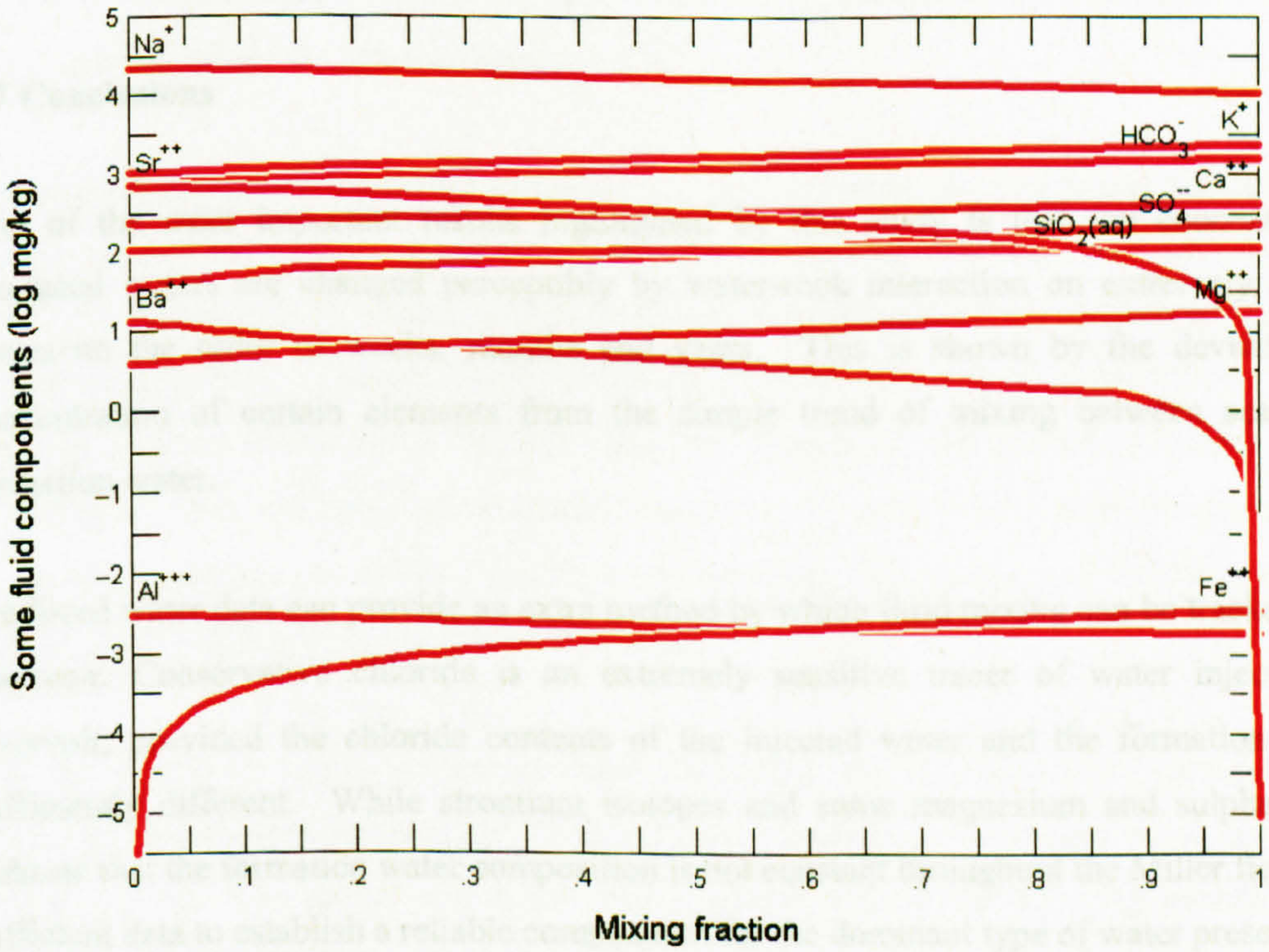

Figure 4.24. Variation in components in the fluid as formation water in the Ekofisk Field is gradually replaced by seawater.

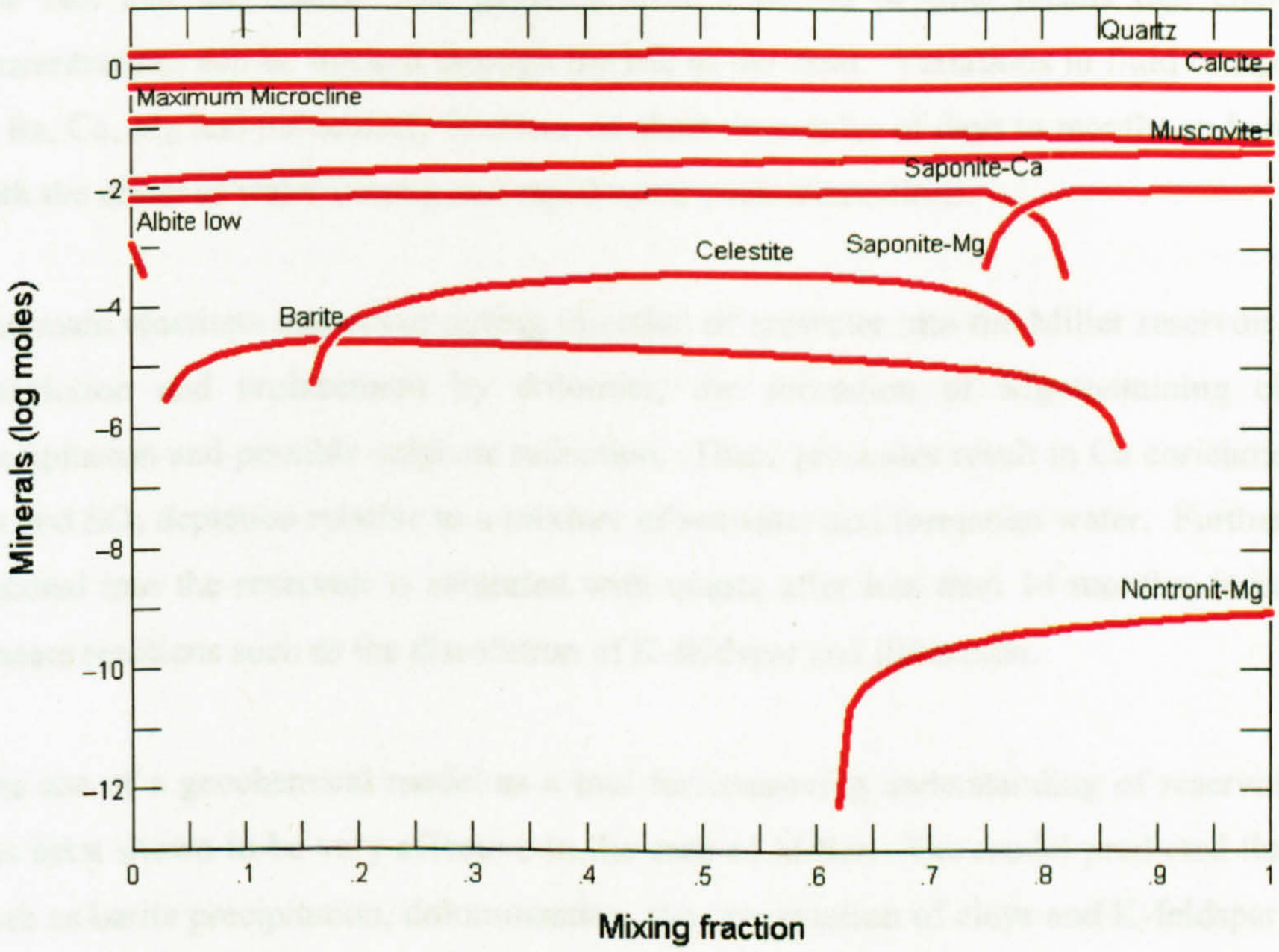

Figure 4.25. Minerals that precipitate as Ekofisk formation water is gradually replaced by seawater

4.7 Conclusions

One of the most important results highlighted by this study is that ion concentrations of produced waters are changed perceptibly by water-rock interaction on extremely short time scales on the order of weeks, months and years. This is shown by the deviation of the concentration of certain elements from the simple trend of mixing between seawater and formation water.

Produced water data can provide an extra method by which fluid mixing can be tracked within a reservoir. Conservative chloride is an extremely sensitive tracer of water injected into a reservoir, provided the chloride contents of the injected water and the formation water are sufficiently different. While strontium isotopes and some magnesium and sulphate outliers indicate that the formation water composition is not constant throughout the Miller field, there is sufficient data to establish a reliable composition for the dominant type of water present.

Deviation of measured produced water analyses from linear mixing lines constructed between the two fluids of differing chloride concentration (formation water and injected water) indicates specific fluid-mineral interactions are occurring in the reservoir and/or well bore.

The fact that the dataset was gathered over a period of time means that changes in ion concentrations can be tracked through the life of the field. Variations in fluid components such as Ba, Ca, Mg and particularly Si occur on short timescales of days to months and are a result of both the effect of water mixing and rapid water-rock interactions.

The main reactions that occur during injection of seawater into the Miller reservoir are: calcite dissolution and replacement by dolomite; the formation of Mg-containing clays, barite precipitation and possible sulphate reduction. These processes result in Ca enrichment and Mg, Ba and SO_4 depletion relative to a mixture of seawater and formation water. Furthermore, fluid injected into the reservoir is saturated with quartz after less than 14 months, indicating rapid silicate reactions such as the dissolution of K-feldspar and illitisation.

The use of a geochemical model as a tool for improving understanding of reservoir processes has been shown to be very effective in the case of Miller. The model predicted that processes such as barite precipitation, dolomitisation, the precipitation of clays and K-feldspar dissolution should occur at Miller reservoir conditions in response to injection of seawater, supporting the hypotheses established from the measured data. In addition, the model has highlighted potential reactions for which there is no evidence in the real dataset, including albitisation of K-feldspar and reactions involving iron-bearing minerals.

Discrepancies between the model-predicted and real behaviour of certain ions (including Ca, Ba and K) are due to reactions in the real system that the model cannot account for. For example, extensive buffering by Ca-bearing phases, slowed precipitation of barite and contamination by K-rich drilling mud. Though GWB modelling supports evidence of water-mixing and water-rock interactions provided by the real data, the success of any model is limited by kinetic constraints. For example, when heated, seawater, in equilibrium with quartz, calcite and hematite, is predicted to precipitate anhydrite; however, data from a real field suggest that this has not occurred, likely due to kinetic limitations.

The model can be easily applied to other water-rock systems with only very few changes, providing a potential method for predicting the reaction of a system to a certain set of circumstances. The model output for these systems reflects the differing mineralogy of the reservoir rock. The model for Central Brae predicted that important reactions would be: the formation of ferro-magnesian clays, reaction between K-feldspar and muscovite and barite equilibrium. At higher temperatures and with a predominantly carbonate mineralogy, the Ekofisk field was predicted to behave somewhat differently. Significant carbonate dissolution

increases the bicarbonate concentration of the water and celestite instead of barite is precipitated.

Though processes such as clay formation and calcite dissolution are described fairly commonly as a feature of diagenesis, it is the speed with which these reactions are documented in Miller that make them particularly interesting. Fast formation of mineral precipitates has been long documented (for example, the formation of barite scale in oilfield production pipes). The field rate of silica release documented here is relevant to the field rate of feldspar-fluid reactions, irrespective of whether silica in the produced Miller fluids is derived from feldspar or quartz dissolution, because it shows the rate at which water can interact with silicate minerals at the field scale.

The detailed mineralogical, chemical and modelling case study of the Miller field provides an insight into the chemical reactions occurring in a typical petroleum reservoir. This information will supplement the global dataset and contribute to the overall understanding of the controls on formation water composition in petroleum reservoirs.

C. GLOBAL DATA ANALYSIS

5. FORMATION WATERS: A GLOBAL SYNTHESIS

5.1 Introduction

Chapter 2 outlined ten closely associated factors which might affect the composition of formation waters (section 2.3). Interaction of formation waters with host rocks (dependent on temperature, pressure, gas partial pressure etc) has been shown to be particularly important in controlling their chemical compositions. It is this that causes the global variation in formation waters from sedimentary basins. The question remains however, whether water-rock interactions as described by authors such as Hanor, Land etc are widely applicable in different geological settings.

The formation water reflects the current mineralogical make-up of the rock; while the geological history of the area may have affected the initial composition of the water and therefore subsequent water-rock reactions. Thus, it is expected that the formation water of a specific rock formation, reservoir or sedimentary basin can be distinguished from waters from other locations. Detailed studies of the San Juan Basin in West Central US and the Miller field in the North Sea (Chapters 3 and 4) have provided new examples of how both natural processes as well as those occurring during the extraction of petroleum can affect specific formation water chemistry. Elevated absolute concentrations of Na in San Juan formation waters have been shown to be the result of interaction with Na-rich smectites. The observation of constant concentrations of Si in waters produced from wells in Miller indicated rapid reaction of water with feldspars and clays. It is important to understand whether these sorts of processes are occurring elsewhere and can be used to interpret water chemistry. In particular, whether having knowledge about the mineralogy of a source rock will enable predictions to be made about the nature of the formation water chemistry.

5.1.1 *Aims and objectives*

The principal objective of this study is to evaluate further the degree to which formation water compositions reflect water-rock interaction processes. That is, to determine the extent to which buffering by certain specific mineral assemblages will account for the observed chemical variation in subsurface pore waters. The study aims to identify and isolate specific mineral-fluid equilibria and assess the relative importance of each in controlling the water compositions from a range of global locations. It is based on water analyses from nine different locations on five continents. Detailed mineralogical information is available for some, but not all of the host formations; identifying links between water chemistry and mineralogy in data-rich areas will assist as a predictive tool in mineralogically data-poor areas. To realise the full information-providing potential of such an extensive dataset it is necessary to identify the relative roles of a

series of different controlling factors. Each individual aspect of water chemistry is best described separately in terms of its possible mineralogical associations, applications and implications. A further objective is to evaluate the influence of mineral-water interaction controls on the practical applications of mineral scaling and CO_2 sequestration. This study adds an extra dimension to the current understanding of formation waters by analysing data from a wide range of contrasting sedimentary basins from around the world.

As a framework for the following discussion, the most important processes affecting the dominant fluid characteristics will be explained in terms of the evolution of a typical formation water. Initially, water buried with sediment already has some inherited characteristics and in time these are modified by detrital mineral-fluid interactions, secondary mineral precipitation and fluid mixing. Although water released through the compaction of shales during diagenesis may have an impact on formation water chemistry, this aspect of the subject is beyond the scope of this study because suitable data is not generally available. An introduction to the dataset will instead be followed by a description of: the origins and importance of inherited salinity; the effects of mineral buffers on the major element composition of formation waters, in particular potassium, sodium, calcium and magnesium; the influence of mixing, including through-flowing and injected waters and the imposition of CO_2 pressure by a coexisting gas.

5.2 Data and data quality

To identify global empirical trends, the dataset must span a wide range of water and rock compositions and be as representative of as many different geological situations as possible. Fortunately, there is a large amount of formation water data in the literature. For this study an extensive propriety database of pore water chemistry was provided by BP and combined with the secondary databases of Bennett (2001) and Yardley (2005), who compiled and published formation water compositions from several geological settings. This has produced an extensive global database of petroleum reservoir formation water chemistry presented in Appendix VI. In addition, the geological setting, history and mineralogical composition of each location for which there is formation water information has also been collated (Appendix VII).

A list of locations included in the database is presented Table 1. The data from each reservoir comprises analysis of various cations and anions. Information relating to TDS, temperature, depth, pressure, pH and isotopic composition is also available in some cases. Elements analysed for in all reservoirs include: Na, K, Mg, Ca, Ba, Cl, and SO_4, commonly with Sr, Si, Br, HCO_3, transition metals and pH. In general however no redox pairs have been analysed.

5.2.1 Data quality

The quality of the data is variable. In many cases, the samples were collected from the water-leg of a separator, but some were collected from the well-head directly, some from repeat formation testers and still other samples are from drill-stem tests. A key problem in quality control is the stability of the sample. Down-hole (and sometimes well-head) samples may precipitate minerals when cooled and degassed for analysis (Collins, I. 2006, pers.comm.) In some cases analyses were carried out over 30 years ago and it is likely that analytical techniques will have improved since then, influencing detection limits at least. In addition, samples from many producing oil and gas fields will have been analysed under operational conditions in production facilities, where emphasis may have been on getting certain valuable information quickly rather than general high quality analysis. It should be noted that some high values can be attributed to contamination of water samples by drilling muds containing a KCl additive, as is common in the North Sea and elsewhere (I. Collins, pers. comm.).

Significant data outliers were rejected from the dataset and all the analyses were subject to charge balance testing. In this way, only the best data were selected to be included in the global synthesis, minimising the possibility of sampling or analytical artefacts. Analytical techniques range from simple titration tests, atomic absorption spectroscopy (AA), inductively coupled plasma – atomic emission spectroscopy (ICP-AES) to ion chromatography. This leads to some discrepancy between the accuracy of different fluid analyses and introduces an element of uncertainty into the data analysis results. Details of analytical techniques are available for some, but not all, of the published water analyses in the original papers cited in Appendix VII.

Some components of reservoir systems play an extremely important role in subsurface reactions, but are very difficult to analyse accurately. Notably, the concentration of bicarbonate ions is directly related to carbonate equilibria and the partial pressure of CO_2, but is affected during sampling as CO_2 can outgas from solution as pressure is reduced during transportation of the fluid to the surface (Carpenter and Miller, 1969; Hutcheon *et al.*, 1993). Uncertainty in bicarbonate values also impacts on pH estimates (Hutcheon *et al.*, 1993), while in addition redox couples are not generally analysed. Instead total sulphur is analysed as sulphate, although there is potential for H_2S degassing alongside CO_2 loss.

It is nonetheless possible to identify general trends among formation waters from different studies by analysing the fluid compositions using simple spreadsheet-produced plots. Anomalies can be identified and interpreted in the context of fluid-rock interactions as discussed in the previous chapters. Cross plots of one ion with another can highlight specific reactions occurring in the reservoir because the constituents of formation waters are subject to fluid-fluid or fluid-rock interactions, (Huseby *et al.*, 2005). The effectiveness of this method has been

illustrated to some extent in the San Juan and Miller case studies (Chapters 3 and 4), but this Chapter provides an insight into whether it can be applied on a global scale.

5.2.2.1 *Geochemical computer modelling of formation waters*

Representative analyses from each location in the global database were subject to thermodynamic analysis using the computer model REACT, as part of the Geochemists' Workbench (GWB) (Bethke, 1996). REACT is a reaction path model that allows the user to specify a particular fluid composition. When no reaction path is required, the programme simply determines the speciation of all the fluid components originally specified, using one of several thermodynamic databases to calculate the activity of each species. The fluid can then be allowed to come to equilibrium at a specified temperature by the precipitation of minerals until the fluid is at equilibrium. For waters of low ionic strength, the *Debye-Huckel* activity model is usually sufficient to provide accurate determinations of water speciations. However, more concentrated solutions are usually better served by using the *Pitzer* equations. Unfortunately, the *Pitzer* database at elevated temperatures is extremely limited and could not account for some important components present in most of the waters e.g. bicarbonate and aqueous silica species.

The speciations of the pore waters were calculated because this is important when calculating the extent of supersaturation of individual minerals. For example, measured Ca in solution could be a mixture of Ca^{2+}, $CaCl^{+}$, $CaHCO_3^{+}$, $CaOH^{+}$, $CaCO_3$, $CaSO_4$ etc, so it would be unreliable to calculate the equilibrium state with respect to calcite by assuming that the Ca analysed was all Ca^{2+}. Unfortunately, some uncertainties remain. For example, the high salinity waters had to be speciated using the *Debye-Huckel* activity equations due to the limitations of the *Pitzer* database. In addition, there are considerable doubts surrounding the accuracy of pH measurements from formation waters due to the potential effects of degassing of CO_2 on release of pressure. Mineral saturation states depend on the relevant cation/hydrogen ratio and inaccurate pH values can lead to significant mistakes in speciation and cause the model to predict incorrectly that certain minerals are saturated. Carbonate species and associated minerals are particularly at risk of misinterpretation due to inaccurate pH values. In some cases pH measurements do not exist at all and in these cases it was necessary to use to the model to calculate pH itself by equilibrium with mineral assemblages thought to be present in the reservoir rock. Despite the limitations, use of the speciated compositions have allowed the saturation states of waters of very different TDS and chemistry to be compared in a quantitative manner.

Following page: **Table 5.1** Representative water analysis from each major location studied together with the calculated speciated concentrations based on the original analysis without any precipitation of saturated solids. Values are in Moles and only species with concentrations greater than 1×10^{-5} are shown. Several water analyses were speciated for each field, and the results for these are shown in raw form in Appendix VIII.

	Alberta Younger		Alberta Older		Angola		Azerbaijan		Central Mississippi		Colombia		Mahakam		GOM 1		GOM 2		GOM 3		Offshore Louisiana		Onshore GOM		San Juan	
	Measured	Speciated	Measured	Speciated	Measured	Speciated	Measured	Speciated	Measured	Speciated	Measured	Speciated	Measured	Speciated	Measured	Speciated	Measured	Speciated	Measured	Speciated	Measured	Speciated	Measured	Speciated	Measured	Speciated
Na+	1.4E+00	1.0E+00	1.6E+00	1.6E+00	2.1E+00	2.0E+00	2.9E-01	2.8E-01	2.6E+00	2.0E+00	8.7E-02	8.7E-02	2.2E-01	2.1E-01	5.3E+00	4.6E+00	3.1E+00	2.9E+00	5.9E-01	5.8E-01	1.3E+00	1.2E+00	1.4E+00	1.3E+00	1.1E-01	1.1E-01
NaCl		2.5E-02		4.3E-02		1.3E-01		2.2E-03		6.1E-01		3.5E-04		9.2E-04		7.8E-01		2.3E-01		9.2E-03		4.6E-02		1.6E-01		2.3E-04
NaSO4-		7.4E-05		4.9E-03				2.2E-05				1.6E-05				7.2E-04		3.0E-04		2.0E-04		1.2E-05				
NaHCO3						1.4E-03		3.1E-03				1.0E-04		4.5E-03		7.4E-04		4.7E-04		2.0E-03		5.9E-04		4.8E-05		1.4E-03
NaCO3-								2.5E-05												1.1E-05						
K+	2.6E-02	9.5E-03	4.9E-02	2.8E-02	8.5E-03	8.2E-03	2.3E-03	2.3E-03	2.3E-01	2.1E-01	8.9E-04	8.9E-04	1.4E-03	1.4E-03	1.7E-02	1.6E-02	3.1E-02	2.9E-02	3.3E-03	3.3E-03	4.7E-03	4.6E-03	1.6E-02	1.5E-02	2.6E-04	2.6E-04
KCl		1.6E-04		6.2E-04		3.3E-04				2.1E-02						1.5E-03		1.6E-03		3.5E-05		1.1E-04		5.4E-04		
KSO4-				1.1E-04																						
Li+	3.2E-03	1.7E-03	5.3E-03	3.5E-03											3.9E-04	3.9E-04	2.6E-03	2.5E-03			5.0E-04	5.0E-04				2.3E-04
Mg++	7.7E-02	7.9E-03	7.6E-02	5.3E-02	3.2E-02	2.6E-02	2.9E-04	2.1E-04	1.6E-01	6.6E-02	6.2E-04	5.9E-04	2.5E-03	1.8E-03	1.1E-01	4.4E-02	3.6E-02	1.9E-02	1.1E-03	8.8E-04	2.4E-02	1.7E-02	1.9E-02	1.2E-02	6.3E-04	5.1E-04
MgCl+		2.4E-03		3.1E-02		1.2E-02				9.5E-02		2.5E-05		1.1E-04		6.2E-02		1.7E-02		1.6E-04		6.3E-03		6.3E-03		2.6E-05
MgSO4				1.8E-03												8.4E-05		2.3E-05								
MgHCO3+						2.5E-04		4.8E-05				1.4E-05		5.9E-04		1.1E-04		3.5E-05		5.7E-05		1.7E-04		3.7E-05		7.8E-05
MgCO3												1.5E-05		2.5E-05						1.1E-05						1.4E-05
Ca++	1.2E-01	1.5E-02	1.6E-01	5.7E-02	1.6E-01	7.6E-02	8.4E-04	5.1E-04	9.9E-01	3.8E-01	1.0E-02	8.3E-03	2.5E-03	1.6E-03	3.1E-01	9.0E-02	2.1E-01	7.6E-02	4.5E-03	3.1E-03	5.1E-02	3.1E-02	1.0E-01	6.4E-02	1.1E-03	8.2E-04
CaCl+		9.1E-03		7.7E-02		8.2E-02		9.2E-05		6.2E-01		8.6E-04		2.2E-04		2.2E-01		1.3E-01		1.1E-03		2.0E-02		4.1E-02		8.3E-05
CaSO4		1.2E-05		1.7E-03								3.3E-05				1.6E-04		8.4E-05		1.4E-05						
CaHCO3+						1.1E-03		1.7E-04				3.4E-04		7.9E-04		2.4E-04		1.5E-04		2.6E-04		3.7E-04		2.1E-04		1.8E-04
CaCO3								7.2E-05				4.9E-04		4.2E-05						6.9E-05						4.4E-05
CaOH+																										
Sr++	2.1E-03	1.8E-03	2.4E-03	2.3E-03	4.2E-03	4.1E-03	4.1E-05	2.1E-05	1.9E-02	1.9E-02	3.6E-04	3.1E-04			4.8E-03	4.8E-03	2.3E-03	2.3E-03	3.7E-04	3.0E-04	7.7E-04	7.4E-04	6.2E-03	6.2E-03	1.8E-04	1.3E-04
SrSO4				5.2E-05																						
SrHCO3+						1.3E-04						3.2E-05				2.8E-05				5.9E-05		2.1E-05		8.9E-05		5.1E-05
Ba++	5.6E-04	5.6E-04	8.2E-06	7.7E-06	3.3E-03	3.1E-03	2.2E-05	2.2E-05	6.3E-04	6.3E-04	1.4E-04	1.4E-04			1.5E-03	1.5E-03	1.5E-04	1.5E-04	1.2E-04	1.2E-04	3.2E-04	3.2E-04	4.4E-03	4.4E-03	2.1E-04	2.1E-04
Fe++	5.0E-06		4.8E-06		1.9E-04	1.9E-05	9.1E-05		2.3E-03						2.7E-03	7.6E-05	2.5E-03	1.9E-04	8.5E-04	2.3E-04	3.5E-04	4.4E-05			2.7E-06	
FeCl+						1.2E-04				1.3E-03						1.3E-03		1.4E-03		5.5E-04		2.5E-04				
FeCl2						5.0E-05				9.4E-04						1.3E-03		9.2E-04		5.9E-05		5.6E-05				
Mn++	2.0E-05	2.0E-05	3.5E-06						1.9E-04	1.9E-04					4.0E-04	3.9E-04					2.4E-05	2.3E-05				
Zn++			0.0E+00				3.1E-05		1.0E-04						8.3E-05						8.3E-07					
ZnCl4--										9.5E-05						7.7E-05										
Ca++																										
CaCl3-								2.4E-05																		
SiO2															7.9E-04	7.9E-04	3.2E-04	3.2E-04			7.8E-04	7.7E-04	1.9E-03	1.9E-03	2.6E-04	2.5E-04
Cl-	1.8E+00	1.1E+00	1.9E+00	1.5E+00	2.5E+00	2.3E+00	2.4E-01	2.4E-01	5.2E+00	3.8E+00	1.0E-01	1.0E-01	1.6E-01	1.6E-01	6.1E+00	5.1E+00	3.6E+00	3.2E+00	5.9E-01	5.8E-01	1.4E+00	1.3E+00	1.6E+00	1.5E+00	8.3E-02	8.3E-02
Br-	3.2E-03	1.7E-03	4.4E-03	3.6E-03			5.5E-04	5.5E-04	3.4E-02	3.4E-02							1.0E-03	1.0E-03	1.1E-03	1.1E-03	1.1E-03	1.1E-03	8.4E-04	8.4E-04		4.8E-05
I-																			2.2E-04	2.2E-04		2.0E-04				
SO4--	1.2E-02	9.4E-05	1.1E-02	5.1E-03	1.3E-04		7.8E-05	5.6E-05			1.4E-04	9.1E-05	4.0E-05	2.9E-05	1.2E-03	2.5E-04	5.8E-04	1.7E-04	5.6E-04	3.4E-04	3.2E-05	1.4E-05	1.8E-05		1.6E-05	1.2E-05
HCO3-					5.7E-03	2.8E-03	4.9E-02	4.4E-02			5.2E-03	4.1E-03	7.9E-02	6.3E-02	1.3E-02	5.6E-04	6.5E-03	4.9E-04	1.8E-02	1.4E-02	3.4E-03	2.3E-03	3.0E-03	4.8E-04	3.2E-02	2.8E-02
CO3--								5.4E-04				1.2E-04		1.1E-04						1.4E-04						1.6E-04
CO2(aq)								1.1E-03				3.9E-05		1.0E-02		1.1E-02		5.4E-03		5.5E-04				2.1E-03		1.1E-03
OH-		1.1E-05						2.4E-05				7.0E-05								1.4E-05						
pH	7.7		6.1		6.1		7.8				8.3		7		5		5.2		7.6				5.9			

Table 5.2. Summary of locations for formation waters included in the global database

Location	Age of host rocks	Reservoir	Major rock type	Reference
Alberta Basin, Canada	Devonian to Cretaceous	Southesk-Cairn carbonate complex;	Carbonate with some sandstone	Connolly *et al.* 1990
Angola, offshore, North of Luanda	Late Cretaceous to Oligocene	Bucomazi petroleum system	Lacustrine and turbiditic sediments	BP (currently producing)
Azerbaijan –Field 1	Late Mesozoic to Cenozoic	Productive Series (Pereiva Suite)	Immature sandstone	BP (currently producing)
Azerbaijan – Field 2	Late Mesozoic to Cenozoic	Productive Series (Pereiva Suite)	Immature sandstone	BP (currently producing)
Central Mississippi	Jurassic and Cretaceous	Norphlet, Smackover and Hosston formations	Sandstones of varying compositions	Carpenter *et al.* 1974
Colombia, Llanos Basin	Late Cretaceous to Eocene	Guadalupe, Mirador and Barco formations	Relatively clean sandstone	BP (currently producing)
Mahakam Basin, Indonesia	Miocene/Pliocene	/	Channel sands	Bazin *et al.*, 1997
North Sea	Devonian to Eocene	Various	Sandstone and carbonate	Warren & Smalley. 1994; Egeberg and Aagaard, 1989
Offshore Gulf of Mexico	Pliocene and Miocene	/	Sandstone + salt, turbidite sands	BP (currently producing)
Offshore Gulf of Mexico – Offshore Louisiana	Jurassic to Miocene	Louann Salt, Norphlet and Smackover Formations, Haynesville Formation and Cotton Valley Group.	Sands + salt	Land *et al.*, 1988
Onshore Gulf of Mexico – Texas Gulf Coast	Oligocene/Micocene	Frio Formation	Muddy sandstone	Hyeong and Capuano, 2001; Kharaka *et al*, 1977
San Juan Basin, Colorado/New Mexico	Upper Cretaceous	Fruitland Formation	Coal beds and muddy sandstone	BP (currently producing)

Table 5.3. Summary of main mineralogy in each location in the global database, note that for some locations information was not always readily available.

Field	Availability of information	Mineralogy
Alberta Basin Older	Readily available	• Carbonates • Bladed calcite cement • Matrix dolomite and anhydrite • Pyrite and chalcopyrite
Alberta Basin Younger	Readily available	• Carbonates, shales and evaporites • Quartz • Zeolites • Various clay minerals including kaolinite
Angola, offshore	Very limited	• Carbonates and siliciclasics
Azerbaijan, Caspian Sea	Limited	• Clastic sediments • Lithic and igneous clasts • Carbonate cemented mudstones
Central Mississippi	Readily available (various formations)	• Quartz, feldspar, dolomite, anhydrite, muscovite, kaolin, chlorite and calcite • Pyrite, celestite, fluorite • Ankerite, dikite and barite
Colombia	Limited	• Quartz • Feldspar, shale and carbonate clasts • Kaolin
Gulf of Mexico Field 1	Limited	• Sands, silts and clays • Allocthonous salt • Kaolin and illite
Gulf of Mexico Field 2	Limited	• Sands, silts and shales • salt
Offshore Louisiana	Readily available (Various formations)	• Carbonate mudstones and sands • Albitising plagioclase and K-feldspar • Authigenic calcite, quartz, chlorite, kaolinite, pyrite, siderite and barite
Onshore Gulf of Mexico	Available	• Illite-smectite • Authigenic quartz, kaolinite, chlorite, and carbonates • Albitising plagioclase
Mahakam Basin	Available	• Quartz, plagioclase and minor muscovite, K-feldspar and detrital calcite • Authigenic kaolinite, illite, quartz and dolomite
San Juan Basin	Available and personally verified	• Quartz • Detrital albite, K-feldspar, mica and lithic fragments • Authigenic siderite, dolomite • Detrital and authigenic clays and quartz overgrowths • Coal

5.2.2. Anions as the basis for water comparisons

Chloride is the most important anion in oil-field formation waters (Collins, 1969), and chlorinity provides a good approximation for salinity. Chloride is conservative in all but the most saline solutions (Hanor, 1994) and therefore presents a useful baseline with which to compare other fluid components. Inevitably, the total concentration of cations increases with increasing chloride due to charge balance constraints, emphasising its role as a master variable (Helgeson, 1969; 1970; Hanor, 1993; 1994). However, because water compositions are buffered by fluid-rock interactions, the concentration of individual cations would not be expected to increase linearly with salinity. Plots were constructed to show the variation in major cation concentration with chloride for all the locations in the global database. Although chloride is usually the main anion, in some waters bicarbonate, sulphate and even organic acids are important or even dominant anions in solution (Hanor, 1994). It was therefore useful to compare cation concentrations with TDS, bicarbonate or sulphate to identify the possible controls on these particular species. Temperature relations are important in establishing the nature of fluid-rock interaction and graphs have been constructed using temperature information wherever available.

5.3 Data Analysis: evidence for controls on formation water compositions

Formation waters from locations included in the database show an extremely wide range of dissolved loads, from as little as 230 mg/l TDS in the San Juan Basin to around 580,000 mg/l TDS in the Gulf of Mexico.

Any reference to a "representative water analysis" indicates one or two real analyses taken from the relevant dataset that are as close to the mean and modal average as possible. In some cases, a particular analysis may have been chosen because of its "typical" composition and because it provided information useful to improve the accuracy of computer modelling e.g. pH. All analyses selected as representative charge balanced to better than ± 10%, assuming that Si and Al dissolve as neutral species.

5.3.1 Inherited characteristics

5.3.1.1 *Origin of fluid salinities*

Chapter 2 presented a brief summary of the processes resulting in high salinity formation waters (section 2.4.1), the most important factors being: the nature of the depositional environment, subaerial evaporation of meteoric and marine waters and dissolution of evaporites. Conventionally, there are two ways to distinguish the origin of high salinity waters: bromide systematics and stable isotopes. Section 2.3.1 provides a detailed description of the background

to the use of bromine to distinguish high salinity fluids of different origin. Briefly, Cl is preferentially partitioned over Br into halogen salts during their precipitation and Br preferentially remains in solution until the final stages of evaporation (Rittenhouse, 1967; Hanor, 1994). Brines formed by the dissolution of halite should have a high Cl/Br ratio (Hanor, 1994; Böhlke and Irwin, 1992; Cann and Banks, 2001) whereas residual bittern brines are rich in Br. Thus, the Cl/Br ratio of formation waters indicates whether an evaporite-related fluid derived its salinity through seawater evaporation or halite dissolution (high ratios = halite dissolution; low ratios = seawater evaporation). This method of analysis is not always appropriate. For example, it may not be useful when applied to waters whose salinity is dependent on meteoric or magmatic inputs.

◆ Alberta Basin - younger (Connolly et al. 1990)
◇ Alberta Basin - older (Connolly et al. 1990)
● Angola (BP)
△ Azerbaijan - Field 1 (BP)
△ Azerbaijan - Field 2 (BP)
○ Central Mississippi (Carpenter et al. 1974)
○ Colombia (BP)
◇ Mahakam basin, Indonesia (Bazin et al., 1997)
+ North Sea - general (Warren & Smalley. 1994)
✳ North Sea - Norway (Egeberg and Aagaard, 1989)
□ Offshore Gulf of Mexico - Field 1 (BP)
□ Offshore Gulf of Mexico - Field 2 (BP)
□ Offshore Gulf of Mexico - Field 3 (BP)
□ Offshore Gulf of Mexico - Offshore Louisiana (Land et al. 1988)
△ Onshore Gulf of Mexico - Texas Gulf Coast (Hyeong and Capuano, 2001; Kharaka et al, 1977)
△ San Juan Basin, Colorado/New Mexico (BP, Snyder et al., 2003)

Figure 5.1. List of locations in global database, together with symbols used in figures. A pull-out version of this Key is included at the end of the thesis for ease of reference.

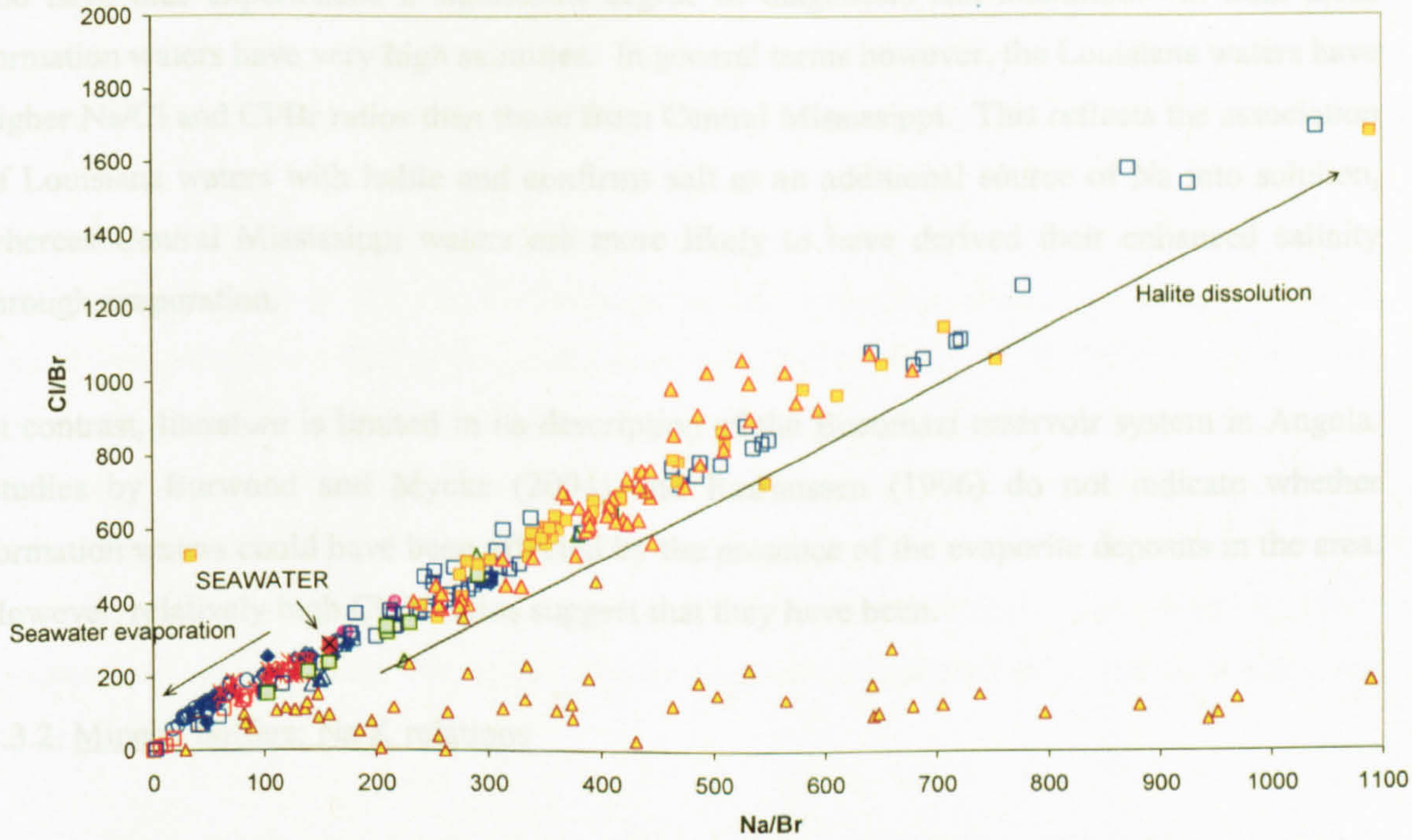

Figure 5.2. Formation waters with high Cl/Br and Na/Br ratios are interpreted to have derived salinity through dissolution of halite. Lower ratios than seawater values indicate a seawater evaporation source. Note anomalous array of San Juan with unusually low Cl/Br ratios due to influence of organics and significant sodium bicarbonate component in these dilute waters.

A plot of Cl/Br against Na/Br (Figure 5.2) thus provides a first approximation of the origin of the salinity of formation waters, seawater evaporation or halite dissolution. All the waters apart from the very low salinity ones from San Juan lie along the seawater evaporation/dissolution trend. This indicates that salinity is a primary feature of formation waters and the Cl/Br ratio is unaffected by mineral-water interactions. There is however, some susceptibility to alteration of the ratio by fluid mixing or by the addition of Br or Na from another source. For example, Figure 5.2 highlights evidence presented in Chapter 3 that waters from the San Juan Basin have unusual Br systematics with anomalously low Cl/Br ratios, likely due to high levels of Br from organics present in coal. The additional Br from this source causes some very low salinity waters to exhibit the same Cl/Br ratios as some extremely concentrated bittern brines. This is because only very small amounts of Br are required to change the ratio in a fluid that has a very low Cl content.

3.3.1.2 *Cl/Br ratios in specific locations*

The data provides a number of examples of how halide systematics may indicate the origin of a particular formation water. In particular, this method is useful because conclusions reached in data-rich areas can provide guidance on data interpretation in data-poor areas. For example, host formations from Central Mississippi (Carpenter *et al.*, 1974; Mancini, 1987) and Offshore Louisiana (Land *et al.*, 1988) are mineralogically complex, relatively old, hot and deeply buried

and have thus experienced a significant degree of diagenesis and alteration. In both areas formation waters have very high salinities. In general terms however, the Louisiana waters have higher Na/Cl and Cl/Br ratios than those from Central Mississippi. This reflects the association of Louisiana waters with halite and confirms salt as an additional source of Na into solution, whereas Central Mississippi waters are more likely to have derived their enhanced salinity through evaporation.

In contrast, literature is limited in its description of the Bucomazi reservoir system in Angola. Studies by Burwood and Mycke (2004) and Rasmussen (1996) do not indicate whether formation waters could have been affected by the presence of the evaporite deposits in the area. However, relatively high Cl/Br ratios suggest that they have been.

5.3.2. Mineral buffers: Na:K relations

Potassium is an extremely common cation in formation waters; the controls on its concentration are relatively well understood. K tends to increase with increasing Cl, however there is some significant scatter in the data (Figure 5.3). Seawater contains only relatively small amounts of K which is concentrated during evaporation until it is removed through precipitation of sylvite (KCl, Fontes and Matray, 1993). Figure 5.3 shows that at low salinities the K/Cl ratio is higher (and therefore the Na/K, lower) than at higher salinities. The higher K levels may be due to the effect of the presence of other anions e.g. sulphate.

The relationship of K with another dominant monovalent cation, Na, is also important. Chapter 2 (section 2.4.3.1) summarises the mineral equilibria that buffer K^+/H^+ and Na^+/H^+ ratios. In particular, it is important to note that the Na/K ratio is used as a geothermometer at higher temperatures (Fournier, 1979) and therefore valuable as an indicator of whether or not equilibrium is approached.

K and Na are important cations in the mineral framework of many siliciclastic petroleum reservoir. It has been suggested that the Na^+/K^+ activity ratios of geothermal waters are controlled by simultaneous equilibrium with albite and microcline (the stable K-feldspar at low temperatures) (Stefánsson and Anórsson, 2000). K-feldspar is commonly present in sedimentary systems along with small amounts of detrital and authigenic albite. In addition, clays provide an important repository for K and Na (Egeberg and Aagaard, 1989; Milliken *et al.*, 1989; Ehrenberg and Nadeau, 1989; Worden and Morad, 2000; Chuhan *et al.*, 2000). Chapter 2 (section 2.4.3.1) illustrates other mineral reactions that could affect the Na/K ratio, including kaolinitisation of K-feldspar and mica in the temperature range 110-140°C and illitisation of kaolin and K-feldspar at still higher temperatures (Smith and Eherenberg, 1989) (reactions 3, 5

and 6, chapter 2) (Aagard *et al.*, 1990; Bjørlykke *et al.*, 1995; Chuhan *et al.*, 2000; 2001). The overall increase in K concentration with Cl could therefore be due to equilibrium with K-bearing silicate minerals responding to charge balance requirements.

5.3.2.1 *Na/K ratios , the temperature effect and alteration*

K-feldspar solubility is affected by temperature and formation waters are thought to be in equilibrium with the mineral at temperatures up to 120°C (Milliken *et al.*, 1989; Chuhan, *et al.*, 2001). However, the fact that the Na/K ratio can be used as a geothermometer indicates the equilibrium also holds at higher temperatures. Stefánsson and Anórsson (2000) suggest it has not yet been convincingly demonstrated that lower temperature waters are in equilibrium with either low-albite or microcline. However, authigenic K-feldspar can form at lower temperatures, so it possible that equilibrium is approached (Aagaard *et al.*, 1990; Worden and Rushton, 1992).

Thus, authigenic K-feldspar precipitation may occur at low temperatures, decreasing the absolute K concentration in the formation water and increasing the Na/K ratio. However, this process is limited to low temperature environments and more common diagenetic dissolution-precipitation reactions related to increasing temperatures tend to release K into solution, thus reducing the Na/K ratio. The concurrent consumption of Na from solution occurring from about 65°C during albitisation in particular affects the Na/K ratio still further. The higher temperature process of illitisation then removes K from the formation water and again increases the Na/K ratio. Therefore, in formation water terms, evidence for these reactions lies in the ratios of the cations involved. Simple Alkali-feldspar equilibration should give a good correlation between Na/K and temperature, but this cannot be seen in the bulk data (Figure 5.4) in which there are over two orders of magnitude of scatter. This may be due to the additional processes occurring in the reservoir. Figure 5.5 illustrates that Na/K ratios are affected by temperature, as albite starts to become the stable feldspar phase for many waters in the database.

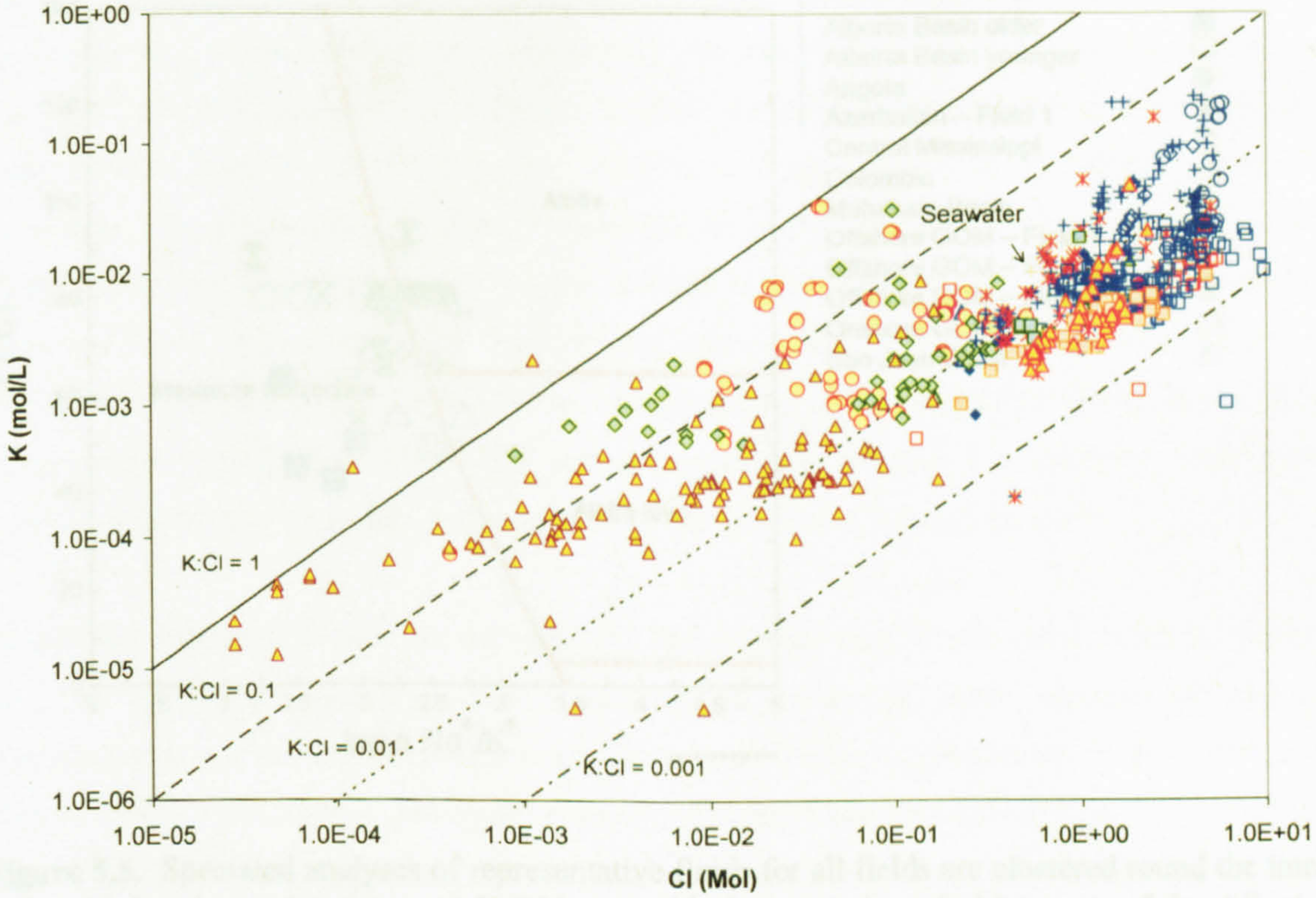

Figure 5.3. Molar concentrations of K and Cl in global formations show a positive correlation although K:Cl ratios decrease with increasing salinity.

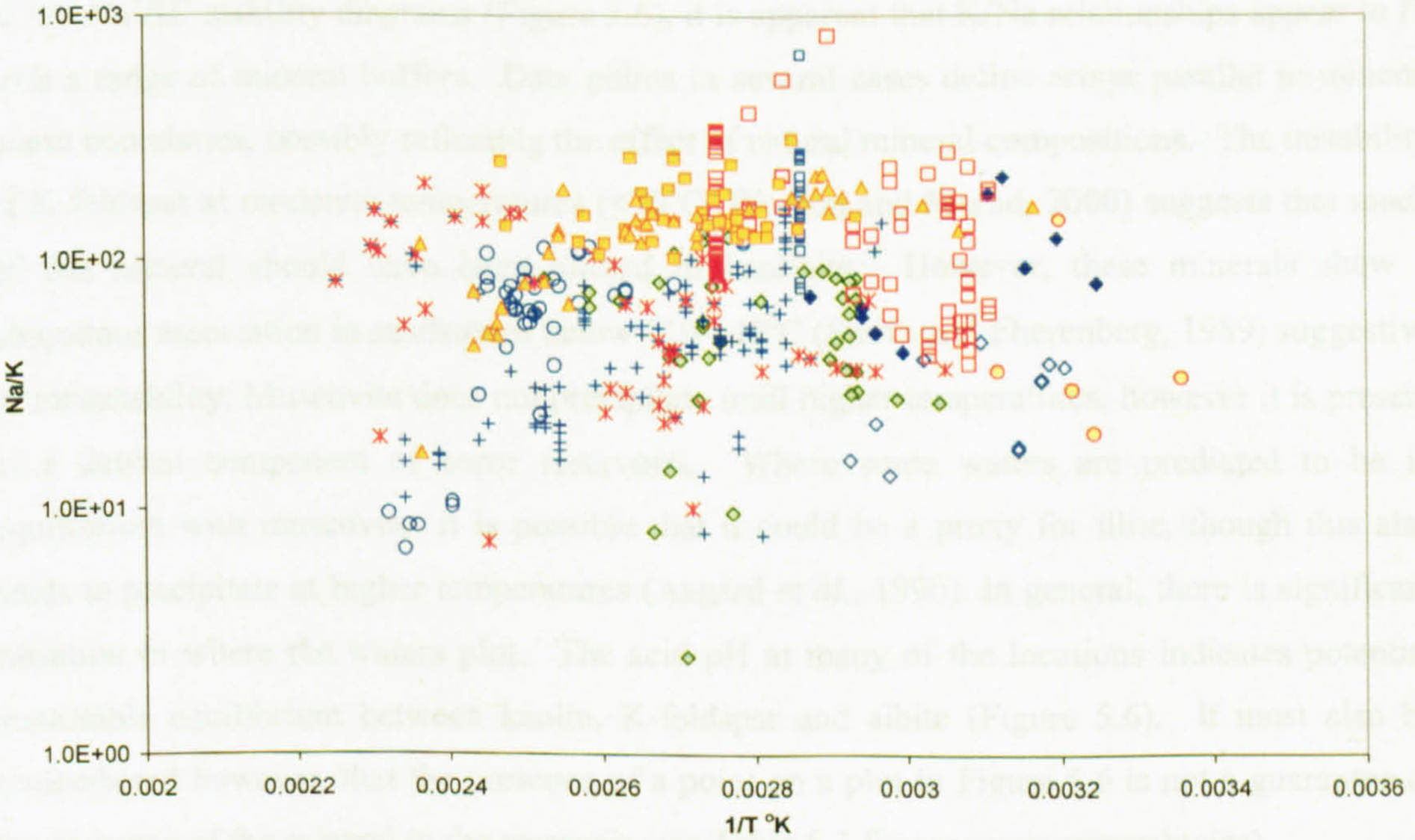

Figure 5.4. The molar Na/K ratio shows little correlation with temperature

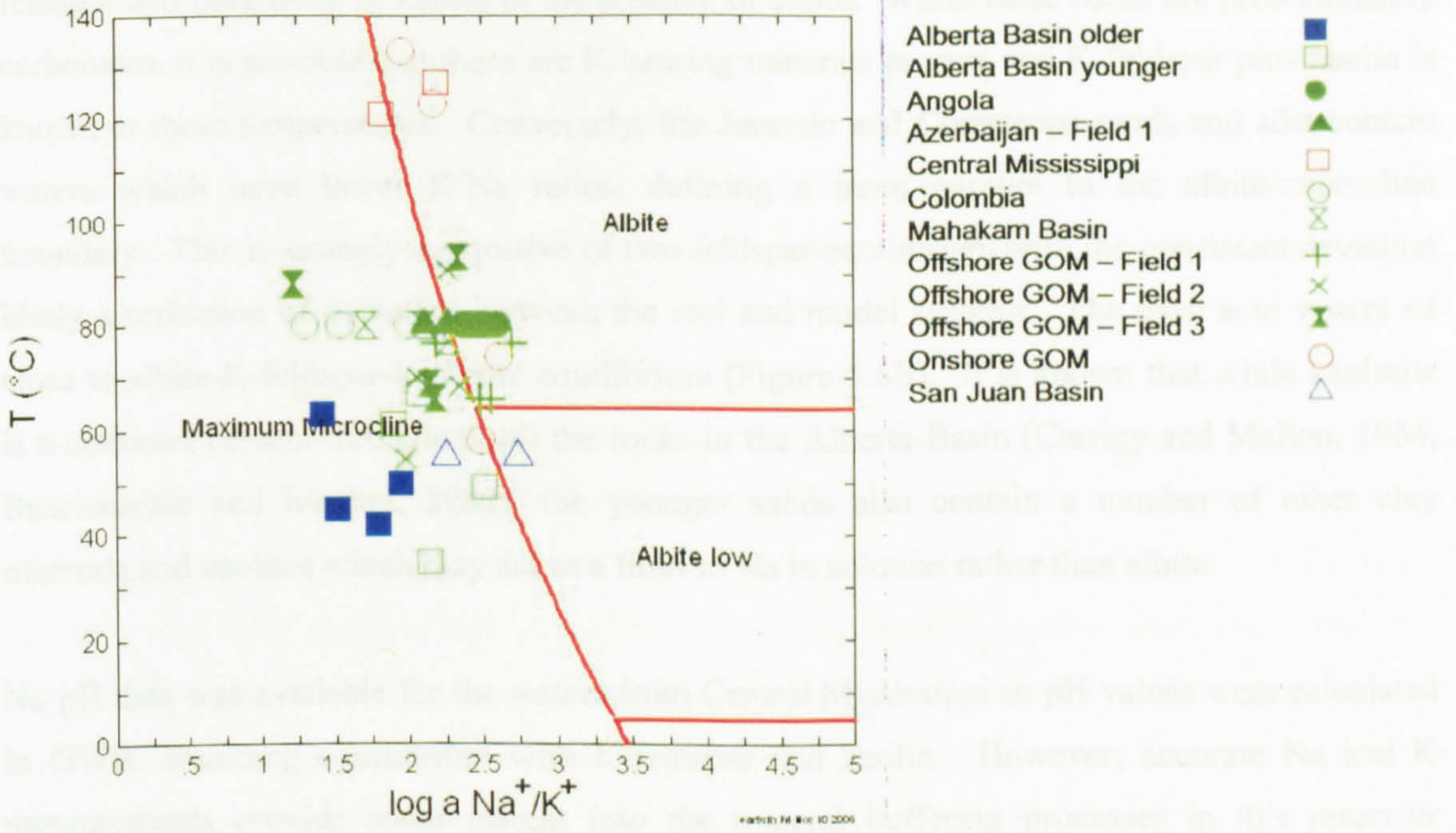

Figure 5.5. Speciated analyses of representative fluids for all fields are clustered round the line of equilibrium between albite and K-feldspar, with the exception of older parts of the Alberta Basin which are firmly in the K-feldspar field.

5.3.2.2 *K-bearing mineral buffers in global petroleum reservoirs*

When GWB speciated water compositions from each location (e.g. Table 1) are plotted on K^+/H^+:Na^+/H^+ stability diagrams (Figure 5.6), it is apparent that K/Na relationships appear to fit with a range of mineral buffers. Data points in several cases define arrays parallel to mineral phase boundaries, possibly reflecting the effect of natural mineral compositions. The instability of K-feldspar at moderate temperatures (<70°C; Worden and Morad, 2000) suggests that much of this mineral should have been altered to kaolinite. However, these minerals show a ubiquitous association in sandstones below 110-140°C (Smith and Eherenberg, 1989) suggestive of metastability. Muscovite does not precipitate until higher temperatures, however it is present as a detrital component of some reservoirs. Where some waters are predicted to be in equilibrium with muscovite, it is possible that it could be a proxy for illite, though this also tends to precipitate at higher temperatures (Aagard *et al.*, 1990). In general, there is significant variation in where the waters plot. The acid pH at many of the locations indicates potential metastable equilibrium between kaolin, K-feldspar and albite (Figure 5.6). It must also be remembered however, that the presence of a point on a plot in Figure 5.6 is not a guarantee of the presence of the mineral in the reservoir (see Table 5.3 for reservoir mineralogies).

The waters from Alberta (Figures 5.6A and B) show different relationships with Na- and K-bearing minerals according the age of the reservoir in which they reside. The waters in rocks of Upper Devonian age (Figure 5.6A) have high K/Na ratios, consistent with equilibrium with K-

feldspar and muscovite or kaolin in the absence of albite. While these rocks are predominantly carbonates, it is possible that there are K-bearing minerals present and K-feldspar plus kaolin is known at these temperatures. Conversely, the Jurassic and Cretaceous sands and silts contain waters which have lower K/Na ratios, defining a trend parallel to the albite-microcline boundary. This is strongly suggestive of two feldspar equilibrium with the consistent deviation likely a reflection of deviation between the real and model systems. The most acid waters sit close to albite-K-feldspar-kaolinite equilibrium (Figure 5.6B). It is known that while kaolinite is a common cement throughout all the rocks in the Alberta Basin (Carrigy and Mellon, 1964, Buschkuehle and Machel, 2002), the younger sands also contain a number of other clay minerals and zeolites which may act as a limit to Na in solution rather than albite.

No pH data was available for the waters from Central Mississippi so pH values were calculated in GWB, assuming equilibrium with K-feldspar and kaolin. However, accurate Na and K measurements provide some insight into the mineral buffering processes in this reservoir (Figure 5.6C). One result is consistent with equilibrium of albite and K-feldspar, but the other fluid is depleted in Na suggesting that no Na-phase was present in the host. Despite this, both feldspars are present in the Smackover Formation (Carpenter *et al.*, 1974; Mancini, 1987) which hosts the fluids analysed in this study. The model suggests that muscovite or illite may be is precipitating under these conditions, and cores have revealed a large proportion of damaged K-feldspars (Mancini, 1987) indicating that alteration reactions are occurring.

The reservoir rocks hosting the Colombian formation waters are pure quartz sandstones with very little additional material (Cazier *et al.*, 1995). These pore waters are unusual in that they have an extremely high K/Cl ratio. In addition, modelling results (Figure 5.6D) suggest equilibrium between K-feldspar and kaolin in the absence of albite.

The Mahakam Basin (Bazin *et al.*, 1997) (Figure 5.6E) is of particular note because it lies at the very lowest salinity end of the formation waters spectrum. The reservoir channel sands contain quartz, plagioclase and minor amounts of muscovite, K-feldspar and detrital calcite. Kaolinite, illite, quartz and dolomite are the main diagenetic mineral phases in the sandstones. Figure 5.6E indicates that the waters are indeed close to being buffered by alkali feldspars with muscovite or in metastable equilibrium with kaolinite.

The two fields studied by Hyeong and Capuano (2001) at the Texas Gulf Coast onshore Gulf of Mexico are known to be experiencing albitisation of K-feldspar at the temperatures and depths from which the analysed fluids were sampled. In support of this, waters from this reservoir all sit within the albite stability field (Figure 5.6F). In addition, it is possible that these waters exhibit low K/Na ratios due to evaporite dissolution.

The San Juan Basin also has anomalously high elemental Na concentrations (see Chapter 3), but this does not result in anomalous K/Na activity ratios. No pH data was available from this Basin so equilibrium with K-feldspar and kaolin was assumed to estimate pH. Figure 5.6G indicates that the waters are buffered by equilibrium with K-feldspar and kaolin, both of which are present in the host lithology. Albite is also known to occur in the San Juan rocks, however, this is not evident from the K/Na ratios.

In addition to evaluating whether equilibrium has been attained at locations whose reservoir mineralogy is relatively well constrained, plots such as those in Figure 5.6 can provide limited information about those with a greater degree of uncertainty if equilibrium can be assumed. Although the three fields in the Gulf of Mexico are in the same general area, their reservoirs clearly differ significantly in terms of reactions controlling formation water chemistry. Field 1 (Figure 5.6H) consistently indicates that kaolin is an important constituent of its reservoir rock, in accordance with evidence from field operators. However, the K/Na ratios sit on the metastable extension of the albite-K-feldspar boundary and the very high salinity means that this fluid analyis is prone to errors in speciations. It could therefore be that the fluids are nearer the metastable albite-K-feldspar-kaolin point than they appear. The pore waters from Field 2 (Figure 5.6I) exhibit a large degree of scatter, though all points lie within the muscovite stability field, at metastable equilibrium between K-feldspar and kaolin. However, these waters are also close to the metastable extension of albite-k-feldspar stability. The scatter in this case may be attributable to the large numbers of separate turbidite reservoirs that make up the single field. Field 3 shows a much closer association with albite, suggesting that this mineral is of greater importance here or that there is an additional source of Na into solution (Figure 5.6J). However, since all three fields give points along the albite-K-feldspar boundary, it could be that much of the difference arises in the effect of errors in the activity model for calculating pH at high salinities, i.e. Field 3 is the least saline its data plot closest to the albite-K-feldspar-kaolin boundary.

There is only a little relevant information in the literature relating to the mineralogy of the offshore Angola oil fields (e.g. Burwood and Mycke, 1996; Gay *et al.*, 2004; Rasmussen, 1996). However, the formation water K-Na systematics (Figure 5.6K) indicate that waters from Angola are relatively tightly clustered in the muscovite stability field, around the point of metastable equilibrium between albite, K-feldspar and kaolin. This assemblage would be reasonably expected to exist in the turbiditic rocks of the region which have a terriginous source, while the low T (80°C) is consistent with its persistence relative to muscovite.

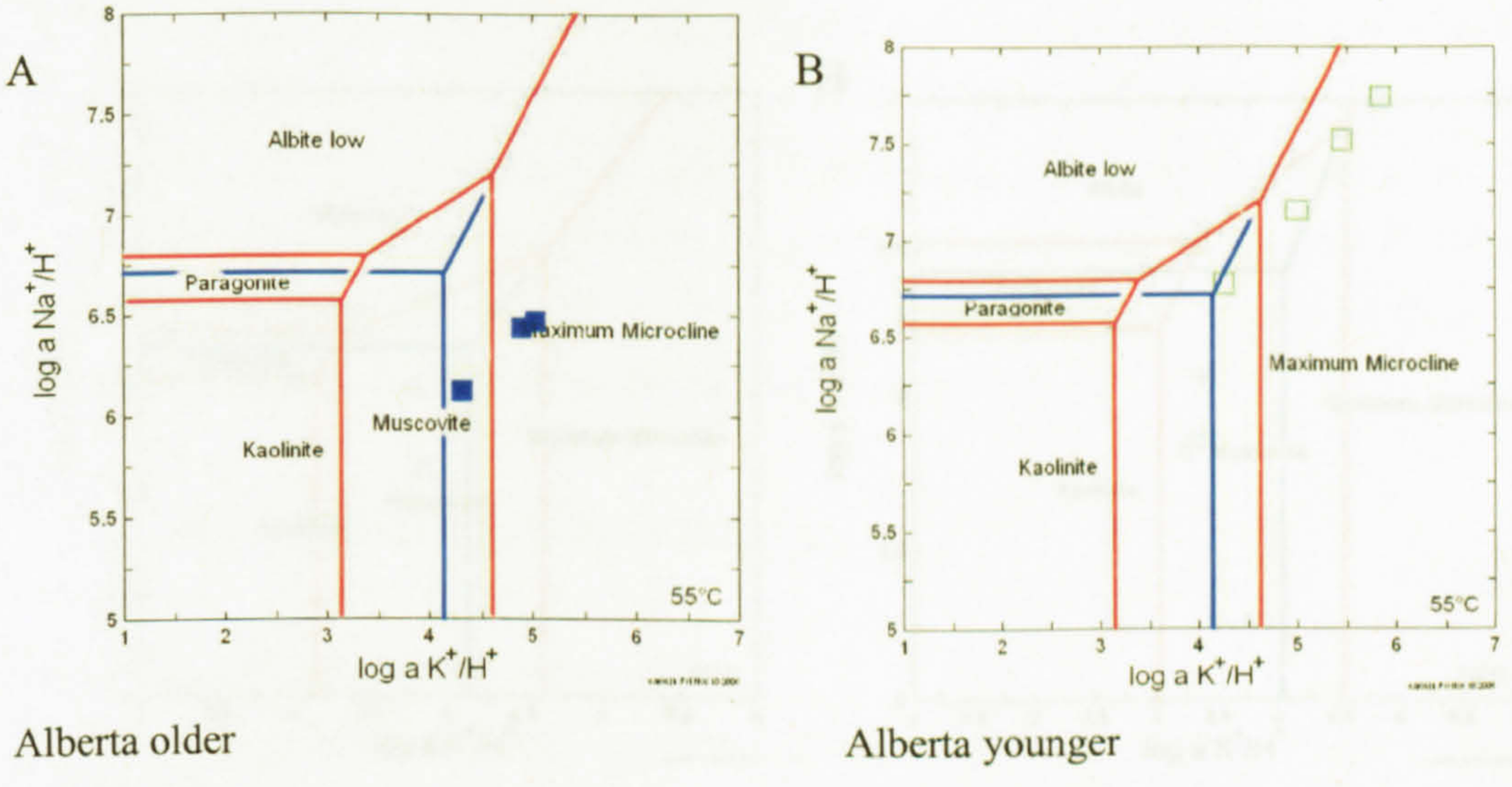

Alberta older

Alberta younger

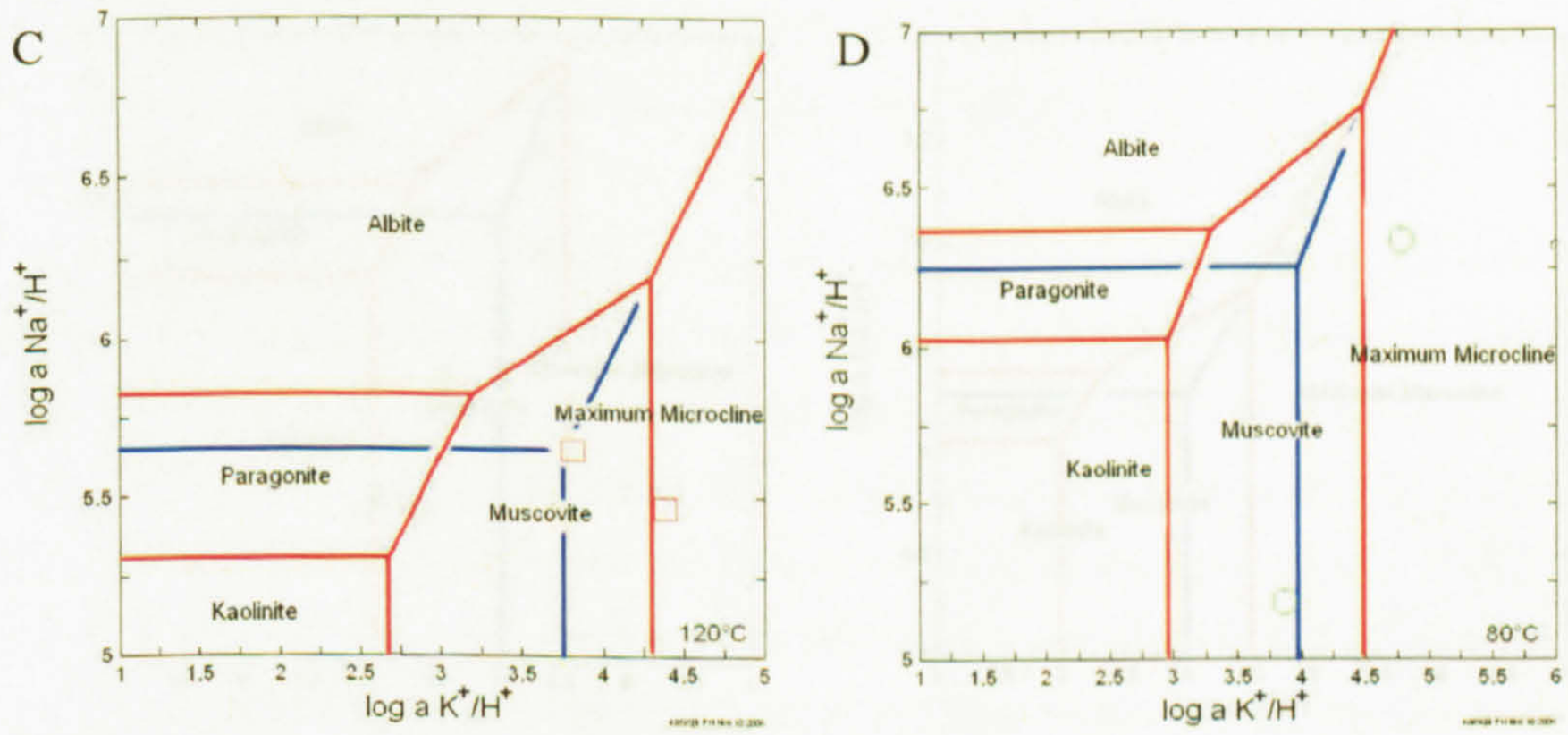

Central Mississippi

Colombia

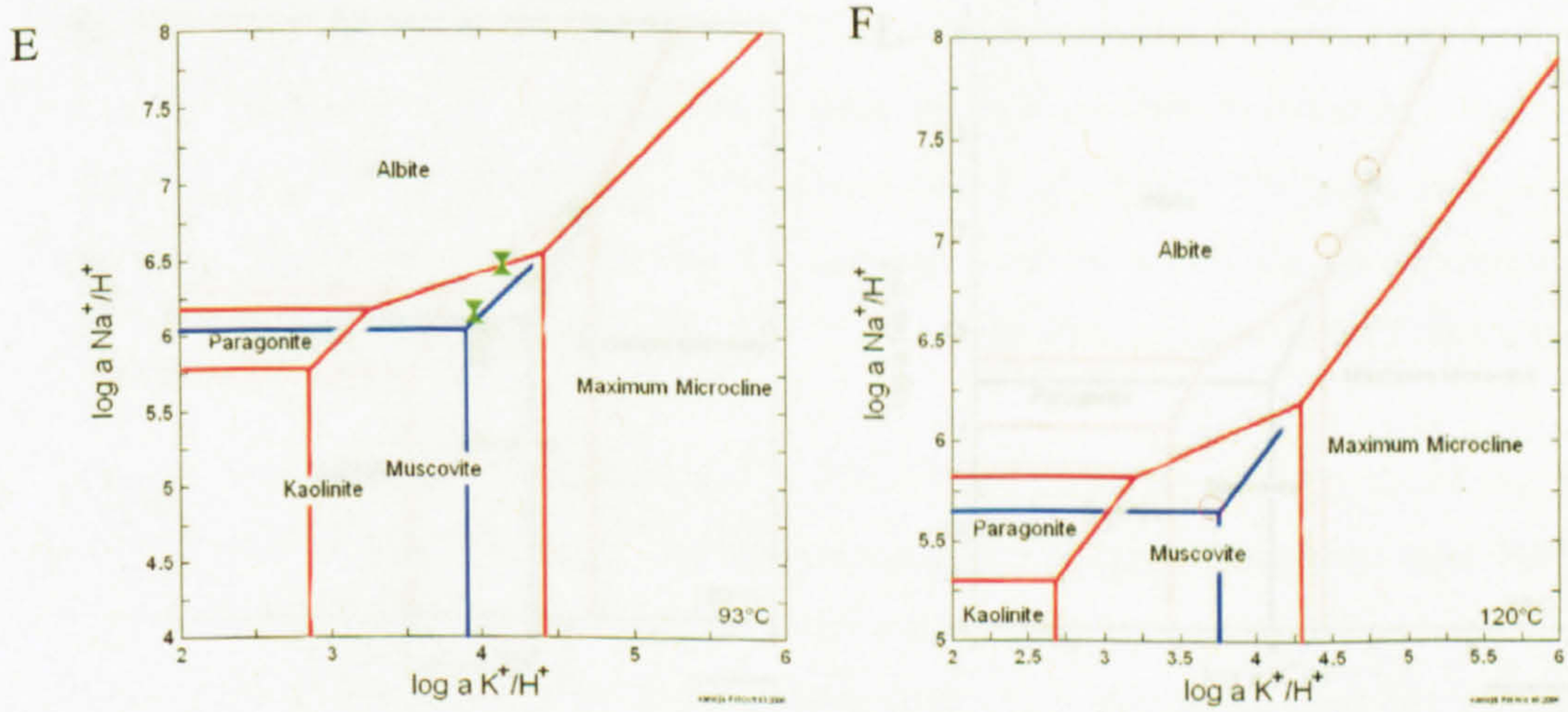

Mahakam Basin

Onshore GOM

Figure 5.6. Mineral stability diagrams for most fields in the global water database, including lines of metastable equilibrium between K-feldspar (maximum microcline) and kaolinite and K-feldspar and albite (lines in red).

G

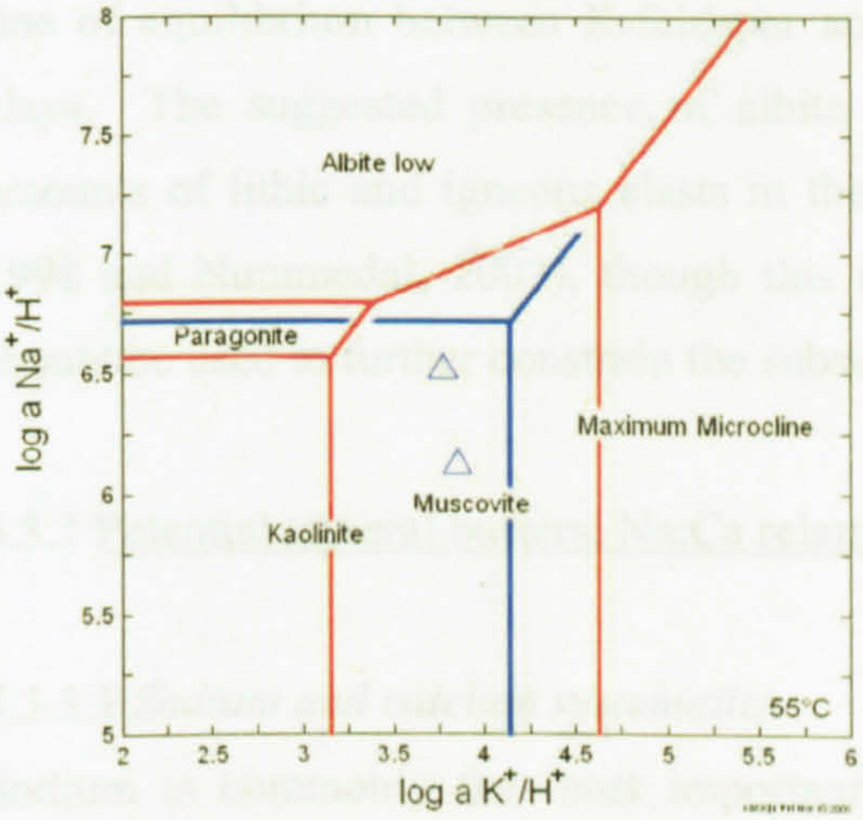

H

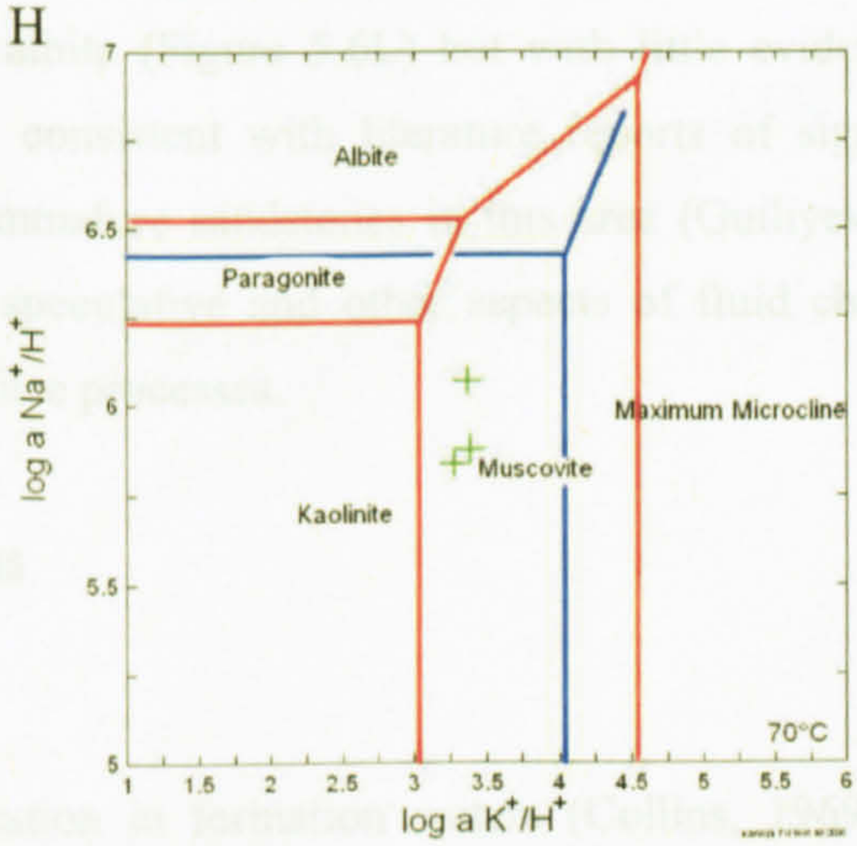

San Juan Basin

I

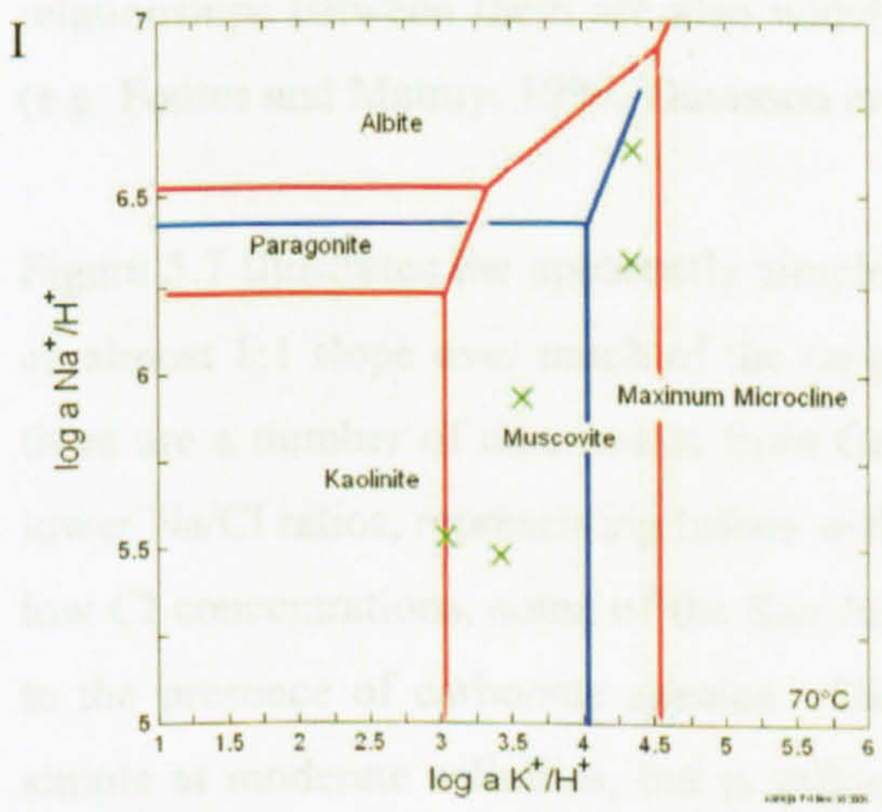

Offshore GOM – Field 1

J

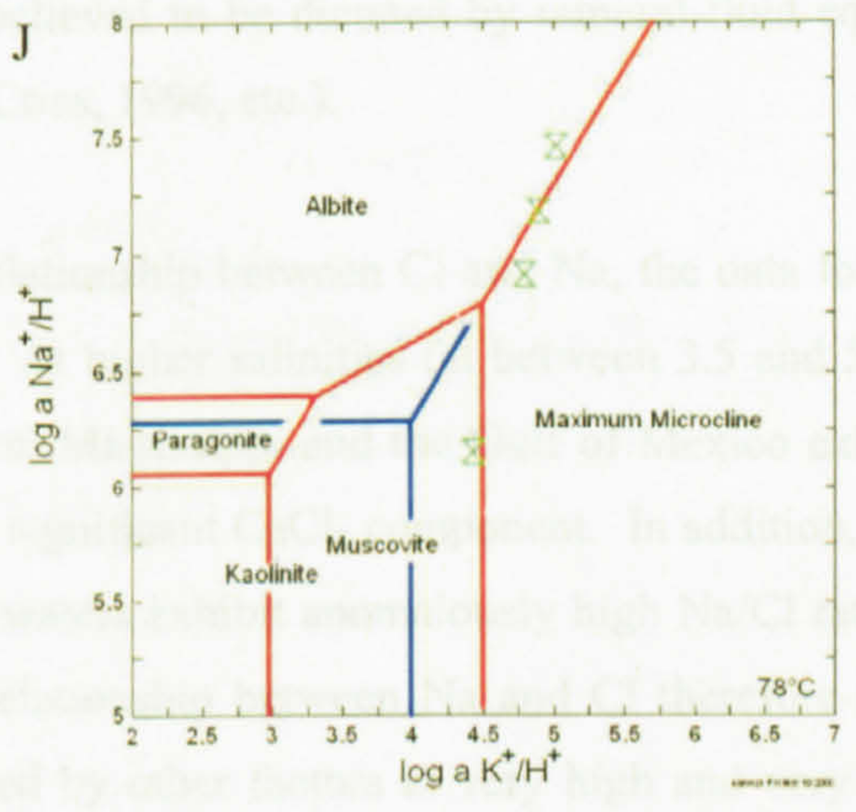

Offshore GOM – Field 2

Offshore GOM – Field 3

K

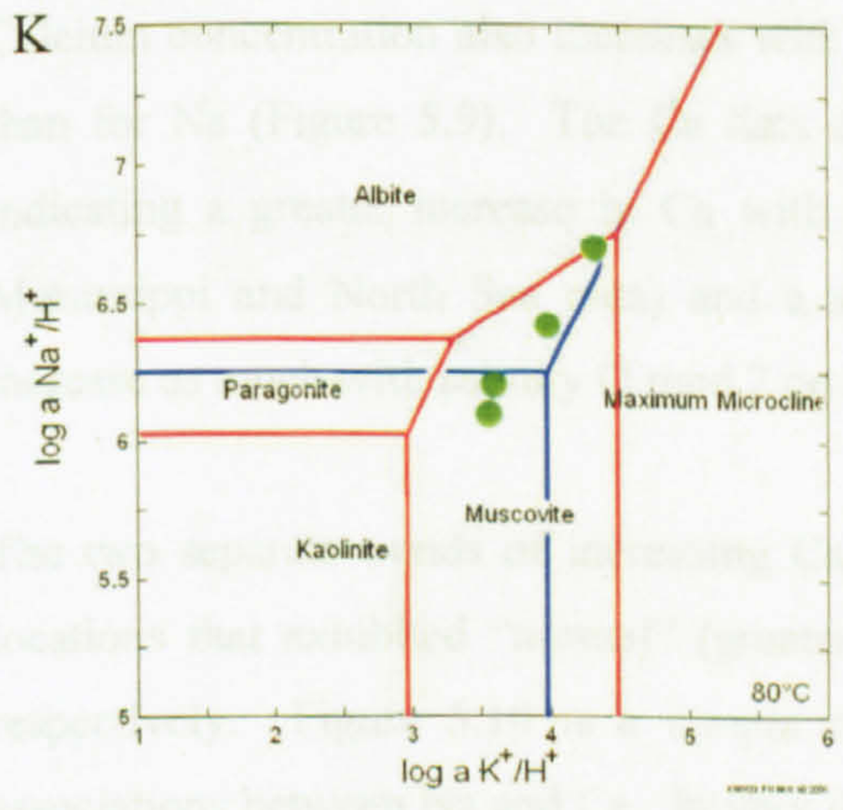

L

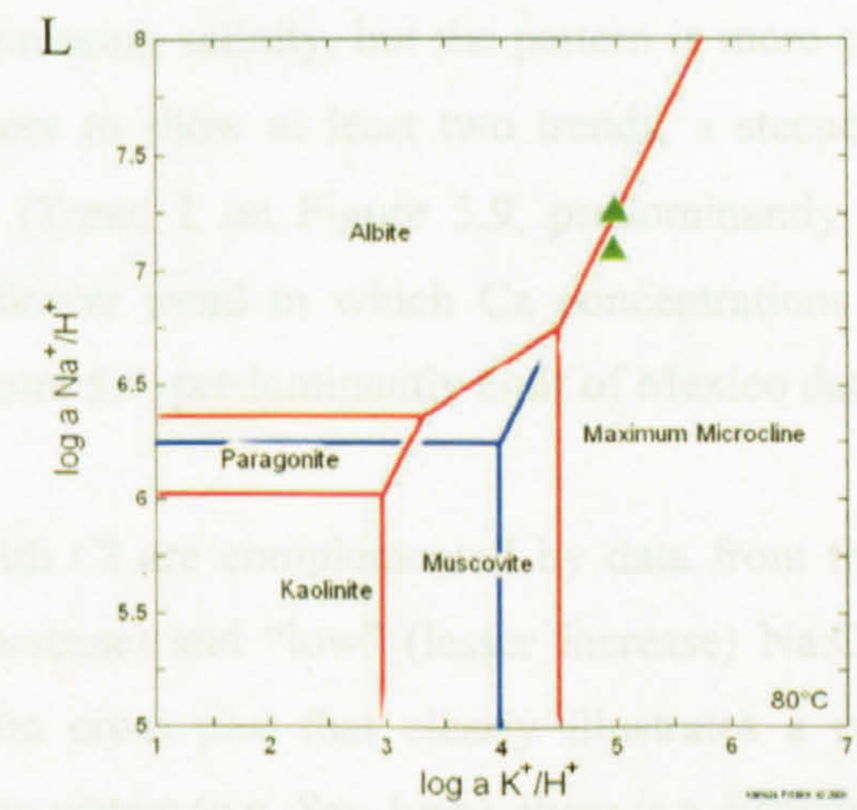

Angola

Azerbaijan – Field 1

Figure 5.6. cont.

The limited data available for Azerbaijan Field 1 indicates the waters again lie directly on the line of equilibrium between K-feldspar and albite (Figure 5.6L) but with little evidence for clays. The suggested presence of albite is consistent with literature reports of significant amounts of lithic and igneous clasts in the immature sandstones in this area (Guiliyev *et al.*, 1998 and Nummedal, 2002), though this is speculative and other aspects of fluid chemistry should be used to further constrain the subsurface processes.

5.3.3 Potential mineral buffers: Na:Ca relations

5.3.3.1 *Sodium and calcium systematics*

Sodium is commonly the most important cation in formation waters (Collins, 1969), with calcium the next abundant. The concentrations of these cations individually and the relationships between them are also widely believed to be dictated by mineral-fluid equilibria (e.g. Fontes and Matray, 1993; Davisson and Criss, 1996, etc.).

Figure 5.7 illustrates the apparently simple relationship between Cl and Na, the data following an almost 1:1 slope over much of the range. At higher salinities (at between 3.5 and 5 M Cl) there are a number of data points from Central Mississippi and the Gulf of Mexico exhibiting lower Na/Cl ratios, representing brines with a significant $CaCl_2$ component. In addition, at very low Cl concentrations, some of the San Juan waters exhibit anomalously high Na/Cl ratios due to the presence of carbonate species. The relationship between Na and Cl therefore appears simple at moderate salinities, but is influenced by other factors at very high and very low Cl concentrations. The relationship is further illustrated in a plot of Na/Cl against Cl (Figure 5.8).

Calcium concentration also increases with increasing salinity, but the pattern is more complex than for Na (Figure 5.9). The Ca data appear to show at least two trends, a steeper curve indicating a greater increase in Ca with Cl (Trend 1 on Figure 5.9, predominantly Central Mississippi and North Sea data) and a shallower trend in which Ca concentrations do not increase as much with salinity (Trend 2 on Figure 5.9, predominantly Gulf of Mexico data).

The two separate trends of increasing Ca with Cl are complemented by data from the same locations that exhibited "normal" (greater increase) and "low" (lesser increase) Na:Cl ratios respectively. Figure 5.10 is a simple cation cross plot that clearly illustrates a range of associations between Na and Ca. In very dilute waters (e.g. San Juan), there is a distinct lack of correlation between these cations, however as formation water concentration (and consequently cation concentration) increases, a clear positive correlation emerges. At higher formation water concentrations, there is again evidence for high Ca/low Na waters (Central Mississippi) and low Ca/high Na waters (Gulf of Mexico), although there are several exceptions to this behaviour.

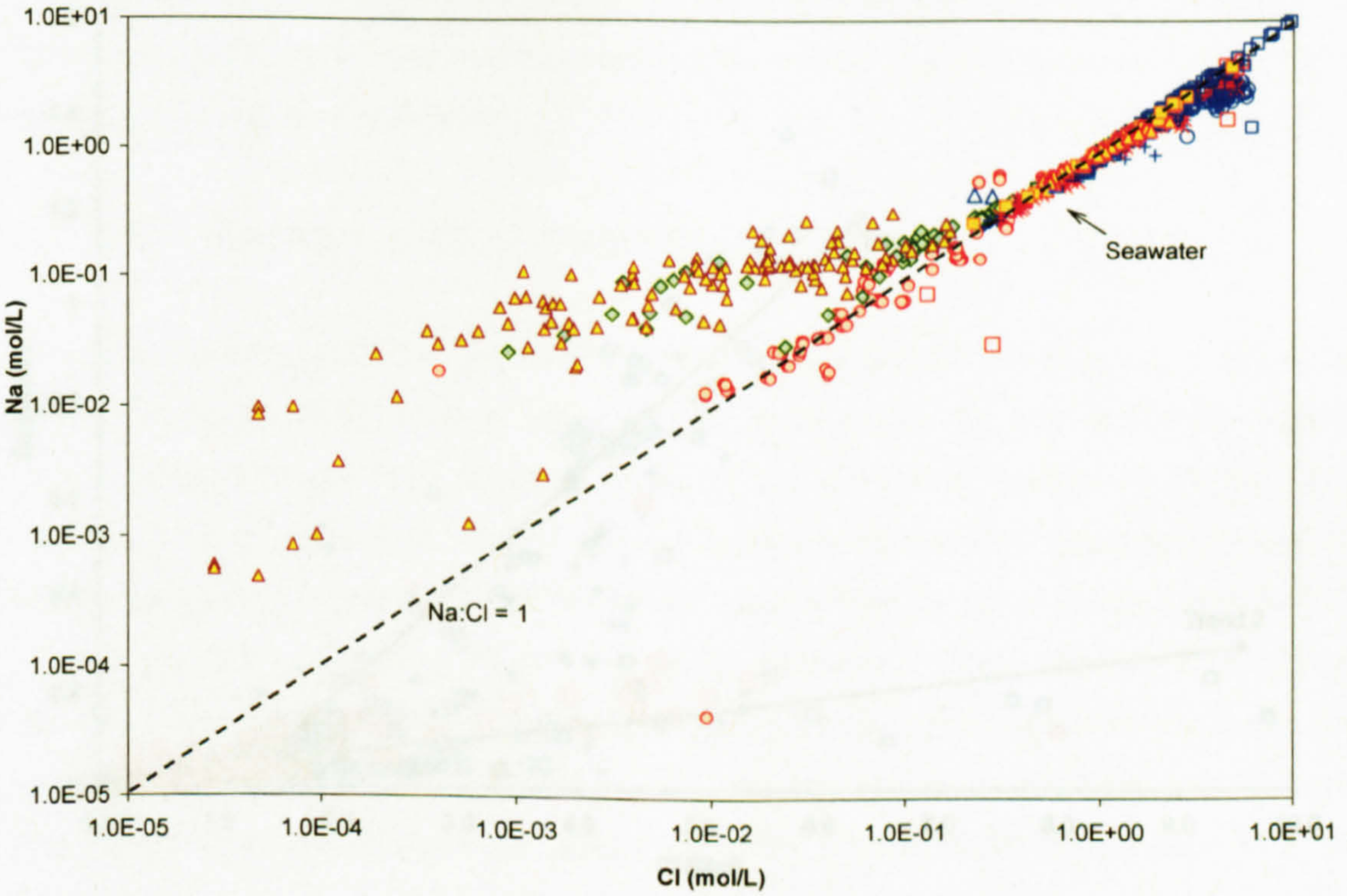

Figure 5.7. Molar concentrations of Na and Cl in global formation waters. Waters show a strong 1:1 positive correlation with slight deviations only at very low and very high salinities. The log scale amplifies the effect of dilute waters. In fact, Na>Cl only when there are other ligands around, and these are only significant when Cl is low.

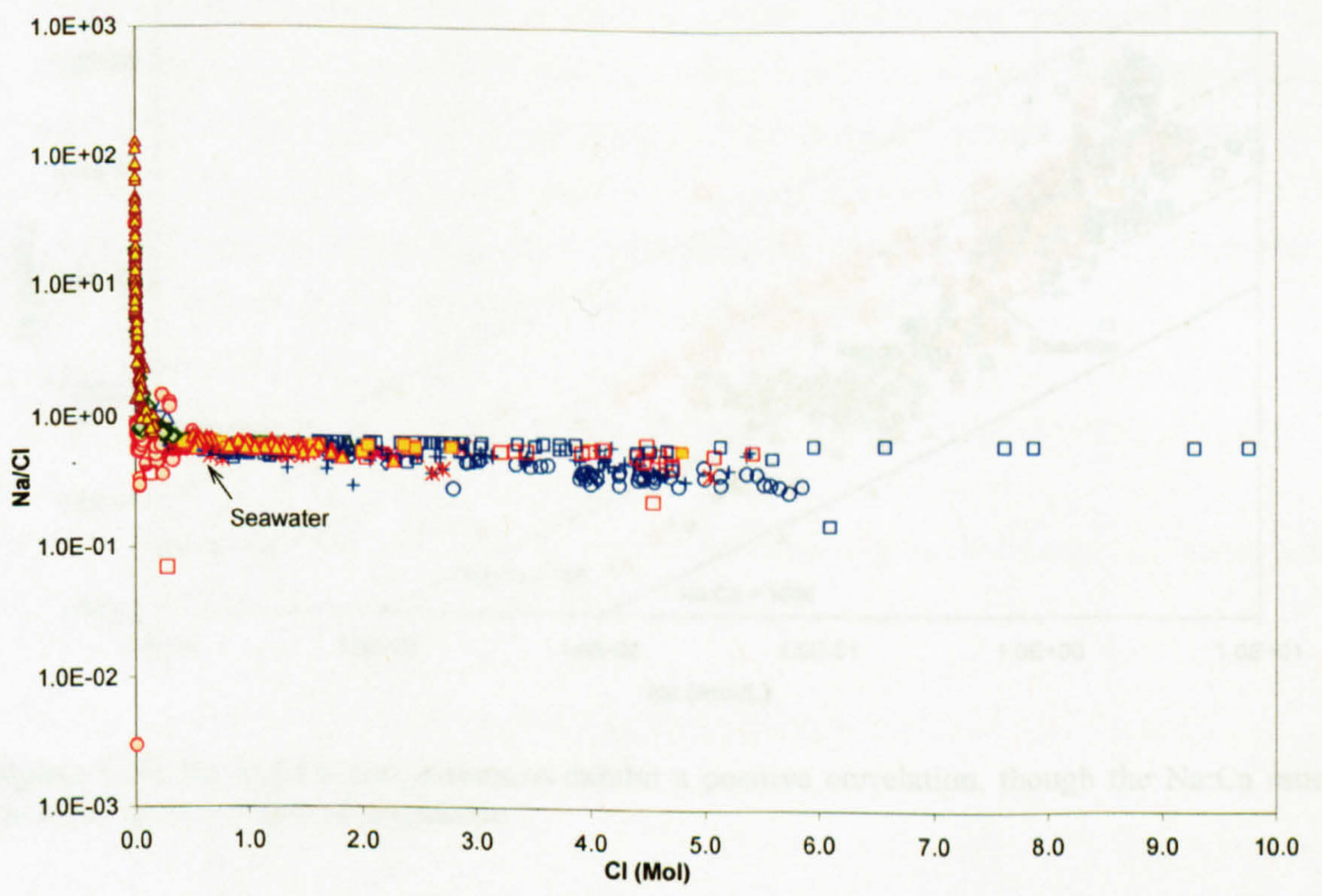

Figure 5.8. The molar Na/Cl ratio in global formation waters is constant at just under 1 at moderate salinities. A proportion of the lower salinity waters contain anomalously high Na, and these correspond with some of those that show relatively high Ca concentrations, discussed later.

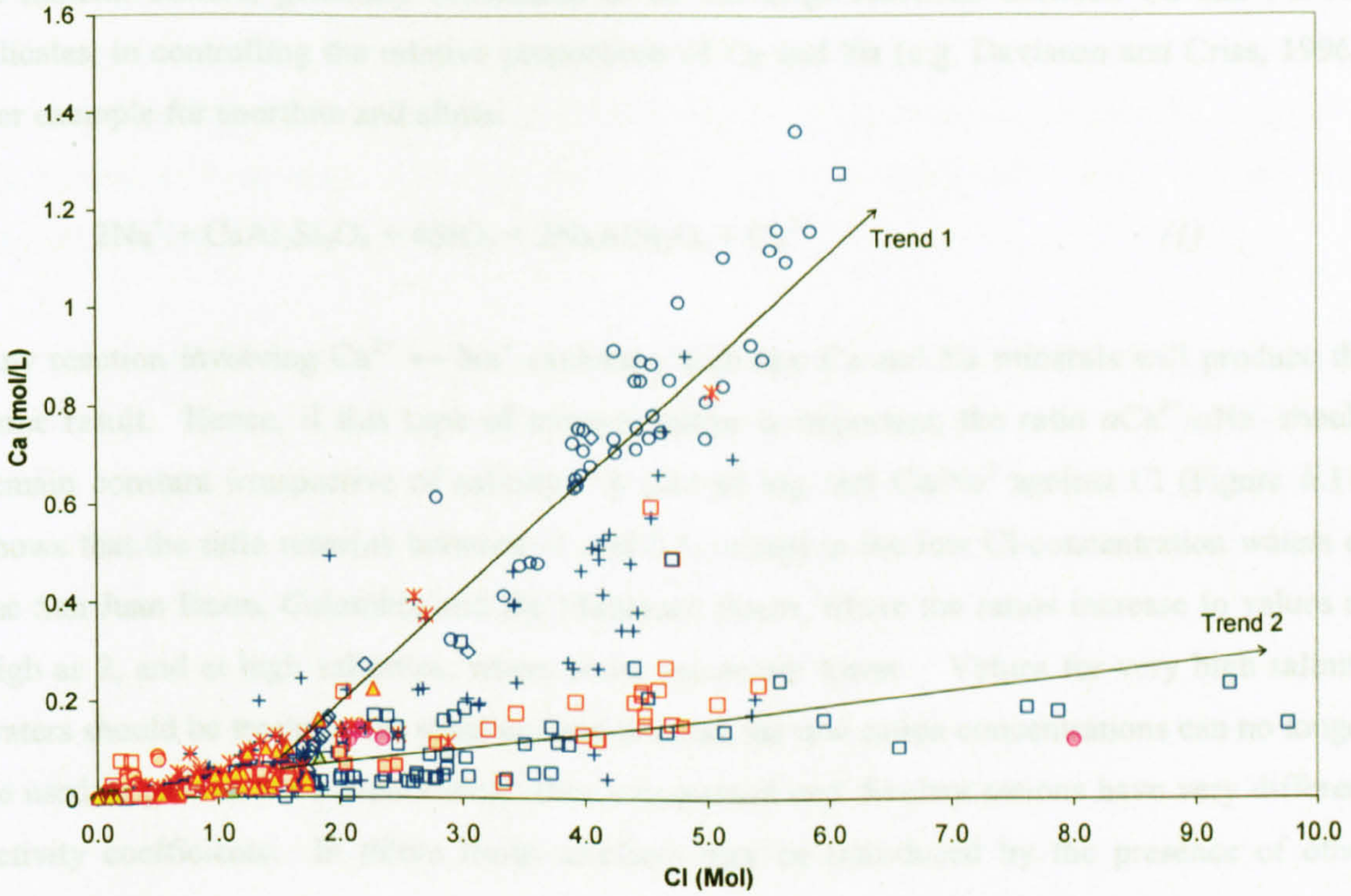

Figure 5.9. Ca concentrations increase with Cl. Note two trends forming at higher salinities.

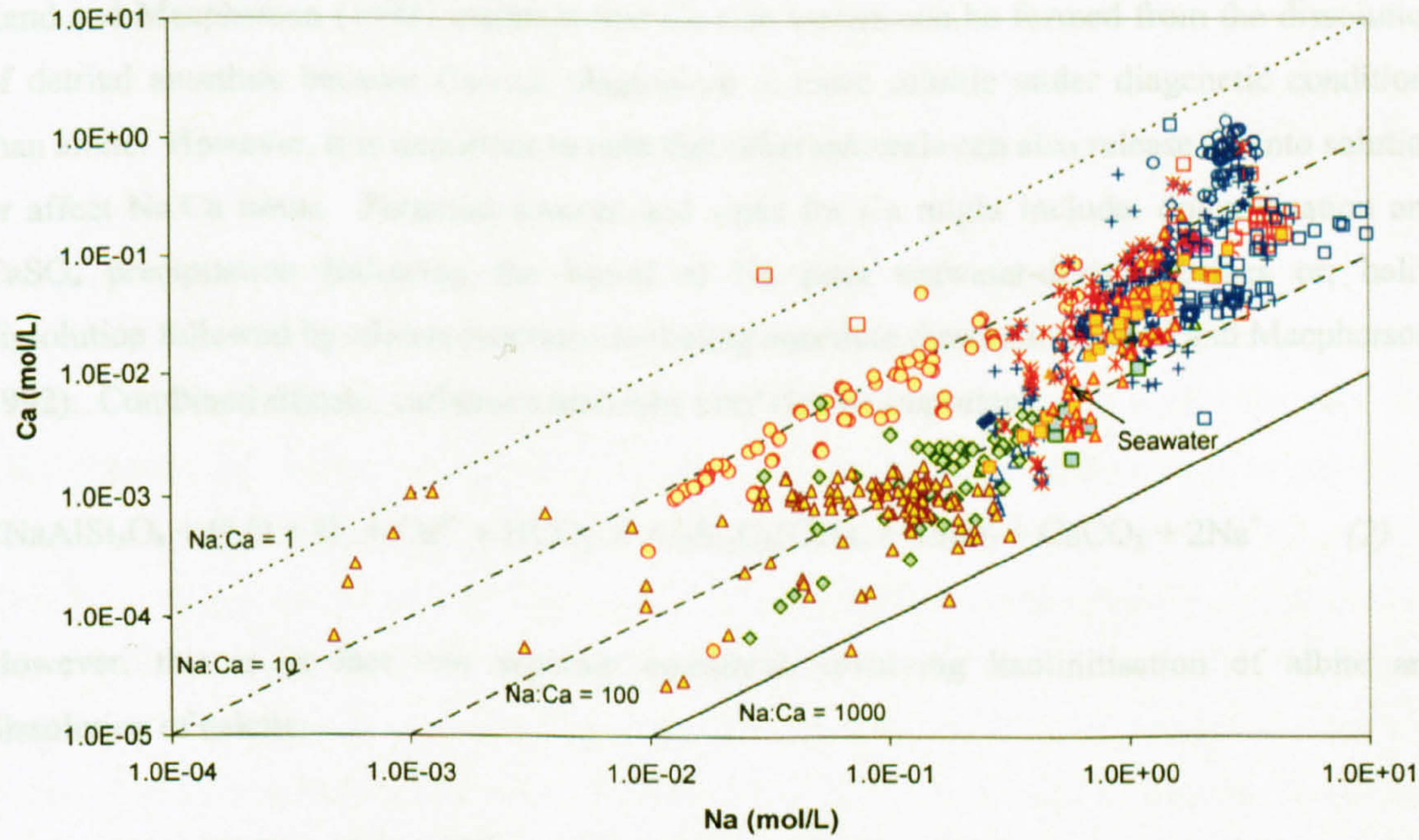

Figure 5.10. Na and Ca concentrations exhibit a positive correlation, though the Na:Ca ratio varies by up to 3 orders of magnitude.

5.3.3.2 *The importance of mineral buffers – albite-plagioclase equilibrium*

Figures 5.11 and 5.12 show the results of further study into Ca and Na systematics of formation waters. The activity ratio $a\mathrm{Ca}^{2+}/a2\mathrm{Na}^{+}$ has been used in the past an indicator of the importance

of mineral buffers, generally considered to be exchange reactions between Ca and Na Al-silicates, in controlling the relative proportions of Ca and Na (e.g. Davisson and Criss, 1996). For example for anorthite and albite:

$$2Na^{+} + CaAl_2Si_2O_8 + 4SiO_2 = 2NaAlSi_3O_8 + Ca^{2+} \qquad (1)$$

Any reaction involving $Ca^{2+} \leftrightarrow Na^{+}$ exchange with any Ca and Na minerals will produce the same result. Hence, if this type of mineral buffer is important, the ratio aCa^{2+}/aNa^{+} should remain constant irrespective of salinity. A plot of log mol Ca/Na^2 against Cl (Figure 5.11) shows that the ratio remains between -1 and 0.5, except in the low Cl-concentration waters of the San Juan Basin, Colombia and the Mahakam Basin, where the ratios increase to values as high as 2, and at high salinities, where some values are lower. Values for very high salinity waters should be treated with some caution because the raw cation concentrations can no longer be used as proxies for ion activities, since monovalent and divalent cations have very different activity coefficients. In dilute fluids artefacts may be introduced by the presence of other species.

5.3.3.3 *Other Ca-mineral buffers: carbonates, sulphates and halite*

Land and Macpherson (1992) maintain that Ca-rich waters can be formed from the dissolution of detrital anorthite because Ca-rich plagioclase is more soluble under diagenetic conditions than albite. However, it is important to note that other minerals can also release Ca into solution or affect Na/Ca ratios. Potential sources and sinks for Ca might include: dolomitisation and $CaSO_4$ precipitation following the burial of Na poor seawater-derived brines or; halite dissolution followed by silicate reactions including anorthite dissolution (Land and Macpherson, 1992). Combined silicate, carbonate reactions may also be important:

$$2NaAlSi_3O_8 + H_2O + H^{+} + Ca^{2+} + HCO_3^{-} = Al_2Si_2O_5(OH)_4 + 4SiO_2 + CaCO_3 + 2Na^{+} \qquad (2)$$

However, this is in fact two separate equilibria, involving kaolinitisation of albite and dissolution of calcite:

$$2NaAlSi_3O_8 + H_2O + 2H^{+} = Al_2Si_2O_5(OH)_4 + 4SiO_2 + 2Na^{+} \qquad (3)$$

$$Ca^{2+} + HCO_3^{-} = CaCO_3 + H^{+} \qquad (4)$$

These reactions are as likely to be occurring in sedimentary reservoir rocks as reaction (1). If mineral buffers control the concentration of Ca and Na in formation waters, it is possible that a combination of silicate- and non-silicate equilibria is responsible for any deviations from Trends 1 and 2 in Figure 5.9. The role of non-silicate equilibria is discussed in more detail in section

5.3.5. Figure 5.12 plots Ca as a proportion of the total major cations (Na+Ca) i.e. XCa, which will increase with Cl if mineral buffers control the Na:Ca relations. The XCa value does increase with salinity, however there are three separate trends reflecting three different types of Ca behaviour in solution. Trends 1 and 2 in Figure 5.12 correspond exactly with the same trends in Figure 5.9.

At higher salinities, high Ca waters such as those from Central Mississippi reflect the continuation of the mineral-buffered trend and the increasing importance of Ca as a cation (Trend 1). At low salinities some waters exhibit anomalously high XCa values (Trend 3) which represent waters in which bicarbonate, not Cl, is the dominant anion. These waters will be discussed in more detail in section 5.3.5.1.

Conversely, Na-rich, Ca-poor waters such as those from the Gulf of Mexico may be those in which mineral buffering is no longer the dominant process due to exceptionally high Na levels derived from evaporite dissolution (Trend 2). If the supply of Na^+ exceeds that required to albitise all the available plagioclase in a sediment (reaction 1), the fluid will be low in Ca relative to the mineral buffering trend, and so is likely to lie along Trend 2 (Figures 5.9, 5.11 and 5.12), rather than Trend 1. Where halite beds are present in the subsurface, halite dissolution is a likely origin for this effect:

$$2NaCl + CaAl_2Si_2O_8 + 4SiO_2 + H_2O = CaCl_2 + 2NaAlSi_3O_8 + H_2O \qquad (5)$$

The process is non-equilibrium and irreversible because the alteration of Ca-rich minerals will proceed to completion before equilibrium (aCa/a^2Na) is attained. A simple model constructed to illustrate this process is shown in Figure 5.13. The model is based on a siliceous rock with 10% porosity by weight. Although plagioclase is rare in many sandstones it is sometimes found, for example in sediments of the US Gulf Coast (Land and Macpherson, 1992) and may have been more common prior to diagenesis, thus it is useful to use as an easily controllable and quantifiable potential source of Ca in the model. For the purposes of the model, the original proportion of calcic plagioclase in the rock is systematically altered. The porosity is filled with water of variable salinity which reacts with all the Ca in the rock until albitisation is complete because either all the Ca or all the Na in the system is within a single phase. For any given amount of plagioclase in the rock, the relative importance of Ca in the final fluid decreases as the amount of salt in the system (the salinity of the pore water) increases. But overall, the proportion of Ca in the pore water increases with the amount of feldspar originally in the rock. The theory of this process can be applied to any Ca-bearing mineral in association with halite, however, to form this trend there must always be only a limited amount present in the rock, so that the final fluid composition is controlled by the original masses available. To summarise,

the blue generic buffering line in Figure 5.13 can be thought of as representing Trend 1, while the red mass limited line represents Trend 2.

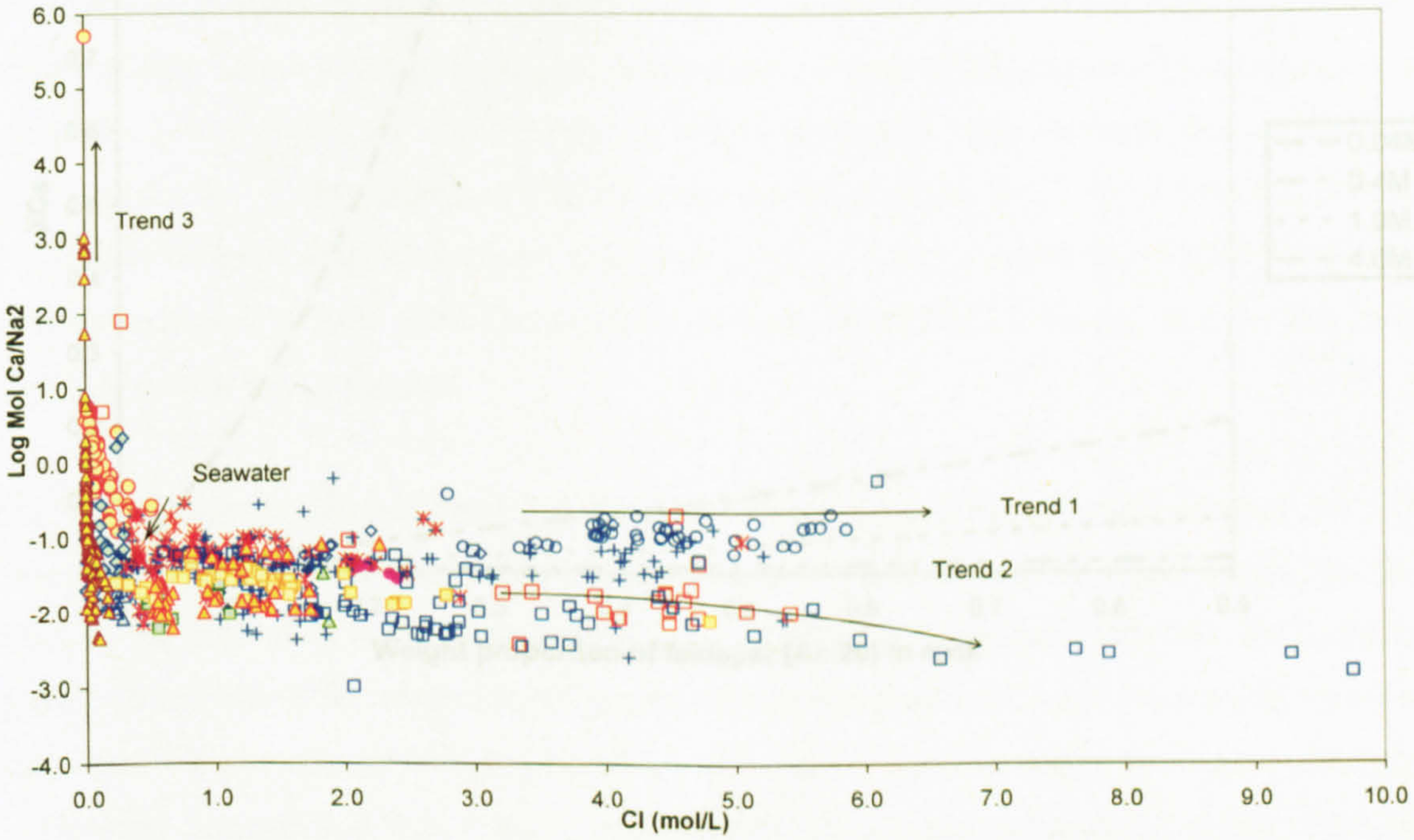

Figure 5.11. The molar Ca/Na^2 ratio is an indicator of mineral buffering, which appears to be occurring at moderate salinities. Deviations can arise through either an absence of buffering or the presence of additional ligands such as bicarbonate.

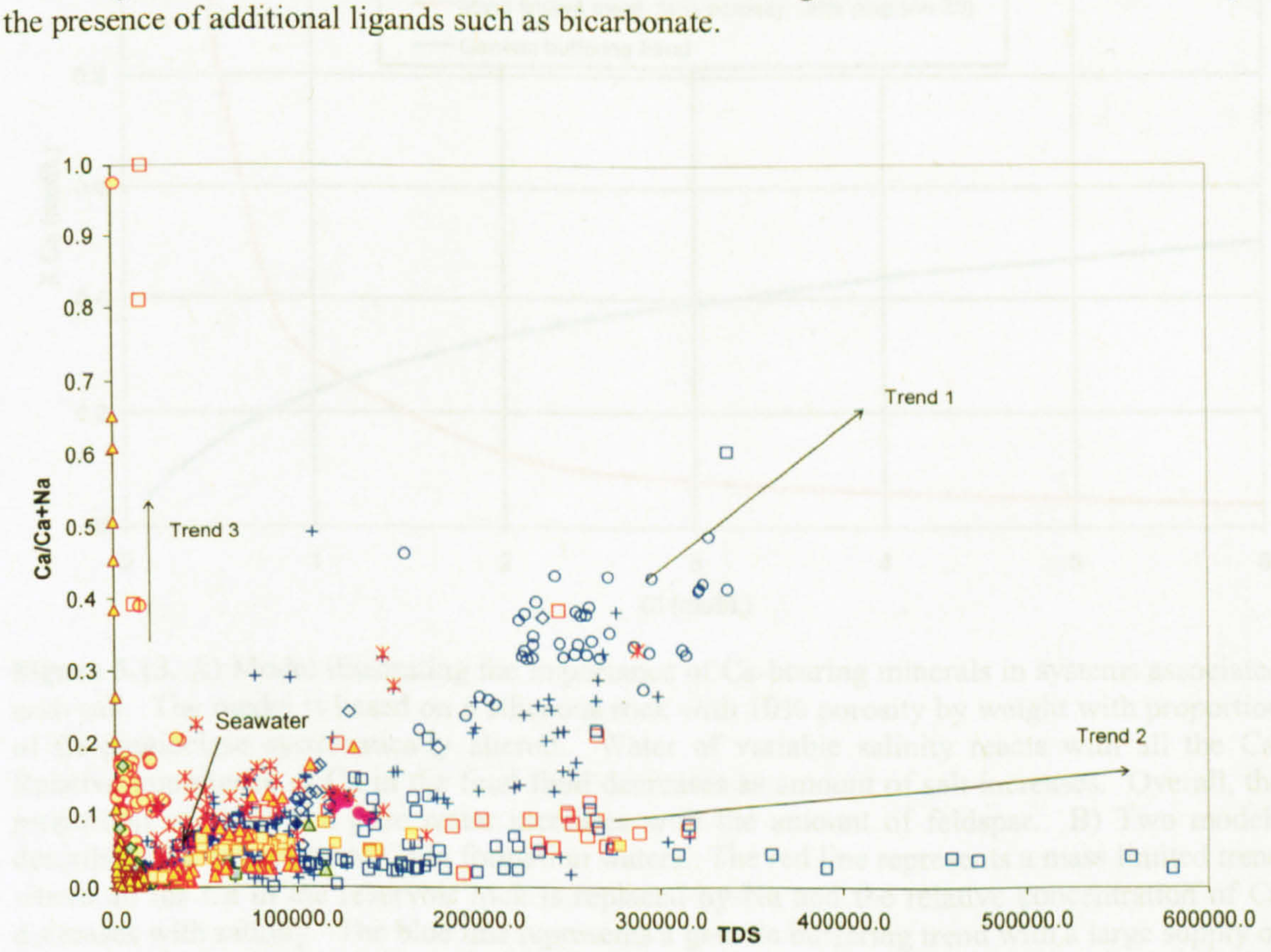

Figure 5.12. XCa (Ca/Ca+Na) variation with total dissolved solids highlights three trends of Ca variation in the global waters

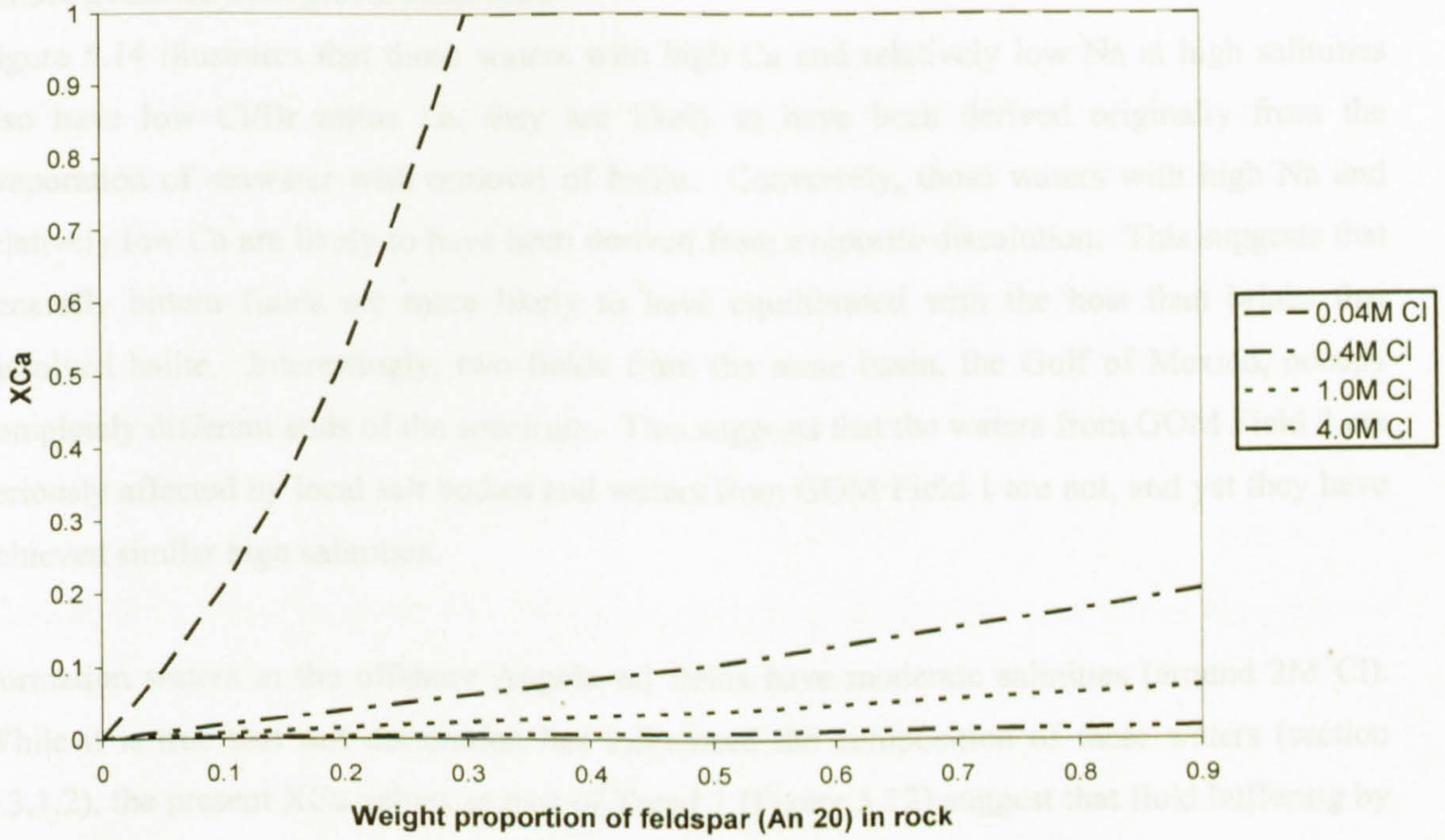

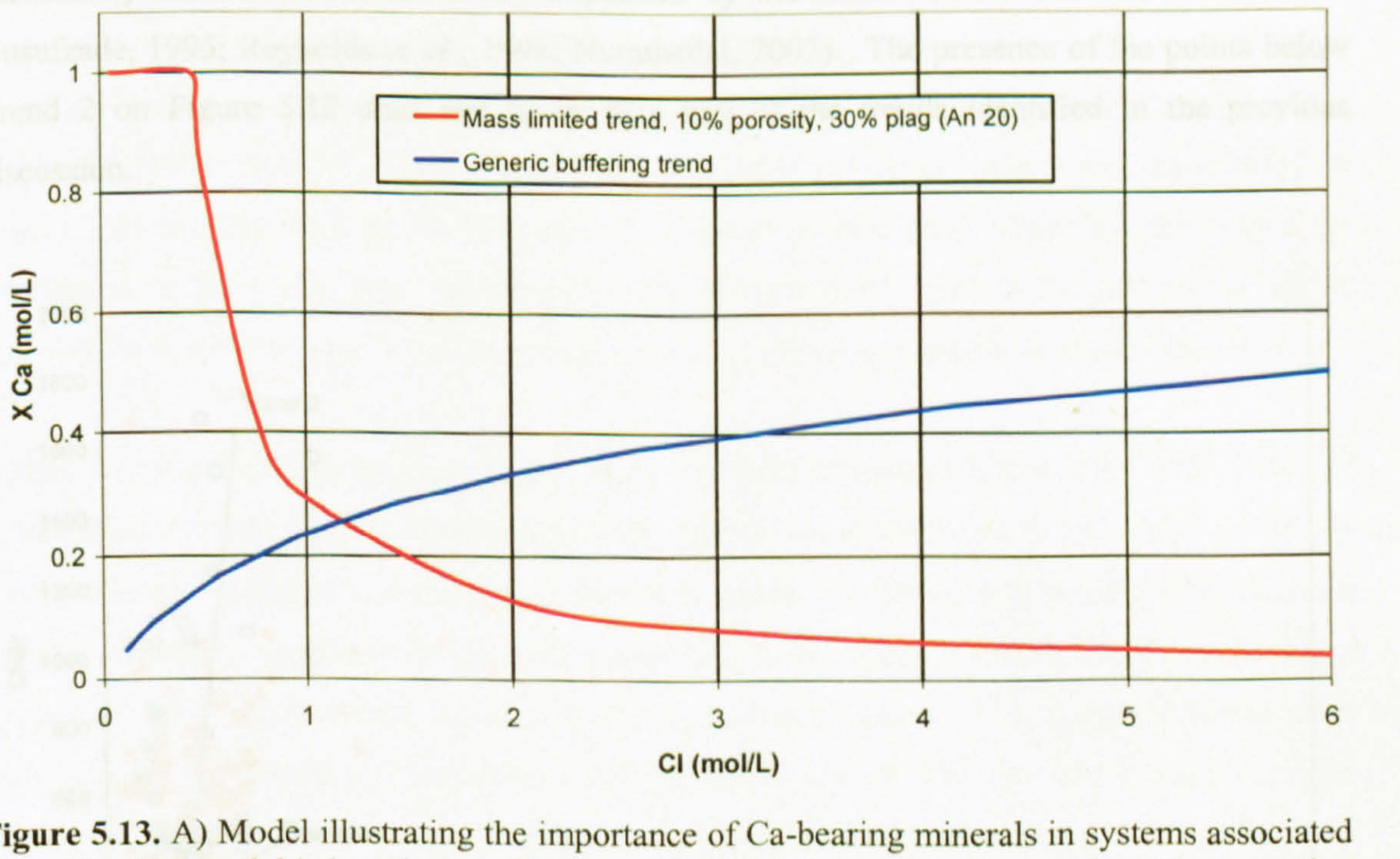

Figure 5.13. A) Model illustrating the importance of Ca-bearing minerals in systems associated with salt. The model is based on a siliceous rock with 10% porosity by weight with proportion of Ca-plagioclase systematically altered. Water of variable salinity reacts with all the Ca. Relative importance of Ca in the final fluid decreases as amount of salt increases. Overall, the proportion of Ca in the pore water increases with the amount of feldspar. B) Two models describing the behaviour of Ca in formation waters. The red line represents a mass limited trend where all the Ca in the reservoir rock is replaced by Na and the relative concentration of Ca decreases with salinity. The blue line represents a generic buffering trend with a large supply of any Ca-bearing mineral. c/f Trend 1 in Figures 5.9 and 5.12

5.3.3.4 *Evidence from global reservoirs*

Figure 5.14 illustrates that those waters with high Ca and relatively low Na at high salinities also have low Cl/Br ratios i.e. they are likely to have been derived originally from the evaporation of seawater with removal of halite. Conversely, those waters with high Na and relatively low Ca are likely to have been derived from evaporite dissolution. This suggests that generally bittern fluids are more likely to have equilibrated with the host than brines that dissolved halite. Interestingly, two fields from the same basin, the Gulf of Mexico, occupy completely different ends of the spectrum. This suggests that the waters from GOM Field 2 are seriously affected by local salt bodies and waters from GOM Field 1 are not, and yet they have achieved similar high salinities.

Formation waters in the offshore Angola oil fields have moderate salinities (around 2M Cl). While it is true that salt dissolution has influenced the composition of these waters (section 5.3.1.2), the present XCa values as part of Trend 1 (Figure 5.12) suggest that fluid buffering by some type of Ca-bearing mineral is still an important control on the Ca and Na concentrations in the water. The pattern of behaviour of Ca and Na in the Azerbaijan formation waters is particularly unusual and is not easily explained by the limited information in the literature (Jusufzade, 1995; Reynolds *et al.*, 1998; Nummedal, 2002). The presence of the points below Trend 2 on Figure 5.12 does not fit in with any of the trends identified in the previous discussion.

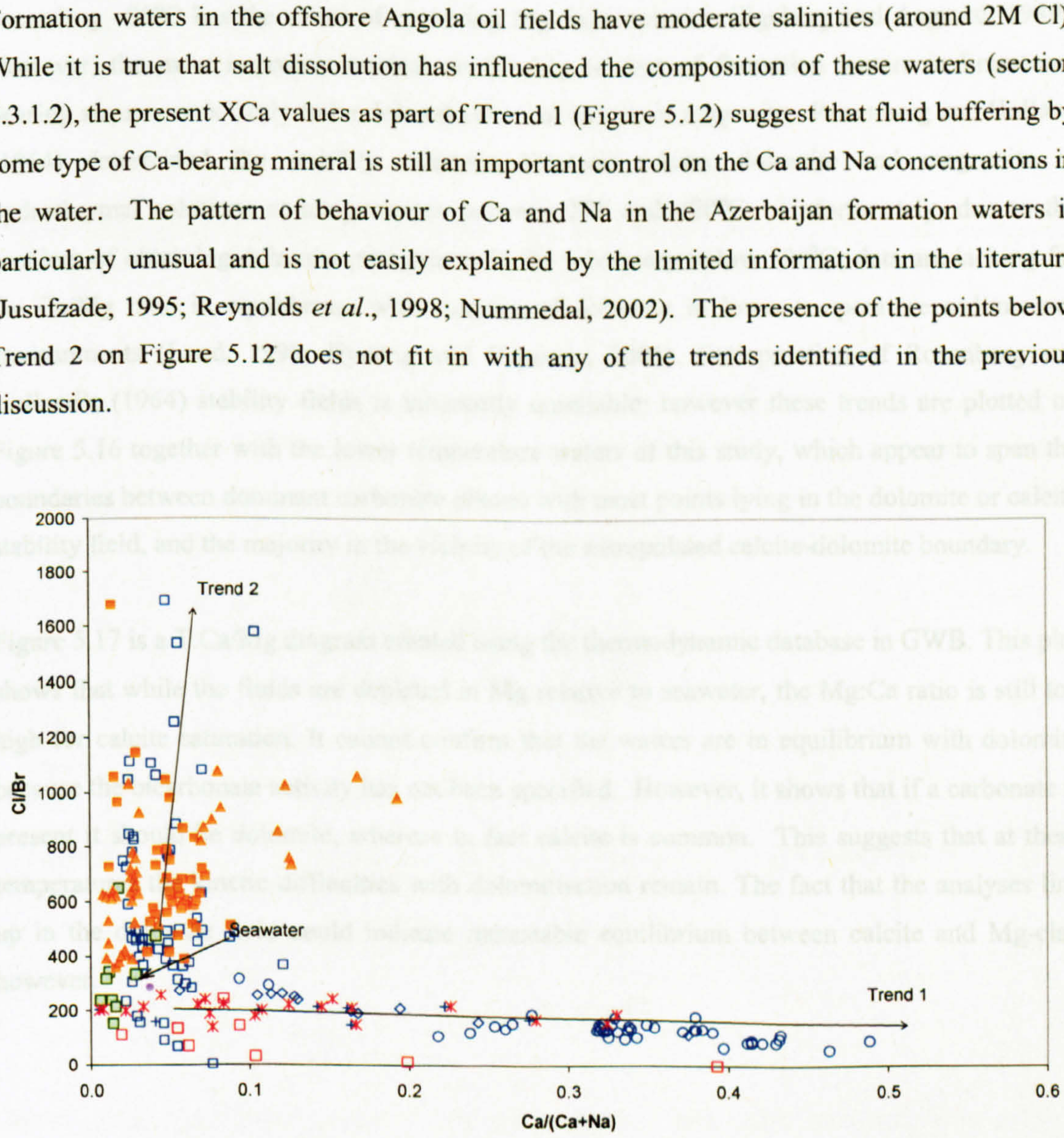

Figure 5.14. High Cl/Br ratios indicate halite dissolution origin. With the exception of Central Mississippi, the GOM Field 1 and some sites in the North Sea, XCa values tend to increase with increasing Cl/Br ratio

5.3.4 Mineral buffers: Ca:Mg relations

Magnesium also displays a positive correlation with Cl, with increasing variation in Mg concentration with increasing Cl. However, there is very little correlation between the Ca/Mg ratio and either Cl concentration (Figure 5.15) or temperature. Waters from all locations exhibit a relative increase in Ca and decrease in Mg when compared with seawater. The following plots are based on bulk analyses without allowance for Ca and Mg speciation. Since these cations complex quite well, the bulk analyses are not a very accurate proxy for the cation ratios, and this may be why the data scatters so much.

Chlorite formation (Humphris and Thompson, 1978), especially from kaolinite at temperatures exceeding ~90°C has the effect of removing Mg from solution (Egeberg and Aagaard, 1989). However, the most important control on the Mg content of formation waters in limestone-bearing sequences is likely to be dolomitisation of calcite or aragonite. Rosenberg and Holland (1964) determined the stability relations between calcite, dolomite and magnesite in hydrothermal solutions at temperatures between 275 and 420°C. Unfortunately, due to the problem of obtaining dolomite precipitates in the laboratory below 100°C, data are lacking for the Ca/Mg ratio in equilibrium with calcite and dolomite in lower-temperature sedimentary environments (Land, 1998; Hyeong and Capuano, 2001). Extrapolation of Rosenberg and Holland's (1964) stability fields is inherently unreliable; however these trends are plotted on Figure 5.16 together with the lower temperature waters of this study, which appear to span the boundaries between dominant carbonate phases with most points lying in the dolomite or calcite stability field, and the majority in the vicinity of the extrapolated calcite-dolomite boundary.

Figure 5.17 is a T:Ca/Mg diagram created using the thermodynamic database in GWB. This plot shows that while the fluids are depleted in Mg relative to seawater, the Mg:Ca ratio is still too high for calcite saturation. It cannot confirm that the waters are in equilibrium with dolomite because the bicarbonate activity has not been specified. However, it shows that if a carbonate is present it should be dolomite, whereas in fact calcite is common. This suggests that at these temperatures the kinetic difficulties with dolomitisation remain. The fact that the analyses line up in the dolomite field could indicate metastable equilibrium between calcite and Mg-clay however.

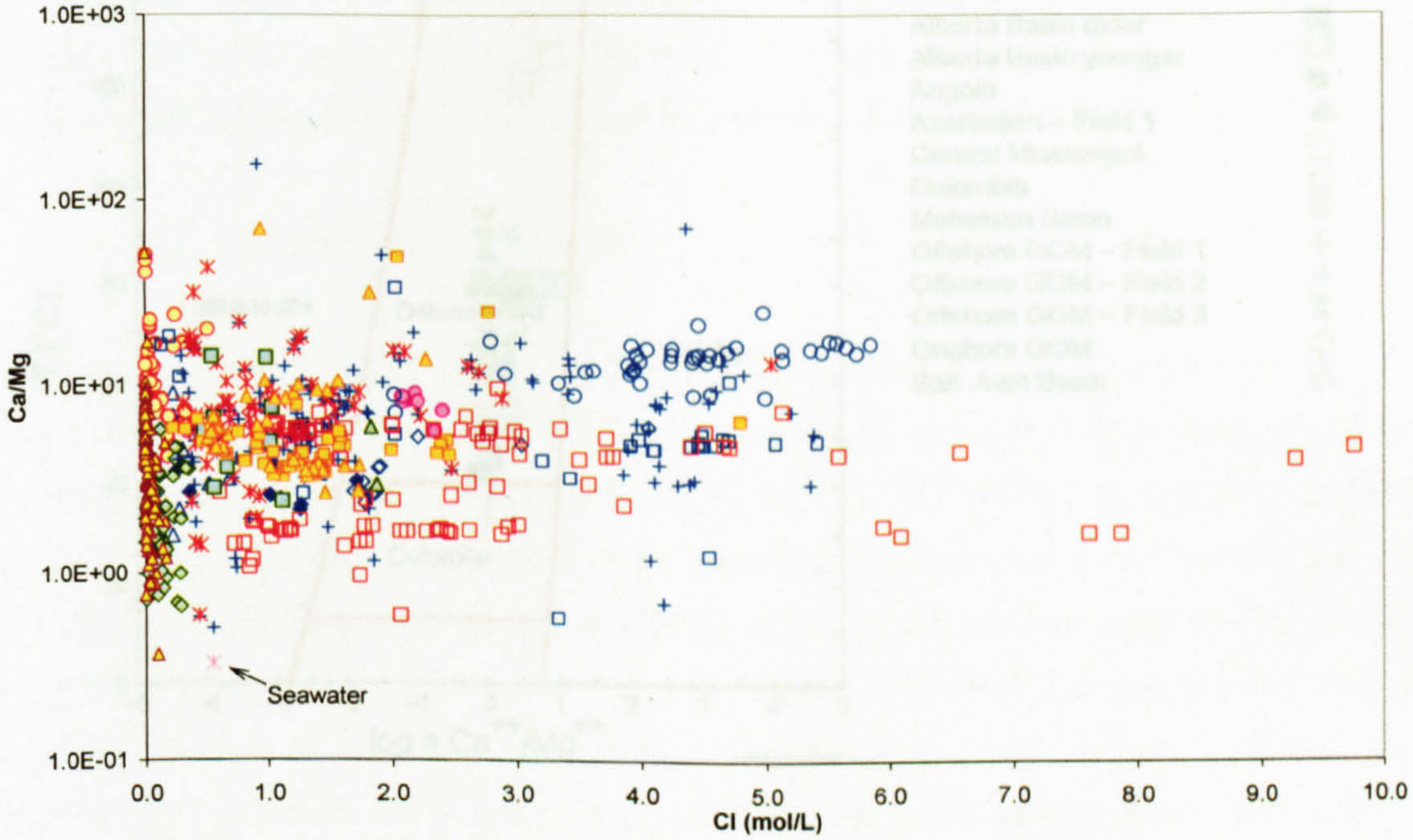

Figure 5.15. Molar Ca/Mg ratios for global formation waters show no discernible correlation with Cl. Note that Ca/Mg ratios are invariably much higher than the seawater value.

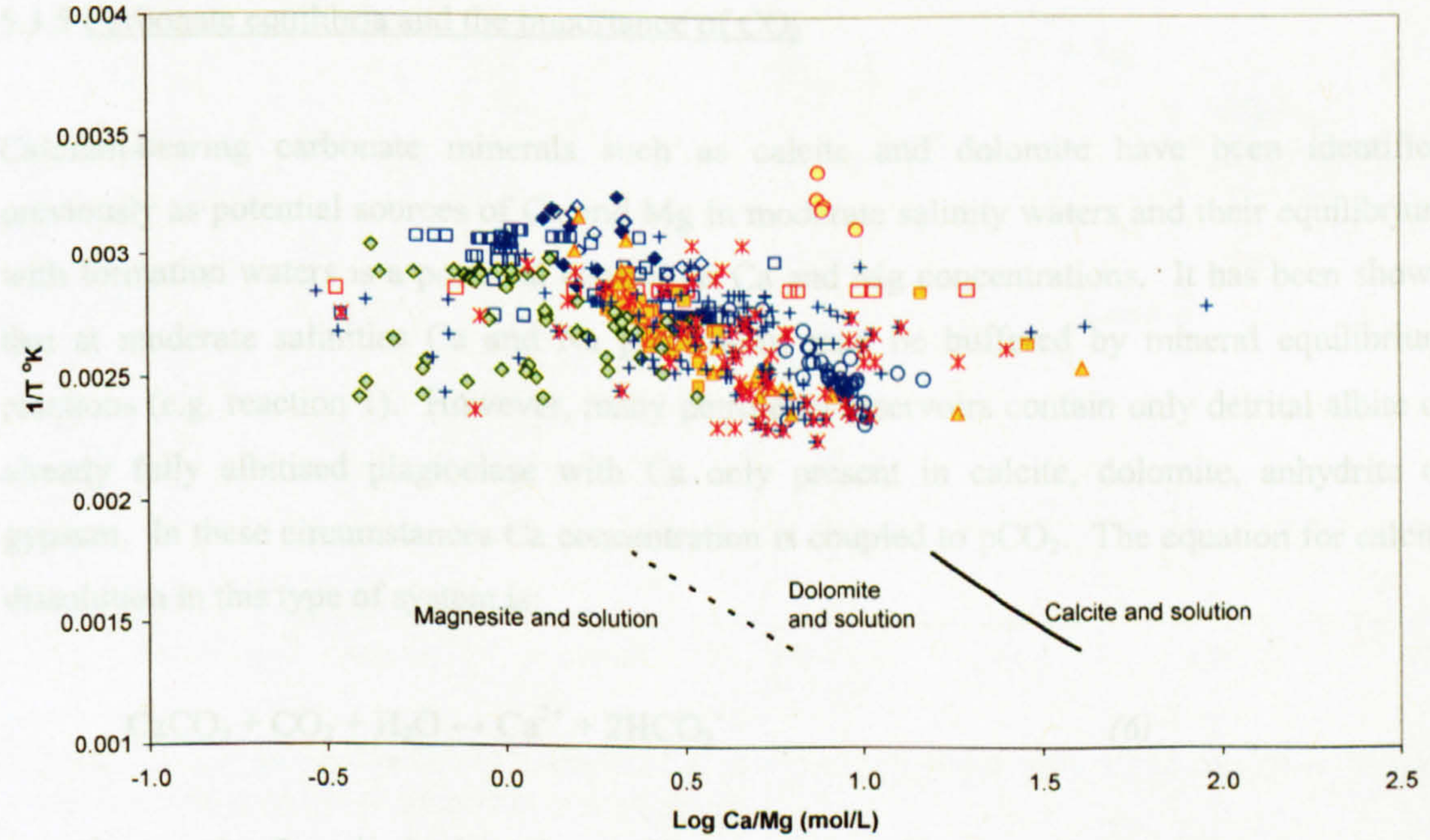

Figure 5.16. Very little change in the molar Ca/Mg ratio with temperature is evident. Extrapolation of high temperature carbonate stability fields after Rosenberg and Holland (1964) is unreliable but most fluids are evidently in equilibrium with either dolomite or calcite and cluster near the extrapolated phase boundary.

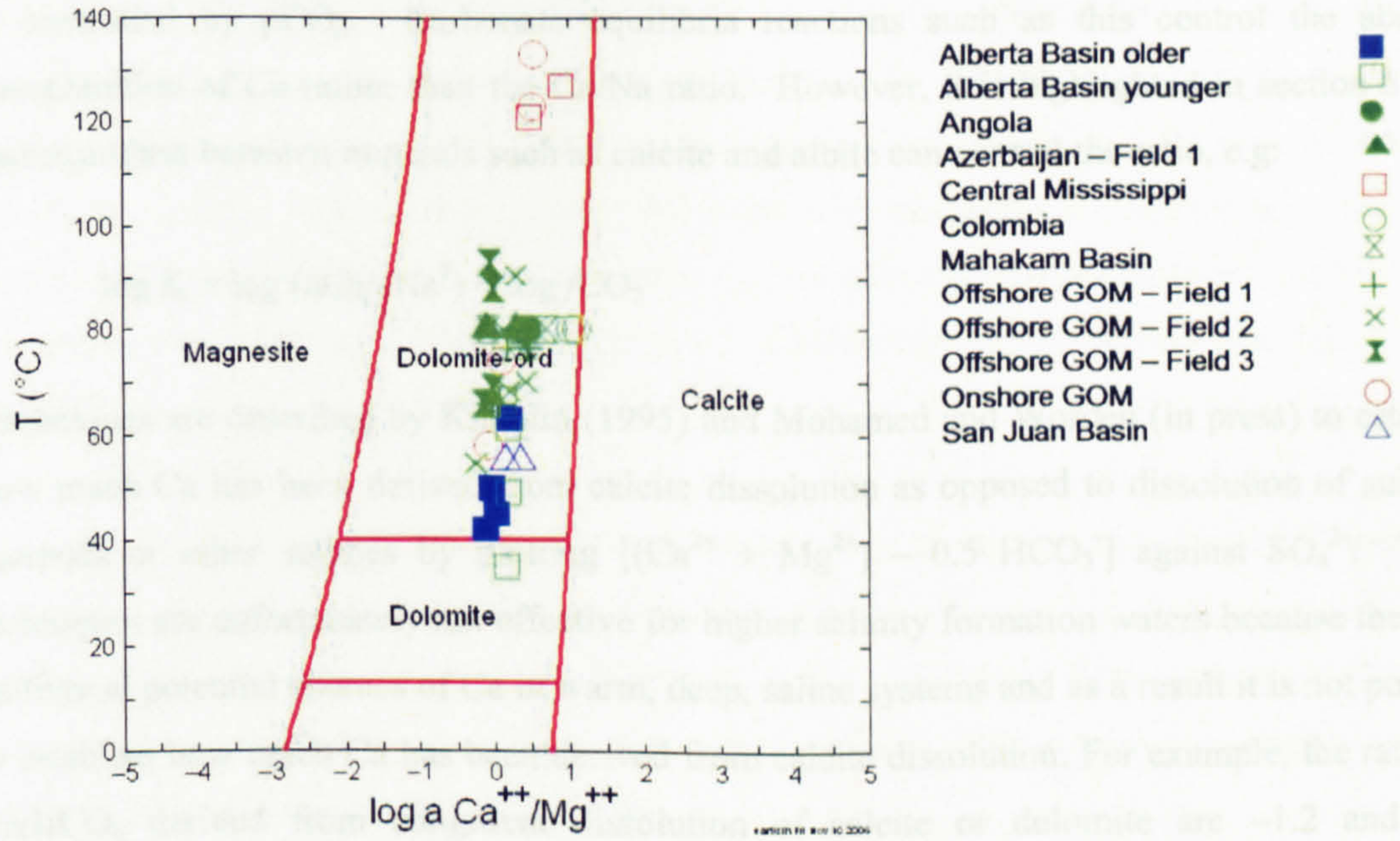

Figure 5.17. Global waters plotted on a stability diagram using Geochemists' Workbench indicate that most waters have a Ca/Mg ratio too low to be in equilibrium with calcite. The ratio may be controlled by equilibrium between calcite and Mg-clay.

5.3.5 Carbonate equilibria and the importance of CO_2

Calcium-bearing carbonate minerals such as calcite and dolomite have been identified previously as potential sources of Ca and Mg in moderate salinity waters and their equilibrium with formation waters is a potential control on Ca and Mg concentrations. It has been shown that at moderate salinities Ca and Na proportions may be buffered by mineral equilibrium reactions (e.g. reaction 1). However, many petroleum reservoirs contain only detrital albite or already fully albitised plagioclase with Ca only present in calcite, dolomite, anhydrite or gypsum. In these circumstances Ca concentration is coupled to pCO_2. The equation for calcite dissolution in this type of system is:

$$CaCO_3 + CO_2 + H_2O \leftrightarrow Ca^{2+} + 2HCO_3^- \qquad (6)$$

(see also reaction 2, earlier) where the equilibrium constant K:

$$K = 10^{-6.0} = \frac{aCa^{2+}\ aHCO_3^{-2}}{pCO_2} \qquad (7)$$

is controlled by pCO_2. Carbonate equilibria reactions such as this control the absolute concentration of Ca rather than the Ca/Na ratio. However, it is highlighted in section 5.3.3.3 that equilibria between minerals such as calcite and albite can control the ratio, e.g:

$$\log K = \log (aCa/aNa^2) + \log fCO_2$$

Techniques are described by Kimblin (1995) and Mohamed and Worden (in press) to establish how much Ca has been derived from calcite dissolution as opposed to dissolution of sulphate minerals or other sources by plotting $[(Ca^{2+} + Mg^{2+}) - 0.5\ HCO_3^-]$ against SO_4^{2-}. These techniques are unfortunately not effective for higher salinity formation waters because there are additional potential sources of Ca in warm, deep, saline systems and as a result it is not possible to establish how much Ca has been derived from calcite dissolution. For example, the ratios of Ca/HCO_3 derived from congruent dissolution of calcite or dolomite are ~1.2 and ~1.4 respectively (Mohamed and Worden, in press), while the ratios for this dataset vary between 0.000545 and ~7000.

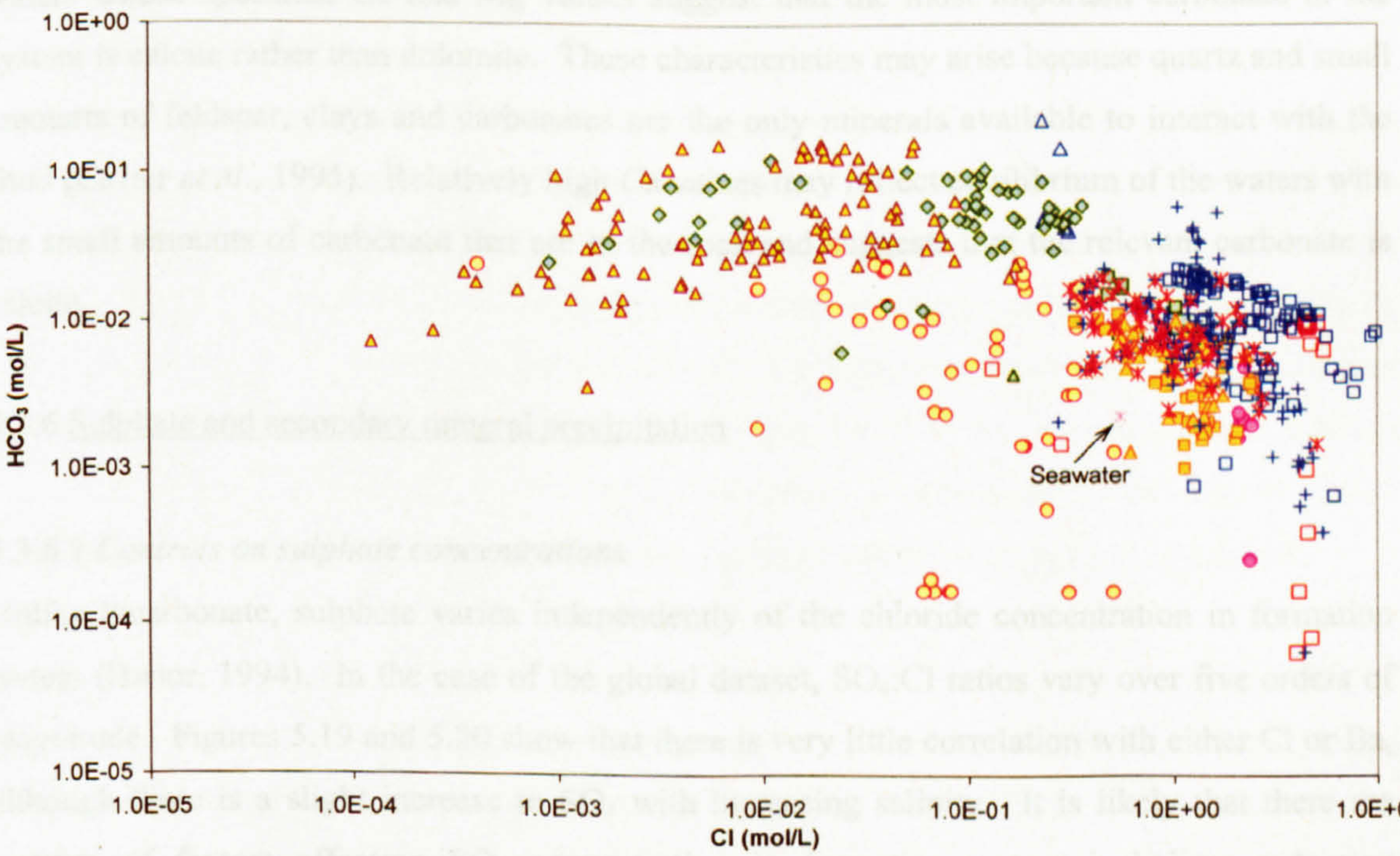

Figure 5.18. Bicarbonate shows a distinctive inverse correlation with Cl at moderate to high salinities, which reverses slightly at low salinities.

5.3.5.1 *Low salinity bicarbonate waters*

Many low-salinity formation waters tend to be Na-HCO_3 dominated (Hanor, 1994). An additional trend highlighted in studying Na and Ca behaviour in this dataset is the relatively high proportion of Ca in the very lowest salinity waters (Trend 3, Figure 5.11). At low

temperatures $CaCO_3$ is more soluble than Ca-silicates (e.g. Maher *et al.*, 2006) and low temperature, low salinity waters are more likely to be dominated by dissolved calcium bicarbonate (Figure 5.18). The inverse correlation between HCO_3 and Cl may be due to a salting-out effect. The activity of water decreases with increasing Cl concentration (salinity), thus reducing the solubility of certain system components e.g. carbonates (see Chapter 4 for a discussion about salting-out with respect to silica solubility). High salinity also reduces CO_2 solubility.

As discussed in Chapter 3, formation water compositions in the San Juan Basin are controlled by bicarbonate concentrations and equilibrium with Na-silicates and coal. Similar trends evident in low salinity waters from Colombia and the Mahakam Basin indicate that similar processes are occurring in these locations despite significant differences in age, temperature and mineralogical composition (See Table 5.3).

5.3.4.3 *Carbonate systematics in specific locations*

Colombian formation waters have extremely high XCa and Ca/Mg ratios and are the only waters whose speciated Ca and Mg values suggest that the most important carbonate in the system is calcite rather than dolomite. These characteristics may arise because quartz and small amounts of feldspar, clays and carbonates are the only minerals available to interact with the fluid (Cazier *et al.*, 1995). Relatively high Ca values may reflect equilibrium of the waters with the small amounts of carbonate that are in the rock and suggests that the relevant carbonate is calcite.

5.3.6 Sulphate and secondary mineral precipitation

5.3.6.1 *Controls on sulphate concentrations*

Unlike bicarbonate, sulphate varies independently of the chloride concentration in formation waters (Hanor, 1994). In the case of the global dataset, SO_4:Cl ratios vary over five orders of magnitude. Figures 5.19 and 5.20 show that there is very little correlation with either Cl or Ba, although there is a slight increase in SO_4 with increasing salinity. It is likely that there are number of factors affecting SO_4 concentration in formation waters including: reduction (biogenic and thermogenic) to sulphide (and therefore organic carbon availability and type, and temperature) and equilibrium with sulphate minerals (Worden *et al.*, 2003; McCartney *et al.*, 2005; Cross *et al.*, 2004).

A major control on the concentration of SO_4 in formation waters is equilibrium with sulphate minerals, particularly barite and anhydrite. Barite solubility is a particular issue in the short term and is an important factor in the prediction of oilfield scales. High levels of Ba and SO_4

cannot coexist due to the insoluble nature of barite. Thus, a strong inverse correlation between the two species might be expected and is conspicuous by its absence (Figure 5.20). Despite this, the vast majority of the data appear to be supersaturated with respect to the barite saturation curve for the relevant temperature and salinity (Figure 5.20). Since saturation is exceeded by orders of magnitude in many cases, these discrepancies merit further evaluation.

Part of the problem may lie in the analysis for SO_4. Until recently SO_4 was derived from AA or ICP-AES measurements of total sulphur (Collins, I. 2006, pers.comm.). These overestimate the SO_4 content in many cases since there are water-soluble reduced sulphur species that can be present. In addition, other aqueous sulphate or bisulphate species may contribute to the overall concentration of SO_4, causing the fluid to appear supersaturated with barite. When the specific activities of the Ba^{2+} and SO_4^{2-} ions (speciated using GWB) are plotted for each location, a number of fluids remain supersaturated (Figure 5.21). The amount of the excess SO_4 present relative to a saturated fluid is plotted for each location on Figure 5.22. It is possible that waters remain supersaturated with respect to barite because slow kinetics have prevented the mineral from precipitating. However, barite scale is known to precipitate extremely rapidly under certain circumstances during the production of hydrocarbons.

An explanation is required for the cause of the apparent poor quality of the remaining supersaturated analyses. A slightly reduced water will have a sulphide as a well as a sulphate component and the sulphide could contribute to an anomalously high measured sulphate value. Unfortunately, no redox pairs were analysed to be able to confirm is this is the case. Figure 5.22 plots the amount of excess sulphate present in the formation water relative to the amount that should be present at barite saturation. It is possible that this excess sulphate actually equates to sulphide measured as part of the total sulphur. In general the fields with the highest saturation ratios are those which appear to have the highest relative proportion of sulphide.

5.3.6.2 *Specific examples*

It has been shown through extensive study of one field in particular (Miller, North Sea, Chapter 4) that controls on SO_4 concentration in waters from producing oilfields are complex. In this case, following mixing of formation water with injected seawater, there was a distinct loss of SO_4 from the mixture that is greater than can be accounted for by precipitation of Ba and Sr sulphate minerals alone. It is likely that this decrease is either due to anhydrite precipitation or to SO_4 reduction. Anhydrite precipitation from a mixture of waters should cause a corresponding drop in Ca concentrations, which is the direct opposite to what was observed. Sulphate reduction at depth is also believed to be responsible for higher levels of HCO_3, as in the San Juan Basin (Chapter 3). However, there is no correlation between HCO_3 and SO_4, probably due to additional limitations imposed by carbonate and sulphate equilibria.

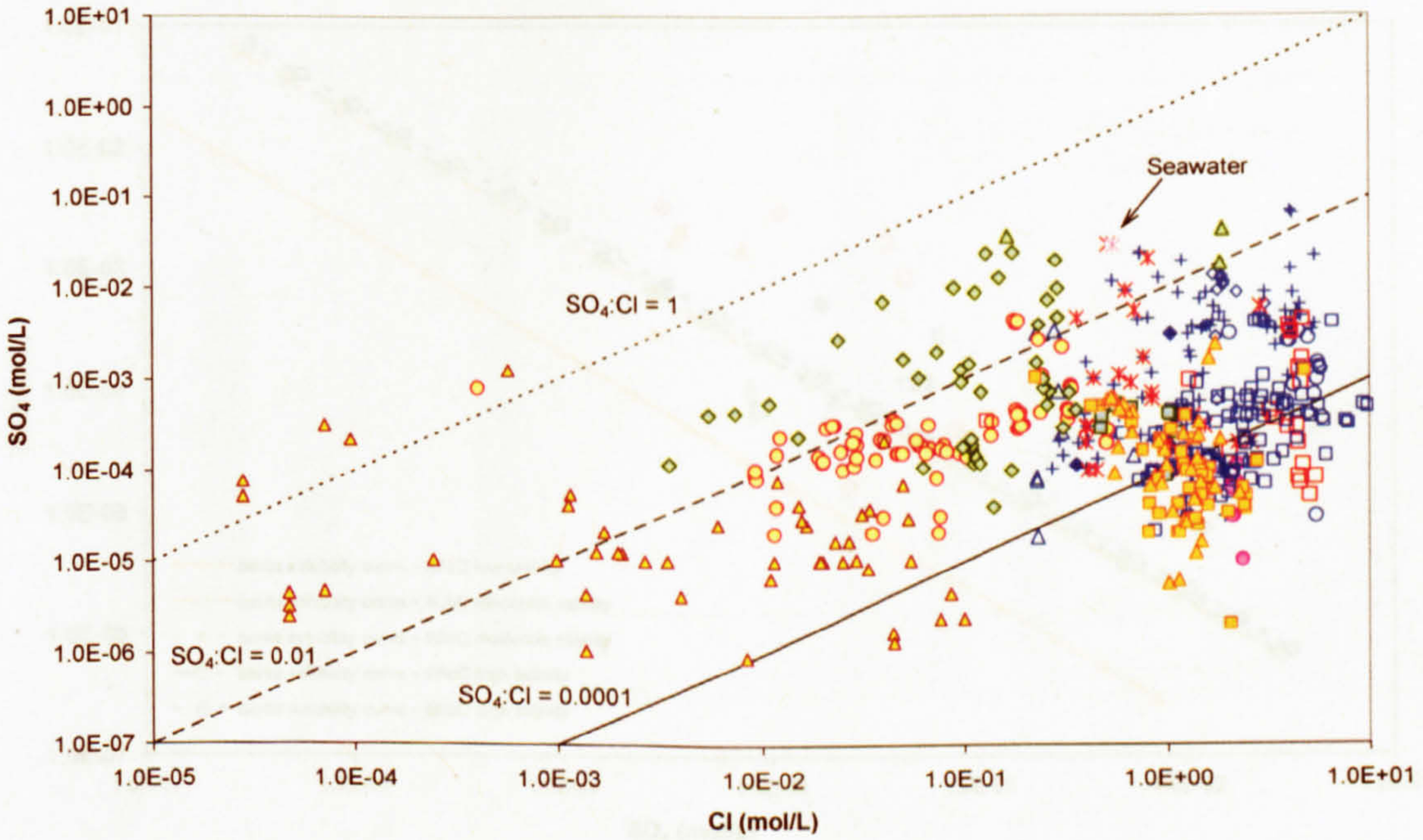

Figure 5.19. Sulphate does not correlate with Cl, and the SO_4:Cl ratio varies over several orders of magnitude

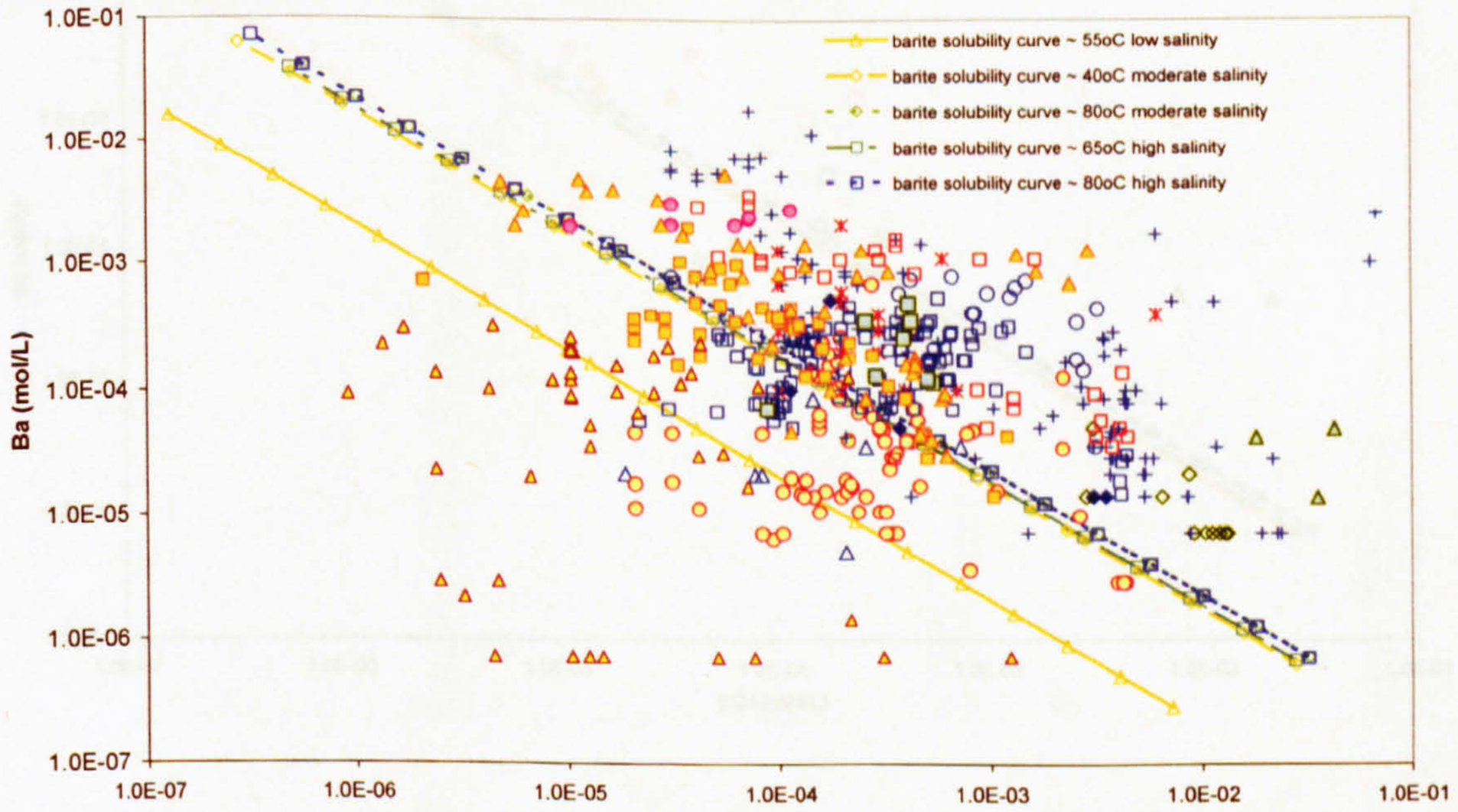

Figure 5.20. Sulphate shows no correlation with Ba. Note that most measured SO_4 and Ba values in global fluids indicate supersaturation with respect to barite.

A

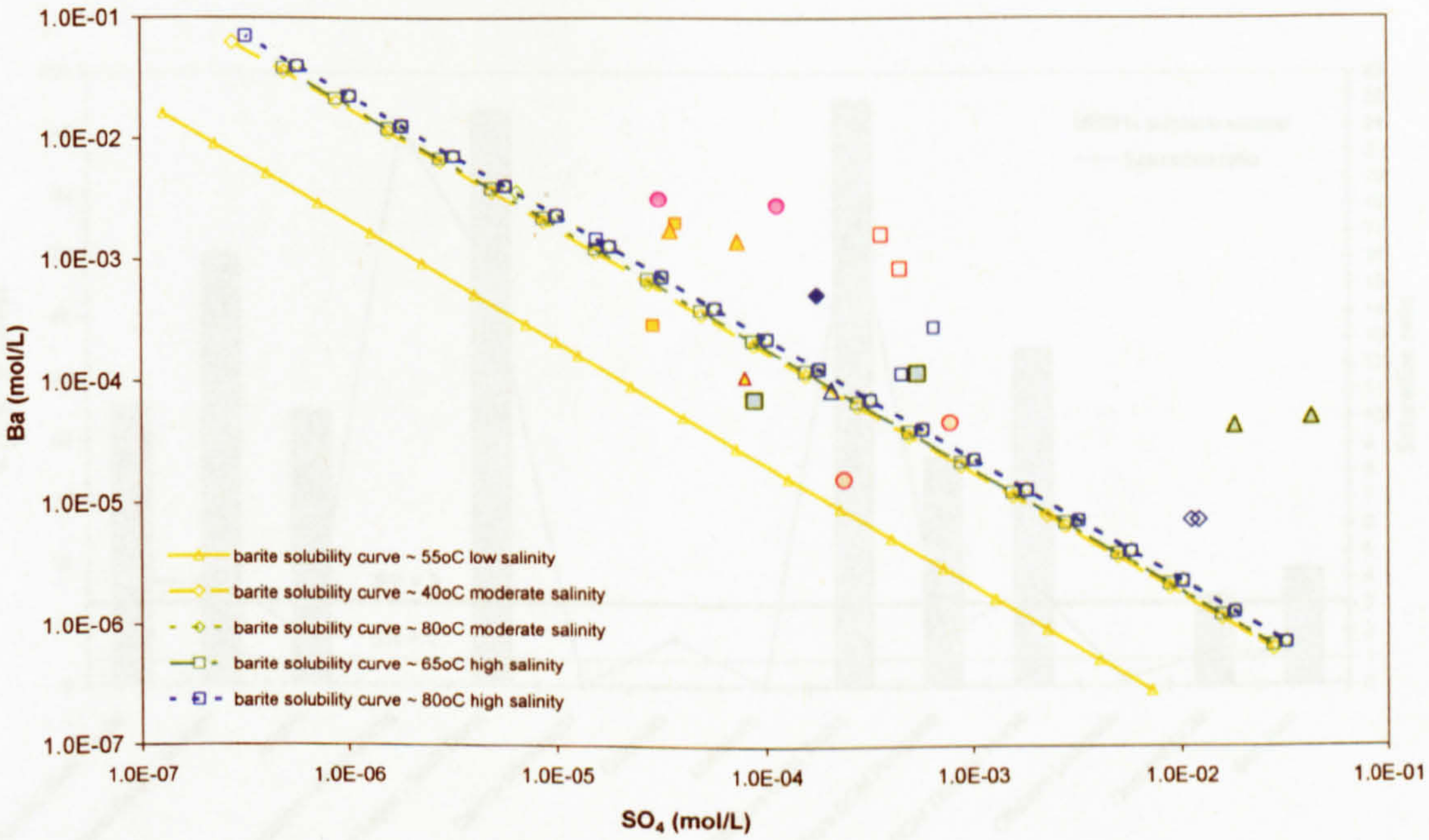

B

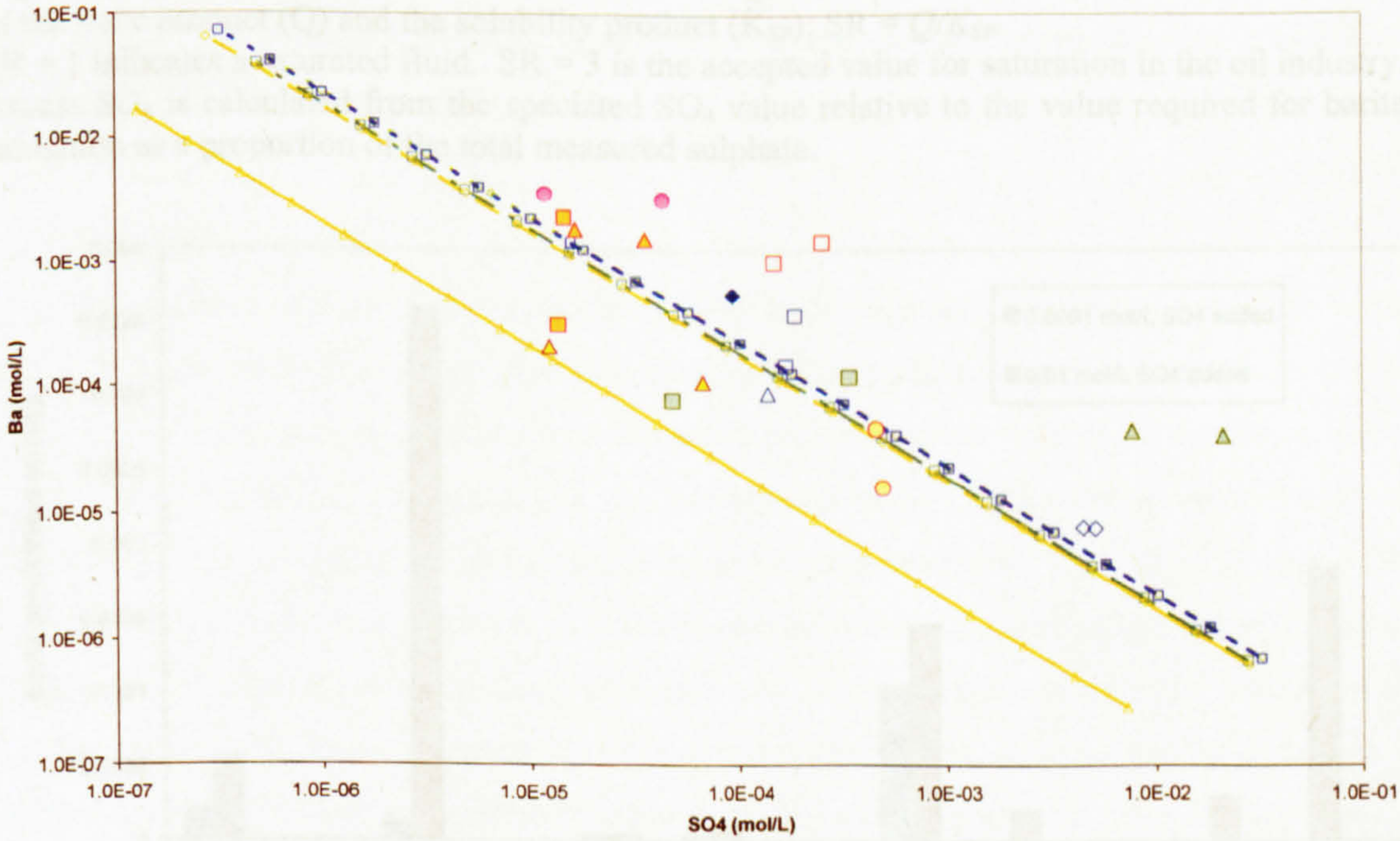

Figure 5.21. A. Molar concentrations of Ba and SO_4 for representative waters from each location in the global database. B. Speciated SO_4 and Ba values for the same anayses. Note some waters remain supersaturated with respect to barite while others are undersaturated or close to saturation.

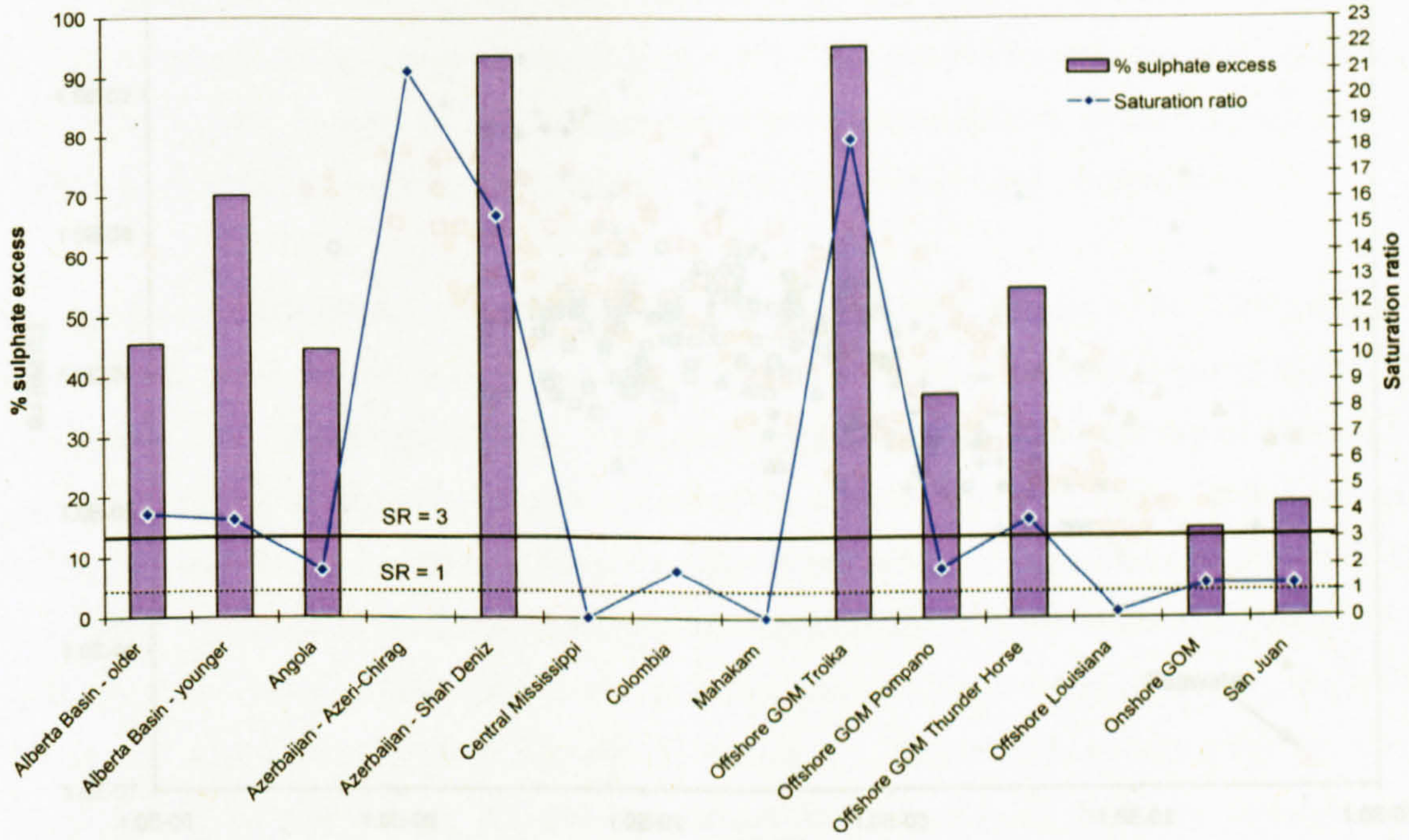

Figure 5.22. Saturation ratios for each location calculated using Geochemists' Workbench. The degree of supersaturation of a water is defined using the saturation ratio (SR) which is the ratio of the ionic product (Q) and the solubility product (K_{SP}): SR = Q/K_{SP}
SR = 1 indicates a saturated fluid. SR = 3 is the accepted value for saturation in the oil industry. Excess SO_4 is calculated from the speciated SO_4 value relative to the value required for barite saturation as a proportion of the total measured sulphate.

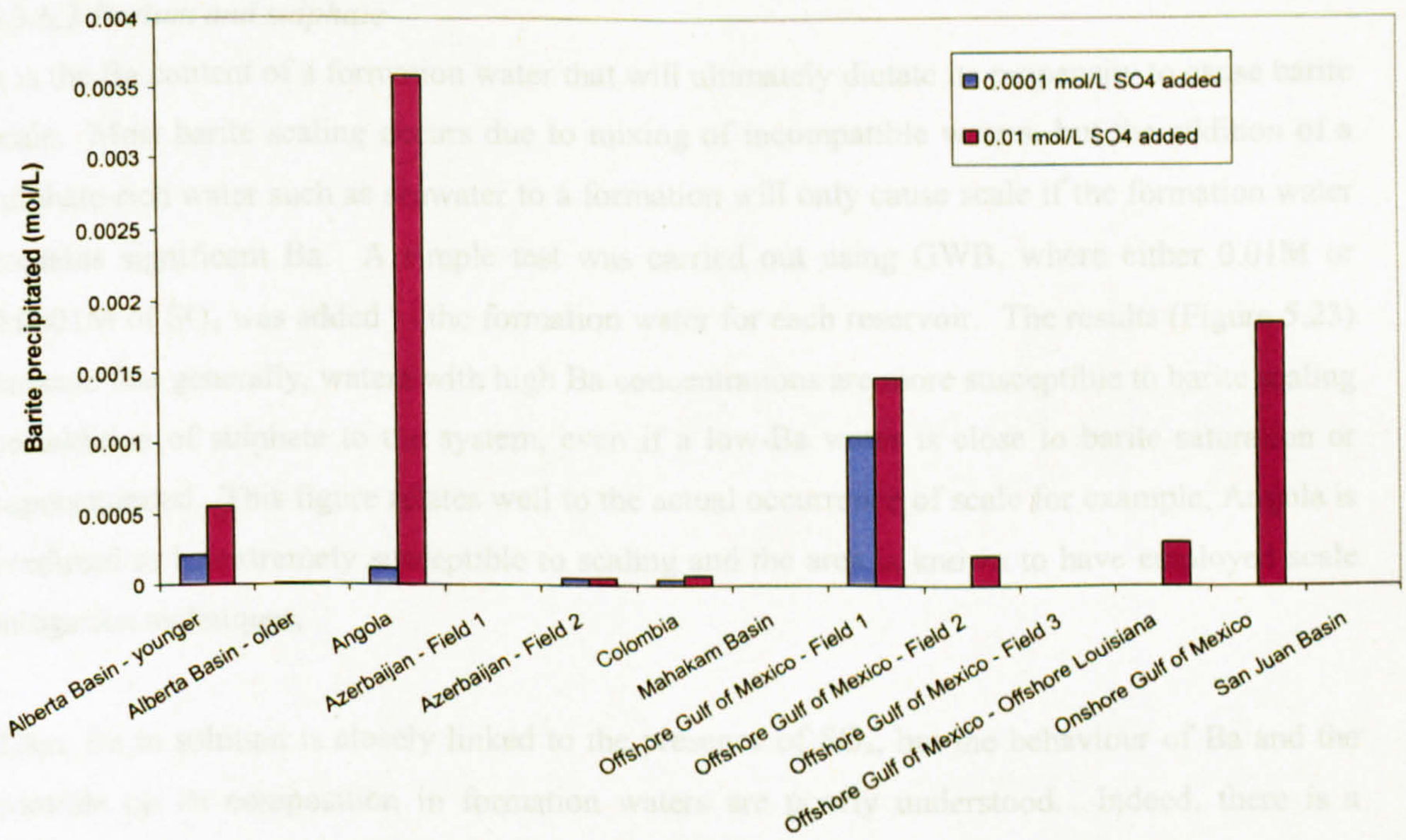

Figure 5.23. Modelled amount of barite precipitated on addition of different amounts of sulphate to the system for each location

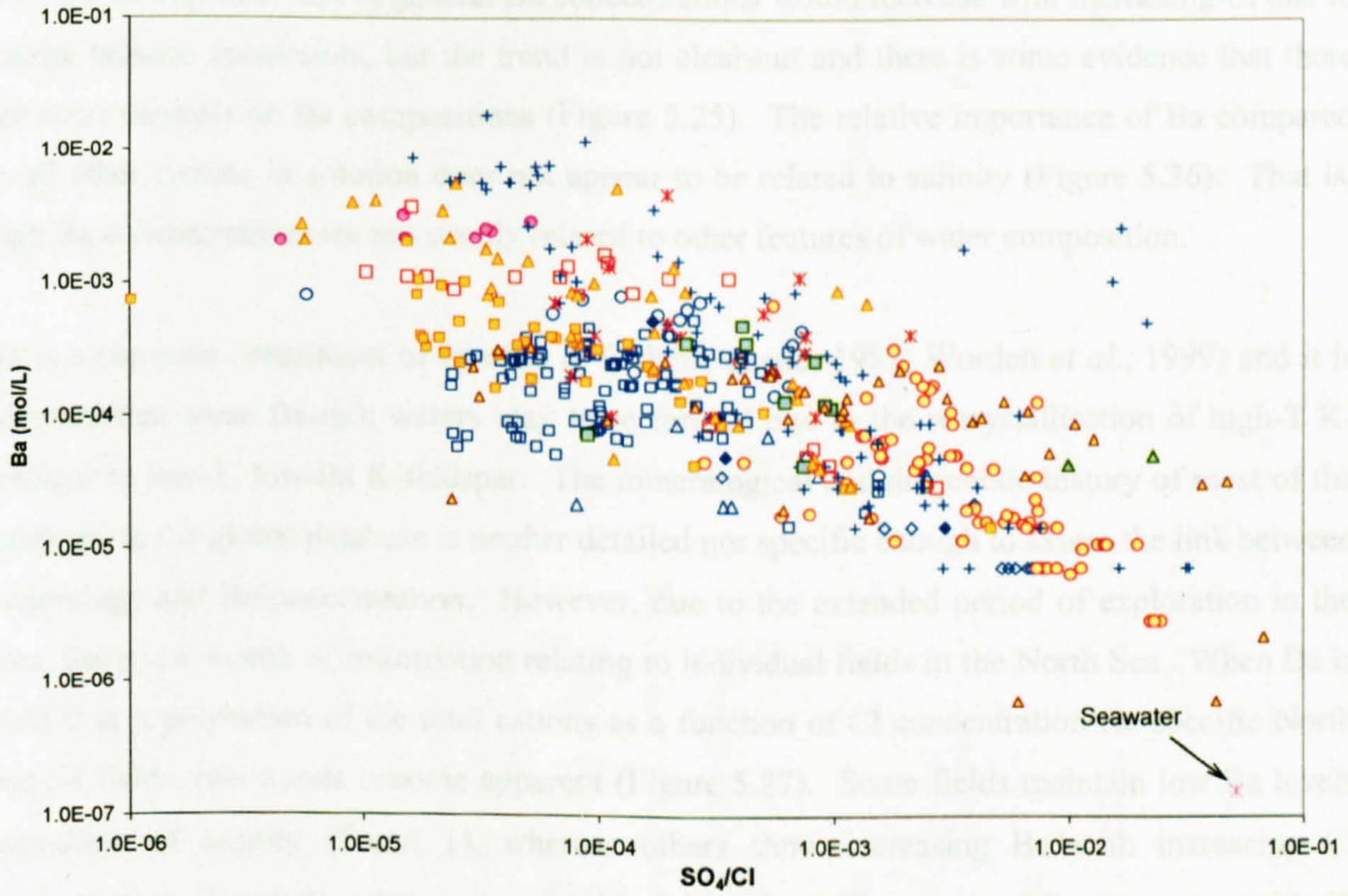

Figure 5.24. The concentration of Ba in solution decreases as the relative importance of SO_4 as an anion increases.

5.3.6.3 *Barium and sulphate*

It is the Ba content of a formation water that will ultimately dictate its propensity to cause barite scale. Most barite scaling occurs due to mixing of incompatible waters, but the addition of a sulphate-rich water such as seawater to a formation will only cause scale if the formation water contains significant Ba. A simple test was carried out using GWB, where either 0.01M or 0.0001M of SO_4 was added to the formation water for each reservoir. The results (Figure 5.23) indicate that generally, waters with high Ba concentrations are more susceptible to barite scaling on addition of sulphate to the system, even if a low-Ba water is close to barite saturation or supersaturated. This figure relates well to the actual occurrence of scale for example, Angola is predicted to be extremely susceptible to scaling and the area is known to have employed scale mitigation techniques.

Thus, Ba in solution is closely linked to the presence of SO_4, but the behaviour of Ba and the controls on its composition in formation waters are poorly understood. Indeed, there is a general trend towards lower Ba at higher relative SO_4 concentrations (Figure 5.24); however while there is also higher Ba at higher Cl concentrations (Figure 5.25), there is no evidence for any significant correlation to any other major species.

It would be expected that in general Ba concentrations would increase with increasing Cl due to charge balance constraints, but the trend is not clear-cut and there is some evidence that there are other controls on Ba compositions (Figure 5.25). The relative importance of Ba compared to all other cations in solution does not appear to be related to salinity (Figure 5.26). That is, high Ba concentrations are not simply related to other features of water composition.

Ba is a common constituent of igneous K-feldspar (Land, 1987; Worden *et al.*, 1999) and it is believed that some Ba-rich waters may have formed due to the recrystallisation of high-T K-feldspar to low-T, low-Ba K-feldspar. The mineralogical and diagenetic history of most of the locations in the global database is neither detailed nor specific enough to assess the link between mineralogy and Ba concentration. However, due to the extended period of exploration in the area, there is a wealth of information relating to individual fields in the North Sea. When Ba is plotted as a proportion of the total cations as a function of Cl concentration for specific North Sea oil fields, two trends become apparent (Figure 5.27). Some fields maintain low Ba levels regardless of salinity (Trend 1), whereas others show increasing Ba with increasing Cl concentration (Trend 2). As a general rule, fields whose Ba concentration increases with Cl tend to be deeper and have less saline formation waters, although variability in temperature is consistent throughout the whole North Sea. Interestingly, the fields containing Ba-rich pore waters all tend to have reservoir rocks from high energy environments, such as fluvial deposits and most commonly, turbidites. Conversely, the low-Ba fields are generally aeolian, deltaic, shallow marine or lacustrine.

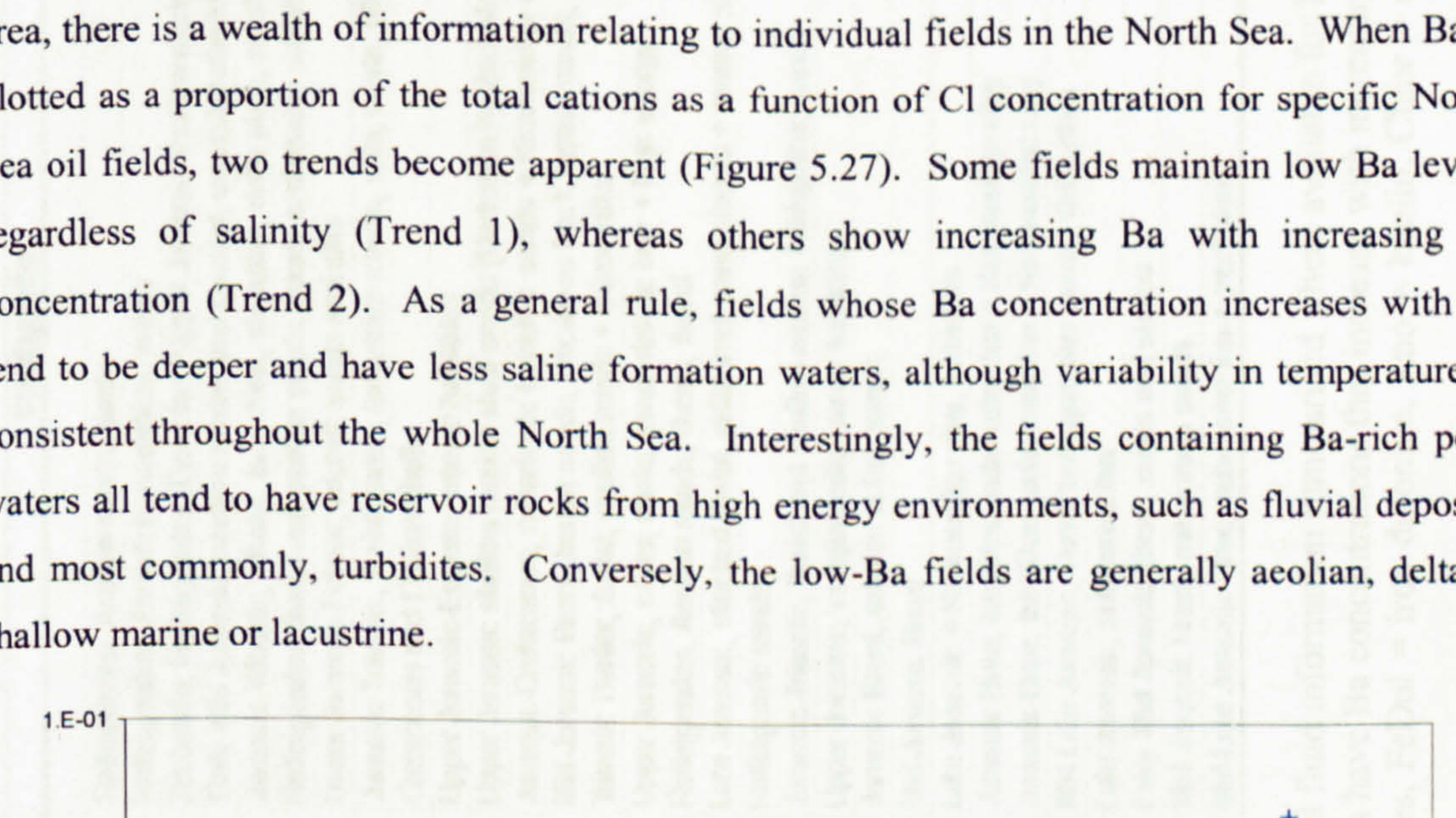

Figure 5.25. Ba concentrations generally increase with increasing salinity, however the trend is not linear and there are additional controls on Ba concentration in formation waters

Trend 1	Trend 2	Temperature (oC)	Depth (m)	Stratigraphy	Mineralogy	TDS
Amethyst		90	2780	Rotleigendes, Aeolian sands, dunes	Qtz, Fsp, Calc, Dol, Ill	
Anglia			2590	Rotleigendes, Zechstein evaporites, sands		250000
Argyll		85	2700	Zechstein, Rotleigendes, Devonian, Upper Jurassic shallow marine sands	Dol Lsts, clean dunes, anhydrite	60000
Beatrice		79	2010	Early-Mid Jurassic, shallow marine and coastal, sands/interbedded clays		58000
Beryl		99	3000-5000	Jurassic-Triassic, alluvial, lacustrine, shoreline, delta plain, sand/shale/coal		40000-100000
Cleeton		80	2770	Rotleigendes, fluvial and aeolian sands, sandy and muddy sabkha deposits	Qtz, FeDol, Kao, Ill authigenic	214000
Clyde		146	3800	Lower Jurassic Fulmar, arkosic sands and silts	Sponges, Qtz, Dol cements	190000
Crawford		87	2600-3900	Jurassic-Triassic, fluvial sands, lacustrine sands, silts, muds, alluvial plain	Chlor cement	80000-160000
Ekofisk		140	3200-4400	Cretaceous and Danian chalk	Low Mg Calc, silica, glauconite et	30000-160000
Guillemot				Upper Jurassic-Eocene, marine turbidites		75000-20200
Gyda		154	4000	Upper Jurassic shallow marine shelf sands (Underlain by Zechstein)	Qtz, minor Ill and carbonate ceme	270000
Highlander		90	3000	Jurassic-Cretaceous, subarkosic turbiditic sands + Kimmeridge clay		85000
Hild		150	4250	Mid-Jurassic Brent, barrier sands, micaeous back barrier sands, lagoonal sh	Ill, Kao, (Calc+Fsp diss), Calc cer	70000
Orwell		167	1540	Triassic Bunter, fluvial, aeolian sands + minor silts		180000
Piper		79		Upper Jurassic, coals, shale, sand, deltaic bay + high energy	Qtz, Calc cements	70000
Ravenspurn		100	3197	Rotleigendes, Aeolian sands, dunes, fluvial	Auth, ill, Qtz, carbonate	265000
Scott		125		Late Jurassic, stacked fluvial, delta front sand sheets + marine shales		125000
Thames		83	2450	Rotleigende sands		250000
	Brent	95	3000	Jurassic-Triassic, fluvial and shallow marine, feldspathic sands	Qtz + carbonate cements	23000
	Central Brae	123	4100	Upper Jurassic, conglomeritic sandy turbidites	Calc cement	120000
	Cormorant	90	2500	Jurassic Brent, arkosic deltaic sands,	Lack det Fsp, Kao, Qtz, Ill cemen	17000
	Don	130		Mid-Jurassic Brent		
	Magnus	115	3050	Late Jurassic + Kimmeridge clay, turbidites	Fsp diss, Kao, Qtz, Calc, FeDol, I	30000
	Miller	120	4000	Jurassic Brae, turbidites, submarine fan + Kimmeridge clay	Qtz, Calc cement, Fsp diss	78000
	North Brae	120	3900	Jurassic Brae, turbidites, submarine fan + Kimmeridge clay		80000
	Osebeg	100	3000	Mid-Late Jurassic, Brent, transgressive sands, delta plain		40000-70000
	South Brae	123	4000	Late Jurassic, submarine fan		80000
	Statfjord	100	3000	Early-Mid Jurassic Brent, sands and shales		23000
	Thistle	100	3345	Mid-Jurassic Brent, micaceous sands	Qtz, Calc	
	Tiffany, Toni and Thelma	140	4000	Mid-Late Jurassic Brae, submarine fan + zechstien		100000

Table 5.4 Temperature, depth stratigraphic, mineralogical and fluid information summarised where available for North Sea oil fields. Trend 1 fields are those which exhibit consistently low Ba concentrations and Trend 2 fields have Ba concentrations that increase with increasing Cl. Abbreviations: Qtz = quartz, Fsp = feldspar, Calc = calcite, Dol = dolomite, Ill = illite, Lsts = limestones, FeDol = iron dolomite, Kao = kaolin, Chlor = chlorite, Auth = authigenic, Det = detrital, Diss = dissolution

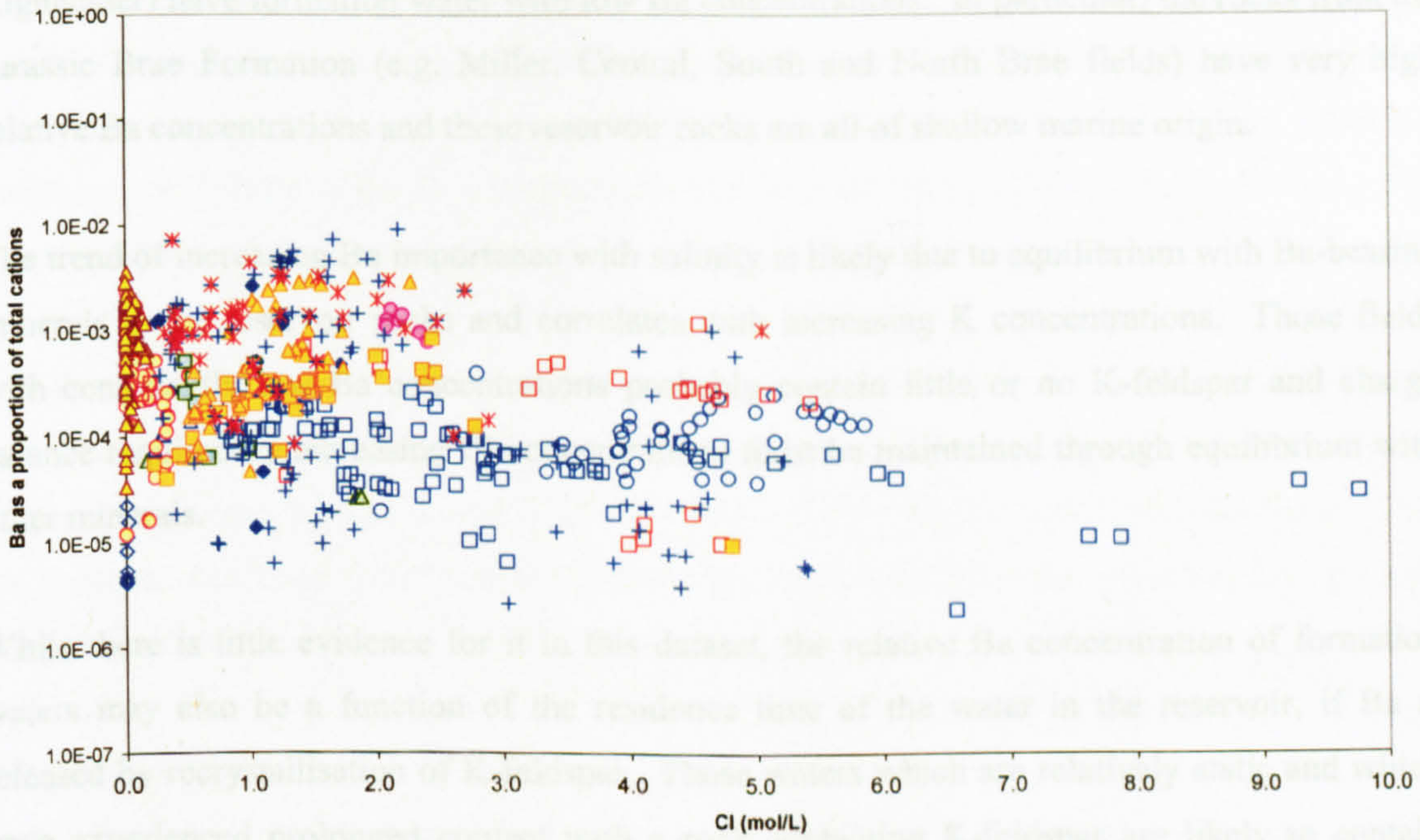

Figure 5.26. The relative importance of Ba as a cation is not affected by changes in salinity.

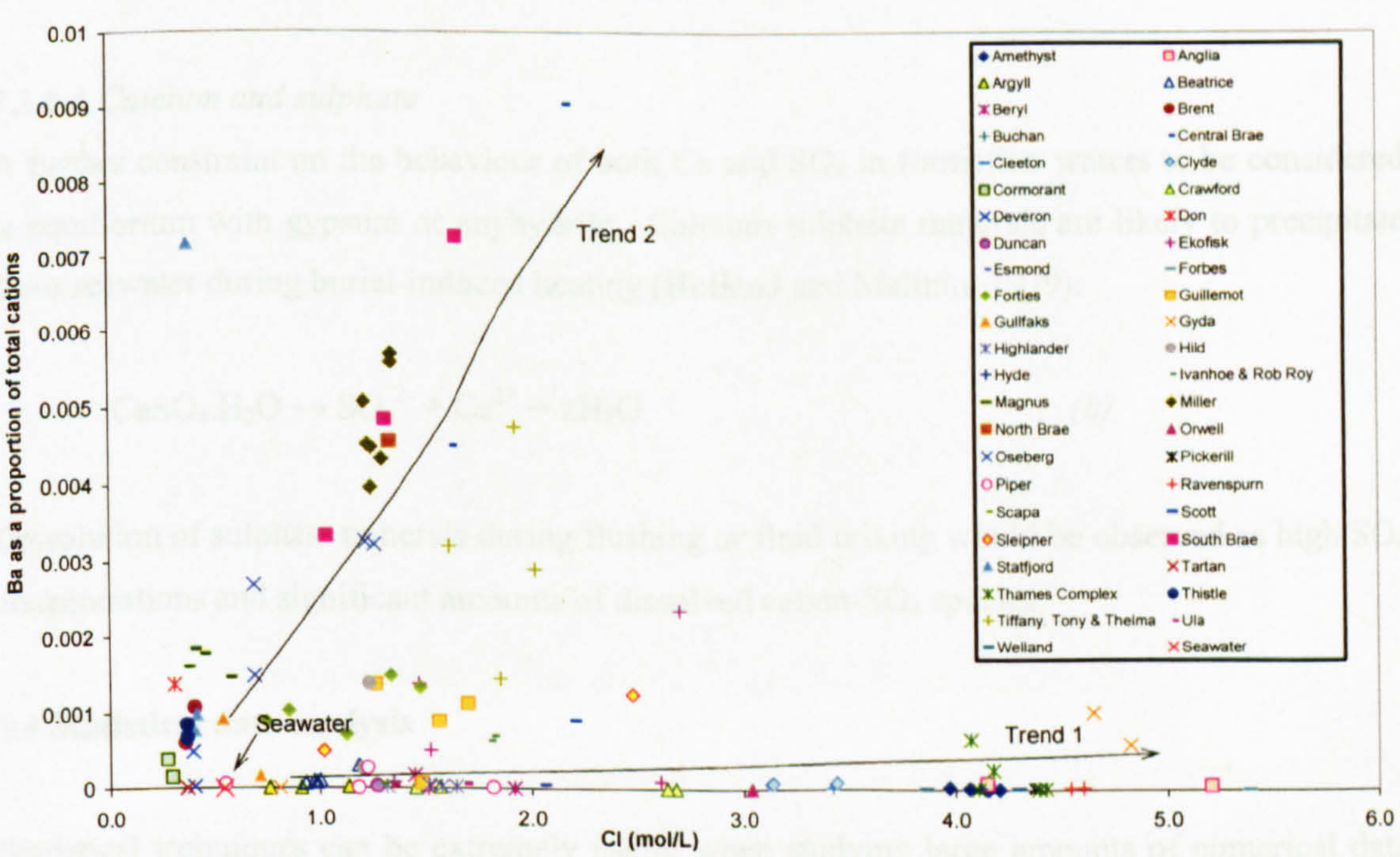

Figure 5.27. North Sea oil fields define two limiting trends when Ba is plotted as a proportion of the total cations. Those formation waters with increasing Ba concentrations tend to be from rocks of Jurassic age containing K-feldspar.

Significantly, the reservoir rocks from all the fields with increasing Ba are Jurassic or Palaeocene in age, while only four fields with Jurassic age rocks (Clyde, Beatrice, Gyda and Highlander) have formation water with low Ba concentrations. In particular, the rocks from the Jurassic Brae Formation (e.g. Miller, Central, South and North Brae fields) have very high relative Ba concentrations and these reservoir rocks are all of shallow marine origin.

The trend of increasing Ba importance with salinity is likely due to equilibrium with Ba-bearing minerals in the reservoir rocks and correlates with increasing K concentrations. Those fields with consistently low Ba concentrations probably contain little or no K-feldspar and charge balance required by increasing Cl concentrations must be maintained through equilibrium with other minerals.

While there is little evidence for it in this dataset, the relative Ba concentration of formation waters may also be a function of the residence time of the water in the reservoir, if Ba is released by recrystallisation of K-feldspar. Those waters which are relatively static and which have experienced prolonged contact with a rock containing K-feldspar are likely to contain more Ba than a dynamic formation water moving through a similar kind of rock, which may have been previously leached of Ba.

5.3.6.4 *Calcium and sulphate*

A further constraint on the behaviour of both Ca and SO_4 in formation waters to be considered is equilibrium with gypsum or anyhydrite. Calcium sulphate minerals are likely to precipitate from seawater during burial-induced heating (Holland and Malinin, 1979):

$$CaSO_4.H_2O \leftrightarrow SO_4^{2-} + Ca^{2+} + 2H_2O \qquad (8)$$

Dissolution of sulphate minerals during flushing or fluid mixing would be observed as high SO_4 concentrations and significant amounts of dissolved cation-SO_4 species.

5.4 Statistical data analysis

Statistical techniques can be extremely useful when studying large amounts of numerical data and are used here to further constrain the main controls on formation water chemistry. Principal components analysis (PCA) and hierarchical cluster analysis (HCA), designed to condense the data and identify general trends, are used to better understand a dataset as detailed as this. These methods of analysis were carried out on the bulk of the global data and the results are presented below.

5.4.1 Principal Components Analysis

PCA is a commonly used technique for finding patterns in data of high dimension and expressing the data in such a way as to highlight their similarities and differences. PCA involves transferring the data such that its (multidimensional) variability (variance) can be expressed using fewer dimensions. The reduced dimensions are known as Principal Components (PCs) and the PC that accounts for most of the variability of the data generally describes the most important aspects of this data (Swan and Sandilands, 1995).

Initial variables included in the analysis were: molar concentrations of Na, K, Mg, Ca, Ba, Cl and SO_4, together with XCa (Ca/Ca+Na) and Na/K ratios. Excel was used with the *statistiXL* add-on to carry out both PCA and HCA techniques. Following the initial analysis, further tests were carried out using fewer initial variables to continue to define the principal data controls (Appendix IX).

5.4.2 PCA Results

Table 5.5. Initial PCA test (test 1) – all data included, 39% of the variability is accounted for by PC1

Explained Variance (Eigenvalues)						
Value	PC 1	PC 2	PC 3	PC 4	PC 5	PC 6
Eigenvalue	3.522	1.162	1.123	1.040	0.810	0.613
% of Var.	39.132	12.912	12.479	11.560	8.999	6.808
Cum. %	39.132	52.044	64.523	76.083	85.081	91.890

Component Loadings (correlations between initial variables and principal components)						
Variable	PC 1	PC 2	PC 3	PC 4	PC 5	PC 6
Na	0.767	0.328	0.305	-0.271	-0.303	-0.074
K	0.593	-0.329	-0.030	-0.221	0.396	-0.548
Mg	0.723	0.179	-0.100	0.160	0.022	0.290
Ca	0.878	-0.086	-0.101	0.258	0.082	0.021
Ba	0.079	-0.448	0.738	-0.212	0.297	0.339
Cl	0.902	0.220	0.216	-0.134	-0.204	-0.041
SO4	0.174	0.113	-0.538	-0.719	0.251	0.274
XCa	0.650	-0.319	-0.294	0.441	0.147	0.173
Na/K	-0.117	0.737	0.203	0.226	0.583	-0.028

The first three principal components account for ~65% of the variance in the dataset. The relative values of the PCs can give an indication if the most important factors affecting fluid composition. For example, PC1 accounts for nearly 40% of the variance and is likely to be related to salinity, on which Cl, Na, Mg, and Ca have a strong dependence; Ba, SO_4 and Na/K values appear to be less dependent on salinity. Similarly, PC2 is correlated with $MgCl_2$, PC3 with BaCl, PC4 with the hardness (alkaline earth metals, Mg + Ca), PC5 with K, Ba and SO_4 and PC6 with Mg, Ba and SO_4. Thus, according to the numbers, most of the variance is due to salinity and then the rest is related to the divalent cations. However, PCA is most useful in

identifying similarities and differences within and between datasets from different locations. Figure 5.28 shows how the data cluster on cross plots of the first three PCs. Seawater is believed to have been a major contributor to many formation waters worldwide. If the original source of formation waters was a dominant control on their compositions, then a "fingerprint" common to seawater-derived waters would be expected in PCA. However, it is clear that most locations occupy distinct areas of the plot, indicating that alternative controls on formation water composition are important.

Changing the original analysis by removing a certain parameter (e.g. Table 5.6) changes the result slightly. However, the relative importance of the different PCs remains unaltered and the formation waters still appear separately on a PC cross plot. It is also useful to note that waters tend to cluster on these plots according to their geographical locations, emphasising the similarities between waters from particular reservoirs.

Table 5.6. PCA test 2 – Na/K ratio removed from analysis, nearly 44% of the variance is accounted for by PC1

Explained Variance (Eigenvalues)					
Value	PC 1	PC 2	PC 3	PC 4	PC 5
Eigenvalue	3.512	1.126	1.056	0.952	0.613
% of Var.	43.902	14.080	13.198	11.903	7.665
Cum. %	43.902	57.981	71.179	83.082	90.746
Component Loadings (correlations between initial variables and principal components)					
Variable	PC 1	PC 2	PC 3	PC 4	PC 5
Na	0.770	0.167	-0.469	-0.326	-0.084
K	0.590	0.078	0.006	0.560	-0.536
Mg	0.726	-0.145	0.082	-0.156	0.303
Ca	0.878	-0.055	0.296	0.025	0.023
Ba	0.075	0.841	-0.092	0.399	0.345
Cl	0.905	0.125	-0.274	-0.238	-0.047
SO4	0.172	-0.567	-0.546	0.513	0.276
XCa	0.646	-0.154	0.600	0.168	0.170

5.4.3 Implications of statistical analysis

The most important information that can be gained from the statistical analyses is that salinity is the overriding characteristic of formation waters and determines much of the variability observed. It is likely, due to the differences observed, that water-rock interactions account for the rest of the variability and are extremely important in determining the present formation water compositions. Significantly, while trends can be identified from individual ion concentrations and ratios, using both traditional and statistical techniques, all the formation water chemistry information available is of no use without further knowledge of the mineralogy of the system.

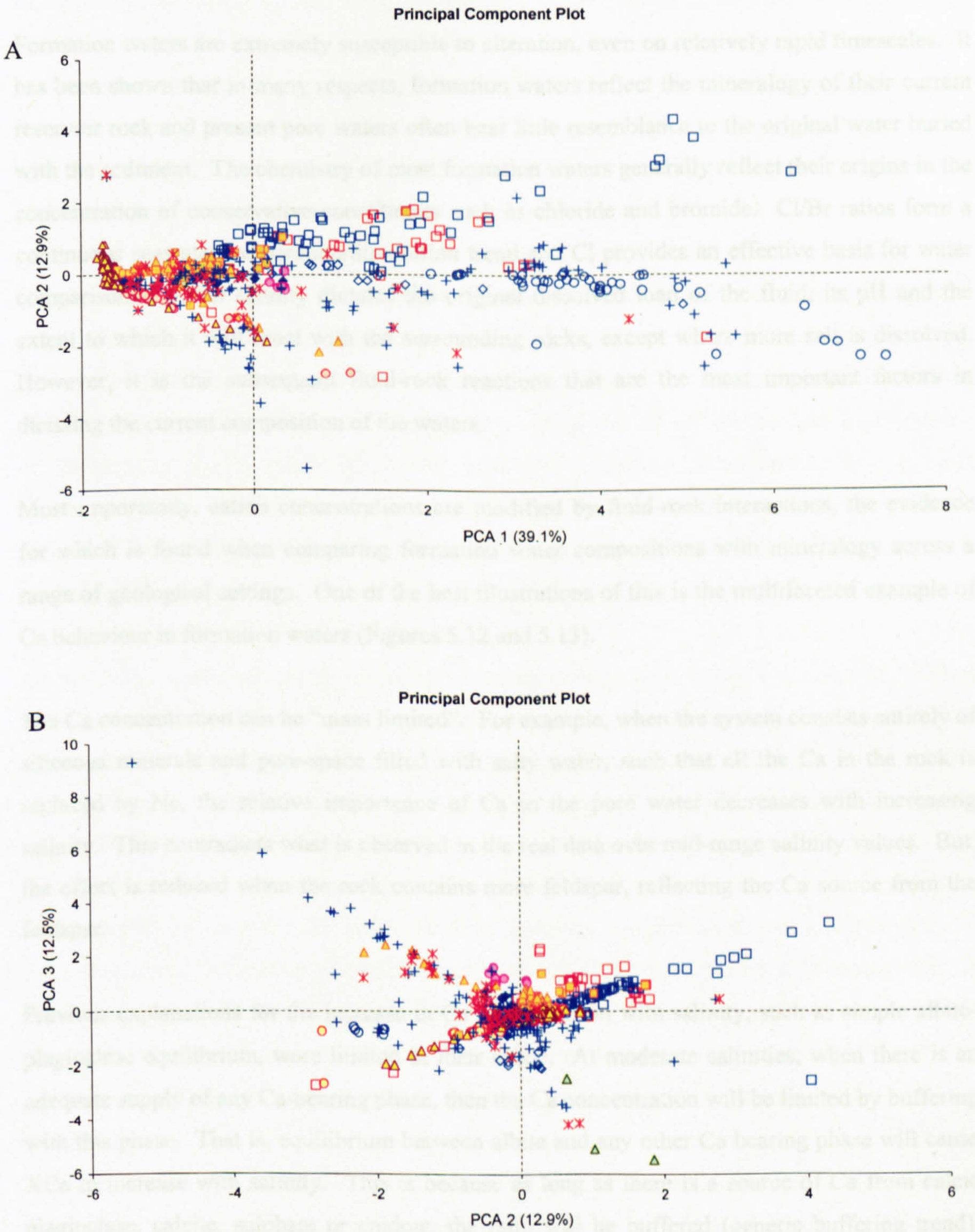

Figure 5.28. Scatter plots showing the distribution of data according to the principal components controlling the variance. A: PC1 and PC2, most of the variance is attributed to PC1, B: PC3 and PC2 account for similar amounts of the variance and the data is scattered at the centre of the plot. Note the clustering of like waters with like on both plots, particularly very high- and very low-salinity waters.

5.5 Discussion and conclusions

Formation waters are extremely susceptible to alteration, even on relatively rapid timescales. It has been shown that in many respects, formation waters reflect the mineralogy of their current reservoir rock and present pore waters often bear little resemblance to the original water buried with the sediment. The chemistry of most formation waters generally reflect their origins in the concentration of conservative constituents such as chloride and bromide. Cl/Br ratios form a continuous seawater evaporation/dissolution trend and Cl provides an effective basis for water comparisons. Initial salinity dictates the original dissolved load of the fluid, its pH and the extent to which it will react with the surrounding rocks, except where more salt is dissolved. However, it is the subsequent fluid-rock reactions that are the most important factors in dictating the current composition of the waters.

Most importantly, cation concentrations are modified by fluid-rock interactions, the evidence for which is found when comparing formation water compositions with mineralogy across a range of geological settings. One of the best illustrations of this is the multifaceted example of Ca behaviour in formation waters (Figures 5.12 and 5.13).

The Ca concentration can be "mass limited". For example, when the system consists entirely of siliceous minerals and pore-space filled with salty water, such that all the Ca in the rock is replaced by Na, the relative importance of Ca in the pore water decreases with increasing salinity. This contradicts what is observed in the real data over mid-range salinity values. But, the effect is reduced when the rock contains more feldspar, reflecting the Ca source from the feldspar.

Previous explanations for the increase in Ca concentration with salinity, such as simple albite-plagioclase equilibrium, were limited in their scope. At moderate salinities, when there is an adequate supply of any Ca-bearing phase, then the Ca concentration will be limited by buffering with this phase. That is, equilibrium between albite and any other Ca bearing phase will cause XCa to increase with salinity. This is because as long as there is a source of Ca from calcic plagioclase, calcite, sulphate or epidote, the ratio will be buffered (generic buffering trend). Then, at higher salinities, the pH decreases and more Ca is likely to dissolve into solution and more CaCl complexes will form, increasing the total amount of Ca in the formation water. Finally, at low salinities, formation waters are dominated by bicarbonate and it is the equilibrium between the formation waters and carbonate minerals that controls the Ca composition.

In addition to Ca, the behaviour of other cations exhibit compelling evidence for the influence of water-rock interactions. Potassium in formation waters appears to be strongly influenced by equilibrium with the K-bearing phases of K-feldspar, mica and illite. The Na/K systematics tend to indicate metastable equilibrium between K-feldspar and albite or K-feldspar and kaolin for most waters at lower temperatures. Waters with higher K/Cl ratios (e.g. low salinity waters such as Colombia and Mahakam) tend to sit in the kaolin stability field, close to the line of metastable equilibrium between K-feldspar and albite.

The details of the controls on Mg (and Ca) compositions of formation waters, particularly with respect to carbonate equilibria, remain uncertain. The foregoing type of data analysis cannot distinguish between influence of carbonates or clay minerals – knowledge of the reservoir mineralogy is required. However, it can be determined that all the waters have Ca/Mg ratios which are too high for calcite saturation. Calcite is a common constituent of many oilfield reservoir mineral assemblages. This suggests Mg concentration in formation waters is controlled either by equilibrium with dolomite or possibly metastable equilibrium between calcite and Mg-clay.

All the fluid constituents examined form continuous global trends, which suggests that different fluid compositions are the result of similar processes occurring under subtly different circumstances. For example, there is a continuous spectrum from high Ca levels at low salinities being controlled by HCO_3 concentrations through moderate-high salinity/high Ca silicate buffered waters to high salinity/low Ca waters dominated by evaporite derived salts. Bicarbonate is inversely correlated with chloride (Figure 13); waters with very low Cl therefore having higher HCO_3 and more influence over carbonate equilibrium allowing relatively more Ca into solution, and waters with very high Cl and low HCO_3 nevertheless also having high Ca levels due to silicate buffering of charge balance. In fact, two major controls on Ca concentration in global formation waters are: the nature of the dominant anion (i.e. Cl or HCO_3) and the origin of the salinity (i.e. seawater evaporation or evaporite dissolution).

However, it should be noted that while trends are evident on a global scale and similar processes occur everywhere, local geology remains a critical factor. For example, two oilfields in the same Gulf of Mexico region, positioned geographically relatively close together, show evidence for two different dominant controls on Ca concentration.

The recognition of the continuous spectrum introduces a degree of predictability into studies of formation waters and suggests that for a given salinity and a given rock type, the cation concentration of the water could be calculated. Thus, the presence of halite indicated by seismic surveys etc could be used to predict whether water will fall in Ca behaviour Trend 1 or 2,

allowing some limited interpretation of the nature of the formation water before ever a water sample is taken. However, due to uncertainties regarding estimates of subsurface pore water chemistry, mineralogy and knowledge gaps in our kinetic and thermodynamic database on many key reactions, uncertainties still exist regarding the controls on many reactions.

5.5.1 *Implications for mineral scaling in oil fields*

Carbonate mineral scaling occurs due to changes in temperature and pressure as oil and water are pumped from the reservoir. $CaCO_3$ becomes more insoluble as the pressure drops and calcite is likely to precipitate. Understanding the controls on Ca and CO_2 in formation waters is therefore important in predicting the likelihood of carbonate scale precipitating. This study has provided information about the controls on Ca concentration in particular. Waters high in Ca are those which are likely to be more susceptible to form calcite scale and these waters tend to include high-salinity waters buffered by Ca-bearing minerals or low-salinity waters with high HCO_3 levels. Those moderate-high salinity waters which are associated with salt bodies are likely to be lower risk.

Barite scale forms due to the interaction of incompatible Ba and SO_4. It has been established through this study that the initial calculated saturation ratio is an unreliable measure of the likelihood of barite scale precipitating. High Ba waters tend to be higher risk and high SO_4 waters lower risk, regardless of whether the water is saturated or supersaturated with regard to barite. Predicting the occurrence of high Ba waters is not trivial, but in the North Sea, those waters which have been associated with K-feldspar bearing rocks for long periods of geological time are more likely to contain high levels of Ba.

5.5.2 *Conclusions and general guidelines*

In studying the waters in this dataset I have identified a number of guidelines that can be applied to most formation waters:

- General trends applicable only on a global scale – not possible to identify local controls.
- General rules
    - *Mineralogy-related*
        - The presence of Ca-bearing minerals will buffer XCa values unless the system is mass limited by the presence of large amounts of salt.
        - K-feldspar/albite equilibrium will buffer Na/K values along the equilibrium boundary unless the ratios are influenced by the presence of micas and clays such as illite and kaolin.
        - The presence of Mg-clays in a reservoir rock can cause Mg/Ca ratios to appear to be in equilibrium with dolomite, even if calcite is the only carbonate phase present.

- Waters which deviate significantly from global trends are likely to have come from very clean reservoirs with few reactive minerals, or reservoirs containing large amounts of unusual minerals.

- Fluid-related

- Salinity higher than TDS = 100000 mg/l and XCa > 0.15 indicates Ca concentration buffered by Ca-bearing silicate, carbonate or sulphate mineral
- Salinity higher than TDS = 100000 mg/l and XCa < 0.15 indicates influence of halite dissolution
- Salinity lower than TDS = 5000 and XCa > ~ 0.06 indicates dominance of bicarbonate (if other indicators are present)
- Low salinity waters with high HCO_3 are likely to have anomalously high relative Na concentrations
- At chlorinities greater than ~1.5 any water with Na/Cl = 1 is likely to have a composition dominated by interaction with halite; waters that have interacted with other minerals will have Na/Cl < 1.
- Waters high in Ba are more susceptible to barite scaling than those with high SO_4, regardless of degree of supersaturation
- Formation water analyses for sulphate are probably unreliable

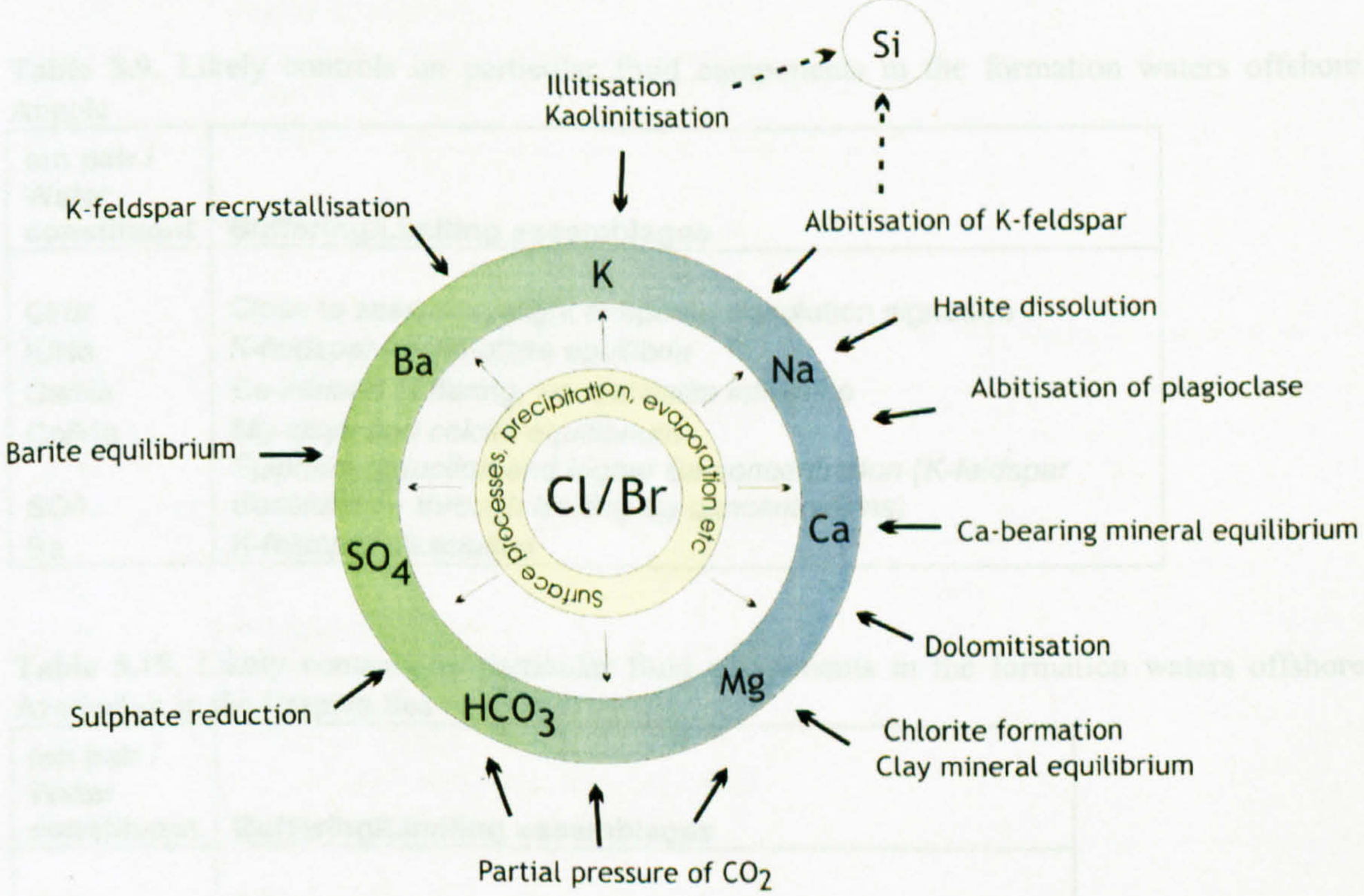

Figure 5.29. Summary diagram illustrating the dominant controls on formation water compositions as determined through past studies and the foregoing data analysis exercise. The origin of the fluid and it's adaptation through surface processes form the basis for any subsequent water-rock interaction and dictate the Cl/Br ratio. Following burial, the composition of any given water is controlled by a number of water-rock interaction processes. However, these processes do not act in isolation and each can be said to have a bearing on a number of others.

Table 5.7. Likely controls on particular fluid components in the formation waters of the Alberta Basin Devonian rocks

Ion pair / Water constituent	**Buffering/Limiting assemblages**
Cl/Br	Seawater evaporation
K/Na	*K-feldspar dissolution as a K-source (Low Na concentrations)*
Ca/Na	Ca-mineral buffering (likely carbonates)
Ca/Mg	Calcite:dolomite equilibrium
SO4	Anhydrite
Ba	*?*

Table 5.8. Likely controls on particular fluid components in the formation waters of the Alberta Jurassic and Cretaceous rocks

Ion pair / Water constituent	**Buffering/Limiting assemblages**
Cl/Br	Seawater evaporation
K/Na	K-feldspar-kaolin equilibrium *(clay mineral reactions)*
Ca/Na	Ca-mineral buffering (likely carbonates and clays)
Ca/Mg	Carbonate cements, clay mineral buffering
SO4	*(K-feldspar dissolution – through limiting Ba concentrations)*
Ba	*K-feldspar dissolution*

Table 5.9. Likely controls on particular fluid components in the formation waters offshore Angola

Ion pair / Water constituent	**Buffering/Limiting assemblages**
Cl/Br	Close to seawater, slight evaporite dissolution signature
K/Na	*K-feldspar-kaolin-albite equilibria*
Ca/Na	*Ca-mineral buffering, no real halite influence*
Ca/Mg	*Mg-clays and calcite equilibrium*
SO4	*Sulphate reduction and higher Ba concentration (K-feldspar dissolution – through limiting Ba concentrations)*
Ba	*K-feldspar dissolution*

Table 5.10. Likely controls on particular fluid components in the formation waters offshore Azerbaijan in the Caspian Sea

Ion pair / Water constituent	**Buffering/Limiting assemblages**
Cl/Br	? Seawater evaporation - Caspian seawater is unusual
K/Na	*K-feldspar/kaolin - Albite/Na-clay equilibrium*
Ca/Na	*Clay minerals/ lithic fragments*
Ca/Mg	*Clay minerals/ lithic fragments*
SO4	*Near barite saturation*
Ba	*Near barite saturation*

Table 5.11. Likely controls on particular fluid components in the formation waters of Central Mississippi, US

Ion pair / Water constituent	**Buffering/Limiting assemblages**
Cl/Br	Seawater evaporation
K/Na	K-feldspar-clay equilibria - kaolin+illite, no additional Na source
Ca/Na	Ca-mineral buffering, carbonates+anhydrite
Ca/Mg	Calcite-dolomite equilibria
SO4	? Anhydrite
Ba	K-feldspar dissolution

Table 5.12. Likely controls on particular fluid components in the formation waters of Colombia in the Llanos basin

Ion pair / Water constituent	**Buffering/Limiting assemblages**
Cl/Br	?
K/Na	K-feldspar, no additional Na source
Ca/Na	Carbonate clasts, low salinity carbonate trend
Ca/Mg	Carbonate clasts
HCO3	Limited numbers of carbonate clasts
SO4	Original sulphate
Ba	*K-feldspar*

Table 5.13. Likely controls on particular fluid components in the formation waters of the Mahakam Basin, Kallimantan, Indonesia

Ion pair / Water constituent	**Buffering/Limiting assemblages**
Cl/Br	?
K/Na	K-feldspar-kaolin
Ca/Na	Carbonate cements and detrital calcite, *additional source of Na ?sodic plagioclase*
Ca/Mg	Calcite-dolomite
SO4	*? Source of SO4 to cause high levels*
Ba	?

Table 5.14. Likely controls on particular fluid components in the formation waters of Offshore Gulf of Mexico, Field 1 in the Green Canyon Area

Ion pair / Water constituent	**Buffering/Limiting assemblages**
Cl/Br	Seawater evaporation
K/Na	Kaolin + *possible K-feldspar alteration*
Ca/Na	Ca-bearing minerals + salt interaction
Ca/Mg	*Mg clays*
SO4	*? Sulphate reduction*
Ba	*K-feldspar*

Table 5.15. Likely controls on particular fluid components in the formation waters of Offshore Gulf of Mexico, Field 2 on the Viosca Knoll

Ion pair / Water constituent	**Buffering/Limiting assemblages**
Cl/Br	Halite dissolution
K/Na	K-feldspar-kaolin + albite/Na-clay
Ca/Na	Mass limited, salt interaction
Ca/Mg	*Mg clays*
SO4	*? Sulphate reduction*
Ba	*K-feldspar*

Table 5.16. Likely controls on particular fluid components in the formation waters of Offshore Gulf of Mexico, Field 3

Ion pair / Water constituent	**Buffering/Limiting assemblages**
Cl/Br	Close to seawater
K/Na	*Albitisation of K-feldspar*
Ca/Na	*Ca mineral buffering*
Ca/Mg	?
SO4	?
Ba	?

Table 5.17. Likely controls on particular fluid components in the formation waters of the Offshore Gulf of Mexico, Offshore Louisiana, Vermillion Block 31

Ion pair / Water constituent	**Buffering/Limiting assemblages**
Cl/Br	Halite dissolution
K/Na	No pH data, likely K-feldspar dissolution
Ca/Na	Mass limited, salt influence
Ca/Mg	Carbonate equilibria - calcite
SO4	Barite equilibrium
Ba	Barite equilibrium

Table 5.18. Likely controls on particular fluid components in the formation waters of the Chocolate/Halls Bayou and West Colombia fields in Brazoria County on the Texas Gulf Coast

Ion pair / Water constituent	**Buffering/Limiting assemblages**
Cl/Br	Halite dissolution
K/Na	K-feldspar-kaolin + albite
Ca/Na	Albitisation of plagioclase + some influence from salt
Ca/Mg	Carbonate equilibria and clay minerals
SO4	? Low sulphate, *barite solubility*
Ba	K-feldspar

Table 5.19. Likely controls on particular fluid components in the formation waters of the northern San Juan Basin, Colorado and New Mexico

Ion pair / Water constituent	**Buffering/Limiting assemblages**
Cl/Br	Influenced by Br from organics
K/Na	K-feldspar-kaolin + influence from Na-clays
Ca/Na	Low temperature carbonate equilibria + clay dissolution
Ca/Mg	Ion exchange, carbonate equilibria
SO4	Oxidation of sulphides and sulphate reduction
Ba	K-feldspar

D. APPLICATIONS

6. THE SIGNIFICANCE OF FORMATION WATER CHEMISTRY FOR CO_2 SEQUESTRATION

6.1 Introduction

Carbon dioxide is a greenhouse gas, part of a group of gases including methane whose increasing concentrations (Figure 6.1) contribute to global warming trends (Broecker, 2006). Evidence has shown that anthropogenic contribution to CO_2 in the atmosphere has caused concentrations to rise progressively in recent years (White *et al.*, 2003). The permanent sequestration of CO_2 from the atmosphere is now considered a viable option to mitigate the effects of increased greenhouse gas emissions (Dove *et al.*, 1998, UK DTI, 2002). One of the most simple and well-researched possibilities is that of subsurface CO_2 storage in pre-existing hydrocarbon reservoirs, for which, in the UK, much of the necessary infrastructure is already in place (White *et al.*, 2003).

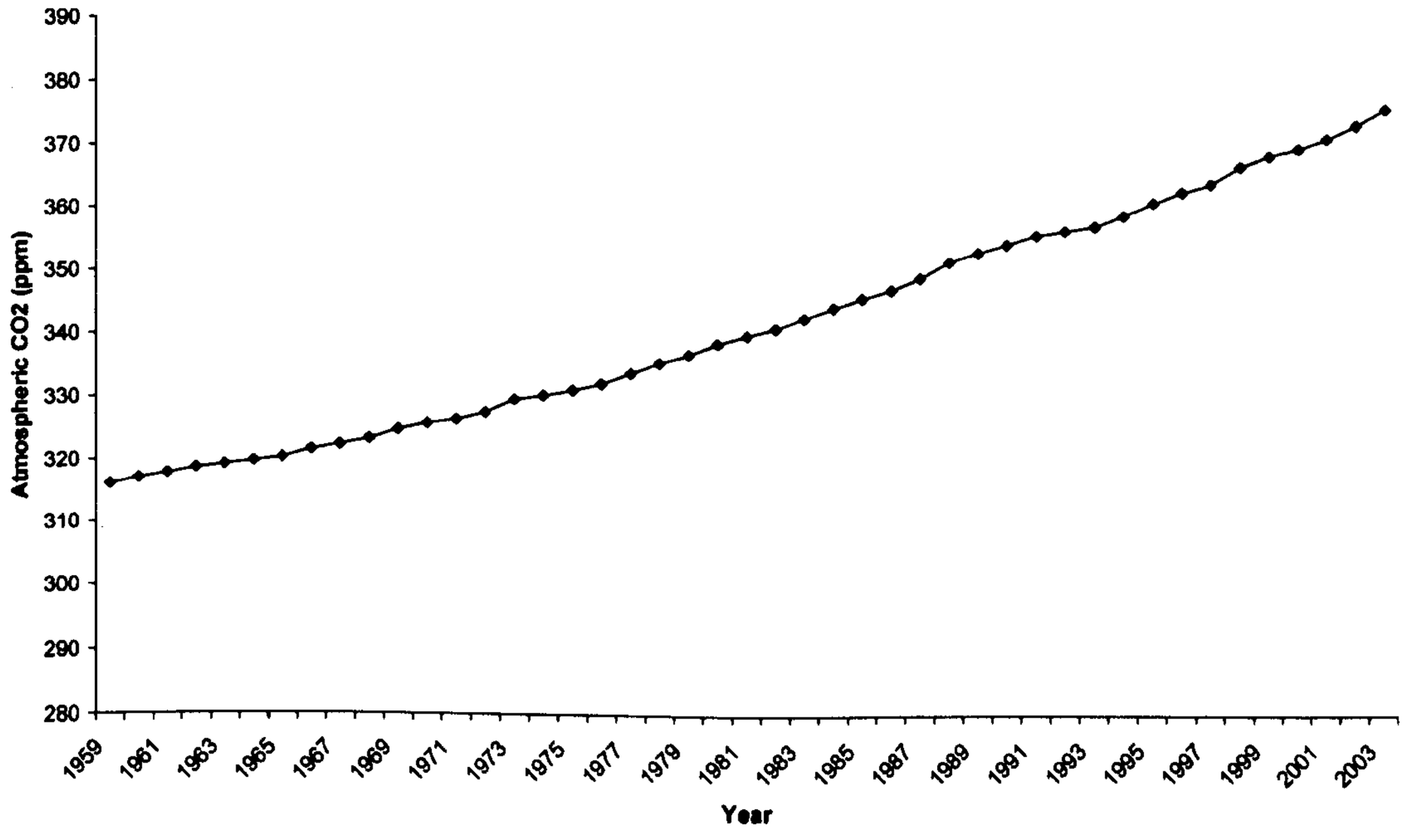

Figure 6.1. Atmospheric average annual CO2 concentrations (ppmv) derived from in situ air samples collected at Mauna Loa Observatory, Hawaii from 1959 to 2003

It was highlighted in Chapter 4 that the success of injecting CO_2 into an oil reservoir for permanent storage depends on a number of reactions and interactions between the gas, the pore water and the host rock and the rate at which these reactions occur. In particular, the most important steps involve the dissolution of the gas into the formation water, the reaction of the dissolved gas with minerals to form stable bicarbonate solutions and the subsequent reaction of bicarbonate with divalent cations to form carbonate mineral (reactions 1-3). An intermediate step that may be potentially damaging to the storage process is the dissolution of carbonate minerals by the water with reduced pH

(Kharaka *et al.*, 2006). This could lead to damage of impermeable seals if restorative processes such as silicate reactions are too slow (e.g. reaction 3).

Carbonic acid dissociation: $CO_2 + H_2O = HCO_3^- + H^+$ *(1)*

Acid neutralisation: $H^+ + CaCO_3 = HCO_3^- + Ca^{2+}$ *(2)*

$3KAlSi_3O_8 + 2H^+ = KAl_3Si_3O_{10}(OH)_2 + SiO_{2(aq)} + 2K^+$ *(3)*

Detailed knowledge of the chemical composition of the formation water and the mineralogy of the reservoir will enable prediction of the behaviour of a system on injection of CO_2, although it is also necessary to understand the relative rates of the different reaction steps, something that is beyond the scope of this study.

6.2 Aims

This study aims to model the effect of CO_2 injection into each of the reservoirs discussed in Chapter 5 (see Table 6.1) using real water compositions together with realistic reservoir mineralogical information. The study is performed in the knowledge that some of the relevant reactions can occur rapidly on the timescales required, but differential rates have not been incorporated in the modelling.

6.3 Past studies

Previously, Gunter *et al.* (1993, 1997) conducted a series of similar geochemical modelling exercises and modelled water-rock reactions driven by the formation of carbonic acid when waste CO_2 is injected into deep aquifers *(Gunter* et al., 1993). The authors concluded that for Na/K-bearing silicate minerals, neutralization of the CO_2 results in development of bicarbonate waters. For Fe/Ca/Mg-bearing minerals, neutralization of CO_2 results in precipitation of siderite, calcite or dolomite with the ionic strength of the formation water remaining relatively constant. Both paths result in substantial trapping and immobilization of CO_2, minimizing the possibility of the CO_2-charged formation water reaching the surface. In addition, they found that experiments carried out at 105°C and 90 bars CO_2 pressure, to test the validity of this mineral-trapping of CO_2 were unsuccessful due to sluggish kinetics of reaction. The most significant change recorded by the reaction products from these experiments was a large increase in alkalinity, which was attributed to very small amounts of water-mineral reaction (Gunter, 1997).

Baines and Worden (2004) examined and modelled natural analogues (including the Miller Field, see Chapter 4) to illustrate the point that carbonate minerals cannot be precipitated without a viable source of available cations. The results were similar to those obtained by Gunter *et al.* (1993, 1997). They concluded that CO_2 added naturally to carbonate rocks or carbonate cemented pure quartz sandstones over geological time causes carbonate minerals to dissolve due to the drop in pH. Once formation water is saturated with CO_2 it will remain as a gas and increase the fluid pressure. On the other hand, they argue that if CO_2 is added to a reactive sandstone with silicates providing active pH buffers, then CO_2 will tend to be sequestered as carbonate minerals, but only on a geological timescale. These authors are pessimistic about how effective these systems may be as storage sites for CO_2. However, they consider "permanent" storage to include only the precipitation of the CO_2 as carbonate minerals, whereas it is possible that simple irreversible dissolution of the gas to bicarbonate ions, with pH buffered by minerals on a rapid timescale may be sufficient, provided that the neutralisation of the acidity is not achieved by reactions that compromise the seals. In addition, the natural analogue processes studied here occurred slowly over extremely long periods of time. In systems experiencing artificial injection, such as those discussed below, carbonate dissolution occurs extremely rapidly and the question is therefore whether reactive sandstones can buffer pH on these much shorter timescales.

Emberley *et al.* (2005) presented the results of studying produced waters from a Canadian carbonate reservoir undergoing CO_2 injection as a form of EOR. After 6 months of injection of CO_2, the authors note that pH had decreased by 0.5 units to a range of 5.9-6.4 from 6.5-7, and alkalinity had increased. The authors indicate that this change is more than likely due to the dissolution of CO_2 in the water. The pH returned to its pre-injection values on a timescale of months. Ca concentration increased and chemical and isotopic data suggest this change in distribution is caused by the dissolution of calcite due to water–rock reactions driven by CO_2. They conclude that addition of CO_2 to water–rock mixtures comprising carbonate minerals causes dissolution of carbonates and production of alkalinity (Emberley *et al.*, 1997). The late increase of pH and the increase of silica in solution suggested silicate minerals were also reactive in great enough amounts to buffer the pH.

Kaszuba *et al.* (2003) carried out experiments in a flexible cell hydrothermal apparatus to determine the extent of fluid–rock reactions, in addition to carbonate precipitation, that may occur in a brine aquifer–aquitard system that simulates a saline aquifer storage scenario. The system was held at 200°C and 200 bars then injected with CO_2 and allowed to react. Results including magnesite precipitation, etch pits in microcline, and mineralization of clays indicated significant dissolution and precipitation of minerals reacting to the perturbed system. Geological sequestration systems are therefore believed to have potential for geochemical reactions that extend beyond simple aqueous

dissolution of CO_2 and dissolution or precipitation of carbonates. These reactions may produce geochemical and geotechnical consequences for sequestration and provide important characteristics for monitoring and evaluation of stored CO_2 (Kaszuba *et al.*, 2003).

To investigate the potential for the geologic storage of CO_2 in saline sedimentary aquifers, Kharaka *et al.* (2006) injected CO_2 at 1500 m depth into a 24-m-thick sandstone section of the Frio Formation on U.S. Gulf Coast. They observed just prior to CO_2 breakthrough to the monitoring well after about 52 hours, the fluid showed sharp drops in pH (6.5–5.7) and increases in alkalinity (100–3000 mg/l as HCO_3) and Fe (30–1100 mg/l). The authors concluded that such rapid dissolution of carbonates could damage the integrity of seals or well cements and lead to leakage.

6.4 Method

Following the method described in Baines and Worden (2004), Geochemist's Workbench (GWB) has been used to model the reactions that might take place on anthropogenic forced addition of CO_2 to different geological systems. The models were all constructed for a rock with 20% porosity (~ 4000cm^3 minerals to ~ 1kg H_2O), with temperature, specific mineralogy (Table 6.1) and mineral proportions, water composition and pH based on values reported in the database. 30g of CO_2 was then progressively added. 30g was chosen rather than 100g used by Baines and Worden (2004) because this is close to the limit of CO_2 saturation in water (Hangx, 2005). Note that close to the injector wells the CO_2 added will be much higher than this in effect, resulting in a free CO_2 phase (Kharaka *et al.*, 2006).

To answer the questions that may be posed about degradation of reservoir properties, fluid displacement, mechanical interaction etc is beyond the scope of this study. However, models for the different reservoirs establish the changing fugacity of CO_2 and potential for formation of bicarbonate ions and carbonate minerals information which is essential for the safe storage of CO_2.

It is important to note that a modelling approach is necessarily limited due to lack of good kinetic data (Baines and Worden, 2004). The following study is simply a means of establishing what *might* happen and for the first time makes use of real mineralogical and water composition data.

Table 6.1. Mineralogical input for each reservoir. Each mineral was included as the free quantity (cm^3) listed here, relative to 1kg H_2O, and was swapped into the basis replacing a relevant cation or anion. Locations in italics indicate failure to model the system; in these cases the effect of adding CO_2 was modelled without minerals present

	Albite	Anhydrite	Ankerite	Anorthite,	Barite	Calcite	Chlorite	Coal	Dolomite	Halite	Illite	Kaolinite	K-feldspar	Muscovite	Pyrite	Quartz
Alberta		50				2000			1500			50			150	250
Angola	*250*			*250*		*500*							*500*			*2500*
Azerbaijan						250					100	150	500			3000
Central Mississippi	200		200		200	200								200		3000
Colombia						150						50	300			3000
Mahakam	*250*			*750*		*125*			*125*		*125*		*500*	*125*		*2000*
GOM Field 1	500									300	350	350	500			2000
GOM Field2	500										125	125	1000			2500
Offshore Louisiana	*250*			*500*		*250*	*250*			*250*		*250*	*250*		*50*	*2000*
Texas Gulf Coast	*250*			*500*		*200*	*200*		*100*		*250*	*250*	*250*			*2000*
San Juan				*100*				*2000*					*200*			*1700*

6.5 Results

6.5.1 Reservoir response to CO_2 injection

Different types of mineral assemblage react to the effects of CO_2 injection in different ways. The following examples outline these differences and highlight the reactions that are most important to the success of any CO_2 sequestration scheme.

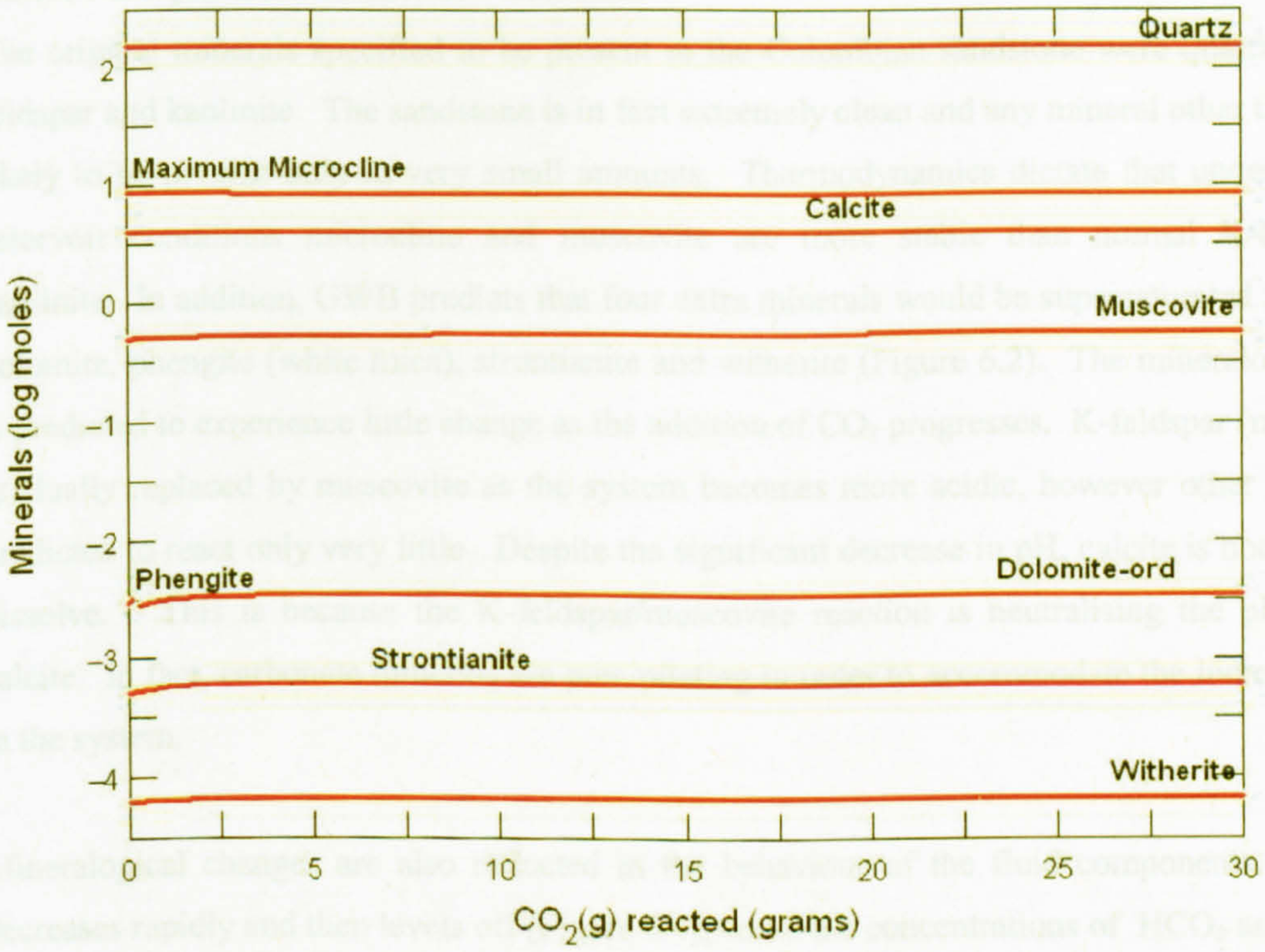

Figure 6.2. Important minerals in the Colombian reservoir system as CO_2 is added. Example of a mineralogically pure sandstone. Plot generated using Gtplot as part of GWB.

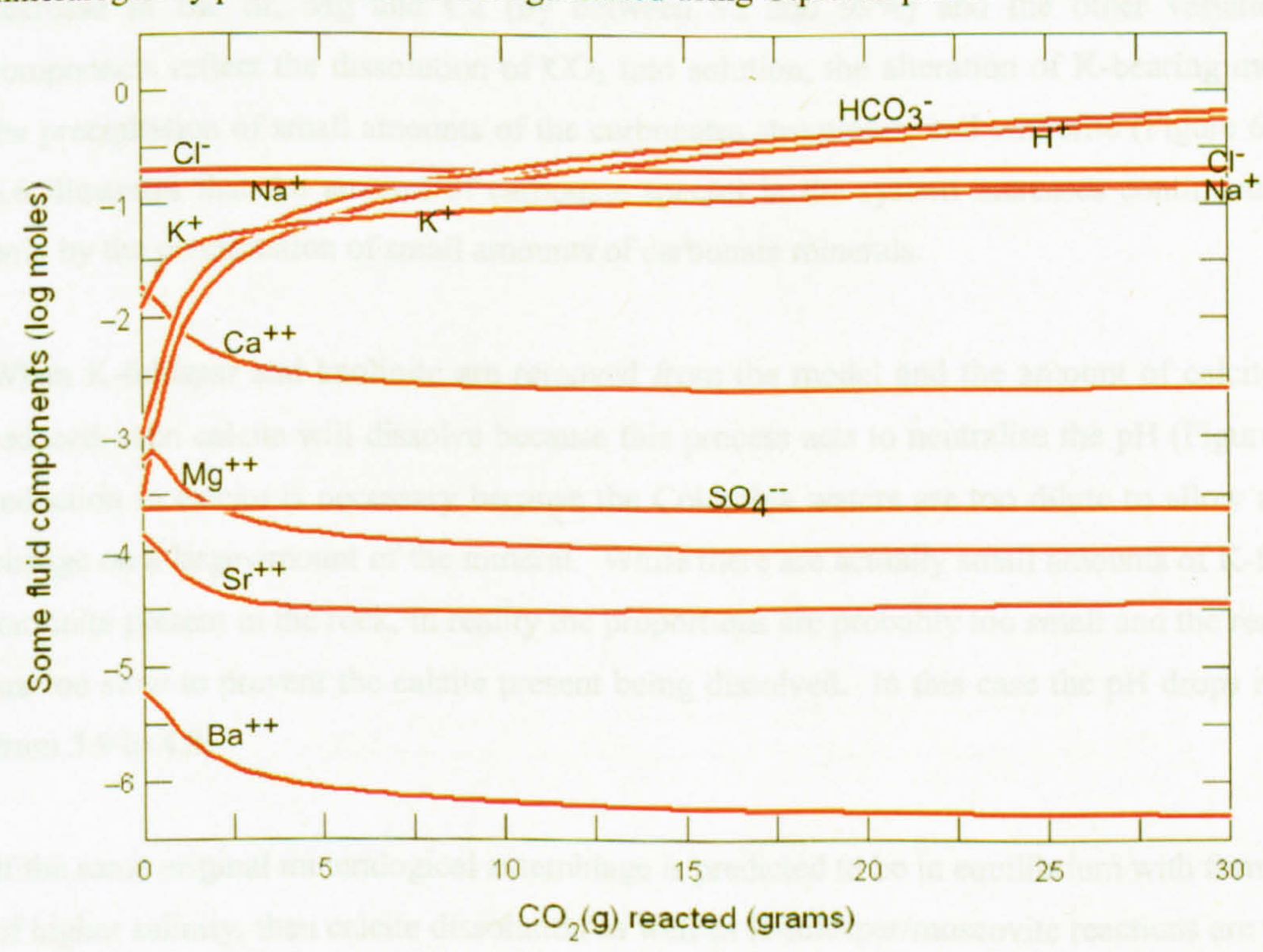

Figure 6.3. Behaviour of fluid components in the Colombian reservoir fluids as CO_2 is added. Example of a mineralogically pure sandstone. Plot generated using Gtplot as part of GWB.

6.5.1.1 *Pure quartzose sandstone – Colombia*

The original minerals specified to be present in the Colombian sandstone were quartz, calcite, K-feldspar and kaolinite. The sandstone is in fact extremely clean and any mineral other than quartz is likely to be present only in very small amounts. Thermodynamics dictate that under Colombian reservoir conditions microcline and muscovite are more stable than normal K-feldspar and kaolinite. In addition, GWB predicts that four extra minerals would be supersaturated at the outset: dolomite, phengite (white mica), strontianite and witherite (Figure 6.2). The mineralogical system is predicted to experience little change as the addition of CO_2 progresses. K-feldspar (microcline) is gradually replaced by muscovite as the system becomes more acidic, however other minerals are predicted to react only very little. Despite the significant decrease in pH, calcite is not predicted to dissolve. This is because the K-feldspar/muscovite reaction is neutralising the pH instead of calcite. In fact, carbonate minerals are precipitating in order to accommodate the increase in HCO_3 in the system.

Mineralogical changes are also reflected in the behaviour of the fluid components. pH clearly decreases rapidly and then levels off (Figure 6.4), while the concentrations of HCO_3 and K increase (Figure 6.3). The change in pH results in a shift in the dominant carbonate species (Figure 6.5) The decrease in Ba, Sr, Mg and Ca (by between 92 and 99%) and the other variation in fluid components reflect the dissolution of CO_2 into solution, the alteration of K-bearing minerals, and the precipitation of small amounts of the carbonates strontianite and witherite (Figure 6.2). Figure 6.6 illustrates that the amount of carbonate species in the system increases continuously, slowed only by the precipitation of small amounts of carbonate minerals.

When K-feldspar and kaolinite are removed from the model and the amount of calcite present is reduced, then calcite will dissolve because this process acts to neutralise the pH (Figure 6.6). The reduction in calcite is necessary because the Colombia waters are too dilute to allow a noticeable change on a large amount of the mineral. While there are actually small amounts of K-feldspar and kaolinite present in the rock, in reality the proportions are probably too small and the reaction times are too slow to prevent the calcite present being dissolved. In this case the pH drops more slowly from 5.9 to 4.8.

If the same original mineralogical assemblage is predicted to be in equilibrium with formation water of higher salinity, then calcite dissolution as well as K-feldspar/muscovite reactions are predicted to act to neutralise the pH (Figure 6.7). This is because a more concentrated fluid can affect a greater amount of calcite than a dilute one. The change in pH is about the same in this case, though overall it is generally higher, dropping from 6.2 to 5.1.

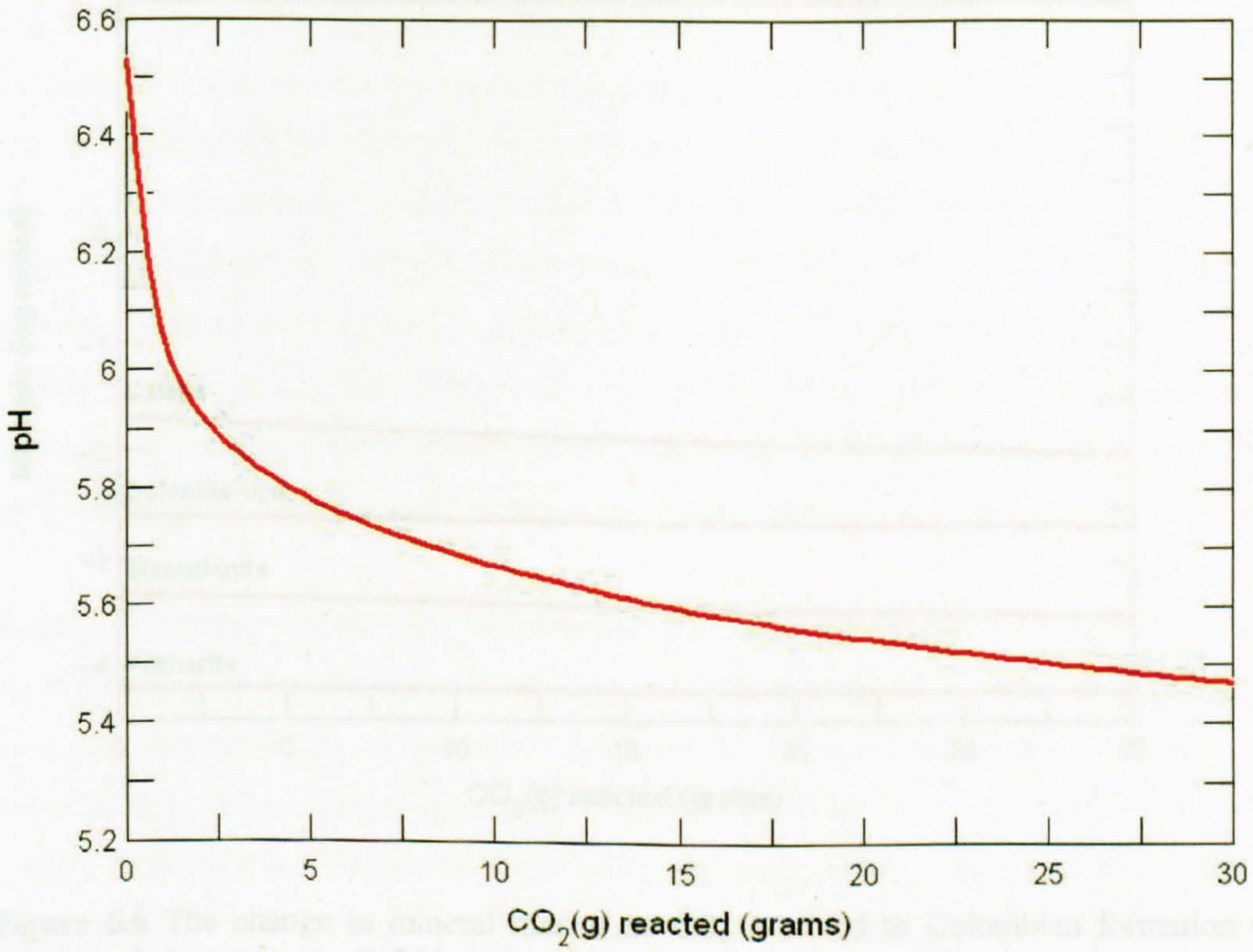

Figure 6.4 pH change in the Colombian water as CO_2 is added. Plot generated using Gtplot as part of GWB.

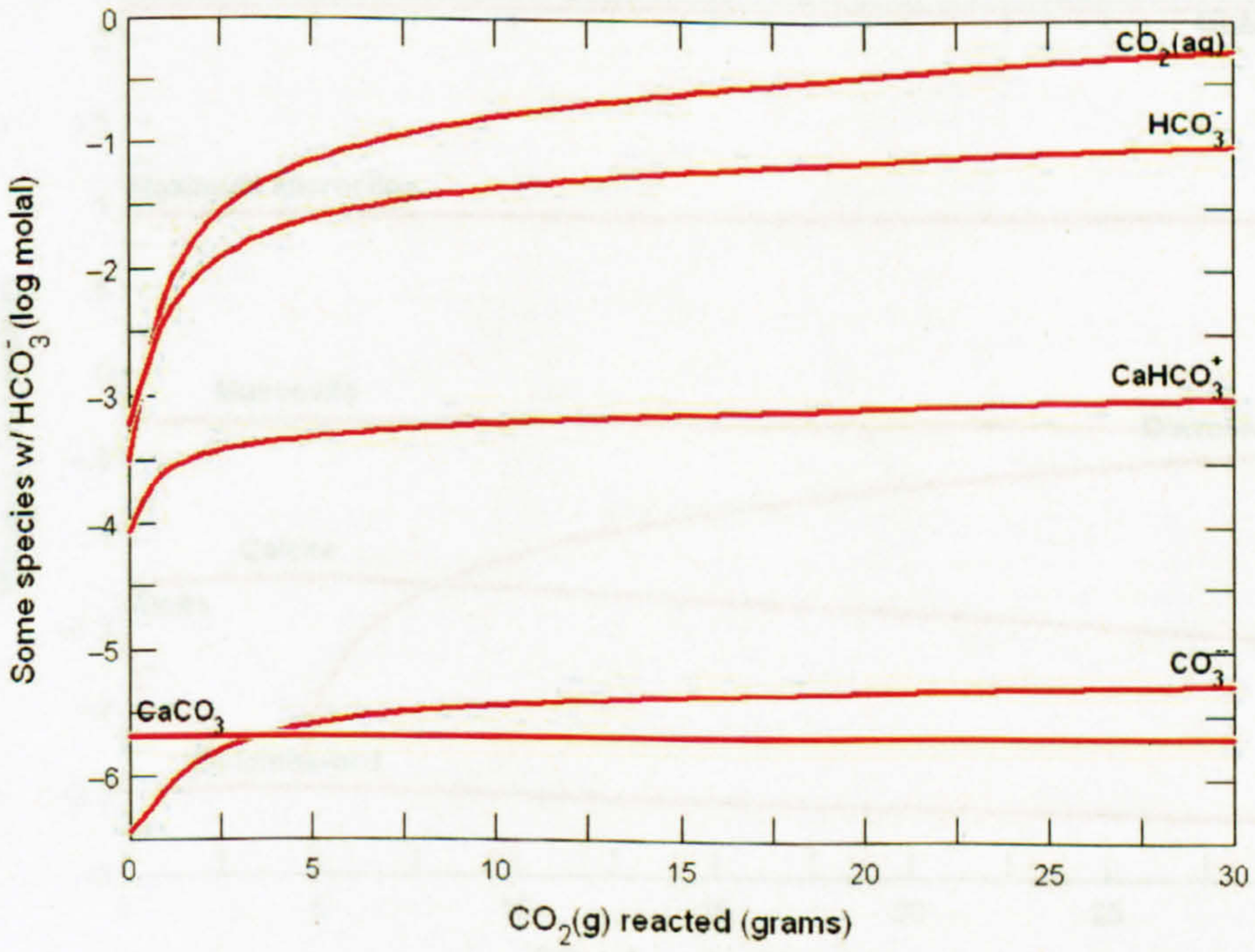

Figure 6.5 Change in carbonate species as CO_2 is gradually added to Colombian waters. Plot generated using Gtplot as part of GWB.

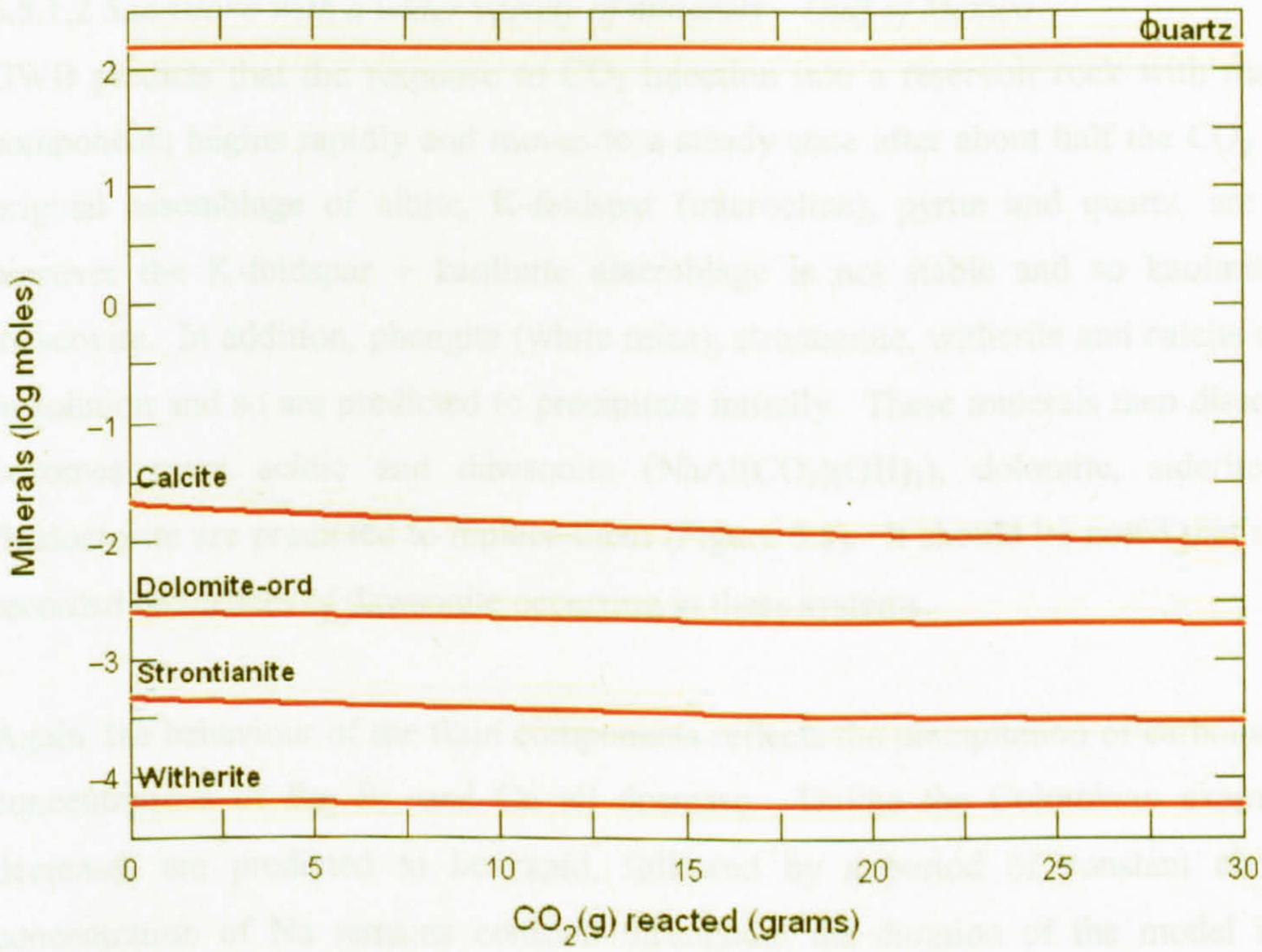

Figure 6.6 The change in mineral masses as CO_2 is added to Colombian formation water in a reservoir that contains no K-feldspar or clays

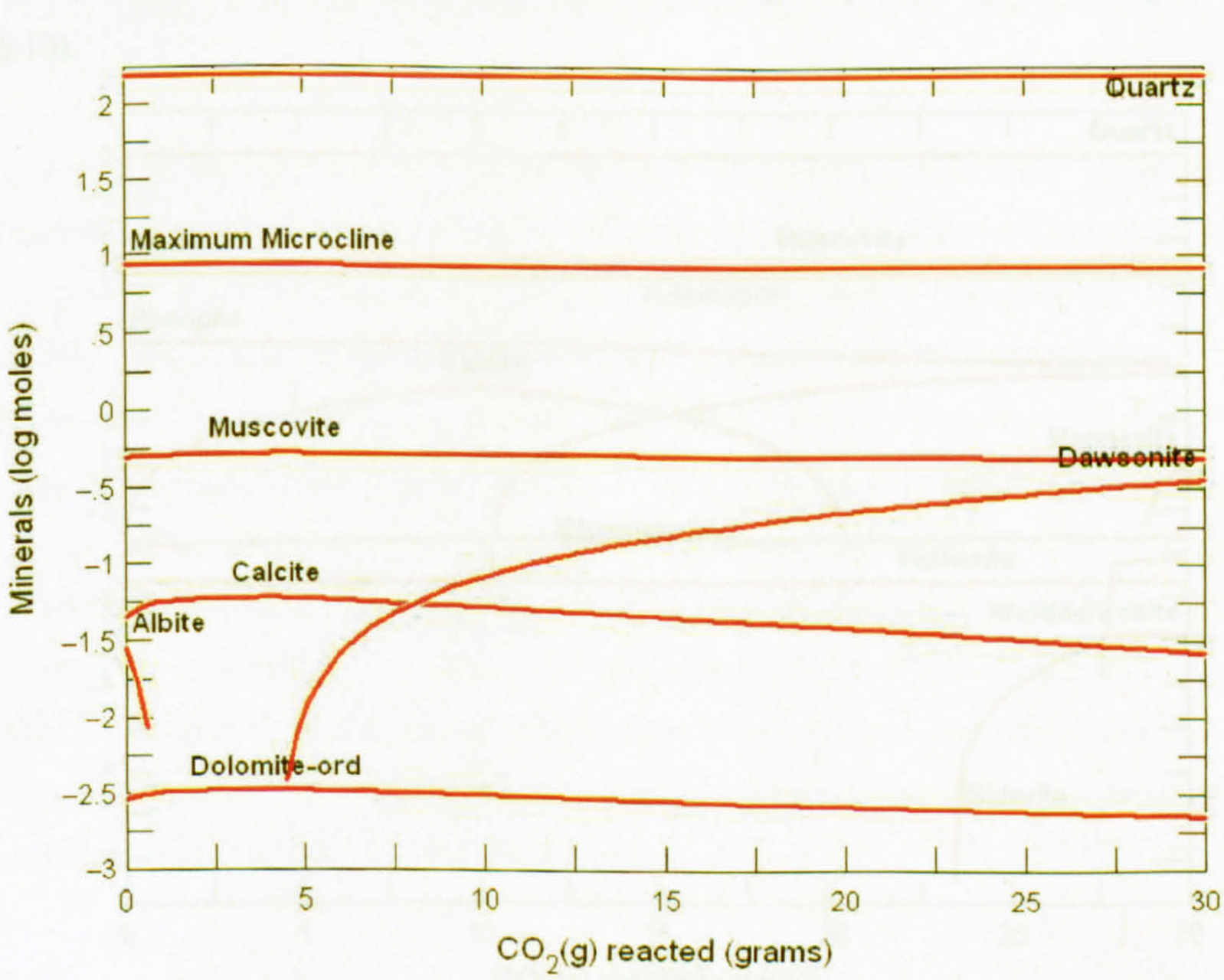

Figure 6.7 The change in mineral masses as CO_2 is added to a reservoir of Colombian mineralogy in equilibrium with high salinity (Cl = 160,000 mg/kg) water

6.5.1.2 *Sandstone with a wider variety of minerals – Gulf of Mexico*

GWB predicts that the response to CO_2 injection into a reservoir rock with many mineralogical components begins rapidly and moves to a steady state after about half the CO_2 has reacted. The original assemblage of albite, K-feldspar (microcline), pyrite and quartz, are present initially, however the K-feldspar + kaolinite assemblage is not stable and so kaolinite is replaced by muscovite. In addition, phengite (white mica), strontianite, witherite and calcite are supersaturated in solution and so are predicted to precipitate initially. These minerals then dissolve as the system becomes more acidic and dawsonite ($NaAl(CO_3)(OH)_2$), dolomite, siderite, magnesite and rhodocrosite are predicted to replace them (Figure 6.8). It should be noted that there are very few recorded incidences of dawsonite occurring in these systems.

Again, the behaviour of the fluid components reflects the precipitation of carbonate minerals as the concentrations of Ba, Sr, and Ca all decrease. Unlike the Colombian example, the stepwise decreases are predicted to be rapid, followed by a period of constant concentration. The concentration of Na remains constant throughout the duration of the model run. K increases slightly, reflecting the reaction of the K-bearing silicates and it is these that also buffer pH which pH decreases only very slightly and then levels off (Figure 6.9). Critically, the concentration of HCO_3 does increase initially, but also does not change beyond the point of 28g CO_2 added (Figure 6.10).

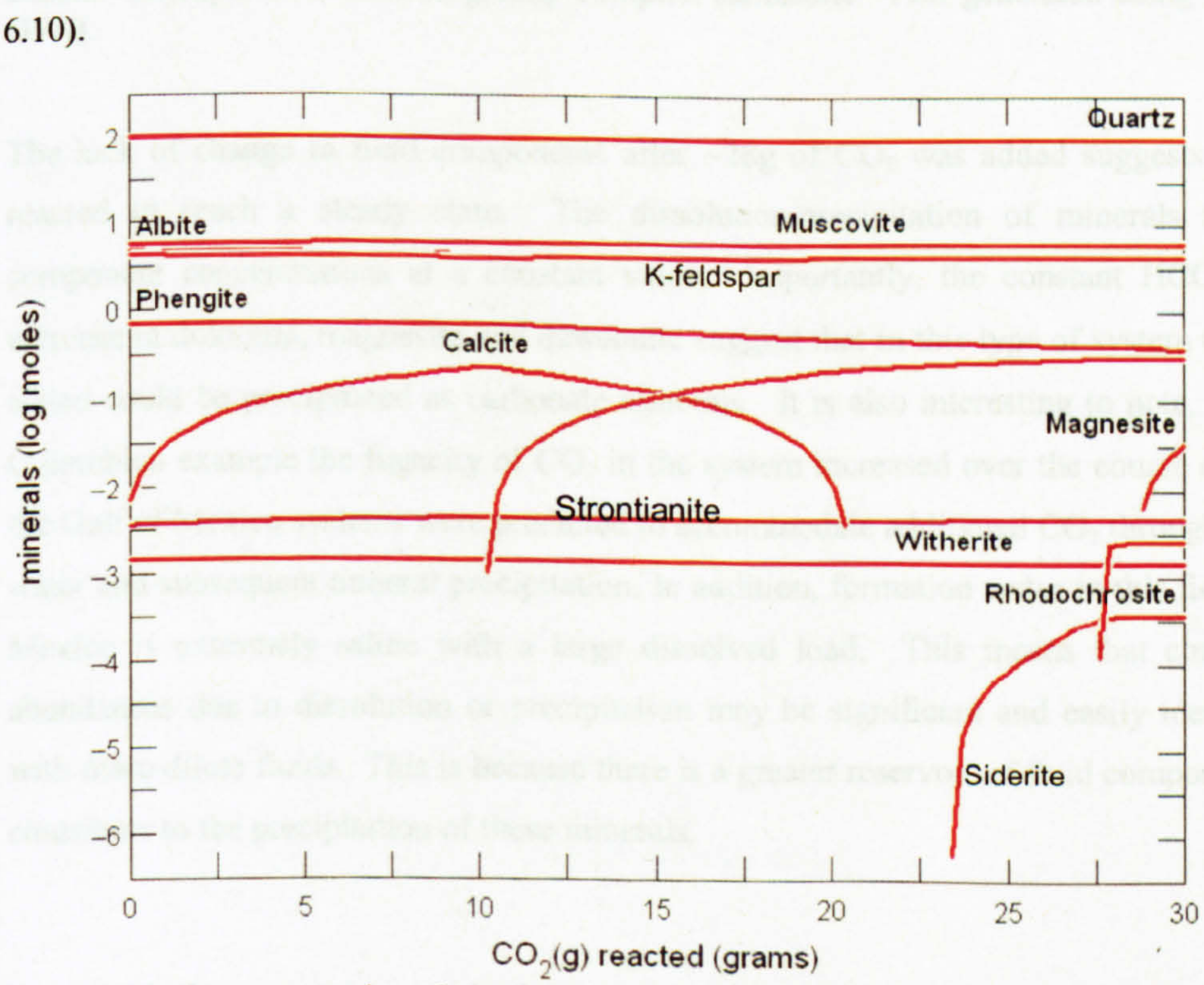

Figure 6.8. Important minerals in the reservoir system of the GOM Field 1 as CO_2 is added. Example of a mineralogically complex sandstone. Plot generated using Gtplot as part of GWB.

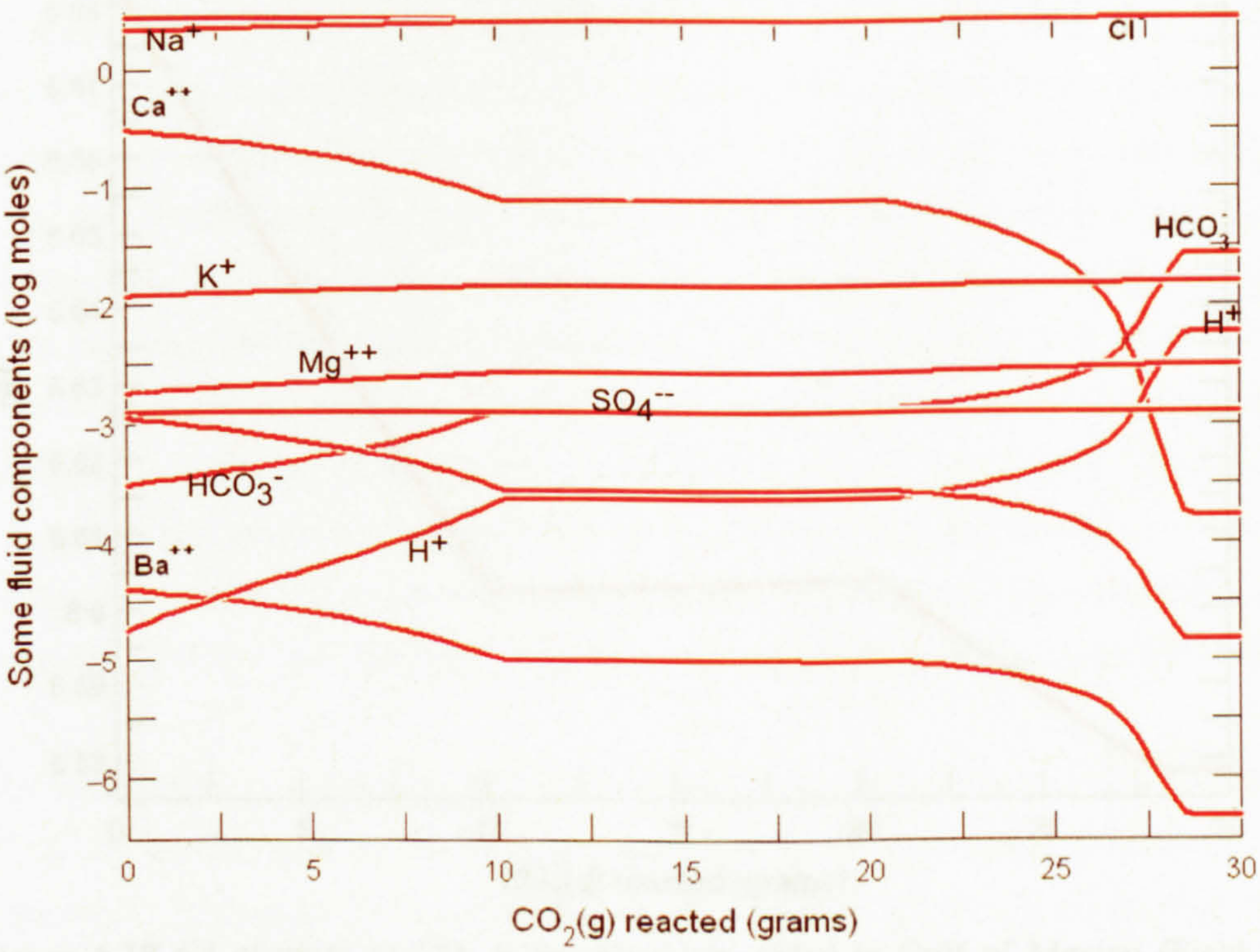

Figure 6.9. Behaviour of fluid components in the reservoir system of the GOM Field 1 as CO_2 is added. Example of a mineralogically complex sandstone. Plot generated using Gtplot as part of GWB.

The lack of change in fluid components after ~28g of CO_2 was added suggests that this system reacted to reach a steady state. The dissolution/precipitation of minerals maintained fluid component concentrations at a constant value. Importantly, the constant HCO_3 value and the increase in dolomite, magnesite and dawsonite suggest that in this type of system CO_2 gas that was added could be precipitated as carbonate minerals. It is also interesting to note, that while in the Colombian example the fugacity of CO_2 in the system increased over the course of the model run, the Gulf of Mexico systems were predicted to accommodate additional CO_2 through dissolution into water and subsequent mineral precipitation. In addition, formation water in this field in the Gulf of Mexico is extremely saline with a large dissolved load. This means that changes in mineral abundances due to dissolution or precipitation may be significant and easily identified compared with more dilute fluids. This is because there is a greater reservoir of fluid components available to contribute to the precipitation of these minerals.

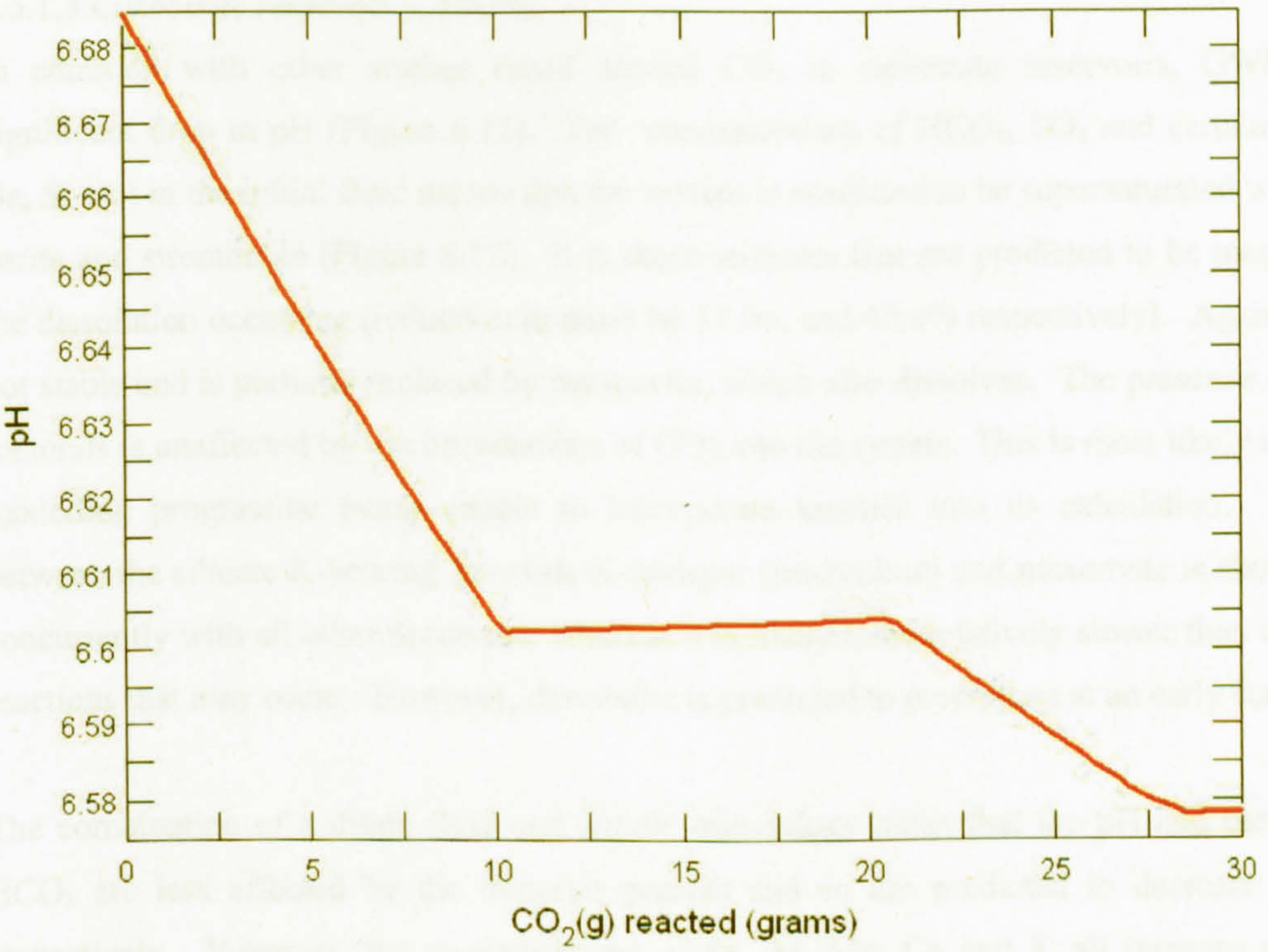

Figure 6.10 pH changes as CO_2 is progressively added to Gulf of Mexico (Field 1) formation waters. Plot generated using Gtplot as part of GWB.

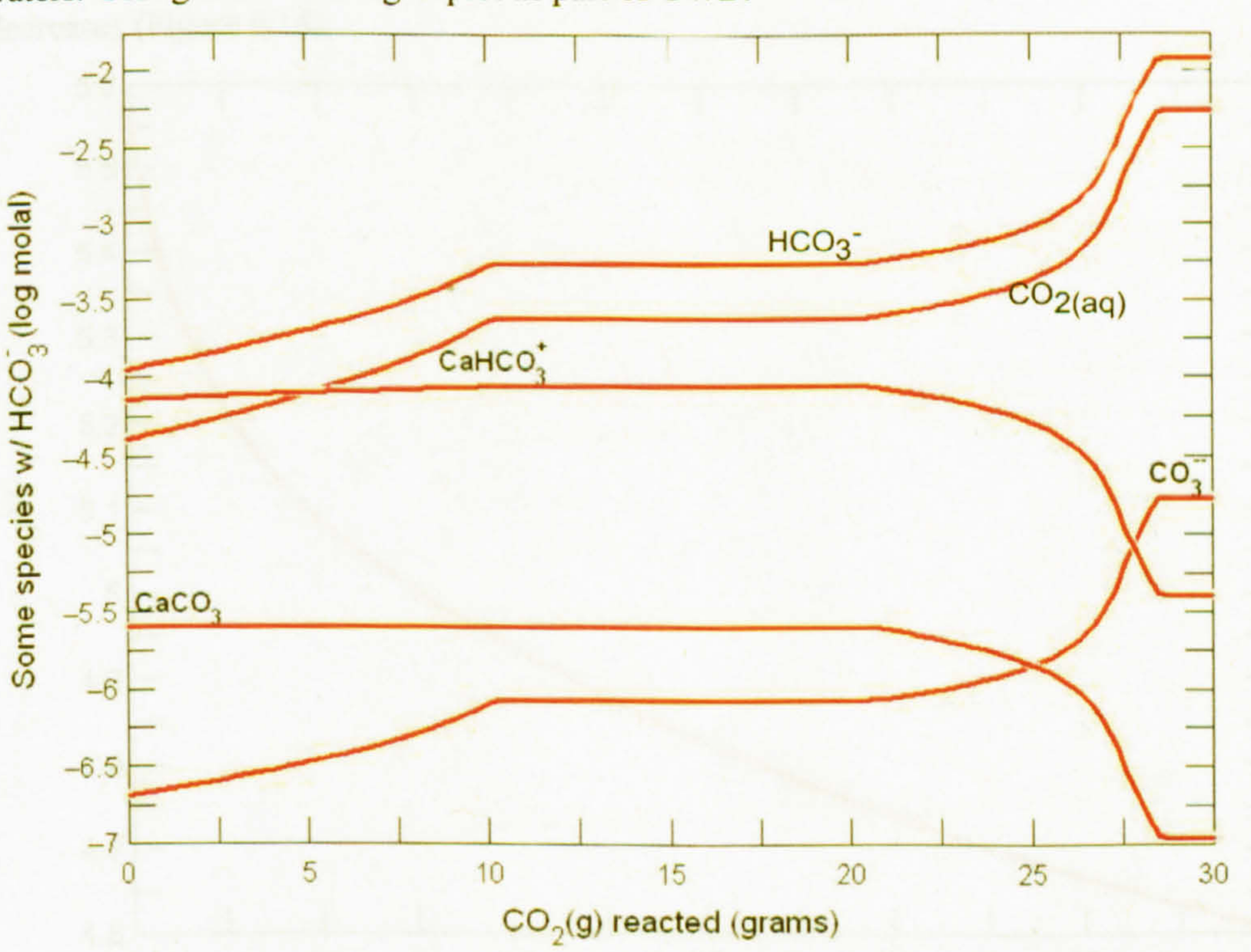

Figure 6.11 Variation in carbonate species as CO_2 is added to waters from Gulf of Mexico Field 1. Plot generated using Gtplot as part of GWB.

6.5.1.3.*Carbonate reservoir – Alberta*

In common with other studies based around CO_2 in carbonate reservoirs, GWB predicts a significant drop in pH (Figure 6.12). The concentrations of HCO_3, SO_4 and certain cations (e.g. Ba, Sr etc) in the initial fluid means that the system is predicted to be supersaturated with respect to barite and strontianite (Figure 6.13). It is these minerals that are predicted to be most affected by the dissolution occurring (reduction in mass by 57.9% and 45.4% respectively). Again, kaolinite is not stable and is partially replaced by muscovite, which also dissolves. The presence of most other minerals is unaffected by the introduction of CO_2 into the system. This is most likely a result of the modelling programme being unable to incorporate kinetics into its calculation. The reaction between the silicate K-bearing minerals K-feldspar (microcline) and muscovite is shown occurring concurrently with all other processes, whereas it is likely to be relatively slower than any carbonate reactions that may occur. However, dawsonite is predicted to precipitate at an early stage.

The combination of a dilute fluid and simple mineralogy mean that the pH and concentration of HCO_3 are less affected by the minerals present and so are predicted to decrease and increase respectively. However, the concentrations of Sr, Ba, Mg, Ca and K all increase as very small amounts of minerals are predicted to dissolve, restricting the pH, only the concentration of Na decreases (Figure 6.14).

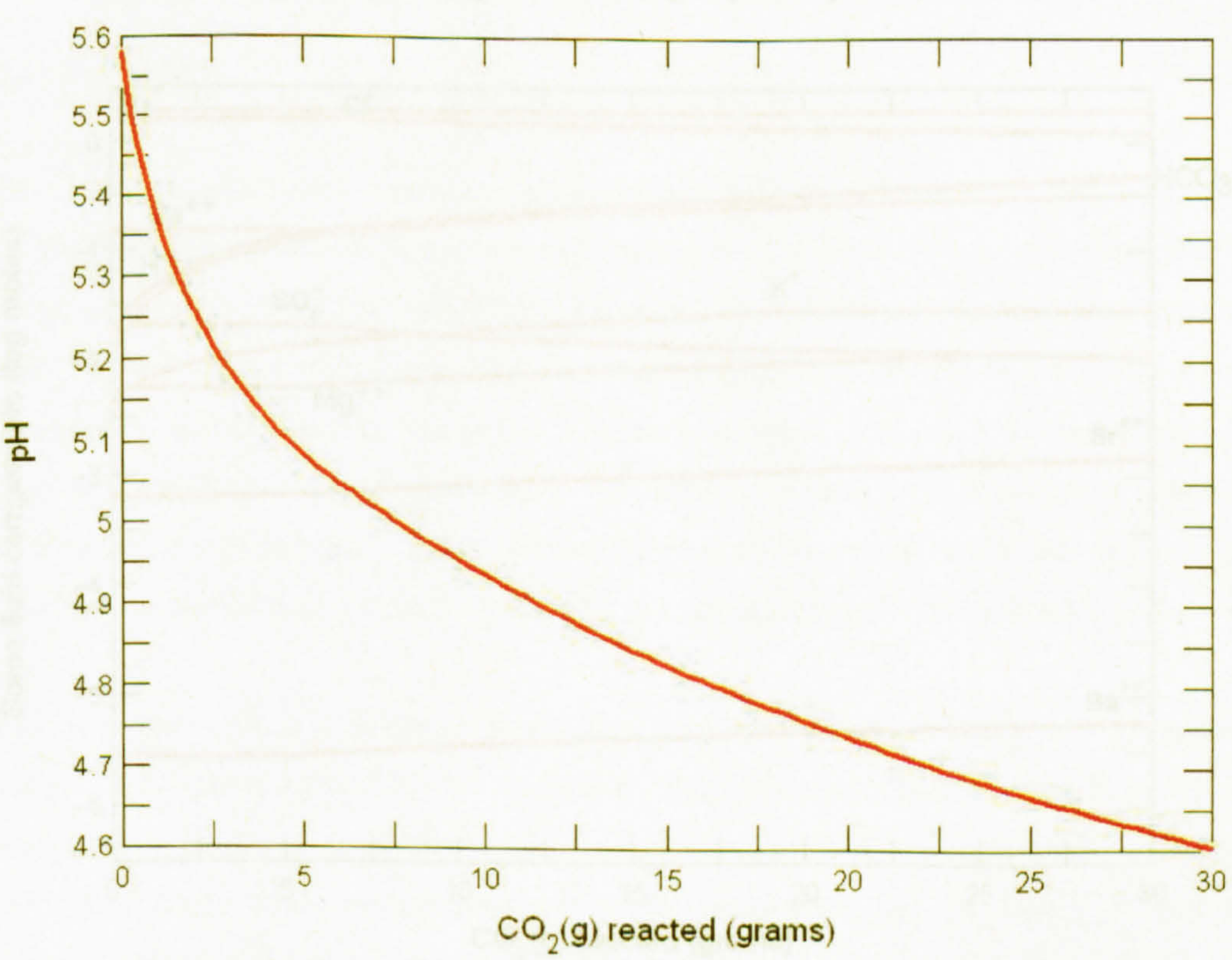

Figure 6.12 Variation in pH as CO_2 is added to Alberta brines. Plot generated using Gtplot as part of GWB.

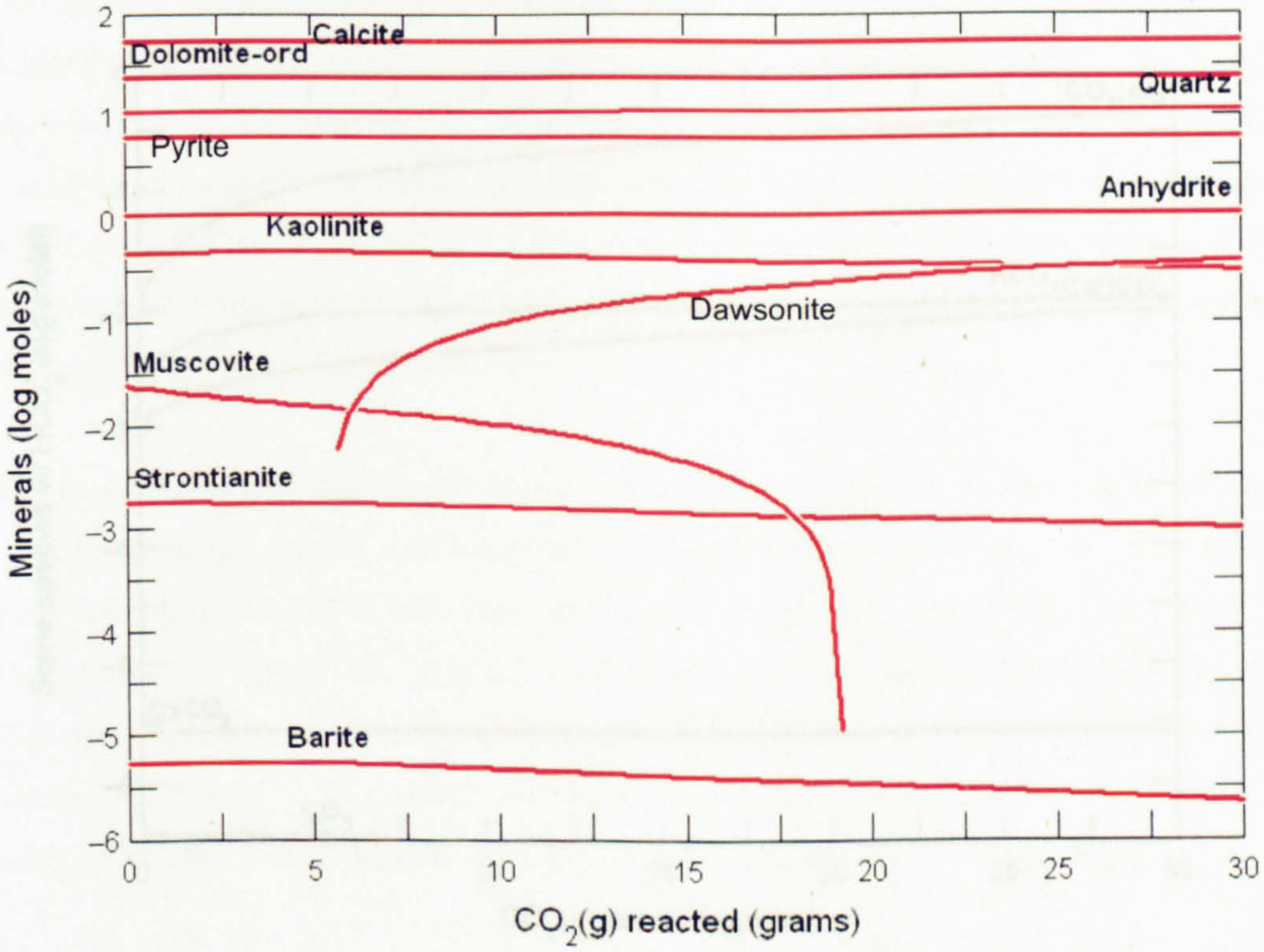

Figure 6.13. Minerals dissolved and precipitated on the addition of CO_2 to the Alberta reservoir fluids with minerals present. Plot generated using Gtplot as part of GWB.

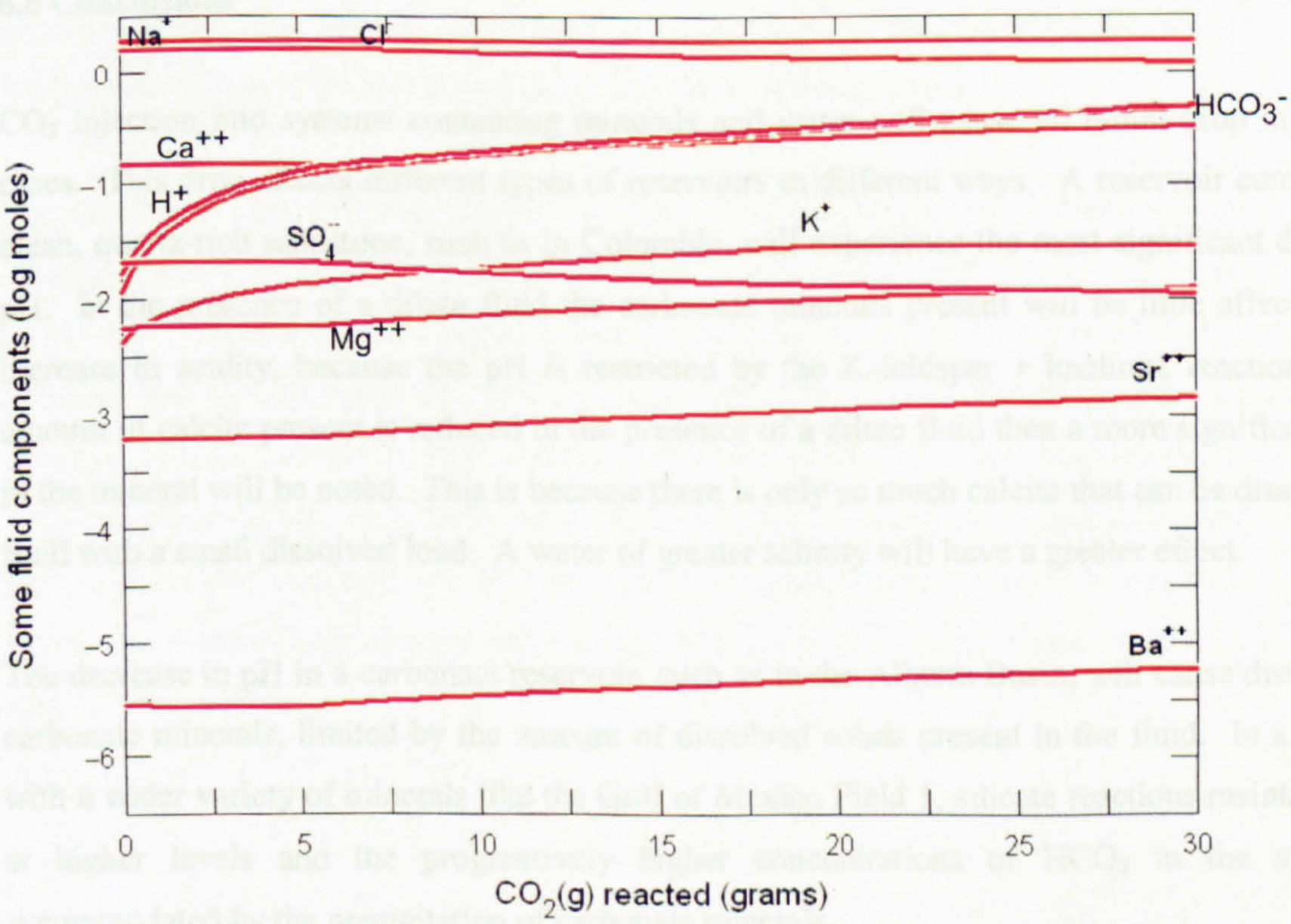

Figure 6.14 Changes in fluid components as CO_2 is added to a the Alberta reservoir fluids in a system containing carbonate and silicate minerals. Plot generated using Gtplot as part of GWB.

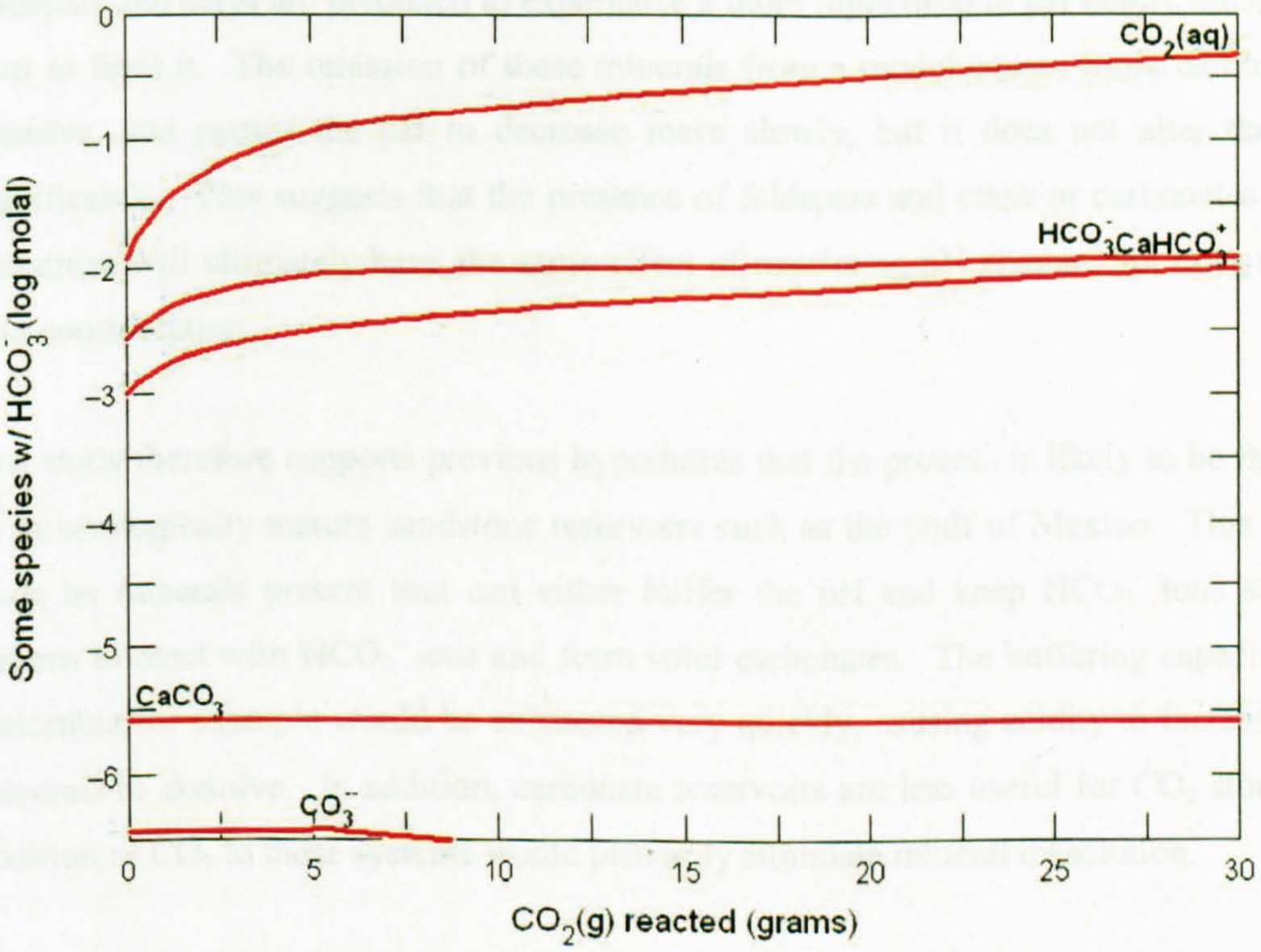

Figure 6.15 Carbonate species in Alberta Basin formation waters as CO_2 is progressively added. Plot generated using Gtplot as part of GWB.

6.6 Conclusions

CO_2 injection into systems containing minerals and water will cause an initial drop in pH in all cases. This drop affects different types of reservoirs in different ways. A reservoir comprising of clean, quartz-rich sandstone, such as in Colombia, will experience the most significant decrease in pH. In the presence of a dilute fluid the carbonate minerals present will be little affected by the increase in acidity, because the pH is restricted by the K-feldspar + kaolinite reactions. If the amount of calcite present is reduced in the presence of a dilute fluid then a more significant change in the mineral will be noted. This is because there is only so much calcite that can be dissolved by a fluid with a small dissolved load. A water of greater salinity will have a greater effect.

The decrease in pH in a carbonate reservoir, such as in the Alberta Basin, will cause dissolution of carbonate minerals, limited by the amount of dissolved solids present in the fluid. In a sandstone with a wider variety of minerals like the Gulf of Mexico Field 1, silicate reactions maintain the pH at higher levels and the progressively higher concentrations of HCO_3 in the system are accommodated by the precipitation of carbonate minerals.

The rapidity of the pH drop is also affected by the type of minerals present. Reservoirs containing feldspars and clays are predicted to experience a more rapid drop in pH before the mineral reactions start to limit it. The omission of these minerals from a model causes more carbonate minerals to dissolve, and causes the pH to decrease more slowly, but it does not alter the change in pH significantly. This suggests that the presence of feldspars and clays or carbonates in large enough quantities will ultimately have the same effect of restricting pH change, but does not take kinetics into consideration.

The study therefore supports previous hypotheses that the process is likely to be far more effective in mineralogically mature sandstone reservoirs such as the Gulf of Mexico. This is because there must be minerals present that can either buffer the pH and keep HCO_3^- ions stable or provide cations to react with HCO_3^- ions and form solid carbonates. The buffering capacity of rocks from Colombia for example would be exhausted very quickly, causing acidity to increase and carbonate minerals to dissolve. In addition, carbonate reservoirs are less useful for CO_2 storage because the addition of CO_2 to these systems would primarily stimulate mineral dissolution.

Simple geochemical modelling indicates that injection of CO_2 into subsurface petroleum reservoirs is a viable option for its long-term storage assuming the buffering capacity of the systems are not exhausted. Geochemical modelling can only provide an idea of what might occur under a certain set of circumstances; however, this study is unique in using real chemical analyses in conjunction with mineralogical information and has produced favourable results.

The equilibrium geochemical modelling used here does not give an indication of the kinetics of chemical reactions. A potential argument against the proposed injection of CO_2 into reservoir rocks is that the reactions required to fix it permanently cannot occur on short enough timescales. In addition, the greater speed of carbonate dissolution relative to silicate reactions could lead to damage of important formations and seals before limiting reactions start to occur. While this remains a possibility, this study has confirmed that feldspar/clay equilibria are important in buffering pH and this, together with evidence of relatively fast reactions from Miller (Chapter 4), means that slow silicate kinetics are not necessarily a valid argument against CO_2 sequestration in appropriate reservoirs.

7. WATERFLOOD MANAGEMENT: PRODUCTION SIMULATION MODELLING

7.1 Introduction

Waterflooding is an EOR technology commonly used to provide pressure support during oil production. Introducing a waterflood to a reservoir initiates additional chemical processes in the system, which must also be understood. Reservoir geologists and production engineers use a number of tools to help them plan waterfloods - one of the most successful and commonly used is the reservoir production simulation model. As with any numerical or computer model, the production forecasts and reservoir information gained from these simulations are only as reliable as the data used to construct them. In other words, to increase the accuracy of a simulation model it is important to incorporate an accurate representation of the distribution of reservoir properties (i.e. permeability, porosity, relative permeability, compressibility etc) in the production simulation. A method of testing whether the reservoir properties are correctly incorporated into the production simulation model is to ensure that the results are consistent with previous production history; a process known as history matching. A key problem with history matches is that they are non-unique because we can never obtain enough measurements from the subsurface to uniquely describe the reservoir (Huseby *et al.*, 2005). A way to reduce this non-uniqueness is to use as much information from the field as possible during both model construction and history matching.

Pore water chemistry data is routinely collected during the production of many reservoirs but is rarely used to aid reservoir characterisation. In the following chapter, the potential use of such data for improving reservoir simulations is investigated. The chapter begins by introducing the concept of production simulation modelling and describing the types of information traditionally used in such a model. The chapter then discusses how studying the chemical composition of the produced water can provide detailed information about reservoir fluid mixing. A simple production simulation model and a case study of the Miller oil field in the North Sea are used to answer some of the questions related to water mixing in the reservoir such as:-

- How does permeability heterogeneity affect the degree of mixing/banking between injected water and the formation water?
- Can specific patterns of injected water breakthrough be predicted?
- What are the mixing patterns of water within the Brae sandstones of the Miller reservoir, and how well are these predicted by a computer simulation?

In addition, new approaches will be introduced for using production simulation models to better effect and simple models will be used to try and understand real data from the Miller field.

Computer simulations incorporate measured and assumed representations of the static reservoir geology. When calibrated by history-matching to observed dynamic data (e.g. oil and water production rates) the models can be used to predict future field behaviour and plan production strategies. Models are commonly used to provide information about future rates of production of oil, gas, formation water and injected water under different field development scenarios and different representations of the uncertain reservoir geology.

When production simulation models are good approximations of the real system they can be used to good effect. The importance of the results of such models is illustrated effectively by the case study example of Miller, where understanding the flow and mixing of formation- and injected-water in the reservoir, now and in the future, is important for predicting the likelihood of barite scale precipitation and producing a strategy for mitigating its effects.

7.1.2 Production simulation models – an introduction

Reservoir simulation is a technique in which a computer-based mathematical representation of the reservoir is constructed and then used to predict its dynamic behaviour. Production simulation models are grid based, the reservoir usually being divided into over 100,000 grid blocks/cells. The reservoir properties (porosity, saturation and permeability etc) and fluid properties (viscosity, PVT) are specified for each cell (Jahn *et al.*, 1998). The grid is obtained from a reservoir model containing many millions of cells and conversion from one to the other is known as upscaling. Most models are based on controlled volume finite difference (Fisher, pers.com. 2006). The production simulation operates based on the principles of balancing the three main forces acting upon the fluid particles (viscous, gravity and capillary forces) and calculating fluid flow from one block to another. Simulation is often used for waterflood design and management.

7.1.3 Water mixing and connate/formation water banking

From a geochemical point of view, fluid mixing, in particular mixing between injected water and formation water, is one of the most interesting processes that take place within an oil/gas reservoir. Critically, it can also be assessed using a reservoir model. As discussed in previous chapters, the degree to which different types of water mix dictates the chemical reactions that occur and the likelihood of scaling taking place. The rate at which injected water is produced at a producing well, relative to the rate of injection and rate and amount of formation water produced, can give a good indication of how much mixing is occurring in the reservoir or the production string. A steady transition between the production of formation water and injected

water suggests that extensive mixing is taking place throughout the reservoir. Conversely, a very sudden change from formation water to injected water being produced implies that very little water mixing has occurred and instead the formation water has been "banked" ahead of the injected water. This is a process known as Connate Water Banking (CWB; though the correct term should be Formation Water Banking) and has significant implications for the prediction of scale formation as well as designing injection strategies. The banking model postulates that the first oil mobilized by the injected water contacts and mobilizes the oil downstream from it, which displaces more oil even further downstream. That is, the first oil produced would be the most downstream oil and the last would be that nearest the injection end (Jones, 1985).

According to Sorbie and MacKay, (2000) Buckley-Leverett theory suggests that CWB occurs behind the water/oil "shock-front". In this ideal case there is a sharp front between the injected waters and connate (formation) waters, and when water breakthrough occurs, the first water produced will be 100% formation water. This will continue until all the formation water is produced, at which point the produced water will change immediately to 100% injected water (Figure 7.1. Sorbie and MacKay, 2000).

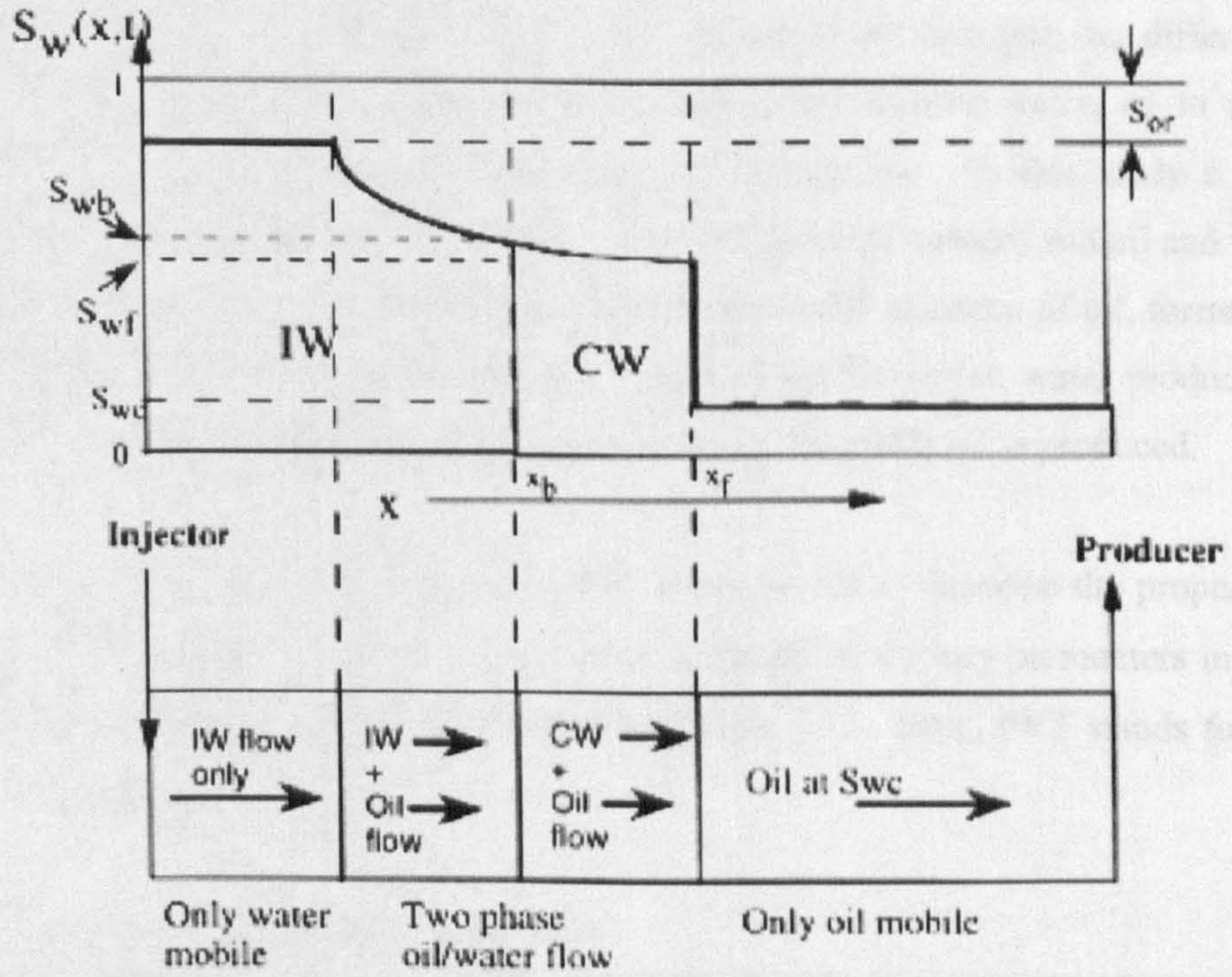

Figure 7.1. Snapshot of the water saturation profile, $S_w(x,t)$, at time t showing CWB; the sharp front between the injected water (IW) and the connate water at $x=x_b$; the single- and two-phase regions which develop. From Sorbie and Mackay, 2000.

7.2 Modelling fluid mixing in a production simulation model

7.2.1 The base case model

To constrain the model input parameters by integrating water compositional data with the computer simulation output, it needed to be possible to systematically alter a number of features of the model (e.g. permeability, oil viscosity, capillary pressure etc). The model output was then studied to determine what effect these changes had on the most relevant parameters e.g. formation water production rate, injected water production rate, breakthrough time etc

The Eclipse 100™ production simulation model (provided by *Rock Deformation Research, Leeds*), which is a fully-implicit, three phase, three dimensional, general purpose blackoil simulator with gas condensate options, was used investigate the controls on water breakthrough within petroleum reservoirs. A basic 2D model was constructed consisting of a 1 cell deep (200 ft), 15 cells (1000 ft each) wide and 9 cells/layers (50 ft each) high (e.g. Figure 7.6). The oil-water contact (OWC) was situated between layers 6 and 7. The reservoir was initially saturated with oil and formation water, according to the capillary pressure curve. The Tracer Tracking option is a keyword within Eclipse that can be used to determine the movement of 'marked' fluid elements during a simulation run. It may be used, for example, to differentiate the movement of water injected by different wells and initial aquifer water, or to predict the variation in salinity or concentrations of other chemical species. In this study a tracer was injected at one end of the reservoir to represent injected water (seawater) and oil and water were produced at the other end. The model calculated the rates and amounts of oil, formation water and the amount of tracer (that is, the injected water) in the formation water produced at each time step. Time step size depended on how quickly all the available oil is produced.

Models of this type are defined using a number of key words to describe the properties of the reservoir and relevant fluids. Table 7.2 is a brief summary of the key parameters in the model used in this study (using accepted industrial units, Table 7.1). Here, PVT stands for pressure, volume and temperature.

Table 7.1. Industry Units and their equivalents

Parameter	**Industry Units**	**SI equivalents and explanations**
Pressure	Psia	1 pound/square inch [absolute] = 6 894.7 pascal
Viscosity	cP	1 centipoise = 0.001 pascal second
Volume	scf	1 standard cubic foot = 0.028 cubic metre
Density	lb/ft^3	1 pound/cubic foot = 16.018 kilogram/cubic metre
Length	ft	1 feet = 0.304 metre
Flow rate	stb/day	1 stock tank barrel = 0.158 cubic metre

Table 7.2 Introducing the key parameters used in the production simulation model

Parameter	**Keyword**	**Features of model**
Water PVT functions	PVTW	• The water formation volume factor at 0 psia is 1.0 rb/Mscf • The water compressibility is 3.03E-06 1/psi • The water viscosity at 0 psia is 0.5 cP
PVT properties of dead oil (no dissolved gas)	PVDO	• The oil phase pressures at increasing depths are 0.0 and 8000.0 psia • The corresponding oil formation volume factors are 1.0 and 0.92 rb/Mscf • The corresponding oil viscosities are 2.0 and 2.0 cP
Rock compressibility	ROCK	• At a reference pressure of 4000 psia, the rock compressibility is 0.30E-05 1/psi
Fluid densities at surface conditions	DENSITY	• The density of oil at surface conditions is 52.0 lb/ft^3 • The density of water at surface conditions is 64.0 lb/ft^3 • The density of gas at surface conditions is 0.0440 lb/ft^3
Tracer information	TRACER	• Two separate tracers, one each associated with the injected water and the formation water
Water/oil saturation functions versus water	SWOF	• When both oil and water are mobile phases, information is needed about water relative permeability, oil-in-water relative permeability and water-oil capillary pressure as functions of the water saturation. Table 6.3 shows a typical model run with unaltered capillary pressure
Tracer concentration	TNUMFIW1	• The keyword specifies the concentration of a tracer in each grid block (1.0 for each block). • The associated stock tank phase of the tracer can only exist in the free state (designated by the letter F)
Equilibration data specification	EQUIL	• The keyword sets the contacts and pressures for conventional hydrostatic equilibrium. • The datum depth is 4000 ft at a pressure of 4000 psia • The depth of the oil-water contact is 4300 ft

Parameter	Keyword	Features of model
Initial tracer concentration versus depth	TVDPFIW1	• The initial tracer concentration values are 0.0 at all depths
General specification data for wells		• This introduces a new well, defining its name, the position of the wellhead, its bottom hole reference depth and other specification data. • There are two wells, an injector (water preferring) and a producer (oil preferring), with a reference depth for bottom hole pressure of 4000 ft.
Well completion specification data	COMPDAT	• Specifies the position and properties of one or more well completions. • In this study, the position of the well completions (perforations) is used as a variable and so changed in each model run, but the well bore diameter at the connection is 1.0 ft.
Control data for production wells	WCONPROD	• The wells are open for production controlled by a liquid rate target of 3* 3000.0 stb/day
Control data for injection wells	WCONINJE	• The injection well is a water injector, open for injection, controlled by surface flow rate target with a surface flow rate target of 2000.0 stb/day
Tracer concentrations for injection wells	WTRACER	• The value of the tracer concentration in the injection stream is 1.0.

Table 7.3 Reservoir water saturation information for a typical model run

Reservoir water saturation	Water relative permeability	Oil relative permeability	Water-oil capillary pressure (psia)
0	0	0.71	50.98
0.05	0	0.69	30.23
0.1	0	0.52	21.54
0.15	0	0.44	16.54
0.2	0	0.36	13.21
0.25	0	0.3	10.81
0.3	0.0172	0.24	8.975
0.35	0.0486	0.19	7.514
0.4	0.0894	0.15	6.319
0.45	0.1377	0.11	5.319
0.5	0.192	0.089	4.467
0.55	0.252	0.064	3.732
0.6	0.318	0.045	3.088
0.65	0.3894	0.03	2.518
0.7	0.4647	0.019	2.011
0.75	0.544	0.011	1.555
0.8	0.627	0.005	1.142
0.85	0.715	0.002	0.766
0.9	0.806	0	0.422
0.95	0.901	0	0.107

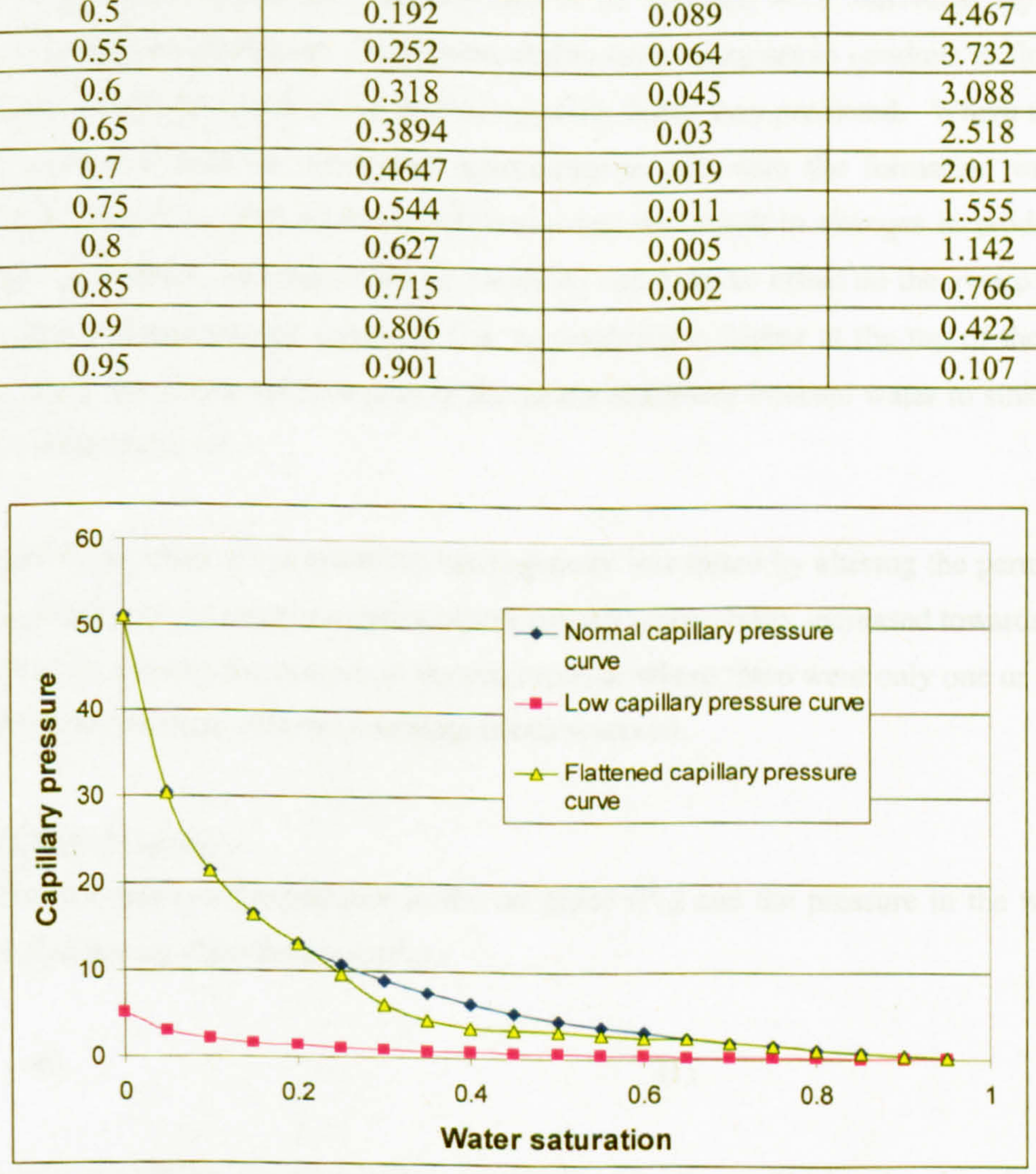

Figure 7.2. Capillary pressure profiles used in this study

7.3 Methods

The ability of the model to take account of reservoir heterogeneities and to determine the dominant controls on the extent of water mixing in reservoirs was assessed. Certain aspects of the model were altered systematically for each run and the results analysed. In the following section, the various parameters are described individually in terms of their influence on water breakthrough.

7.3.1 Permeability

Reservoirs in clastic sedimentary basins tend to be layered, with individual layers having different average permeabilities. High permeability layers may act as conduits to flow and can cause injected water to arrive at the producing wells faster than predicted. Where this occurs, injected water will have an additional opportunity to mix with the formation water. This enhances the possibility that reactions will occur that will result in changes in produced water chemistry. In addition, heterogeneous permeability can have an effect on the sweep efficiency. For example, a coarsening-up sequence (i.e. permeability is higher at the top of the reservoir) might improve the sweep because gravity forces the shallower injected water to sink lower and so flush out any extra oil.

In the model, the effect of permeability heterogeneity was tested by altering the permeability of each individual layer to create scenarios where overall permeability increased towards the top of the reservoir or towards the bottom of the reservoir, or where there were only one or two higher permeability layers in an otherwise homogeneous reservoir.

7.3.2 Capillary Pressure

The difference between the pressure in the oil phase (P_O) and the pressure in the water phase (P_W) is called the capillary pressure (P_C) :

$$P_c = P_W - P_O \qquad (1)$$

The pressure needed for the oil to enter a particular pore throat (P_c) is related to the interfacial tension (σ), the radius of the capillary tube/pore throat (r_t) and the contact angle between the water and the rock surface (θ) by:

$$P_c = \frac{2\sigma\cos\theta}{r_t} \qquad (2)$$

Figure 7.2 shows a capillary pressure curve, illustrating that the greater the capillary pressure, the more oil is present in the pore spaces relative to water; thus creating a situation where water-

water mixing is less likely to occur. A pressure-depth plot (Figure 7.3) highlights the fact that the higher a point is above the free water level, the higher the capillary pressure and the more oil that can get into the pore space. Changing the capillary pressure curve to lower values increases the amount of formation water above the free water level relative to the standard values (cf. Figures 7.5 and 7.10).

Table 7.4 Parameter variation details for models 1-4

Model	Permeability	Vertical permeability	Capillary pressure curve	Oil Viscosity cP	Perforation position
1	Either homogeneous permeability at 50 or 100 mD in all cells (runs 1a and b), or heterogeneous permeability varying from 50 – 800 mD (runs 1c to 1f), or higher permeability layer of 1000 mD against a background of 50 mD (runs 1g to 1l)	= 1/10 horizontal permeability	normal capillary pressure profile	2	varying locations
2	Either homogeneous permeability at 50 mD for all cells (runs 2a, b and g), or heterogeneous permeability varying from 50 – 800 mD (runs 2c to 2f)	= 1/10 horizontal permeability	variable capillary pressure profile (see 7.2)	2	layers 1, 2 and 5
3	Homogeneous permeability and then either heterogeneous permeability varying from 50 – 800 mD (runs 3a and b), or higher permeability layer of 1000 mD against a background of 50 mD (runs 3c and d)	= 1/10 horizontal permeability	normal capillary pressure profile	0.1 0.2 0.5 1.0 2.0 10.0 20.0	layers 1, 2 and 5
4	Heterogeneous permeability varying from 50 – 800 mD (all models)	= horizontal permeability	normal capillary pressure profile	2.0 20.0	layers 1, 2 and 5

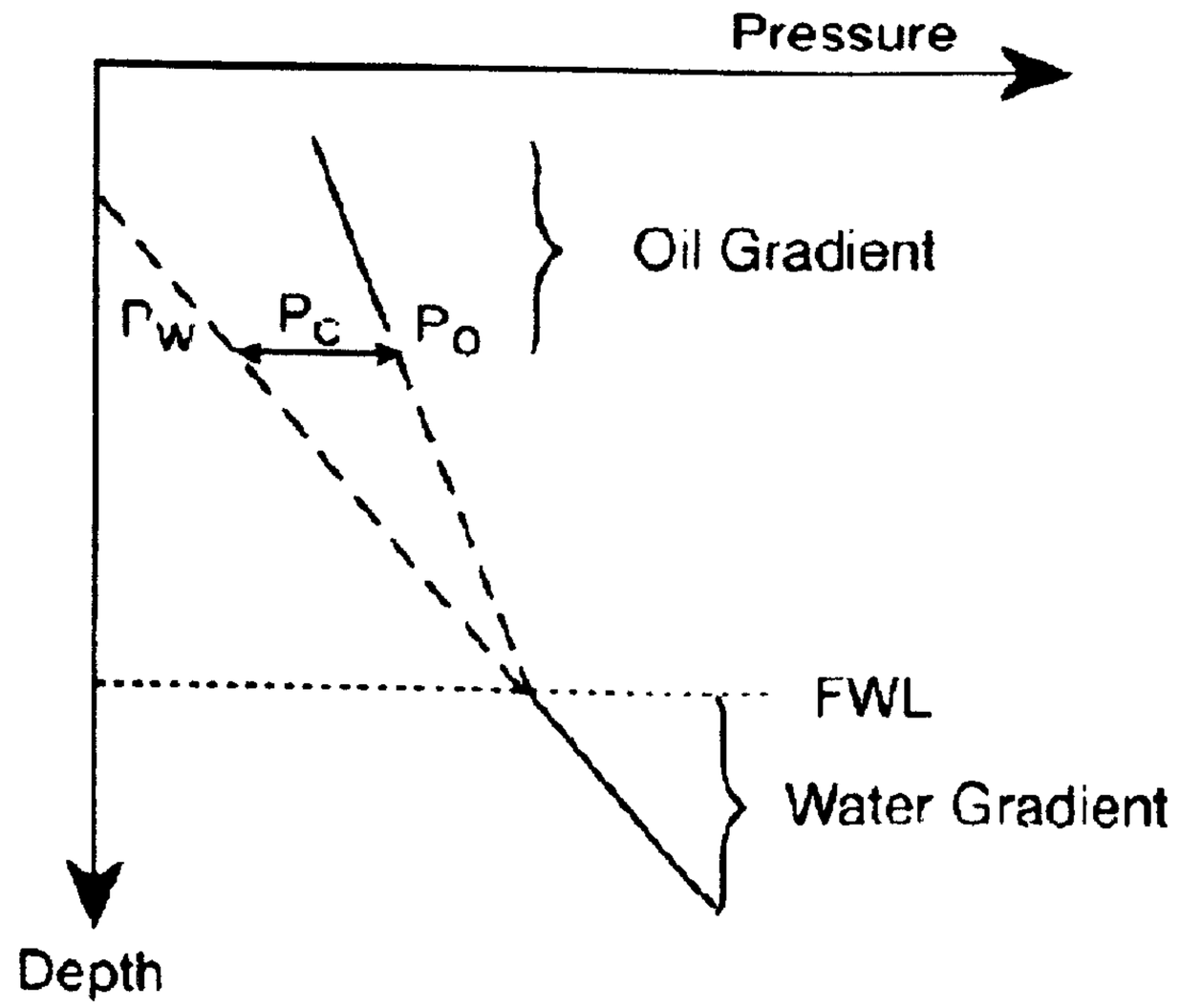

Figure 7.3. Pressure-depth plot illustrating the relationship between oil and water pressure and capillary pressure. From Jahn *et al.*, 1998.

The shape of the capillary pressure curve was varied by reducing the pressures in the standard curve by a factor of 10, or by flattening a portion of the standard curve to create a different shape. These changes were expected to have an effect on both amount of oil and water in place and the reaction of those fluids to the injection of water into the reservoir.

7.3.3 Relative permeability and mobility ratio

Relative permeability is the ratio of effective permeability of a particular fluid at a particular saturation to absolute permeability of that fluid at total saturation (equation 2). The mobility of a fluid is defined as the ratio of its permeability to viscosity. When water is displacing oil in the reservoir, the mobility ratio determines which of the fluids moves preferentially through the pore space (Jahn *et al.*, 1998). The mobility ratio for water displacing oil is defined as:

$$\text{Mobility ratio (M)} = (k_{rw}/\mu_w)/(K_{ro}/\mu_o) \qquad (2)$$

Where k_{rw} is the relative permeability to water, μ_w and μ_o are viscosities of water and oil respectively and k_{ro} is the relative permeability to oil. If the mobility ratio is greater than 1 (i.e. oil is less mobile) then there will be a tendency for water to move preferentially through the reservoir and will give rise to an unfavourable displacement front which is termed viscous fingering. If the mobility ratio is less than unity (i.e. the oil is more mobile) then there will be a stable displacement front. Altering the viscosity of the oil will change the nature of the displacement front and may affect the degree to which mixing occurs in the reservoir (Larue and Friedman, 2005).

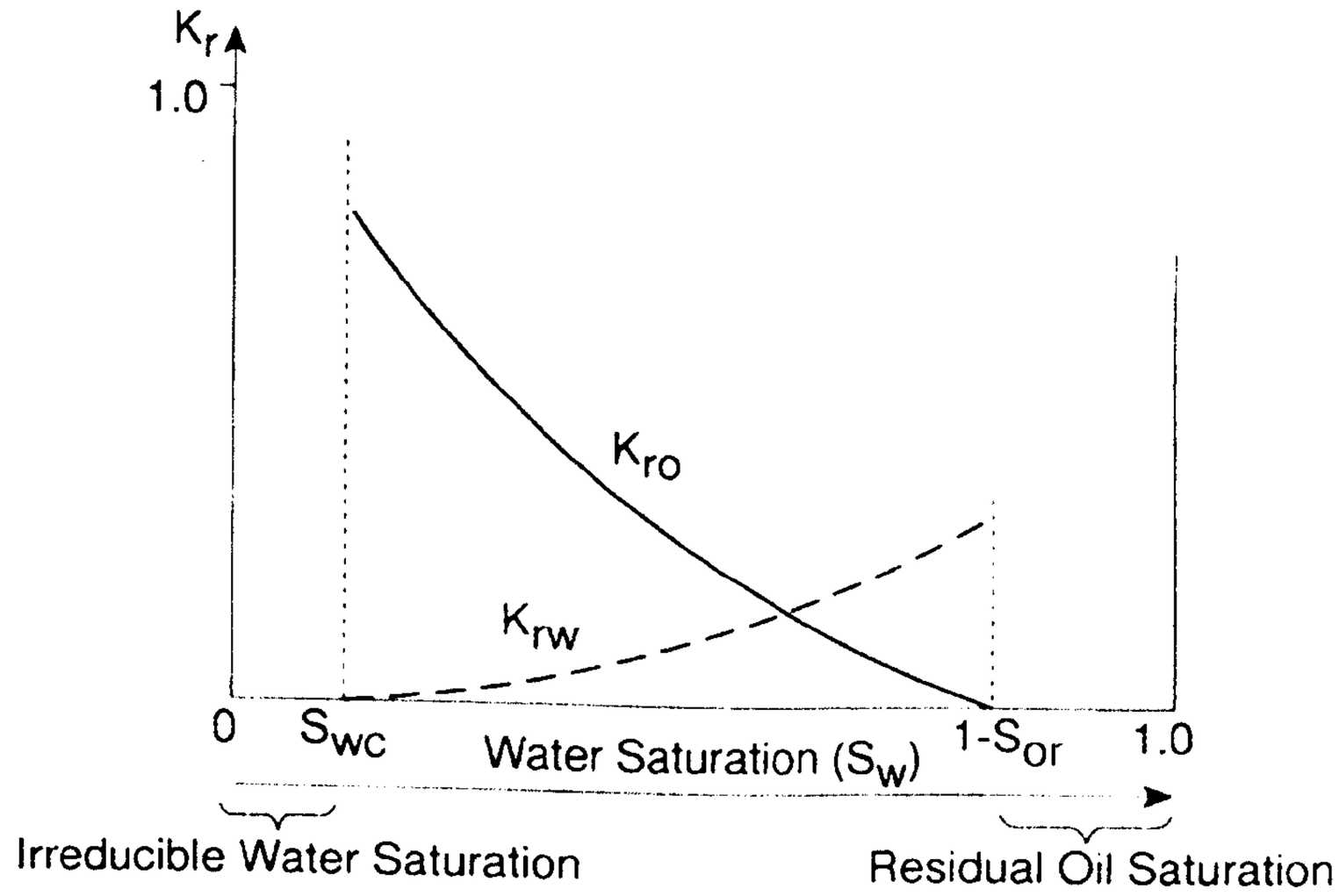

Figure 7.4. Relative permeability curve for oil and water. From Jahn *et al.*, 1998.

In the model, the viscosity of the oil was varied between 0.1 and 20 cP, while either maintaining all other parameters constant, or altering the permeability.

7.3.4 Vertical permeability

In most sedimentary basins and in most reservoir models it is assumed that lateral permeability is greater than vertical permeability. A truly homogeneous reservoir with respect to permeability is likely to allow fluids to travel more freely between layers, which will have an effect on how much the injected water can mix with the formation water.

In the model, the vertical permeability was set to be the same as the horizontal, creating either a completely homogeneous reservoir, or a layered reservoir in which each layer had equal horizontal and vertical permeability.

7.3.5 Perforation position

In addition to the main factors controlling the output of the model, importance of the number and location of perforations through which water was injected (i.e. the well completion data) was assessed for each model, by altering the locations of the perforations in a number of different runs. Completion strategies are often aimed at identifying ways of optimising production. Here, the model is used to assess how the position of the perforations could affect water production/mixing.

7.3.6 Altering management strategies

It is common practise to halt injection or production at one or several wells in an oilfield for reasons of maintenance, scale mitigation or a change in production strategy. The cessation of pumping may allow fluids to flow back, mix and interact with one another in new ways.

A number of runs were carried out on an otherwise unchanging system in order to assess the effect of shutting in a well. Injection and production were stopped for either 3 days or a year, early, mid-term or late in the life of the wells.

7.4 Results

Each model was set to run for the equivalent of 5000 days (over 13 years) or for as long as oil could still be produced from the reservoir and while the progress of injected water incursion and oil replacement could be tracked through time. Production and injection rates were monitored continuously while the total amounts of water and oil produced, as well as the images that show the location of the oil and waters apply to the final situation at the end of the run. Appendix IX contains tables outlining the precise specification of each model.

In all cases, comparisons were made between a "base case" model and models in which fluid properties had been altered. The base case consisted of a homogeneous reservoir with permeability of 100 mD, a normal capillary pressure profile, oil viscosity of 2 cP, vertical permeability = $1/10^{th}$ horizontal permeability, no shut-in periods and perforations in layers 1,2 and 5 in both the injector and the producer. Figures 7.4 and 7.5 shows the changing production rates through time of injected water, formation water and oil in the base case and Figure 7.6 shows how the computer programme FloViz™ was used to image the changing reservoir system.

7.4.1 Model 1. Permeability Variation

Prior to an in-depth study of the effect of permeability variation on the reservoir system, simple changes were made to the base case model in order to note the overall changes to be expected from permeability heterogeneity. All other reservoir and fluid properties were held constant (Figure 7.6).

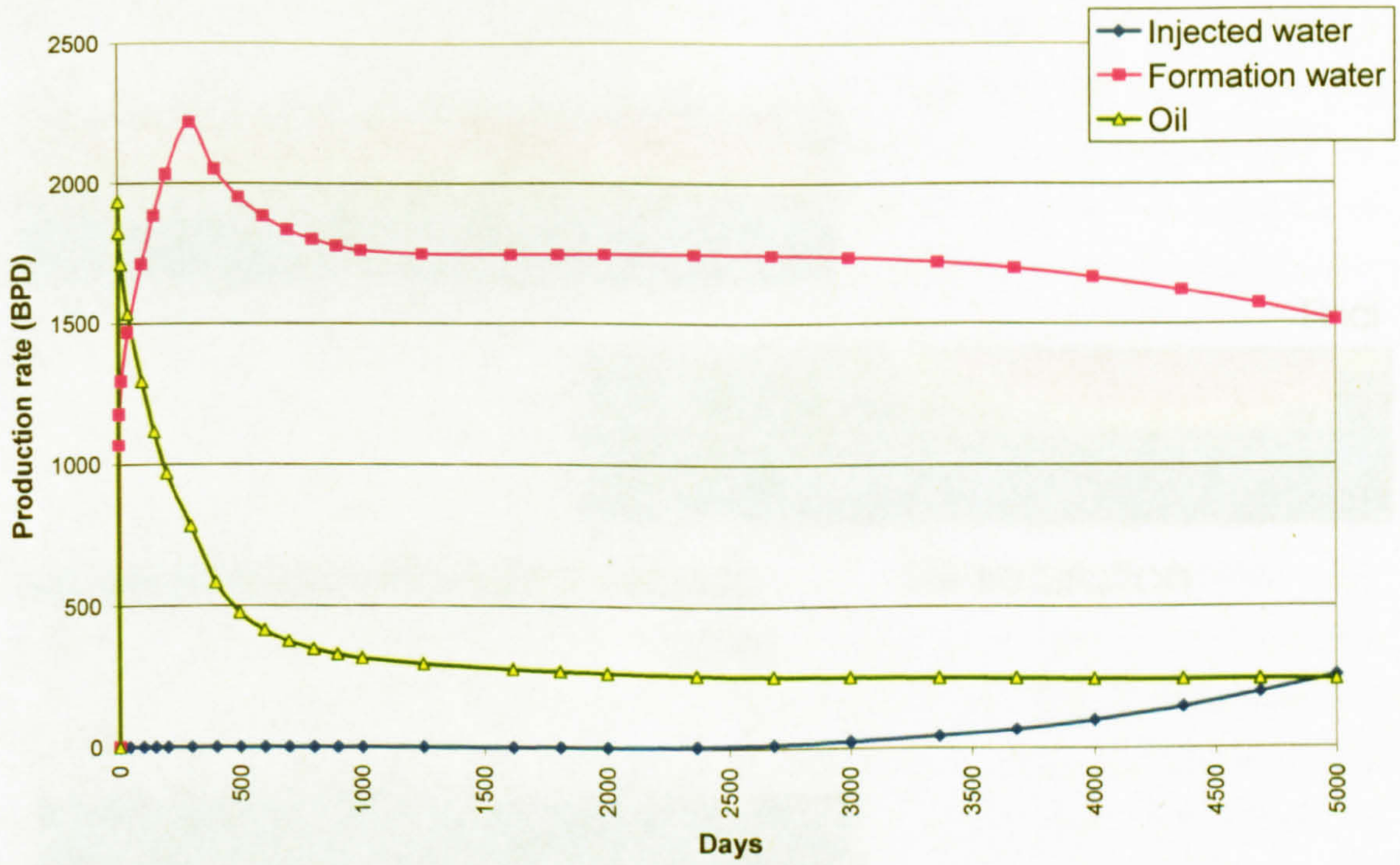

Figure 7.5. Production rates of reservoir fluids as modelled for the "base case" scenario of a homogeneous reservoir, with standard values for capillary pressure and oil viscosity, and no changes made to the management of the wells.

The model predicted a homogeneous reservoir will produce far less injected water at a slower rate than a similar reservoir with one or two high permeability horizons, but that these reservoirs will produce less formation water overall. In all cases, there was predicted to be a rapid increase in the rate of formation water production as oil production rate decreased, with a subsequent decline as injected water breakthrough occurred. The model predicted that a reservoir in which the permeability increases with increasing depth will have the highest total water production because the water is able to flow more easily through those layers which had a lower initial oil saturation. This also explains why this type of reservoir produced the smallest amount of oil at the lowest rate.

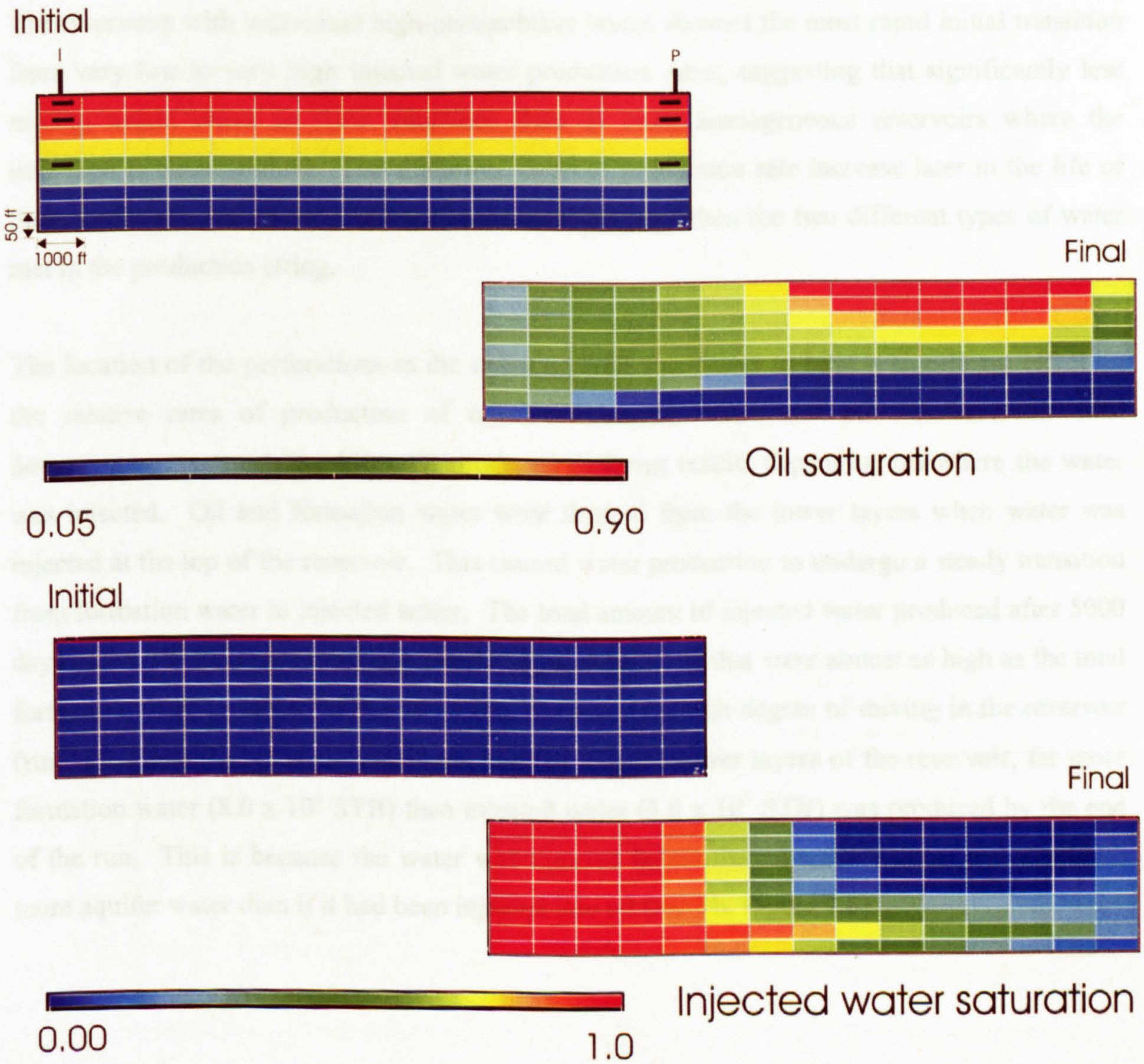

Figure 7.6. Images from the programme FloViz showing a lateral view of the 2D reservoir, illustrating oil, injected water and total water saturation at the beginning and end of runs for the "base case" model outlined in section 7.4. Note initial view for oil saturation shows location of injecting (I) and producing (P) wells and the layers in which the wells are perforated.

The reservoirs with individual high-permeability layers showed the most rapid initial transition from very low to very high injected water production rates, suggesting that significantly less mixing would occur in these situations than in more homogeneous reservoirs where the transition is more gradual. The shallower slope of production rate increase later in the life of these wells was due to the predicted increase of mixing when the two different types of water met in the production string.

The location of the perforations in the injecting well was found to have a significant effect on the relative rates of production of injected/formation water and oil. A reservoir with homogeneous permeability (50 mD) produced different results depending on where the water was injected. Oil and formation water were flushed from the lower layers when water was injected at the top of the reservoir. This caused water production to undergo a steady transition from formation water to injected water. The total amount of injected water produced after 5000 days (4.0×10^6 STB) reflected this trend and reached levels that were almost as high as the total formation water produced (4.9×10^6 STB), suggesting a high degree of mixing in the reservoir (run 1a). Conversely, when water was injected into the lower layers of the reservoir, far more formation water (8.0×10^6 STB) than injected water (3.0×10^5 STB) was produced by the end of the run. This is because the water was injected below the oil-water contact and displaced more aquifer water than if it had been injected into oil (run 1b, Figure 7.8).

A

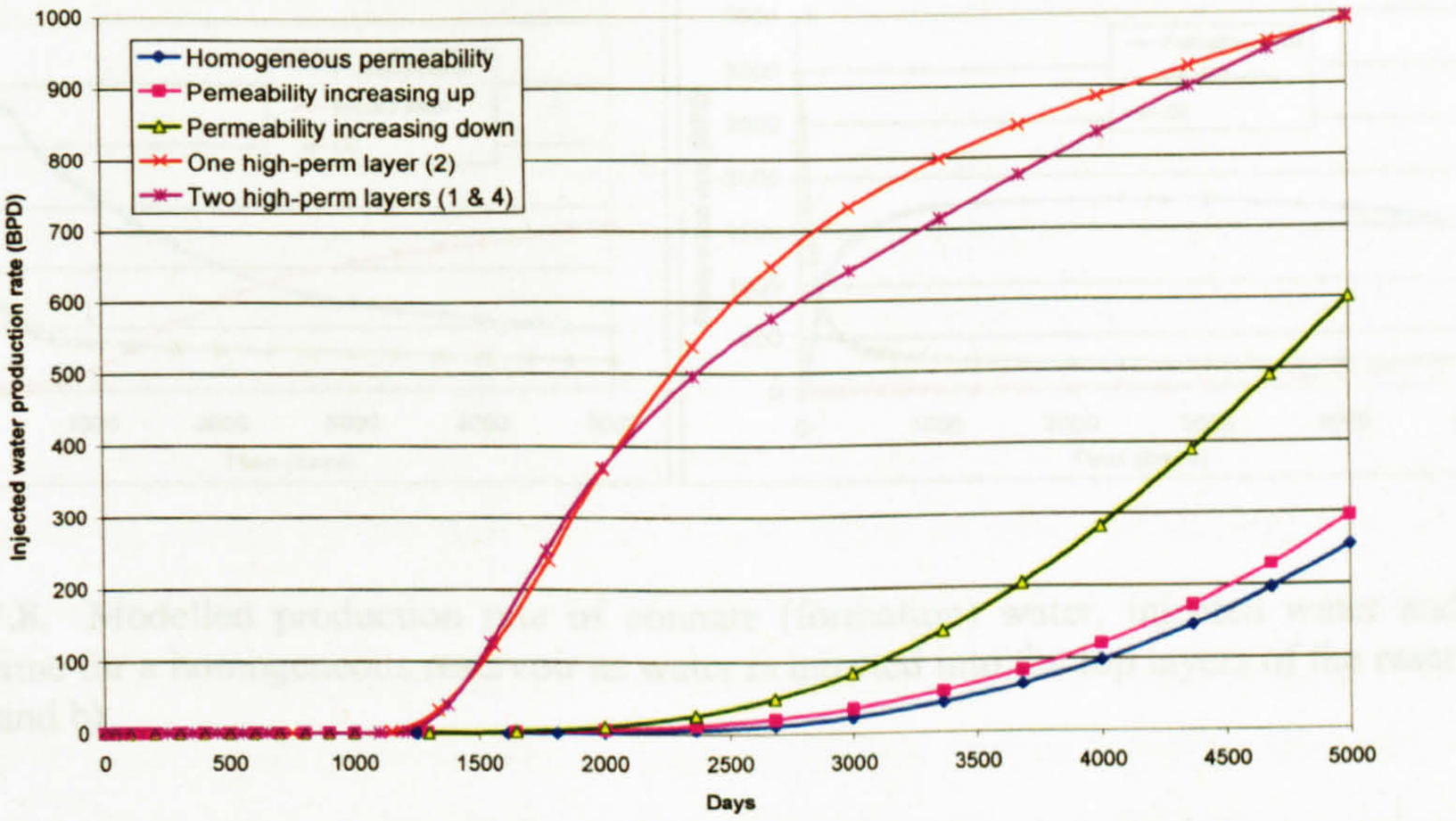

B

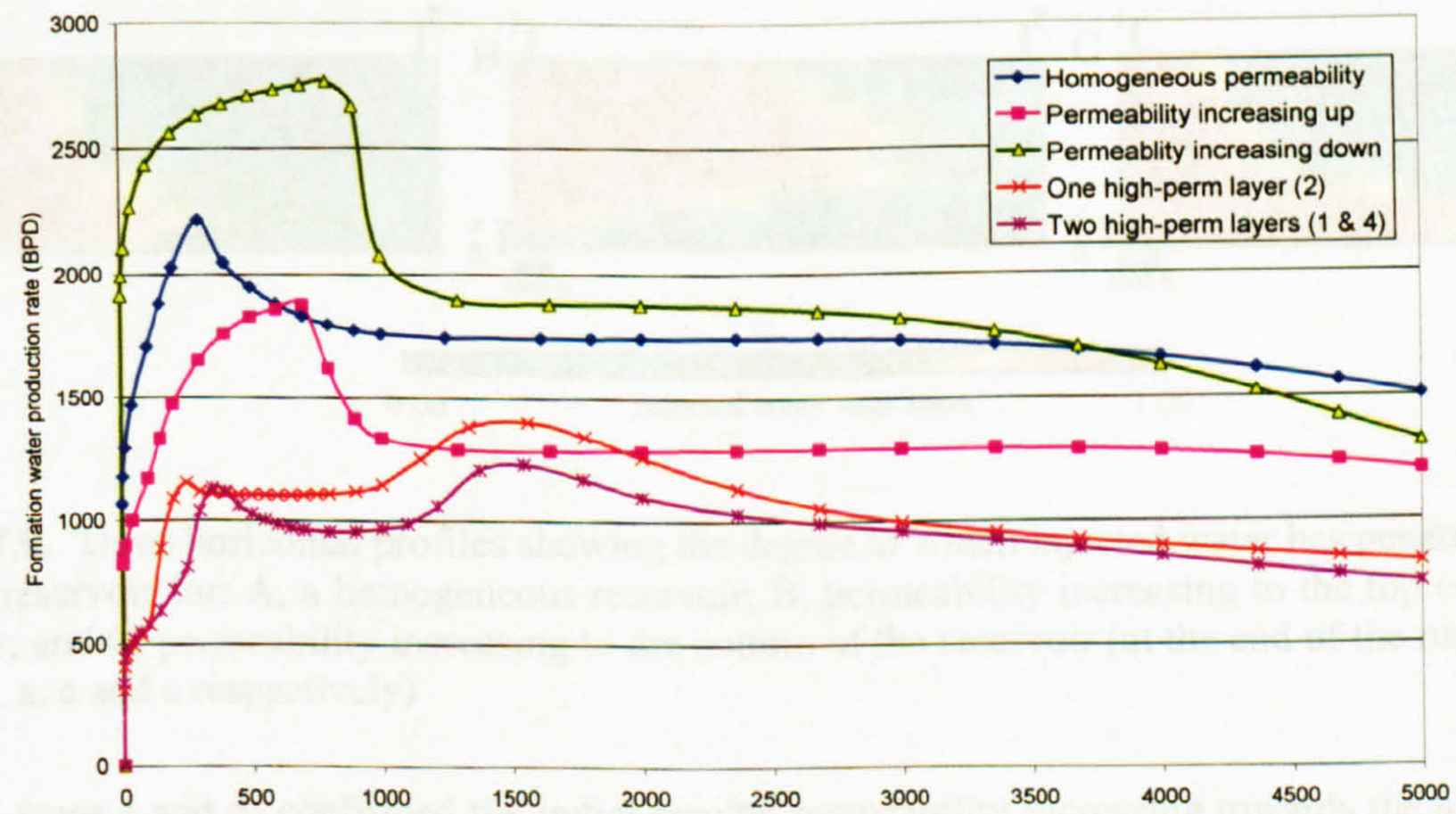

C

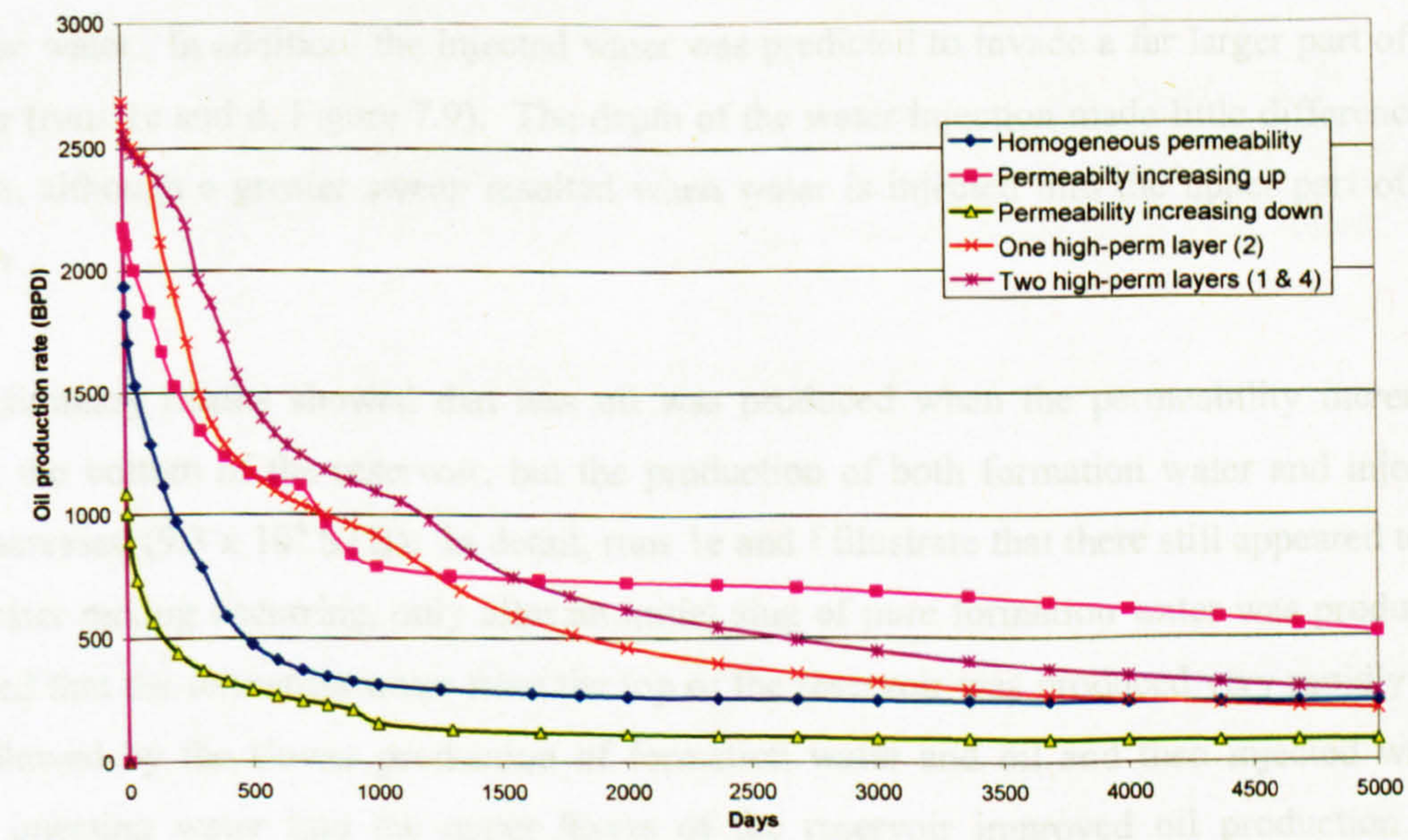

Figure 7.7. Production rates of: A) injected water, B) formation water and C) oil for five reservoirs with different permeabilities

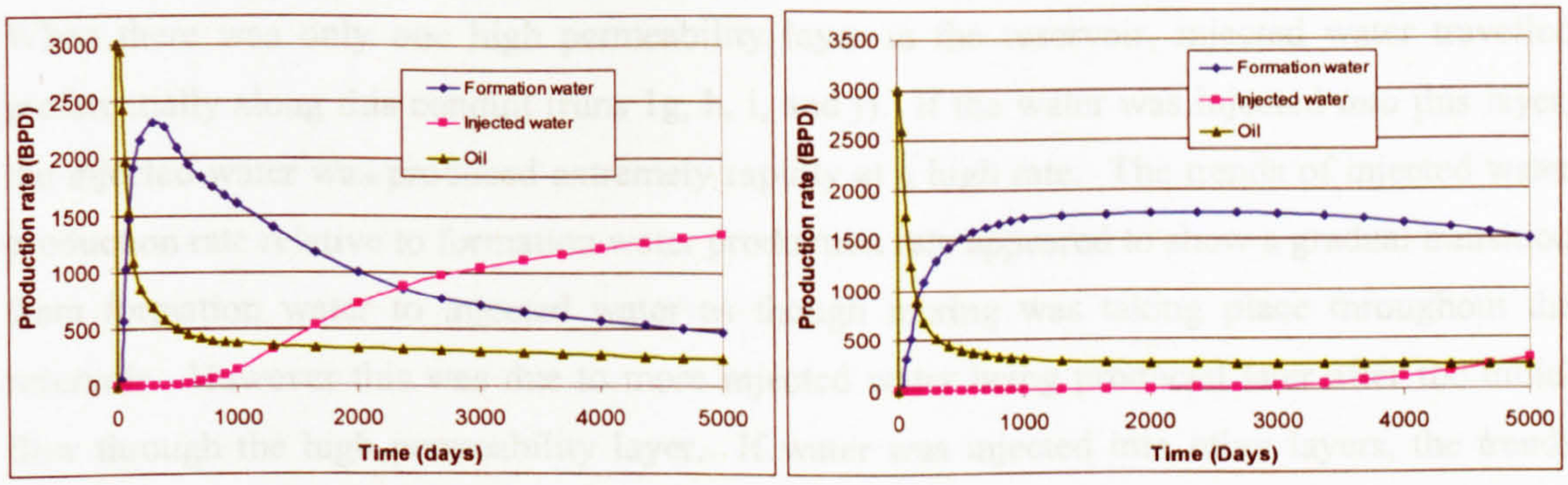

Figure 7.8. Modelled production rate of connate (formation) water, injected water and oil through time for a homogeneous reservoir as water is injected into the top layers of the reservoir (runs 1a and b)

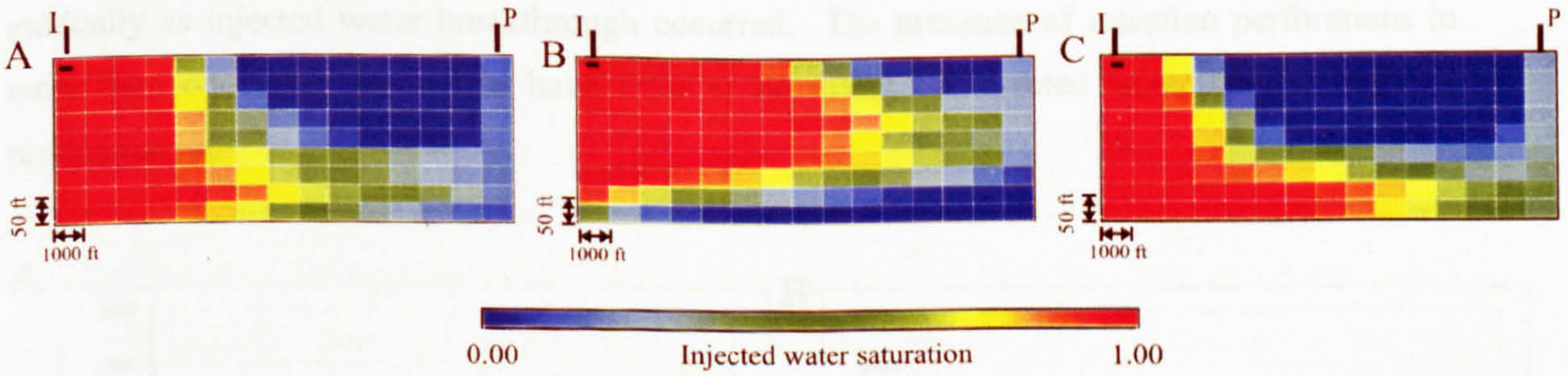

Figure 7.9. Three horizontal profiles showing the degree to which injected water has penetrated into the reservoir for: A, a homogeneous reservoir; B, permeability increasing to the top of the reservoir; and C, permeability increasing to the bottom of the reservoir (at the end of the run for model 1, a, c and e respectively)

Model 1 (runs c and d) confirmed the initial results: permeability increasing towards the top of the reservoir caused a far greater amount of oil to be produced, along with large amounts of formation water. In addition, the injected water was predicted to invade a far larger part of the reservoir (runs 1c and d, Figure 7.9). The depth of the water injection made little difference in this case, although a greater sweep resulted when water is injected into the upper part of the reservoir.

The preliminary results showed that less oil was produced when the permeability increased towards the bottom of the reservoir, but the production of both formation water and injected water increased (9.3×10^6 STB). In detail, runs 1e and f illustrate that there still appeared to be some water mixing occurring, only after an initial slug of pure formation water was produced. It seemed that the formation water from the top of the reservoir was produced very rapidly and was followed by the slower production of formation water and oil and then injected water. Again, injecting water into the upper layers of the reservoir improved oil production and decreased water production by a small amount compared to injection at greater depths.

When there was only one high permeability layer in the reservoir, injected water travelled preferentially along this conduit (runs 1g, h, i, and j). If the water was injected *into* this layer, the injected water was produced extremely rapidly at a high rate. The trends of injected water production rate relative to formation water production rate appeared to show a gradual transition from formation water to injected water as though mixing was taking place throughout the reservoir. However this was due to more injected water being produced later after the initial flow through the high permeability layer. If water was injected into other layers, the trends showed a similar pattern but the total amount of injected water produced was reduced and the production rate was slower, with a longer delay before the onset of injected water production. The location of the high permeability layer also had an effect; highly permeable upper layers of the reservoir caused more injected water to be produced and showed a very distinctive pattern with a slug of formation water being produced initially and then the amount decreasing gradually as injected water breakthrough occurred. The presence of injection perforations in more than one layer seemed to have little or no effect on injected water breakthrough or production rate.

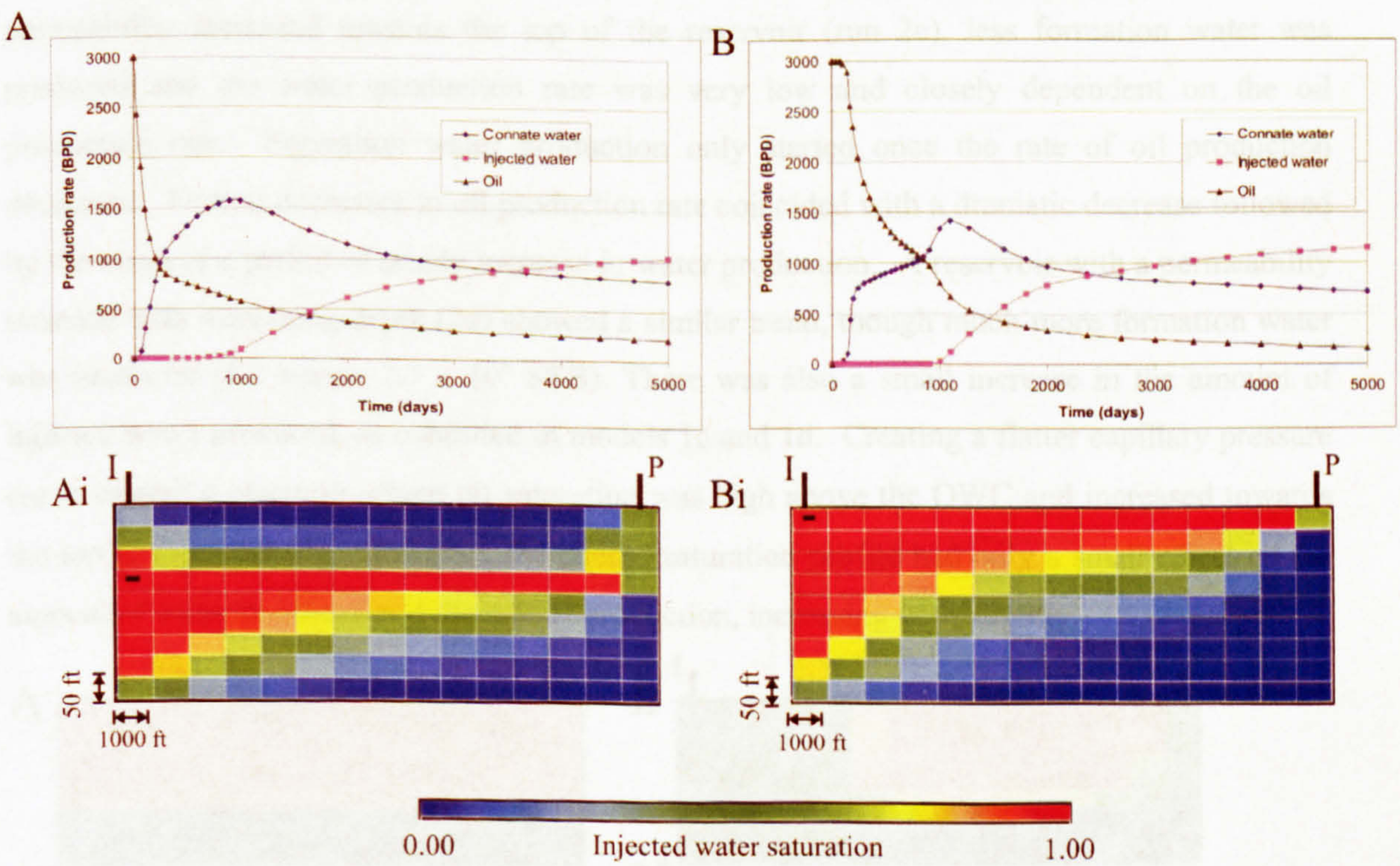

Figure 7.10. A: production rate data and (Ai) injected water profile for a reservoir with a high permeability layer above the OWC, with water injected *into* this layer. B: production rate data and (Bi) injected water profile for a reservoir with a high permeability layer at the reservoir surface, with water injected *into* this layer (at the end of the run for runs 1g and 1h).

7.4.2 Influence of the shape of the capillary pressure curve

Lowering the capillary pressure required for non-wetting phases to enter pore-space had the effect of altering the oil saturation profile (Figure 7.12). In a homogeneous reservoir containing rocks with large pore-throats and a narrow size distribution (i.e. a low capillary pressure) the oil was at extremely high saturation immediately adjacent to the oil-water contact (OWC) and up to the reservoir surface. At low capillary pressure the total amount of water produced was very low, particularly injected water. However, fluid production rates at low capillary pressure were extremely sensitive to permeability heterogeneities. Reservoirs with permeability increasing upwards were predicted to have very little water breakthrough at all and to produce a large proportion of the oil initially in place, while the opposite can be said for reservoirs with permeability increasing downwards. At high capillary pressures, permeability had a smaller effect on fluid production rates.

In a homogeneous reservoir, at low capillary pressure, the formation water production rate was extremely rapid to begin with and the rate slowed with time (run 2a. Figure 7.11). When permeability increased towards the top of the reservoir (run 2c), less formation water was produced and the water production rate was very low and closely dependent on the oil production rate. Formation water production only started once the rate of oil production decreased. Further decreases in oil production rate coincided with a dramatic decrease followed by the onset of a period of steady increase in water production. A reservoir with a permeability increase with increasing depth (2d) showed a similar trend, though much more formation water was produced (8.3 versus 2.7 x 10^6 STB). There was also a small increase in the amount of injected water produced, as exhibited in models 1c and 1d. Creating a flatter capillary pressure curve created a reservoir where oil saturation was high above the OWC and increased towards the top of the reservoir. However, the altered saturation profile had only a small effect on the amount of water produced and the rate of production, increasing both slightly.

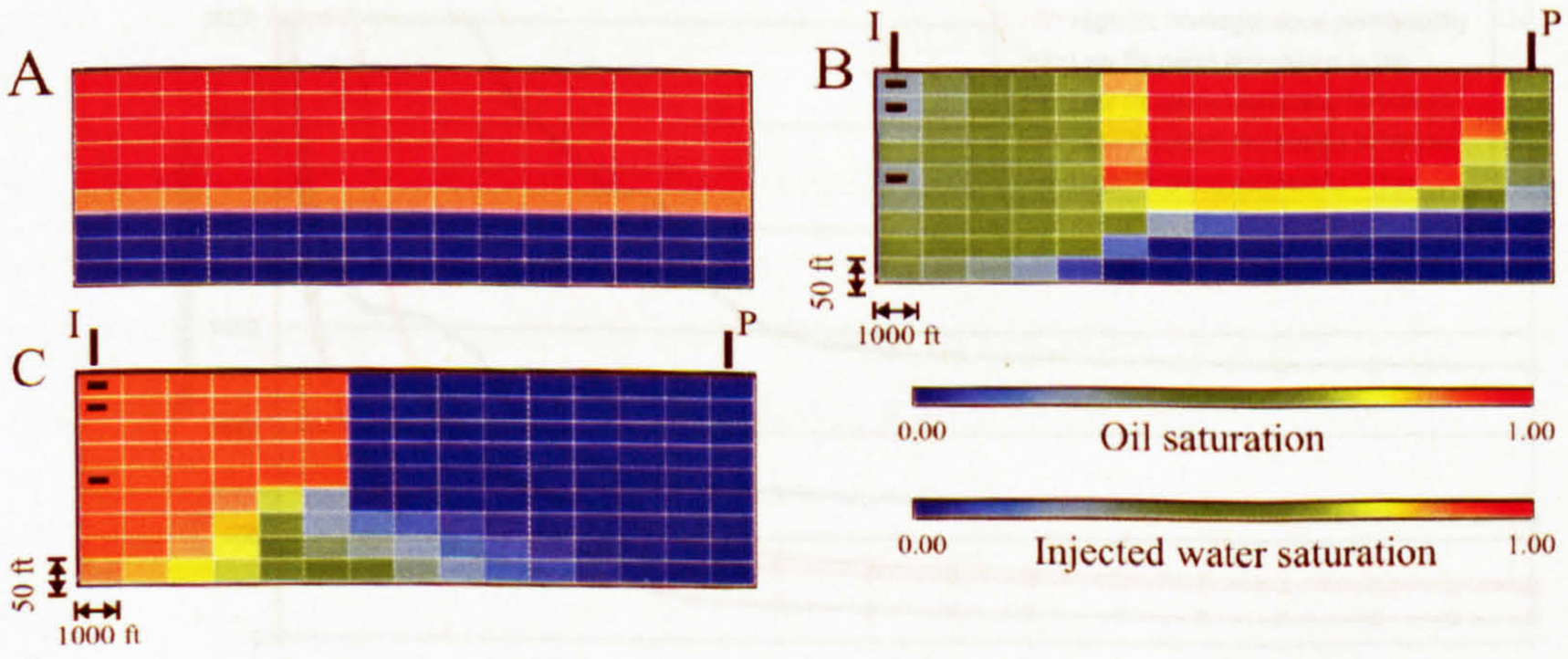

Figure 7.11. Model 2a. A, Oil saturation in a reservoir with lowered capillary pressure; B, Oil saturation in the same reservoir after oil production for 13 years; C, injected water saturation in the same reservoir after oil production for 13 years. Note different scale for image C and the abrupt contact between injected water and original reservoir waters.

A

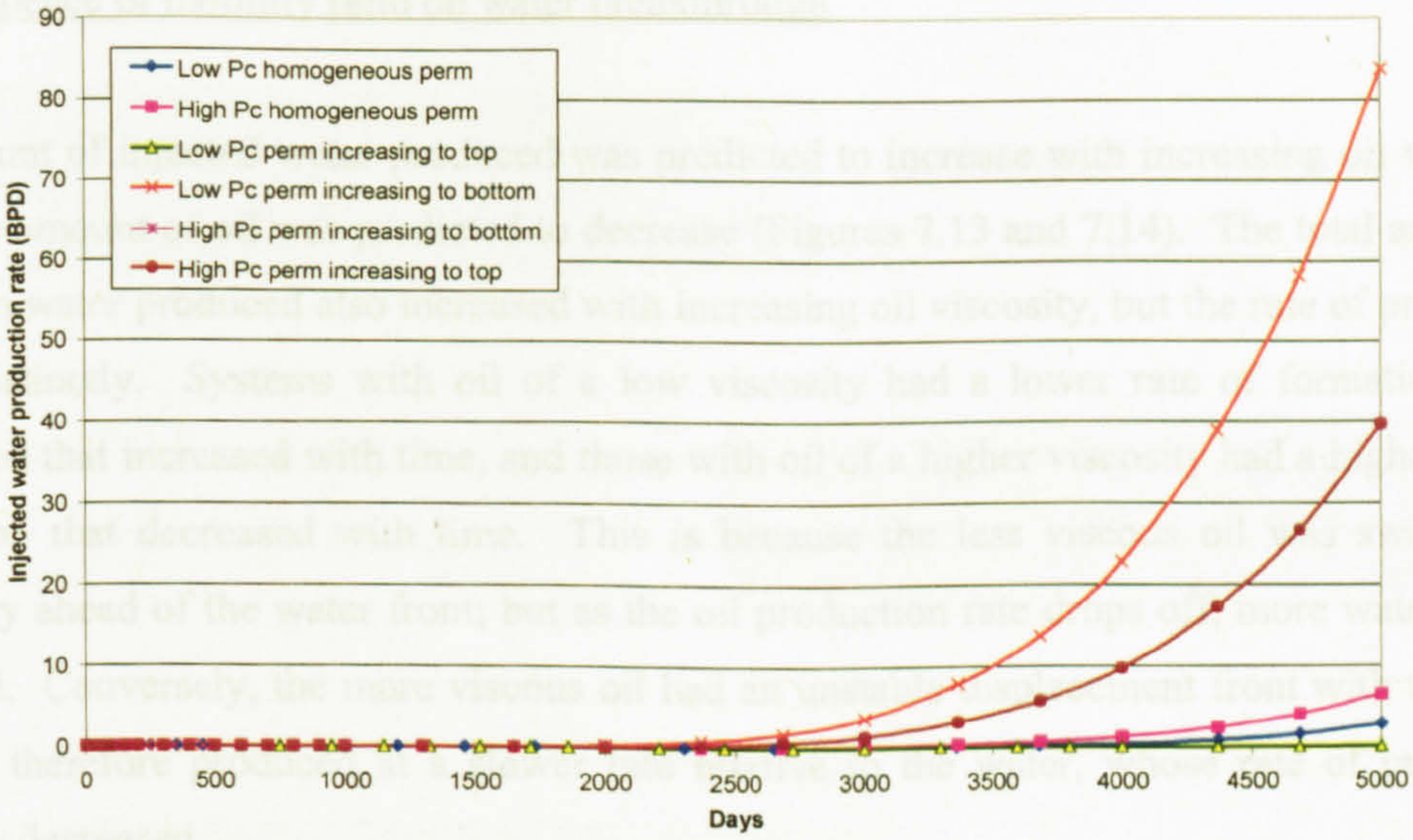

B

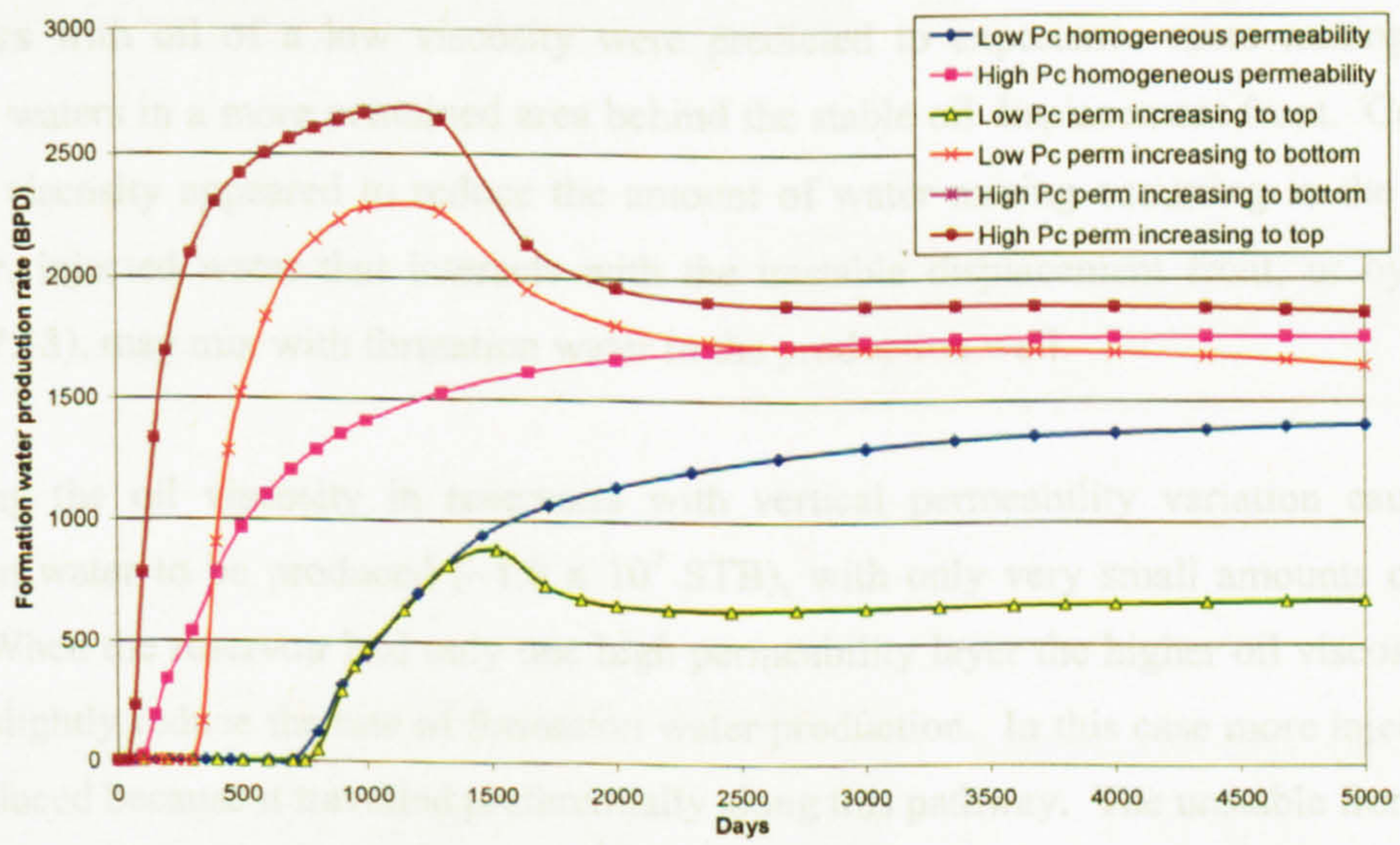

C

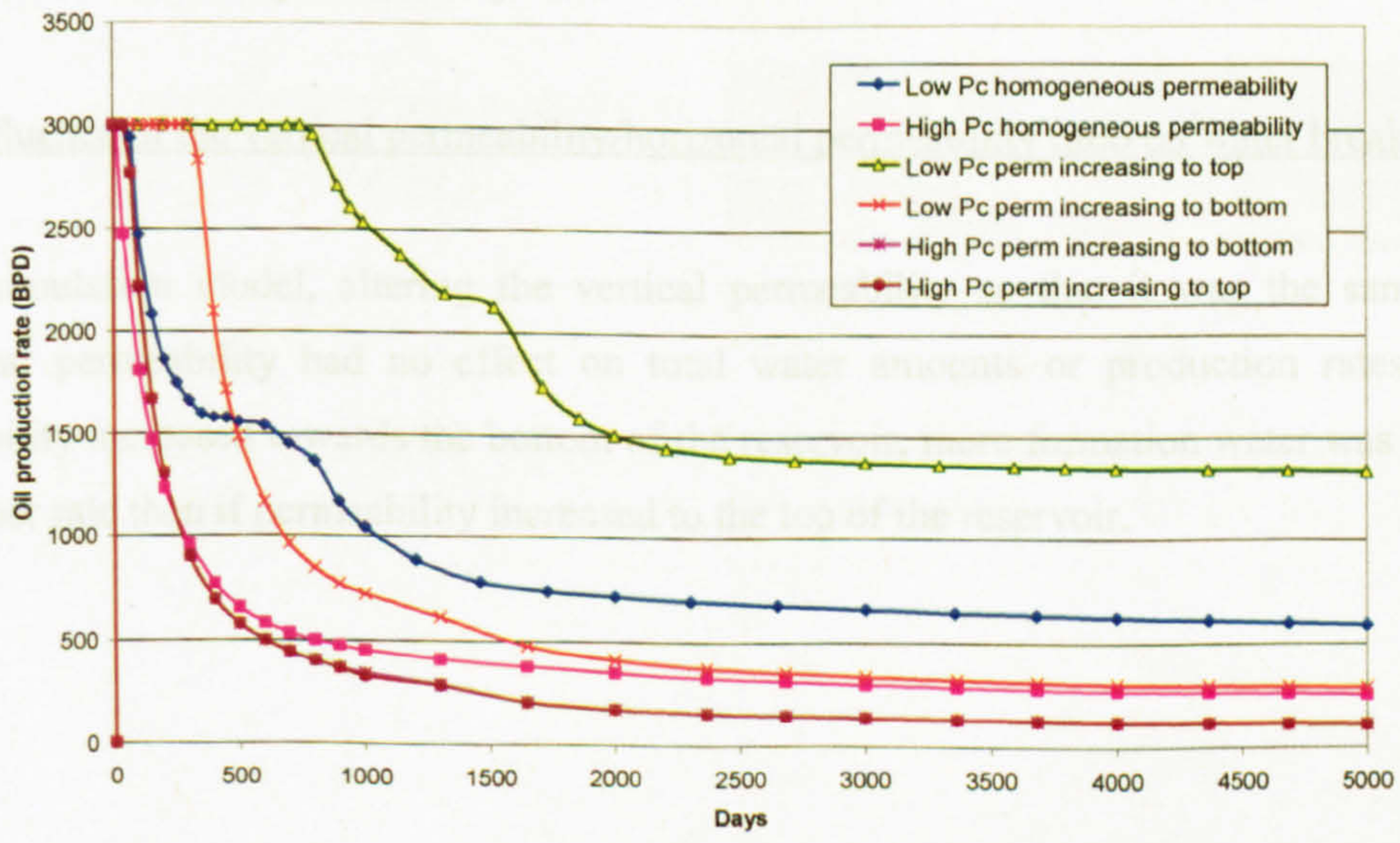

Figure 7.12. Production rates of: A) injected water, B) formation water and C) oil for two capillary pressure profiles in 3 reservoirs with different permeabilities

7.4.3 Influence of mobility ratio on water breakthrough

The amount of injected water produced was predicted to increase with increasing oil viscosity, while the amount of oil was predicted to decrease (Figures 7.13 and 7.14). The total amount of formation water produced also increased with increasing oil viscosity, but the rate of production varied distinctly. Systems with oil of a low viscosity had a lower rate of formation water production that increased with time, and those with oil of a higher viscosity had a higher rate of production that decreased with time. This is because the less viscous oil was swept more efficiently ahead of the water front; but as the oil production rate drops off, more water can be produced. Conversely, the more viscous oil had an unstable displacement front with the water and was therefore produced at a slower rate relative to the water, whose rate of production gradually decreased.

Reservoirs with oil of a low viscosity were predicted to experience more mixing between different waters in a more contained area behind the stable oil displacement front. Conversely, high oil viscosity appeared to reduce the amount of water mixing occurring in the reservoir. However, injected water that interacts with the unstable displacement front, or by-passes it (Figure 7.13), may mix with formation water in the production well.

Increasing the oil viscosity in reservoirs with vertical permeability variation caused more formation water to be produced (~1.0×10^7 STB), with only very small amounts of injected water. When the reservoir had only one high permeability layer the higher oil viscosity served to only slightly reduce the rate of formation water production. In this case more injected water was produced because it travelled preferentially along this pathway. The unstable front between the water and the high viscosity oil suggested that a relatively large degree of mixing could be predicted to be occurring in such a system.

7.4.4 Influence of the vertical permeability/horizontal permeability ratio on water breakthrough

In the simulation model, altering the vertical permeability so that it was the same as the horizontal permeability had no effect on total water amounts or production rates. If the permeability increased towards the bottom of the reservoir, more formation water was produced at a higher rate than if permeability increased to the top of the reservoir.

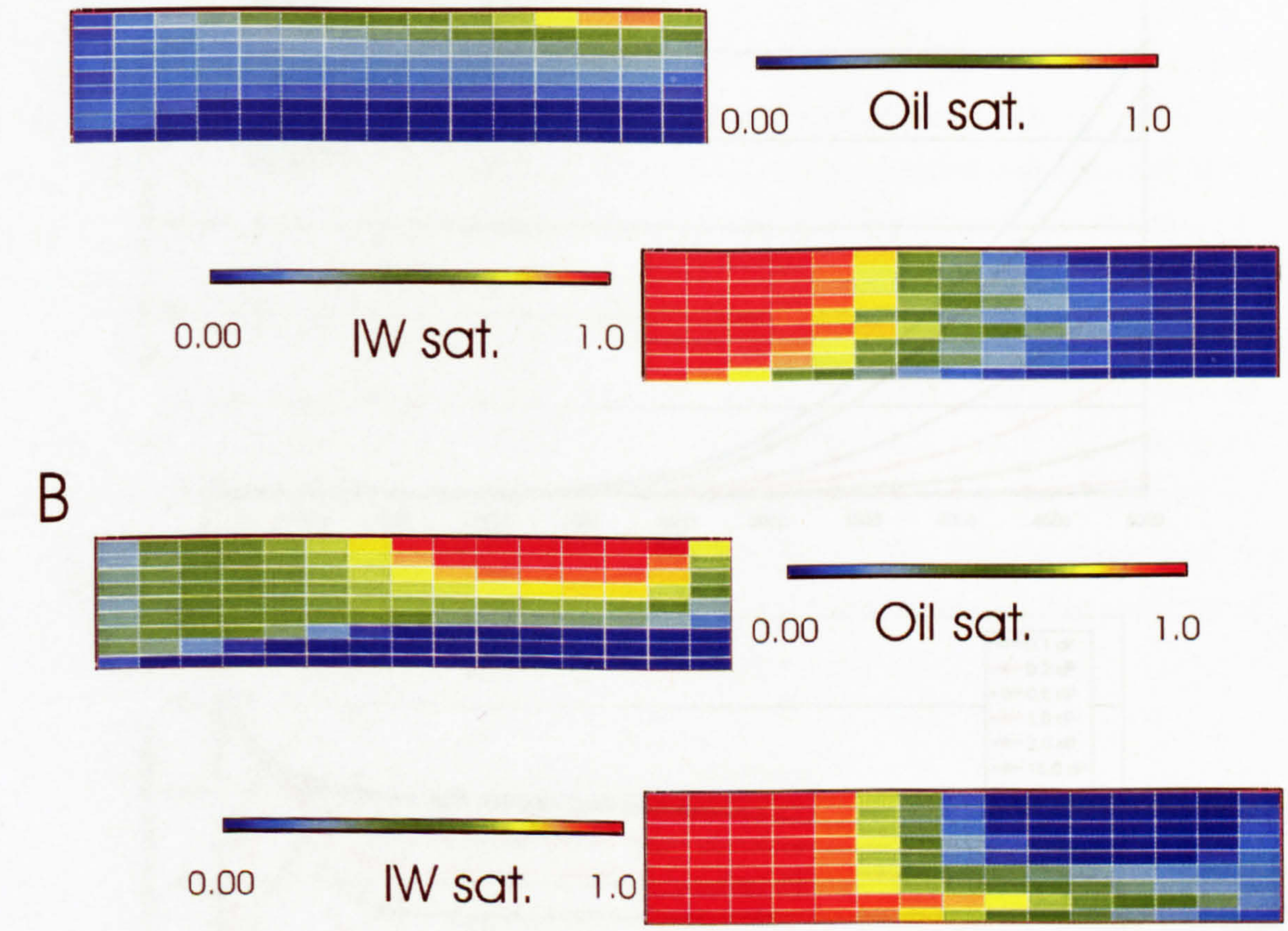

Figure 7.13. Images illustrating the oil and injected water (IW) saturation profiles in the reservoir at the end of a model run with oil viscosities of A) 0.2, B) 2.0 and C) 20.0 cP respectively.

A

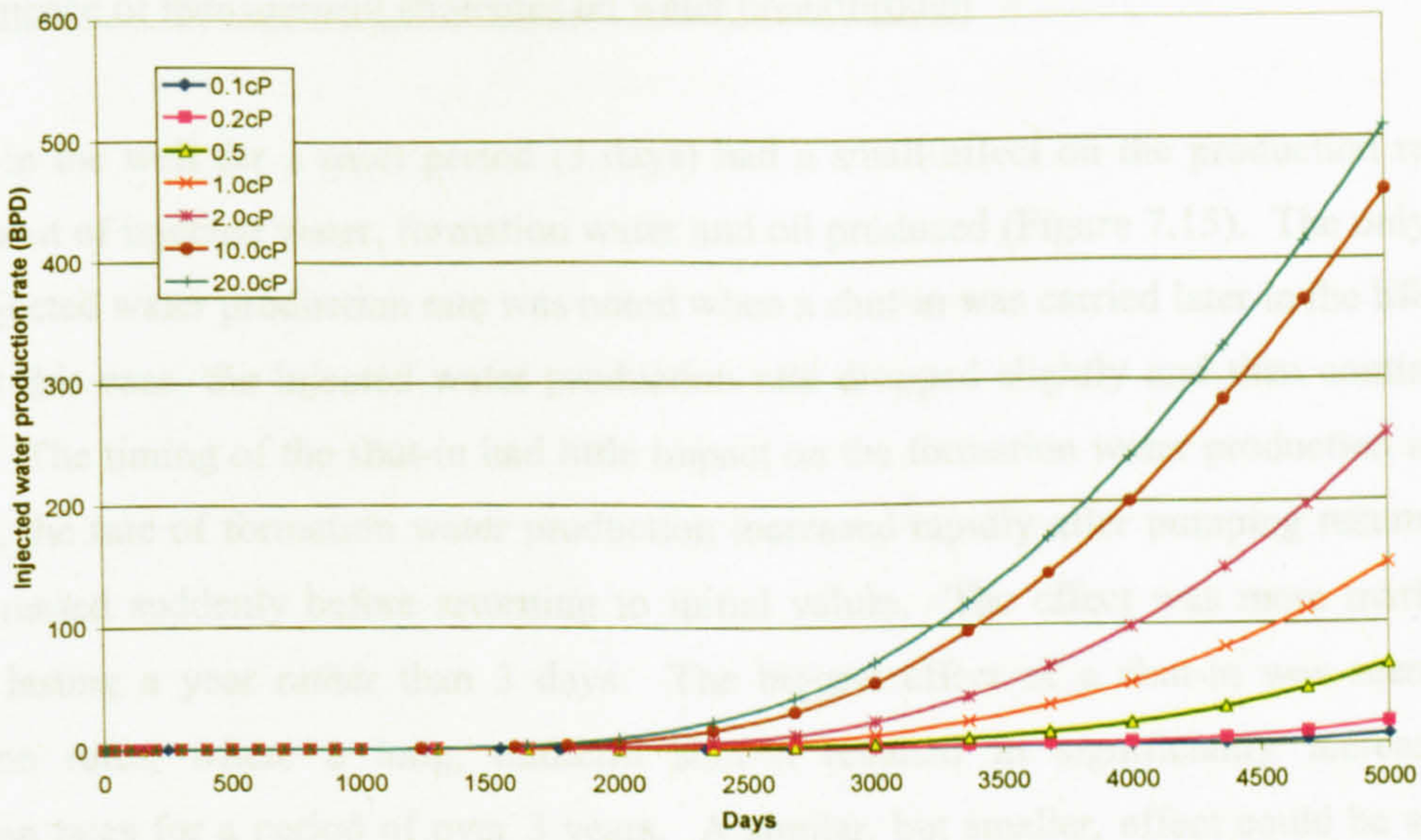

B

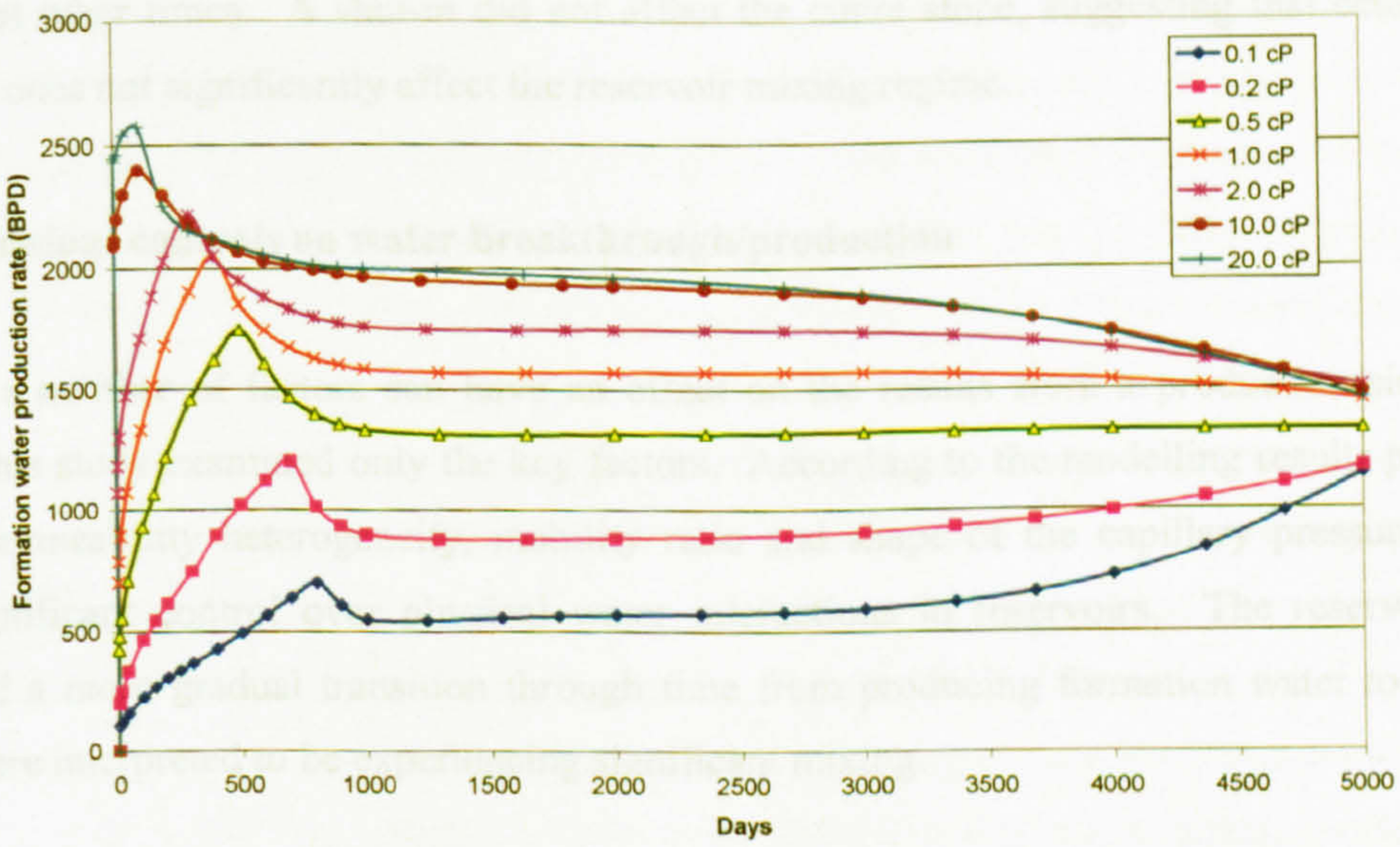

C

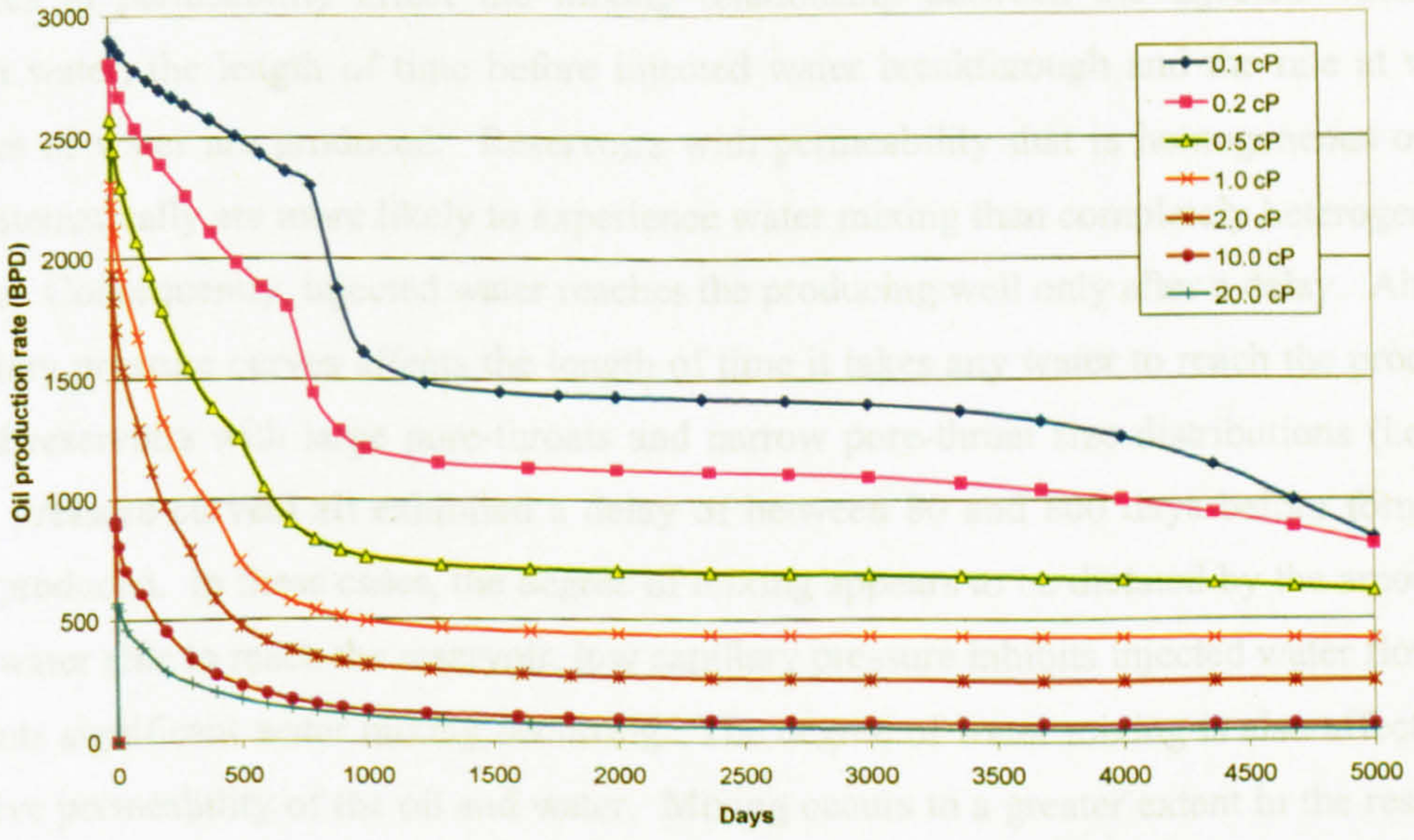

Figure 7.14. Production rates of: A) injected water, B) formation water and C) oil for seven reservoirs with oil of differing viscosity

7.4.5 Influence of management strategies on water breakthrough

Shutting-in the well for a short period (3 days) had a small effect on the production rate and total amount of injected water, formation water and oil produced (Figure 7.15). The only effect on the injected water production rate was noted when a shut-in was carried later in the life of the field. In this case, the injected water production rate dropped slightly and then continued to increase. The timing of the shut-in had little impact on the formation water production rate. In all cases, the rate of formation water production increased rapidly after pumping resumed and then decreased suddenly before returning to initial values. The effect was more marked for shut-ins lasting a year rather than 3 days. The biggest effect of a shut-in was seen in oil production rates, where a long, midterm shut-in resulted in significantly increased oil production rates for a period of over 3 years. A similar, but smaller, effect could be seen for shut-ins at other times. A shut-in did not affect the curve slope, suggesting that cessation of pumping does not significantly affect the reservoir mixing regime.

7.5 Discussion: controls on water breakthrough/production

Clearly, a number of factors can have an effect on the results from a production simulation model; this study examined only the key factors. According to the modelling results presented above, permeability heterogeneity, mobility ratio and shape of the capillary pressure curves have significant control over physical water interactions in reservoirs. The reservoirs that exhibited a more gradual transition through time from producing formation water to injected water were interpreted to be experiencing significant mixing.

Differences in permeability affect the mixing relationship between the injected water and formation water, the length of time before injected water breakthrough and the rate at which both types of water are produced. Reservoirs with permeability that is homogeneous or that varies systematically are more likely to experience water mixing than completely heterogeneous reservoirs. Consequently, injected water reaches the producing well only after a delay. Altering the capillary pressure curves affects the length of time it takes any water to reach the producer. Modelled reservoirs with large pore-throats and narrow pore-throat size distributions (i.e. low capillary pressure curves) all exhibited a delay of between 80 and 800 days before formation water is produced. In these cases, the degree of mixing appears to be dictated by the amount of injected water able to reach the reservoir, low capillary pressure inhibits injected water flow and so prevents significant water mixing occurring. The degree of water mixing is also affected by the relative permeability of the oil and water. Mixing occurs to a greater extent in the reservoir in systems with low viscosity oil, however a system with higher viscosity oil may be more at risk from water mixing occurring in the well bore. The model did not predict that altering

reservoir management strategies has any impact on the mixing regime or fluid flow in the reservoir at all. However, it will be demonstrated later that shutting in a well may have a significant effect on fluid flow and it may be that the model is not equipped to interpret this fully.

Two dominant production rate profiles arise from differences in the nature of injected water incursion. As the oil production rate inevitably declines, formation water from the oil leg is produced at a higher rate, if there is a steady supply of injected water (having experienced larger amounts of mixing in the reservoir) then the formation water production rate will decline gradually. Conversely, if only very small amounts of injected water are reaching the production well then the formation water production rate declines much more rapidly.

Most mixing occurs in a homogeneous reservoir. However, with a favourable capillary pressure, the next highest potential for mixing occurs when permeability increases to the top of the reservoir but water is injected at greater depth, or when permeability increases to the bottom of the reservoir and water is injected at shallower levels. A low capillary pressure inhibits injected water flow, but a mixing zone is likely to be spread over a wide area of the reservoir.

Even a very simple model has the capacity to reflect real changes in reservoir properties in a realistic way. However, this implies that small heterogeneities could have big effects on modelling results and emphasises the need for detailed knowledge of the reservoir properties. This problem is traditionally overcome by having a range of models that span the likely range of values of the key properties. However, water compositional data should provide an extra dimension that reduces the number of iterations required to produce a useable model. In the case study that follows, real production data were compared with results predicted by a production simulation model in order to establish the accuracy of the model determine which, if any, of the above properties (e.g permeability, capillary pressure) appear to influence the efficacy of the model. A real case study will also provide evidence of the usefulness of produced water chemistry in characterising a reservoir and supporting production simulation models.

A

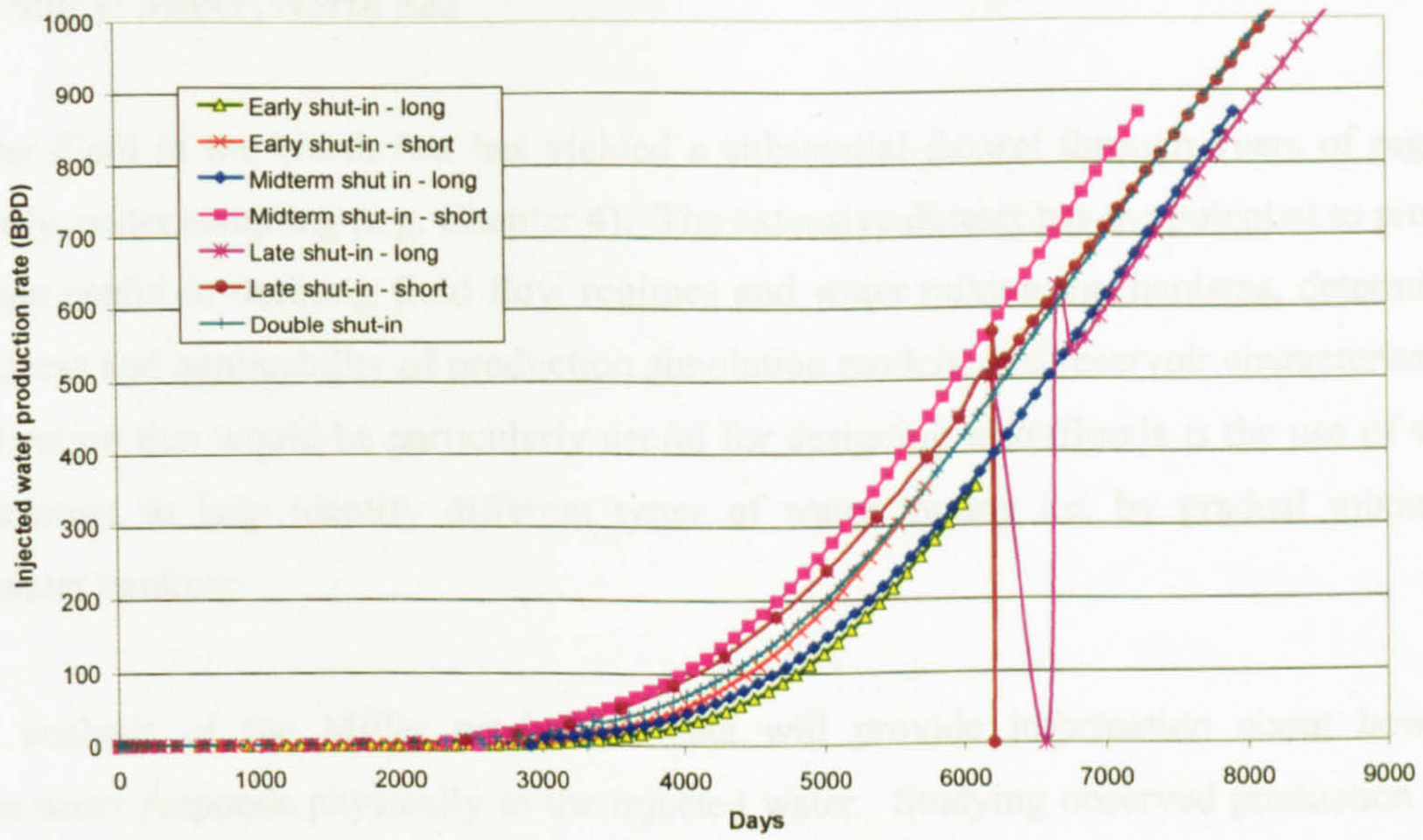

B

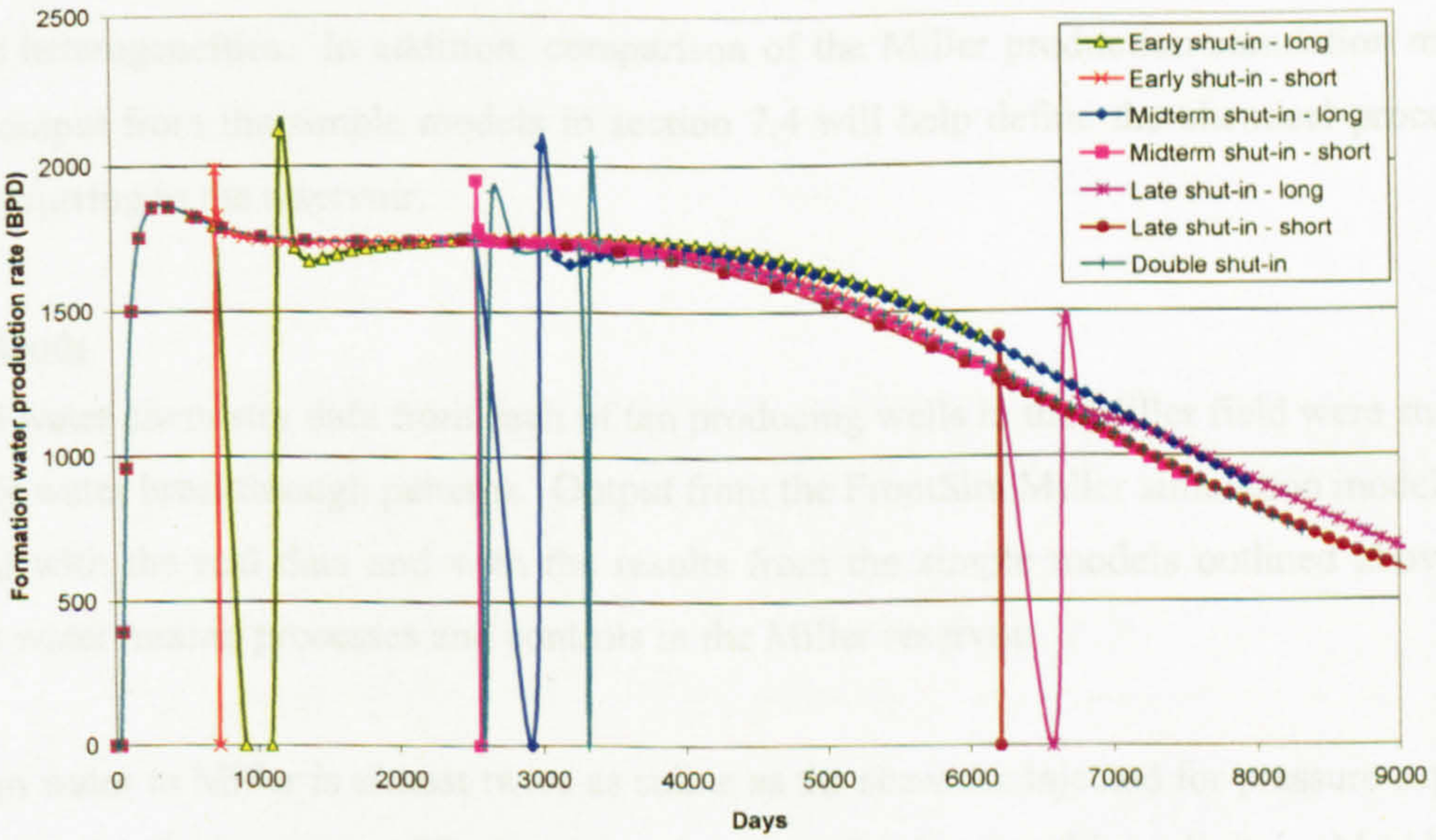

C

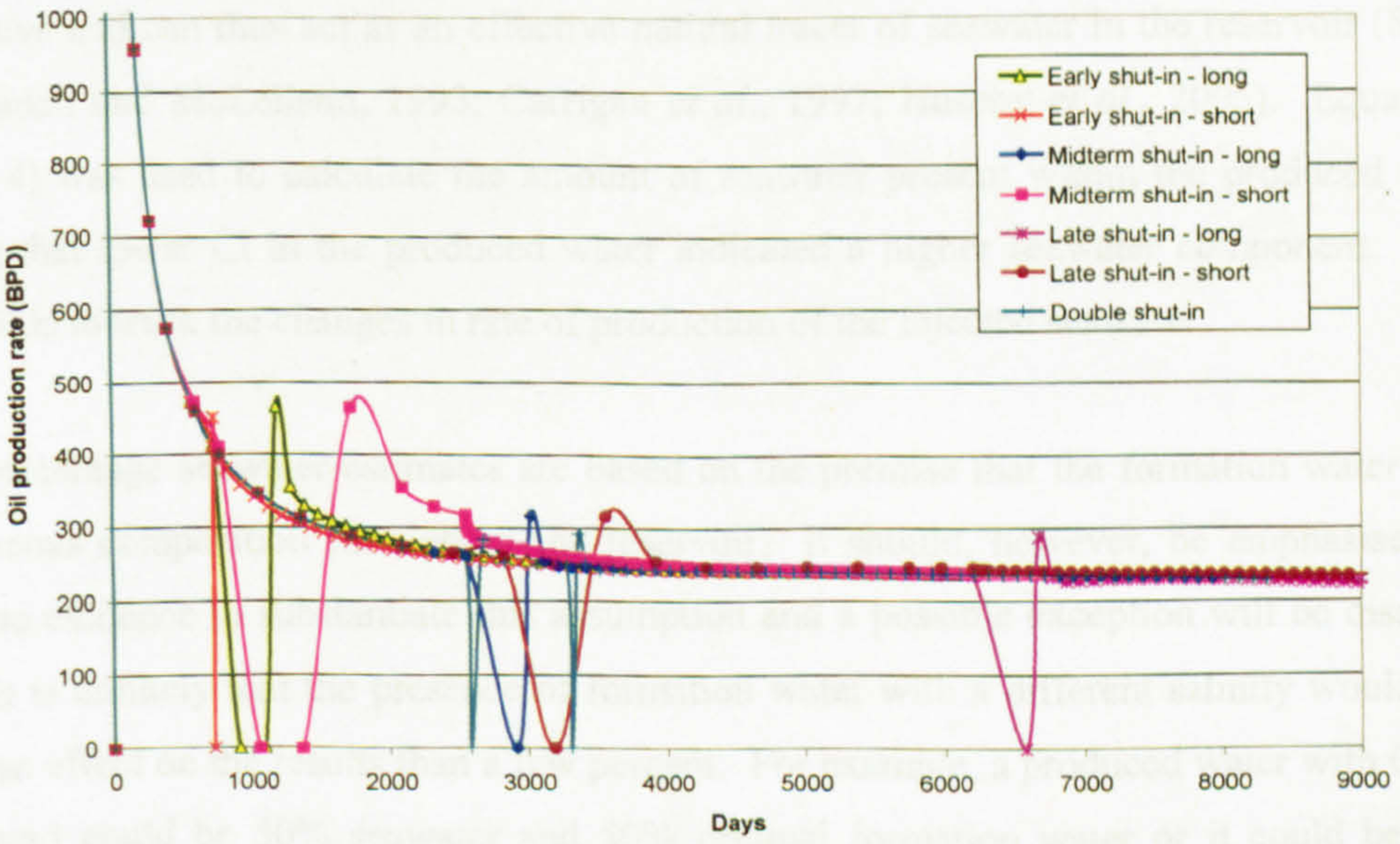

Figure 7.15. Production rates of: A) injected water, B) formation water and C) oil for the same reservoir experiencing different management strategies

7.6 Case Study: Miller, North Sea

The Miller Field in the North Sea has yielded a substantial dataset through years of regular, almost daily, water sampling (e.g. Chapter 4). The extensive dataset has the potential to provide information useful in defining fluid flow regimes and water mixing mechanisms, determining the usefulness and applicability of production simulation models, and reservoir characterisation. One application that would be particularly useful for designing waterfloods is the use of water data simulation to help identify different types of water mixing i.e. by gradual mixing or connate water banking.

Detailed analysis of the Miller production data will provide information about how the formation water responds physically to the injected water. Studying observed production rates will allow identification of variation in water mixing styles in the reservoir and highlight important heterogeneities. In addition, comparison of the Miller production simulation model with the output from the simple models in section 7.4 will help define the chemical processes that are occurring in the reservoir.

7.6.1 Methods

Produced water chemistry data from each of ten producing wells in the Miller field were studied to identify water breakthrough patterns. Output from the FrontSim Miller simulation model was compared with the real data and with the results from the simple models outlined above, to constrain water mixing processes and controls in the Miller reservoir.

Formation water in Miller is almost twice as saline as the seawater injected for pressure support and enhanced oil recovery. The main anion contributing to this salinity, chloride, is conservative and can thus act as an effective natural tracer of seawater in the reservoir (Slentz, 1981; Braden and McLelland, 1993; Carrigan *et al.*, 1997; Huseby *et al.*, 2005). Equation 1 (Chapter 4) was used to calculate the amount of seawater present within the produced water, assuming that lower Cl in the produced water indicated a higher seawater component. Thus, was possible to track the changes in rate of production of the injected seawater.

All the percentage seawater estimates are based on the premise that the formation water had a homogeneous composition throughout the reservoir. It should, however, be emphasised that there is no evidence to substantiate this assumption and a possible exception will be discussed below. It is unlikely that the presence of formation water with a different salinity would have more of an effect on the results than a few percent. For example, a produced water with Cl of ~ 30,000 mg/l could be 50% seawater and 50% original formation water or it could be some combination of seawater with two different formation waters, or 100% different formation

water. The additional formation water would have to have a salinity close to seawater (~20,000 mg/l) to invalidate the model completely; if it had only 30,000 mg/l Cl, then any produced water with less than 30,000 mg/l would still be exhibiting some seawater influence. In the example given above, the maximum uncertainty would be 50%, which is substantial, but not enough to render the model obsolete.

7.6.2 Results

First oil was produced in 1992, however the majority of the data relating to rates and amounts of hydrocarbons and water produced dates only as far back as 1995. Thus, the following results apply mostly to changes occurring in the field between 1995 and January 2004.

7.6.2.1 *Water incursion patterns*

Five different patterns of water incursion into the reservoir were identified and the ten wells could be divided among these groups accordingly (Figure 7.16). The behaviour of the wells in each group is discussed below. Figure 7.17 is a map of the Miller field, including the relative positions of all the producing wells.

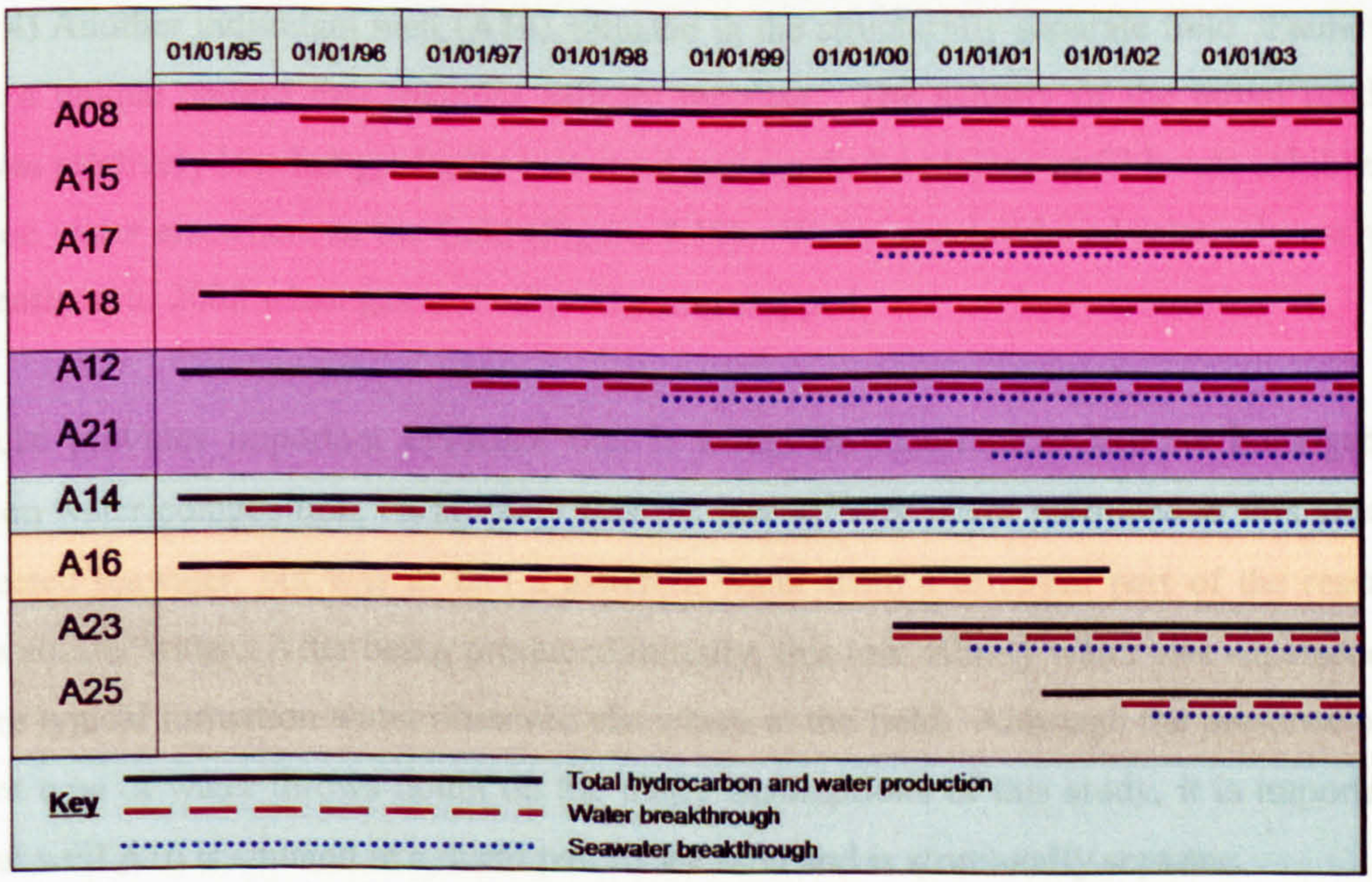

Figure 7.16. Providing an overview of the production information of each of the main ten wells studied. Each line (solid, dashed or dotted) begins when production starts and ends if and when production ceases.

Group 1) Four wells (**A08, A15, A17** and **A18**) appear to have produced only a small amount of water and experienced little seawater breakthrough. The concentrations of chloride and

sulphate in the produced water remained consistently high and low respectively. Well A17 showed evidence for slight seawater incursion, but this did not exceed 27% of the water produced.

Group 2) Two of the ten wells (**A12** and **A21**) showed a slightly greater seawater component overall and appeared to show a gradual increase and decrease in the amounts of sulphate and chloride respectively. This indicates progressive mixing of a high-sulphate, low-chloride water (seawater) with a low-sulphate, high-chloride water (formation water) over time. These wells started producing at the same time as the previous four, yet behave slightly differently. Water breakthrough at A12 occurred relatively early (1998) and generally had a seawater component of between 25 and 50%. Breakthrough at A21 occurred around two years later and the transition to very large seawater components was rather more rapid.

Group 3) A single well (**A14**) showed a much more rapid transition to a high seawater component. This well is situated some distance (about 2.5km in either case) from the two main groups of wells and started to produce water fairly early in its life (Figure 7.18). The apparent seawater component was consistently above 40% (where measured).

Group 4) Another individual well (**A16**), situated in the structurally separate field "Panhandle" showed a unique pattern that includes salinity increase. The salinity of the initial produced water was relatively low but gradually increased and reached a plateau at Cl levels exhibited by formation water elsewhere in the field (Figure 7.19). Water was produced relatively early and consistently until 2002 when gas and oil production stopped.

Well A16 provides important evidence that it would be incorrect to assume homogeneous formation water composition. It is likely that the low salinity water produced in this area was not injected seawater, but was in fact a different water from a different part of the reservoir, perhaps aquifer water. After being produced initially, this low salinity water was superseded by the more typical formation water observed elsewhere in the field. Although the presence of this different type of water throws doubt on the major assumptions of this study, it is important to note that well A16 is situated in a distal part of the field and is structurally separate.

Group 5) The final two wells (**A23** and **A25**) started producing late in the life of the field and this was reflected in the rapid onset of water production and the consistently high seawater component in the produced water. Mixed water was produced from these wells from the start of production in 2001 and 2002 respectively

January
2002

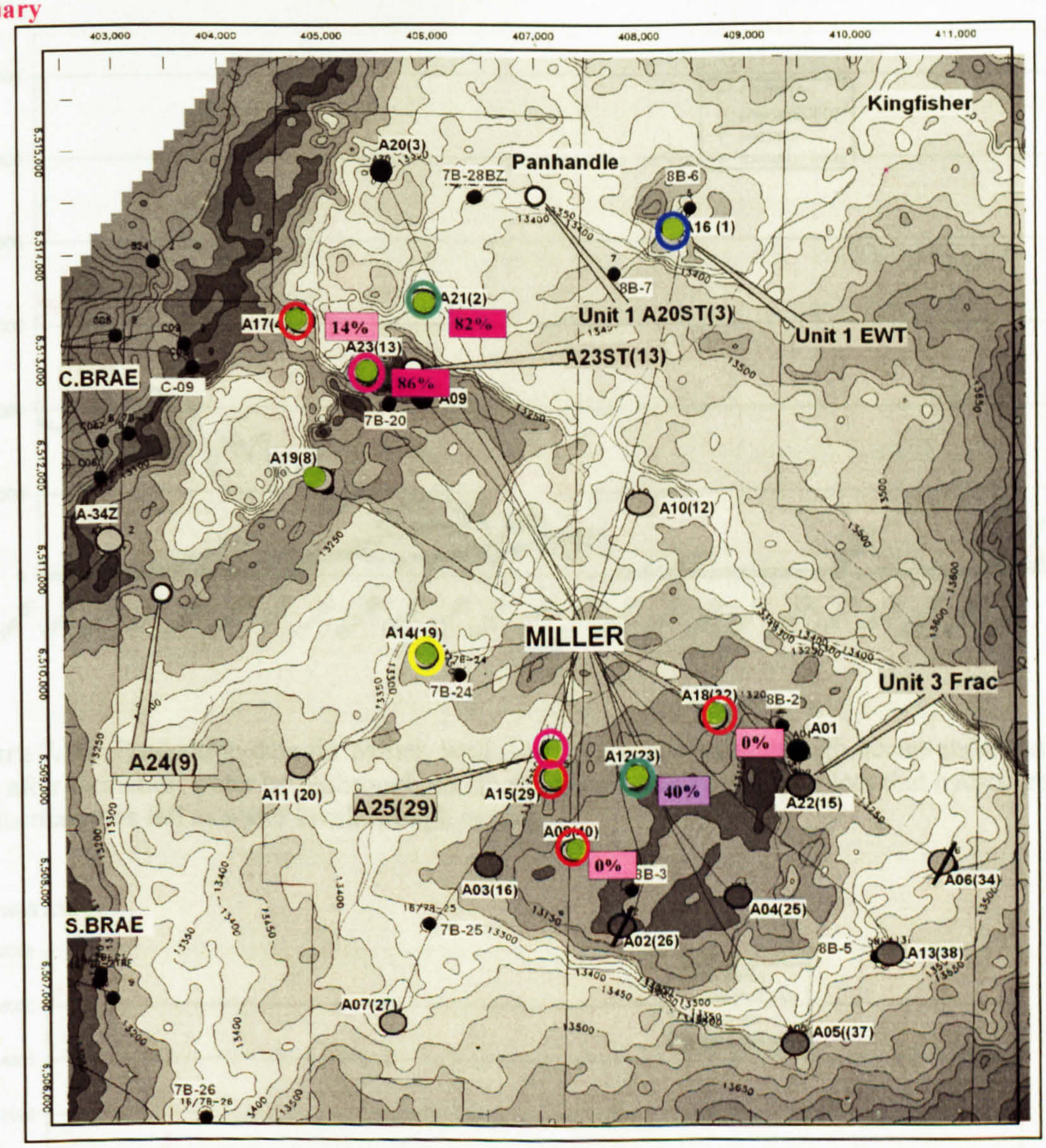

MILLER FIELD STATUS

Top Reservoir Depth Map
(CI 25 Ft)

0%
25%
50%
75%

Percentage Seawater incursion

Little water breakthrough, no seawater

Seawater component, gradual fluid mixing

Seawater component, more rapid fluid mixing

Salinity increases (?decreasing seawater)

Mixing prior to water production

Exploration/Appraisal well

Abandoned Well

Producer

Water injector

AGI Injector

CRI – Cuttings injection

Suspended well

Drill Option

Figure 7.17. Top reservoir depth map of the Miller Field showing the locations of the main wells (injectors and producers) and highlighting the different patterns of seawater incursion over the field.

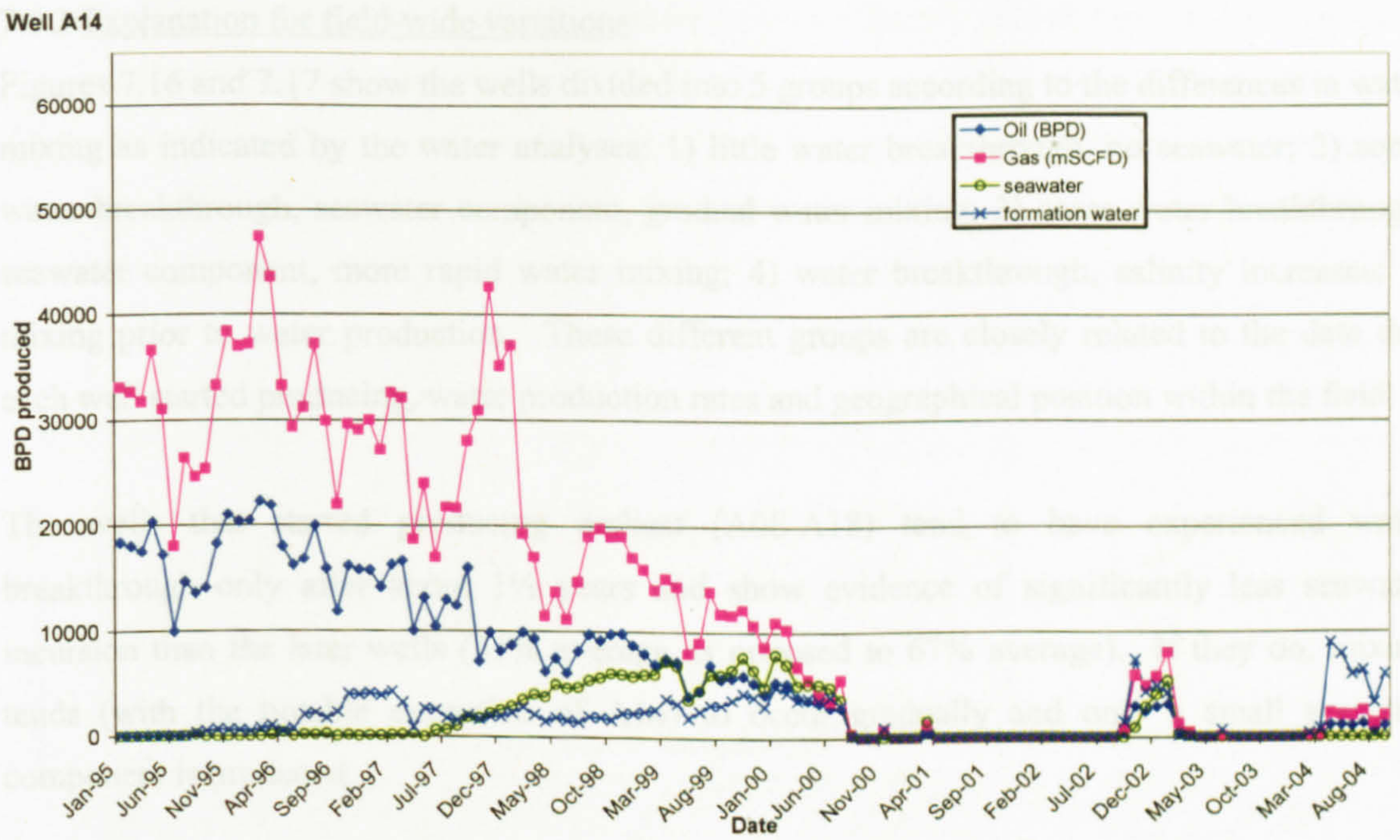

Figure 7.18. Production data for Miller, well A14. Seawater breakthrough occurs more than a year after formation water breakthrough and increases relatively rapidly. Note that hydrocarbon production rates fall as water breakthrough occurs.

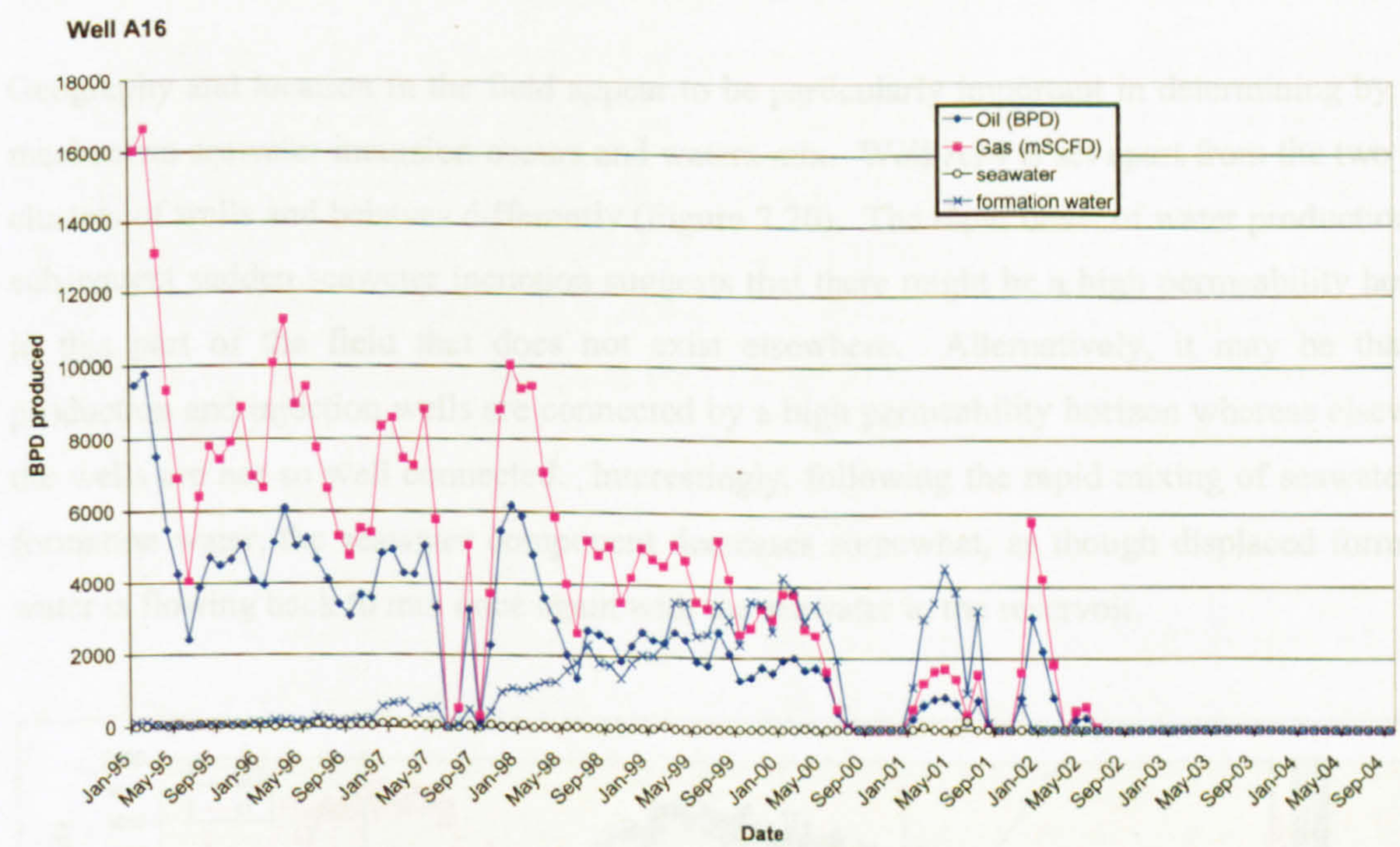

Figure 7.19. Production data for Miller, well A16. Seawater breakthrough never really occurs and formation water breakthrough occurs very late in the life of the well. Note that hydrocarbon production rates fall as water breakthrough occurs. Note different scale to Figure 7.14.

7.6.3 Explanation for field-wide variations

Figures 7.16 and 7.17 show the wells divided into 5 groups according to the differences in water mixing as indicated by the water analyses: 1) little water breakthrough, no seawater; 2) some water breakthrough, seawater component, gradual water mixing; 3) some water breakthrough, seawater component, more rapid water mixing; 4) water breakthrough, salinity increases; 5) mixing prior to water production. These different groups are closely related to the date that each well started producing, water production rates and geographical position within the field.

The wells that started producing earliest (A08-A18) tend to have experienced water breakthrough only after about 1½ years and show evidence of significantly less seawater incursion than the later wells (41% average as opposed to 67% average). If they do, mixing tends (with the notable exception of A14) to occur gradually and only a small seawater component is produced.

Significantly, the younger wells (A23 and A25) both exhibit considerably higher seawater concentrations, possibly because the seawater will already have mixed with the formation water in the reservoir prior to production. It is also clear that increased seawater incursion relates to increased overall water production rates and that at this time gas and oil production rates fall.

Geography and location in the field appear to be particularly important in determining by what mechanism seawater incursion occurs and waters mix. Well A14 is set apart from the two main clusters of wells and behaves differently (Figure 7.20). The rapid onset of water production and subsequent sudden seawater incursion suggests that there might be a high permeability horizon in this part of the field that does not exist elsewhere. Alternatively, it may be that the production and injection wells are connected by a high permeability horizon whereas elsewhere the wells are not so well connected. Interestingly, following the rapid mixing of seawater and formation water, the seawater component decreases somewhat, as though displaced formation water is flowing back to mix once again with the seawater in the reservoir.

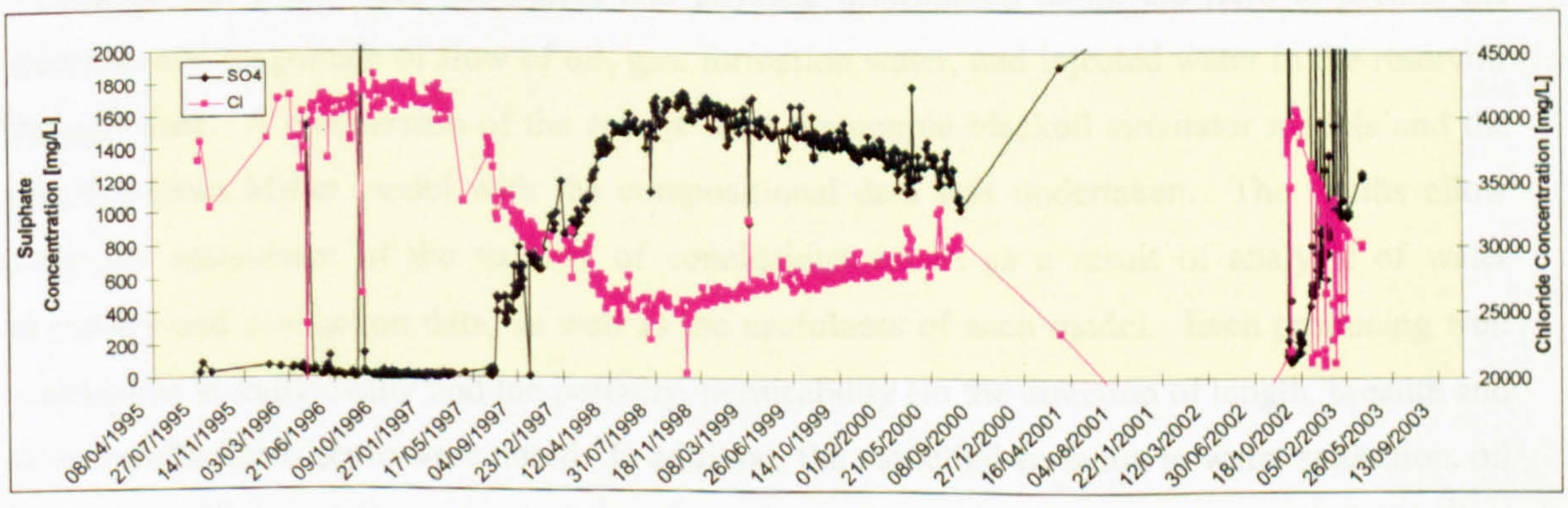

Figure 7.20. Variation in sulphate and chloride concentration in produced water over time for well A14, note rapid decrease in chloride followed by gradual increase (refer to Figure 7.15).

The salinity increase of well A16 is also interesting because, situated at some distance from the main field, it behaves in an entirely different way from any other well (Figure 7.21). It is possible that some mixing with seawater occurred before production started and then the supply of seawater declined, or that part of the produced water is from a different aquifer which may not be laterally extensive over the whole field.

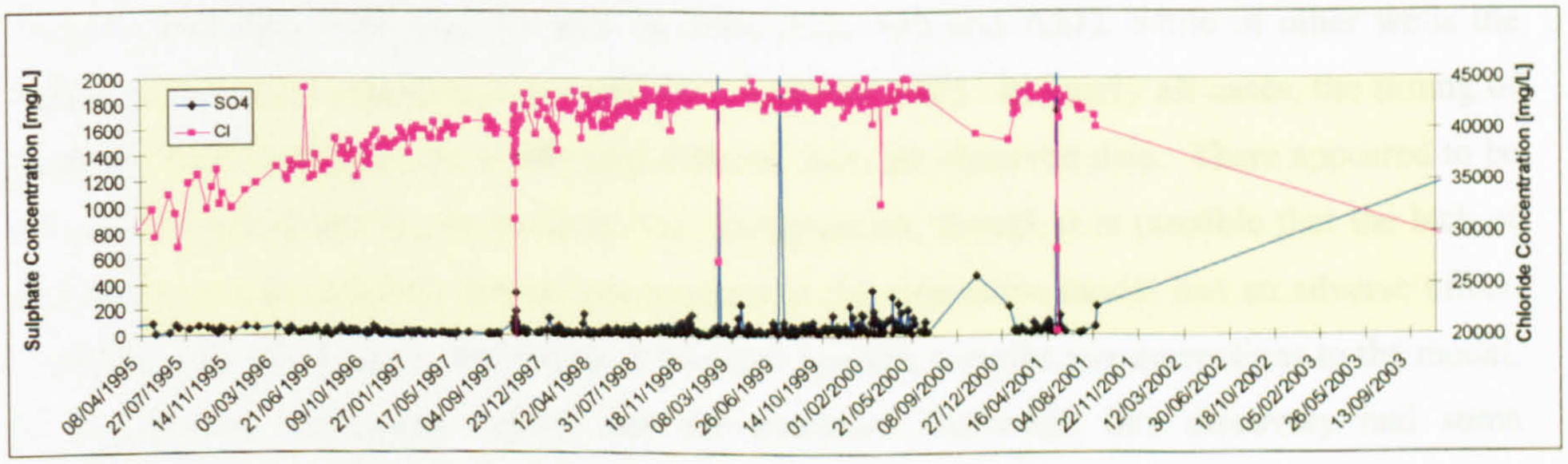

Figure 7.21. Variation in sulphate and chloride concentration in produced water over time for well A16, note gradual increase in chloride

In addition to these localised examples of geographical influence, it is possible to identify a larger trend that fits in with the geological structure of the area. The wells that tend not to be subject to significant seawater incursion are all situated in topographic lows and are separated from each other and the injectors by other topographic features. The wells that show more seawater influence sit mostly on a NW-SE trending line through the centre of the field and are generally on topographic highs. It is possible that these wells bear the brunt of the seawater influence because seawater is less dense than formation water and tends to fill the higher areas of the field first.

7.6.4 Production simulation model

The FrontSim production simulation model is a streamline model, which differs from a blackoil simulation but which uses geological and physical information about the field to predict the direction and magnitude of flow of oil, gas, formation water, and injected water in the reservoir through time. A comparison of the results from the simple blackoil simulator models and the real FrontSim Miller model with the compositional data was undertaken. The results allow objective assessment of the validity of conclusions drawn as a result of analysis of water chemistry and production data, as well as the usefulness of each model. Each producing well was looked at individually and the porosity, permeability (in the direction of length, breadth and depth) and relative depth were noted. In addition, the modelled variation in water saturation, oil saturation and seawater concentration over time were examined and compared with the data gathered from the producing field.

The analyses were undertaken on the understanding that the model had been fully history-matched. However, part way through the study, some further history-matching tests were carried out. It was discovered that, although the oil and water production rates predicted by the model matched very well with the observed data, the same could not be said for seawater (injected water) concentration and production rates (for example, Figure 7.22 and Figure 7.23).

In some wells the model predicted that less seawater would be produced than was actually the case, for example, well A14 (as well as A08, A12, A15 and A21), while in other wells the model predicted the opposite (e.g. well A17, A18 and A25). In nearly all cases, the timing of seawater breakthrough in the model also differed from the observed data. There appeared to be no simple explanation for, or trend in, the discrepancies, though it is possible that the lack of any means to take capillary forces into account in the streamline model had an adverse effect. Unfortunately, due to time constraints, it was not possible to make any corrections to the model, or to add any correction factors into the analysis. Although this discovery had some implications for the results of the model analysis, most of the results enabled exciting conclusions to be drawn. Despite the quantitative discrepancies, the general trends produced by the model compared favourably with what was observed in the real situation and provided some useful information and explanations for patterns of seawater incursion.

7.6.4.1 *Qualitative model results: comparisons with real data*

Injectors. The model, which has been history-matched to accurately reflect the real situation, provides additional information about injection wells. There are therefore no comparisons to be made. However, the relevant information relating to the injection wells can be summarised as follows. The Wells A5, A6 and A7 were the original injectors supporting the early producers, and these were gradually superseded by wells A10 and A11, which went on to provide pressure support for the greater proportion of the producing wells. The injectors are situated in deeper areas to allow the water to flow up-dip to the producers and the data show that the wells that experience more influence from seawater sit mostly on a NW-SE trending line through the centre of the field and are generally situated on structural highs.

Producers. The model predicted that the wells situated in the southern part of the field experienced little injected water breakthrough (that is until 2002, when the model ends). Water compositional data confirm that the wells in this area indeed do not experience large amounts of seawater incursion; however, the pattern is not at all homogeneous. Wells A08, A15 and A18 show no evidence of seawater incursion, rather than the ~20% predicted by the model. The real exception is A12 in which water breakthrough occurred relatively early (1998) and generally had a seawater component of between 25 and 50%. This suggests that there is an extra component of complexity/heterogeneity that the model cannot account for.

Situated on its own in the centre of the field, A14 was predicted to have relatively rapid water breakthrough following the rapid removal of oil from the reservoir, due to high permeability layers and direct influence from the two major injectors A10 and A11. The observed data shows a similar pattern, but seawater was predicted to breakthrough almost a year later by the model than actually occurred. The observed rapid increase of the proportion of injected water in the produced water, coupled with the comparative lack of mixing between the two waters suggested that this might be one well in the field that showed reasonable evidence for connate water banking. The model, however, provides no evidence of this type of behaviour and instead predicts that injected water breakthrough is gradual, implying mixing is occurring.

The northern wells were all predicted to be influenced more by injectors A10 and A11 and to experience water breakthrough and injected water incursion sooner in their lives than the southern wells. The model appears to include a higher permeability layer towards the north west of A10 causing wells A17 and A21 to have been directly and severely affected by the injected water from this well. It is observed that the northern wells do indeed experience water breakthrough relatively much earlier and the produced water generally does have a larger component of seawater. However, A17 experiences very little seawater incursion and it may be that a large proportion of the injected water from A10 is actually produced in A21 before it ever reaches A17.

The two wells that started producing late in the life of the field, A23 and A25, were predicted to be affected by injected water incursion almost immediately on commencement of production, which supports what is observed. The instantaneous production of seawater suggests that extensive mixing must have taken place in the reservoir prior to production, indicating that connate water banking is extremely unlikely to have occurred to any great extent in Miller.

A

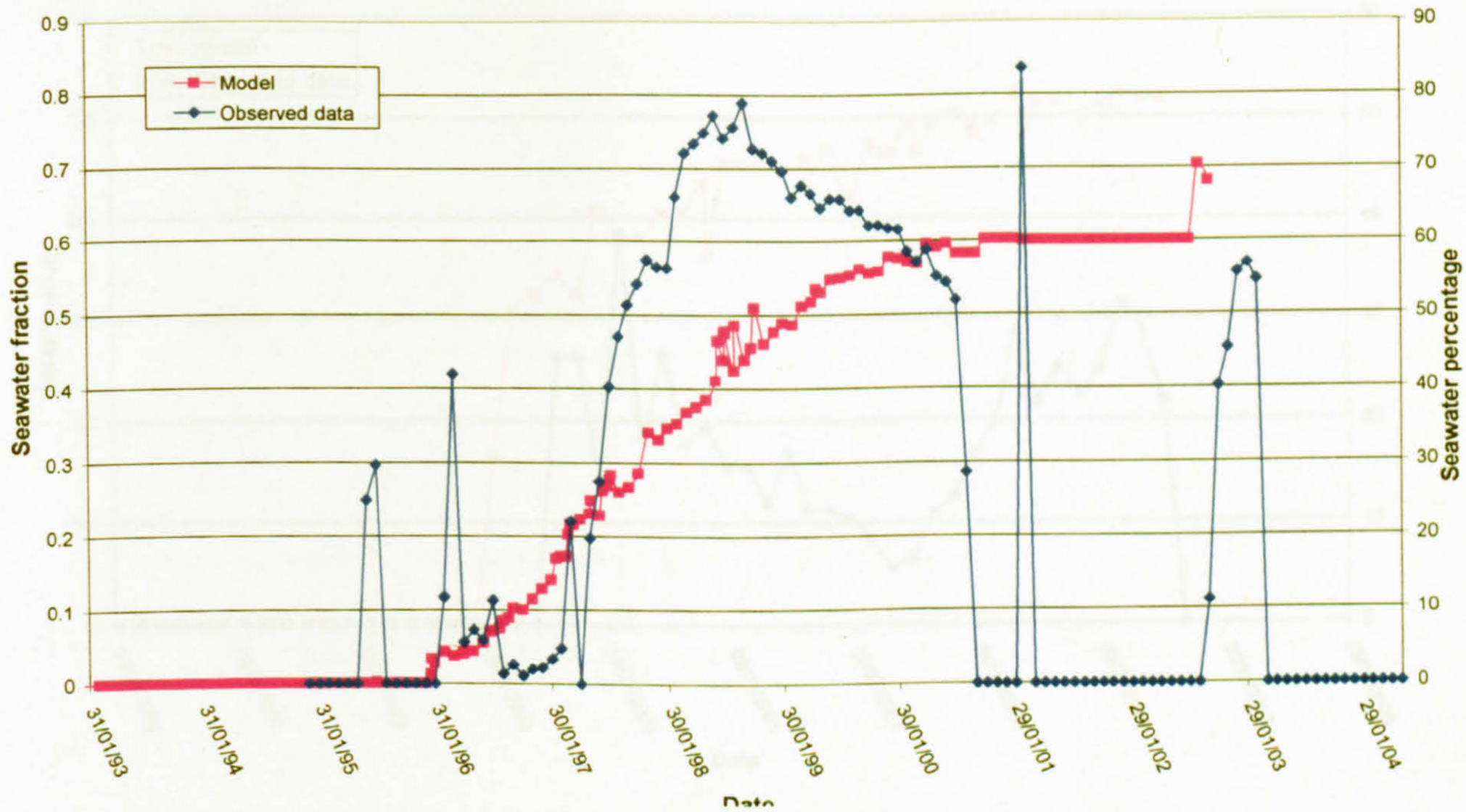

B

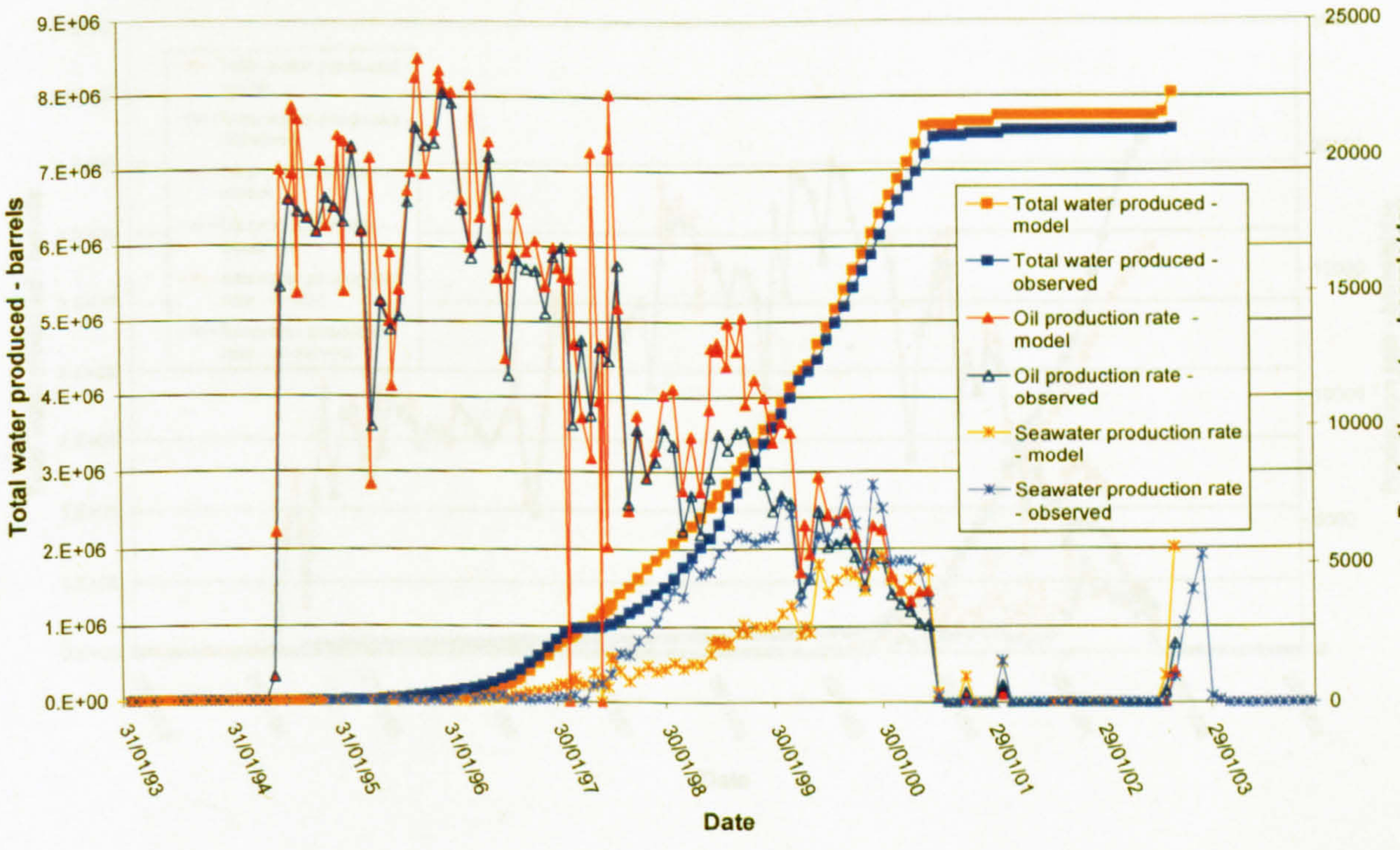

Figure 7.22. Comparisons between the model predictions and observed data for well A14: A) the seawater concentration in the produced water through time, as observed and predicted; B) total water produced, oil production rate and seawater production rate as predicted by the FrontSim model and as observed. Note that, for total water production and oil production rate the match between the predicted and the real data is very good, but that there is a large discrepancy for the seawater production rate.

A

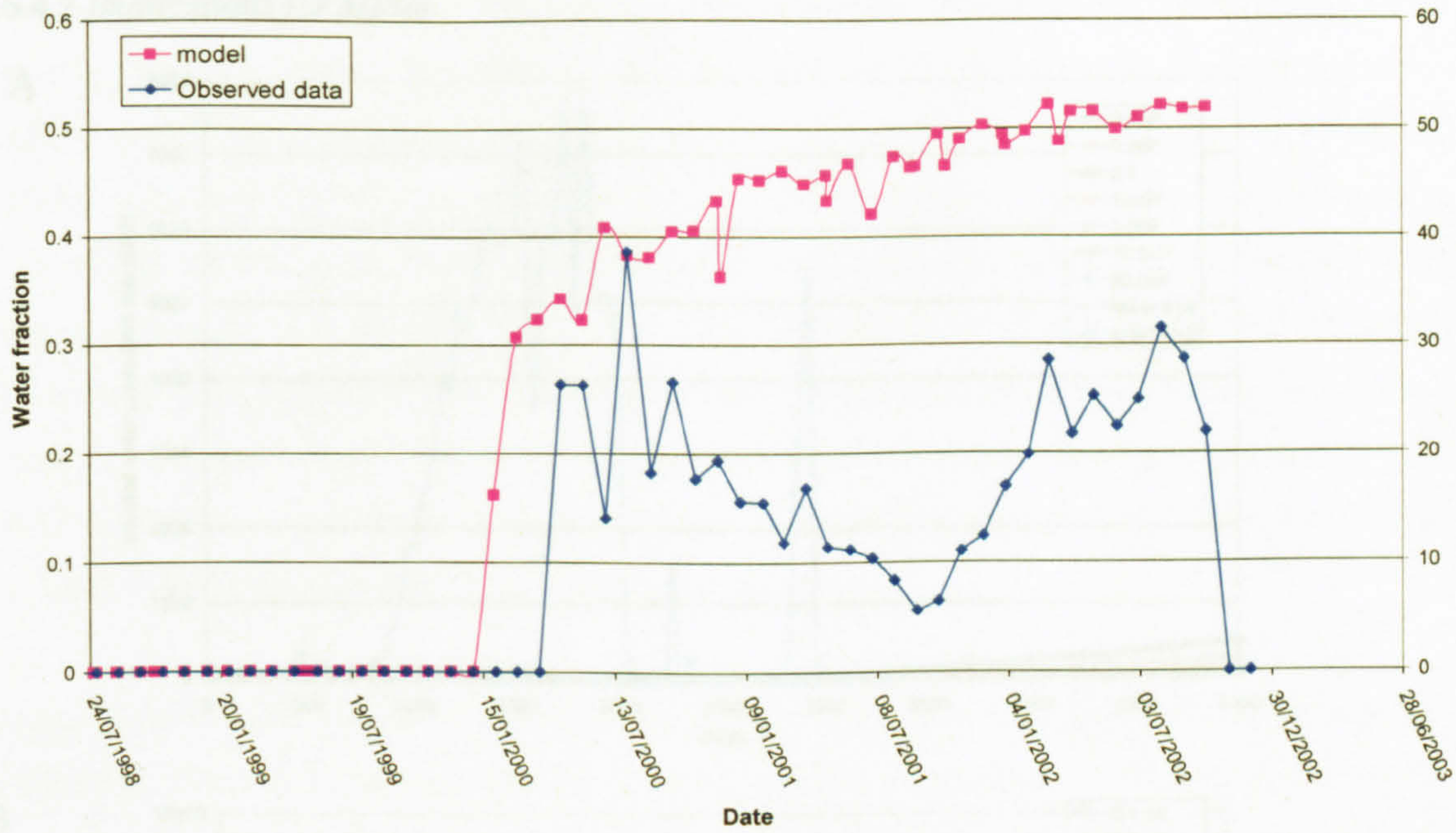

B

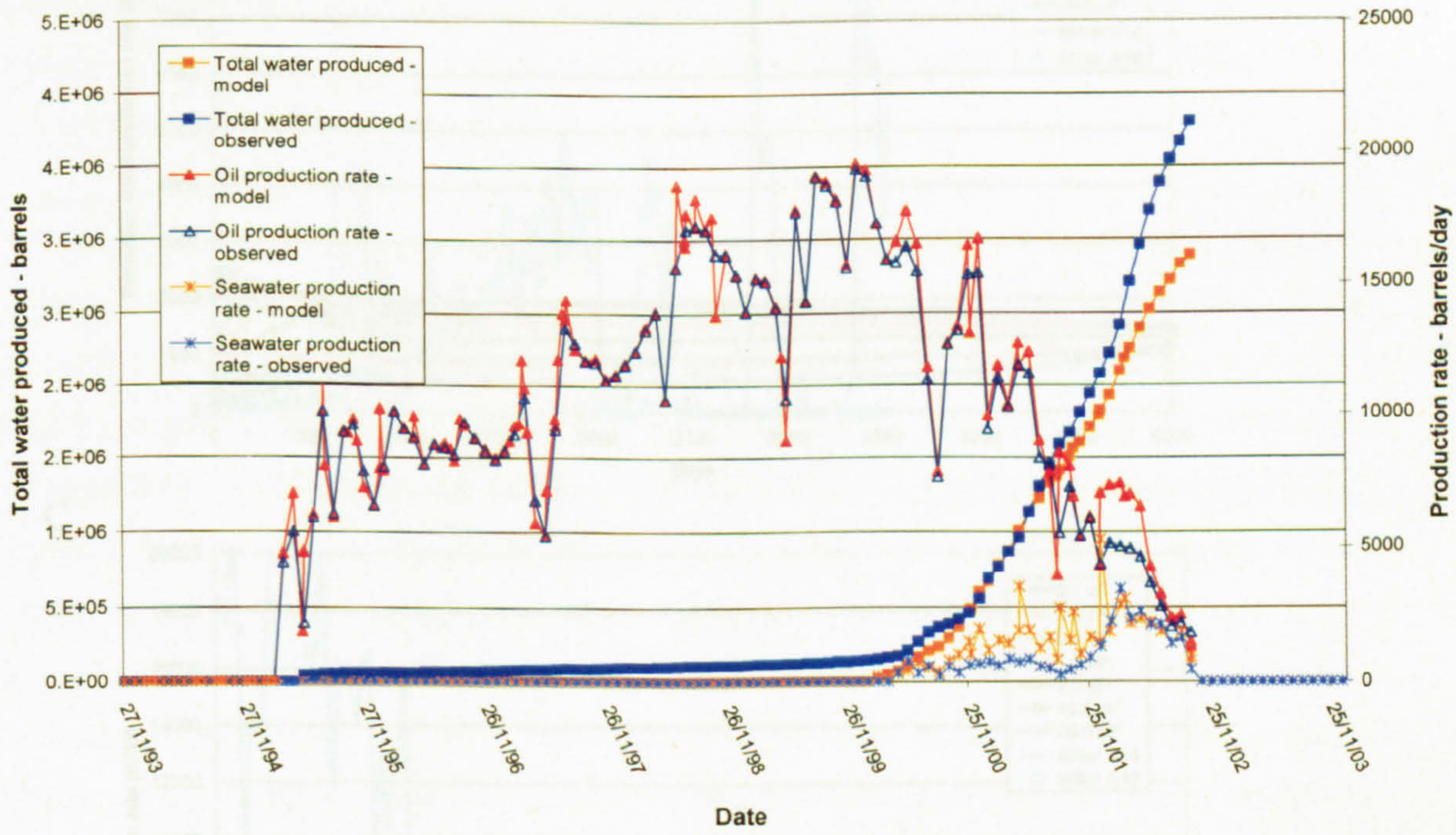

Figure 7.23. Comparisons between the model predictions and observed data for well A17: A) the seawater concentration in the produced water through time, as observed and predicted; B) total water produced, oil production rate and seawater production rate as predicted by the FrontSim model and as observed. Note that, for total water production and oil production rate the match between the predicted and the real data is very good, but that there is a large discrepancy for the seawater production rate.

7.6.4.2 *Implications for Miller*

A

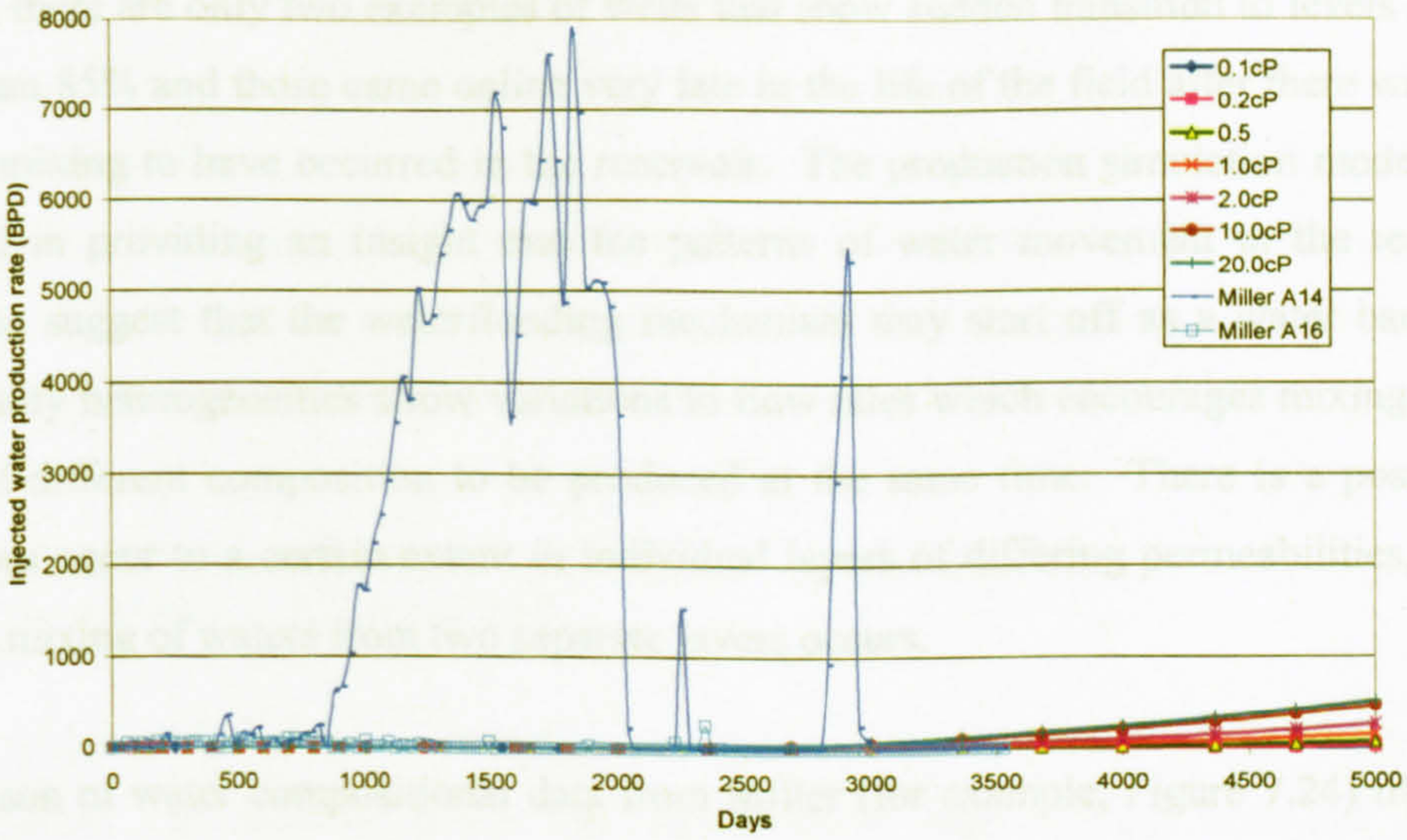

B

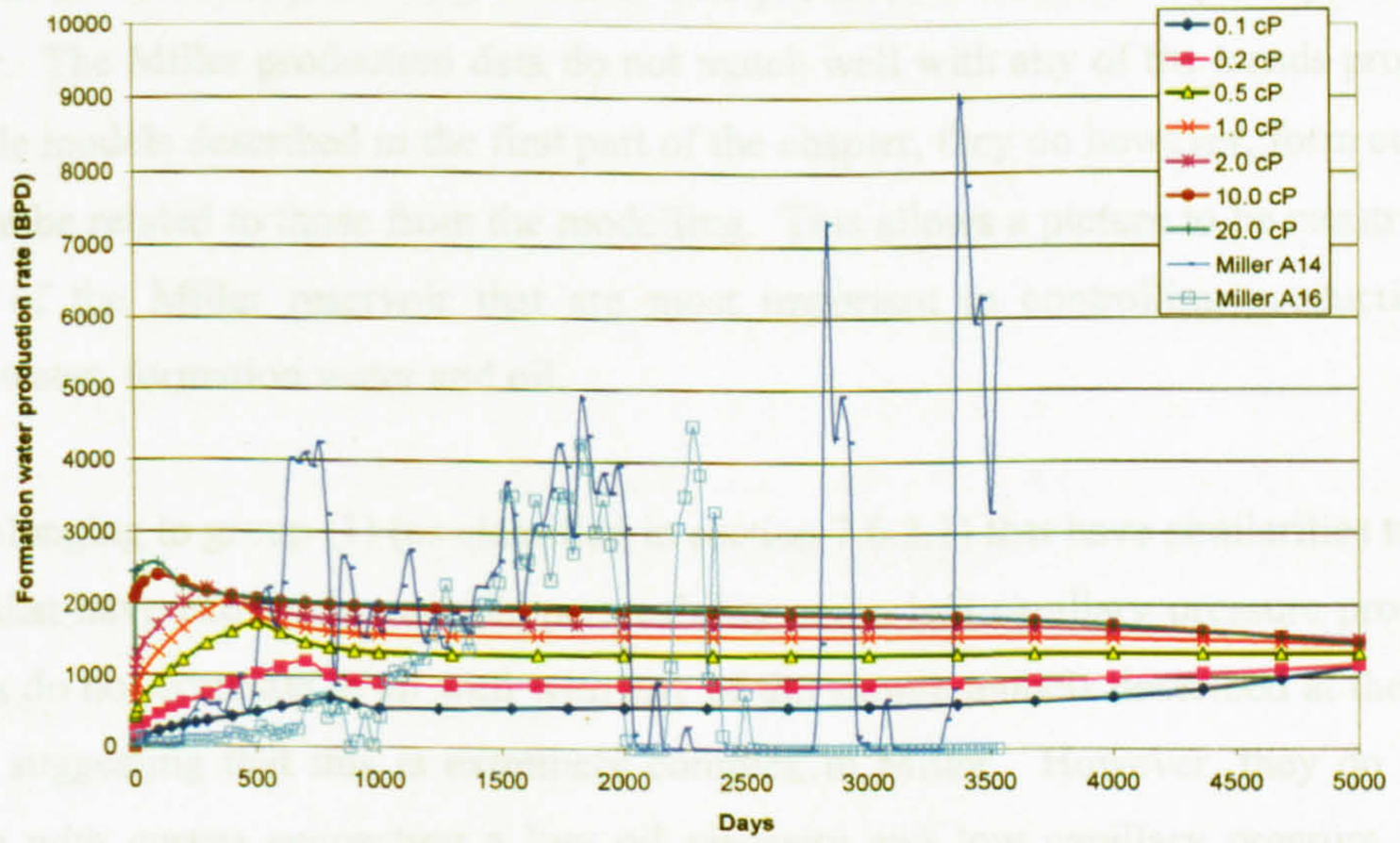

C

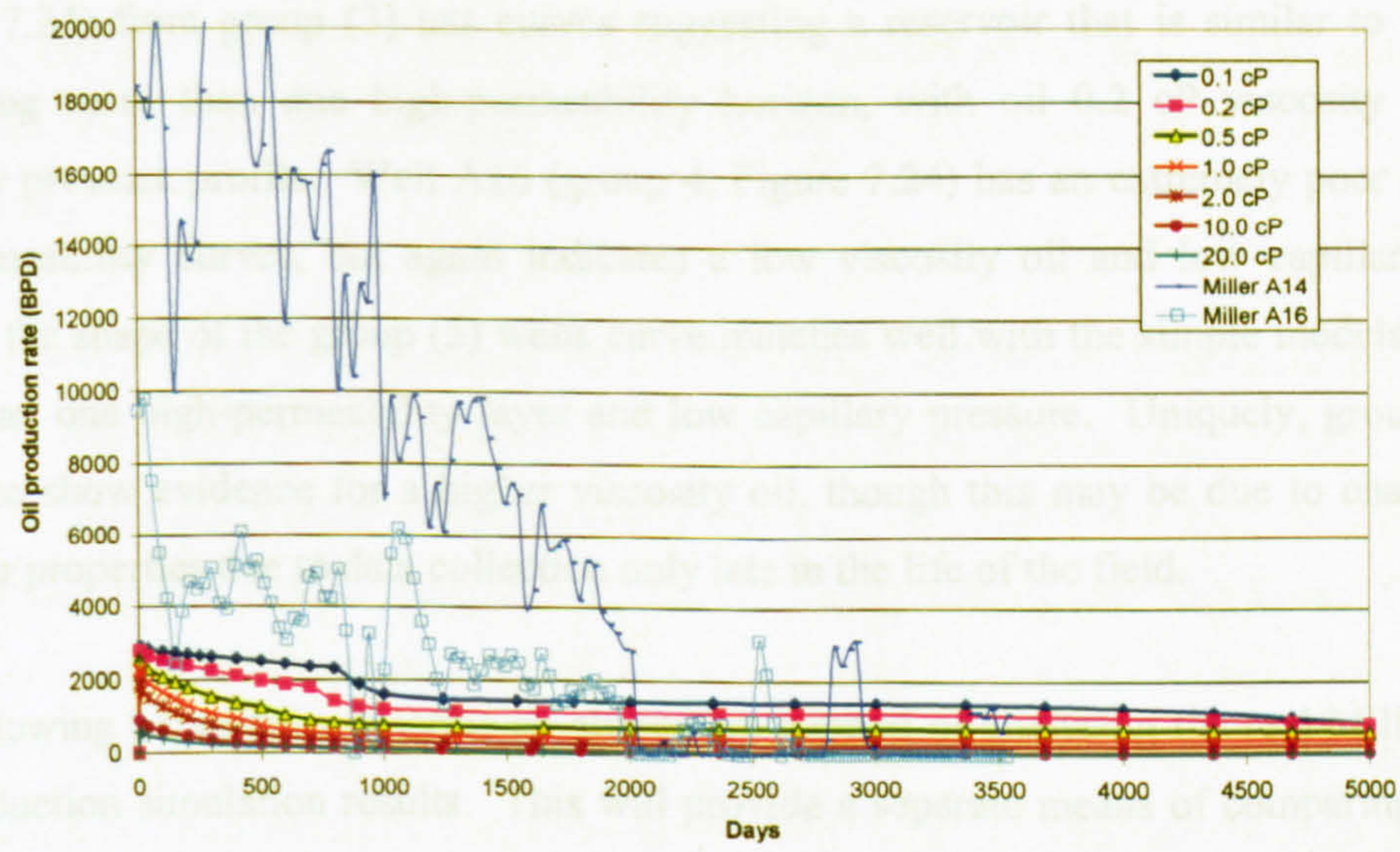

Figure 7.24. Illustrating how real production data from the Miller oil field relate to trends predicted by the Eclipse production simulator, using the example of effect of variable oil viscosity on A) injected water production rate, B) formation water production rate and C) oil production rate.

Water chemistry data suggests that mixing is an important process in the Miller Field. For example, there are only two examples of wells that show sudden transition to levels of seawater higher than 85% and those came online very late in the life of the field after there was plenty of time for mixing to have occurred in the reservoir. The production simulation model proved to be useful in providing an insight into the patterns of water movement in the reservoir and seemed to suggest that the waterflooding mechanism may start off as a water bank, but that permeability heterogeneities allow variations in flow rates which encourages mixing and allows waters of different composition to be produced at the same time. There is a possibility that CWB does occur to a certain extent in individual layers of differing permeabilities, but that at the well, mixing of waters from two separate layers occurs.

Comparison of water compositional data from Miller (for example, Figure 7.24) illustrates the difficulties involved in producing a model that produces a reasonable portrayal of a specific reservoir. The Miller production data do not match well with any of the trends produced from the simple models described in the first part of the chapter, they do however, form curves whose shape can be related to those from the modelling. This allows a picture to be constructed of the features of the Miller reservoir that are most important in controlling production rates of injected water, formation water and oil.

Wells belonging to group (1) (as classified in section 7.6.2.1) that have similarities to the simple models that have extremely variable permeability and a low capillary pressure profile. Group (2) wells do not correlate at all well with any of the simple models described at the start of the chapter, suggesting that this is extremely complex in Miller. However, they do consistently correlate with curves suggesting a low oil viscosity and low capillary pressure. Well A14 (Figure 7.24) from group (3) has curves suggesting a reservoir that is similar to the models containing more than one high-permeability horizon, with oil 0.2 cP viscosity and a low capillary pressure profile. Well A16 (group 4, Figure 7.24) has an extremely poor match with the permeability curves, but again indicates a low viscosity oil and low capillary pressure. Finally, the shape of the group (5) wells curve matches well with the simple models containing more than one high-permeability layer and low capillary pressure. Uniquely, group (5) wells appear to show evidence for a higher viscosity oil, though this may be due to changes in the reservoir properties due to data collection only late in the life of the field.

The following paragraphs describe an alternative method of analysing the real Miller data and the production simulation results. This will provide a separate means of comparing predictive results with real ones to determine the accuracy of the models as well as explaining the trends shown in the real data. A number of parameters that characterise the simulation output are

compared with input parameters for the Miller data, the Miller FrontSim model and the Eclipse models.

Average permeability/oil viscosity (k/μ) is a measure of the ease with which fluids flow through the reservoir, a high value indicating relative ease of flow and a low value indicating constricted flow. The Dykstra-Parsons coefficient is a measure of the heterogeneity of a series of values, in this case, the permeability variation in the reservoir. The value is calculated by

$$Vdp = \frac{\text{(permeability at } 50^{th} \text{ percentile} - \text{permeability at } 84^{th} \text{ percentile)}}{\text{permeability at } 50^{th} \text{ percentile}}$$

with a value of 0 being completely homogeneous and a value of 1 being completely heterogeneous. In order to assess the importance of ease of fluid flow and permeability heterogeneity on the waterflood and reservoir management, average permeability (mD)/oil viscosity (cP) and the Dykstra-Parsons coefficient were plotted against: time to water breakthrough (days or pore volumes injected), time to injected water breakthrough (pore volumes injected), time to 50% watercut (pore volumes injected), initial watercut value (%) and the rate of increase of injected water proportion (stb/day/day). The amount of time taken for changes to occur within a petroleum system is dependent on the size of the reservoir and the rate at which water is injected into it. Therefore, the number of pore volumes of water injected is used as a measure of time wherever possible to eliminate uncertainty between different datasets. However, in some cases change may occur with no injection and in these situations, measuring time in days is an adequate alternative.

Figure 7.25 shows the time to water breakthrough in days and pore volumes with respect to k/μ and Vdp, and indicates that water takes longer to breakthrough in reservoirs in which oil flows easily but that water breakthrough occurs sooner in reservoirs with very heterogeneous permeability.

When injected water is considered separately, some differences become apparent in that reservoirs with high k/μ tend to allow faster injected water breakthrough (Figure 7.26). It is possible that this discrepancy arises because a reservoir with high k/μ is extremely permeable to oil. This allows the hydrocarbons to reach the producing well rapidly with little influence from formation water. However, by the time the water reaches the well, the relatively unrestricted flow of injected water will have reached the formation water and mixed. In addition, a reservoir with extremely heterogeneous permeability is likely to have a number of high permeability horizons, allowing fast transport of water and injected water to the producing well.

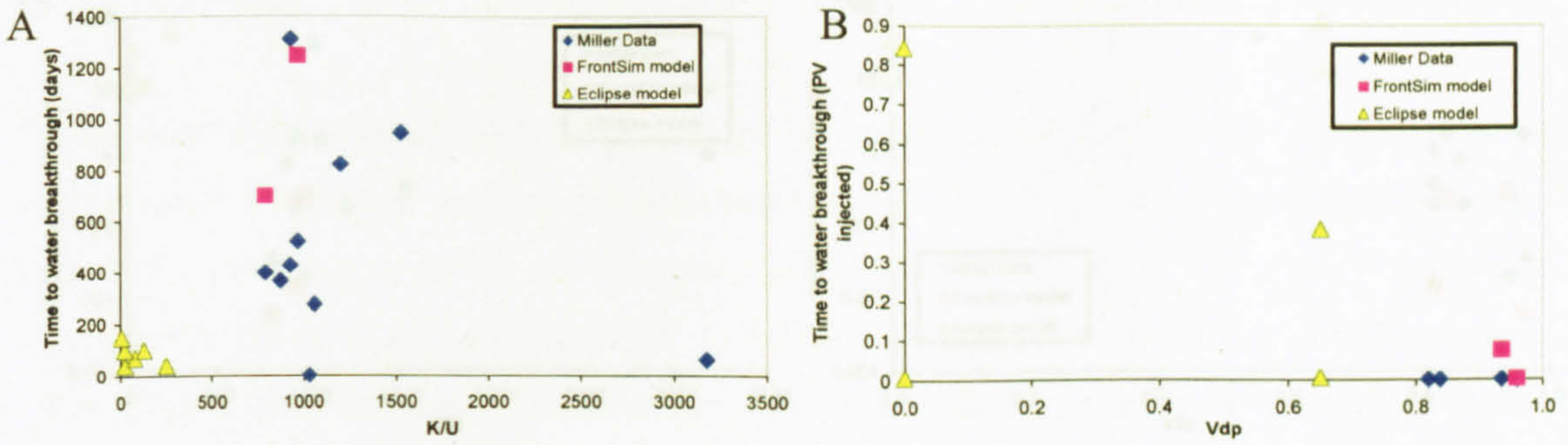

Figure 7.25. Time, in either days or pore volumes injected, to water breakthrough as a function of a) K/U and b) Vdp

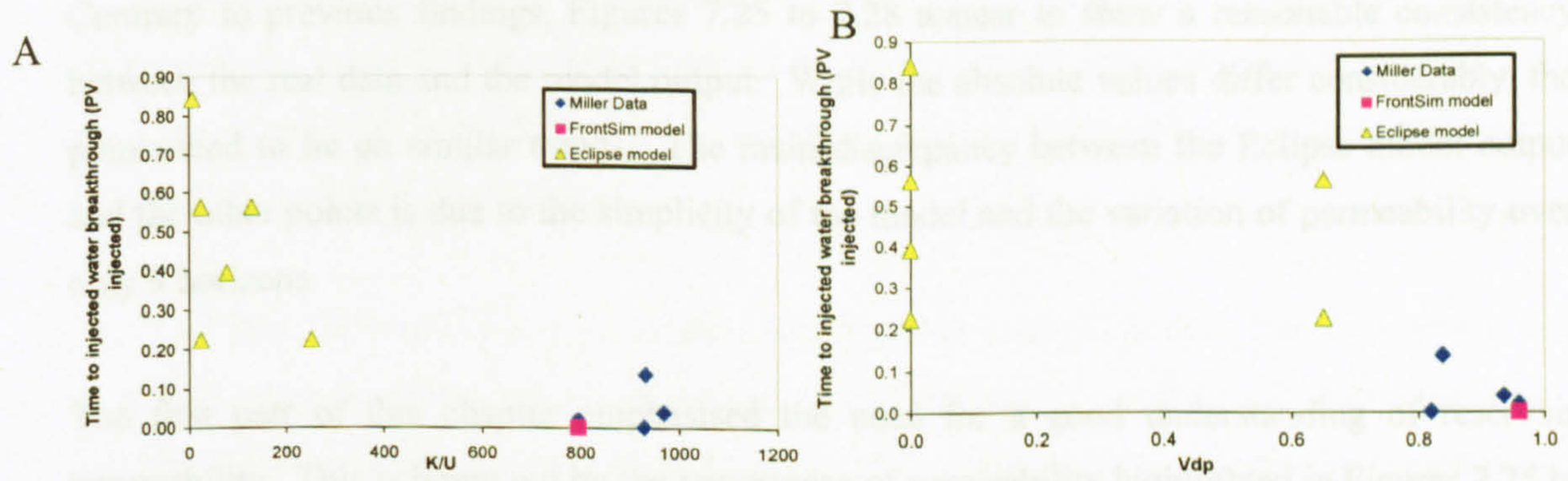

Figure 7.26. Time, in pore volumes injected, to injected water breakthrough as a function of a) k/μ and b) Vdp

The amount of time until 50% water cut is reached is a measure of how much influence water breakthrough has on the system. For example, if a well experiences rapid water breakthrough with a slow progression to 50% watercut, this may be more manageable than a well with slower water breakthrough but a very rapid progression to high water production. Figure 7.27 illustrates that generally the greater the ease of flow through the reservoir, the less time taken to 50% watercut.

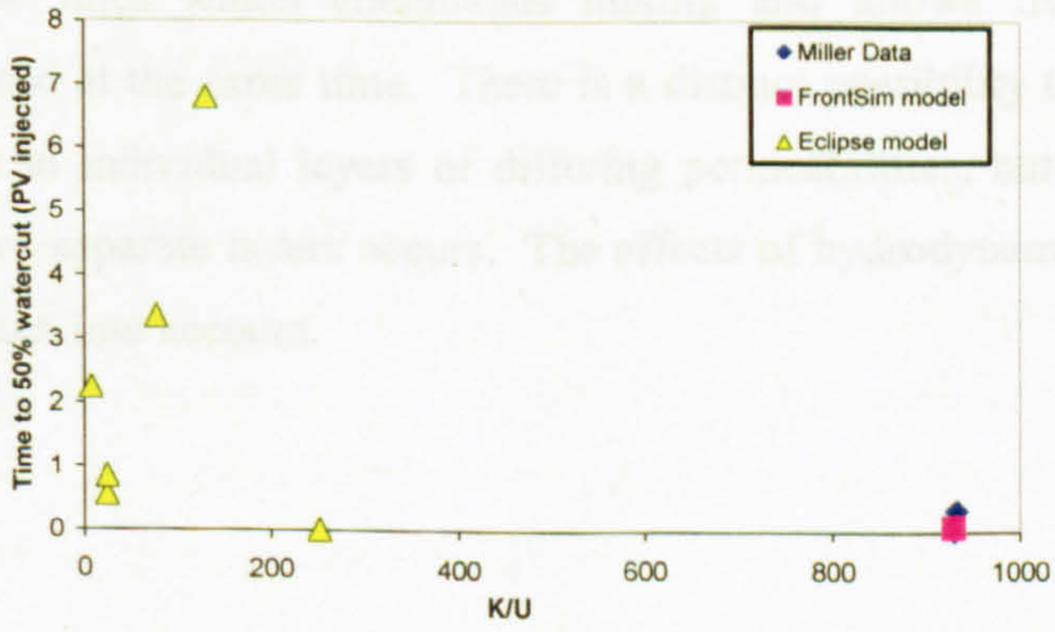

Figure 7.27. Time, in pore volumes injected, to 50% watercut as a function of k/μ

The size of the initial watercut is also important, a smaller percentage obviously being more desirable, and while the k/μ value appears to have little influence over this parameter, the more heterogeneous the reservoir, the smaller the initial watercut is likely to be.

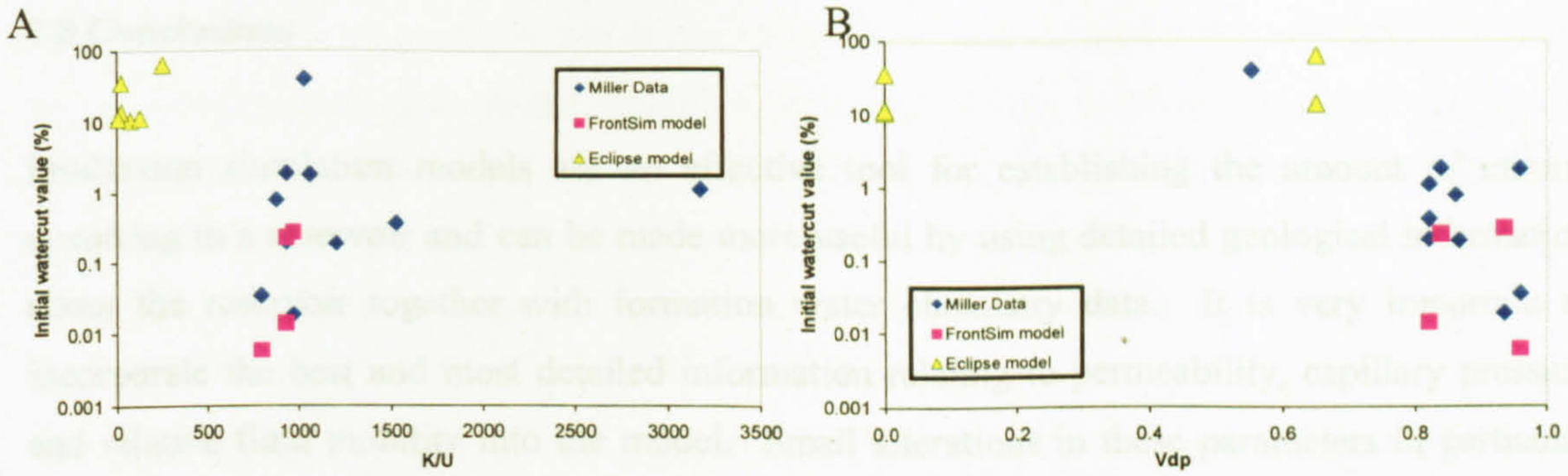

Figure 7.28. Initial watercut value as a function of a) k/μ or b) Vdp

Contrary to previous findings, Figures 7.25 to 7.28 appear to show a reasonable consistency between the real data and the model output. While the absolute values differ considerably, the points tend to lie on similar trends. The main discrepancy between the Eclipse model output and the other points is due to the simplicity of the model and the variation of permeability over only 9 horizons

The first part of this chapter emphasised the need for a good understanding of reservoir permeability. This is borne out by the importance of permeability highlighted in Figures 7.25 to 7.28. Oil viscosity and capillary pressure are also important and the information in the model relating to these appears to be reliable. Discrepancies between the streamline model results and the real production data for Miller can be ascribed both to the lack of detailed permeability information in the model, and the inability of the streamline model to take into account different capillary pressures.

The patterns in the way fluid appears to move in the reservoir model suggest that the waterflooding mechanism may start off as a water bank, but that permeability heterogeneities allow variations in flow rates which encourages mixing and allows fluids of different composition to be produced at the same time. There is a distinct possibility that banking does occur to a certain extent in individual layers of differing permeabilities, but that at the well, mixing of waters from two separate layers occurs. The effects of hydrodynamic dispersion and diffusion must also be taken into account.

7.8 Conclusions

Production simulation models are an effective tool for establishing the amount of mixing occurring in a reservoir and can be made more useful by using detailed geological information about the reservoir together with formation water chemistry data. It is very important to incorporate the best and most detailed information relating to permeability, capillary pressure and relative fluid mobility into the model. Small alterations in these parameters in particular can cause significant changes to a model output. Reservoirs with permeability that is homogeneous or that varies systematically are more likely to experience water mixing than reservoirs with heterogeneous permeability. Low capillary pressure inhibits water flow and prevents water mixing. More mixing occurs in systems containing low viscosity oil than high, but high viscosity oil may increase the risk of water mixing in the well bore – of significance in the prediction of scale precipitation.

The Vdp and Dykstra-Parsons parameters also provide a useful insight into how production simulation models reflect real situations and enable comparisons to be made with data from a producing field. Again, the model and the real data indicate that permeability heterogeneity significantly affects flow of the different fluids through the reservoir. The greater the heterogeneity, the faster water breakthrough is likely to be. The results show that a model can be consistent with real data, but that careful, ongoing analysis of model accuracy should be undertaken.

An extremely effective way of testing a model output is to compare it with real production data. Although it is often neglected, a good match of modelled and real injected water breakthrough can significantly improve all aspects of a model. The best way to track injected water breakthrough in a real situation is to use changes in the water chemistry, provided the end-members of injected and formation waters are well constrained.

Studying the measured and modelled data from Miller highlighted the risks of using reservoir modelling to understand fluid flow and mixing in complex reservoirs. Chloride concentration in produced water was used to calculate the proportion of the produced water that had been injected. This data was used to identify five different patterns of injected water incursion in the Miller reservoir including 1) minor water breakthrough, 2) gradual water breakthrough and progressive mixing, 3) rapid injected water breakthrough and minor mixing, 4) dominant formation water, or alternative formation water and 5) extremely rapid water breakthrough – mixing prior to production. These different patterns are the result of variable production strategies, geographical position of the wells and permeability heterogeneity in the reservoir.

Comparison of the measured Miller data with the Streamline computer model highlighted some significant problems with model reliability. Although it was possible to "tweak" the model enough to provide an accurate prediction of oil behaviour over the life of the field, the water production data (particularly injected water) remained ambiguous and inaccurate, possibly causing misinterpretation of the scaling risk associated with waterflooding.

Results from the first part of the study indicate that it is theoretically possible to produce accurate predictions using a computer model. It should be possible to predict patterns of water breakthrough and mixing in a reservoir, given enough information about the rock properties. While this kind of detailed information is rarely available when needed, a reasonable approximation can be reached provided the modeller has a reasonable understanding of the geology in the system. The importance of a well understood and characterised reservoir to work with cannot be emphasised enough.

Discrepancies between the streamline model results and the real production data for Miller can be ascribed both to the lack of detailed permeability information in the model and the inability of the streamline model to take into account different capillary pressures. These problems are partly the result of a lack of understanding of the importance of carefully history matching produced water as well as oil data when the model was created originally.

Production simulation modelling can therefore be an extremely useful tool in managing oil production from a specific field. Two of the most valuable uses for produced water data are as part of reservoir models in A) the tracking of injected water in the reservoir and B) assessing the reliability of production simulation models. If studied in enough detail, Cl as a tracer can provide a useful indication of the extent of mixing in the reservoir, the location of any potentially high permeability layers and the degree to which vertical permeability differs from horizontal.

Model 1. Varying permeability

Model ref.	Permeability (mD)									Perforations								
	Layer									Layer								
	1	2	3	4	5	6	7	8	9	1	2	3	4	5	6	7	8	9
1a	50	50	50	50	50	50	50	50	50	X								
1b	50	50	50	50	50	50	50	50	50									X
1c	800	700	600	500	400	300	200	100	50	X								
1d	800	700	600	500	400	300	200	100	50									X
1e	50	100	200	300	400	500	600	700	800	X								
1f	50	100	200	300	400	500	600	700	800									X
1g	50	50	50	1000	50	50	50	50	50				X					
1h	1000	50	50	50	50	50	50	50	50	X								
1i	1000	50	50	50	50	50	50	50	50				X					
1j	50	50	50	1000	50	50	50	50	50	X								
1k	50	50	50	1000	50	50	50	50	50	X	X			X				
1l	1000	50	50	50	50	50	50	50	50	X	X			X				

Model 2. Varying capillary pressure

Model ref.	Capillary Pressure Profile	Permeability (mD)									Perforations								
		Layer									Layer								
		1	2	3	4	5	6	7	8	9	1	2	3	4	5	6	7	8	9
2a	Lower	50	50	50	50	50	50	50	50	50	X	X			X				
2b	Higher	50	50	50	50	50	50	50	50	50	X	X			X				
2c	Lower	800	700	600	500	400	300	200	100	50	X	X			X				
2d	Lower	50	100	200	300	400	500	600	700	800	X	X			X				
2e	Higher	50	100	200	300	400	500	600	700	800	X	X			X				
2f	Higher	800	700	600	500	400	300	200	100	50	X	X			X				
2g	Flat curve	50	50	50	50	50	50	50	50	50	X	X			X				

Model 3. Varying mobility ratio

Model ref.	Oil Viscosity (cP)	Permeability (mD)									Perforations								
		Layer									Layer								
		1	2	3	4	5	6	7	8	9	1	2	3	4	5	6	7	8	9
3a	20	50	100	200	300	400	500	600	700	800	X	X			X				
3b	20	800	700	600	500	400	300	200	100	50	X	X			X				
3c	20	50	50	50	50	50	1000	50	50	50	X	X			X				
3d	20	50	50	50	50	1000	50	50	50	50	X	X			X				

Model 4. Vertical permeability the same as horizontal

Model ref.	Vertical permeability = horizontal permeability?	Permeability (mD)									Perforations								
		Layer									Layer								
		1	2	3	4	5	6	7	8	9	1	2	3	4	5	6	7	8	9
4a	Yes	50	100	200	300	400	500	600	700	800	X	X			X				
4b	Yes	800	700	600	500	400	300	200	100	50	X	X			X				
4c	Yes	800	700	600	500	400	300	200	100	50	X	X			X				
4d	Yes	50	100	200	300	400	500	600	700	800	X	X			X				

E. CONCLUSIONS

8.0 CONCLUSIONS

Water-rock interactions are of great significance in terms of the controls on formation water compositions.

The nature of the dominant control on those fluids that reside in the subsurface has been the subject of some controversy over a number of years. In particular, authors have disagreed over the degree of influence of water-rock interactions compared with fluid origin, and over which processes in particular control such ratios as Na:Ca, Ca:Mg, Ca:HCO_3 and Ba:SO_4. Findings here indicate that water-rock interactions are far more important than any other potential control except in the case of chlorinity. In addition, a number of reactions are common to all similar reservoirs, so that formation water compositions reflect the mineralogy of the relevant host-rocks. This study has helped to reduce the controversy by providing evidence from an integrated dataset.

The San Juan case study provided a snapshot in time of a low-salinity system affected by leaching of Na-rich bentonites caused by high bicarbonate concentrations as well as by ion exchange and reduction reactions involving coal beds. While previous isotopic studies established that the basin is not throughflowing, but recharged through meteoric input and basinal upwelling, detailed analysis of formation water chemistry was able to create a useful picture of the additional processes occurring in the system. Variation in Cl concentrations supports previous hypotheses that this area is experiencing significant meteoric recharge in the northwest. In addition, Ca and Na behaviour provide evidence for dissolution of Ca-bearing minerals and the leaching of the abundant bentonite clay, present in the area as the devitrification product of ash falls. These processes likely predominate over simple ion exchange.

In the San Juan Basin, the generation of bicarbonate by coalbed or methane oxidation has a great effect on the chemistry of the waters. Another likely source for this is the dissolution of Ca carbonate minerals at the basin margins. The study of low salinity-high bicarbonate waters has contributed significantly to the understanding of formation waters on a global scale as was examined in more detail in Chapter 5.

In contrast, the Miller case study showed a picture of changes on a production timescale of a saline system affected by fluid mixing and mineral-water reactions. In particular, Ca, Mg, Ba and SO_4 are affected by calcite dissolution and replacement by dolomite, clay formation, barite precipitation and possible sulphate reduction. Fluid injected into the reservoir is saturated with quartz after less than 14 months, indicating a rapid equilibration of the fluid with the silicate system.

Tracking of produced fluid compositional changes through time provides a useful monitor of fluid mixing mechanisms and chemical reactions. This is particularly useful for comparison with reservoir simulation models. An in depth understanding of specific reservoir properties is required to realise the potential of production simulation models. In particular, variations in permeability heterogeneity, fluid properties (including viscosity, density relative permeability) and capillary pressure can all affect a model output and should be as accurate as possible. A substantial amount of fluid mixing can be seen to be occurring in the Miller field from the water chemistry, however, reproduction of real results by the model is extremely difficult to achieve.

While very different systems, San Juan and Miller actually help define different parts of a single, continuous spectrum encompassing all global formation waters. Continuity arises through the action of similar mineralogically-dependent reactions on formation waters of differing starting compositions.

Cation concentrations are modified by water-rock interactions, even in low salinity waters at low temperatures. Similar reactions occur in a variety of different settings and, post burial, the global variation is due to differences in mineralogy in different locations. The evidence for the different reactions is found when comparing formation water compositions with mineralogy across a range of geological settings. The most important reactions in petroleum reservoirs include: K-feldspar dissolution, alteration and recrystallisation; clay mineral formation (e.g. kaolinitisation and illitisation of K-feldspar) and interaction of formation waters with dolomite and Mg-containing clays and sulphate reduction. For example, widespread equilibrium of pore waters with Ca-containing silicate, carbonate and sulphate minerals in all situations means that there is a continuous trend of relative Ca concentration with salinity (TDS), from very low to very high salinity waters, encompassing most formation waters.

It has also been demonstrated that some silicate reactions can occur extremely rapidly once a system has been disturbed. In particular, silicate reactions that constrain pH and release Si into solution have been shown to occur on a timescale of less than 14 months in the Miller field. While it remains true that non-equilibrium assemblages do occur (e.g. kaolinite + K-feldspar), fluid compositions appear to reflect mineralogy.

A deeper understanding of water chemistry in petroleum reservoirs will allow reservoir engineers, production chemists, geochemists and geologists in the industry to perform their roles more effectively. Information provided by formation water analyses from a single location has tremendous application. Given the knowledge gained through this study, it should be possible to

make an informed set of deductions about the nature of the host-rock mineralogy and the potential response of the whole system to the introduction of fluids with compositions varying from fresh water to seawater to CO_2.

Rapid reactions between water and clays/feldspars help to constrain pH even when the system is perturbed, for example by injection of water or CO_2. Modelling results indicate that reservoirs with a wide range of different minerals therefore tend to be the most effective at maintaining a stable system, while clean sand and carbonate reservoirs are more susceptible to formation or seal damage through dissolution of carbonate minerals. Salinity of the formation water is also a factor in determining how much pH will respond to injection however. A system containing feldspars and clays may react rapidly enough to prevent significant damage to a seal caused by carbonate dissolution in some cases.

This study has also highlighted some remaining uncertainties to be resolved by future work:

- Formation water analyses may be of variable quality, and the quality may be hard to evaluate.
- It would be extremely useful to develop a rigorous method for determining the controls on Mg in formation waters, in particular distinguishing between the influence of carbonate and clay minerals.
- Which other practical applications could benefit from an improved understanding of this subject? A potential use for this data is as part of a detailed study into oilfield mineral scale prediction. These data analysis techniques used in conjunction with lithological study and geochemical modelling could provide a useful predictive model, in an age when making the most of current resources is becoming more and more important. An additional direct practical application of formation water data would be to include it as a further constraint within reservoir simulation models.

References

Aagaard, P., Egeberg, P.K., Saigal, G.C., Morad, S. and Bjørlykke, K., 1990, Diagenetic albitisation of detrital K-feldspars in Jurassic, Lower Creatceous and Tertiary clastic sedimentary reservoir rocks from offshore Norway, II. Formation water chemistry and kinetic considerations, *Journal of Sedimentary Petrology*, **60**, 575-581.

Aase, N.E. and Walderhaug, O., 2005, The effect of hydrocarbons on quartz cementation: diagenesis in the Upper Jurassic sandstones of the Miller Field, North Sea, revisited, *Petroleum Geoscience*, **11**, 215-223

Abercrombie, H.J., Hutcheon, I.E., Bloch, J.D. and de Caritat, P., 1994, Silica activity and the smectite-illite reaction, *Geology*, **22**, 539-542

Aplin, A.C. and Warren, E.A.; 1994, Oxygen isotopic indications of the mechanisms of silica transport and quartz cementation in deeply buried sandstones, *Geology*, **22**, 847-850

Appelo, C.A.J. and Willemsen, A., 1987, Geochemical calculations and observations on salt water intrusions, I. A combined geochemical/mixing cell model, *Journal of Hydrology,* **94**, 313-330.

Ayers, W.B., Ambrose, W.A.Jr. and Yeh, J.S., 1994, Coalbed methane in the Fruitland Formation, San Juan Basin; depositional and structural controls on occurrence and resources, In (Ayers, W.B.Jr. and Kaiser, W.R. eds.) Coalbed methane in the Upper Cretaceous Fruitland Formation, San Juan Basin, New Mexico and Colorado, *New Mexico Bureau of Mines and Mineral Resources*, **146**, 13-40

Banks, D.A., Giuliani, G., Yardley, B.W.D. and Cheilletz, A., 2000, Emerald mineralization in Colombia: fluid chemistry and the role of brine mixing, *Mineralium Deposita*, **35**, 699-713

Banks, D.A., Boyce, A.J., Samson, I.M., 2002, Constraints on the Origins of Fluids Forming Irish Zn-Pb-Ba Deposits: Evidence from the Composition of Fluid Inclusions, *Economic Geology*, **97**, 471-480.

Barclay, S.A., Worden, R.H., Parnell, J., Hall, D.L. and Sterner, S.M., 2000, Assessment of Fluid Contacts and Compartmentalisation in Sandstone Reservoirs Using Fluid Inclusions: An Example from the Magnus Oil Field, North Sea, *AAPG Bulletin*, **84**, 489-504.

Barclay, S.A. and Worden, R.H., 2000, Geochemical modelling of diagenetic reactions in a sub-arkosic sandstone, *Clay Minerals*, **35**, 57-67

Barclay, S.A. and Worden, R.H., 2000a, Petrophysical and Petrographical analysis of quartz cement volumes across oil-water contacts in the Magnus Field, northern North Sea, In (Worden, R.H. and Morad, S eds.) Quartz Cementation in Sandstones, *Special Publication of the International Association of Sedimentologists,* **29**, 1-20, Blackwells, Oxford, UK

Bazin, B., Brosse, E. and Sommer, F., 1997, Chemistry in oil-field brines in relation to diagenesis of reservoirs 1. Use of mineral stability fields to reconstruct *in situ* water composition. Example of the Mahakam Basin, *Marine and Petroleum Geology*, **14**, 481-495

Bazin, B., Brosse, E. and Sommer, F., 1997, Chemistry in oil-field brines in relation to diagenesis of reservoirs 2. Reconstruction of palaeo-water composition for modelling illite diagenesis in the Greater Alwyn area (North Sea), *Marine and Petroleum Geology*, **14**, 496-511

Bethke, C.M., 1996, *Geochemical Reaction Modeling, Concepts and Applications*, Oxford University Press, New York, 371p

Biester, H., Selimovic, D., Hemmerich, S. and Petri, M., 2006, Halogens in pore water of peat bogs – the role of peat composition and dissolved organic matter, *Biogeosciences*, **3**, 53-64

Billings, G.K., Hitchon, B. and Shaw, D.R., 1969, Geochemistry and origin of formation waters in the Western Cancda Sedimentart Basin, 2. Alkali Metals, *Chemical Geology*, **4**, 211-223

Birkle, P., Rossilio Aragon, J.J., Portugal, E. and Fong Aguilar, J.L., 2002, Evolution and origin of deep reservoir water at the Activo Luna oil field, Gulf of Mexico, Mexico, *Bulletin of the American Association of Petroleum Geologists*, **86**, 457-484

Bjørkum, P.A., Oelkers, E.H., Nadeau, P.H., Walderhaug, O. and Murphy, W.H., 1998, Porosity Prediction in Quartzose Sandstones as a Function of Time, Temperature, Depth, Stylolite Frequency and Hydrocarbon Saturation, *American Association of Petroleum Geology Bulletin*, **82**, 637-648

Bjørkum, P.A., Walderhaug, O. and Nadeau, P.H., 2001, Thermally driven porosity reduction: impact in basin subsidence, In (Shannon, P.M., Haughton, P.W.D. and Corcoran, D.V. eds.) The Petroleum Exploration of Ireland's Offshore Basins, *Geological Society Special Publications*, **188,** 385-392

Bjørlykke, K and Egeberg, P.K., 1993, Quartz cementation in sedimentary basins, *The American Association of Petroleum Geologists Bulletin*, **77**, 1538-1548

Bjørlykke, K. and Grant, K., 1994, Salinity variations in North Sea formation waters: implications for large-scale fluid movements, *Marine and Petroleum Geology*, **11**, 5-9

Bjørlykke, K., Aagaard, P., Egeberg, P.K. and Simmons, S.P., 1995, Geochemical constraints from formation water analyses from the North Sea and the Gulf Coast basins on quartz, feldspar and illite precipitation in reservoir rocks, In (Cubitt, J.M. and England, W.A. eds.) The Geochemistry of Reservoirs, *Geological Society Special Publication*, **86**, 5-32

Bjørlykke, K., 1996, Lithological control on fluid flow in sedimentary basins, In (Jamtveit, B. and Yardley, B.W.D., eds.) Fluid flow and transport in rocks: Mechanisms and effects, Chapman and Hall, London

Bjørlykke, K., 1997, Mineral/Water Interaction, Fluid Flow and Frio Sandstone Diagenesis: Evidence from the Rocks: Discussion, *The Bulletin of the American Association of Petroleum Geologists*, **81**, 1534-1535

Bjørlykke, K., 1998, Clay mineral diagenesis in sedimentary basins – a key to the prediction of rock properties. Examples from the North Sea Basin, *Clay Minerals*, **33**, 15-34

Blake, R.E. and Walter, L.M., 1999, Kinetics of feldspar and quartz dissolution at 70-80°C and near-neutral pH: Effects of organic acids and NaCl, *Geochimica et Cosmochimica Acta*, **63**, 2043-2059

Bloch, S., Lander, R.H. and Bonnell, L., 2002, Anomalously high porosity and permeability in deeply buried sandstone reservoirs: Origin and predictability, *Bulletin of the American Association of Petroleum Geologists*, **86**, 301-328

Böhlke, J.K. and Irwin, J.J., 1992, Laser microprobe analyses of Cl, Br, I and K in fluid inclusions: Implications for sources of salinity in some ancient hydrothermal fluids, *Geochimica et Cosmochimica Acta*, **56**, 203-225

Bottrell, S.H., Moncaster, S.J., Tellam., J.H., Lloyd, J.W., Fisher, Q.J. and Newton, R.J., 2000, Controls on bacterial sulphate reduction in a dual porosity aquifer system: the Lincolnshire Limestone aquifer, England, *Chemical Geology*, **169**, 461-470.

Braden, J.C. and McLelland, W.G., 1993, Produced Water Chemistry Points to Damage Mechanisms Associated With Seawater Injection, SPE paper 26045, 167-178

Broecker, W.S., 2006, The Holocene CO2 rise: Anthropogenic or natural? *Eos (Transactions, American Geophysical Union)*, **87**, 27

Brosse, É., Matthews, J., Bazin, B., Le Gallo, Y. and Sommer, F., 2000, Related quartz and illite cementation in the Brent sandstones: a modelling approach, In (Worden, R.H. and Morad, S eds.) Quartz Cementation in Sandstones, *Special Publication of the International Association of Sedimentologists,* **29**, 1-20, Blackwells, Oxford, UK

Burley, S.D., 1984, Patterns of diagenesis in the Sherwood Sandstone Group (Triassic), United Kingdom, *Clay Minerals*, **19**, 403-440

Burwood, R. and Mycke, B., 1996, Coastal Angola and Zaire: A Geochemical Contrast of the Lower Congo and Kwanza Basin Hydrocarbon Habitats, *Bulletin of the American Association of Petroleum Geologists*, **80**, 1277

Buschkuehle, B.E. and Machel, H.G., 2002, Diagenesis and palaeofluid flow in the Devonian Southesk-Cairn carbonate complex in Alberta, Canada, *Marine and Petroleum Geology*, **19**, 219-227

Cann, J.R. and Banks, D.A., 2001, Constraints on the genesis of the mineralization of the Alston Block, Northern Pennine Orefield, northern England, *Proceedings of the Yorkshire Geological Society*, **53**, 187-196

Carpenter, A.B. and Miller, J.C., 1969, Geochemistry of saline subsurface water, Saline County, Missouri, *Chemical Geology*, **4**, 135-167

Carpenter, A.B., Trout, M.L. and Pickett, E.E., 1974, Preliminary Report on the Origin and Chemical Evolution of Lead- and Zinc-Rich Oil Field Brines in Central Mississippi, *Bulletin of the Society of Economic Geologists*, **69**, 1191-1206

Carpenter, A.B. 1978, Origin and Chemical evolution of brines in sedimentary basins, *Oklahoma Geological Survey Circular,* **79**, 60-77.

Carrigan, W.J., Nasr-El-Din, H.A., Al-Sharidi, S.H. and Clark, I.D., 1997, Geochemical Characterisation of Injected and Produced Water from Palaeozoic Oil Reservoirs in Central Saudi Arabia, SPE paper 37270, 591-600

Carrigy, M.A. and Mellon, G.B., 1964, Authigenic clay mineral cements in Cretaceous and Tertiary Sandstones of Alberta, *Journal of Sedimentary Petrology*, **34**, 461-472

Cazier, E.C., Hayward, A.B., Espinosa, G., Velandia, J., Mugniot, J-F. and Leel, W.G. Jr., 1995, Petroleum Geology of the Cusiana Field, Llanos Basin Foothills, Colombia, *Bulletin of the American Association of Petroleum Geologists*, **79**, 1444-1463

Chuhan, F., Bjørlykke, K. and Lowrey, C., 2000, The role of provenance in illitization of deeply buried reservoir sandstones from Haltenbanken and North Viking Graben, offshore Norway, *Marine and Petroleum Geology*, **17**, 673-689.

Chuhan, F., Bjørlykke, K. and Lowrey, C., 2001, Closed system burial diagenesis in reservoir sandstones – Examples from the Garn Formation at Haltenbanken area, offshore mid-Norway, *Journal of Sedimentary Research*, **71**, 14-25

Coleman, M.L., 1985, Geochemistry of diagenetic non-silicate minerals: kinetic considerations, *Phil. Trans. R. Soc. Lond. A.* **315**, 39-56

Collins, A.G., 1975, Geochemistry of oilfield waters, developments in petroleum science I, Elsevier, Oxford, pp 496

Connolly, C.A., Walter, L.M., Baadsgaard, H. and Longstaffe, F.I., 1990, Origin and Evolution of formation waters, Alberta Basin, Western Canada Sedimentary Basin, I. Chemistry, *Applied Geochemistry*, **5**, 375-395

Connolly, C.A., Walter, L.M., Baadsgaard, H. and Longstaffe, F.I., 1990, Origin and Evolution of formation waters, Alberta Basin, Western Canada Sedimentary Basin, II. Isotope systematics and water mixing, *Applied Geochemistry*, **5**, 397-413

Conti, A., Sacchi, E., Chiarle, M., Martellini, G. and Zuppi, G.M., 2000, Geochemistry of the formation waters in the Po plain (Northern Italy): an overview, *Applied Geochemistry*, **15**, 51-65

Craig, H., 1961, Isotopic Variation in Meteoric Waters, *Science*, **133**, 1702-1703

Cross, M.M., Manning, D.A.C., Bottrell, S.H., and Worden, R.H., 2004, Thermochemical sulphate reduction (TSR): experimental determination of reaction kinetics and implications of the observed reaction rates for petroleum reservoirs, *Organic Geochemistry*, **35**, 393-404

Curtis, C.D., 1985, Clay mineral precipitation and transformation during burial diagenesis, *Phil. Trans. R. Soc. Lond. A*. **315**, 91-105

Curtis, C.D., Coleman, M.L. and Love, L.G., 1986, Pore water evolution during sediment burial from isotopic and mineral chemistry of calcite, dolomite and siderite concretions, *Geochimica et Cosmochimica Acta*, **50**, 2321-2334

Davisson, M.L. and Criss, R.E., 1996, Na-Ca-Cl relations in basinal fluids, *Geochimica et Cosmochimica Acta*, **60**, 2743-2752

Dickson, J.A.D., 2002, Fossil echinoderms as monitor of the Mg/Ca ratio of Phanerozoic oceans, *Science*, **298**, 1222-1224

Dobson, L.M. and Buffler, R.T., 1997, Seismic Stratigraphy and Geologic History of Jurassic Rocks, Northeastern Gulf of Mexico, *Bulletin of the American Association of Petroleum Geologists*, **81**, 100-120

Dove, P.M. and Rimstidt, J.D., 1994, Silica-water interactions, In (Heaney, P.J., Prewitt, C.T. and Gibbs, G.V., Eds.) Silica: physical behaviour, geochemistry and materials applications, *Reviews in Mineralogy*, **29**, 259-308

Drever, J.I., 1997, The geochemistry of natural waters: surface and groundwater environments, Prentice Hall, Upper Saddle River, N.J., USA

Eastoe, C.J., Long, A. and Knauth, L.P., 1999, Stable chlorine isotopes in the Palo Duro Basin, Texas: Evidence for preservation of Permian evaporite brines, *Geochimica et Cosmochimica Acta*, **63**, 1375-1382

Eastoe, C.J., Long, A., Land, L.S. and Kyle, J.R., 2001, Stable chlorine isotopes in halite and brine from the Gulf Coast Basin: brine genesis and evolution, *Chemical Geology*, **176**, 343-360

Egeberg, P.K. and Aagaard, P., 1989, Origin and evolution of formation waters from oil fields on the Norwegian shelf, *Applied Geochemistry*, **4**, 131-142

Eggenkamp, H.G.M., Kreulen, R and Koster van Groos, A.F., 1995, Chlorine stable isotope fractionation in evaporites, *Geochimica et Cosmochimica Acta*, **59**, 5169-5175

Ehrenberg, S.N. and Nadeau, P.H., 1989, Formation of diagenetic illite in sandstones of the Garn Formation, Haltenbanken area, Mid-Norwegian continental shelf, *Clay minerals*, **24**, 233-253

Emberley, S., Hutcheon, I., Shevalier, M., Durocher, K., Mayer, B., Gunter, W.D. and Perkins, E.H., 2005, Monitoring of Fluid–rock interaction and CO_2 storage through produced fluid sampling at the Weyburn CO2-injection enhanced oil recovery site, Saskatchewan, Canada, *Applied Geochemistry*, **20**, 1131-1157

Emery, D., Smalley, P.C. and Oxtoby, N.H., 1993, Synchronous oil migration and cementation in sandstone reservoirs demonstrated by quantitative description of diagenesis, *Philosophical Transactions of the Royal Society of London*, **344**, 115-125

Fassett, J.E., 1975, Fruitland Formation Coal Deposits of San Juan Basin, New Mexico and Colorado, *Bulletin of the American Association of Petroleum Geologists*, **59**, 908

Fisher, Q. J., Knipe, R.J and Worden, R.H., 2000, Microstructures of deformed and non-deformed sandstones from the North Sea: implications for the origin of quartz cement in sandstones, In (Worden,

R.H. and Morad, S eds.) Quartz Cementation in Sandstones, *Special Publication of the International Association of Sedimentologists,* **29**, 1-20, Blackwells, Oxford, UK

Fontes, J.Ch. and Matray, J.M., 1993, Geochemistry and origin of formation brines from the Paris Basin, France. 1. Brines associated with Triassic salts, *Chemical Geology*, **109**, 149-175.

Fouillac, C. and Michard, G., 1981, Sodium/lithium ratio in water applied to geothermometry of geothermal reservoirs, *Geothermics*, **10**, 55-70

Fournier, R.O., 1983, A method of calculating quartz solubilities in aqueous sodium chloride solutions, *Geochimica et Cosmochimica Acta*, **47**, 579-586

Frape, S.K. and Fritz, P. 1987, Geochemical trends from groundwaters from the Canadian Shield, In (Fritz P. and Frape S.K. eds.) *Saline Water and Gases in Crystalline Rocks,* Geological Association of Canada Special Paper **33**, 5-18.

Garland, C.R., 1993, Miller Field: reservoir stratigraphy and its impact of development, In (Parker, J.R., ed.) *Petroleum Geology of Northwest Europe: Proceedings of the 4th Conference*, Geological Society, p.401-414

Gay, A., Lopez, M., Cochonat, P. and Sermondadaz, G., 2004, Polygonal faults-furrows related to early stages of compaction – upper Miocene to recent sediments of the Lower Congo Basin, *Basin Research*, **16**, 101-116

Girard, J-P., Muntz, I.A., Johansen, H., Lacharpagne, J-C. and Sommer, F., 2002, Diagenesis of the Hild Brent Sandstones, northern North Sea: Isotopic evidence for the prevailing influence of deep basinal water, *Journal of Sedimentary Research*, **72,** 746-759.

Glassman, J.R., 1992, The fate of feldspar in the Brent Group reservoirs, North Sea: a regional synthesis of diagenesis in shallow, intermediate and deep burial environments. In (Morton, A.C., Haszeldine, R.S., Giles, M.R. and Brown, S. Eds.) Geology of the Brent Group, *Geological Society of London Special Publication*, **61**, 329-350

Gluyas, J. and Coleman, M., 1992, Material flux and porosity changes during sediment diagenesis, *Nature*, **356**, 52-54

Gluyas, J., Garland, C., Oxtoby, N.H. and Hogg, A.J.C., 2000, Quartz cement: the Miller's Tale, In (Worden, R.H. and Morad, S eds.) Quartz Cementation in Sandstones, *Special Publication of the International Association of Sedimentologists,* **29**, 1-20, Blackwells, Oxford, UK

Glynn, P.D. and Plummer, L.N., 2005, Geochemistry and the understanding of ground-water systems, *Hydrogeology Journal*, **13**, 263-287

Graf, D.L., 1982, Chemical osmosis, reverse chemical osmosis, and the origin of subsurface brines, *Geochimica et Cosmochimica Acta*, **46**, 1431-1448

Gunter W.D., Perkins E.H., and McCann T.J., 1993, Aquifer disposal of CO2-rich gases: reaction design for added capacity, *Energy Conversion and Management,* **34**, 941-948

Gunter, W.D., Wiwchar, B and E.H. Perkins, 1997, Aquifer disposal of CO2-rich greenhouse gases: extension of the time scale of experiment for CO2-sequestering reactions by geochemical modelling, *Mineralogy and Petrology*, **59**, 129-140

Hangx, S.J.T., Behaviour of the CO2-H2O system and preliminary mineralisation model and experiments, In *Subsurface mineralisation:Rate of CO2 mineralisation and geomechanical effects on host and seal formations*, www.co2-cato.nl/modules.php?name=Downloads&d_op=getit&lid=71

Hanor, J.S., 1993, First order controls on the composition of basinal brines, *Geofluids extended abstracts*, In (Parnell, J. ed.).

Hanor, J.S, 1994, Origin of saline fluids in sedimentary basins, In (Parnell, J. ed.) *Geofluids, Origin, Migration and Evolution of Fluids in Sedimentary Basins,* Geological Society Special Publications, **78,** 151-174

Hanor, J.S., 2002, Reactive transport involving rock-buffered fluids of varying salinity, *Geochimica et Cosmochimica Acta*, **65**, 3721-3732

Hoefs, J., 2004, Stable Isotope Geochemistry, Springer-Verlag, Berlin Heidelberg, Germany

Helgeson, H.C., 1970, Description and interpretation of phase relations in geochemical processes involving aqueous solutions, *American Journal of Science*, **268**, 415-438

Helgeson, H.C., Murphy, W.M. and Aagaard, P., 1984, Thermodynamic and kinetic constraints on reaction rates among minerals and aqueous solutions. II. Rate constants, effective surface area and the hydrolysis of feldspar, *Geochimica et Cosmochimica Acta*, **48**, 2405-2432

Helgeson, H.C., Knox, A.M., Owens, C.E. and Shock, E.L., 1993, Petroleum, oil field waters, and authigenic mineral assemblages: Are they in metastable equilibrium in hydrocarbon reservoirs? *Geochimica et Cosmochimica Acta,* **57**, 3295-3339

Hitchon, B., Billings, G.K. and Klovan, .E., 1971, Geochemistry and origin of formation waters in the Western Canada Basin – III. Factors controlling chemical composition, *Geochimica et Cosmochimica Acta*, **35**, 567-598

Hoefs, J., 2004, Stable Isotope Geocchemistry, Berlin Heidleberg, Germany, Springer-Verlag

Holland, H.D. and Malinin, S.D., 1979, The solubility and occurrence of non-ore minerals, In (Barnes, H.J. ed) *Geochemistry of Hydrothermal Ore Deposits*, Wiley-Interscience, New York

Humphris, S.E. and Thompson, G. 1978, Hydrothermal alteration of oceanic basalts by seawater, *Geochimica et Cosmochimica Acta,* **42**, 107-125

Hurst, A. and Nadeau, P.H., 1995, Clay Microporosity in Reservoir Sandstones: An Application of Quantitative Electron Microscopy in Petrophysical Evaluation, *Bulletin of the American Association of Petroleum Geologists*, **79**, 563-573

Huseby, O., Chatzichristos, C., Sagen, J., Muller, J., Kleven, R., Bennett, B., Larter, S., Stubos, A.K. and Adler, P.M., 2005, Use of natural geochemical tracers to improve reservoir simulation models, *Journal of Petroleum Science and Engineering*, **48**, 241-253

Hutcheon, I. and Abercrombie, H., 1990, Carbon dioxide in clastic rocks and silicate hydrolysis, *Geology*, **18**, 541-544

Hutcheon, I., Shevalier, M. and Abercrombie, H.J., 1993, pH buffering by metastable mineral-fluid equilibria and evolution of carbon dioxide fugacity during burial diagenesis, *Geochimica et Cosmochimica Acta*, **57**, 1017-1027

Hyeong, K and Capuano, R.M., 2001, Ca/Mg of brines in Miocene.Oligocene clastic sediments of the Texas Gulf Coast: Buffering by calcite/disordered dolomite equilibria, *Geochimica et Cosmochimica Acta*, **65**, 3065-3080

Icenhower, J.P. and Dove, P.M., 2000, The dissolution kinetics of amorphous silica into sodium chloride solutions: Effects of temperature and ionic strength, *Geochimica et Cosmochimica Acta*, **64**, 4193-4203

Jamtveit, B. and Yardley, B.W.D., 1997, Fluid flow and transport in rocks: an overview, In (Jamtveit, B. and Yardley, B.W.D., eds.) Fluid flow and transport in rocks: Mechanisms and effects, Chapman and Hall, London

Jones, S.J., 1985, Some Surprises in the Transport of Miscible Fluids in the Presence of a Second Immiscible Phase, SPE12125

Jones, B.F. and Bodine Jr. M.W. 1987 Normative Salt characterization of Natural Waters, In (Fritz P. and Frape S.K .eds) *Saline Water and Gases in Crystalline Rocks,* Geological Association of Canada Special Paper **33**, 5-18.

Jorgensen, B.B., Isaksen, M.F. and Jannasch, H.W., 1992, Bacterial Sulfate Reduction Above 100 degrees C in Deep-Sea Hydrothermal Vent Sediments, *Science*, **258**, 1756-1757

Jusufzade, K.B., 1995, The oil and gas potential of the South Caspian Sea, *Bulletin of the American Association of Petroleum Geologists*, **79**, 1224-1225

Kaiser, W.R., Swartz, T.E. and Hawkins, G.J., 1994, Hydrologic framework of the Fruitland Formation, San Juan Basin, In (Ayers, W.B.Jr. and Kaiser, W.R. eds.) Coalbed methane in the Upper Cretaceous Fruitland Formation, San Juan Basin, New Mexico and Colorado, *New Mexico Bureau of Mines and Mineral Resources*, **146,** 133-163

Kaszuba, J.P., Janecky, D.R. and Snow, M.G., 2003, Carbon dioxide reaction processes in a model brine aquifer at 200°C and 200 bars: implications for geologic sequestration of carbon, *Applied Geochemistry*, **18**, 1065-1080

Khain, V.E. and Polyakova, I.D., 2004, Oil and Gas Potential of Deep- and Ultradeep-Water Zones of Continental Margins, *Lithology and Mineral Resources*, **39**, 530-340

Kharaka, Y.K., Cole, D.R., Oak, S.D., Gunter, W.D., Knauss, K.G., Freifeld, B.M., 2006, Gas-water-rock interactions in Frio Formation following CO2 injection: Implications for the storage of greenhouse gases in sedimentary basins, *Geology*, **34**, 577-580

Kimblin, R. T., 1995. The chemistry and origin of groundwater in Triassic sandstone and quaternary deposits, northwest England and some UK comparisons. *Journal of Hydrology*, **172**, 293-311.

Kleven, R. and Alstad, J., 1996, Interaction of alkali, alkaline-earth and sulphate ions with clay minerals and sedimentary rocks, *Journal of Petroleum Science and Engineering*, **15**, 181-200

Klusman, R.W., 2003, A geochemical perspective and assessment of leakage potential for a mature carbon dioxide-enhanced oil recovery project and as a prototype for carbon dioxide sequestration; Rangely field, Colorado, *AAPG Bulletin,* **87**, 1485-1507

Krauskopf, D., 1957, Dissolution and precipitation of silica at low temperatures, *Geochimica et Cosmochimica Acta*, **10**, 1-26

Land, L.S. and Milliken, K.L., 1981, Feldspar diagenesis in the Frio Formation, Brazoria County, Texas Gulf Coast, *Geology*, **9**, 314-318

Land, L.S., 1987, The major ion chemistry of saline brines in sedimentary basins, In (Baanavar, J.R., Koplik, J. and Winkler, K.W. eds.), Physics and Chemistry of Porous Media II: Ridgefield, Conn., *American Institute of Physics Conference Proceedings*, **154**, 160-179

Land, L.S., Macpherson, G.L. and Mack, L.E., 1988, The geochemistry of saline formation waters, Miocene, Offshore Louisiana, *Transactions – Gulf Coast Association of Geological Societies*, **38**, 503-512

Land, L.S., 1991, Evidence for vertical movement of fluids, Gulf Coast sedimentary basin, *Geophysical Research Letters*, **18**, 919-922

Land, L.S. and Macpherson, G.L., 1992, Origin of Saline Formation Waters, Cenozoic Secion, Gulf of Mexico Sedimentary Basin, *Bulletin of the American Association of Petroleum Geologists*, **76**, 1344-1362

Land, L.S., 1995, Na-Ca-Cl saline formation waters, Frio Formation (Oligocene), South Texas, USA: Products of diagenesis, *Geochimica et Cosmochimica Acta,* **59**, 2163-2174

Land, L.S., 1998, Failure to Precipitate Dolomite at 25°C from Dilute Solution Despite 1000-Fold Oversaturation after 32 years, *Aquatic Geochemistry*, **4**, 361-368

Land, L.S. and Milliken, K.L., 2000, Regional loss of SiO_2 and $CaCO_3$ and gain of K_2O during burial diagenesis of Gulf Coast mudrocks, USA, In (Worden, R.H. and Morad, S eds.) Quartz Cementation in Sandstones, *Special Publication of the International Association of Sedimentologists,* **29**, 1-20, Blackwells, Oxford, UK

Larter, S.R. and Aplin, A.C., 1995, Reservoir geochemistry: methods, applications and opportunities, In (Cubitt, J.M. and England, W.A. eds.) The Geochemistry of Reservoirs, *Geological Society Special Publication*, **86**, 5-32

Larter, S.R., Aplin, A.C., Corbett, P.W.M., Ementon, N., Chen, M. and Taylor, P.N., 1997, Reservoir geochemistry: A Link Between Reservoir Geology and Engineering? *SPE Reservoir Engineering*, **12**, 12-17

Larue, D.K. and Friedman, F., 2005, The controversy concerning stratigraphic architecture of channelized reservoirs and recovery by waterflooding, *Petroleum Geoscience.*, **11**, 131-146

Laubach, S.E. and Tremain, C.M., 2005, Tectonic setting of the San Juan Basin, In (Ayers, W.B.Jr. and Kaiser, W.R. eds.) Coalbed methane in the Upper Cretaceous Fruitland Formation, San Juan Basin, New Mexico and Colorado, *New Mexico Bureau of Mines and Mineral Resources*, **146**, 9-11

Lawrence, J.R. and Taylor, H.P. Jr., 1971, Deuterium and oxygen-18 correlation: Clay minerals and hydroxides in Quaternary soils compared to meteoric waters, *Geochimica et Cosmochimica Acta*, **35**, 993-1003

Le Gallo, Y., Bildstein, O. and Brosse, E., 1998, Coupled reaction-flow modelling of diagenetic changes in reservoir permeability, porosity and mineral compositions, *Journal of Hydrology*, **209**, 366-388

Lowenstein, T.K, Timofeeff, M.N., Brennan, S.T., Hardie, L.A. and Demicco, R.V., 2001, Oscillations in Phanerozoic seawater chemistry: Evidence from fluid inclusions, *Scicence*, **294**, 1086-1088

Lowenstein, T.K., Hardie, L.A., Timofeeff, M.N. and Demicco, R.V., 2003, Secular variation in seawater chemistry and the origin of calcium chloride basinal brines, *Geology*, **31**, 857-860

Lundegard, P.D. and Land, L.S., 1989, Carbonate equilibria and pH buffering by organic acids – response to changes in p_{CO2}, *Chemical Geology*, **74**, 277-287

Lynch, F.L., Mack, L.E. and Land, L.S., 1997, Burial Diagenesis of illite/smectite in shales and the origin of authigenic quartz and secondary porosity in sandstones, *Geochimica et Cosmochimica Acta*, **61**, 1995-2001

Macaulay, C.I., Haszeldine, R.S. and Fallick, A.E., 1992, Diagenetic Pore Waters Stratified for at Least 35 Million Years: Magnus Oil Field, North Sea, *American Association of Petroleum Geologists Bulletin,* **76**, 1625-1634

Machel, H.G., 2001, Bacterial and thermochemical sulfate reduction in diagenetic settings – old and new insights, *Sedimentary Geology*, **140**, 143-175

Mackay, E.J. and Sorbie, K.S., 2000, Brine Mixing in Waterflooded Reservoirs and the Implications for Scale Prevention, SPE 60193

Mackenzie, F.T. and Kump, L.R., 1995, Reverse Weathering, Clay Mineral Formation and Oceanic Element Cycles, *Science*, **270**, 586-587

Maher, K., Steefel, C.I., DePaolo, D.J. and Viani, B.E., 2006, The mineral dissolution rate conundrum: Insights from reactive transport modelling of Uranium isotopes and pore fluid chemistry in marine sediments, *Geochimica et Cosmochimica Acta,* **70**, 337-363

Marchand, A.M.E., Haszeldine, R.S., Macaulay, C.I., Swennan, R., and Fallick, A.E., 2000, Quartz cementation inhibited by crestal oil charge: Miller deep water sandstone, UK North Sea, *Clay Minerals*, **35**, 201-210

Marchand, A.M.E., 2001, Diagenesis and porosity preservation in deepwater oilfield sandstones, Unpublished PhD Thesis, University of Edinburgh

Marchand, A.M.E., Haszeldine, R.S., Smalley, P.C., Macaulay, C.I. & Fallick, A.E. (2001), Evidence for reduced quartz cementation rates in oil-filled sandstones. Geology 29, 915-918

Marchand, A.M.E., Macaulay, C.I., Haszeldine, R.S. and Fallick, A.E., 2002, Pore water evolution in oilfield sandstones: Constraints from oxygen isotope microanalysis of quartz cement, *Chemical Geology*, **191**, 285-304

Marroquìn, I.D. and Hart, B.S., 2004, Seismic attribute-based characterization of coalbed methane reservoirs: An example from the Fruitland Formation, San Juan Basin, New Mexico, *Bulletin of the American Association of Petroleum Geologists*, **88**, 1603-1621

McBride, E.F., Macpherson, G.L, Diggs, T.N. and Mack, L.E., 1988, Petrography, stable isotope geochemistry and diagenesis of Miocene sandstones, *Transactions – Gulf Coast Association of Geological Societies*, **38**, 513-523

McBride, B.C., Weimer, P. and Rowan, M.G., 1998, The Effect of Allochthonous Salt on the Petroleum Systems of Northern Green Canyon and Ewing Bank (Offshore Louisiana), Northern Gulf of Mexico, *Bulletin of the American Association of Petroleum Geologists*, **82**, 1083-1112

McCartney, R.A., Williams, J.C. and Coghlan, G., 2005, Processes Determining the Composition of Produced Water From Subsea Fields and Implications for Scale Management – Birch Field, UKCS, SPE 94869

McKinley, J.M., Worden, R.H. and Ruffell, A.H., 2003, Smectite in sandstones: a review of the controls on occurrence and behaviour during diagenesis, In (Worden, R.H. and Morad, S eds.) Clay mineral cements in Sandstones, *Special Publication of the International Association of Sedimentologists*, **34**, 109-128, Blackwells, Oxford, UK

Michael, K. and Bachu, S., 2002, Origin, chemistry and flow of formation waters in the Mississippian-Jurassic sedimentary succession in the west-central part of the Alberta Basin, Canada, *Marine and Petroleum Geology*, **19**, 289-306

Milliken, K.L., McBride, E.F. and Land, L.S., 1989, Numerical Assessment of dissolution versus replacement in the subsurface destruction of detrital feldspars, Oligocene Frio Formation, South Texas, *Journal of Sedimentary Petrology*, **59**, 740-757

Milliken, K.L. and Land, L.S., 1991, Reverse weathering, the Carbonate-Feldspar System, and Pore Water Evolution during Burial of Sandstones, *Bulletin of the American Association of Petroleum Geologists*, **75**, 636

Mohamed, E.A. and Worden, R.H., 2006, Geochemical evolution of groundwater in the Triassic Sherwood Sandstone aquifer in the Liverpool area, UK, *Applied Geochemistry*, In Press.

Monnin, C., 1999, A thermodynamic model for the solubility of barite and celestite in electrolyte solutions and seawater to 200°C and to 1kbar, *Chemical Geology*, **153**, 187-209

Monnin, C., Jeandel, C., Cattaldo, T. and Dehairs, F., 1999, The marine barite saturation of the world's oceans, *Marine Chemistry*, **65**, 253-261

Monnin, C., Wheat, C.G., Dupre, B., Elderfield, H. and Mottl, M.M., 2001, Barium Geochemistry in sediment pore waters and formation waters of the oceanic crust on the eastern flank of the Juan de Fuca Ridge (ODP Leg 168), *Geochemistry Geophysics Geosystems 2*, No. 2000GC000073, Jan 8

Neve, L. 2004, Quantification of the mineralogy of siliciclastic sedimentary rock: A comparative study, *unpublished MSc thesis, University of Leeds.*

Nicolle, G., Boibien, C., Ten-Haven, H.L., Tegelaar, E. and Chavagnac, Ph., 1997, Geochemistry: A Powerful tool for Reservoir Monitoring, SPE paper 37804, 395-401

Nummedal, D., 2002,Hydrocarbons of the South Caspian Basin: How Exploitation Depends on the Understanding of the Neogene Palaeoclimate, *Bulletin of the American Association of Petroleum Geologists*, **86**, 194-195

Oelkers, E.H., Bjørkum, P.A. and Murphy, W.M., 1996, A petrographic and computational investigation of quartz cementation and porosity reduction in North Sea sandstones, *American Journal of Science*, **296**, 420-452

Oelkers, E.H. and Schott, J., 1998, Does organic acid adsorption affect alkali-feldspar dissolution rates? *Chemical Geology*, **151**, 235-245

Oelkers, E.H., Bjørkum, P.A., Walderhaug, O., Nadeau, P.H and Murphy, W.M., 2000, Making diagenesis obey thermodynamics and kinetics: the case of quartz cementation in sandstones from offshore Mid-Norway, *Applied Geochemistry*, **15**, 295-309

Østvold, T. and Randhol, P., 2001, Kinetics of $CaCo_3$ Scale Formation. The influence of Temperature, Supersaturation and Ionic composition, *Society of Petroleum Engineers*,

Pearson, F.J., 1994, Models of mineral controls on the composition of saline groundwaters of the Canadian Shield, In (Fritz P. and Frape S.K .eds) *Saline Water and Gases in Crystalline Rocks,* Geological Association of Canada Special Paper **33**, 39-51

Prosser, D.J., McKeever, M.E., Hogg, A.J.C. and Hurst, A., 1995, Permeability heterogeneity within massive Jurassic submarine fan sandstone from the Miller Field, northern North Sea, UK. In: (Hartley, A.J. and Prosser, D.J. eds) Characterisation of Deep Marine Clastic Systems, *Geological Society of London Special Publicaation*, **94**, 201-219

Rasmussen, E.S., 1996, Structural evolution and sequence formation offshore South Gabon during the Tertiary, *Tectonophysics*, **266**, 509-523

Reynolds, A.D., Simmons, M.D., Bowman, M.B.J., Henton, J., Brayshaw, A.C., Ali-Zade, A.A., Guiliyev, I.S., Suleymanova, S.F., Ateava, E.Z., Mamedova, D.N. and Koshkarly, R.O., 1998, Implications of Outcrop Geology for Reservoirs in the Neogene Productive Series: Ashperon Peninsual, Azerbaijan, *Bulletin of the American Association of Petroleum Geologists*, **82**, 25-49

Riese, W.C., Pelzmann, W.L. and Snyder, G.T., 2005, New insights on the hydrocarbon system of the Fruitland Formation coal beds, norther San Juan Basin, Colorado and New Mexico, In (Warwick, P.D. ed) Coal Systems Analysis, *Geological Society of America Special Paper*, **387**, 73-111

Rittenhouse, G., 1967, Bromine in oilfield waters and its use in determining possibilities of origin of these waters, *Bulletin of the American Association of Petroleum Geologists*, **51**, 2430-2440

Rosenberg, P.E. and Holland, H.D., 1964, Calcite-Dolomite-Magnesite Stability Relations in Solutions at Elevated Temperatures, *Science*, **145**, 700-701

Saigal, G.C., Morad, S., Bjørlykke, K., Egeberg, P.K. and Aagaard, P., 1988, Digenetic albitisation of detrital K-feldspar in Jurassic, Lower Cretaceous and Tertiary clastic reservoir rocks from offshore Norway, I. Textures and origin, *Journal of Sedimentary Petrology*, **58**, 1003-1013

Schmid, S., Worden, R.H. and Fisher, Q.J., 2004, Diagenesis and reservoir quality of the Sherwood Sandstone (Triassic) Corrib Field, Slyne Basin, west of Ireland, *Marine and Petroleum Geology*, **21**, 299-315

Schmid, S., Worden, R.H. and Fisher, Q.J., 2006, Carbon isotope stratigraphy using carbonate cements in the Triassic Sherwood Sandstone Group: Corrib Field, west of Ireland, *Chemical Geology*, **225**, 137-155

Schmulovich, K.I., Yardley, B.W.D. and Graham, C.M., 2005, The solubility of quartz in chloride solutions at 400°-800°C and 0.1-0.9 GPa, *Geochimica et Cosmochimica Acta*, **69**, A823

Scott, A.R., Kaiser, W.R. and Ayers, W.B. Jr., 1994, Thermogenic and Secondary Biogenic Gases, San Juan Basin, Colorado and New Mexico – Implications for Coalbed Gas Producibility, *Bulletin of the American Association of Petroleum Geologists*, **78**, 1186-1209

Skilbrei, O.B., Hallenbeck, L.D. and Sylte, J.E., 1990, Comparison and Analysis of Radioactive Tracer Injection Response With Chemical Water Analysis Into the Ekofisk Formation Pilot Waterflood, SPE paper 20776, 559-569

Slentz, L.W., 1981, Geochemistry of reservoir fluids as a unique approach to optimum reservoir management, SPE paper 9582, 37-48

Smalley P.C. and Warren, E.A., 1994, The Miller Field. In, (Warren, E. A. and Smalley, P.C. eds.), North Sea Formation Waters Atlas, Geological Society Memoir, **15**, 52

Smalley, P.C., Dodd, T.A., Stockden, I.L., Råheim, A. and Mearns, E.W., 1995, Compositional heterogeneities in oilfield formation waters: identifying them, using them, In (Cubitt, J.M. and England, W.A. eds.) The Geochemistry of Reservoirs, *Geological Society Special Publication*, **86**, 5-32

Smalley, P.C. and Hale, N.A., 1996, Early Identification of Reservoir Compartmentalisation by Combining a Range of Conventional and Novel Data Types, *SPE Formation Evaluation*, paper 30533, 163-169

Smalley, P.C., England, W.A., Muggeridge, A., Abacioglu, Y. and Cawley, S., 2004, Rates of reservoir fluid mixing: implications for interpretation of fluid data, From (Cubitt, J.M., England, W.A. and Larter, S. eds) *Understanding Petroleum Reservoirs: towards an Integrated Reservoir Engineering and Geochemical Approach*, Geological society special publications, **237**, 99-113

Smith, J.T. and Eherenberg, S.N., 1989, Correlation of carbon dioxide abundance with temperature in clastic hydrocarbon reservoirs: relationship to inorganic chemical equilibrium, *Marine and Petroleum Geology*, **6**, 129-136

Snyder, G.T., Riese, W.C., Franks, S., Fehn, U., Pelzmann, W.L., Gorody, A.W. and Moran, J.E., 2003, Origin and history of waters associated with coalbed methane: ^{129}I, ^{36}Cl, and stable isotope results from the Fruitland Formation, CO and NM, *Geochimica et Cosmochimica Acta*, **67**, 4529-4544

Sorbie, K.S. and Mackay, E.I., 2000, Mixing of injected, connate and aquifer brines in waterflooding and its relevance to oilfield scaling, *Journal of Science and Engineering*, **27**, 85-106

Spears, D.A., 2005, A review of chlorine and bromine in some United Kingdom coals, *International Journal of Coal Geology*, **64**, 257-265

Stefánsson, A. and Anórsson, S., 2000, Feldspar saturation state in natural waters, *Geochimica et Cosmochimica Acta*, **64**, 2567-2584

Steuber, T. and Vezier, J, 2002, Phanerozoic record of plate tectonic control of seawater chemistry and carbonate sedimentation, *Geology*, **30**, 1123-1126

Swan, A.R.H. and Sandilands, M., 1995, Introduction to Geological Data Analysis, Blackwell Science, Oxford

Taylor, H.P., 1997, Oxygen and Hydrogen Isotope Relationships in Hydrothermal Mineral Deposits, In, (Barnes, H.L. ed.) *Geochemistry of Hydrothermal Ore Deposits, 3rd*, Wiley, New York, 227-271

Todd, A.C., Yuan, M.D. and McCracken, I.R., 1994, *Sulphate and carbonate scale prediction in North Sea oil and gas fields*, In (Warren, E.A. and Smalley, P.C. eds) North Sea Formation Waters Atlas, Geological Society Memoir, **15**, 105-113

Ullyott, J.S. and Nash, D.J., 2006, Micromorphology and geochemistry of groundwater silcretes in the eastern South Downs, UK, *Sedimentology*, **53**, 387-412

United Kingdom Department of Trade and Industry (DTI), (2002), *Our energy future – creating a low carbon economy*. Energy White Paper. http://www.dti.gov.uk/energy/whitepaper

Verma, M.P., 2000, Chemical thermodynamics of silica: a critique on its geothermometer, *Geothermics*, **29**, 323-346

Von Damm, K.L., Bischoff, J.L. and Rosenbauer, R.J., 1991, Quartz solubility in hydrothermal seawater: an experimental study and equation describing quartz solubility for up to 0.5 M NaCl solutions, *American Journal of Science*, **291**, 977-1007

Walderhaug, O., 1994a, Temperatures of quartz cementation in Jurassic sandstones from the Norwegian continental shelf – evidence from fluid inclusions, *Journal of Sedimentary Research*, **64**, 311-323

Walderhaug, O., 1994, Precipitation rates of quartz cement in sandstones determined by fluid inclusion microthermometry and temperature-history modelling, *Journal of Sedimentary Research*, **64**, 324-333

Walter, L.M., Stueber, A.M. and Huston, T.J., 1990, Br-Cl-Na systematics in Illinois basin fluids: Constraints on fluid origin and evolution, *Geology*, **18**, 315-318

Warwick, P.D., 2005, Coal systems analysis: A new approach to the understanding of coal formation, coal quality and environmental considerations, and coal as a source rock for hydrocarbons, In (Warwick, P.D. ed) Coal Systems Analysis, *Geological Society of America Special Paper*, **387**, 1-8

Weimer, P., Rowan, M.G. McBride, B.C. and Kligfield, R., 1998, Evaluating the Petroleum Systems of the Northern Gulf of Mexico Through Integrated Basin Analysis: An Overview, *Bulletin of the American Association of Petroleum Geologists*, **82**, 865-877

Weimer, P., Crews, J.R., Crow, R.S. and Varnai, P., 1998, Atlas of Petroleum Fields and Discoveries, Northern Green Canyon, Ewing Bank, and Southern Ship Shoal and South Timbalier Areas (Offshore Louisiana), Northern Gulf of Mexico, *Bulletin of the American Association of Petroleum Geologists*, **82**, 878-917

White, C.M., Strazisar, B.R., Granite, E.J., Hoffman, J.S. and Pennline, H.W., 2003, Sequestration and capture of CO_2 from large stationary sources and sequestration in geological formations – Coalbeds and deep saline aquifers, *Journal of the Air and Waste Management Association*, **53**, 645-715

Wilson, T.P. and Long, D.T., 1984, The behaviour of bromide during the dissolution of halite at 25°C and 1 atm, *Geological Society of America Abstracts with Programmes*, pp 697

Worden, R.H. and Rushton, J.C., 1992, Diagenetic K-feldspar textures: a TEM study and model for diagenetic feldspar growth, *Journal of Sedimentary Petrology*, **62**, 779-789

Worden, R.H., Smalley, P.C. and Oxtoby, N.H., 1995, Gas Souring by Thermochemical sulfate reduction at 140°C, AAPG Bulletin, 79, 854-863

Worden, R.H., Coleman, M.L. and Matray, J-M., 1999, Basin scale evolution of formation waters: A diagenetic and formation water study of the Triassic Chaunoy Formation, Paris Basin, *Geochimica et Cosmochimica Acta*, **63**, 2513-2528

Worden, R.H. and Morad, S., 2000, Quartz cementation in oil field sandstones: a review of the key controversies, In (Worden, R.H. and Morad, S eds.) Quartz Cementation in Sandstones, *Special Publication of the International Association of Sedimentologists*, **29**, 1-20, Blackwells, Oxford, UK

Worden, R.H. and Morad, S., 2003, Clay minerals in sandstone: controls in formation, distribution and evolution, In (Worden, R.H. and Morad, S eds.) Clay mineral cements in Sandstones, *Special Publication of the International Association of Sedimentologists,* **34**, 3-41, Blackwells, Oxford, UK

Worden, R.H., Smalley, P.C. and Barclay, S.A., 2003, H_2S and diagenetic pyrite in North Sea sandstones: due to TSR or organic sulphur compound cracking? *Journal of Geochemical Exploration*, **78-79**, 487-491

Yardley, B.W.D. and Graham, J.T., 2002, The origins of salinity in metamorphic fluids, *Geofluids*, **2**, 249-256

Yardley, B.W.D., 2005, Metal Concentrations in Crustal Fluids and Their Relationship to Ore Formation, *Economic Geology*, **100**, 613-632

Zeigler, K., Coleman, M.L. and Howarth, R.J., 2001, Palaeohydrodynamics of fluids in the Brent Group (Oseberg Field, Norwegian North Sea) from chemical and isotopic compositions of formation waters, *Applied Geochemistry*, **16**, 609-632

Zhou, Z. and Ballantine, C.J., 2006, ^4He dating of groundwater associated with hydrocarbon reservoirs, *Chemical Geology*, **226**, 309-327